

NASA-CR-3611 19830008725

NASA CR-3611

DESERT LANDFORMS OF SOUTHWEST EGYPT: A BASIS FOR COMPARISON WITH MARS



NF02127

BEST

AVAILABLE

COPY

**DESERT LANDFORMS OF
SOUTHWEST EGYPT:
A BASIS FOR COMPARISON
WITH MARS**

Farouk El-Baz and Ted A. Maxwell, Editors
National Air and Space Museum
Smithsonian Institution
Washington, DC

Prepared for
The Planetary Geology Program,
Office of Space Science and Applications,
National Aeronautics and Space Administration
Under Grant No. NSG-7486

The enhanced Landsat image on the cover shows Gebel Uweinat, an 1800 m high mountain located at the borders of Egypt, Libya and Sudan. The dark, elongated streak surrounding the mountain is created by the predominant northerly winds characteristic of this part of the Western Desert of Egypt. Relationships between topographic features and wind streaks in southwestern Egypt show many similarities to those observed on Mars.

DEDICATION

C. VANCE HAYNES

Department of Geology
University of Arizona
Tucson, Arizona 85721

With respect and admiration we dedicate this volume to the late W. B. Kennedy Shaw, archaeologist, historian, botanist, and pioneer explorer of the Libyan Desert (Western Desert of recent literature). Born in Northumberland in 1901, Shaw was trained in forestry at University College, Oxford and in 1923 took a forestry job in Sudan. In Khartoum he met Douglas Newbold, who became Governor of Kordofan Province the year after his epic "Desert Odyssey of 1000 Miles" (Newbold, 1924), and together in 1926 they mapped the Merga depression, discovered Burg El-Tuyur (hill of the birds), and explored the desert between Merga and Selima on the last scientific camel expedition in the Western Desert (Newbold and Shaw, 1928). In 1930 they gave up the use of camels and joined R. A. Bagnold in exploring the sand sea, Gilf Kebir, Uweinat and the Selima sand sheet with Model A Fords (Bagnold, 1931). During the discussion of their presentation to the Royal Geographical Society, Shaw presented one of the few published accounts of the plight of refugees from Kufra in 1931. The skeleton we found at Black Hill is probably one of them (see Haynes; Chapter 9).

A further journey with Bagnold (1933) was made in 1932 from Kharga to Uweinat, Sarra Wells, El-Fasher, El-Atrun, Merga, Laqiya, and Selima covering over 6000 miles. Three years later Shaw (1936a) organized his own expedition and covered over 6300 miles to explore parts of the sand sea, Gilf Kebir, Wadi Howar, and Wadi Hussein. This led to new discoveries of rock paintings, numerous archaeological sites in Wadi Howar, and an unmapped depression between Merga and Selima.

His desert expertise was put to more practical use in 1940 when he left the Palestine Department of Antiquities to join the Long Range Desert Group as Intelligence Officer and later the Special Air Service. His book "Long Range Desert Group" (Shaw, 1945) is now a collector's item.

Those of us who are fortunate enough to travel the deserts west of the Nile are frequently reminded of those who have gone before (see McHugh; Chapter 2) by their tracks on the stony parts of the desert floor, by the wind-swept remains of their camp sites, and by the names of places such as Burg El-Tuyur, a remote but conspicuous outcrop within the Great Selima Sand Sheet in northern Sudan. This year, upon finding this lonely rock and viewing the single engraving of a Neolithic steer that Newbold and Shaw had found 54 years earlier, the thrill of discovery was mixed with one of sadness. Bill Shaw died 23 April 1979.

**Page Missing in
Original Document**

FOREWORD

R. A. BAGNOLD
Rickwoods
Mark Beech
Edenbridge, Kent
England

It is now more than half a century since I first went to Egypt. Motor transport, introduced during the First World War, was still largely confined to the few existing roads. I very soon became interested in the possibilities it offered of reaching, at a cost we could afford, the many famous antiquities of the Middle East, then accessible only with difficulty and at considerable expense in time and money. The possibilities grew with our experience, and we turned, inevitably, to those of penetrating the still largely mysterious vastness of the Egypto-Libyan Desert far beyond camel range. Ahmed Hassenein, later Hassenein Pasha, had made his epic camel journey of some 2000 miles but three years previously, crossing for the first time ever the entire desert from north to south; from Sallum on the Mediterranean coast, via the then little-known Kufra group, an oasis then the center of Senussi influence, to El Fasher far away in the Sudan (see map on following page). On the way he discovered for the civilized world the existence of the solitary Uweinat-Arkenu massif with its permanent water supply from isolated local rainfall on the mountain, and its prehistoric rock drawings and paintings. This modest man, uniquely half a Bedouin by birth, a Balliol scholar by education and a diplomat by profession, could probably alone have achieved such a journey at the time. His book The Lost Oases is a mine of information.

The discovery of Uweinat's water supply broke the biological barrier that had limited all previous attempts to penetrate westwards from southern Egypt. As an immediate result, Prince Kemal el Din led two successive expeditions southwestwards from Kharga Oasis, organized in the grand manner and including geologists, surveyors and others. He discovered and traversed the foot of the long high cliff line which he named the Gilf Kebir, however, without exploring the plateau above. He reached and surveyed the Uweinat massif and was able to push on westward as far as the deep well-shaft of Maaten Sarra dug by El Mahdi Senussi. To the north, though, there still remained the 400 mile long physical barrier of the Great Sand Sea whose westward extent was then unknown. Its huge parallel dune chains remained uncrossed until 1932.

To those few of us whose interests extended beyond the confines of the Nile Valley it was a stimulating time of new discoveries. John Ball, director of the new Egyptian Desert Survey and one of the fathers of desert exploration had just shown that a single common artesian aquifer in the Nubian Sandstone underlay the whole desert, outcropping wherever wind erosion had proceeded to a sufficient depth. In order to do this, he had collated altitudes above sea level of the



Sketch map showing route of Hassanein Bey through the Libyan Desert (drawn by H. A. Bumstead, 1924; courtesy National Geographic Magazine).

standing water in all the oases and known wells and water holes. His map, with surface contours superimposed on those of the artesian water table neatly explained the mystery of how the oases could exist.

Life in a rainless land depends entirely on a continued supply of artesian water. The populations of the inhabited oases have for ages been limited by the natural rate of supply. That of the tiny oasis of Qara has, for instance, traditionally been limited to forty people. As early as 1921 a development company started pumping from newly sunk bore-holes in Kharga Oasis. The immediate rapid draw-down in all the existing wells and springs caused the whole project to be abandoned. But now the lesson seems to have been forgotten, or deliberately ignored. The present very large-scale Libyan irrigation project in the neighborhood of Kufra is causing a fall in the artesian water level amounting to one meter per year.

The Egypto-Libyan desert is vulnerable to Man's activities in another, very different sense. Having been subjected to wind erosion for a great period of time, evidence of its past successive human occupations are all concentrated together on the present surface. Hence if appreciable progress is ever to be made in the interpretation of the human past in this desert it seems probable that special methods involving comparative statistics concerning the surface density and distribution of the various types of artifacts will be necessary. This seems to apply particularly to the rock drawings and paintings. Some of the latter are far more spectacular than those at Uweinat. They are of at least three different kinds, often found together on the wall of the same cave or protected recess. The differences of style and theme are so great that the artists must have belonged to peoples of different ages and cultures. But when the paintings were done and by what successive peoples we have no direct means of estimating. The most promising approach, which has not been hitherto attempted, appears likely to be a wide-ranging and coordinated statistical survey, covering as much as possible of the paintings belt across north Africa, aimed at correlating the type or types of painting (recorded in some agreed standard color-photographic format), together with the character of the location (always in my experience a water-source), with the relative densities of the artifact types found nearby. But, alas, human nature is such that the temptation to pick up and remove ancient artifacts seen lying on the ground is almost irresistible. Even now the original statistical pattern of artifact distribution must in some places have already spoilt. Almsy discovered an exceptionally fine and well-preserved picture gallery in a cave beneath a western outlier of the Gilf. Being an artist he spent some time copying the paintings, and being also a cigarette smoker he unconsciously ground the ends into the sand floor (why not, in such a remote region?). Some years later, Ronald Peel and I happened to scoop away the few centimeters of sand and cigarette ends from beneath one of the paintings. There, on the floor, still intact, lay small lumps of all four of the original mineral pigments. We re-buried them.

There is, in this wonderful desert, unlimited scope for many more scientific expeditions similar to that reported in this book. But for the sake of posterity it is to be hoped (I fear probably in vain) that mankind's craving for exploitation will not lead to the exhaustion of the accumulated past, whether of water or of archaeology, in the same way as is now happening in the case of fossil fuels.

**Page Missing in
Original Document**

CONTENTS

DEDICATIONiii
C. Vance Haynes

FOREWORD v
R. A. Bagnold

Chapter 1. JOURNEY TO EGYPT'S FARTHEST CORNER 1
Farouk El-Baz

Chapter 2. A CHRONICLE OF RESEARCH AND EXPLORATION IN
THE GILF KEBIR-UWEINAT MOUNTAIN REGION 21
William P. McHugh

Chapter 3. DESERT NAVIGATION 27
C. Vance Haynes and Ted A. Maxwell

Chapter 4. THE VIEW FROM SPACE 37
Farouk El-Baz

Chapter 5. LINEATION PATTERNS OF THE CENTRAL WESTERN DESERT 51
H. A. El-Etr and A. R. Moustafa

Chapter 6. GEOLOGY OF THE SOUTHWESTERN DESERT OF EGYPT. 57
Bahay Issawi

Chapter 7. BASEMENT ROCKS OF THE GILF-UWEINAT AREA. 67
Ahmed Atif Dardir

Chapter 8. CRATER FORMS IN THE UWEINAT REGION 79
Farouk El-Baz and Bahay Issawi

Chapter 9. THE DARB EL-ARBA'IN DESERT: A PRODUCT OF QUATERNARY
CLIMATIC CHANGE. 91
C. Vance Haynes

Chapter 10. WIND PATTERNS IN THE WESTERN DESERT. 119
Farouk El-Baz and R. W. Wolfe

Chapter 11. BARCHANS OF THE KHARGA DEPRESSION. 141
Nabil Sayed Embabi

Chapter 12. SAND SHEET AND LAG DEPOSITS IN THE
SOUTHWESTERN DESERT 157
Ted A. Maxwell

Chapter 13. COATINGS ON SAND GRAINS FROM SOUTHWESTERN
EGYPT. 175
Farouk El-Baz and Donna Prestel

| | | |
|----------------------|---|------|
| Chapter 14. | GEOLOGY OF THE SOUTHERN GILF KEBIR PLATEAU AND VICINITY, WESTERN DESERT, EGYPT | .189 |
| | Maurice J. Grolier and Patricia A. Schultejann | |
| Chapter 15. | THE INTERPLAY OF FLUVIAL, MASS-WASTING AND EOLIAN PROCESSES IN THE EASTERN GILF KEBIR REGION . . . | .207 |
| | John F. McCauley, Carol S. Breed and Maurice J. Grolier | |
| Chapter 16. | BOULDER TRACKS ON HILLSLOPES IN SOUTHWEST EGYPT AND SIMILAR FEATURES ON THE MOON. | .241 |
| | Farouk El-Baz | |
| Chapter 17. | ANALOGS OF MARTIAN EOLIAN FEATURES IN THE WESTERN DESERT OF EGYPT | .247 |
| | Ted A. Maxwell and Farouk El-Baz | |
| Chapter 18. | CHARACTERISTICS OF ROCK POPULATIONS IN THE WESTERN DESERT AND COMPARISON WITH MARS | .261 |
| | J. B. Garvin | |
| Chapter 19. | EROSIONAL PATTERNS OF THE GILF KEBIR PLATEAU AND IMPLICATIONS FOR THE ORIGIN OF MARTIAN CANYONLANDS. . . | .281 |
| | Ted A. Maxwell | |
| Chapter 20. | ARCHAEOLOGICAL INVESTIGATIONS IN THE GILF KEBIR AND THE ABU HUSSEIN DUNEFIELD | .301 |
| | William P. McHugh | |
| Chapter 21. | NEOLITHIC FAUNAL REMAINS IN THE GILF KEBIR AND THE ABU HUSSEIN DUNEFIELD, WESTERN DESERT, EGYPT . . . | .335 |
| | Achilles Gautier | |
| Chapter 22. | THE FLORA OF GEBEL UWEINAT AND NEIGHBORING REGIONS, SOUTHWEST EGYPT. | .341 |
| | Loutfy Boulos | |
| REFERENCES | | .349 |

Chapter 1

JOURNEY TO EGYPT'S FARTHEST CORNER

FAROUK EL-BAZ

National Air and Space Museum
Smithsonian Institution
Washington, D.C. 20560

ABSTRACT

The Gilf Kebir-Uweinat expedition of 1978 was organized to verify geologic interpretations of Apollo-Soyuz photographs. These photographs and Landsat images showed features that are reminiscent of those depicted by Mariner and Viking missions to Mars. It was therefore intended to field study these features in order to better understand their morphologic analogs on Mars. For two weeks, an inter-disciplinary group of sixteen researchers investigated the extremely arid tracts across 2500 km from Kharga Oasis south-southwest to the border intersection of Egypt, Libya and Sudan. The convoy of vehicles consisted of six Soviet Gaz desert jeeps, two Volkswagen type 181 cars, two 4.5-ton tanker trucks for water and gasoline, and one 12-ton lorry loaded with food and camp supplies. The findings of the expedition lend support to other indications that climate change played a significant role in the formation of the eastern Sahara. These findings also reveal that correlations between the eolian features in southwestern Egypt and the wind-blown patterns on the surface of Mars will result in a better understanding of eolian activity on both planets.

INTRODUCTION

The seeds of the 1978 expedition to southwestern Egypt were planted four years earlier during the planning for astronaut observations and photography on the Apollo-Soyuz Test Project (ASTP). As principal investigator for the "Earth Observations and Photography" ASTP experiment, I was responsible for selecting and flight-scheduling of sites for study from Earth orbit (El-Baz and Mitchell, 1976). At the same time, a joint research project between the Smithsonian Institution and Ain Shams University was organized to study "Desert Erosion and Sand Movement in Egypt".

Study of the photographs of the Western Desert of Egypt taken prior to ASTP revealed interesting eolian features, although detailed study of some required additional photography. Thus, the area of Uweinat Mountain was selected as one of the primary sites of obser-

vation on the ASTP mission. When the mission was accomplished in July 1975, the ASTP astronauts were debriefed on what they observed. Further study of their observations and the photographs they obtained added to the significance of the locality, particularly in terms of analog correlations with wind-blown features on Mars (El-Baz, 1977, p. 80).

In the course of discussions with colleagues from both the United States and Egypt, it became apparent that a field investigation of the Uweinat region utilizing the added perspective of Earth orbital photographs would be very worthwhile. The purposes of the investigation were manifold, and included:

1. Field checking of photogeologic interpretations based on Apollo-Soyuz observations and photographs as well as Landsat images.
2. Study of wind-blown features revealed in the Earth orbital photographs and images for comparison with eolian features revealed on the surface of Mars by Mariner 9 and Viking 1 and 2 spacecraft.
3. Investigation of fluvial landforms, particularly the dry wadis of the Gilf Kebir plateau, for comparison with martian channels.
4. Collection of information on the Quaternary and Recent deposits that may be significant to the understanding of the origin of the Western Desert of Egypt.
5. Gathering data on prehistoric human habitation in the region for a better understanding of the environmental factors that prevailed in the region during the past few thousand years.
6. Study the potential of the southern and southwestern parts of the Western Desert of Egypt in terms of agriculture and/or economic mineral deposits.

Because of the above, it was necessary to put together a multidisciplinary team of investigators for the expedition, and it also became necessary to secure funding from various sources to support the journey. The trip was made possible through the cooperation of many individuals and numerous agencies in both the United States and Egypt. The group assembled in Cairo and proceeded from Kharga Oasis to Bir Tarfawi West, to the Gilf Kebir, Uweinat Mountain, and back (Fig. 1.1). Field work was conducted during two weeks between 25 September and 8 October, 1978. Preliminary results of the expedition were published in the Geographical Journal (El-Baz and others, 1980).

THE TEAM

The scientific investigation team was composed of seven American and nine Egyptian specialists in the fields of geology, planetology, Quaternary geology, geography, archaeology, and botany, including:

Loutfy Boulos, National Research Center, Cairo: Botanist specializing in plant taxonomy with much experience in desert flora, who visited the Uweinat region in 1968.

Carol Breed, U.S. Geological Survey, Flagstaff, Arizona: Geologist with much experience in the classification of dune types from orbital images and in the formation of sand dunes.

Atif Dardir, Geological Survey of Egypt, Cairo: Geologist specializing in igneous petrology and economic mineral deposits.

Hamid Dowidar, Geology Department, Ain Shams University, Cairo: Graduate student (Ph.D), presently working on the structural setting of the southern part of the Western Desert.

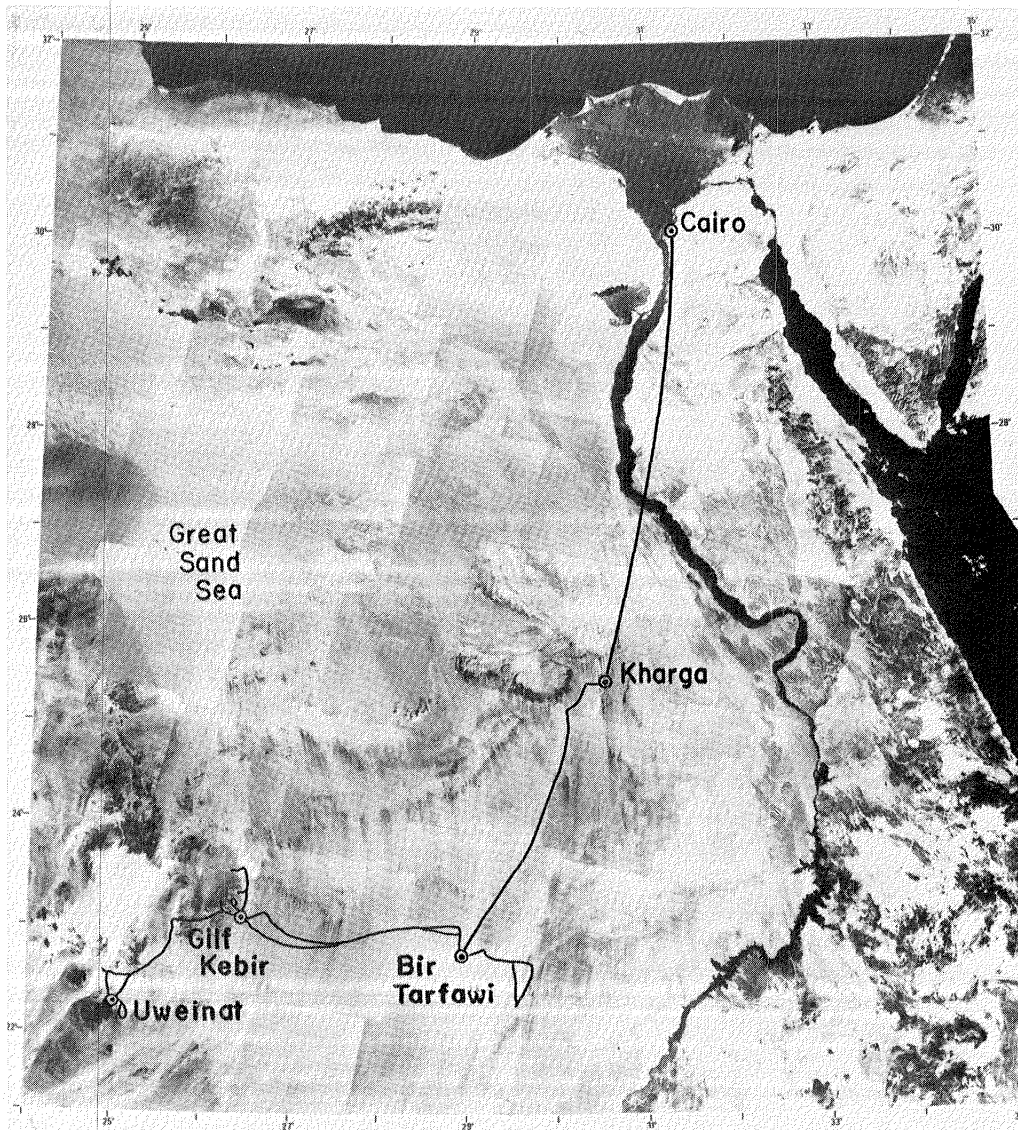


Figure 1.1 Generalized route of the 1978 journey to Gilf Kebir and Uweinat as plotted on a Landsat image mosaic of Egypt.

Farouk El-baz, National Air and Space Museum, Smithsonian Institution, Washington, D.C.: Geologist specializing in desert studies and planetary geology; Co-Principal Investigator of the research project on "Desert Erosion and Sand Movement in Egypt", and Science Advisor to President Sadat.

Hassan El-Etr, Geology Department, Ain Shams University, Cairo: Structural geologist and Co-Principal Investigator of the research project on "Desert Erosion and Sand Movement in Egypt".

Nabil Embabi, Geography Department, Ain Shams University, Cairo: Geomorphologist who specializes in dune forms and rates of sand transport; now teaching at the University of Qatar, Doha.

Maurice Grolier, U.S. Geological Survey, Flagstaff, Arizona: Astrogeologist with much experience of mapping of planetary surfaces with photographs from space.

Vance Haynes, Departments of Anthropology and Geosciences, University of Arizona, Tucson, Arizona: Quaternary geologist who spent eight field seasons in the Western Desert of Egypt.

Mohamed Ibrahim, Geological Survey of Egypt, Cairo: Geologist who is charged with field investigation in the Western Desert.

Bahay Issawi, Geological Survey of Egypt, Cairo: Senior geologist and field guide of the expedition who mapped the area in 1971.

Ted Maxwell, National Air and Space Museum, Smithsonian Institution, Washington, D.C.: Geologist specializing in geomorphology and sedimentology who was charged with the radio transmissions to the Nimbus-6 satellite.

John McCauley, U.S. Geological Survey, Flagstaff, Arizona: Astrogeologist with much experience in planetary geology and specialist on eolian features of Mars.

William McHugh, GAI Consultants, Inc., Kansas City, Missouri: Archaeologist who investigated the implements collected by Oliver Myers in 1938 from archaeological sites in the Gilf Kebir.

Adel Moustafa, Geology Department, Ain Shams University, Cairo: Geologist now working on a Ph.D. in photogeology at the Geology Department, University of Texas at Austin.

Mahmoud Youssef, Geology Department, Ain Shams University, Cairo: Geologist who specializes in remote sensing particularly the use of Landsat data.

In addition, Hatim Farid, science editor of Cairo's October Magazine joined the expedition. He wrote several articles on the expedition and its results in October (Farid, 1978). Sixteen employees of the Geological Survey of Egypt supported the expedition as drivers, mechanics, and cooks, making a total of 33 participants.

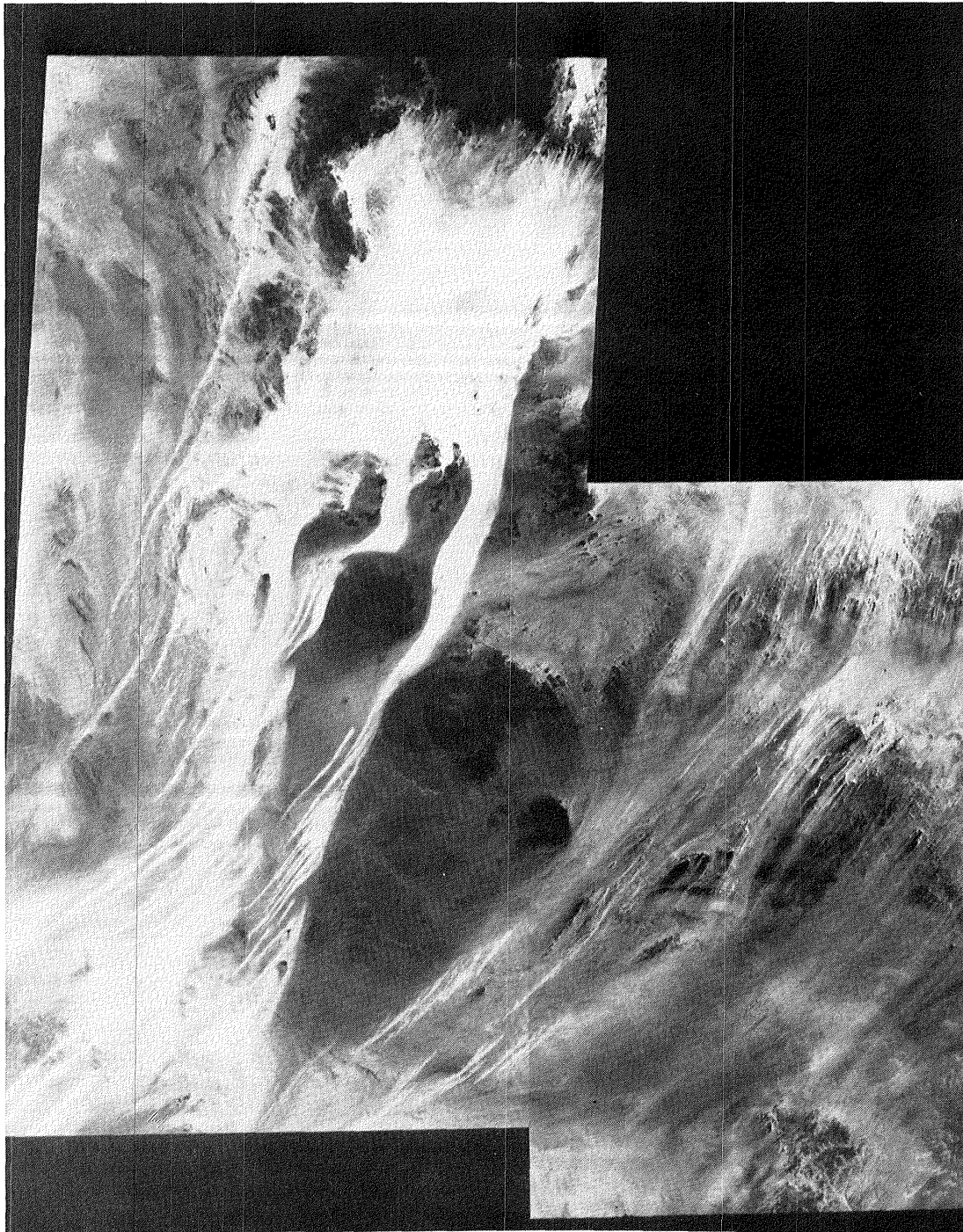


Figure 1.2 Computer generated mosaic of Landsat images of the Uweinat region showing bright streaks of sand over darker rock surfaces. (Courtesy of Goddard Space Flight Center).

LOGISTICS

When the trip was first planned in 1977, the Military Survey of Egypt was to provide necessary logistical support. However, in the summer of 1978, the Military Survey decided to postpone their expedition to Uweinat. This necessitated organizing the logistical support through the Geological Survey of Egypt.

In preparation for the trip, I took care of administrative arrangements and secured the necessary approvals from the American and Egyptian Governments. Hassan El-Etr acted as quartermaster, and was responsible for procurement of field supplies and food. Vance Haynes duplicated photographs of areas visited by previous expeditions and William McHugh provided team members with reprints of O. H. Myers' unpublished maps of archaeological sites in the Gifl Kebir area. The Smithsonian Institution procured a small scale mosaic of computer-enhanced Landsat images of the Uweinat area (Fig. 1.2) and the U.S. Geological Survey prepared enlargements of selected Landsat images along the route.



Figure 1.3 Photographs of some of the vehicles used on the journey including a water tank truck (top), the truck that carried food and camping supplies shown here during an attempt to get it unstuck (middle), and a VW "thing" parked near the bones of a camel, with a camel caravan in the background in the Darb El-Arba'in (bottom).

The basic logistical support was provided by the Egyptian Air Force and the Geological Survey of Egypt. The Egyptian Air Force very kindly flew the scientists from Cairo to Kharga and back in a Convair-280 airplane usually reserved for military staff. Bahay Issawi supervised the preparation of Geological Survey vehicles and the selection of support personnel. The organization was very carefully done with regards to schedules, itinerary, transportation of personnel and supplies, camping, sanitation, and cooking. All vehicles, except for the two German Volkswagen cars, were Soviet made as other equipment that found its way into the civilian sector of the Egyptian economy before termination of Soviet aid in the early seventies. The convoy of vehicles (Fig. 1.3) included: One 12-ton 3-axle truck, which carried tents, bedding, food and medical supplies, and some drinking water and fuel; one 4.5-ton tanker truck for gasoline; one 4.5-ton tanker truck for drinking water, and six 4-wheel drive 7-seater 1969 Gaz Jeeps. It is beyond the scope here to evaluate in detail the performance of these vehicles in the field. Breakdowns were minor and few, mostly due to engine overheating. Air ventilation inside the passenger cab was a little inadequate, but system redundancy was superb. Only once did one Jeep run out of gas, and rescue from the lead Jeep came within one-half hour.

The southern part of the Western Desert of Egypt consists to a large extent of a discontinuous eolian peneplain (Fig. 1.4). It extends for hundreds of kilometers, and is interrupted here and there by sand seas, low ridges, escarpments, dissected plateaus, and shallow flat-bottomed valleys. The surface is covered by thin, densely-packed sand sheets mantled in places by desert lags ranging in size from sand to granule, cobble stones. The landscape is old, and the sand and the lag are mature, making travel at speeds of 60-80 km/hr across the trackless desert a surprisingly easy accomplishment. In places, this speed can be maintained over continuous distances of hundreds of kilometers. Our guides navigated from one major landmark to another, but dead reckoning by compass was also used. The large truck, and at least one of the two 4.5-ton tankers traveled one day ahead of the convoy, so that camp could be set up before the arrival of the passenger Jeeps. Only the 12-ton truck had some difficulty in negotiating the worst areas of loose sand.

For planning purposes, the rule of thumb used by the Geological Survey of Egypt in calculating water rations adequate for work in the desert is: 3 gallons per day, per scientist; 1.5 gallons per support personnel. As a matter of fact, century-old experience proves that corpulent, let alone obese persons, drink more water than lean ones. Thus, a very severe selection process favoring lean workers over fat ones is applied to Egyptian labor working in the desert. These water rations and also gasoline rations are augmented from 10 to 50 percent to take into account leaks and other unforeseen contingencies. Upon completion of the journey and return to Kharga Oasis, there was a 500-gallon (2-ton) surplus in the water truck, representing a 50 percent redundancy on the party's actual requirements, and therefore a large margin of safety.

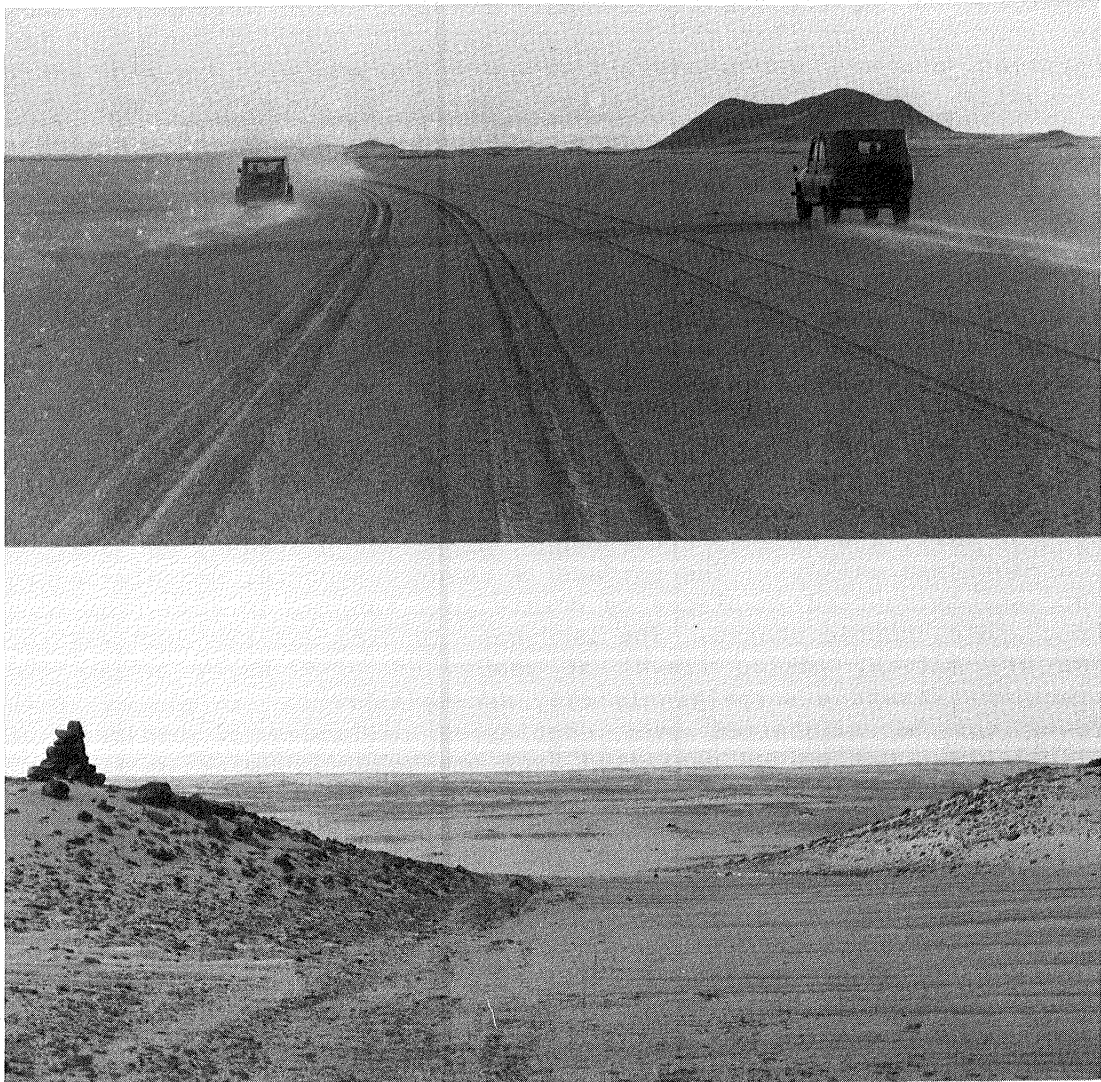


Figure 1.4 Photographs illustrating the peneplained nature of the Western Desert of Egypt. Photograph at bottom shows cairns along the Darb El-Arba'in.

Camping in the open, in light sleeping bags, was quite possible and even pleasurable, both at the northern slope of Gebel Uweinat and 100 km south of Kharga Oasis. Nevertheless, we stayed most of the time in 2-man or larger conical tents. These, like the cone-shaped or multifaceted pyramidal hills in the regional landscape, seem to

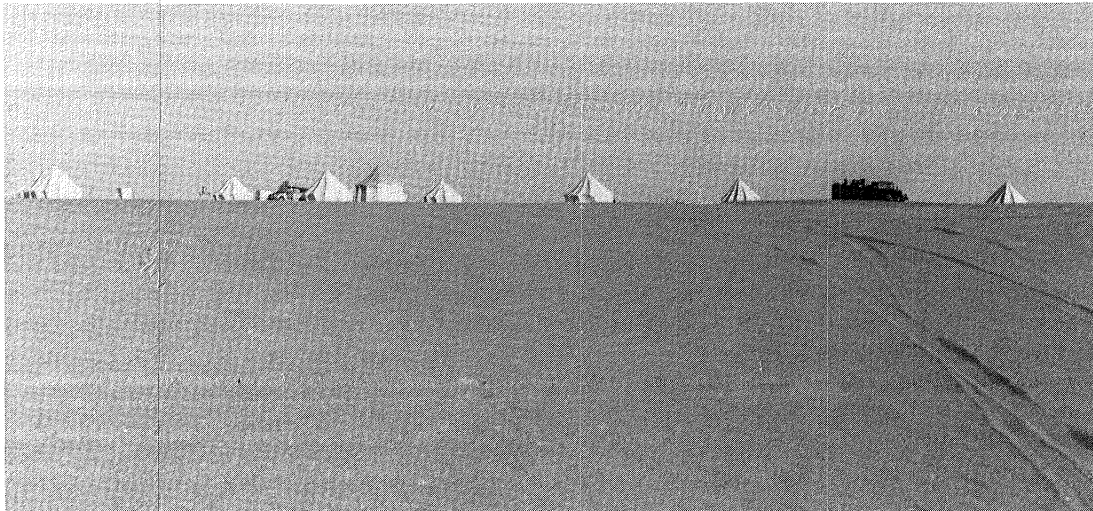


Figure 1.5 Camp at Bir Tarfawi West showing the wind-resistant conical tents.

conform to the shape offering the least resistance to the wind (Fig. 1.5). Sanitation practices current in any military camp were observed. Food, cooked in the Egyptian style, was adequate, and hot tea was the main beverage. Egyptian wine and stronger alcoholic drinks were available to those who liked them. Fresh meat, besides canned meat, was provided by live domesticated ducks brought from a duck-raising ranch at Kharga Oasis (Fig. 1.6).

Time of travel was ideal. Temperatures ranging up to 40°C rarely became a problem, except in midday, because of the low moisture content in the air. The breeze was surprisingly constant (average wind velocity: 20 km per hour), except around Gebel Uweinat, where the weather was very calm. Flies were found at some oases and around Gebel Uweinat, probably because of the nearby presence of herds of

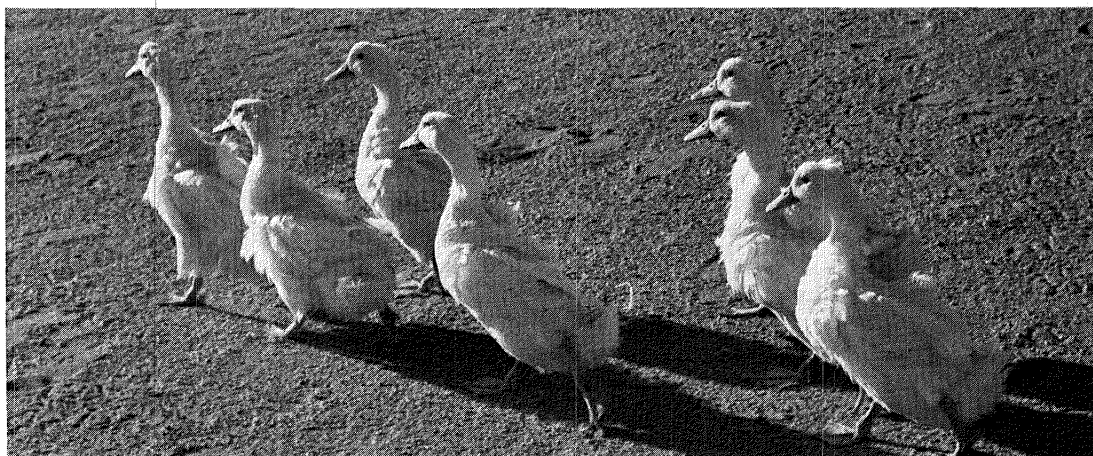


Figure 1.6 White ducks from Kharga that provided the fresh meat supply during the journey.

domesticated goats and occasional feral donkeys and wild gazelles.

THE ROUTE

Our expedition greatly benefited from the knowledge gained from thirteen previous journeys to Uweinat from various localities in Egypt, particularly the 1938 Bagnold expedition (Bagnold and others, 1939). Based on this knowledge, we plotted our route on maps and space photographs and were thus ready to begin. On the morning of 25 September 1978, our plane departed from Cairo's Almaza Airport, and during the next two hours we observed and photographed many interesting features from the air. At Kharga we met with the jeeps that had arrived a day earlier from Cairo. We used some time to study the Kharga "mud lions", which are wind sculpted yardangs of lacustrine deposits with blunt fronts and aerodynamically shaped bodies. On the following day we started our drive to the south-southwest.

From Kharga we drove west on the Kharga-Dakhla asphalt road and at the 60-km mark we made a turn toward the south-southwest, leaving the last asphalt surface we saw for the rest of the trip. Our target was Bir Tarfawi West (Fig. 1.1) where the heavy vehicles awaited. We reached our destination long after sunset.

In the vicinity of the camp at Bir Tarfawi West we visited a patch of burned organics along an ancient, now dry, lake shore. Because of the known age of gastropods and snails embedded in the dry lake strata, archaeologists were able to assign a relative age to the abundant manmade artifacts in these strata. The visited site, Vance Haynes noted, may have hosted human settlements at least 30,000 years ago. The water at the well dug by the Geological Survey of Egypt was reached at 2 m depth. As we drove toward a red-colored field of barchan dunes, we encountered flint implements that were estimated to be about 6,000 years old. A few inches in the soil below, Vance Haynes found pieces of ostrich egg shells.

On 28 September we headed east to Qaret El-Maiyit, which is Arabic for "hill of the dead", because of the human skeleton that was discovered there in 1922. The exposed granitic rock (Fig. 1.7) displayed a long down-wind tail of dark surface that was surrounded by light-colored sand on either side. The streak appeared very similar to those photographed by Viking spacecraft in the Cerberus region of Mars (El-Baz and Maxwell, 1979a; Chaikin and others, 1980). Weathered products of orthoclase from intervening pegmatite veins in the granite gave this tail a dark red tone. Nearby were large sandstone and granite blocks arranged in crude circles; we assumed that these represented an ancient human settlement (Fig. 1.8). We continued the drive towards the fabled Darb El-Arba'in caravan route, which is nearly 20 km wide where we intersected it. At its border we examined the mineralized products of a geyser, which turned out to be mostly silica and iron.

As we continued the exploration southeastward toward Bir Sheb, we came upon a ghost settlement at Bir Kurayim that was established by the Egyptian Desert Development Organization in 1964. The buildings,

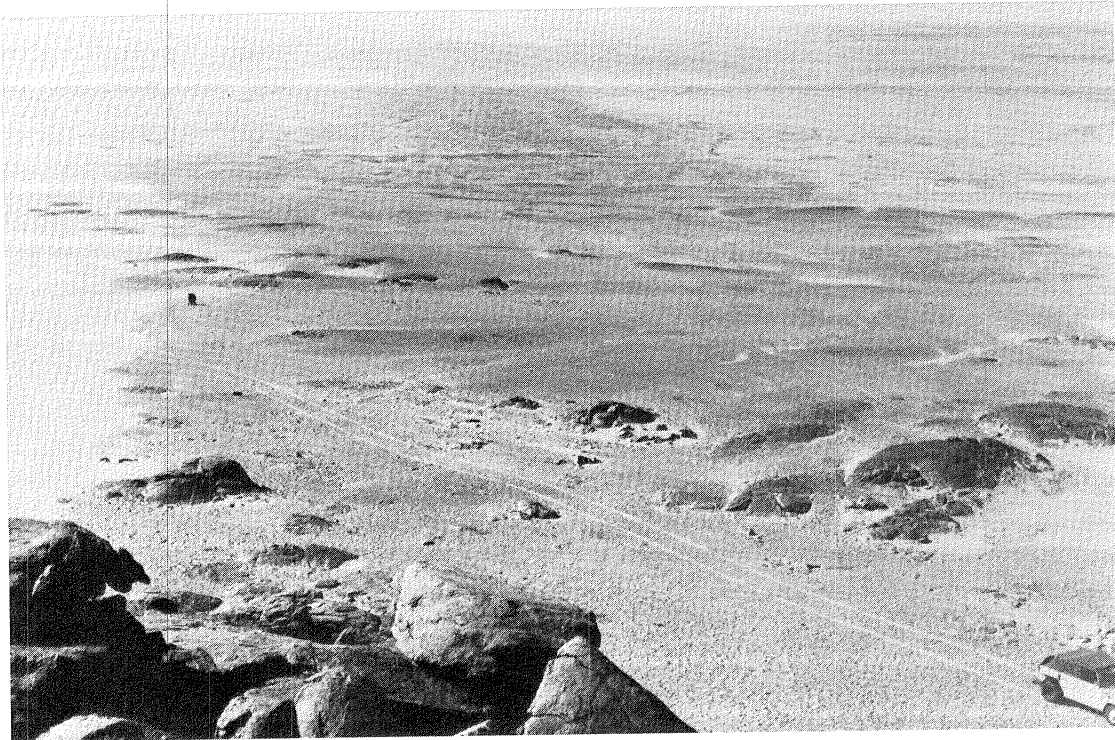


Figure 1.7 Granitic rocks of Qaret El-Maiyit in the foreground with a dark tail surrounded by sand deposits in the background.



Figure 1.8 Remains of a prehistoric house, marked by large rocks arranged in a 4 m diameter circle.

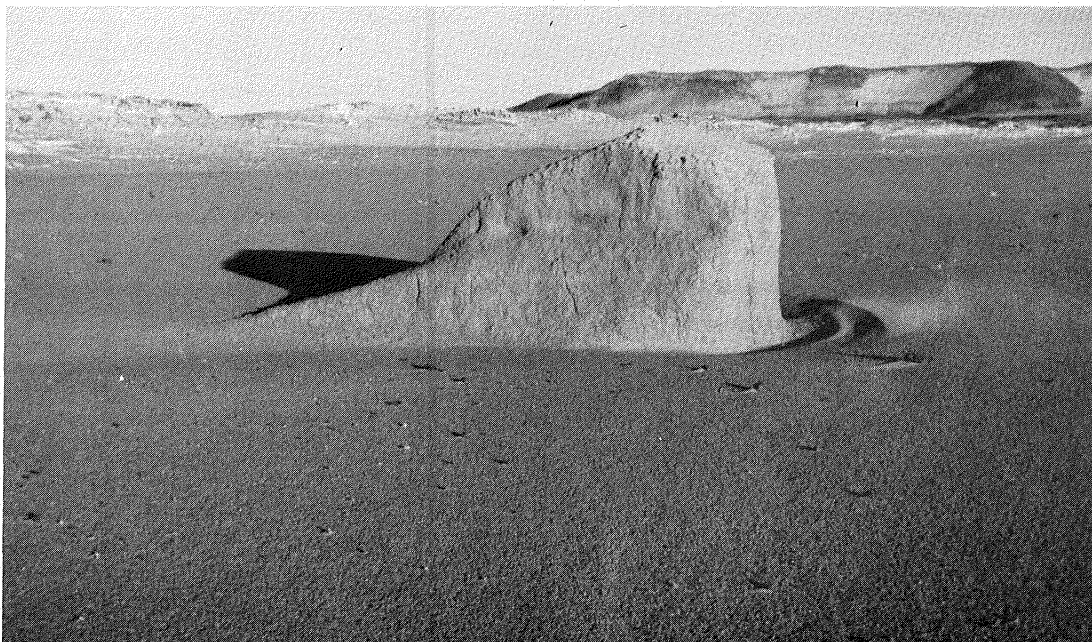


Figure 1.9 A typical 2 m high yardang with a blunt side facing the wind.

which were half-filled with sand, were made of galvanized metal and glass, materials one would least expect in a desert environment.

On the following day, we were up at sunrise to break camp. We drove north for 32 km to a block of conglomerate that sprung from the featureless plain. Saleh, the most conscientious of our support crew erected a 2 m high cairn on top of it to lead other drivers. Along the route we stopped several times to wait for the heavy vehicles. It took many men to get these unstuck using two huge chain ladders. At one stop a sheet of sand, a few grains thick, moved hurriedly along the surface. The wind velocity was measured to be 16 km/hr. It appeared that most grains were rolling rather than saltating on the surface.

We continued westward on 30 September and with the morning light our first stop was to study a field of yardangs (Fig. 1.9). Several of these were 2 m high and exhibited very straight windward faces. As we approached the southeastern scarps of the Gilf Kebir we headed to "Bagnold's camp" (Fig. 1.10). The 1938 tracks of his trip were partly covered by a 1 km longitudinal dune. The side of the dune adjacent to the camp site had partly submerged the low structure. Wooden boxes at the site showed the effects of wind erosion; a piece of wood that was 13 mm in thickness on the nailed side, was only 2 mm thick at the exposed surface. We established camp at the entrance of Wadi Wassa near the southeasternmost tip of the Gilf Kebir (Fig. 1.11).

On 1 October 1978, we traveled northward to Wadi Mashi. On top of the Gilf Kebir, William McHugh discovered a site where implements were strewn near "core" blocks of quartzite, from which they were

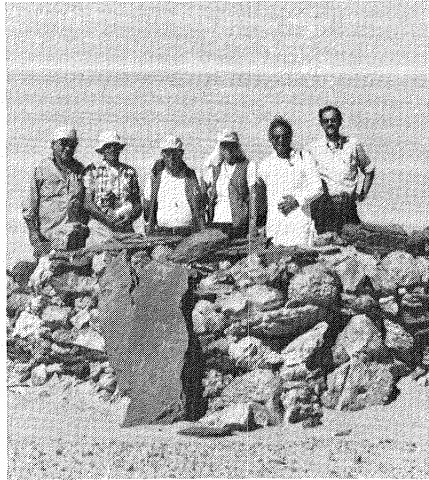


Figure 1.10 Group assembled at the site of the camp erected in 1938 by Bagnold and his team of explorers at the southeastern edge of the Gilf Kebir plateau.

chipped, perhaps 100,000 years ago. Geologists studied the fluvial landforms that were highly modified by wind action as the archaeologist studied the site down to 20 cm below the surface. At the head of Wadi Mashī we noticed the smooth dome-like appearance of basalt hills. The columnar basalt pieces were dense and fine grained inside, but pitted by wind action on outer surfaces (Fig. 1.12). Back at camp we decided to break the expedition into two groups, one to stay at the Gilf, and the other to head for Uweināt Mountain to the southwest.

For the next three days two-thirds of the expedition investigated details of Wadi El-Bakht and Wadi Ard El-Akhdar. At Wadi El-Bakht, the archaeological site of neolithic age discovered by Oliver Myers in 1938 was studied. Geologists examined the wind and water erosion in the lower part of the wadi. Pebbles and cobbles of friable sandstone on the floodplain showed abundant evidence of wind erosion in the form



Figure 1.11 Setting of the camp at Gilf Kebir as depicted in drawing by Hamid Dowidar.

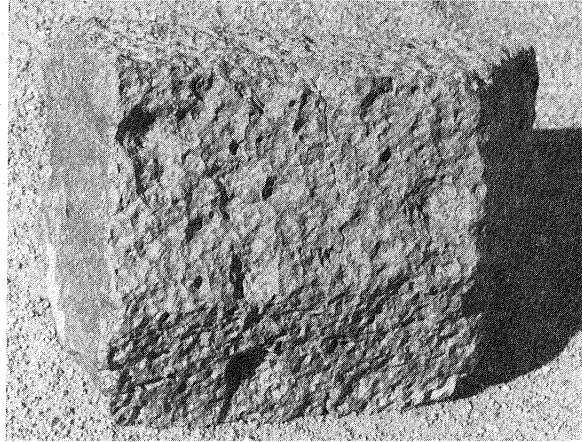


Figure 1.12 A block of columnar basalt, 30 cm long, with a pitted outer surface and a dense, fine-grained interior exposed at left.

of delicately-etched projections along bedding planes aligned with the wind. The team also studied the relationships of falling and climbing dunes, yardangs and ripples, and surveyed the wadis' topographic profiles.

At Wadi Ard El-Akhdar, the Gilf party excavated additional archaeological sites, surveyed the topography and investigated the relationships of present setting to the blockage of a narrow part of the wadi. The wadi constriction must have been blocked in prehistory to allow water to form a lake upstream. Members of the team were divided in opinion; some maintained that a presently active dune must have blocked the wadi, while others argued that sand is not good enough for a dam and the blockage must have been by a wedge of fanglomerate, parts of which were exposed in the wadi wall at the constriction. The controversy lingered on.

Meanwhile, the Uweinat party headed westward in Wadi Wassa, whose floor kept a record of rainy seasons in the form of mud layers. The team's botanist, Loutfy Boulos, once again was able to put his expertise to use (Fig. 1.13) since the expedition had left the last plants behind at Bir Tarfawi West. From the condition of vegetation, he estimated that it had not rained there for approximately 20 years. The party left the Gilf Kebir through a pass, 10 km north of Wadi Diyaq, where kaolinized material was exposed at the base of the cliffs. The Mehashimat, a low lying and highly fractured plateau, loomed in the distance as the mountains of Gebel 1114 and Peter and Paul appeared. All of a sudden, the sandstones of the Gilf Kebir gave way to dark volcanic rocks of basalts and trachytes with surrounding aprons of flagstones and pea-size pebbles. Some volcanic craters appeared to be marked crater rims, without any volcanic rock within. By nightfall the Uweinat party arrived at the north entrance of a small unnamed valley just west of Karkur Talh where we found many trees, petroglyphs in caves, and a prehistoric milling stone (Fig. 1.14).

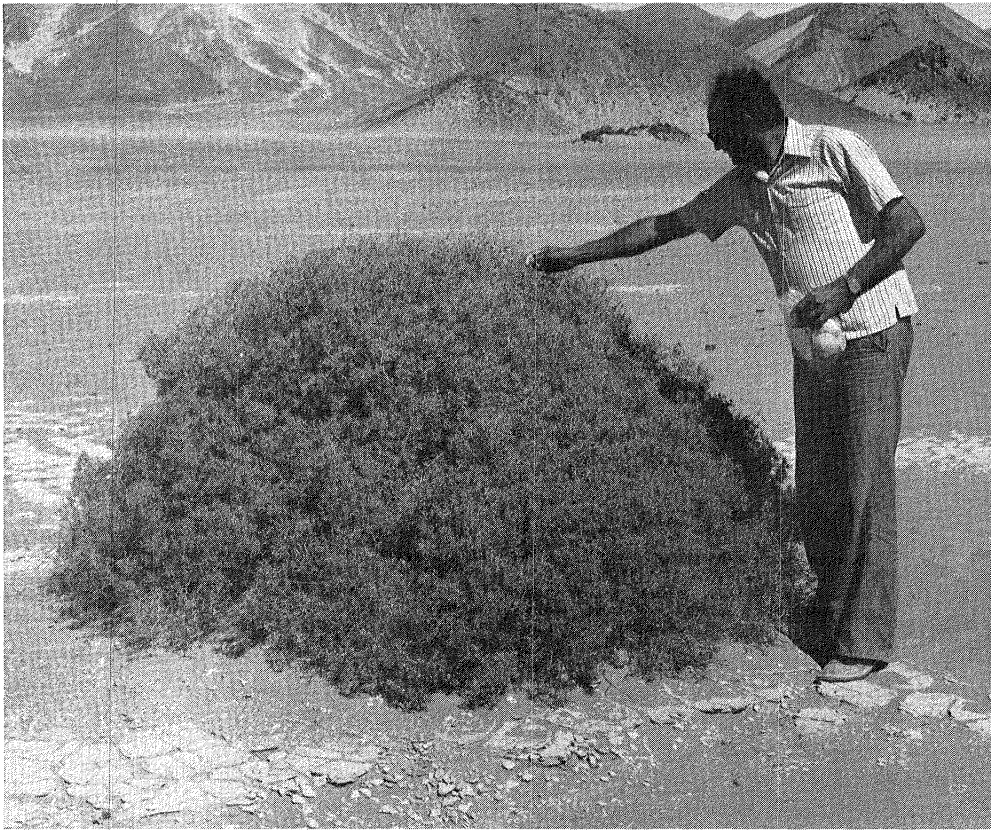


Figure 1.13 Botanist Loutfy Boulos samples a Zilla spinosa in Wadi Wassa at the southern edge of the Gilf Kebir. Mud-cracked surface surrounds the plant.

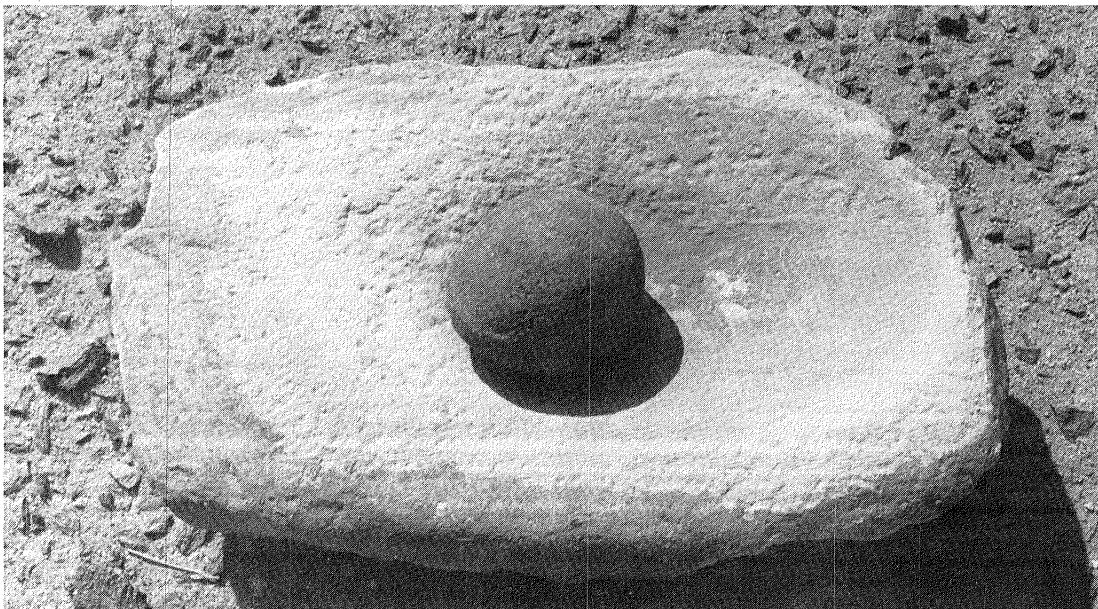


Figure 1.14 A 40 cm wide milling stone with its spherical grinding stone from a valley, Karkur Talh, in Gebel Uweinat.

Exploring the northern slopes of Gebel Uweinat we were most impressed by the power of wind, which came from the north. The wind had sculpted the rock into eerie shapes of frozen dinosaurs and other giant animals. The exposed rock surfaces were all pitted. Where sand grains were lodged in these pits they twirled around as the wind gusted, enlarging the pits. Fluted rock surfaces formed from pits that were lined up in rows (Fig. 1.15).

On the return journey from Uweinat we wanted to achieve the last objective before rejoining the other party at the Gilf Kebir. This was reaching the broad sand mass just east of Gebel Babein. I wanted to sample the sand there in order to compare it to sand samples from other parts of the Great Sand Sea that were collected on an earlier expedition. This would increase the geographic spread of our samples and allow us to study the reddening of sand as the distance from source increases. We were unable to find an active slip face on the dune. The sand was accumulated in a giant whaleback dune with gentle slopes. On top of the dune, approximately 1 km away from the desert surface, we encountered pencil-sized, tube-like pieces of rock. Nothing could have carried these objects to the eastern flank of the whaleback dune but a fierce wind storm.

The reunited party broke the Gilf Kebir camp on the morning of 5 October 1978 and headed eastward back to Bir Tarfawi West. We passed by remains of World War II; an English army truck that was disassembled with pieces strewn in the sand. The engine hood had created a small wind shadow that resulted in the formation of an 8 m sand tail in its lee. The heavy trucks were left to return at their own slow pace with one jeep for emergencies.

During the return trip, several areas of iron-rich sandstone were noted. In one place, hematite was exposed as a thinly laminated red layer of unknown depth (Fig. 1.16); we dug over 40 cm without reaching the base. Within this red layer were dark brownish-black nodules of iron and manganese oxides. We drove for 11 km over this iron ore, which we estimated to be about 150 km west of Bir Tarfawi. We recommend to the Geological Survey of Egypt the assessment of the economic potential of this particular deposit.

We arrived back at Kharga about midday on 6 October. The first item on the agenda was to shave and shower for the first time since we left Kharga eleven days earlier. After a meal that was more like a banquet, a group assembled to study the Kharga barchan dunes. In the evening we met with local geologists, hydrologists, engineers, and agricultural experts to discuss our findings on the expedition and the pros and cons of large scale agricultural development in the New Valley province. It was stated that although underground water supplies were plentiful, the irrigation schemes were wasteful of the water. Also, the available data did not allow a resolution of whether or not the underground water supply was being replenished from the south and west.

On the following day the party was again split into two groups; one headed toward the plateau north of Kharga depression, and the

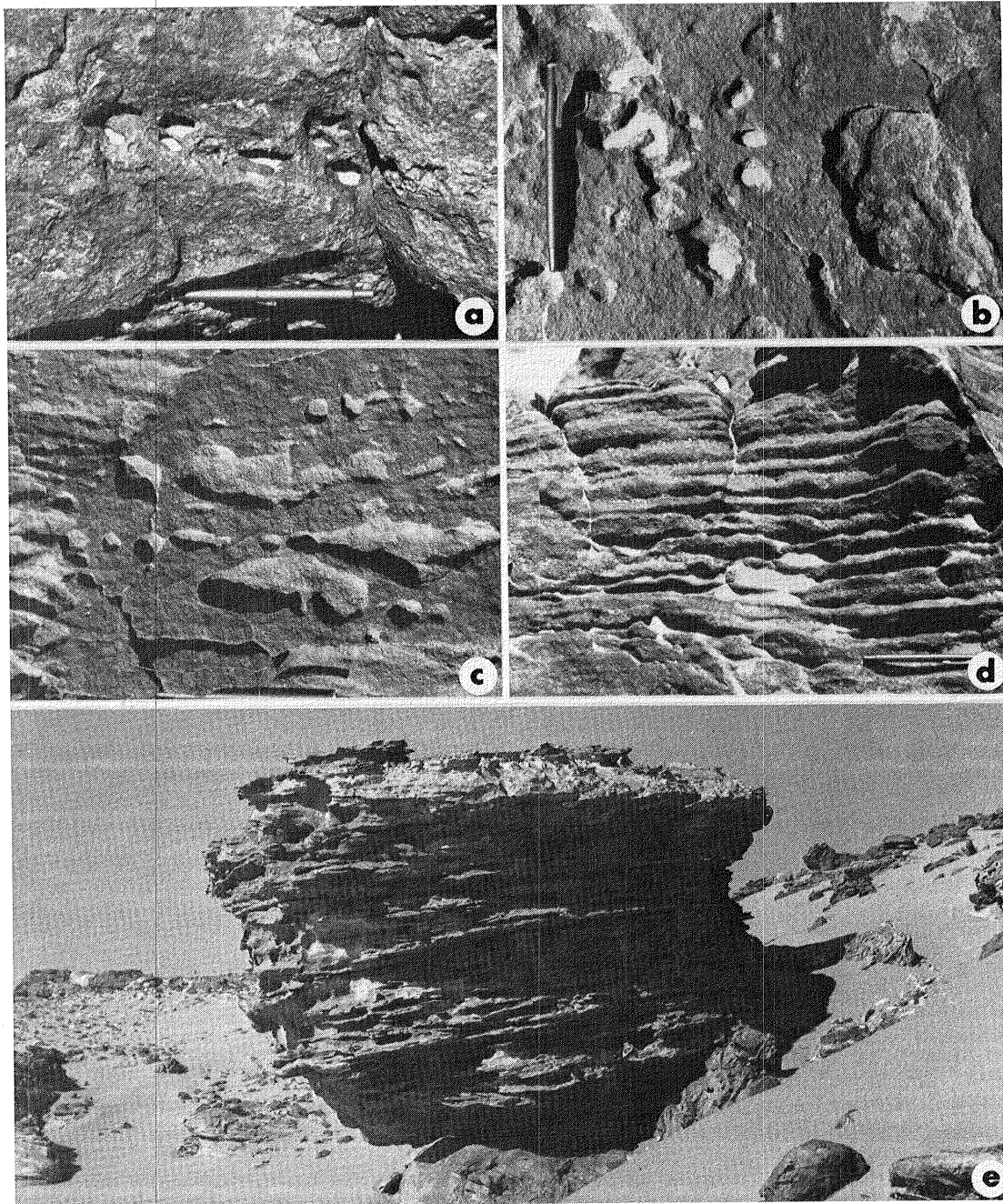


Figure 1.15 Photographs showing the effects of sand-blasting of sandstone rocks along the northern face of Gebel Uweinat showing elongate pits (a;b), coalescent pits (c), flutes (d), and the appearance of a pitted and fluted rock (e).

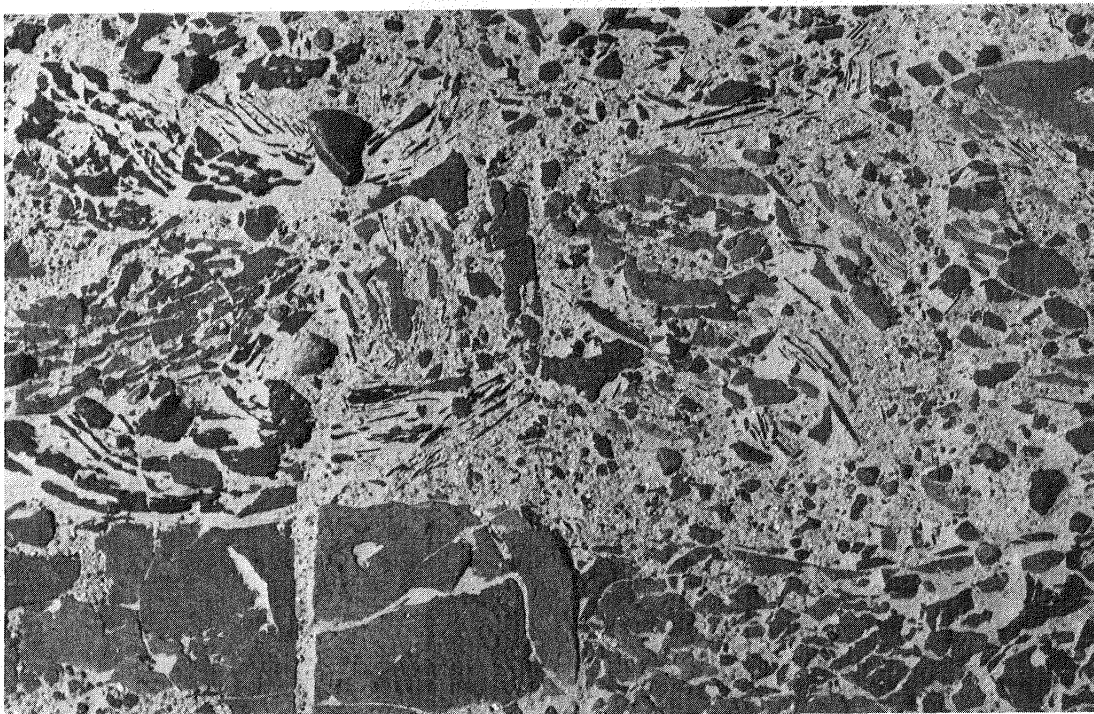
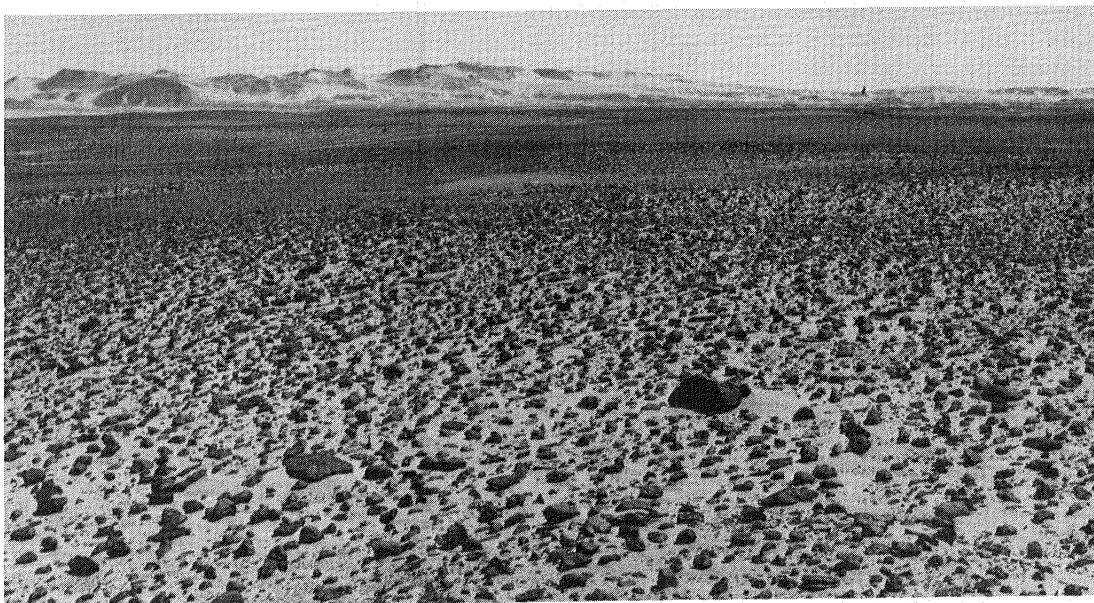


Figure 1.16 Dark hematitic nodules cover the surface 150 km west of Bir Tarfawi (top), and thinly laminated hematitic sandstone (bottom).

other headed south towards Baris Oasis. On top of the plateau more of the wind-formed features were studied. There, the wind had carved yardangs in the extremely resistant crystalline limestone. Within the depression, the other group observed mounds that marked ancient springs, which were aligned along north-south trending faults. Fault boundaries were marked by tamarisk trees and bamboo growths in the

salty soil. We also studied remains of irrigation canals built in Roman times and lined with palm tree bark. Evidence of deflation of the soil by wind was clear everywhere. At Ein El-Shorafa, Vance Haynes estimated that nearly 55 m of soil had been deflated during the past 3000 years, or 18 mm per year. In the evening, the two groups returned to Kharga to exchange experiences and discuss the findings.

The field work at Kharga ended in the morning of 8 October 1978. Some of the hours of the day were spent in sorting of the samples and separating those to be left at Kharga. One of the results of the expedition was to interest the local unit of the Geological Survey to keep samples from all expeditions at the newly established Kharga Museum. In the afternoon our plane was ready to fly us back to Cairo. As it took off, the lighting was perfect for a view of the enormous concentration of yardangs north of Kharga, probably one of the largest fields in the world. We reached Cairo at sunset, ending a most interesting expedition and starting new thoughts on desert landforms and wind-blown features on both Earth and Mars.

ACKNOWLEDGMENTS

Numerous organizations and individuals significantly contributed to the success of this journey. The financial support of the following institutions is acknowledged: Ain Shams University for providing food, photomosaics and some camping needs; the Egyptian Air Force for providing an airplane to transport the scientists between Cairo and Kharga; the Geological Survey of Egypt for making available the necessary vehicles, gasoline, support personnel, and camp equipment; the National Geographic Society for making available the two Volkswagen type 181 vehicles; Goddard Space Flight Center for providing a Landsat mosaic of the Uweinat region and the transmitting apparatus and satellite tracking data; and the New Valley Governorate for providing the space for lodging, meals, and lectures and seminars at Kharga.

International travel was also financed by several organizations, including: the National Air and Space Museum (for T. Maxwell); the National Geographic Society (for V. Haynes); the National Science Foundation (for the author); the Smithsonian Foreign Currency Program (for C. Breed and J. McCauley); and the U.S. Geological Survey (for M. Grolier). William McHugh paid his own way. The Planetary Geology Program Office of the National Aeronautics and Space Administration (NASA) covered the salaries of C. Breed and J. McCauley during the expedition.

Maurice Grolier supplied the author with information for the section of this paper dealing with "logistics". The National Air and Space Museum, Smithsonian Institution, supported the preparation of the camera-ready manuscripts for this book. Ann W. Gifford of the Center for Earth and Planetary Studies at the National Air and Space Museum drafted many of the illustrations. This book could not have been produced without the unstinting work of Donna J. Slattery of the same Center, who typed numerous versions of the manuscripts.

**Page Missing in
Original Document**

Chapter 2

A CHRONICLE OF RESEARCH AND EXPLORATION IN THE GILF KEBIR-UWEINAT MOUNTAIN REGION

WILLIAM P. MCHUGH
G. A. I. Consultants Inc.
Pittsburgh, Pennsylvania 15146

ABSTRACT

Six decades of exploration and research in southwestern Egypt and northwestern Sudan are reviewed. After the initial discovery of Gebel Uweinat in 1923 by Hassanein Bey and the pioneer explorations of northern Sudan by Newbold and Shaw, the area became a popular destination for explorers and arid lands scientists. By the middle and late 1930's, archaeological investigations were an important component of these expeditions, and clear evidence of once widespread human occupation in late prehistoric times became apparent. World War II terminated scientific study in the area, although it was used by British forces raiding the Italian Libyan outposts. Scientific research commenced again in the 1960's with expeditions by British, Egyptian, Belgian, and Libyan groups, with archaeology an important element of the Belgian expedition. The 1970's saw only two reported expeditions to the Gilf Kebir-Gebel Uweinat before the 1978 expedition of the Geological Survey of Egypt and the Smithsonian Institution reported in this volume.

RESEARCH AND EXPLORATION: PRE-1940

The Gilf Kebir and Gebel Uweinat remained outside the pale of scientific knowledge until the middle of the 1920's. Although W. J. Harding-King may have seen the Gilf Kebir in the distance in 1909 (Harding-King, 1913), and Dr. John Ball and a Lt. Moore approached the northeast outliers of the Gilf Kebir in 1918, it was not until April, 1923, that either the Gilf or Uweinat were actually reached by explorers. In that year, Ahmed H. Haasanein Bey, an Egyptian diplomat and explorer, discovered Gebel Uweinat to be temporarily inhabited by about 150 Goran tribesmen under a Sheikh Herri, and also discovered some prehistoric rock engravings (Hassanein Bey, 1924a; 1924b; 1925).

At the same time, Douglas Newbold, a British colonial servant in the Anglo-Egyptian Sudan, made an extended journey into northwestern Sudan and discovered widespread artifactual remains and rock engravings at Zolat el Hammad and Gebel Tageru (Newbold, 1924). In 1927, Newbold, accompanied by W. B. K. Shaw, made a second journey into northwest Sudan, again on camel, reaching Merga (Nukheila) Oasis (19°03'N, 26°15'E) and Burg El-Tuyur (29°95'N, 27°41'E), where they discovered rock engravings, and Selima Oasis (21°23'N, 29°20'E). Newbold authored an article on the rock pictures and archaeology of the Libyan Desert in Antiquity (1928) and he and Shaw authored a second

article in the Sudan Notes and Records (1928) on the general results of the journey.

In early 1925, Prince Kemal El-Din Hussein led an expedition of Citroen (half-track) motorcars into the southern Libyan Desert and formally discovered and named the Gilf Kebir which he saw on his route from Kharga Oasis to Gebel Uweinat. Dr. John Ball of the Desert Survey of Egypt accompanied the prince on this expedition (Ball, 1927; 1928). In 1926, the prince made a second trip to Uweinat, this time following the eastern cliffs of the Gilf Kebir. Kemal El-Din published the results of his expeditions in *La Geographie* (Hussein, 1928) and the *Revue Scientifique Illustrée* with Abbe Breuil (1928). The latter article concerns the rock engravings of Gebel Uweinat, the first publication devoted solely to the rock art of Uweinat.

In 1928, H. J. L. Beadnell made a quick trip to Gebel Uweinat and discovered an easy car-route from Bir Tarfawi (22°55'N, 28°55'E) (Clayton, 1937). In the winter of 1930-31, P. A. Clayton made a triangulation survey from the Nile Valley to Gebel Uweinat and then north along the Darb El-Arba'in (the forty day track) to Kharga Oasis. On April 2, 1931, he made a rapid, one-day plane-table survey of the western cliffs of the Gilf Kebir mapping this stretch for the first time (Clayton, 1933; 1937). At 23°34'N, 25°16'E on the western side of the Gilf Kebir, Clayton discovered some rock engravings and milling stones at the mouth of a large wadi, the first of several such discoveries made in this area.

In October and November of 1930, R. A. Bagnold led the first of his three expeditions to Uweinat and the Gilf Kebir (Fig. 2.1). He skirted the eastern cliffs of the Gilf, paralleling Prince Kemal El-Din's route of 1926. Newbold, Shaw, and others accompanied Bagnold on this journey which took them to Gebel Uweinat, Gebel Kissu, Wadi Howar, and Selima Oasis (Bagnold, 1931; Bagnold and others, 1931). Shaw reported the botanical results of this (and the 1932) expedition (Shaw, 1931; Shaw and Hutchinson, 1931; 1934) and on the rock art of Uweinat (Shaw, 1934).

In the spring of 1932, an expedition led by Robert C. E. Clayton and Count L. de Almasy, including P. A. Clayton and H. G. J. Penderel, made a reconnaissance of the western and northern parts of the Gilf Kebir using a small, two-seater Gipsy I Moth airplane for flights across the Gilf Kebir. On these flights, the long wadis of the northern Gilf were discovered, but their actual exploration was not accomplished until a few years later. R. C. E. Clayton died within the year and the results of this expedition are known only from the short note published by Rodd (1933).

In late 1932, R. A. Bagnold led his second expedition to the Gilf-Uweinat area and explored far to the south and west of Uweinat (Bagnold, 1933). An important member of the party was Dr. K. S. Sandford, a geologist who made observations which are still the primary source of much of our knowledge on the geology and geomorphology of this vast area (Sandford, 1933a; 1933b; 1935a; 1935b; 1936).

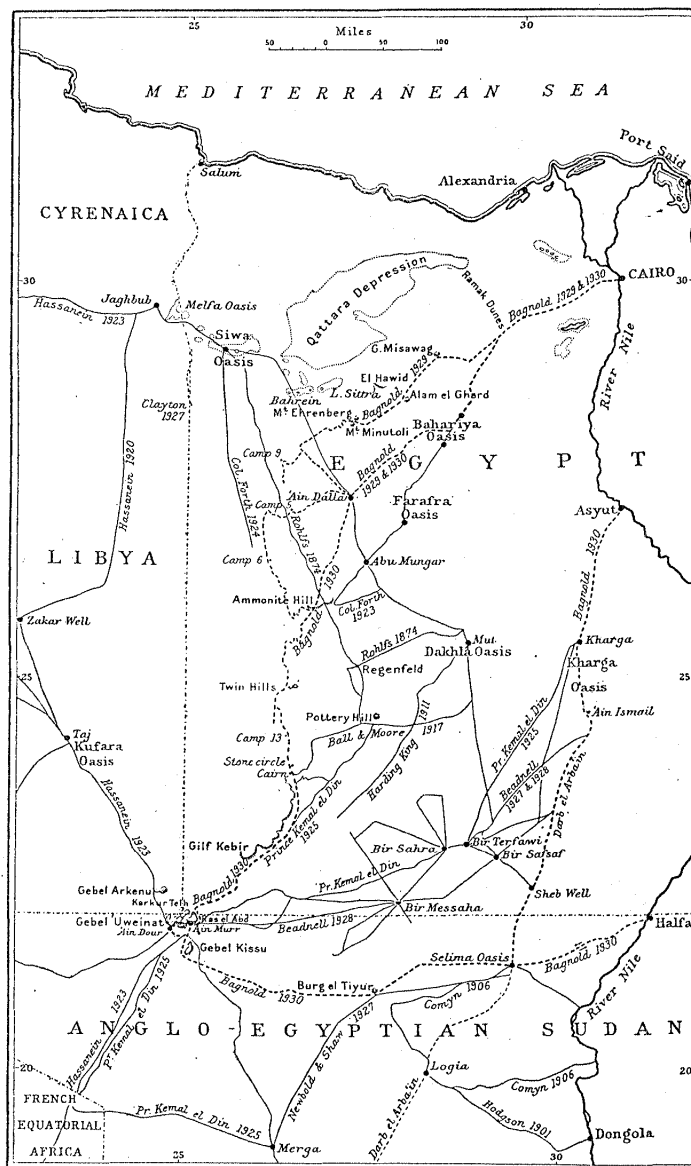


Figure 2.1 Map of Southeastern Gifl Kebir and vicinity, from Bagnold, 1931.

In March and April, 1933, P. A. Clayton, Lady R. C. E. Clayton, and Lt. Comm. Roundell made a survey of the northern part of the Gifl Kebir. At the same time, H. W. G. J. Penderel, Count L. de Almsy, Dr. L. E. Kadar, Hans Casparius, and Dr. R. A. Bermann surveyed the northeastern and western parts of the Gifl Kebir. Almsy went on to Gebel Uweinat, where he met an Italian group. The Italians had established a frontier outpost there after capturing Kufra Oasis in 1931. According to Almsy (1936), his driver discovered the painted caves at Ain Doua and brought them to the attention of Count L. di Caporiacco who published a description of them (1933; di Caporiacco et P. Graziosi, 1934). Almsy also published two travelog-type descriptions of his explorations in the Libyan Desert (1936, 1940).

The first purely archeological expeditions to the Gilf-Uweinat and surrounding areas were those led by Leo Frobenius in 1933 and 1934-35. The purpose of these expeditions was to investigate the rock pictures and archeology of the Libyan Desert, which resulted in the major monograph on the rock art of the area by Hans Rhotert (1952). The expedition members also made collections of artifactual materials from the locales of the rock pictures and elsewhere but unfortunately these were destroyed in World War II (Rhotert, pers. comm.). The Frobenius expeditions recorded, by manual and photographic means, the rock engravings and paintings from the northern and western Gilf Kebir, from Gebel Uweinat, and from a number of localities in northern Sudan. Rhotert's 1952 monograph provides us with the most comprehensive collection of representations of the rock art of the southern Libyan Desert.

In 1935, W. B. K. Shaw led a party to the southern part of the Gilf Kebir where they discovered a single shelter with painted pictures and some scant artifactual remains. Shaw reported the results of this expedition, which covered much more than the southern Gilf, in several articles (1936a; 1936b; 1936c), and Michael H. Mason wrote a popular account of the journey (1926).

The final pre-war scientific expedition to the Gilf-Uweinat area was again led by R. A. Bagnold in the winter and spring of 1938. It was actually a combined expedition with Bagnold and R. F. Peel responsible for the geological research, and Oliver H. Myers and Hans A. Winkler responsible for the investigations of the archeological sites and the rock art. Sir Robert Mond provided the financial support for Myers' and Winkler's participation. A number of publications resulted from this combined expedition: a multi-authored preliminary report in the *Geographical Journal* (Bagnold and others, 1939) including Myers' contribution to the archeological investigations, the articles on the archeology, geology, geomorphology, rock art, and ethnography by Peel (Peel, 1939a; 1939b; 1941; 1942), and the article and monograph on the rock art of Gebel Uweinat, the southern Gilf, Dakhla, and the west bank of the Nile by Winkler (1939a; 1939b). Because of the outbreak of World War II and his sudden involvement and permanent separation from the artifactual materials collected on this expedition, Myers was unable to publish a description of them or his interpretations of their significance. He did leave three short, unfinished manuscripts outlining some of his ideas (Myers, not dated; a, b, c). McHugh (1971) has studied part of the Myers collection and has published the results of this analysis and his paleographic and cultural ecological reconstructions in three papers (McHugh, 1974a; 1974b; 1975).

RESEARCH AND EXPLORATION: POST-1940

During the early part of World War II after the Italians had declared war on the British, the Gebel Uweinat and southern Gilf Kebir were used as a staging area by the British Long Range Desert Group (LRDG) for reconnaissance and military operations against the Italian outposts in southeastern Libya (Bagnold, 1945; Wright, 1945; and Shaw, 1945). The desert patrols accomplished a considerable amount of

mapping in eastern Libya, but collected no further archeological data during the war. During the 1978 expedition, we found evidence of the presence of LRDG in the form of stripped lorries and concentrations of empty petrol cans in three localities near the eastern Gilf.

The earliest post-World War II expedition to the Gilf-Uweinat area was that of the Royal Military Academy, Sandhurst, England, to Gebel Archenu and southeastern Libya in 1962. This expedition was led by M. A. J. Williams and D. N. Hall (1965). In April, 1967, a group comprised of members of the U.S. Naval Medical Research Unit Number Three (NAMRU-3), Cairo, the Egyptian Ministry of Health, and the Egyptian Desert Reclamation Department, journeyed to Uweinat to collect mammals and their ectoparasites, insects, and botanical specimens. This expedition has been reported on by Dale J. Osborne, medical zoologist, and Karl V. Krombein, Smithsonian entomologist (Osborne and Krombein, 1969). This group concentrated its activities in the Karkur Murr, in the southeastern part of Uweinat in the Sudan, and briefly visited Karkur Talh in the northwestern part of Uweinat. The NAMRU-3 group collected 55 plant species, six mammalian species, and 30 species of wasps.

In the fall and winter of 1968-69, a joint Belgian-Libyan contingent went to Uweinat for a period of several months. The Libyan contingent consisted of Dr. Loutfy Boulos, botanist and leader, Prof. Rashid Hamdy, zoologist, Dr. Mohamed El-Mokahel, mycologist, all from the University of Libya, and a military and police support group (Boulos, pers. comm., 1978). The Belgian contingent consisted of J. Leonard (leader and botanist), J. Klerkx (geologist), X. Misonne (zoologist), J. de Heinzelin and P. Haesarts (Quaternary geologists), and F. Van Noten (prehistorian), in addition to a military support group (Leonard, 1969, p. 102; Van Noten, 1978, p. 12). The Belgians concentrated their investigations in the Karkur Talh and connecting wadis, and in the plain to the north in order to intensively study a restricted area rich in rock art (Karkur Talh) and prehistoric settlements. The Belgian effort has resulted in two publications, the multi-authored preliminary report (Leonard, 1969) and Van Noten's monograph on the rock art of Karkur Talh and connecting wadis (Van Noten, 1978).

In November, 1968, an expedition representing the Geological Survey of Egypt under M. H. Hermina and M. A. El-Hinnawi, and individuals from several other organizations (Prof. S. M. El Shazly, Atomic Energy Institute, Dr. R. El Tahlawy, Assiut University, and M. Habib, Desert Development Organization) conducted a reconnaissance trip to Uweinat and the Gilf Kebir (B. Issawi, pers. comm.). In December, 1971, the Geological Survey of Egypt under Dr. Bahay Issawi returned to the Gilf and Uweinat accompanied by Dr. Robert Giegengack, University of Pennsylvania geologist. They camped at the eastern end of Wadi Wassa in the southern Gilf (where the 1978 expedition camped), made a trip to Uweinat, and attempted but failed to reach the silica glass area north of the Gilf. On his return, Issawi surveyed the northeastern flank of the Gilf in late January and early February, 1972. Giegengack and Issawi have published their review of the silica glass problem in Annal V of the Geological Survey of Egypt (1975), and

Issawi has published or reported on other results of the expedition (Issawi, 1973a).

In February, 1975, a group from the Combined Prehistoric Expedition consisting of Fred Wendorf, Vance Haynes, Rushdi Said, and Romauld Schild made a brief trip to the southern Gilf and visited the large Upper Acheulean site investigated by Myers as well as the locale of the lake sediments and neolithic settlements in upper Wadi el Bakht (Wendorf and others, 1976; 1977). Haynes (pers. comm.) collected ostrich egg shell from the surface of the lake sediments which has provided the first ^{14}C date from the southern Gilf (7280 BP \pm 90; SMU-273). The Wadi El-Bakht and Wadi Ard El-Akhdar to the west were two objectives of the 1978 expedition.

The early expeditions to the Gilf Kebir and Gebel Uweinat are most important because they fixed the location and determined the broad nature of these two physiographic features and because they laid the basis for future research. Bagnold conducted experiments and made observations on the movement of sand when in the field and combined these data with laboratory data in his pioneer work, The Physics of Blown Sand and Desert Dunes (1941), still an important work on this subject. K. S. Sandford and R. F. Peel made extremely important contributions to our understanding of the geology and geomorphology of the southern Libyan Desert and to arid land geomorphology in general. W. B. K. Shaw made the first extensive collections of the flora of this region. The investigations of Newbold, Rhotert, Shaw, and Winkler, especially, brought the remarkable rock art of this area to notice.

In addition, although only two of the pre-World War II expeditions to the Gilf-Uweinat and surrounding areas were primarily or largely motivated by archeological considerations, these early expeditions revealed that this part of the southern Western Desert had formerly supported a varied native fauna and extensive human populations in prehistoric times as evidenced by the rock art and the widespread sites of human settlement. Finally, the knowledge of this area gained by some individuals was later employed in military operations against the Italians in Libya during World War II.

In the subsequent 35 years, expeditions to the Gilf-Uweinat area have been intermittent but gradually increasing in frequency. The geological, paleogeographic potential of this vast area is now more widely appreciated and its multidisciplinary promise will attract more scientists to this incredibly beautiful and barren area. Oil exploration is already underway and tourists cannot be far behind.

ACKNOWLEDGMENTS

I would like to express my appreciation to Bahay Issawi, Farouk El-Baz, Vance Haynes, Loutfy Boulos, and Dale Osborne for their help in preparing this chapter.

Chapter 3

DESERT NAVIGATION

C. VANCE HAYNES

Departments of Geosciences and Anthropology
University of Arizona
Tucson, Arizona 85721

TED A. MAXWELL

National Air and Space Museum
Smithsonian Institution
Washington, D.C. 20560

ABSTRACT

Navigation in the Western Desert of Egypt has traditionally been done by using celestial sightings with a theodolite, using a sun compass developed during the 1930's, relying on native guides who are familiar with the terrain, and most frequently by dead reckoning using a compass and odometer readings. As an improvement on the dead reckoning method, a vertical card compass was used on this expedition mounted on the windshield of one of the vehicles. In addition, a satellite-relayed remote access measurement system (RAMS) was used as a check on our positions as plotted by dead reckoning. For stationary satellite transmissions, the locations computed by the RAMS system were accurate to within 3.4 km, while for transmissions en route, the computed positions were much less accurate than those derived from traditional methods of navigation.

INTRODUCTION

During the early days of Western Desert exploration, navigation was either celestial, by the use of theodolite (Hassanein Bey, 1925; Hussein, 1928) or by Bedouin guides who navigate by making use of various combinations of landmarks, sun angle, Polaris, experience, intuition, and luck (Harding-King, 1925). Normally, the former method was the most precise. In the 1930's Bagnold (1953) and his associates navigated by use of his sun compass, and by astronomic observations with theodolite at evening halts (Newbold, 1931). Further refinements were made by the Long Range Desert Group (LRDG) during World War II and later (Hall, 1967). During the 1978 trip, we were equipped with a transmitter that relayed a signal via Nimbus satellite to a ground receiving station. The position of the transmitter was computed nominally three times a day, so that our location could be determined and compared to navigated locations.

NAVIGATION METHODS

Dead reckoning by magnetic compass and odometer is somewhere in between celestial navigation and the use of native guides in

both simplicity and accuracy. Some guides, however, have little or no difficulty relocating an area as long as there is reasonably good visibility. Some, in fact, have remarkable abilities in this regard. Two such guides, Saleh and Ayed Marif Salem have worked for the Geological Survey of Egypt in this capacity for years, and accompanied us on this journey.

The main problem with dead reckoning is in the use of magnetic compasses (Sheppard, 1970). With hand-held compasses, such as the Brunton type, one must step away from the magnetic vehicle, sight along the desired heading and select a landmark (rock, hill, contact between color changes, etc.) as far ahead as visibility and terrain will allow. In irregular or broken ground this is not usually very far, and one must rapidly select alternate marks along the heading as hills and dips obscure the initial mark. As the landmark is approached, it is sometimes possible to prolong the heading by lining up with another distant object, but this can lead to serious error if true direction is not checked frequently.

On the flat, featureless sand sheets where there are no landmarks, one must rely on a properly compensated compass mounted on the windshield. Dead reckoning in this way, while less accurate, is faster and less tedious than with the seemingly incessant stops needed with the hand-held compass, but the main difficulty is overriding by the liquid-filled compass as one bumps along over irregular surfaces. In extensive areas of broken terrain, frequent stops are needed to allow the compass to settle and to line up a new mark. Because such marks are seldom more than a few kilometers away, one is constantly looking for additional marks farther ahead and alternate marks in between as the main target disappears from view. Only those who have experienced this kind of desert driving can appreciate how exhausting it can be. One often does not realize the degree of their fatigue until the stop at the end of the day, but an objective successfully reached makes it all worthwhile.

Wherever possible, the objective of dead reckoning should be a clearly recognizable or identifiable landmark, and the route must be faithfully plotted on the map. Only in this way are discrepancies apt to be discovered in time to be usefully corrected. With this degree of care and a distinct landmark as the day's objective, one is impressed with the accuracy with which distant locations can be reached. After a field season or two, as one becomes more familiar with the landscape, a high degree of confidence can be attained. This is the stage at which one has to guard against being overconfident and therefore careless. The desert is notorious for the unforeseen to happen. In a sandstorm visibility is commonly reduced to only a few meters, and patterns or tracks on the desert surface can be obliterated in minutes.

One of the most common mistakes of desert travel is the attempt to rely on old tracks. It is incredible how subtly the wrong track can lead one astray, and now with ever more people motoring in the Western Desert, such as petroleum exploration parties, scientific expeditions, and even desert tours, there are many tracks that are not

a part of the traditional routes of Bagnold or the LRDG. In following one's own tracks, distance and direction records should be faithfully continued as a check and as a backup in case the tracks have been obliterated. This is particularly true at night, and more than one desert traveler has been embarrassed by going the wrong way on his outbound tracks.

A significant factor noticed when being guided by a native guide was a bias for the left whenever a choice had to be made in deviating from the main course. In one case, it was apparent from dead reckoning that we were veering too far to the south from our intended southwesterly heading (Haynes and others, 1979). By knowing the direction in which we were off course we were able to head due north and pick up the lost caravan track. When dead reckoning over long distances, it can be useful to maintain a slight bias in order to err toward familiar ground or to know on which side an objective may be in case it is missed.

When avoiding difficult ground such as dunes, the most reliable procedure is to take a new course until the obstacle can be passed by one or two more straight legs. In so doing, one is often tempted by apparent short cuts that can lead to cul de sacs. Needless to say, it takes very few deviations of this type to introduce large errors in one's navigation. One solution is to have a second vehicle (it is always best to proceed with no less than two vehicles in desert travel), wait while the first explores the route. If a way through is found, the second vehicle can proceed after a preset waiting time. If not the first vehicle can return and pick up where it left off. All of these cautions and good intentions are not, however, always followed.

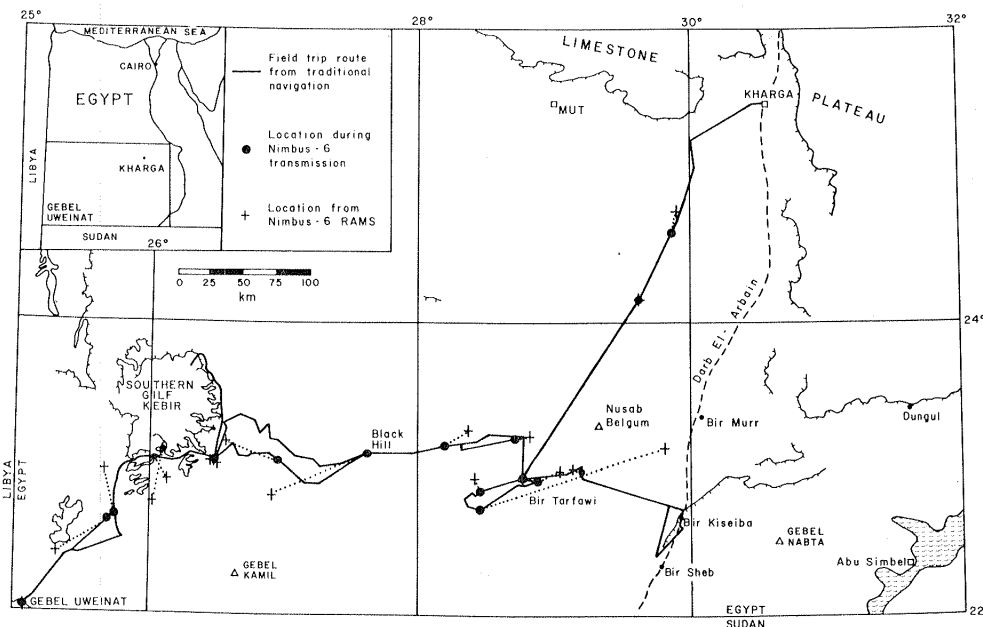


Figure 3.1 Route map showing comparison of navigated route to that obtained from Nimbus-6 RAMS satellite tracking.

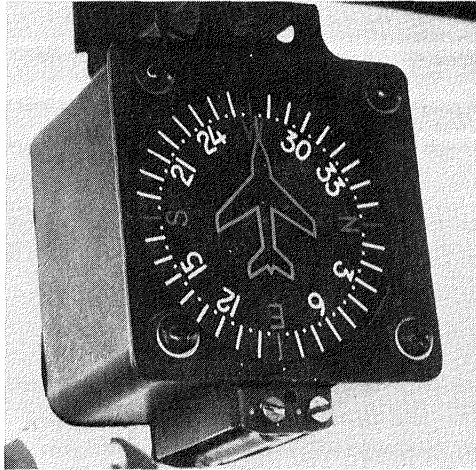


Figure 3.2 Vertical card compass mounted on windshield of Volkswagen Type 181 desert vehicle.

Vertical Card Compass

On the present journey while being guided by Saleh and Ayed we maintained a dead reckoning course log and map plot (Fig. 3.1) by use of a properly compensated vertical card magnetic compass manufactured for aircraft by Hamilton Instruments, Inc., Houston, Texas. The advantages of this instrument over the standard liquid filled compass is that the motion is damped so there is essentially no override, and vibrations are not detrimental. Thus, the compass can be read while underway even over fairly rough terrain. With the compass mounted on the windshield of our Volkswagen Type 181 (Fig. 3.2), and centered between the two seats, both the driver and navigator could monitor it. Over rough ground, the navigator advised the driver of any course corrections necessary, leaving him free to maintain visual contact with the route. Also, the driver advised the navigator whenever a significant change in course was made or anticipated.

Periodically, the vertical card compass was checked by Brunton, with declination properly set, by either sighting back along the tracks if straight, or by sighting along the long axis of the vehicle from far enough in front to avoid its magnetic effect. If mapped landmarks were in view and positively identified, we would check our position by resection.

NIMBUS-6 RAMS EXPERIMENT

In addition to these traditional methods of desert navigation, the Nimbus-6 RAMS (Remote Access Measurement System) was used to obtain location data that would aid in plotting the field trip route. The system operates by transmission of a signal from the ground to a satellite, which is then relayed to a ground receiving station where frequency shifts in the transmitted signal are converted into ground locations by knowing the precise orbital track. The RAMS system was used for three reasons: 1) Available map coverage of the Gebel Uweinat - Gilf Kebir region is limited to 1:500,000 scale maps made

on the basis of surveys done before and during World War II; 2) Uncertainties in the accuracy of desert navigation (essentially mileage and azimuth recordings) made an alternate means of plotting sample locations desirable; and 3) In order to test the "search and rescue" capabilities of the RAMS, and in the absence of any other means of communication, the transmitter was equipped with a switch that would relay a message signalling an emergency situation.

Logistics

The ground-based platform for the Nimbus-6 RAMS communications link consists of three parts; a power supply, transmitter and antenna. A 12 volt Gel Cel battery (fully charged before the trip) provided power to the transmitter continuously for two weeks. The transmitter (manufactured by Handar) had the capability to send messages on four channels during each transmission. For our use, however, it was pre-set for no message transmission during normal operation, and full-scale transmission on the first channel during an emergency. During operation, both battery and transmitter (wrapped in 1-inch foam for cushioning) were kept on the rear floor of the vehicle. No problems were encountered with either the transmitter or the battery.

Locating the antenna (manufactured by CHU Associates) at the highest point of a canvas-covered vehicle was much more difficult. A wooden antenna mount made before the trip proved unsuitable after one day in the field. Consequently, the antenna was bolted to the body of the vehicle (Fig. 3.3). This position resulted in 90-100° loss of the (circular) radiation pattern of the antenna, but using the predicted pass time, an attempt was made to favorably orient the vehicle with the antenna facing the spacecraft.

Results

The results of the Nimbus-6 RAMS calculated locations and those from navigation while en route are presented in Table 3.1. As a minimum, at least one location per day was expected, although up to three per day were possible. Before the trip, it was not known whether the Nimbus-6 communications link would be operating during the nighttime passes in order to provide additional coverage. For the 11 days of the Gilf Kebir - Gebel Uweinat trip, 31 transmissions were received at Goddard Space Flight Center in Greenbelt, Maryland. During the emergency test procedure on October 13, 2 transmissions were received. Of these 33 transmissions, sufficient data were received for computing 22 locations.

Locations computed from RAMS do not compare well with those plotted from the more traditional methods of desert navigation (Fig. 3.1). During the trip a record of mileage and direction was kept independently by both authors; one familiar with the terrain (C.V.H.), and one unfamiliar with the terrain (T.A.M.). Despite this observational bias, over one stretch of 367 km (from Bir Sahara to the Gilf Kebir), the final navigated positions fall within 10 km of each other. However, of the 22 total locations computed by the RAMS, only 11 were within 10 km of the navigated positions. Of these 11 locations, 9

Table 3.1 Comparison of Nimbus - RAMS and Navigated Tracking Data.

| Day | Local Time | No. Transmissions Received | Location Method* | Error** | RAMS CALCULATED | | NAVIGATED | | Difference (km) |
|--------|------------|----------------------------|------------------|---------|----------------------|-------|-----------|-------|-----------------|
| | | | | | LAT. | LONG. | LAT. | LONG. | |
| 9/26 | 12:44pm | 9 | 1PP | 96.6 | 24.79 | 29.87 | 24.58 | 29.83 | 16 |
| (9/27) | 12:09am | 15 | 1PP | 100.0 | 22.93 | 28.76 | 22.93 | 28.76 | ±3 |
| 9/27 | 10:28am | 12 | 1PP | 99.9 | 22.99 | 29.03 | 22.91 | 28.90 | 14 |
| | 12:01pm | 13 | 1PP | 100.0 | 23.16 | 29.79 | 22.66 | 28.42 | 150 |
| | 1:50pm | 10 | 1PP | 99.9 | 22.89 | 28.43 | 22.83 | 28.77 | 6 |
| | 11:41pm | 3 | - | - | no location computed | | | | - |
| 9/28 | 11:21am | 25 | 2PP | 21.0 | 23.00 | 29.13 | 23.00 | 29.23 | 12 |
| | 10:49pm | 10 | 1PP | 38.7 | 22.91 | 28.76 | 22.80 | 28.52 | ±3 |
| 9/29 | 12:24pm | 12 | 1PP | 100.0 | 23.23 | 28.80 | 23.20 | 28.70 | 10 |
| | 2:16pm | 4 | 1PP | 58.9 | 23.29 | 28.80 | 23.20 | 28.43 | 8 |
| (9/30) | 12:05am | 3 | - | - | no location computed | | | | - |
| 9/30 | 10:04am | 3 | - | - | no location computed | | | | - |
| | 11:11pm | 12 | 1PP | - | 23.03 | 26.45 | 23.05 | 26.45 | ±3 |
| (10/1) | 2:51am | 2 | - | - | no location computed | | | | - |
| 10/1 | 11:03am | 23 | 2PP | 48.0 | 23.06 | 26.45 | 23.05 | 26.45 | ±3 |
| | 12:48pm | | | | | | | | |
| (10/2) | 12:27am | 3 | - | - | no location computed | | | | - |
| 10/2 | 10:25am | 9 | 1PP | 99.2 | 22.94 | 26.12 | 23.05 | 26.03 | 15 |
| | 12:08pm | 21 | 2PP | 37.0 | 22.98 | 25.66 | 22.67 | 25.76 | 33 |
| | 1:55pm | | | | | | | | |
| 10/3 | 11:35am | 19 | 2PP | 45.0 | 22.05 | 25.11 | 22.05 | 25.11 | ±3 |
| | 1:13pm | | | | | | | | |

| | | | | | | | | | |
|------|---------|----|-----|-------|-------|-------|-------|-------|----|
| 10/4 | 10:45am | 9 | 1PP | 60.3 | 22.43 | 25.32 | 22.65 | 25.72 | 48 |
| | 2:18pm | 5 | 1PP | 50.2 | 22.78 | 26.00 | 23.10 | 26.08 | 40 |
| | 11:59pm | 12 | 1PP | 100.0 | 23.05 | 26.45 | 23.05 | 26.45 | ±3 |
| 10/5 | 10:07am | 6 | 1PP | 99.8 | 23.19 | 26.56 | 23.08 | 26.92 | 44 |
| | 11:58am | 25 | 2PP | 32.0 | 22.81 | 26.89 | 23.07 | 27.58 | 76 |
| | 1:35pm | 10 | 1PP | 99.0 | 24.15 | 29.61 | 24.17 | 29.57 | ±3 |
| | 11:18pm | 10 | 1PP | 99.0 | 24.15 | 29.61 | 24.17 | 29.57 | ±3 |
| 10/6 | 12:53pm | 11 | 1PP | 50.3 | 25.45 | 30.51 | 25.45 | 30.51 | ±3 |

Emergency Test

| | | | | | | | | | |
|-------|---------|----|-----|-------|----------------------|-------|-------|-------|---|
| 10/13 | 11:35am | 15 | 1PP | 100.0 | 28.50 | 29.14 | 28.45 | 29.35 | 7 |
| | 11:00pm | 3 | - | - | no location computed | | | | - |

* 1PP: one pass position; 2PP: two pass position (Location is computed for first transmission time).

** Test for accuracy; on one pass position, 100.0 is best score. On two pass positions, 50.0 is best score.



Figure 3.3 Nimbus-6 RAMS antenna mounted on rear of Volkswagen Type 181 desert vehicle.

were from camp or otherwise stationary positions. The average difference between RAMS and navigated locations is 3.4 km for stationary transmissions, and 36.3 km for transmissions while en route (tracking data are summarized in Table 3.2).

The lack of correspondence of navigated versus RAMS-calculated positions most likely results from a combination of several factors, although orbit geometry, placement of the antenna, and the roughness of the terrain are thought to be most important. For example, the 12:01 PM location on September 27 (discrepancy of 150 km) was transmitted from the middle of the Abu Hussein dune field while the

Table 3.2 Summary of Nimbus - RAMS Tracking Data.

| | |
|--|---------|
| Total No. Transmissions received | 33 |
| Total No. Locations computed | 22 |
| Minimum expected locations (No. days in field) | 11 |
| DISCREPANCIES | |
| No. Locations in camp or stationary | 9 |
| Average error of stationary locations | 3.4 km |
| No. Locations while <u>en route</u> | 13 |
| Average error of <u>en route</u> locations | 36.3 km |
| Total Locations computed | 22 |
| Total Locations < 10 km off | 11 |

vehicle was making a wide turn from west to north. The angle from horizontal to the spacecraft at this time was 85°, greater than the 10°-80° needed for optimum locations.

The test of the emergency switch on October 13 performed as expected, and indicated that the battery had remained fully charged. The battery voltage was further confirmed upon return to Goddard Space Flight Center, and no significant loss of power had taken place throughout the trip.

Recommendations

Equipment. Neither the transmitter nor battery created any problems during the trip. However, for the extremely rough terrain, suitable means of strongly anchoring the antenna is necessary. Since most desert vehicles have canvas tops, the antenna cannot be bolted directly to the top of the vehicle, as the struts that support the roof are not strong enough to support the antenna. Any vertical-pole mount must be secured by guy lines attached as close as possible to the top of the antenna. Judging from the results of this experiment, however, the most important consideration is keeping the antenna stationary for the duration of a pass. Consequently, predictions of pass times are a necessity, as are predictions of the groundtrack (spacecraft sub-point) so that a proper antenna-spacecraft orientation can be maintained. Even this mode of operation can create problems for a large caravan, since it means that at least one of the vehicles must stop for each pass. At present, however, this seems to be the only feasible method to improve the accuracy of location data.

Data Handling. During this experiment, two-pass positions were calculated for 5 of the locations. Although these locations would theoretically be more accurate than one-pass positions, the actual location of the transmitter had changed several tens of kilometers between the times of the two transmissions. A potential improvement in the calculation procedure would be the capability to calculate these transmissions as one-pass positions.

Potential for Remote Desert Studies

In spite of the large discrepancies in location resulting from this experiment, the Nimbus-6 RAMS has great potential for studies of the remote regions of the world. With suitable accuracy, this system will aid future desert studies by:

1. Allowing a group (or several groups) to remain in the field with a communication device that could be relied on in an emergency situation.
2. Providing location data that would be useful for both locating samples and checking navigation.
3. Providing real-time data (locations while still in the field) that could be used for field checks on the locations of known landmarks and other features, and for correcting the field trip route during travel.

4. Adding two-way communication with the outside world. In addition to the added sense of security, this would provide an internal test on the operating condition of the system.

ACKNOWLEDGMENTS

The use of the Nimbus-6 RAMS transmission equipment was made possible through the courtesy of NASA/Goddard Space Flight Center. We are particularly indebted to W. W. Conant and G. Gilbert for their assistance with the system. B. Issawi provided us with supplementary route information after the trip.

Chapter 4

THE VIEW FROM SPACE

FAROUK EL-BAZ

National Air and Space Museum

Smithsonian Institution

Washington, D.C. 20560

ABSTRACT

No systematic aerial photographs were ever obtained of the southwestern part of the Western Desert of Egypt. This lack of aerial photographs increases the value of images taken from space in studying the landscapes of this part of the desert. Coverage from space of the Western Desert of Egypt includes data from the manned missions of Gemini IV through XII, Apollo 7 and 9, Skylab 2, 3, and 4, and particularly the Apollo-Soyuz Test Project. It also includes images obtained by the unmanned Landsat spacecraft and weather satellites such as Meteosat. Detailed study of the landforms in this desert is hampered by the low resolution of space images and photographs. It is recommended that high resolution photographs of this desert be taken by the Large Format Camera on the Space Shuttle. Such photographs should be used in making large-scale topographic maps of the Western Desert, particularly its southwestern part. Other data that may be helpful in the future include the television (RBV) images from Landsat 3 and stereo, high resolution images from the French SPOT spacecraft.

INTRODUCTION

The Western Desert occupies 681,000 km², more than two-thirds the land area of Egypt. It is basically a rocky platform crossed in places by parallel belts of sand dunes. The generally flat terrain is broken by numerous depressions that enclose oases, and in the southwestern part, by the Gilf Kebir sandstone plateau and the granitic mountains of the Uweinat region (Said, 1962).

Aerial photographic coverage of this desert is patchy. The only part that is adequately photographed is the coastal strip; much of the coverage was obtained during World War II. Also, the western borders of the Nile Valley were photographed along with the oases, because of their value to agricultural and other economic development. The rest of the desert, particularly the southwestern part has never been systematically photographed by aerial cameras.

The lack of aerial photographs increases the value of those taken from Earth orbit. Since the advent of NASA's manned space program, orbital photographs have been used to provide information on remote, inaccessible and unexplored areas. Because of their large regional

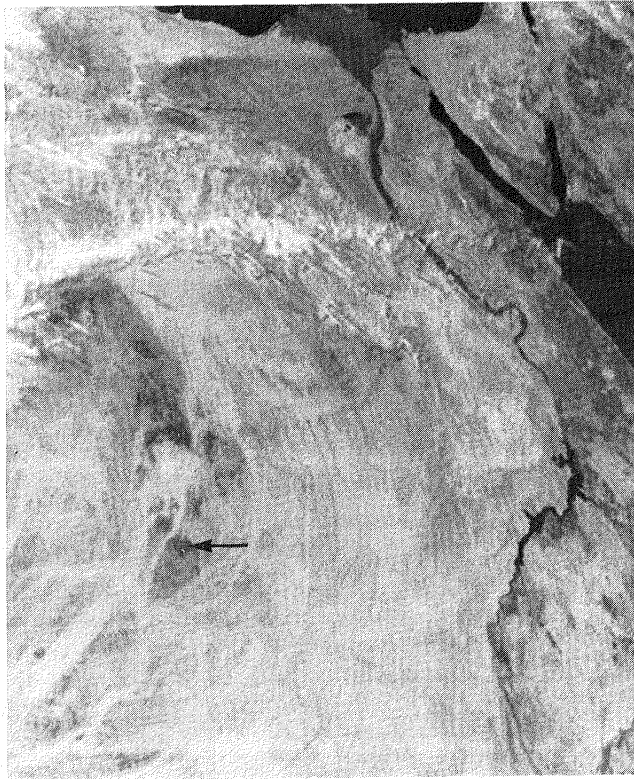


Figure 4.1 Enlargement of Meteosat image, at 2.5 km resolution, showing Egypt and parts of Libya and Sudan. Arrow points to the Uweinat Mountain (photo courtesy of G. Hunt).

coverage, these photographs provided a new perspective and an effective tool to study large-scale landforms. These photographs were later supplemented by images obtained by unmanned satellites such as Landsat and Meteosat (Fig. 4.1).

Table 4.1 lists the usable photographs and images covering parts of the deserts of Egypt. This list is here provided to allow ordering individual frames from NASA. The list includes those obtained on the Gemini IV through XII (55 frames), Apollo missions 7 and 9 (15 frames), Skylab missions 2, 3 and 4 (40 frames), Apollo-Soyuz Test Project (53 frames). Of nearly 500 images with less than 30% cloud cover from Landsat satellites, 65 reasonably cloud free images from Landsat 1 alone provide complete coverage of the deserts of Egypt (Table 4.2; Fig. 4.2).

ASTRONAUT PHOTOGRAPHS

All the American astronauts who orbited the Earth agreed that the view from space was wondrous. During the Mercury, Gemini and early Apollo flights it was quickly realized that trained astronauts were able to expertly describe observed phenomena and adequately photograph significant features (El-Baz, 1977).

Table 4.1 Earth Orbital Photographs Covering the Egyptian Deserts

| <u>GEMINI IV</u> | <u>GEMINI XII</u> | <u>SKYLAB 2</u> | <u>APOLLO-SOYUZ</u> | |
|-------------------|-------------------|-----------------|---------------------|--------------|
| S-65-34664 | S-66-62986 | SL2-106-1142 | 70 mm Camera | 70 mm Mapper |
| S-65-34665 | S-66-62987 | SL2-106-1143 | | |
| S-65-34668 | S-66-63081 | SL2-106-1144 | AST-1-048 | AST-16-1246 |
| S-65-34776 | S-66-63476 | | AST-1-049 | AST-16-1247 |
| S-65-34779 | S-66-63477 | <u>SKYLAB 3</u> | AST-1-050 | AST-16-1248 |
| S-65-34780 | S-66-63478 | SL3-115-1884 | AST-1-051 | AST-16-1249 |
| S-65-34781 | S-66-63479 | SL3-115-1885 | AST-2-126 | AST-16-1250 |
| S-65-34782 | S-66-63480 | SL3-115-1886 | AST-2-127 | AST-16-1251 |
| S-65-34783 | S-66-63481 | SL3-115-1900 | AST-2-128 | AST-16-1252 |
| S-65-34784 | S-66-63482 | SL3-115-1901 | AST-2-129 | AST-16-1253 |
| | S-66-63529 | SL3-115-1917 | AST-2-130 | AST-16-1254 |
| <u>GEMINI V</u> | S-66-63530 | SL3-115-1918 | AST-2-131 | AST-16-1255 |
| S-65-45569 | S-66-63531 | SL3-115-1919 | AST-2-132 | AST-16-1256 |
| S-65-45606 | S-66-63532 | SL3-115-1920 | AST-2-133 | AST-16-1257 |
| S-65-45697 | S-66-63533 | SL3-115-1921 | AST-2-134 | AST-16-1258 |
| S-65-45608 | S-66-63534 | SL3-118-2158 | AST-2-135 | AST-16-1259 |
| S-65-45626 | | SL3-122-2620 | AST-2-136 | AST-16-1260 |
| S-65-45736 | <u>APOLLO 7</u> | SL3-129-3076 | AST-2-137 | |
| S-65-45778 | AS7-5-1622 | SL3-129-3077 | AST-2-138 | 35 mm Camera |
| | AS7-6-1693 | | AST-2-139 | |
| <u>GEMINI VII</u> | AS7-6-1694 | <u>SKYLAB 4</u> | AST-2-140 | AST-31-2633 |
| S-66-63535 | AS7-8-1905 | SL4-138-3769 | AST-9-553 | AST-31-2634 |
| S-65-63748 | AS7-8-1906 | SL4-138-3770 | AST-9-554 | AST-31-2635 |
| S-65-63749 | AS7-11-1999 | SL4-138-3771 | AST-9-555 | |
| S-65-63849 | AS7-11-2000 | SL4-138-3772 | AST-9-556 | |
| S-65-63850 | AS7-11-2003 | SL4-138-3773 | AST-9-557 | |
| S-65-64006 | AS7-11-2006 | SL4-138-3790 | AST-9-558 | |
| | AS7-11-2008 | SL4-138-3815 | AST-13-843 | |
| <u>GEMINI X</u> | AS7-11-2009 | SL4-138-3369 | AST-13-844 | |
| S-66-45678 | | SL4-190-6993 | AST-13-845 | |
| S-66-45679 | <u>APOLLO 9</u> | SL4-194-7219 | AST-13-846 | |
| S-66-45680 | AS9-20-3176 | SL4-194-7220 | AST-13-847 | |
| S-66-45681 | AS9-20-3177 | SL4-194-7221 | AST-13-848 | |
| | AS9-23-3521 | SL4-194-7222 | AST-13-849 | |
| <u>GEMINI XI</u> | AS9-23-3522 | SL4-194-7254 | AST-13-850 | |
| S-66-54528 | | SL4-194-7255 | AST-13-851 | |
| S-66-54529 | | SL4-194-7256 | AST-13-852 | |
| S-66-54530 | | SL4-194-7257 | | |
| S-66-54531 | | SL4-194-7258 | | |
| S-66-54662 | | SL4-194-7259 | | |
| S-66-54663 | | SL4-194-7261 | | |
| S-66-54664 | | SL4-194-7262 | | |
| S-66-54776 | | SL4-208-8143 | | |
| S-66-54777 | | | | |
| S-66-54778 | | | | |
| S-66-54893 | | | | |
| S-66-54895 | | | | |

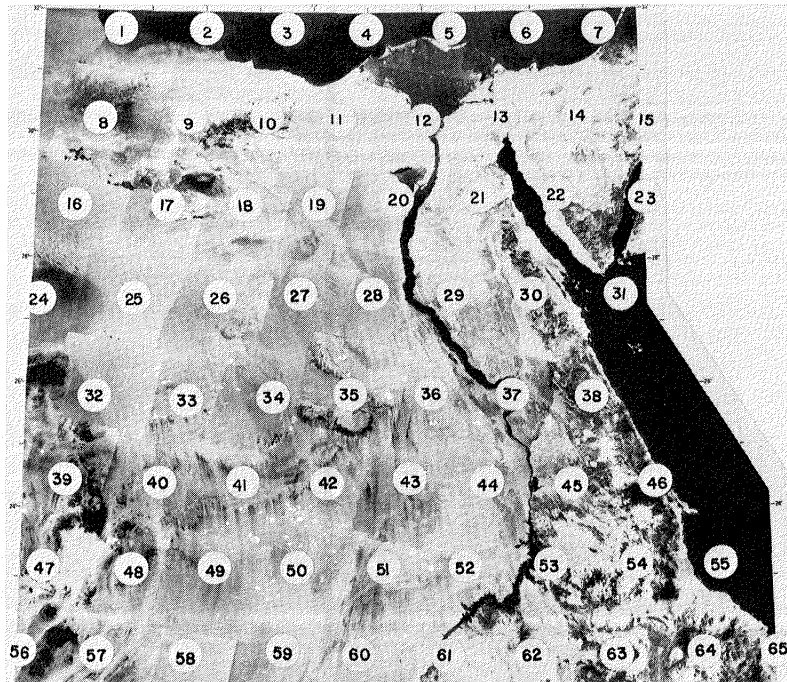


Figure 4.2 Landsat 1 coverage of Egypt; image numbers correspond to those listed in Table 4.2.

At the start of the American manned space flights, Mercury 6 through 9, an informal surface observation and photography experiment was conducted. The most valuable photographs were obtained on Mercury 9 by astronaut Gordon Cooper, who also made several observations that

Table 4.2 Landsat 1 Frames Providing Complete Coverage of Egypt.

| | | | |
|------------------|------------------|------------------|------------------|
| 1. E-1187-08230 | 17. E-1204-08182 | 33. E-1113-08132 | 49. E-1112-08083 |
| 2. E-1204-08173 | 18. E-1113-08123 | 34. E-1058-08065 | 50. E-1165-08023 |
| 3. E-1113-08114 | 19. E-1058-08060 | 35. E-1165-08014 | 51. E-1110-07570 |
| 4. E-1058-08051 | 20. E-1039-08001 | 36. E-1110-07561 | 52. E-1109-07511 |
| 5. E-1039-07592 | 21. E-1110-07552 | 37. E-1109-07502 | 53. E-1144-07453 |
| 6. E-1164-07541 | 22. E-1145-07493 | 38. E-1144-07444 | 54. E-1107-07394 |
| 7. E-1145-07484 | 23. E-1108-07434 | 39. E-1204 08194 | 55. E-1214-07341 |
| 8. E-1169-08231 | 24. E-1205-08243 | 40. E-1113-08135 | 56. E-1042-08193 |
| 9. E-1204-08180 | 25. E-1204-08185 | 41. E-1112-08080 | 57. E-1131-08144 |
| 10. E-1113-08121 | 26. E-1113-08130 | 42. E-1201-08022 | 58. E-1112-08085 |
| 11. E-1058-08053 | 27. E-1058-08062 | 43. E-1110-07563 | 59. E-1165-08025 |
| 12. E-1039-07595 | 28. E-1039-08004 | 44. E-1109-07504 | 60. E-1110 07572 |
| 13. E-1074-07541 | 29. E-1110-07554 | 45. E-1108-07450 | 61. E-1141-07285 |
| 14. E-1145-07491 | 30. E-1145-07500 | 46. E-1107-07392 | 62. E-1144-07455 |
| 15. E-1144-07432 | 31. E-1108-07441 | 47. E-1204-08200 | 63. E-1143-07401 |
| 16. E-1205-08241 | 32. E-1042-08182 | 48. E-1131-08141 | 64. E-1214-07344 |
| | | | 65. E-1091-07482 |

showed that he was able to see more than expected. These results generated considerable interest among the scientific community and encouraged plans for additional experiments on later missions.

Photographs on these missions were obtained using handheld Hasselblad cameras (Cortright, 1968). The 70 mm format allowed enlargement of the originals without affecting the sharpness of the photographs. Color film was used, which increased the value of the data. Scientists working with astronaut-obtained photographs were able to discriminate subtle changes recorded on the film because of the high sensitivity of the human eye to color. Particularly in photographs of desert regions, color was a significant factor, and variations in the color were found to be meaningful (El-Baz, 1978a), thus adding to the scientific content of space-borne photographs.

The first useful photographs of the Western Desert of Egypt were obtained by the Gemini missions. These photographs provided views of the remote southwestern regions and allowed mapping of the morphology (Pesce, 1968). One particular photograph with large regional coverage (S-66-54528) vividly portrayed the flow directions of sand dune belts among the topographically-high plateaus and granitic mountains (Fig. 4.3).

A near vertical view of the Uweinat Mountain was also obtained by the Gemini XI mission (S-66-54776). Taken from an altitude of 482 km, the photograph showed the details of the mountains of Uweinat,



Figure 4.3 The eastern Sahara as viewed by Gemini XI, photograph number S-66-54528.

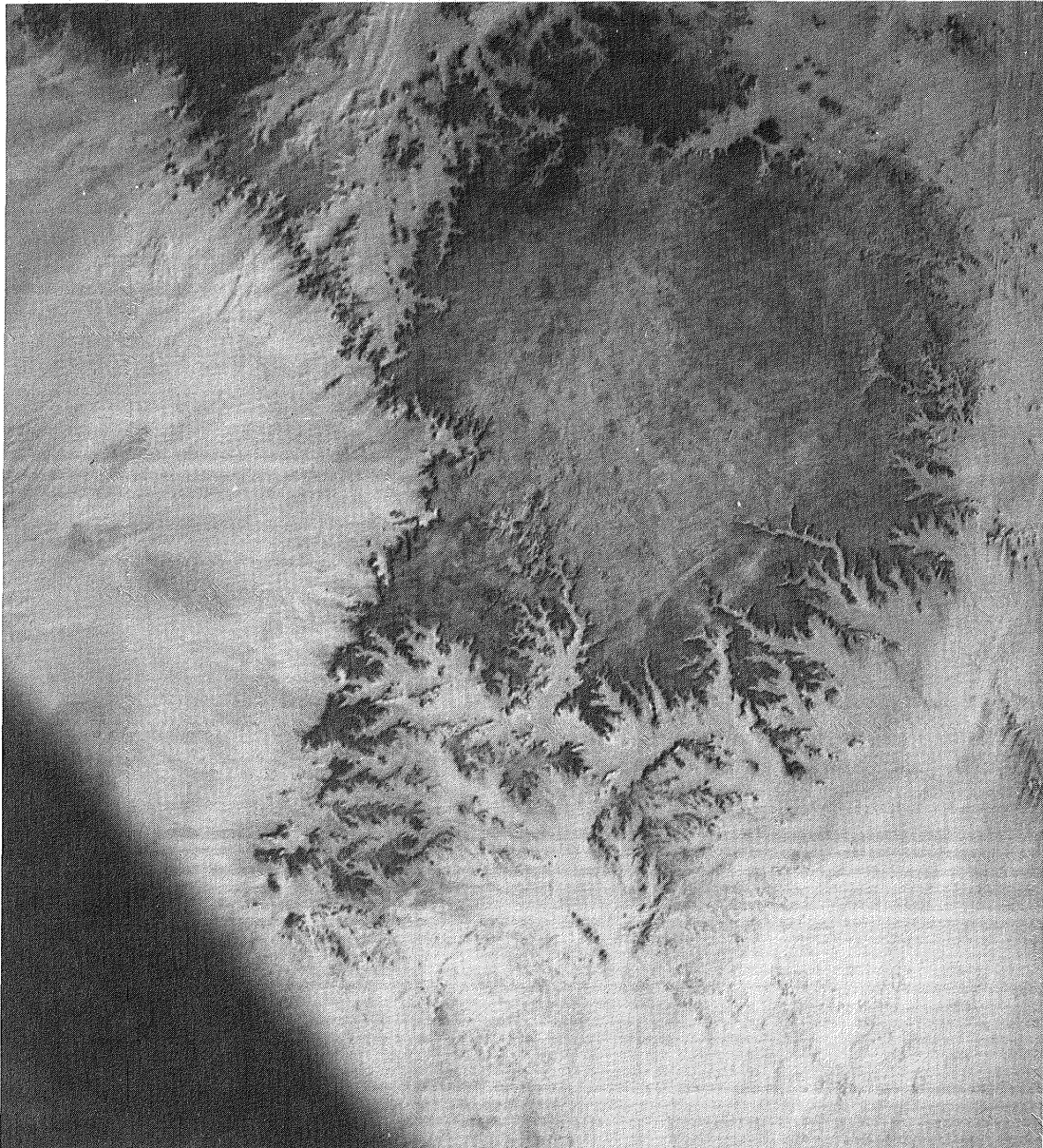


Figure 4.4 Apollo 7 view of the Gilf Kebir plateau. Width of photograph at top is approximately 140 km.

Archenu, Kissu, and Babein, all of which are circular granitic intrusions (Pesce, 1968, p. 62). The same view showed details of the southern Gilf Kebir and the diversity in the directions of dune belts as they made their way between the topographic highs.

Perhaps the best photograph of the Gilf Kebir plateau was obtained by Apollo mission 7 (Fig. 4.4). The southern half of the

Gilf was depicted as a flat and smooth-surfaced plateau with straight western borders. The photograph clearly displayed the numerous deep canyons particularly in the southeastern border. The canyons were clearly formed by water erosion under rainy conditions, which prevailed over 8,000 years ago. These canyons were morphologically compared to similar gorges in the martian canyonlands (Maxwell and El-Baz, 1979).

Apollo mission 9 obtained two noteworthy photographs of the southern part of the Western Desert of Egypt. The first, AS9-23-2533, depicted the Uweinat Mountain region, particularly the sand dune belts in southwest Egypt (Nicks, 1970). The second, AS9-20-3176, showed the vast plains of the southeastern part of the desert. In this photograph east-west trending scarps were clearly displayed along with patches of light-colored deposits, which marked the sites of ancient playa deposits of former lakes.

The Skylab astronauts also obtained useful photographs of the southern part of the Western Desert of Egypt. Two photographs in particular provided new information on the Darb El-Arba'in Desert (as named by Vance Haynes in this volume), in the southeast (SL4-138-3770), and on the extension of features in the southwest part deep into Sudan (SL3-115-1900). In the latter photograph, it is clear that the light-colored streaks in Egypt extend into the Sudan with a distinct veering towards the southwest (Fig. 4.5). The scarps and isolated hills typi-



Figure 4.5 Skylab 3 photograph of the southwestern desert of Egypt and the northwestern desert of Sudan, showing the curved nature of eolian streaks (SL3-115-1900).

cal of the Western Desert are also prevalent in northwestern Sudan. The numerous color variations in this photograph are not yet fully understood.

Photography of the deserts of Egypt was considered a major objective on the Apollo-Soyuz Test Project (ASTP). ASTP photographs were obtained with one Nikon and two Hasselblad 70mm cameras (Table 4.1). One 70mm camera was bracket-mounted and was equipped with an intervalometer and reseau plate to provide stereo mapping photography. The second camera had a single lens reflex mechanism for handheld photography. Some photographs were taken with a color sensitive film (SO-242) that was specifically selected for desert photography (El-Baz, 1977).

The ASTP photographic coverage is shown in Figure 4.6. Some of the photographs covered areas previously photographed on earlier missions, for example the Uweinat Mountain region (Fig. 4.7). This allowed making comparisons of the two data sets to study changes with time. Using a Bausch and Lomb model ZT-4 Zoom Transfer Scope, one photograph can be projected onto another, despite differences in obliquity and scale, by optically rotating, stretching, and enlarging one of the photographs.

One such comparison was made of the Uweinat Mountain region (Slezak and El-Baz, 1979). As shown in Figure 4.7, the wind-deposited

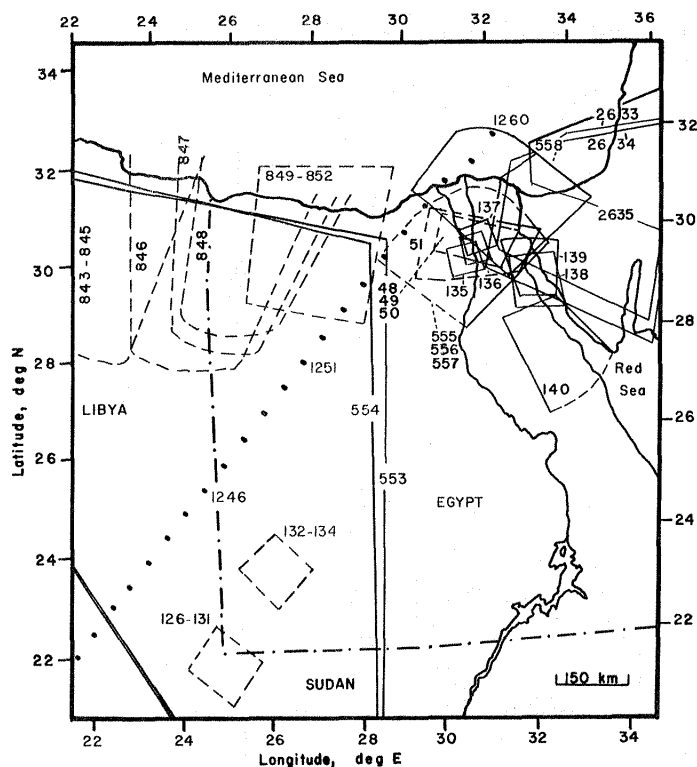


Figure 4.6 Photographic coverage of Egypt from the Apollo-Soyuz Test Project. Numbers are listed in Table 4.1.

sand between the mountain highs is much lighter in color than the surroundings. The region was analyzed in an effort to determine the temporal changes that may have occurred between the time of the Apollo 9 photograph that was taken in 1969 (AS9-23-3533) and the ASTP photographs that were taken in 1975 (AST-2-126, 127, 129, and 130). It was found that the lateral shift distance of sand in the region was 2.5 km in 6 years, or more than 400 m per year (Slezak and El-Baz, 1979, p. 269).

LANDSAT IMAGES

The unmanned Landsat satellites operate from the relatively high altitude of approximately 920 km. Landsat spacecraft are in a near-polar orbit (81° inclination) and travel around the Earth every 103 minutes. Therefore, they fly over the same area of the Earth every 18 days. Each spacecraft is equipped with scanners that image portions of the Earth on selected orbit.

The Landsat multispectral scanners produce images representing four different bands of the electromagnetic spectrum. The four black-and-white bands are designated as follows: band 4 for the green spectral region (0.5 to 0.6 microns); band 5 for the red spectral region (0.6 to 0.7 microns); band 6 for the near-infrared region (0.7 to 0.8 microns); and band 7 also for the near-infrared region (0.8 to 1.1 microns).

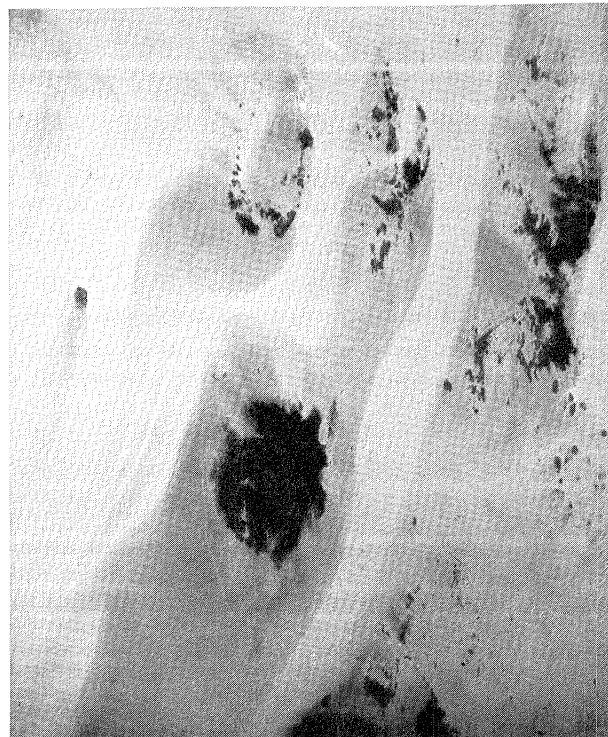


Figure 4.7 Apollo-Soyuz photograph of the Uweinat Mountain region. Note the bright sand dune belts between the topographic highs (AST-2-127).

Light reflectance data from the four scanner channels are converted first into electrical signals, then into digital form for transmission to receiving stations on Earth. The recorded digital video data are re-formatted into computer compatible tapes and/or converted at special processing laboratories to black-and-white photo images. The images from the four bands can be recorded on four black-and-white films from which photographic prints are made in the usual manner.

Because each of the four bands records a different range of radiation, the black-and-white images generated for each band display different sorts of information. Combinations of three or four of the bands produce false-color composites. Such composites covering the total area of Egypt (Fig. 4.2), have been made, annotated and published (El-Baz, 1979a).

The effective resolution of Landsat images at 1:1,000,000 scale is approximately 400 m. However, the Landsat data can be computer-enhanced to produce images at 1:250,000 scale and larger. The effective resolution of enhanced images becomes about 150 m, which is double the size of individual picture elements (one "pixel" = 80 m). However, linear and very high-contrast features the size of a pixel can be detected in such enhanced images.

The difference between the standard and enhanced Landsat products is shown in Figure 4.8. The standard image shows part of the Nile Valley in the upper right corner and the Kharga Depression in the lower left. Terrain characteristics are barely discernible in this image. Only the bright-colored dune belts within the dark-floored Kharga depression are barely visible. However, the enhanced image of part of the Kharga depression clearly displays the lineated nature of the yardang field north of Kharga. This image also shows the texture of sand dune belts and the road that connects Kharga with Dakhla Oasis to the west and the Nile Valley to the northeast.

To date, only a few images covering the Western Desert oases and the Uweinat Mountain - Gilf Kebir region have been enhanced. The cost of this computer enhancement, over \$1,000 per image, has limited the amount of Landsat images that are fully utilizable in photogeologic interpretations.

Landsat spacecraft 1, 2 and 3 were also equipped with a television camera system referred to by the acronym RBV, for return beam vidicon. This system was shut down early in Landsat 1 operation and only worked occasionally on Landsat 2. Digital images from the RBV contain additional information, in the visible range, to the multispectral data. For this reason it was recently recommended to NASA to acquire RBV images of the Western Desert from Landsat 3.

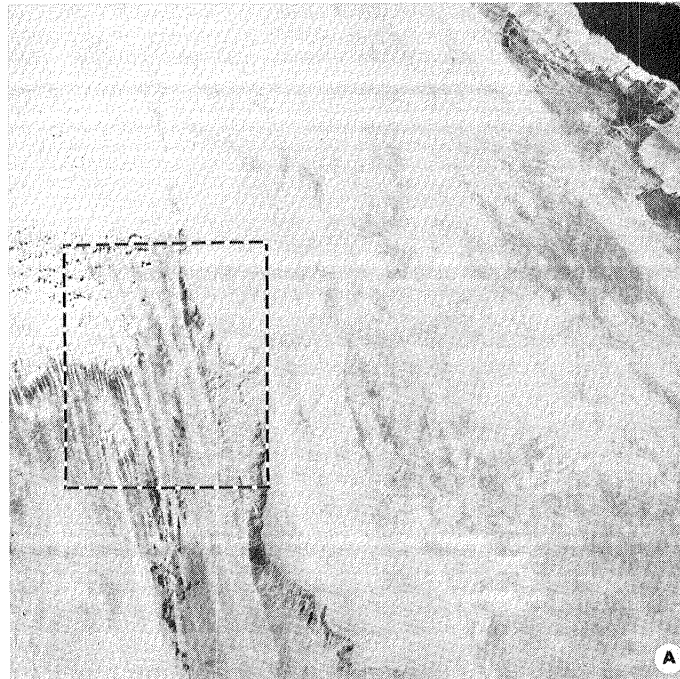


Figure 4.8 (A) Landsat image of the Kharga depression (lower left) and part of the Nile Valley (upper right corner); (B) Computer enhanced part of image marked by a box in (A).

RECOMMENDATIONS FOR FUTURE MISSIONS

The Large Format Camera

The Space Shuttle program will allow the application of what has been learned on previous space missions to better photograph the Earth from orbit. The earliest such use will be of the "Large Format Camera" (LFC; as shown in Fig. 4.9) to allow the acquisition of mapping quality, vertical, stereo, color, and high-resolution photographs from orbit. Photographs from this camera can be used for mapping utilizing conventional techniques and instruments without costly electronic and digital enhancement or image correction.

The LFC derives its name from the size of its individual frames; 45.7 cm in length and 22.9 cm in width. Its 305 mm, f/6 lens has a $40^\circ \times 74^\circ$ field-of-view. The film will be driven by a forward motion compensation unit as it is exposed on a vacuum platen (El-Baz and Ondrejka, 1978).

The LFC system resolution will be 100 lines/mm (1000:1 contrast) to 88 lines/mm (2:1 contrast). This means a photo-optical resolution of 10 to 20 m from an altitude of 260 km. The camera will have the ability to utilize a number of films, including Kodak high resolution black-and-white (3414), color (SO-356), and color infrared (SO-131) in magazines with a capacity of 1,200 m of film. Also an electronic filter changer will permit different films to be used during a single mission.

Orthophotomaps may be made from LFC orbital photographs at scales of 1:100,000 and 1:50,000. The operating framing rate of 80% will provide the required base/height ratio for topographic mapping with 20 m contours (Doyle, 1979).

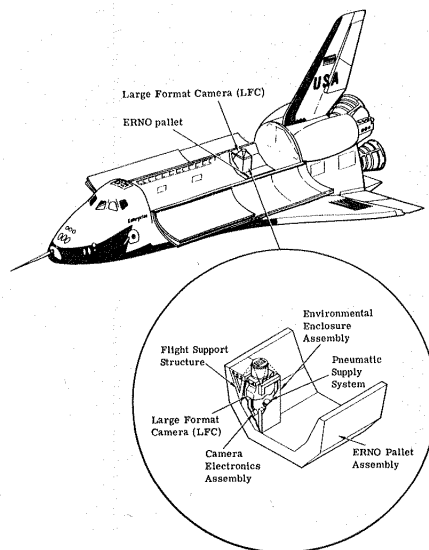


Figure 4.9 Sketch illustrating the deployment of the Large Format Camera (LFC) in the Space Shuttle cargo bay (from El-Baz and Ondrejka, 1978, p. 716).

Both the resolution and the geometric accuracy of the LFC make it very suitable for photography of the southern part of the Western Desert of Egypt. It is recommended that such photographs be taken to allow geologic interpretations and the making of large scale topographic maps. High resolution photographs and accurate topographic maps are required for detailed study of this region, both for its development potential and for analog correlation with the martian deserts.

The SPOT System

The European Space Agency has adopted the SPOT system as one of its major earth observation programs. SPOT is a multi-mission platform that was initiated as part of the national space program of France (Honvault, 1980), with the first satellite to be launched in 1985 using an Ariane rocket.

The basic data acquisition system is composed of two imaging instruments in the visible and near-infrared spectra within a 60 km field-of-view. These instruments utilize the recently-developed "linear array" detector technology rather than the Landsat type "scanners". The detectors will allow the acquisition of images with the ground resolution of 20 m in the multispectral (3 band) mode, and 10 m in the panchromatic mode.

SPOT instruments will also be able to acquire stereoscopic images of the same area of the Earth. This will be accomplished by a mirror placed in the opening of each instrument that may be swiveled $\pm 26^\circ$. This mirror will allow the instruments to acquire images of areas as distant from the satellite groundtrack as 400 km. With the satellite placed in a sun-synchronous 98.7° inclination orbit at 822 km above Earth, it will cover the globe in 26 days, with access to a given area at an average of 2.5 days. The platform mass of SPOT is 920 kg with a maximum payload mass of 800 kg. With the solar power panels extended it will measure 6 m in length by 12 m in width. The spectral bands of each sensor will cover the following ranges: (a) 0.50 - 0.59 microns, 0.61 - 0.69 microns, and 0.79 - 0.90 microns for the three multispectral bands (20 m resolution); and (b) 0.50 - 0.90 microns for the panchromatic sensor (10 m resolution).

Both the resolution and the stereo coverage of the panchromatic sensor make it suitable for photography of subtle topographic features, such as those of the Western Desert. SPOT images should be obtained of this desert for use in photogeologic interpretations and for analog correlations with features of Mars.

**Page Missing in
Original Document**

Chapter 5

LINEATION PATTERNS OF THE CENTRAL WESTERN DESERT

H. A. EL-ETR and A. R. MOUSTAFA

Department of Geology
Faculty of Science
Ain Shams University
Abbasia, Cairo, Egypt

ABSTRACT

Multi-band Landsat images (scale 1:1,000,000 and 1:500,000) were used to delineate the photo lineations of an area approximately 281,280 km² in the central Western Desert. A total of 481 lineaments were detected, of which 197 linear features are in the Bahariya region (41,750 sq km). For comparison purposes, aerial photographs (scale 1:60,000) and mosaics (scale 1:100,000) were used to identify the detailed lineation pattern of the main part of the Bahariya region (approximately 18,530 sq km). In this case, a total of 8,326 lineaments were identified. The study shows that regional photo lineation pattern of the central Western Desert is characterized by a strong preferred orientation in the NW to NNW and ENE directions. Local deviations, however, also occur in the Bahariya region. These are attributed mainly to lithostratigraphic control.

Space imagery is valuable in deciphering regional lineations that may be obscured in aerial photographs and mosaics. Such lineations control, to a substantial degree, the shapes of the Siwa, Bahariya, and Farafra Depressions. Aerial photography, however, is still an indispensable source of data with significant details of direct bearing on the local and semi-regional scales and provides a high resolution medium for checking the details and "ground meaning" of regional features on space imagery.

INTRODUCTION

Photo lineations are defined as natural linear or curvilinear features of any length, including topographic, physiographic, lithologic, structural, vegetation, or soil zonal alignment, visible primarily on aerial photographs (El-Etr, 1976). Lineaments detected in surface or near surface rocks may reflect significant linear structures (e.g. faults) in the basement rocks underlying the sedimentary section (Hodgson and others, 1976) or they may be expressions of smaller or shallower linear structures originating in the surface or near surface rocks (e.g. related to the joint and fracture systems of these rocks). The advent of space imagery has provided a powerful tool for the direct identification of regional lineaments (10 km to >100 km).

Space images provide wide coverage, revealing lineations which cannot be detected on aerial photographs, and providing means for spatial correlation between widely separated features. The Landsat images used in this study are recorded in four spectral bands designated 4 through 7; the first two are in the range of the visible light and the other two in the near-infrared range. Band 7, at 0.8 to 1.1 microns is especially useful and has the following unique capabilities: (a) effective penetration of thin clouds and contrails under certain conditions and (b) definition of water/land interface with high precision, enabling detection and identification of rather small circular and linear water bodies (Williams and Carter, 1976). Aerial photographs, although they cover smaller ground areas, do so at higher resolution and provide more details of lineations detected in space images. Both types of data are employed in this study.

PROCEDURE OF STUDY

The technique of quantitative photo lineation analysis was discussed by El-Etr (1967 and 1976) and reviewed recently by El-Etr and Abdel Rahman (1976). In the present study, this technique is adopted for both space images and aerial photographs. The first step is to study the single band images (1:1,000,000) and plot the detected lineations on the corresponding 1:500,000 images. Reliability orders are then assigned, the first order denoting the most pronounced lineations and the third order the most subtle. The lineations are annotated with lengths recorded in kilometers and orientations (azimuth) in classes of 10° of arc for later construction of frequency curves. The detected lineations are next checked on the false-color images (scale 1:1,000,000), and compiled on a false-color mosaic.

The principal parameters used in the present study for the identification of photo lineations are persistent linear topographic expressions of scarps, ridges, and wadis, and linear features separating geologic units of different tone, texture or pattern. Features interpreted as faults, fractures, and joints are also included.

LINEATIONS OF THE CENTRAL WESTERN DESERT

The studied area of the Western Desert covers approximately 281,280 km² between latitudes 26°00'N and 30°30'N, and longitudes 24°E to 30°E. A total of 482 linear features with a total length of 6,488 km were detected (Figure 5.1). A high lineation density is apparent in and adjacent to the depressions which contain oases. A pronounced lineament system in the Giarabub-Siwa region consists mainly of north-westerly to west-northwesterly and east-northeasterly trends. In Bahariya, northeast to east northeast and northerly trends are conspicuous. The eastern part of Farafra is characterized by relatively low lineation density. This region is underlain by relatively nonresistant Cretaceous chinks and shales, but the western part of Farafra, including El-Quss Abu Said Plateau shows a much higher lineation concentration with pronounced northwesterly to west-northwesterly and northeasterly trends. This part of the depression

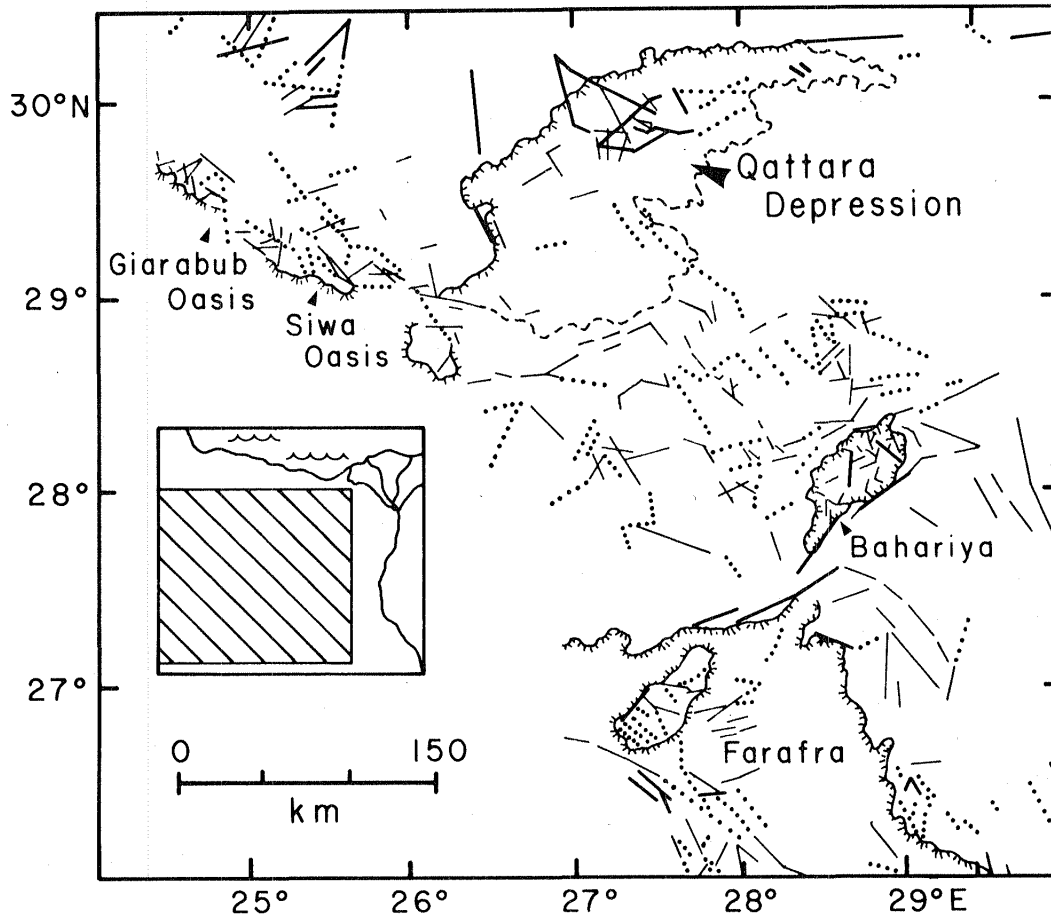


Figure 5.1 Lineations of the central Western Desert detected from Landsat images. First order lineations shown by thick solid lines, second order lineations shown by dotted lines, and third order lineations shown by thin solid lines.

is capped by more resistant Paleocene and Eocene limestone beds.

Belts of high lination density also connect the oases depressions. For example, a well-defined belt extends southeasterly from Giarabub through Siwa and the smaller Sitra and Nuweimisa depressions to Bahariya. This belt diffuses in a broader belt extending southeasterly from the southern part of Qattara to Bahariya. The Bahariya and Farafra oases are connected by a narrow belt oriented northeasterly to east-northeasterly, and Farafra and Dakhla (further south) are connected by a north-northwesterly oriented belt. Such belts outline the boundaries of the physiographic provinces of the central Western Desert.

Lination density is evidently controlled by the underlying lithology and the extent of unconsolidated surficial materials (desert pavement, sand dunes, and sand sheets) under which bedrock exposures are concealed. Southeast of Qattara for example, the low lination

concentration is a function of the presence of the poorly indurated clastic Moghra Formation of Miocene age (Said, 1962) as well as partial concealment by sand dunes south of Qattara. Another low lineation density characterizes the Great Sand Sea (west of the depressions in Fig. 5.1). A higher lineation density is present on the indurated Marmarica Plateau (north of Siwa). The massive Eocene limestones exposed in the Bahariya-Farafra region are characterized by a high lineation concentration.

LINEATIONS OF THE BAHARIYA REGION

The Bahariya region was used as an experimental test site to check the validity of space imagery in comparison with conventional aerial photography. Accordingly, the lineation pattern of this region was identified twice, once from space images (Fig. 5.2) and another time from aerial photographs. The designation "Bahariya region" is used to mean the inner oasis-containing depression and a portion of the surrounding area. The region studied is bounded by longitudes 27°20'E to 30°00'E and latitudes 27°30'N to 29°00'N. It is approximately 41,750 km² in area.

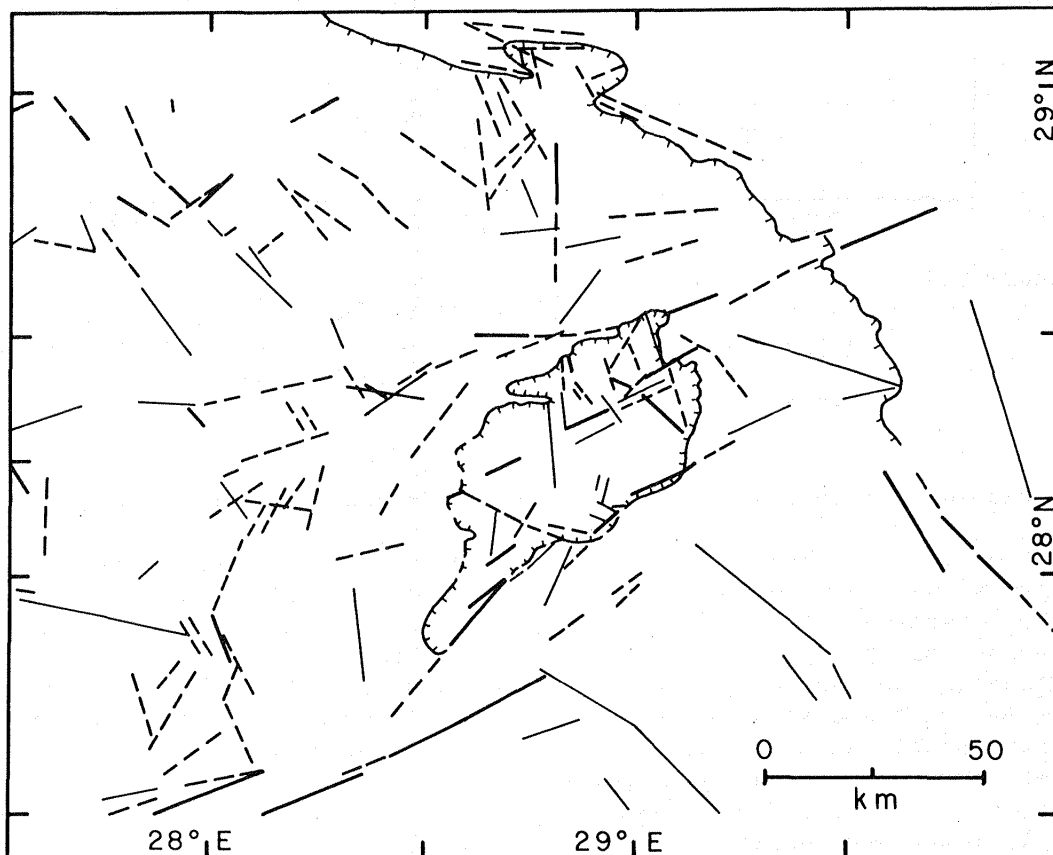


Figure 5.2 Lineations of the Bahariya region detected from Landsat images. First order lineations shown by thick solid lines, second order lineations shown by thick dashed lines, and third order lineations shown by thin solid lines.

Cretaceous and Oligocene clastic rock units, as well as four main basaltic occurrences are exposed in the inner depression. The floor and walls of the outer depression are formed mainly of indurated Eocene limestone. Further east on the outer plateau, gravel spreads of Oligocene to Lower Miocene are superposed on the Eocene limestones. Northwards, Oligocene sands and gravels are exposed followed by the Miocene Moghra Formation. South southeasterly moving sand dunes of Ghard Abu Muharik, Ghard Ghorabi and others are found in the floor of the outer depression to the northeast and east of the inner depression.

The lineation pattern of the Bahariya region shown in Figure 5.2 includes the same linear features expressed in Figure 5.1, but they are here better expressed due to the larger scale of this map. The lineations have a greater concentration in the depression than on the surrounding plateau (outside the second scarp marked in Fig. 5.2). A total of 197 linear features totalling 2,101 km are illustrated. A significant portion of these lineaments bound the straighter parts of the scarp. The photo lineation pattern of the Bahariya region was identified stereoscopically on aerial photographs (scale 1:100,000). The area studied approximates 18,530 km² and is bounded by longitude 28°00'E to 29°48'E and latitude 27°44'N to 29° 12'N. A total of 8,326 linear features were detected. The total length of lineaments is measured as 6,207 km. There are 3,690 first and second order lineaments totalling 3,376 km; 4,636 third order lineaments total 2,831 km.

Construction of more than 140 frequency curve plots based space image and air photo lineation data was carried out to ascertain the predominant lineament trends. Analysis of the orientations derived on the basis of Landsat images shows significant trends of east-northeast and north-northwest to northwest. Air photo lineations also display significant east-northeast and north-northwest trends, although there is much more scatter and peaks are more broad than in the case of space image lineation trends.

Table 5.1 Comparison of Landsat and Air Photo Lineations.

| | Landsat Pattern | Air Photo Pattern |
|----------------------------|--------------------------|------------------------|
| Original Scales | 1:1,000,000 1:500,000 | 1:100,00 1:60,000 |
| Total Area Studied | 41,750 km ² | 18,530 km ² |
| Total Number of Lineations | 197 | 8,326 |
| Total Length of Lineations | 2,101 km | 6,207 km |
| Average Lineation Length | 10.6 km | .75 km |
| Significant Trends | ENE, NNW to NW | ENE, NNW |

A comparison of the characteristics of the space image and air photo lineation patterns is summarized in Table 5.1. Several conclusions can be drawn from the comparison:

1. The long linear features seen on space images are commonly seen to consist of several pieces in air photos due to local (natural or mechanical) detail.
2. A single linear feature in a space image may actually consist of linear belts of en echelon lineations; this can be determined by examination of the corresponding aerial photograph.
3. Because of resolution limitations, small-sized lineation detected in air photos may be missed completely in space images. This may induce an element of difference in the prominent trends detectable in each pattern
4. The number of lineations in the air photo is statistically valid to allow the construction of isopleth-type concentration (density) maps. Such is not the case in the space images. Lineation density variation is a good index for the recognition of lithologic variations and concealment by surficial unconsolidated materials.

Chapter 6

GEOLOGY OF THE SOUTHWESTERN DESERT OF EGYPT

BAHAY ISSAWI

Geological Survey of Egypt
Abbasia, Cairo, Egypt

ABSTRACT

The Precambrian - Lower Paleozoic granites, granite gneisses, orthogneisses and other igneous and metamorphic rocks form the basal shelf of southern Egypt over which deposition of clastics and carbonates took place through most of the Phanerozoic. Basement outcrops have been recorded and mapped from many areas in southwest Egypt, stretching from the Nile in the east to Uweinat in the far west (El-Ramly, 1972). North of latitude 24°N, small outcrops are associated with fault lines of relatively minor vertical displacements, approximately 100 m. However, north of latitude 25°N, the Precambrian-Lower Paleozoic igneous rocks sink below the surface and are not exposed. The Gilf Sandstone, best exposed at the Gilf Kebir plateau is unfossiliferous, and a Jurassic to Upper Cretaceous age is assigned based on its stratigraphic placement and lateral equivalence to fossiliferous beds on the surface and in the subsurface in the Kharga/Dakhla region. Based on litho- and biostratigraphic correlations with Upper Cretaceous-Lower Tertiary units, the same age is preferred for the Nubia Formation, which resulted from deposition in several basins on the uneven pre-existing surface. Structural contouring on the base of the Duwi (Phosphate) Formation indicates that two basins and three highs were responsible for individual depositional centers ranging in age from the Paleozoic in the west to the Mesozoic in the east. Alternating periods of wet and dry climates characterized the Quaternary, which resulted in widespread fluvial, lacustrine and eolian deposits.

PALEOZOIC SANDSTONES

The accumulation of continental facies over the igneous shelf began during the early Paleozoic in southwest Egypt near Uweinat. Cambro-Ordovician sediments were recorded in the nearby Libyan outcrops by Burollet (1963) and Mahrholz (1965), but their possible extension into Egypt was questioned by Issawi (1978). Devonian-Carboniferous strata, however, are known from Uweinat and western Gilf Kebir areas. The total thickness of the exposed Paleozoic section reaches a maximum of 300 m in the area of Gebel Kamil. North of the Uweinat area, igneous rocks (rhyolites, phonolites, syenites, and trachytes) were noticed interbedded within the sedimentary

section. Farther north, the Paleozoic section loses its igneous interbeds, and sandstone with clay intercalations dominate. Samples collected from the area west of the Gilf Kebir near the Libyan border have yielded Devonian spores and pollen. Lithologically, the sandstone beds are medium- to coarse-grained, poorly sorted, quartzitic, very hard, partly ferruginous and partly kaolinized especially at the base. Primary structures are rare, although contortion and microfolds are common in the area of Gebel Kamel.

Klitzsch (1978) claimed the occurrence of a thick section (50 m) of tillite at Wadi Abd El-Malik. Above the tillite is a 100 m thick unit of sandstone and mudstone, including traces of trilobites which can be assigned to the Silurian-Devonian.

The most important factors which distinguish the Paleozoic section are:

1. The base is kaolinized with mica flakes and angular quartz pebbles and grains.
2. Conglomerates are common in the lower part of the section, formed of subangular to subrounded pebbles of both igneous and sedimentary derivations.
3. Interbedded igneous sills and dikes are most common in the south; the sills may reach a thickness of 20 m.
4. The sandstone is coarse-grained, partly massive quartzite, and partly fine-grained, and soft and flaky, including plant remains in Karkur Talh.

In the area between Gebel Uweinat and the Gilf Kebir plateau, the sedimentary section fills concavities and irregularities in the underlying basement surface. On a regional basis, Gebels Uweinat, Arkenu, Babein, and Nazar in the south and southwest, and the igneous bodies near Gebel Kamel form a huge, discontinuous ring-like structure inside which the Paleozoic section was deposited. This cratonic basin is nearly encircled by basement rocks, and might have been breached in post-Paleozoic times in a northerly direction. Whiteman (1971) has indicated that a comparable situation may exist to the northwest and southeast of Uweinat, suggesting that the mountain created a barrier between two huge basins sloping northwest towards Kufra in Libya, and east to southeast towards Selima Oasis in Sudan.

During a recent visit to Lagiat El-Arba'in and Lagiat Umran in Sudan (20°00'N and 28°25'E), however, a nearly identical stratigraphic situation was encountered. Granites and granite gneisses comparable to those north of Gebel Uweinat were observed overlain by a thick (>50 m) varicolored sandstone section with minor red clay bands near the base. The sandstone is characterized by irregular quartz pebbles, is partly kaolinized, occasionally cross-bedded, and contains ferruginous pockets and micas. At Lagiat El-Arba'in, the sandstone contains huge trunks of fossil wood approximately 20 m in length. The wood is metamorphosed to a white, rock like marble.

The sandstone section gets progressively thicker as the Egyptian border is approached. In places south of 22°N and west of 27°E, the basement crops out again similar to the situation inside Egypt north of 22°N. Consequently, it is possible that the Paleozoic section extends southwards into Sudan to the Lagia area, and even farther south to join the Paleozoic exposures around Wadi Howar as suggested by Vail (1978). In the western Sudan, Rodis and Iskander (1963) and Rodis and others (1964) recorded the presence of several cratonic basins with clastic deposits. The thickness of this section is 300 to 500 m, and the deposits are believed to be of Upper Cretaceous age.

THE GILF SANDSTONE

The Gilf Sandstone overlies the Paleozoic section with a significant unconformity, especially prominent at the western cliffs of the Gilf Kebir, where kaolinized sandstone and sub-rounded, white, quartz, egg-like gravels mark the contact. The sequence covers the nearly vertical cliffs of the Gilf plateau and its surface. Farther to the northwest, it covers the ground surface between the Great Sand Sea to the east, and continues westward into Libya. North of 25°N, it dips below the fossiliferous Upper Cretaceous beds. In the south and southeast, the Gilf beds overlie the nearly endless and vast plain covered by Paleozoic sandstones.

The section is over 200 m thick and is composed of sandstone which is dominantly fine-grained with occasional ferruginous and manganiferous dark bands, pebble-beds, and several hard quartzitic beds. The base is kaolinized, although the top is always hard and quartzitic, and forms a wall over the basal-sloped beds, which makes the plateau inaccessible except for passes in the northeast and northwest. The beds are generally unfossiliferous; even fossil wood is not observed. Primary structures, ripple marks and cross bedding are common in places, dipping 30° (on the average) to the northeast.

Klitzsch (1978) classified the Mesozoic sandstone in southwest Egypt into seven units, three of which were assigned to the Jurassic and the others to the Cretaceous. He believed that some of these units extend from the Kharga-Dakhla region to the Uweinat-Gilf Kebir region. Surprisingly, Klitzsch belittled the value of facies change in his cross section indicating consistent units between Kharga and the Gilf Kebir, a distance of 600 km (Klitzsch, 1978; p. 516). Instead, his correlations depend primarily on Lingula and plant remains; no index fossils were mentioned. The boundaries between his units are impossible to follow in the field and are not consistent with our concepts on Egyptian stratigraphy.

Instead, we believe the stratigraphic position of the Gilf Sandstone is determined by the following facts:

1. Dipping of the Gilf beds to the north and northeast where they disappear under the Cretaceous sandstone and shale section best exposed in the Abu Ballas area.

2. To the west, the upper beds interfinger with the basal member of the Nubia Sandstone (the Taref Sandstone Member), suggesting that they are coeval.

3. The subsurface clastic section in Kharga and Dakhla Oases, which lies below the outcropping Taref, is thus equivalent to the main part of the Gifl Sandstone.

4. The subsurface section in the oases belongs partly to the Jurassic (Saad and Ghazaley, 1976). It is thus logical to assume that the Gifl Sandstone is Jurassic at base and Upper Cretaceous (the part equivalent to the Nubia Sandstone) at top.

THE NUBIA FORMATION

In light of recent work, it is now necessary to restrict the term "Nubia Formation" to sandstone beds exposed in parts of southern Egypt and northern Sudan. These beds are associated with a suite of litho- and biostratigraphic units belonging mainly to the Upper Cretaceous and Lower Tertiary. The lower contact of the Nubia with the underlying igneous rocks is uneven, which might represent the development of several depositional basins contiguous to each other. Continental conditions dominated, with minor marine incursions. The southward facies change of the northerly marine beds, and the continuously younger sandstone to the south both mark a general flooding of the area during the late Cretaceous to early Tertiary with minor breaks. In southern Egypt, it is possible to recognize several phases in which the organic and detrital deposits alternate in time and space. Thus, although there was a general transgression, intricate relations suggest that there was fluctuation between the gain of sea over land and vice versa.

The maximum exposed thickness of the Nubia is approximately 100 m, whereas its cumulative thickness (surface and subsurface) south of 23°N may be no greater than 350 m. The dip of cross-bedding is generally to the north, but northeast and northwest dips are not uncommon, indicating a southern highland mass supplying the clastics. Thus, the Nubia Sandstone is a heterochronous megafacies which can be correlated with different Upper Cretaceous-Lower Tertiary units exposed to the north.

UPPER CRETACEOUS - LOWER TERTIARY SEDIMENTS

Fossiliferous sediments represent two major embayments in southern Egypt, and follow two troughs: Dakhla to the west, and the main plateau just west of the Nile. The sediments are clastics at base, clays with sands, phosphate and marly intercalations at the middle, and carbonates with clay and minor sand interbeds at the top. The beds are generally fossiliferous, deposited under supratidal, tidal and infratidal environments. Generally, the beds dip gently to the north at 1° to 2°, except near structural lines where locally very steep angles of dip were recorded. The age of this section is Upper Cretaceous, Paleocene and Lower Eocene, and the thickness of the section averages 400 m.

VOLCANICS

Olivine basalts and dolerites are the most widespread igneous rocks in the area. These occur in a variety of forms; creating plateaus, cinder cones, dikes, and sills in the different types of sandstones. In one case only, at Darb El-Arba'in, the basalt was observed cutting the Paleocene limestone forming a volcanic plateau (Issawi, 1971). The recent age determination of the volcanics in southern Egypt relegates them to the time span between the late Cretaceous and early Oligocene (Meneisy and Kreuzer, 1974).

Trachyte and phonolite plugs and cones represent much older volcanics, and are present in the area south of the Gilf Kebir and northeast of Uweinat. These are most probably associated with the Hercynian movement which affected southwest Egypt during the late Paleozoic.

The volcanic distribution in southwest Egypt suggests an extremely unstable surface during the times of eruptions. Many features were developed, including fused and jointed sandstone, and baking, hardening and ferrugination of the sandstone beds. Chalcedony sheets, especially prevalent at Darb El-Arba'in, are always associated with the sites of the eruptions.

QUATERNARY DEPOSITS

The Quaternary history of southwestern Egypt is much more complex than the Paleozoic and Mesozoic history. The oldest sediments contain Acheulean remains, 180,000 years B.C., found in Balat (Dakhla Oasis), in east Kharga and in the Bir Sahara area. Mousterian (100,000 years B.C.), Aterian (40,000 years B.C.), Neolithic (9,000 years B.C.) and younger sites are widespread in the desert. Studies of these artifacts and associated sediments indicate several alternating wet and dry phases during the Pleistocene. The wet phases filled huge lakes at Bir Sahara and Bir Tarfawi which dried up in times of aridity.

Quaternary lacustrine and associated deposits cover huge areas in southern Egypt (approximately 150 x 100 km), which can be related to fluctuations in climatic conditions and to the rise and fall of the underground water level. The level of underground water is no doubt related to climatic factors, hence the local alternation of water fall and aridity has had a great impact on both the type of sediments and human occupations.

The presence of conglomerates, wash sheets and extensive mud pans indicates that huge amounts of water were available during the formation of these features. On the other hand, dried-up springs, tufa deposits and deflation features indicate the water filled local basins that were later dessicated under more arid conditions.

STRUCTURES

The main factors controlling the structural framework in southwest Egypt are: 1) Tensional forces leading to a great number of

east-west faults, and 2) Vertical or diagonal uplift of the basement rocks. The faults are mostly normal, and may strike in places up to several hundred kilometers (e.g. the Kalabsha - Tarfawi fault). They generally trend east-west, but may deviate a few degrees either to the north or south. Other trends (north-south) are also present, but are of less importance. The displacement along an individual fault varies from a few meters to a few hundred meters. En echelon, antithetic and step faults are common. Tearing is conspicuous along some of these structural features, and in places (e.g. west of Dungul) the horizontal displacement may reach up to 750 m.

Hinge and pivot faults are also present, and thrusting has occurred in two areas; west Dungul and Gebel Kalabsha. Igneous rocks, granites and volcanic bodies are present along the course of some faults, especially those cutting the sandstone units. The fault planes have been hardened by silica solution, which produces sandstone dikes of considerable length.

Uplift of the Basement Rocks

Due to the thin cover of sediments, the uplift of the basement rocks is significant in the structural pattern of the area. This is apparent in Darb El-Arba'in area and farther east, where the sedimentary beds are highly tilted around the igneous bodies. Hogbacks are common, and even overturned beds are present in some places near the uplifted igneous masses. At Qarn Ginah, Kharga Oasis, the high angles of dip of the sandstone beds and the steep, nearly closed anticlines indicate that the depth to basement is not great nearby.

The effect of basaltic (and other volcanic) eruptions gives rise, also, to ring-like dikes of sandstone which, in places, completely surround the volcanic mass and may be topographically higher than the mass itself.

The effect of arching, coupled with fault block movement against sufficient friction results in very complicated, short, interlocked features. Where varied lithologies are present, beds are twisted and wrinkled, giving rise to a series of interlocking or en echelon folds. However, where vertical movements disturb the sandstone section, beds are faulted rather than folded. It is here that sandstone dikes are most common.

Folding

Structural contouring on the base of the Duwi (Phosphate) Formation or its isopach equivalent reveals two major basins (Dakhla in the west, and the "Plateau Basin" in the east), and three major highs (Chephren in the east, Tarfawi in the middle and Uweinat in the west). These structural features trend generally north to northeast. The northwest trend present in Libya reflects a Caledonian phase of structural development older than any affecting southwest Egypt, and is not believed to be present in Egypt (Klitzsch, 1966; 1970; 1971).

The earlier structural orogenic cycle recorded in the southwestern desert is the Hercynian, which took place during the late Paleozoic - Early Mesozoic. This is followed by the Alpine cycle which continued during most of the Mesozoic and the Tertiary. The rocks affected are Paleozoic in age to the west, and Lower Eocene in age to the east and north. It seems probable that stresses started in the southwest and extend with time to the east and north. Thus, while the Uweinat high is a Paleozoic feature, the Tarfawi high is Mesozoic, and the Chephren high is Upper Cretaceous to Paleocene in age. The Dakhla basin is probably Jurassic in the south, ranging to Cretaceous and Paleocene in the north. The Plateau Basin is mainly an Upper Cretaceous-Lower Tertiary feature.

LITHOFACIES STUDY

Both the tectonic map (Fig. 6.1) and the lithofacies isopach map (Fig. 6.2) show the distribution and thickness of different lithologic units in southwest Egypt. Two major basins of deposition cover most of the area discussed. The Plateau Basin in the east (Issawi, 1971) is covered by Upper Cretaceous-Lower Tertiary sediments. The basin becomes progressively deeper to the north, and shallower to the south, where igneous patches delineate its southern boundary. The basement relief map (GPC, 1979) shows a depth to basement of slightly less than that shown in Figure 6.2, especially in the northern part of the basin. To the west, the southern extension of the Dakhla basin is superimposed on an undulated, warped basement surface.

The sediments within these basins are marine carbonates in the Plateau basin (Upper Cretaceous-Lower Tertiary) and continental clastics (Jurassic-Cretaceous) in the southern part of the Dakhla basin. Marine deposits of Upper Cretaceous-Lower Tertiary age are present in the northern part of the Dakhla basin.

The basement relief map indicates nearly the same picture. The main difference is that the basement map (GPC, 1979) shows the Gebel Kamil high trending northeast as far as Kharga, and truncating the Tarfawi high north of 23°30'N. In the present work, the Tarfawi high is continued northward towards Kharga, though it may shift eastwards near latitude 23°N, where it occupies the Kharga depression.

GEOLOGICAL HISTORY

The oldest exposed rocks are the basement granites, granodiorites and granite gneisses representing the northern part of the African Shield. The area west of Bir Sahara was apparently active during the early Paleozoic and into the early Mesozoic. The area east of Bir Sahara most probably remained a stable positive feature during all the Paleozoic.

Lower Paleozoic sediments have a rather restricted distribution in this part of southern Egypt. Only a very limited thickness of clastics rests directly on the basement, suggesting either that thin Lower Paleozoic cover was deposited, or that deposition was balanced by erosion. In contrast to the early Paleozoic history, the Middle

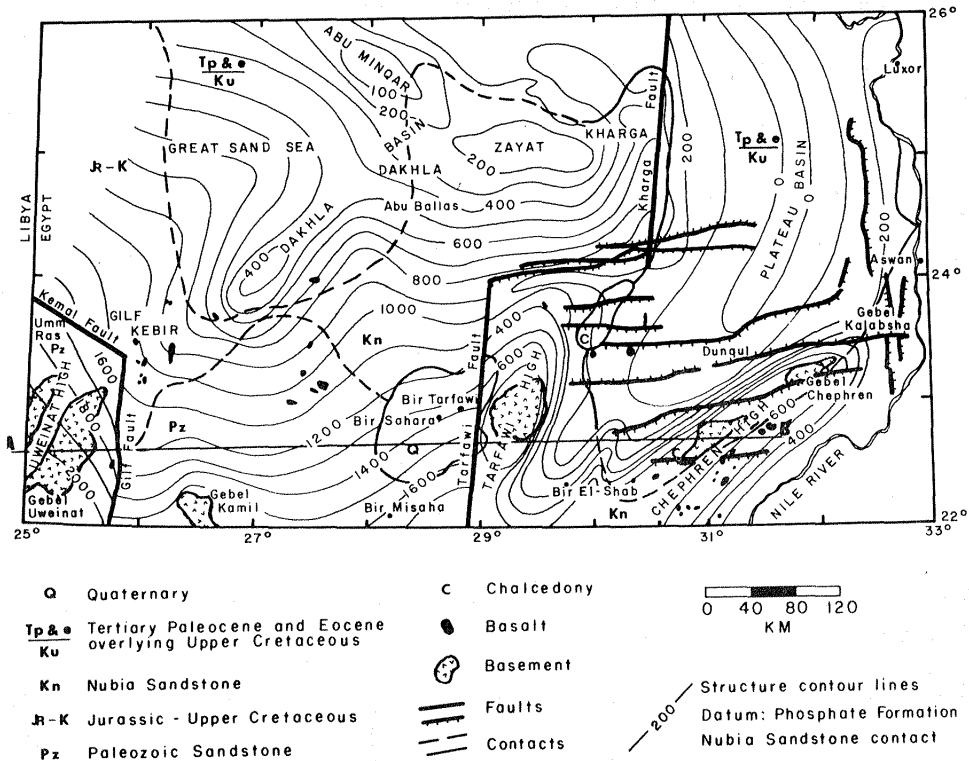


Figure 6.1 Provisional tectonic map of southwest Egypt; line A-B near 23°N is cross section shown in Figure 6.3.

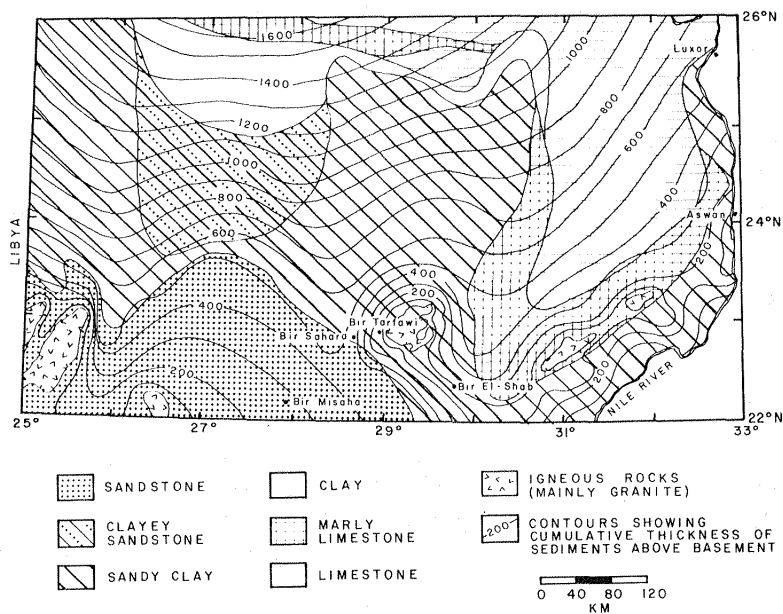


Figure 6.2 Provisional lithofacies - isopach map of southwest Egypt. The depositional trough northeast of Bir Tarfawi is here called the Plateau Basin, whereas the trough northeast of Uweinat may represent a southward extension of the Dakhla basin.

(Devonian) and Upper (Carboniferous) Paleozoic sediments are well represented west of Bir Sahara. The Uweinat high (Fig. 6.3) started during the end of the early Paleozoic, and began the separation of this region into large intercratonic basins occupying most of southwestern Egypt. The sediments deposited in these basins are exclusively clastics; coarse-grained continental facies accumulated on the platform fringing the southern shield. Subsidence of these intercratonic basins might have been initiated during deposition, but was later emphasized by continued warping. On the swells which separate the neighboring basins, Devonian sediments are absent, and the Carboniferous section is punctuated by unconformities marked by the volcanic injections and intrusions of the Gebel Uweinat area. A basal unconformity almost everywhere marks the base of the Devonian and is represented by relatively thick conglomerate bands. A similar unconformity is also found within the carboniferous section.

The positive area to the east of Bir Sahara and other basement highs constitutes a dissected Lower Paleozoic shield, in contrast to the peripheral cratonic platforms which received and retained Middle to Upper Paleozoic deposits. By the close of the Paleozoic, the basins in southwestern Egypt were further delineated by the rise of the Tarfawi high in the east. The area to the west of Bir Sahara was still active, as indicated by the many trachyte and phonolite volcanic plugs. These volcanics probably represent the end of the Hercynian movement which preceded the stability of the Mesozoic.

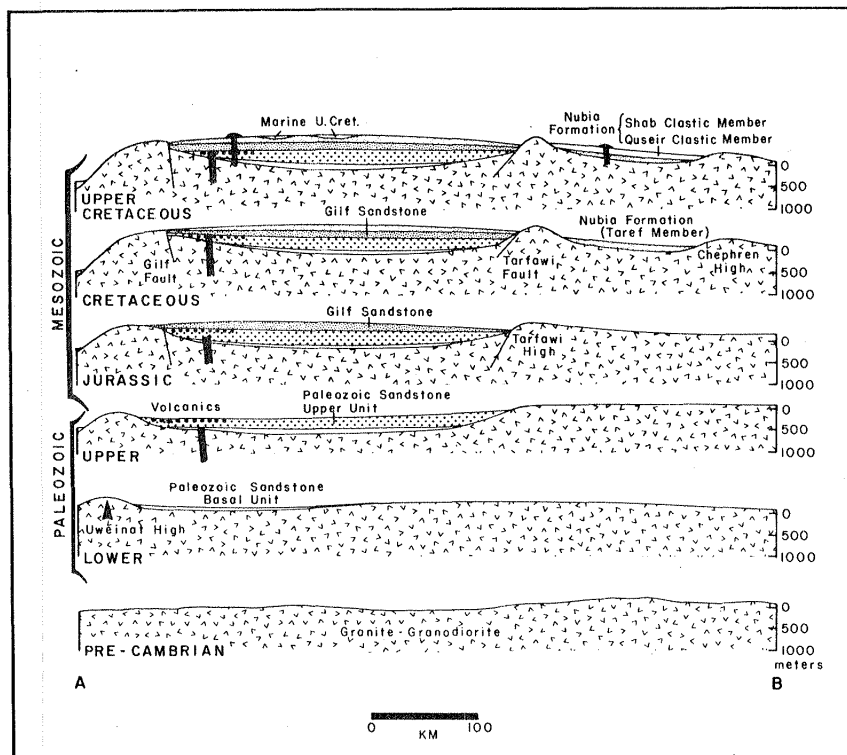


Figure 6.3 Cross sections showing Paleozoic and Mesozoic depositional events of southwestern Egypt. East-west line A - B is located at approximately 23°N (Fig. 6.1).

Cratonization of the western area was emphasized by the thick continental deposits of the Gifl Sandstone during most of the Jurassic and Cretaceous. Also during the Cretaceous, movement of the area to the east of Bir Sahara was initiated by the rise of the Chephren high. Continental clastics continued to pour into the basins both east and west of Bir Sahara, giving rise to the top-most part of the Gifl Sandstone or the equivalent Taref Clastic Member of the Nubia Formation.

The late Cretaceous is marked by a marine transgression over the area. The Quseir Clastic and Shab Clastic Members of the Nubia Formation were deposited in the south, while more marine facies were deposited in the north. Thus, the phosphatic and fossiliferous Dakhla Shale beds were deposited in the Dakhla - Kharga region at the same time as the continental fluviatile Nubia Formation in the south (Issawi, 1972; 1973b).

On a broad scale, the tectonic stability of southwestern Egypt seems to move from southwest to northeast. Even tensional stresses leading to faulting moved also in this direction with time. So, while the southern part of the Tarfawi fault is a Jurassic feature, its northern continuation to Kharga is most probably Cretaceous in age.

During the Paleocene and early Eocene, seas covered the eastern part of the area, and thick and varied marine sediments were deposited. The final phase of instability is characterized by two features: 1) tensional faults with local thrusts (at Kalabsha and west Dungul areas), and 2) the large number of basaltic extrusions and minor doleritic intrusions. The age of these intrusions ranges from Upper Cretaceous to Lower Oligocene. Chalcedony sheets well-developed along the Darb El-Arba'in are associated with the sites of volcanic eruptions. Tensional readjustment together with vertical or oblique movements of the basement rocks, and to a lesser degree compressional forces, gave the area its final structural setting after the later Cretaceous. After the early Oligocene, the area reached complete stability, proceeding from west to east.

The Quaternary was a period of very active fluvial and lacustrine sedimentation. Tufa and travertine deposits, gravels and other sedimentary sequences indicate either runoff or seepage of underground water. However, arid phases alternated with the wet phases, and deflation carved many of the Western Desert depressions presently associated with sand dunes and sheets.

Chapter 7

BASEMENT ROCKS OF THE GILF-UWEINAT AREA

AHMED ATIF DARDIR

Geological Survey of Egypt
Abbasia, Cairo, Egypt

ABSTRACT

Early work on the basement rocks of southwestern Egypt resulted in the discovery of gneisses and crystalline schists intruded by granite in the Uweinat-Archenu region. Both plutonic and extrusive volcanic rocks exist in the southwestern desert, ranging from coarse-grained granite at Abu Bayan, to extrusive basalts at Gebel Uweinat. The time sequences of basement rocks are based on two major orogenies occurring in the middle and late Precambrian. The Precambrian basement rocks investigated during the 1978 expedition consist of old granitoids exposed south of the Gilf Kebir, young granitoids east of Bir Sahara, and a few dikes and veins that cross-cut the granite of Qaret El-Maiyit. Quartz trachyte and syenite plugs intrude both basement rocks and later Paleozoic sandstones, suggesting a Jurassic to Cretaceous age of foreland platform volcanism. During the mid-Tertiary to Quaternary small basic extrusions were widespread in the Gilf-Uweinat region, forming dikes, cones and sheets of small lateral extent. Economic mineral prospects for the Gilf-Uweinat region remain high, and deposits of iron, manganese and vanadium should be investigated more fully.

INTRODUCTION

The Western Desert of Egypt south of 24°N latitude is characterized by a monotonous, nearly horizontal surface with very gently northerly dipping sandstones ranging from Paleozoic to Cretaceous in age. Sand dunes are the most common landform, while other Quaternary deposits are of local importance. The sedimentary cover unconformably overlies the Precambrian basement crystalline rocks, which form a part of the north African Shield (Khein, 1971). The sedimentary cover thins out southwards, giving way to crystalline basement rocks. In this part of Egypt, both the basement rocks and the overlying sedimentary cover form part of a wide peneplain surface, with hummocks higher than 8 m rarely disturbing the monotony of the landscape.

Both the basement complex and the overlying sedimentary cover are intruded by alkaline volcanic rocks. These rocks form high cones, plugs and dikes, and are believed to be of Paleozoic-Mesozoic age. Basic extrusions in the form of cones, sheets and flows represent the latest phase of volcanic activity within this particular area. The age of the basic extrusions ranges from Tertiary to Quaternary.

During the Gifl-Uweinat expedition, several Precambrian basement outcrops were examined, in addition to the Mesozoic and Tertiary-Quaternary volcanics.

PREVIOUS WORK

Basement rocks in the southwestern desert were first mentioned during Hassanein Bey's expedition (Hassanein Bey, 1924b). Later, Prince Kemal El-Din Hussein made two visits to the Gifl Uweinat area, accompanied by Dr. Ball in the first (1924-1925) and by Menchikoff in the second (1928). Until the late 1930's, the samples brought by Hassanein Bey and the observations and samples of Ball and Menchikoff from the Kemal El-Din expeditions (Hussein, 1928) remained the only available geological information on the basement rocks of the Western Desert of Egypt (Menchikoff, 1926).

Hume (1934; 1935) gave an elaborate account of the distribution, age and character of the "fundamental Precambrian rocks in the Western Desert of Egypt," based on the data of the above-mentioned expeditions. In addition, his own observations were made on Gebel Abu Bayan south of Kharga Oasis. According to Hume (1934), the oldest basement rocks are the gneisses and crystalline schists. Their existence was first recorded by Ball in the Uweinat-Archenu region, and form part of a large exposure surrounded on all sides by fan-shaped plains of Nubia Sandstone. The fundamental member of this rock series is a typical grey gneiss, which is intruded by great masses of granite.

In the Uweinat-Arkenu region, thick, highly-inclined crystalline schists are cross-cut by volcanic rocks, pegmatites, and quartz veins. Referring to Menchikoff's observations, Hume (1934) mentioned that the schists in the Gebel Uweinat vicinity appear in the vertical walls of the valleys, where they have been protected by the sandstone. According to Hume, these rocks are of pre-Archean age.

Plutonic rocks were identified from specimens collected during Hassanein Bey's expedition. These were found to be a coarsely crystalline, grey hornblende granite. The work of Menchikoff (1928) also showed the presence of quartz diorites, alkaline aegirine granite, and alkaline quartz syenites with sodic amphibole. The existence of several granitic centers was recorded by Beadnell in the area between Bir Tarfawi and Gebel Uweinat (Hume, 1935).

The Abu Bayan granites, first discovered by H. G. Lyons in 1894 were found to be coarse-grained hornblende granites containing large crystals of orthoclase (Hume, 1935). In this area, Hume could differentiate not only the grey hornblende granite, but also nearly every type of rock known in the Eastern Desert of Egypt. Hume (1935) assigned a Metarchean to Epiarchean age to these rocks. Pegmatite dikes and quartz veins were mentioned briefly by Menchikoff (1928). The dikes crossing the Abu Bayan granites appear to belong to a felsite dolerite association, and do not cross the Nubia Sandstone (Hume, 1935). Hume assigned a late Cambrian age to these rocks.

Volcanic rocks in this region consist of the alkaline rhyolites and trachytes at Gebel Kissu, and phonolites with aegirine and basalts at Gebel Uweinat. The volcanics are in the form of dikes which pierce not only the metamorphic and igneous rocks, but enter the Nubia Sandstone as well (Hume, 1935). Hume stated also that the dikes recorded by Menchikoff (1928) in Gebel Uweinat penetrate the Nubia Sandstone and therefore may be of Cretaceous or post-Cretaceous age.

New contributions to our knowledge on the basement geology of the Western Desert have been made by Issawi (1968; 1971) who had the chance to investigate, map, outline and identify most of the basement outcrops. The samples collected by him were given to M. F. El-Ramly of the Egyptian Geological Survey, and results of the identifications were published by El-Ramly in 1972, appearing in the geological map of the basement rocks in the south Western Desert (scale 1:1,000,000).

The basement exposures in the Darb El-Arba'in area, in Kurkur-Dungul area, and in the Gilf-Uweinat area were described in detail by Issawi (1968; 1971). Attention was also given to the prominent basement landmarks, and to the flat lying, peneplained basement rocks which are concealed by thin sand sheets.

BASEMENT ROCKS

Akaad and El-Ramly (1961) proposed a classification of the basement rocks in Egypt deduced "from definite and certain field relations of the ground actually studied and where distinct metasedimentary and sedimentary rock groups and local unconformities have been mapped" (Akaad and El-Ramly, 1961; p. 20). The sequence of events upon which this classification is based consists of two main orogenies. The first orogeny reached its climax at the middle of the Precambrian, after the sedimentation of pelites, semi-pelites, calcareous pelites and marls (now represented by gneisses of Migif-Hafafit). The emplacement of granite and volcanics has not yet been identified in outcrop, but they are present as pebbles in the next sedimentary group.

The second orogeny attained its maximum during the late Precambrian after sedimentation of greywackes, mudstones, pelites and semi-pelites in a geosyncline. This was followed by or contemporaneous with volcanic eruptions and intrusion of ultrabasic bodies. The second orogeny is contemporaneous with the emplacement of gabbros and diorites followed by grey granites, now referred to as old granitoids.

The last cycle of events is represented by periods of volcanism (old volcanics), sedimentation (Hammamat group), and tectonism (intrusion of young granitoids). The Precambrian ended with a period of igneous intrusions represented by the post-granite dikes.

El-Shazly (1964) presented a classification for the basement rocks based on the structural development of Egypt. He defined three major stages of structural development:

1. Geosynclinal and main orogenic stage constituting the main bulk of Precambrian 1. This stage includes geosynclinal sediments, volcanics and synorogenic plutonites.

2. Post-geosynclinal and late orogenic stage, including sediments and associated volcanics followed by late orogenic and post-orogenic plutonites.

3. Foreland volcanic stage, including the alkaline volcanics and plutonites, and basic volcanics.

In 1972, the Geological Survey of Egypt published a geologic map of the basement rocks of Egypt (El-Ramly, 1972) in which the term "old granitoids" was introduced for the later granites and granodiorites, and the "young granitoids" was introduced to replace "red and pink granite". More recently, the area of Gebel Uweinat region in Sudan and its extension in Libya and Egypt was studied by Vail (1978), who constructed a preliminary 1:2,000,000 geological map of the area (Fig. 7.1). He presented a tentative sequence of the basement rocks of the Sudan and adjacent areas, but considered the sequence of events to be preliminary.

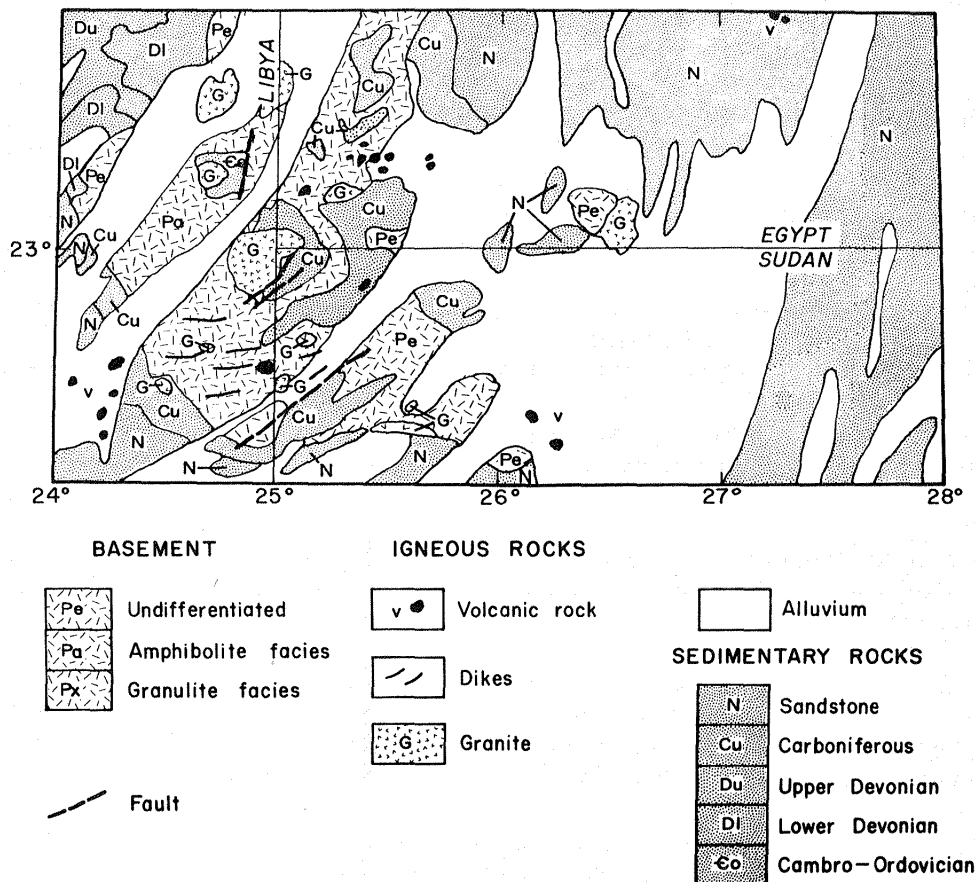


Figure 7.1 Geologic map of Gebel Uweinat area, after Vail, 1978.

GEOLOGICAL SETTING OF BASEMENT ROCKS IN THE GILF-UWEINAT REGION

The basement rocks investigated during the Gilf-Uweinat expedition were found to represent two distinct stages in the tectonic evolution of Egypt and North Africa. The first stage may be related to the Arabo-Nubian shield which protrudes north and northeastward from the centrally located African shield underlying thick platform sediments. The second stage may be related to the early foreland platform volcanic stage of El-Shazly (1964), and may represent the late Jurassic-early Tertiary (Alpine) stage of activation of the African platform (Dardir, 1973).

In this study, the Precambrian basement rocks and other rocks of magmatic affiliation are dealt with according to their orogenic evolution using the classification of El-Ramly (1972). The location of the investigated sites is shown in Figure 7.2.

Precambrian Basement Rocks

The outcropping Precambrian basement rocks occur in three main classes: old granitoids, young granitoids and acidic dikes.

Old Granitoids. Rocks of this group cover extensive areas near Gebels Peter and Paul, El-Mihashamat near the Libyan border (Fig. 7.3), south of the Gilf Kebir, southeast of Gebel Uweinat, and surrounding Ras El-Abd, south of the Egypt-Sudan border. These rocks are mainly composed of granites and granodiorites with minor occurrences of diorites.

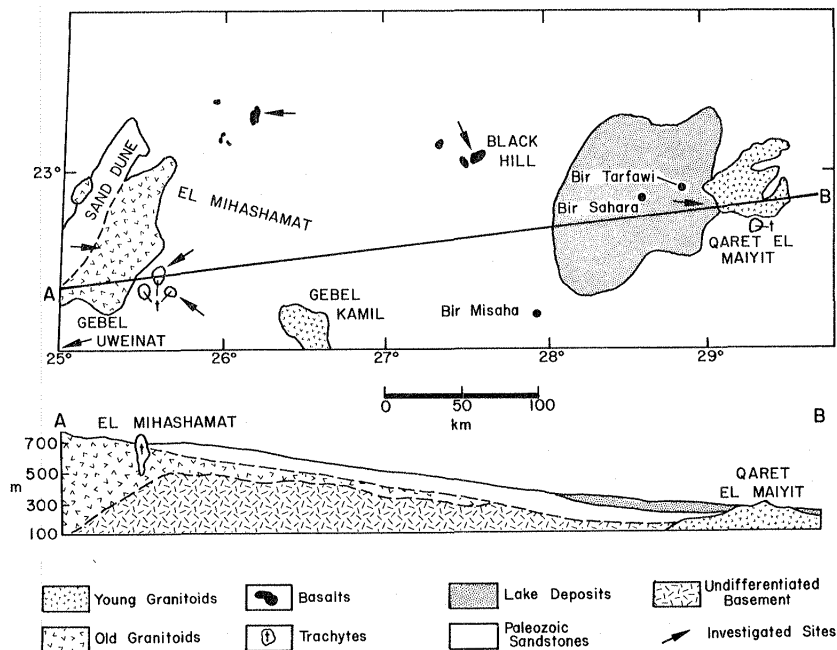


Figure 7.2 Location of basement outcrops investigated (arrows) during the 1978 Gilf-Uweinat expedition. Cross section below shows relationships among old and young granitoids, and overlying Paleozoic sandstones.



Figure 7.3 Remnants of granitoid exposures severely modified by wind erosion. Intense weathering along joint planes produced the present discontinuous basement relief.

Surrounding Gebels Peter and Paul, the country is covered by a coarse-grained, xenolithic hornblende granodiorite which forms low knolls 1 to 2 m high. These rocks weather into large spheroidal bodies 0.5 - 2.0 m in diameter (Fig. 7.3). The old granitoids are unconformably overlain by up to 15 m of Paleozoic sandstones and local thin sand sheets. In thin section, the rock is medium-grained, subhedral, granular and moderately deformed. It is similarly composed of plagioclase, quartz and orthoclase, although mafics are represented by biotite and hornblende, which show parallel orientation.

Mid-way between Gebel Uweinat and Ras El-Abd, cataclased granite-granodiorite prevail. The rock is coarse- to medium-grained, and has an approximately level surface. Issawi (1978) recorded an exposure of orthogneiss-granite near longitude $26^{\circ}30'E$ and the Egyptian-Sudanese border, within which he identified the presence of two small gabbro outcrops.

Near Ras El-Abd, the country is composed of gneissic hornblende diorite. In thin section the rock is composed of andesine, quartz and abundant mafics, including hornblende, biotite and augite. Most likely, the specimens brought by Hassanein Bey (1924b) and Menchikoff (1928) were collected from these exposures. On the Libyan side of Gebel Uweinat, basement rocks near the alkaline intrusions are composed of charnockitic gneiss exhibiting granulitic metamorphism, and granite gneiss injected by migmatites and locally granitized (Klerks, 1978). The charnockitic gneiss provides an age of 2670 m.y., while the anatectic granites gave 1540 m.y. Klerks (1978) assumes that the magmatization is contemporaneous with the anatexis. Although the age of the main metamorphic event affecting the gneisses is uncertain,

preliminary interpretation suggests that their age is close to 2790 m.y. In thin section these rocks are composed of quartz, K-feldspar and minor plagioclase. The quartz shows strong cataclasis, and biotite and quartz show subparallel alignment.

The plain west and southwest of the Gilf Kebir is covered by grey, medium- to fine-grained granodiorite. The basement outcrops extend for more than 100 km in a northeasterly direction with an average width of about 30 km (Fig. 7.2). The southwestern side is covered by a sand dune separating these basement outcrops from those along the Egyptian-Libyan border and farther to the west (Gebel Babein).

Young Granitoids. East of Bir Sahara, an extensive outcrop of young granitoid occupies a wide area which has been leveled to the ground surface forming part of the Atmur El-Kibeish peneplain. An elevated part of the young granitoid (Qaret El-Maiyit, Fig. 7.4) rises 20-25 m above the ground level. The hill is composed of massive, coarse- to medium-grained red granite. This young granitoid mass was investigated and mapped by Issawi (1971).

The rocks of Qaret El-Maiyit include granite, medium-grained quartz adamellite and biotite-hornblende granodiorite. Xenoliths are 2-3 cm in length, have an angular outline, and are composed of fine-grained, light grey diorites. Albitization and microclinization are well developed.

According to Hume (1935), these rocks are most likely late Precambrian in age. The young granitoid intrusions may belong to the Late Baikal, or Saliarck phase of folding (Dardir, 1973). El-Shazly (1964) regarded similar rocks in the Eastern Desert of Egypt to be late orogenic plutonites.

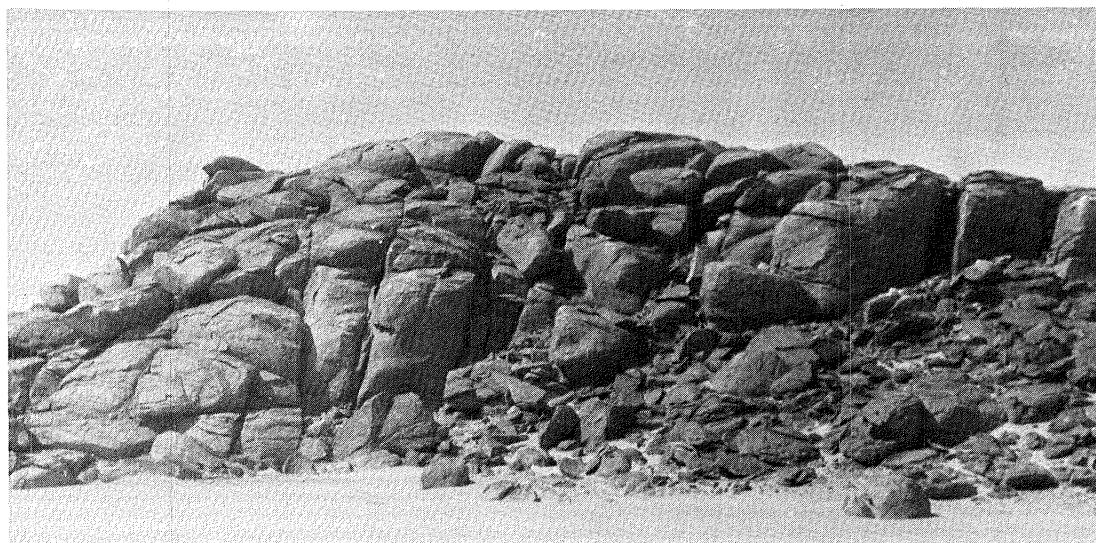


Figure 7.4 Young granitoids exposed at Qaret El-Maiyit, east of Bir Sahara. Note the intensive vertical jointing.



Figure 7.5 Andesite dike cross-cutting granite of Qaret El-Maiyit. Dike is 1 m wide.

Dikes and Veins. Very few dikes and veins were recorded, except for some pegmatite and aplite veins and one andesite dike (Fig. 7.5) cutting the young granitoids of Qaret El-Maiyit. These are thin veins, never exceeding 1 m in thickness. The pegmatites are coarse-grained, and have variable orientations. They are composed of microcline, microcline perthite and oligoclase; quartz occurs in the interstitial spaces between the feldspar crystals. Aplites are composed of microcline, microcline perthite and little quartz.

The dikes and veins belong to post-orogenic stage of El-Shazly (1964). Intrusion of these dikes represents a transitional phase between the orogenic and platform stages which took place at the end of the Precambrian (Hume, 1935).

Foreland Platform Volcanics

Quartz Trachytes, Syenites and Rhyolites. The quartz trachytes (phonolites) form relatively high plugs and elongated dikes with steep slopes rising up to 200 m above the surrounding plain. Although sporadically distributed, they pierce not only the basement rocks, but also the Paleozoic sandstones. The most important of these are Gebel 1114 (after Issawi, 1978), Gebels Peter and Paul (Fig. 7.6) and the northern edge of Gebel Uweinat (the largest of these bodies). The crystalline quartz trachytes and overlying sandstones are cut by deep ravines.

The quartz trachytes show microcrystalline texture on their outer boundary, becoming subhedral and even coarsely porphyritic towards the core. They are concentrated in the area south and southwest of the

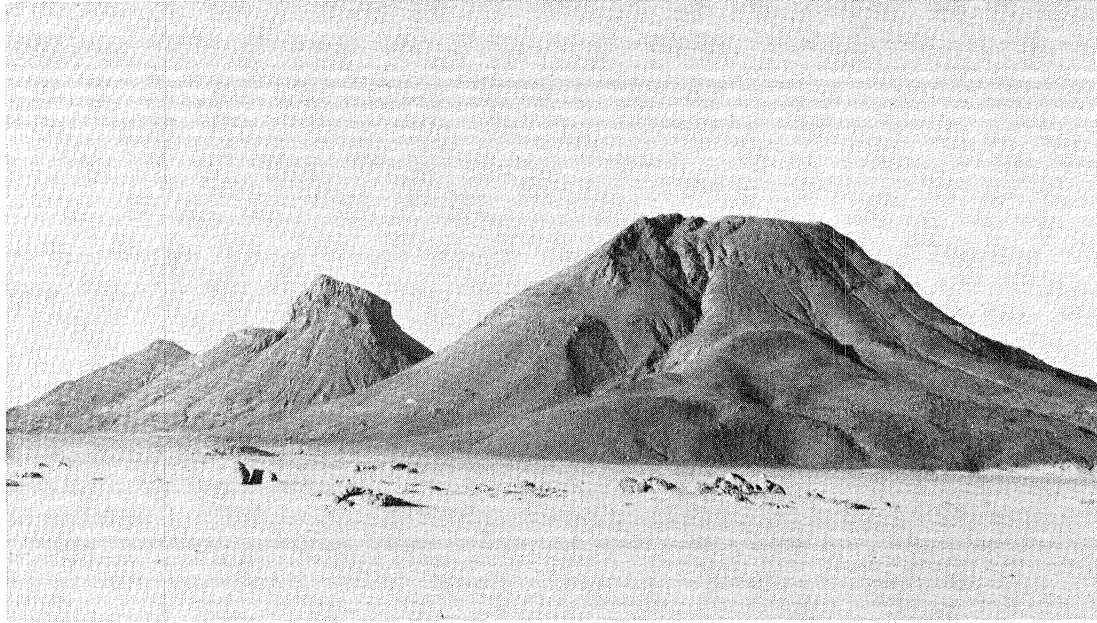


Figure 7.6 Trachyte plugs south of the Gilf Kebir; known as Gebels Peter and Paul. Eroded bedrock in the foreground consists of granitoid outcrops.

Gilf Kebir, and are distributed around Gebel Uweinat, and its eastern and southeastern surroundings. The intruded sandstones are highly indurated and silicified due to thermal effects, which led Menchikoff (1928) and Hume (1935) to consider these quartziferous sandstones as crystalline schists. The sandstones are also impregnated with small pockets and veinlets of manganese.

Syenite and carbonatite plugs intruding the Cretaceous sandstones are present southeast of Kufra basin 100 km west of Gebel Uweinat in Libya (Doughri and others, 1978). The syenite here is light-colored and fine- to medium-grained, and the carbonatite was noticed occupying the center of one of these syenite plugs. These plugs contain up to 730 ppm Ce, 700 to 7200 ppm Ba, 1330 ppm Zr, 2100 ppm Y, 1600 ppm Sr, 340 ppm Rb, and 100 ppm U. The forms of these plugs are similar to those of the Eastern Desert of Egypt, and may indicate that the intrusion was explosive in nature similar to those described by Akaad and Noweir (1964).

The northern part of Gebel Uweinat is composed of quartz trachyte (previously referred to as phonolite). The rock is fine-grained, formed of trachytic matrix which includes phenocrysts of euhedral perthite or sanidine with minor orthoclase and rare quartz. The core samples are porphyritic and coarse-grained. Grain size decreases outwards towards the periphery, and alkaline ferromagnesian minerals (aegirine or riebeckite) are common.

Basic Rocks. Basic extrusions in the form of dikes, volcanic cones and volcanic sheets are present in many parts of the Gilf-Uweinat

area. The extrusions are of relatively small size, though their aerial distribution is very wide. The basic rocks are either doleritic or olivine basalts. The doleritic basalts predominate in the area limited by longitude 27°00' to 27°30'E, latitude 23° to 24°N, whereas olivine basalts crop out south of the Gilf Kebir and north of Gebel Uweinat (Issawi, 1978). These rocks cross-cut both the Precambrian basement rocks, and the Paleozoic and Mesozoic sandstones.

Issawi (1978) suspected that these basic rocks might be of Quaternary age, since their geomorphic patterns are not yet adapted to the very recent fluvial regime prevailing in the area. However, El-Shazly (1964) is of the opinion that the emergence of land in mid-Tertiary produced deep fractures which led to the extrusions.

The petrographic study of the samples collected at Wadi Mashi revealed for the first time the presence of olivine-enriched picrite. A lamprophyre dike 1 m in thickness was also discovered cutting the sandstones of Wadi Karkur Talh in a N-S direction. It extends for some 400 m, and exhibits onion-shaped weathering (Fig. 7.7). The rock is a coarse-grained spassertite, with angular texture, and is composed mainly of augite and sanidine, with secondary minerals that include carbonate, iron oxides, chlorites and zeolites.

MINERAL RESOURCES

Recently discovered economic mineral deposits in the Western Desert are few in number, although they are characterized by their large reserves and great areal distribution. For example, the reserves of the Bahariya iron ore are approximately 265 million tons. The explored areas of the Abu Tartur phosphate deposit are 900 million tons, and the kaolin deposits at Kalabsha amount to 16.5 million tons.



Figure 7.7 Lamprophyre dike cross-cutting Paleozoic sandstones at Gebel Uweinat. Note onion-shaped spheroidal weathering.

Prospects for economically valuable mineral deposits may also be present in the Gilf-Uweinat area.

Iron and manganese deposits were discovered by Issawi (1971) 420 km south of Kharga near 27°30'E and 23°10'N. The area of these deposits is a wide plain of about 50 km². Two iron ore types were recognized: 1) Goethite-hematite ore (50-60% Fe) and 2) Highly ferruginous fine-grained sandstones, which represent the major part of the deposit. Four samples were chemically analyzed; the results are shown in Table 7.1.

Rich manganese pockets (23% Mn) are common intercalations associated with the iron in the sandstone of the surrounding country rock. Manganese veinlets were also noticed in many places among the sandstones of Gebel Uweinat (Fig. 7.8), and nodular manganese masses were noticed in the volcanic rocks of Gebel Uweinat by Ball and Sandford (1971).

The basement rocks of southwest Egypt present another potential deposit. Large mineral deposits have been discovered in the basement and protosedimentary cover of the ancient platforms. Detailed geological exploration of the basement outcrops and the thin sedimentary cover may lead to the discovery of iron and manganese ore deposits, copper-nickel deposits, titanium ores, gold and uranium. In addition, a carbonatite agglomerate plug of 500 m in diameter was discovered 109 km west of Gebel Uweinat in the Libyan territory. The plug contains up to 730 ppm Ce, 2100 ppm Nb, 900 ppm Y, 100 ppm W, and 950 ppm Th.

Table 7.1 Analysis of Iron Deposits from the Black Hill Region.*

| Sample No. | Fe _{tot.} | FeO | Fe ₂ O ₃ | SiO ₂ | MnO ₂ | CaO | P | V** | Al ₂ O ₃ |
|------------|--------------------|-------|--------------------------------|------------------|------------------|------|------|-----|--------------------------------|
| 1 | 24.5 | 0.75 | 34.14 | 36.10 | 0.15 | 2.59 | 1.52 | - | 14.70 |
| 2 | 25.1 | 14.51 | 19.74 | 55.15 | 1.00 | 2.59 | 1.05 | 140 | 1.70 |
| 3 | 58.3 | 3.16 | 79.90 | 6.57 | 0.37 | 2.46 | 0.82 | 252 | 1.20 |
| 4 | 15.1 | 2.75 | 18.59 | 51.10 | 12.00 | 1.91 | 0.96 | 196 | 5.00 |

* Samples 1,2 and 4 represent the low grade siliceous ore, sample 3 represents the goethitic ore.

** Vanadium in parts per million.

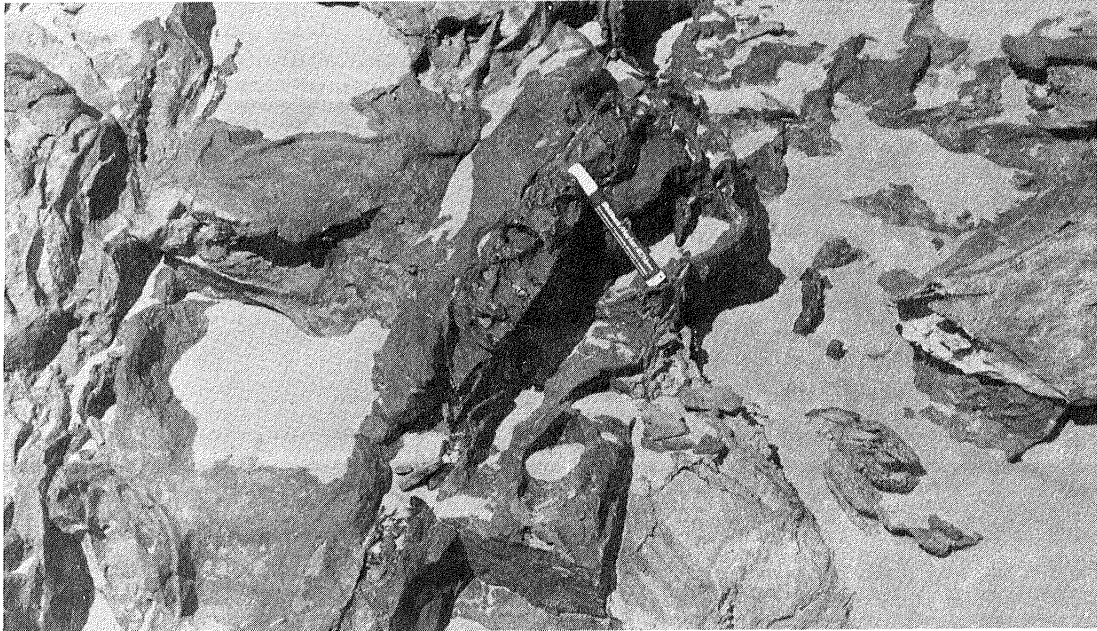


Figure 7.8 Manganese veinlets cross-cutting Paleozoic sandstones north of Gebel Uweinat.

CONCLUSIONS

The basement outcrops of southwest Egypt represent parts of the north African platform which occupies the extensive north and central parts of the African continent. Alternating episodes of uplift and subsidence within the North African platform resulted in the outcropping of the basement rocks and the formation of intracratonic basins, where thick sediments were deposited. These uplifts are now represented by Regabat, Tuarig, Tibesti, and Uweinat, while the sedimentary basins consist of Tayden, Morzoq and Kufra. Eastward continuity of this series of uplifts is present in huge outcrops of the Arabo-Nubian shield (Khein, 1971). By the end of the Precambrian, many of the basement highs were subjected to peneplanation, while the filled depressions were preserved. Later, younger sediments covered both the peneplained surfaces and the depressions.

The outcropping of Precambrian rocks is dissected in an east-west direction, where they are overlain by Paleozoic sandstones. These sandstones are intruded by alkaline rocks of probable Jurassic age, comparable to those of Nigeria which had previously been assigned a Carboniferous, or late Cretaceous age similar to the Eastern Desert outcrops (Khein, 1971).

Mineral prospects of the area are encouraging, but a systematic geologic program is needed to cover this remote area. The iron ores discovered by Issawi (1971) and investigated by the present expedition need further detailed work. Spectral analysis of the few samples shows large amounts of vanadium and the area may actually represent a vanadium deposit rather than an iron ore deposit.

Chapter 8

CRATER FORMS IN THE UWEINAT REGION

FAROUK EL-BAZ
National Air and Space Museum
Smithsonian Institution
Washington, D.C. 29560

BAHAY ISSAWI
Geological Survey of Egypt
Abbasia, Cairo
Egypt

ABSTRACT

The Uweinat area contains three different varieties of crater forms, namely: 1) two multi-ringed impact structures in southeast Libya, including the Oasis astrobleme and the BP structure, and two other craters of possible impact origin; 2) simple, breached, and complex volcanic craters northeast of Gebel Uweinat, some of which may be maars and other cryptoexplosion structures; and 3) a complex of large circular, shallow depressions east of Gebel Kissu in north-west Sudan. Because the number and variety of crater forms in the Uweinat area is unique, additional photogeologic interpretations are required based on computer-enhanced Landsat images or high resolution photographs from the Shuttle. These interpretations will allow detailed correlations of crater forms in this region with similar features on planetary bodies such as the Moon, Mars and Mercury.

INTRODUCTION

The eastern part of the Sahara where the borders of Egypt, Libya and Sudan meet is underlain by a Precambrian complex of metamorphic and intrusive rocks (Sandford, 1935c; Said, 1962; and Pesce, 1968). This complex is one of many that crop out in the middle of the Sahara, separating it into northern and southern parts. This "Oweinat series" (Hume, 1934, p. 55) of metamorphics is intruded by granites with subordinate rhyolites, which are believed to be of post-Carboniferous age (Pesce, 1968, p. 62). Four major intrusions average approximately 20 km in diameter including the mountains known as Gebel Babein, El-Bahri, Arkenu, and Uweinat (Fig. 8.1).

The Precambrian rocks are surrounded by hard quartzitic sandstones with highly consolidated conglomerate and syenite porphyry sheets, which are interbedded with sandstones, phonolites and trachyte sills, all of Paleozoic age (Issawi, 1980). In these Precambrian and Paleozoic rocks, Upper Cretaceous - Lower Oligocene (Meneisy and Kreuzer, 1974) basaltic and doleritic extrusions form isolated cones. Farther from the Uweinat region, only the continental Nubia Sandstone of late Mesozoic age abounds. This sandstone unit is partially



Figure 8.1 Apollo-Soyuz photograph (AST-2-127) of the Uweinat area in the eastern Sahara. Numbers identify the mountains of Babein (1), El-Bahri (2), Arkenu (3), and Uweinat (4).

covered by sand dunes and sand sheets of Quaternary age.

This area of the eastern Sahara exhibits an unusually large number of circular features, which resemble craters photographed on other planetary surfaces. In this paper features observed in Earth orbital photographs of this region will be discussed with emphasis on planetary analogies, including:

1. Multi-ringed impact structures in southeast Libya, including the "BP structure" and the "Oasis astrobleme."
2. Numerous vents including cryptoexplosion structures north-east of Gebel Uweinat in southwestern Egypt.
3. A complex of circular structures in northwest Sudan, located east-southeast of Uweinat and east of Gebel Kissu.

IMPACT STRUCTURES IN SOUTHEAST LIBYA

A stereo strip of color photographs was taken of southeastern Libya and southwestern Egypt by the Apollo-Soyuz Test Project (ASTP) mission of July 1975 (El-Baz and Mitchell, 1976). This strip included a photograph of the region of Kufra Oasis. Approximately 119 km north-northeast of Kufra, the photograph depicted a distinct, multi-ringed astrobleme (Fig. 8.2). The term "astrobleme" refers to an ancient circular feature of impact origin (Dietz, 1961, p. 51). These

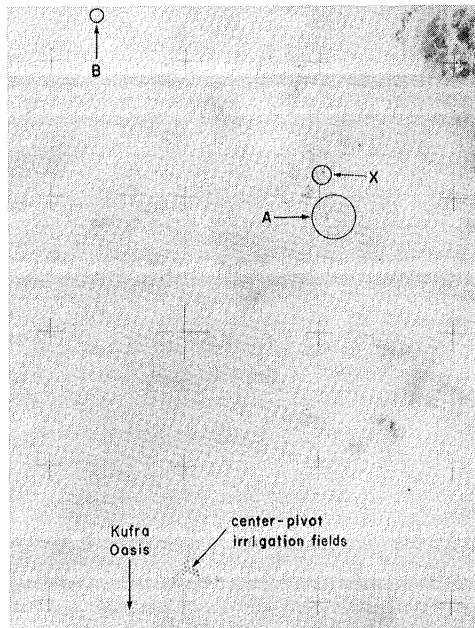


Figure 8.2 The region of Kufra Oasis in southeast Libya as photographed by the Apollo-Soyuz mission (AST-15-1244). Marked are the Oasis astrobleme (A), the BP structure (B), and a circular feature of unknown origin (X).

terrestrial features are of significant interest in comparative planetology because they constitute analogs to impact craters on planetary bodies such as the Moon, Mars and Mercury.

This circular feature was named "Oasis structure", because it was called to the attention of J. R. Underwood by geologists from the Oasis Oil Company of Libya. French and others (1974) estimated its diameter to be 11.5 km. However, study of Landsat images and Apollo-Soyuz photographs by Dietz and McHone (1979, p. 185) revealed an overall diameter of 17 km. Dietz and McHone renamed the structure the "Oasis astrobleme", further establishing its extraterrestrial origin.

The ASTP photograph of the Oasis astrobleme clearly shows a prominent central dome, about 5 km in diameter. The dome is outlined by resistant beds that form a series of discontinuous hills. There is also a faint indication of a 1 km diameter central ring, which may be a collapse structure. Thus, the multiple rings of the Oasis astrobleme (1, 5 and 17 km in diameter) make it appear similar in gross morphology to experimental explosion craters, for example the craters produced in alluvium by detonation of TNT charges.

Jones (1977) discussed several complex craters produced by detonation of TNT charges at the Defense Research Establishment, Suffield, Canada. Both the Snowball Crater and the Prairie Flat Crater particularly resemble the Oasis astrobleme. The Prairie Flat Crater was made on unconsolidated alluvial sands, in silts and clays with the

water table at 6.7 m below the surface, and the sandstone bedrock at approximately 60 m depth. The resulting crater had an average rim crest diameter of 85.5 m with four inward sloping ridges measuring 43 m, 37 m, 32 m, and 17 m (Roddy, 1977, p. 227).

Multi-ringed craters abound on the Moon and the terrestrial planets, as exemplified by the well-preserved Orientale basin on the lunar west limb (Fig. 8.3). The inner part of the Orientale basin that is filled with basaltic mare material is 300 km across, and the basin exhibits four rings that are 320, 480, 620, and 920 km across. A fundamental concern in studying Orientale and similar basins on planetary bodies is the need to correctly interpret the apparent crater diameter and the structural meaning of the rings (Roddy, 1977, p. 230). Although the Orientale basin is 54 times larger than the Oasis feature, detailed study of the latter may shed more light on the formation of multi-ringed structures on planetary bodies.

The impact origin of the Oasis astrobleme has already been well established by studies of shock metamorphic effects, especially planar structures in quartz (French and others, 1974). The structure can only be dated as post-Early Cretaceous, which is the age of the Nubia Sandstone that is affected by the event (Dietz and McHone, 1979). It has been speculated that the Oasis astrobleme could possibly be the site of origin of the highly siliceous "Libyan Glass", which is also believed to have been produced by meteorite impact (Underwood, 1979).

Approximately 10 km north-northeast of the Oasis astrobleme is another circular structure (Fig. 8.2). To our knowledge, no one has explored this feature in the field, although it is rather close to the Oasis astrobleme. It shows a partial ring that is approximately 2.5 km

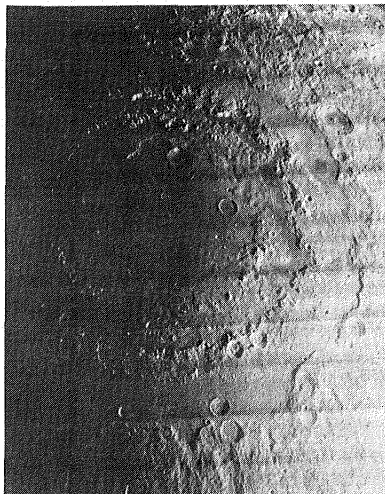


Figure 8.3 The Orientale basin on the western limb of the Moon as photographed by Lunar Orbiter IV (Frame M-187). The central part of the basin is filled with basaltic mare material; only patches of this mare material occur within the middle and outer rings of the basin.

in diameter and is visible on both Landsat images and Apollo-Soyuz photographs. It was labeled "twin site" by El-Baz and Mitchell (1976, p. 54). Based on photogeologic interpretations of the Apollo-Soyuz photographs, it is probable that this smaller circular feature is also an impact crater. However, the resolution of the orbital photographs does not allow recognition of internal structure or rings.

Some 80 km north of the Oasis astrobleme is another multi-ringed crater, approximately 2.8 km in diameter. It is known as the "BP structure", because it was first discovered by British Petroleum geologists working in southeastern Libya (Martin, 1969). The name was used incorrectly to identify the Oasis astrobleme by El-Baz and Mitchell (1975, p. 54).

The BP structure, which is 165 km northeast of Kufra Oasis, shows a distinct central peak and two rings (Fig. 8.4). The outer ring of hills, 2.8 km in diameter, has a maximum relief of about 20 m and is composed of sandstone beds that dip inward at angles ranging from 3° to 15°. The inner ring of hills, 2 km in diameter, is more structurally deformed than the outer ring with inward dip angles of 20° to 40° (French and others, 1974).

Because of its 600 m diameter, central peak, and the double ring, the BP structure may be considered an analog to many craters on the Moon and the terrestrial planets. For example, the ratio of the central peak to crater size (1:4.6) is similar to that of lunar craters such as Icarus and Theophilus (see, for example Masursky and others, 1978, p. 163). Also the same ratio of the two rings of the BP structure (2:2.8 km) is similar to that of the two rings of the crater Shroedinger (210:300 km; see Kosofsky and El-Baz, 1970, p. 106).



Figure 8.4 Aerial view of the "BP structure", a meteorite impact crater in southeastern Libya. The outer rim is 2.8 km in diameter; it encloses an inner ring and a large central peak (Courtesy of J. R. Underwood).

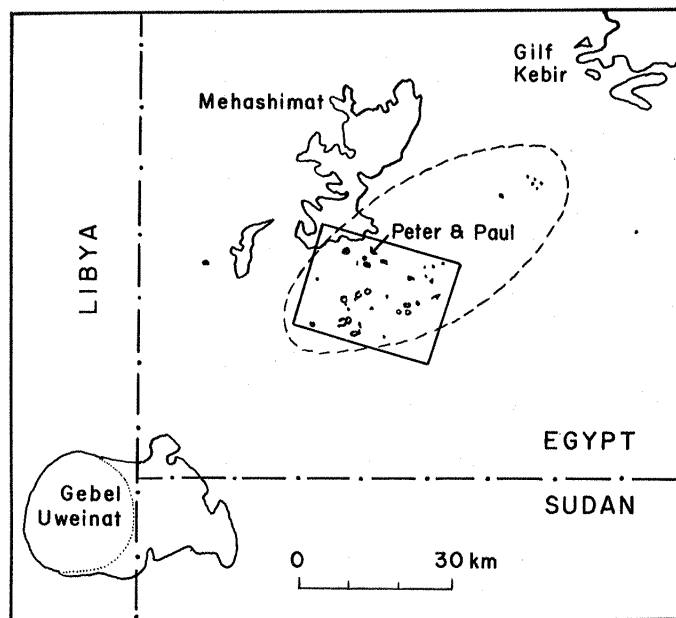


Figure 8.5 Sketch map of the fields of volcanic craters between the Gifl Kebir plateau and Gebel Uweinat in southwest Egypt. Compare with map by Peel (1939b, p. 300).

In addition to the craters discussed above, French and others (1974, p. 1425) mention another structure 160 km east-northeast of the Kufra Oasis that is elliptical, with a 3.5 km long axis trending north and a 1.8 km short axis trending east. In spite of the unique abundance of impact craters in this region, the resolution of orbital photographs is not sufficient to make more complete morphologic interpretations of these features. Using computer enhanced Landsat images or higher resolution photographs, the morphology of these crater forms could be more precisely compared to craters of impact origin on other planetary surfaces.

VOLCANIC CRATERS IN SOUTHWEST EGYPT

The vast plain between Gebel Uweinat and the Gifl Kebir plateau is marked by many crater-like features. Several of these craters were discovered by P. A. Clayton in 1931 and studied in detail by Sandford (1933c; 1935b). Later, Peel (1939b) discovered other groups of craters during the journey to the Gifl and Uweinat with R. A. Bagnold in 1938. Photographs and images taken from space provide a better perspective of their distribution (Fig. 8.5) compared to the detailed map of Peel (1939b, p. 300). These images also show the variety of crater forms in the region (Fig. 8.6).

Craters in this region cover areas varying from 100 km² to a few tens of square meters. In plan view, they are nearly circular, and some rise 200 m above the encompassing flat surface. The outer parts of the circles are made of Paleozoic sandstone, whereas volcanic rocks are piled inside, sometimes rising higher than the sandstone walls. A

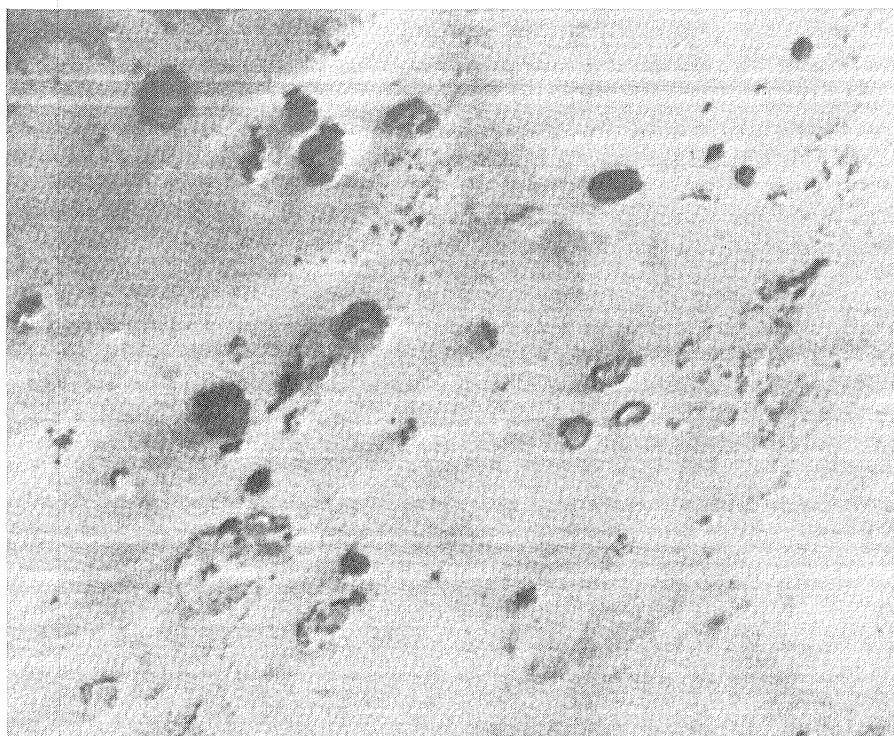


Figure 8.6 Enlargement of Landsat image (E-1131-08141) of area marked in Figure 8.5. The image shows the variety of volcanic features.

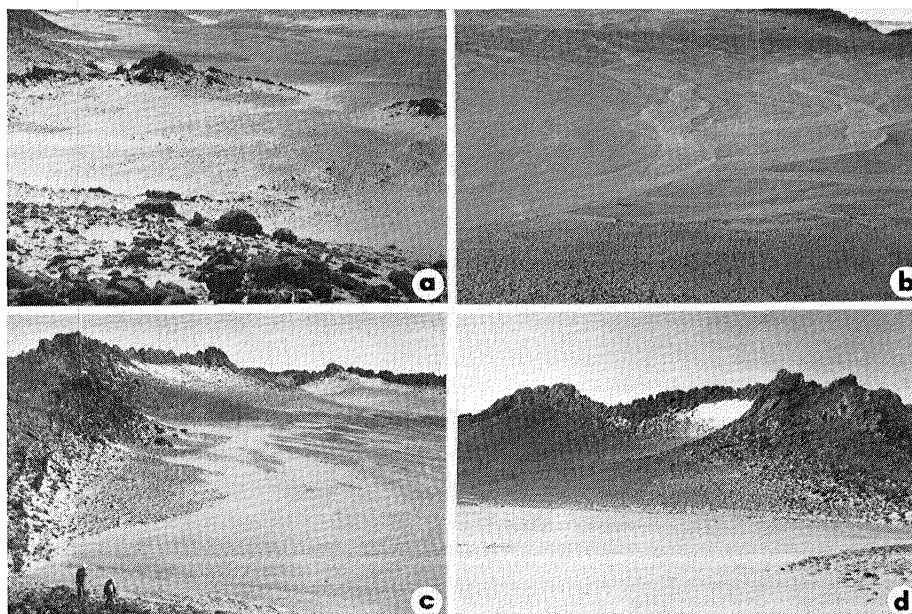


Figure 8.7 Photographs of crater forms in southwestern Egypt; a small crater within a larger feature showing multiple maar-like eruptions (a); crater floor with a drainage pattern from occasional rains in the area (b); and nearly vertical strata at rims of craters (c and d).

narrow gully may be found between the sediments and the volcanics. However, in some craters the volcanics are plastered on the sandstone leaving no gap in between, and filling the whole area inside the ring-like structure. In some of these craters the interior volcanics stand nearly vertical without any sandstone around, e.g. Peter and Paul (Fig. 8.7). The lack of sandstone rims results from the outer sandstones wearing away by wind erosion faster than the volcanics inside. In some cases, the erosion is incomplete, leaving low hummocks of sandstone at the foot of the vertical volcanics.

The sandstone "ring" may be completely closed, or may be breached by a wadi that drains the structure. The volcanic debris is thus distributed long distances away from the main mass. A few blocks lie at the foot of the rims, probably produced by gravity (mass wasting) and wind erosion.

The volcanics generally consist of trachytes and olivine basalts. The trachytes cross-cut and are interbedded in the Paleozoic sandstone together with phonolites, rhyolites and microsyenites. Only the trachytes form piles of considerable thickness, protruding 80 m above the sandstones, e.g., in the Ras El-Abd area; basalt has never been observed to form such features. The complex trachytes, phonolites, microsyenites and rhyolites are believed to be associated with the Hercynian orogeny which affected the area during the late Paleozoic.

The eruption of the volcanic bodies greatly affected the nearby sediments in a number of ways. The sandstone was baked, metamorphosed, and hardened. Dull glass-like quartz occurs within the sandstone of a crater east of Gebel Uweinat, along the Egypt-Sudan border. Chalcedony is also usually associated with the basaltic extrusions. The bedding is usually disturbed, and vertical to overturned beds are not uncommon (Fig. 8.7). Sandstones near the volcanic masses typically exhibit columnar jointing, especially near the basalts on the top of the Gilf Kebir. Ferruginous and manganiferous pockets and lenses were recorded from near the basalts of the Black Hill, the top of the Gilf Kebir, and the Uweinat area.

Our observations during the 1978 reconnaissance indicate that there are several craters that may best be described as cryptoexplosion structures. In such cases, the sandstone layers at the rim are nearly vertical (Fig. 8.7) and there are no volcanic rock exposures in the central portion of the craters. One crater displays a gentle dome of sediments in the middle. Similar sandstone rings are common in the area west of the Nile at Abu Simbel, where very intricate topographic features of sandstone were mapped by the second author. The bedding is almost obscured where the sandstone walls rise 29 to 30 m above the surrounding plains. In many cases, basalt cones occur inside the wall circles, whereas in others the volcanics are not exposed on the surface. The effect of heat and most probably gas emanations may result in more or less the same features.

The available photographs and the brief field survey do not rule out the presence of impact craters in this region. The area between Uweinat and the Gilf Kebir (dashed area in Figure 8.5) should be

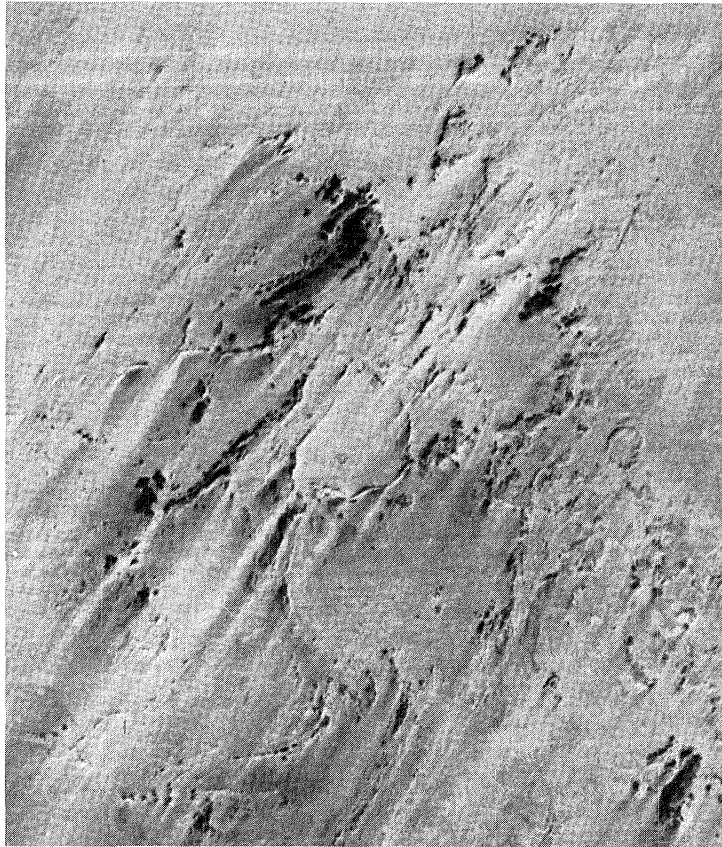


Figure 8.8 Enlargement of Landsat image (E-1131-08144) of area southeast of Gebel Uweinat showing circular features in wind-striated terrain.

studied in detail to examine this possibility. Some of the impact craters may have been overlooked because of the abundance of volcanic craters and other volcanic landforms. The situation is reminiscent of Meteor Crater in Arizona. Its origin may not have been recognized if it occurred in the middle of the volcanic field some 60 km to the northwest.

CIRCULAR FEATURES IN NORTHWEST SUDAN

Landsat images reveal the presence of a group of peculiarly circular features (Fig. 8.8) in an area centered approximately 130 km east-southeast of Gebel Uweinat. This area of northwestern Sudan has not yet been explored, and therefore, the nature of these circular features cannot be ascertained.

The circularity of the features is indicated largely by a few discontinuous arcs and knobs. The terrain appears to have been heavily modified by eolian action, and the relatively dark surface is striated by light-colored streaks that trend from northeast to southwest (Fig. 8.8). These bright streaks appear to be accumulations of sand in the form of sheets or dunes (El-Baz and Maxwell, 1979b; El-Baz and others, 1979a).

The circularity of these features is also accentuated by a difference in the texture of the terrain inside and outside the features. Inside the circular structures, the surface is relatively smooth and flat. Outside the terrain is hummocky and lineated. These characteristics are similar to those in old, cratered terrains in the lunar highlands (see Masursky and others, 1978), in the southern hemisphere of Mars (see Mutch and others, 1976), and the plains of Mercury (see Davies and others, 1978).

The largest of these features is approximately 14 km; two others are about 8 km and 7 km, and the smallest is 2.5 km in diameter. Although the nature of these features is not fully understood, they may represent: 1) ancient impact scars on the Precambrian basement; 2) remnants of buried volcanoes; or 3) unusually oriented outcrops of rocks that were more resistant to erosion than the surrounding sandstone.

The 1:1,000,000 scale map of the region shows that all exploration journeys have missed or bypassed the desolate region in which the circular features occur. The map, which was published in 1961 by the British D Survey, War Office and Air Ministry (Jebel 'Uweinat, Map series 1301, sheet NF-35, edition 6-GSGS) indicates that the following explorers visited areas adjacent to the region: Hassanein in 1923, Prince Kemal El-Din in 1925, Bagnold in 1930 and 1932, Sweeting in 1934, Shaw in 1935, and Miskin in 1942.

As shown in Figure 8.9, none of these explorers traveled through the area that encompasses the circular features. The closest approach was made by Sweeting in 1934. The area may have been avoided because

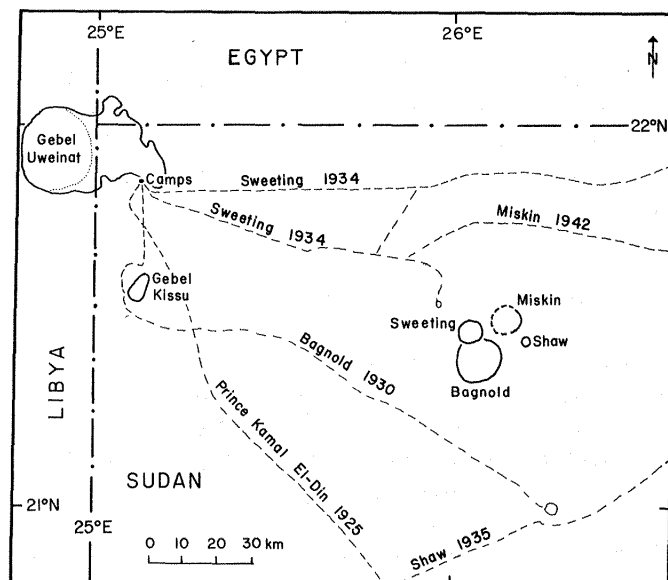


Figure 8.9 Sketch map of circular features southeast of Gebel Uweinat and their proposed names. The features are named after the early explorers who came nearest to the locality.

of the roughness of the terrain, with no especially high mountain peaks to intrigue the travelers. The existence of the circular structures was not known before the Landsat images were obtained in 1972.

The area in which these structures are located displays numerous features that are similar to streaked areas in the Cerberus region of Mars (El-Baz and Maxwell, 1979a), thus adding to the importance of the locality with respect to comparative planetological studies. To allow easy reference to the circular structures in the future, it is here proposed to name them after those early explorers that came closest to the locality. As shown in Figure 8.9, these names and their corresponding circular structures are: Bagnold (14 km), Miskin (8 km), Sweeting (7 km), and Shaw (2.5 km). It is expected that field investigations of these structures will be of value to understanding the crater forms not only on the Earth, but also on other planetary bodies.

**Page Missing in
Original Document**

Chapter 9

THE DARB EL-ARBA'IN DESERT: A PRODUCT OF QUATERNARY CLIMATIC CHANGE

C. VANCE HAYNES

Departments of Geosciences and Anthropology
University of Arizona
Tucson, Arizona 85721

ABSTRACT

The Darb El-Arba'in Desert, as dry as any place on Earth, is today an eolian-derived landscape with no large integrated drainage systems, but there is clear evidence of past periods of wetter climate separating the longer periods of hyperaridity. On the basis of recent research a number of hypothetical concepts are expressed for further consideration and testing in order to better understand land-climate interrelationships during the Quaternary Period. The alternations from moist to dry and the attendant changes in processes acting upon rocks with differential resistance caused by silicification and ferruginization are believed to be main factors in shaping the landscape. A combination of archaeological and radiocarbon dating has allowed some rates of wind erosion to be approximated.

Depressions appear to be the result of a combination of structural weaknesses, salt weathering and wind erosion. The effects of these factors in the more uniform rocks appear to be the creation of extensive flat areas as the land is lowered during interpluvials to levels controlled by water tables. What have been called desert pediplains are more likely the result of wind action rather than water.

The oases depressions were blown out to essentially their present configuration and depth before about 200,000 years ago when Late Acheulean people utilized artesian springs on the depression floors. Since then two major pluvial periods, one during Mousterian-Aterian time and one during Terminal Paleolithic-Neolithic time, are in evidence in the stratigraphic record which reveals smaller epicycles within pluvials. Human occupation of the Darb El-Arba'in Desert corresponds to pluvial periods, but these are out of phase with the late Pleistocene glacial stages of the northern hemisphere.

Pleistocene interpluvials appear to have been even drier than the present, and pre-Late Acheulean wind erosion appears to have been cumulatively greater than all that has occurred since then. Remnants of relict terra rossa soils in solution cavities on the Egyptian Plateau suggest the presence of an early or pre-Pleistocene karst terrain preceeding eolian processes that have been predominant since the end of terra rossa soil development.

INTRODUCTION

In the earliest geography, that of Herodotus in the 5th century B.C., western Egypt is known as the land of the Libyans. The desert west of the Nile Valley has, therefore, long been known as the Libyan Desert or since World War II, as the Western Desert. But there is a portion of this vast area that is even drier than the rest and therefore different in both life (ecology) and form (geomorphology). In some ways it is similar in appearance to Mars (Bagnold, 1978; Haynes, 1978; El-Baz, 1978b). It should have a separate name, and therefore I shall call it the Darb El-Arba'in Desert after the ancient caravan route that traverses the middle of it. The Arba'in (short for Darb El-Arba'in) Desert (Fig. 9.1) as here defined includes much of what has been referred to as the Libyan Desert or the Western Desert but excludes the area north of the Great Sand Sea. Specifically, it is an area of about 400,000 km² that lies south of the Eocene Limestone (Libyan) Plateau, west of the Nile, north of Wadi Howar in Sudan, and east of the border with Libya and the Ennedi Mountains in Chad. Traversing the length of this vast desert from NNE to SSE is the ancient caravan route, Darb El-Arba'in, all but abandoned since the end of the slave trade (Shaw, 1929). Literally, Darb El-Arba'in is Road of the Forty, but the origin and meaning of the name is obscure. Murray (1967) disagreed with Shaw's (1929) contention that forty was the number of days caravans spent on the road and suggested instead that it stood for the forty companions of Mohamed.

Rainfall over most of this area is less than a millimeter per year and individual storms at a particular place may be decades apart (Bagnold, 1954). In the area of Kharga and Dakhla Oases in the north, the only population centers in the area, daily average wind velocities range between 4.3 and 18.5 km/hr throughout the year and the daily average relative humidity is between 28 and 56 percent, with an average potential evaporation rate at Kharga on the order of 5,000 mm/yr (Ezzat, 1974). This is 25% greater than that of the Salton Basin in the Imperial Valley of California in the United States.

Bedrock in the Arba'in Desert is composed mostly of the Cretaceous Nubia Formation (Said, 1962) made up of cross-bedded sandstones with numerous interbedded shales (Hermina and Issawi, 1971). The Nubia Formation is underlain by Precambrian granites and granite gneisses except in the southwestern corner of Egypt where Paleozoic sediments are present (Issawi, 1973a; Klitszch and others, 1979). On the Limestone Plateau and in a few outliers to the south, Tertiary limestones and shales overlie the Nubia Formation, which is locally intruded by basalts believed to be of late Tertiary or early Pleistocene age (Issawi, 1971). Nubian sandstone (used here in the general sense of any sandstone member of the Nubia Formation) forms the main aquifer of north Africa, and is one of the great aquifers of the world.

The Arba'in Desert, as dry as any place on Earth, is today an eolian-derived landscape with no integrated drainage systems. Aside from the inactive wadis descending the limestone plateau, the only vestiges of former rivers are a few sinuous ridges of wind resistant channel gravels (inverted wadis), most common near the Nile

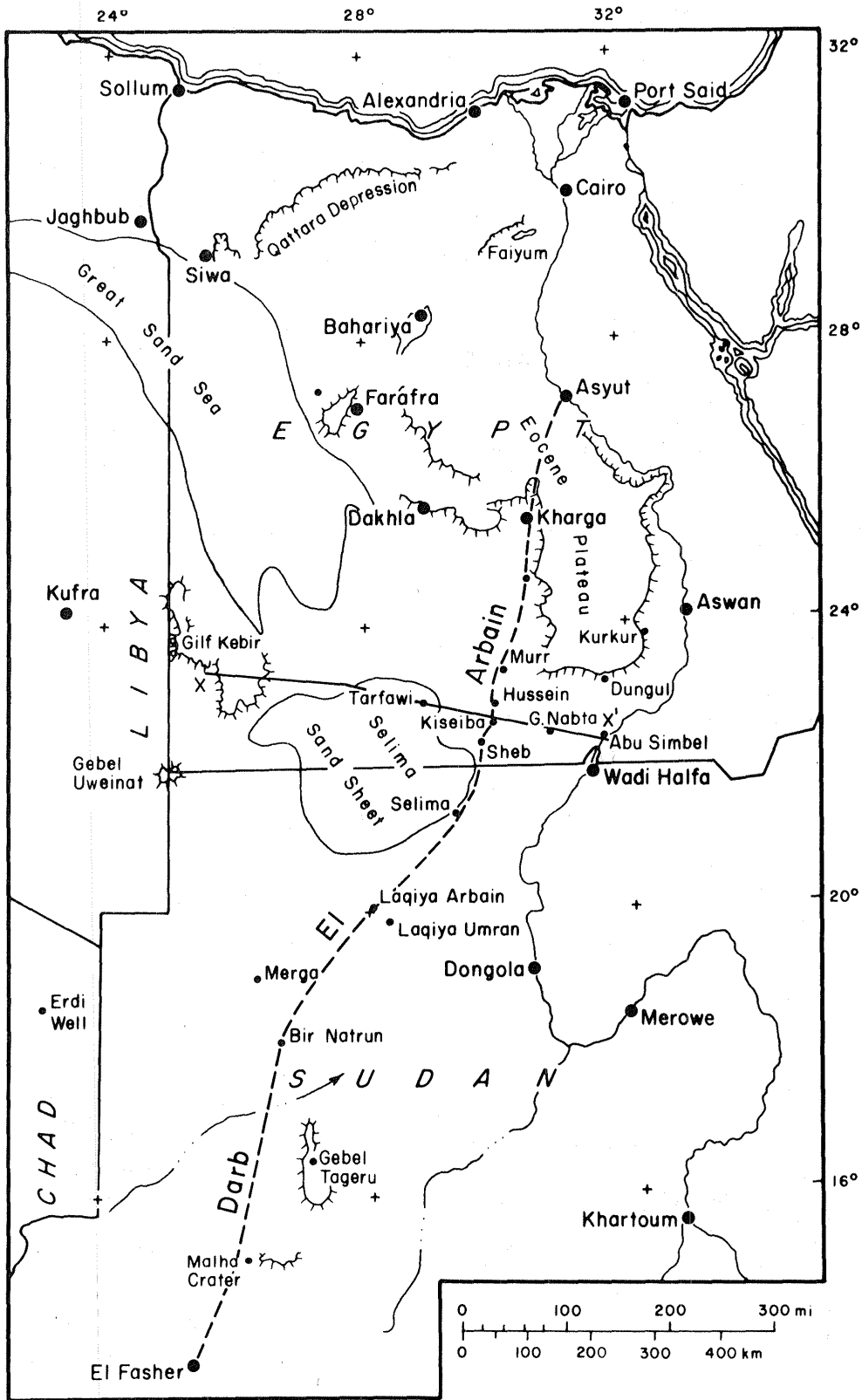


Figure 9.1 Map of the Darb El-Arba'in track between El-Fasher, Sudan, and Asyut, Egypt.



Figure 9.2 Alluvial hamada at the base of Black Hill displays runnels attesting to occasional rains.

(Giegengack, 1968). Elsewhere, the only evidence of recent running water consists of small dry runnels at the base of slopes (Fig. 9.2).

The landscape consists of nearly flat plains separated by escarpments and erosional remnants (inselbergs) without typical pediments (Fig. 9.3). Deflational hollows range in size from meters to many tens of kilometers, and were created by differential wind erosion on a large scale (Fig. 9.4). Alluvial fans are relatively small and essentially inactive. Structural control is obvious in only a few places and many structures are truncated (Fig. 9.5).

PAST CLIMATES

Evidence for Pleistocene oscillation from one climatic regime to another in the Arba'in Desert was first presented by Caton-Thompson and Gardner (1932). They found four levels of spring deposits along

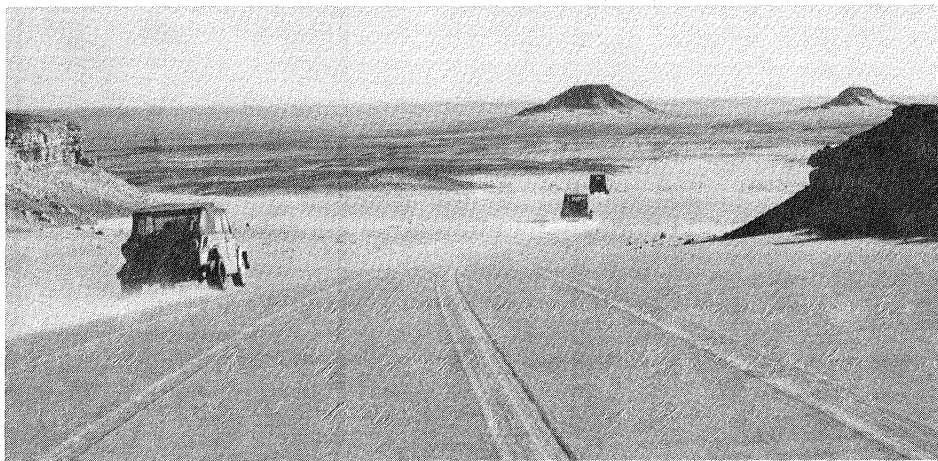


Figure 9.3 Two hills as viewed from the Kiseiba escarpment are capped by resistant quartzite.

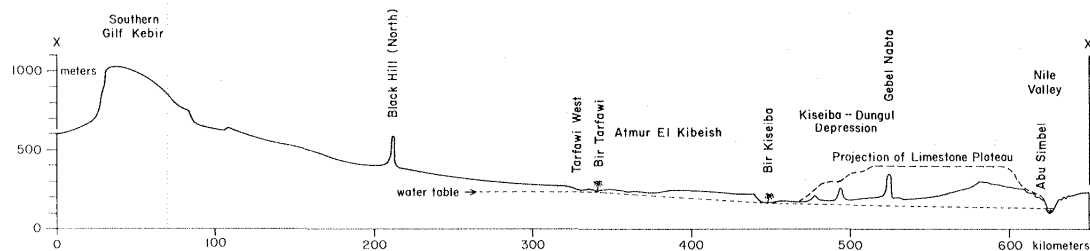


Figure 9.4 Geologic profile from Gifl Kebir to Abu Simbel.

the sides of the Kharga depression, which represent four wet phases of climate separated by arid periods of severe wind erosion and successive lowering of the desert floor. Spring deposits exposed on this floor contained late Acheulean hand axes in situ indicating that the wind had eroded to the present level by about $200,000 \pm 100,000$ years ago, a modern estimate for the age of the late Acheulean culture (Wendorf and others, 1976; 1977). Butzer and Hansen (1968, p. 85) found evidence for at least six Quaternary pluvial episodes in the Nubian Nile Valley.

Pleistocene climatic oscillations are evident from the important archaeological excavations conducted in the Dike area (Schild and Wendorf, 1975) and in the area of Bir Tarfawi (Wendorf and others, 1976; 1977; Wendorf and Schild, 1980). After late Acheulean occupation of springs, the water table dropped, man and central African type fauna disappeared, and the depressions were deepened by wind as the

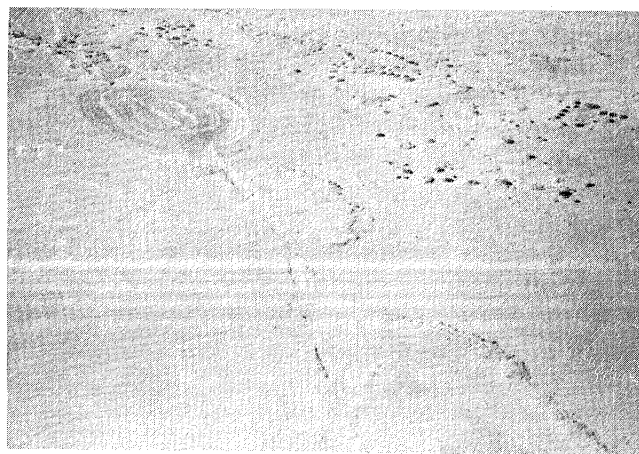


Figure 9.5 The dome of Gebel Mara and bifurcated fault have been truncated by wind action.

climate turned hyperarid and stayed so for tens of thousands of years. Sometime after approximately 60,000 BP, a relatively wet climate returned and the water table rose. Ponds filled the Tarfawi and Tarfawi West basins, and man appeared, again in the stratigraphic record in the form of Mousterian hunters of big game animals. Mousterian and later Aterian people occupied the Tarfawi basins several times between 60,000 and 25,000 BP, in response to times of high ground-water levels that occurred between periods of wind erosion and partial dune filling of the basins.

After approximately 30,000 BP, the Arba'in Desert was too arid for human occupation for essentially 20,000 years. Not until the onset of pluvial conditions at about 10,000 BP did man and animals again return to the desert. This time, Terminal Paleolithic and Neolithic peoples brought domesticated animals with them, probably from central Sudan. They eventually practiced agriculture around the margins of intermittent playa lakes that dried up and were eroded three times during the Holocene. By 5,000 BP the present hyperarid climate had set in.

It is these alternations from moist to dry that are undoubtedly the significant cause of the present landforms of the Arba'in Desert. Two entirely different systems of expending nature's energy are represented. Solar energy is, of course, the ultimate source, but under moist climates (at best, semiarid in this part of Africa), vegetation grows, soils form, and the rocks at the earth's surface are weakened and broken down into smaller, more resistant minerals by the higher chemical energy promoted by moisture. If the climate is so wet that rivers flow, then running water cuts channels and otherwise erodes the land into the familiar topography of valleys and ridges. This condition has not prevailed in this area since Acheulean time at the latest. For the past 200,000 years, running water has played a minor role in shaping the surface of the land.

Under hyperarid climates, like that of today, water plays practically no role at all because there is so little. Measurable rain falls only once every 40 years or so and is immediately absorbed by the sand and porous rocks. Although puddles may form in lower spots, they evaporate almost as fast as formed. Instead of water, air heated by the sun becomes the mobile agent of erosion as winds sweep the land. Without water the plants die, and loose soil, no longer protected by plants, blows away. As the land surface is lowered by wind erosion, evaporation from the water table occurs. Salts form, expand, and further weaken the rock at the surface, allowing more of it to blow away which enhances further evaporation. Thus, the ultimate limit on wind scour and deflation is the water table.

WIND PHENOMENA

Nowhere is the work of persistent, unidirectional wind more apparent than it is in the Arba'in Desert. From a microscopic scale to that of satellite images, wind has influenced every fraction of the land. Every stone is polished, pitted, grooved, or frosted to one degree or another by pelting sand, silt, or clay; and each can take on

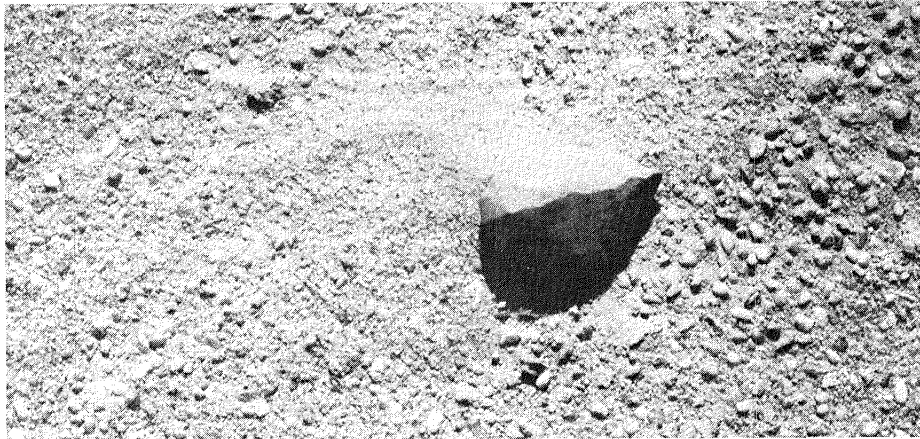


Figure 9.6 An acheulean hand ax has been converted into a ventifact (eolized) and rests on a pebble sheet.

a variety of oft-repeated, faceted shapes (ventifacts, dreikanter). Artifacts that have remained exposed are sand blasted more or less in proportion to their age. Some Acheulean hand axes are barely recognizable (Fig. 9.6), whereas Neolithic tools seldom show more than a light rounding of formerly sharp edges.

A concretion-capped protrusion, about 2 cm long, on a fragment of Kurkur limestone was found on the deflated floor of a Neolithic playa lying oriented into the prevailing wind (Fig. 9.7). The playa was deflated sometime after 5000 BP which suggests that the minimum rate of abrasion of this limestone is 0.004 mm/yr under these particular localized conditions. The actual rate, however, is probably much greater because the time of exposure and optimum orientation of the specimen was probably less than 5000 years. Concrete at the base of the fence posts at the north end of Kharga airport has been abraded back as much as 7 cm since their installation in 1965 (Fig. 9.8); this

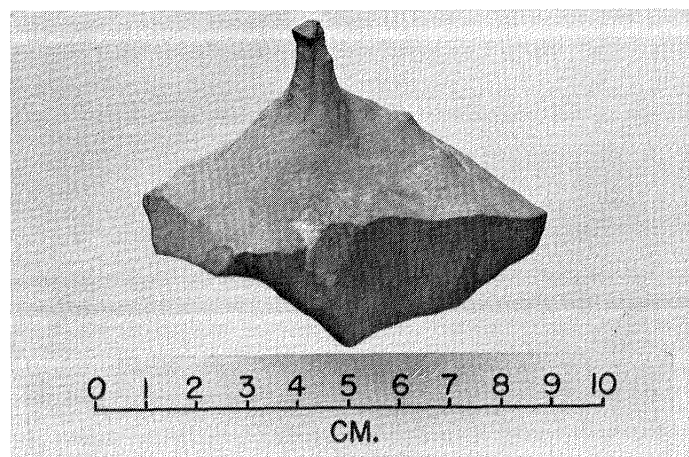


Figure 9.7 Ventifact of Kurkur Limestone with a protrusion caused by a more wind-resistant inclusion.

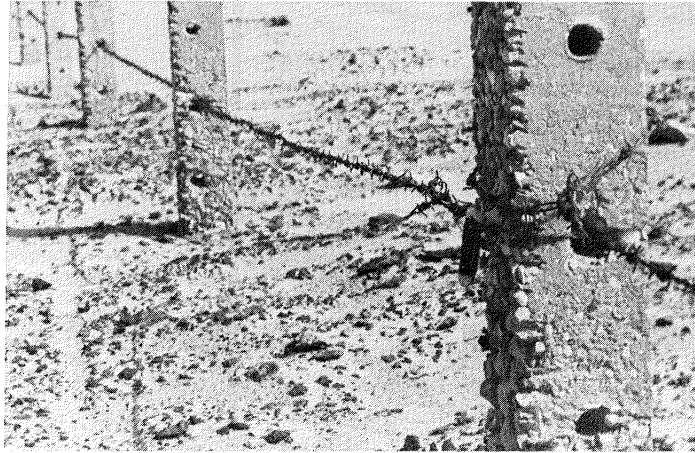


Figure 9.8 Sandblasted fence posts at Kharga airport in 1976 were constructed in 1965.

indicates a rate of abrasion of 2 mm/yr. Other posts in the same row show little or no abrasion.

On top of Bargat El-Shab are the last remaining outliers of the Tertiary limestone that caps the Eocene Plateau 60 km to the north (Issawi, 1971). The vestiges of limestone on a nearby hill are no more than a few scattered, boulder size ventifacts (Haynes, 1980a). Many erosional remnants are undercut by sandblasting at the level of the surrounding surface (Fig. 9.9), and flaggy outcrops commonly produce a shingle armor that protects lower slopes. In regions of broken ground, isolated positive features disturb the air stream and create horseshoe-shaped vortices (Greeley and others, 1974a) which allow only a minimum accumulation of sand on the leeward side. Other hills have longitudinal dunes attached to the leeward sides, and still other remnants have annular hollows or moats which reflect the horseshoe-shaped wind vortex that formed them. It is clear that every weakness in the

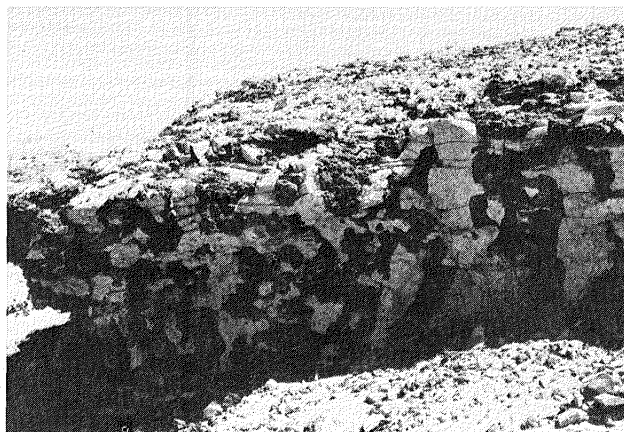


Figure 9.9 Highly silicified and ferruginous caprock of the Gifl Kebir is contact metamorphic zone associated with basaltic intrusions.



Figure 9.10 Wadi bed descending the escarpment at Um Dabadib has been flattened and wind scoured into bed forms unrelated to stream flow.

bedrock is taken advantage of by the wind, and that no outcrop has escaped at least some modification by the wind. Hills become aerodynamically shaped into yardangs, and limestone-capped mountains such as Gebels Nabta (Fig. 1d in Haynes, 1980a) and Shirshir (Plate 29 in Hume, 1925) become grooved into giant north-south flutes separated by sandblasted and pitted limestone. An outstanding example of a truncated dome is Gebel Marawa (Fig. 9.5), which was mapped by Issawi (1968).

The Pleistocene erosive force of the wind is everywhere manifest in the Arba'in Desert, but nowhere more so than near the remote Roman outpost of Um Dabadib at the foot of the northern escarpment of the Kharga depression. Here, dry river channels extend from the steep slopes out to playa flats where they disappear under mud deposits of the Neolithic pluvial. The channels are much older and probably date to Acheulean times. Every cobble and boulder exposed in the streambed has been truncated and fluted by wind action (Fig. 9.10). The predominance of wind over water in shaping the landscape in the past 200,000 years is abundantly clear at Um Dabadib, where the present bedform is the result of eolian and not fluvial action.

POSITIVE TOPOGRAPHIC FEATURES

Many positive features of the Arba'in Desert are due to differential resistance caused by silicification and ferruginization of formerly permeable sandstones (Fig. 9.9). This solution hardening is a major factor in creating topographic relief, and many flat-topped hills are maintained by a protective cap of hardened sandstone (Fig. 9.3). These zones, some of which cross cut sedimentary structure, appear to be unrelated to the small basaltic intrusions in the area, which are commonly encased in a zone several meters thick of contact metamorphosed (silicified) sandstone displaying pronounced columnar jointing (Fig. 9.11). The ferruginized zones probably represent



Figure 9.11 Columnar jointing in metamorphosed sandstone reveals the shallow presence of a basaltic intrusion.

groundwater mineralization from a time when the land surface was much higher than it is now. Said (1975) has suggested that some of these erosion resistant small hills may represent old spring sites. Among the more common features of the Holocene playa deposits (mud pans) in the Arba'in Desert are numerous playa remnants in the form of yardangs (Fig. 9.12). In some basins, these aerodynamic shapes are the dominant outcrop form, but there are other basins such as Nabta playa (Haynes, 1980a) in which they are absent, and the deflational remnants are simply flat to undulating floors of playa mudstones in spite of the removal of several meters of sediment.

The relatively soft consistency of the mud deposits is an apparent factor in the formation of yardangs because they are not as common in bedrock remnants. Where they do occur in bedrock, such as in the extreme northwest corner of the Kharga depression, their formation appears to have been augmented by joints which occur in troughs



Figure 9.12 Yardangs of Neolithic-age playa muds at Laqiya Umran.



Figure 9.13 Air view of the Eocene Plateau between Kharga and Asyut showing yardangs, megaflutes, and troughs aligned with the prevailing wind. A few do not conform to the prevailing northerly winds. (ca 1.5 km across base of photo).

between yardangs. Similar structural control may occur on the Limestone Plateau which is covered with innumerable yardangs (Fig. 9.13).

The main positive features of the Arba'in Desert are Gebel Uweinat (1893 m), the Gilf Kebir plateau (1000+ m), and the Eocene Limestone Plateau (400+ m), which apparently owe their existence to their great resistance to erosion. These features pre-date late Acheulean time, with an age estimate of $200,000 \pm 100,000$, as indicated by the distribution of artifact concentrations on the surface and in situ at the base of the great escarpments at Dakhla, Kharga, and the Gilf Kebir. Pluvial-interpluvial cycles before then are revealed by only a few remnants of lacustrine deposits armored by silica nodules, by inverted wadis in what is now a waterless desert, and by the terrace deposits of the Kharga depression and the Nile Valley (Sandford and Arkell, 1933; de Heinzelin, 1968; Giegengack, 1968; Butzer and Hansen, 1968). These cycles probably extended back at least to the beginning of the Pleistocene.

The resistance of the Gilf Kebir to wind erosion is most likely due to the protective cap of silicified sandstone. This mineralization may be due to ground water heated by the basaltic intrusions that crop out on the top of the plateau (Peel, 1939b). The baking of sandstone is intense in some areas (Fig. 9.9). At one time before the onset of Pleistocene pluvial-eolian cycles, the Gilf Kebir was probably connected with the Limestone Plateau.

Penetrating the 300 m high cliffs that surround much of the Gilf are relatively long narrow wadis or canyons that end abruptly as box canyons. Wadis in the southern Gilf are located mostly on the east side and are floored by colluvium and alluvium with terraces up to 3 m high composed of red, clayey sand with gravel lenses (Fig. 9.14).



Figure 9.14 Many wadis in the southern Gilf Kebir expose a terrace of clayey sand alluvium under alluvial fan gravels.

The rather angular courses of these wadis, and the lack of any significant catchments led Peel (1941) to suggest that they may have been caused by ground water sapping at the base of cliffs in karstic fashion as the surrounding land was lowered. Another possibility is that former catchment areas were present in shales or softer beds that may have overlain the plateau, but are now destroyed by deflation. The surface of the southern plateau has a significant slope to the east (Fig. 9.4), the side with the longest drainages, and recent mapping by Issawi (1973a) reveals the presence of northward dipping shales off the northern end of the Gilf Kebir that probably extended over it at one time. Until the wadi deposits themselves are studied and the Pleistocene chronology better understood, the origin of the wadis must remain in doubt. This view is shared by Maxwell (1980) who has initiated new systematic analyses of the Gilf wadis.

The Limestone Plateau is capped by dense Tertiary limestone, the surface of which is severely sandblasted and wind scoured into hillocks (yardangs) and furrows that parallel the prevailing wind direction (Sandford, 1933a; Plate 28 in Hume, 1925). On closer inspection there are numerous troughs and elongated hollows extending in other directions as well (Fig. 9.13), and patches of red, terra rossa soils exposed in quarry walls extend down into solution features in the limestone (Fig. 9.15). The pipe-like fillings of terra rossa are the remnants of what must have once been a thick, continuous soil over the Limestone Plateau. The present highly irregular surface appears to be the result of solution and soil development under karstic conditions, subsequently truncated and modified severely by eolian processes. Erosion remnants reveal more than one episode of red soil formation. The karst may have been initiated by a subtropical climate in Pliocene time with subsequent shorter or less intense intervals of intense eolian action. Subsequent pluvials have not left the large-scale evidence of solution and soil development on the limestones as did the earliest episode.



Figure 9.15 Limestone quarry in the Eocene Plateau southwest of Asyut reveals terra rossa soil in solution cavities.

The karst undoubtedly formed when the water table stood closer to the general level of the major solution features. This was most likely before the major depressions of the Arba'in Desert had approached their pre-Acheulean depth. It is clear, therefore, that throughout the Pleistocene there has been a net decline in the level of the regional water table until it reached its present level within Nubian sandstone aquifers as so eloquently proposed by Ball (1927).

The highest elevation in the Western Desert is the top of Gebel Uweinat (1893 m) in the extreme northwest corner of Sudan where it joins Egypt and Libya. This relatively flat-topped mountain (Hussein, 1928) is composed of granitic basement rocks overlain by Paleozoic sandstones, both of which have been intruded by syenite (Issawi, 1973a). A prominent bench, possibly an abandoned pediment, between 800 and 1200 m surrounds the higher mountain mass which is radially drained by several canyons containing acacia trees, grasses and low shrubs, indicating the presence of shallow groundwater recharged by infrequent rains. Though isolated by relatively flat plains, the mountain is large enough to cause orographic rain. Alluvial terraces in Wadi Talh indicate at least one episode of Holocene aggradation, and several of Pleistocene age (de Heinzelin et al., 1969). The canyon walls are famous for their fine, though relatively inaccessible rock art mostly of Neolithic or later age (Winkler, 1939a; Van Noten, 1978). Neolithic artifacts occur in ancient stabilized dunes on or interbedded with the alluvium and now undergoing deflation. The single episode of earlier aggradation is represented by a higher terrace composed of well-rounded quartzite boulders (Fig. 9.16) representing a magnitude of discharge that has not occurred in recent time (Haynes, 1980b). Similar terraces have been observed at Gebel Archenu and farther to the west (Williams and Hall, 1965).

In the Nile valley east of the Arba'in Desert, Butzer and Hansen (1968) describe several surfaces (pediplains) believed to represent successive cycles of stability and denudation during late Tertiary and Pleistocene time. Similar surfaces, such as those at Gebel Nabta (Haynes, 1980a), Black Hill (Fig. 9.17), Gilf Kebir (Fig. 9.18;

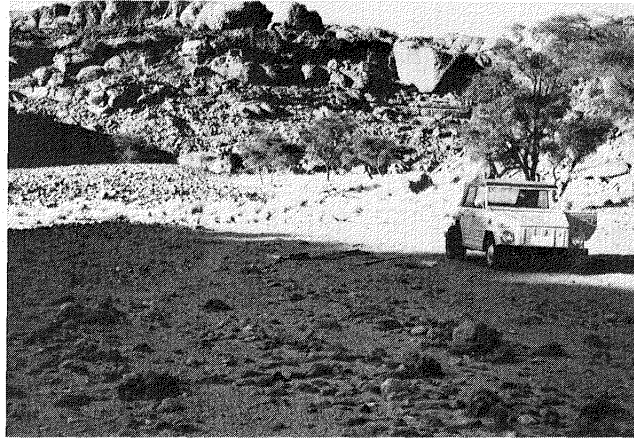


Figure 9.16 Rounded-boulder terrace in Wadi Talh, Uweinat.

Haynes, 1980b) and elsewhere (Sandford, 1935a; Said, 1975), occur in the Arba'in Desert but their origins and correlation to the Nile Valley must await more detailed study.

NEGATIVE TOPOGRAPHIC FEATURES

Whereas some major depressions appear to coincide with faults (for example, the Kharga depression), the negative topographic areas are principally due to deflation of shales or sandstones weakened by salt weathering following dessication of former lakes, or by evaporation of an exposed capillary fringe. The process can be witnessed today at the remote salt lake of Merga in northwestern Sudan where deflation in a formerly much larger lake basin has exposed the water table. Nubian sandstone around the western margin of the present lake is very friable due to the high content of efflorescent salts (Haynes and others, 1979). Whenever it does rain, these salts may be leached or washed from the surface to leave another highly deflatable covering



Figure 9.17 Erosional surfaces around the base of Black Hill are covered with fan gravels. Acheulean hand ax was found on the prominent bench in the middle ground.

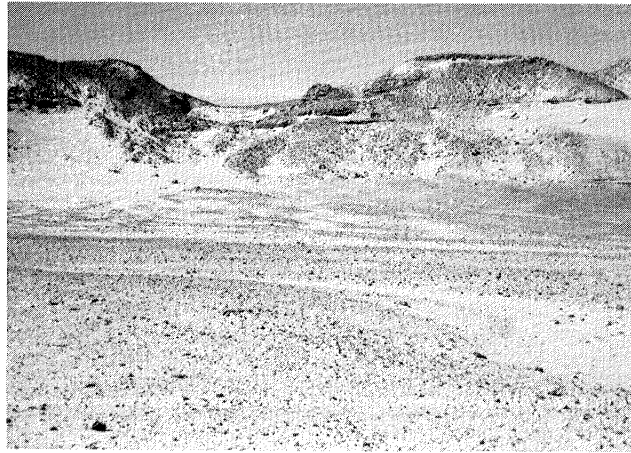


Figure 9.18 A prominent ridge projecting eastward from the Gilf Kebir contains a channel filled with current-bedded sand and is capped with alluvial-fan gravels. Alluvial fan deposits at the footslope farther out of the picture to the right contain Late Acheulean hand axes (Myers, 1939).

of loose sand as in the process of basin formation described by Judson (1950).

The largest depression of the Arba'in desert is that at Kharga, which extends southward for 220 km along the western edge of the limestone plateau, is up to 40 km wide, and is only 1 m above sea level at its lowest point. A fault runs the length of the Kharga depression (Beadnell, 1909) and artesian springs are known to have occurred there as far back as Acheulean times (Caton-Thompson, 1952). As with practically all of the hundreds of smaller depressions of the Arba'in Desert, the Kharga depression held playa lakes in Neolithic times.

Another topographically depressed area occurs in the eastern part of the Arba'in Desert between Bir Kiseiba (Fig. 9.4) and Dungul, a spring below the southern part of the Limestone Plateau. The plateau, known as the Sinn El-Kedab in this area, forms the northern boundary of the depression (Fig. 9.1). Subdepressions are numerous in this little known area and many contain Neolithic age playa deposits, the most important of which are at Nabta Playa. Extensive archaeological excavations there have permitted radiocarbon dating and a redefinition of the prehistory from Terminal Paleolithic time, 9,500 to 8,500 years ago, through Neolithic times, 8,000 to 6,000 years ago (Wendorf and others, 1976; 1977; Wendorf and Schild, 1980).

A northeast-southwest aligned depression 80 km northwest of Laqiya Arba'in in Sudan (Fig. 9.19) was explored in 1935 (Shaw, 1936a) and is unusual in that it is located in a relatively flat stony plateau, bounded by cliffs, and is relatively deep for its width. The depression is not aligned with the prevailing wind direction, and has two parallel branches. A southerly arm may connect it with the main

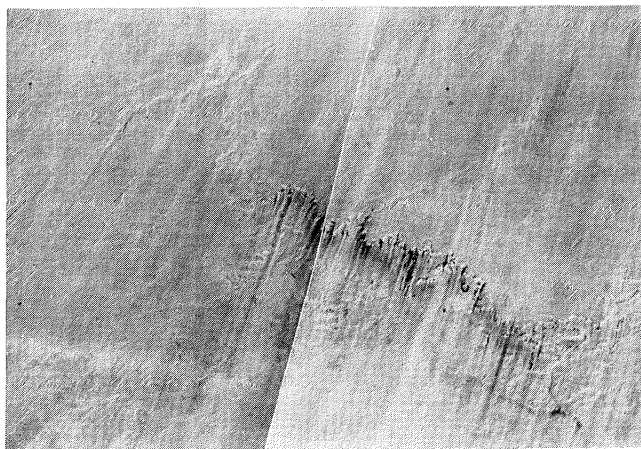


Figure 9.19 Landsat view of the Laqiya depression showing linear depressions to the northwest (upper left).

Laqiya depression. Its form and alignment with what appears to be the local structural fabric suggests that it is structurally controlled. The unintegrated branches indicate that it is not derived from a stream course, but may have formed by deflation as the water table fluctuated in a sandstone fracture weakened at the surface by leaching of cement or salt weathering. As suggested for the canyons in the Gifl Kebir (Peel, 1941), it could also have formed via spring discharge and sapping. This process does occur in some karst terrains, but would have occurred here only if it was at one time connected with the Laqiya depression.

ORIGIN OF THE DEPRESSIONS

From observations in many depressions of the Western Desert, from the Qattara in the north to Merga in the south, I am of the opinion that most if not all are the result of eolian corrasion and deflation of beds weakened by leaching of cement and salt efflorescence (Knetsch and Yallouze, 1955). The mechanism is self-enhancing, once started by the development of an initial area of internal drainage. Each wetting allows new salts to form upon drying, and crystallization and recrystallization of expanding salts weakens the cementing of the sedimentary matrix and loosens grains for their plucking by the wind. Thus, basins will expand at the expense of weaker rocks and at a rate in proportion to the frequency of cycles of wetting and drying. The driest (hyperarid) part of a climatic cycle would not be as effective as the transitional parts. The transition from wet to dry would appear to be optimal because it would take less time for vegetation and soil to be destroyed than to be reestablished.

Once the water table is approached by the basin floor, efflorescence by evaporation from the capillary fringe would further aid deflation as long as evaporation exceeded recharge (i.e. a net decline of the water table). If at this stage the water table were to rise significantly, artesian springs could emerge, some eruptively as mentioned below.

The occurrence of faults or fractures could augment corrasion not only because of physical weaknesses, but by bringing ground water to the surface where evaporation and efflorescence would aid the comminution of rocks (Knetsch and Yallouze, 1955). The fault trace itself may maintain a positive relief within the basin, as it does in parts of the Kharga depression, because of cementation, wetness, and a concentration of vegetation.

The same effect can be seen in the Qattara depression where, in spite of statements to the contrary (Ezzat, 1974; Murray, 1952), a fault occurs along the northern scarp (S. Zaghloul, personal communication) and several springs are located along it. The depth of the depression is apparently in a steady state because seasonal water table fluctuations show no net trend, possibly because of support from sea water. Also, the main mineral of the salt crusts and sabkhas is halite (NaCl) which is neither efflorescent nor crumbly and can form wind resistant deposits especially when mixed with sand. It is significant that the Qattara fault is at right angles to the prevailing wind with the depression leeward, whereas the Kharga fault is parallel to the wind with the elongated depression along both sides. It is the only major depression of the Arba'in desert so oriented with respect to the prevailing wind.

ORIGIN OF EXTENSIVE FLAT AREAS

The center of the Arba'in Desert, a remarkably flat area 400 km north-south and 300 km east-west, is broken only by a few hills and scarps. As Peel (1966) has pointed out, it approaches being the ultimate peneplain. Much of the area, the Atmur El-Kibeish or plain of the sheep, is nearly level with elevations between 200 and 300 m surrounded by more broken ground with elevations between 300 and 400 m to the north and south. It rises as much as 600 m westward as the Gifl Kebir plateau and Gebel Uweinat are approached (Fig. 9.4). Much of the nearly level area is covered by smooth sand sheets on which one can drive motor vehicles at relatively high speed for an hour or more on a single heading and see no topographic break on the horizon in any direction (Fig. 9.20). In a few places elongate groups of barchans

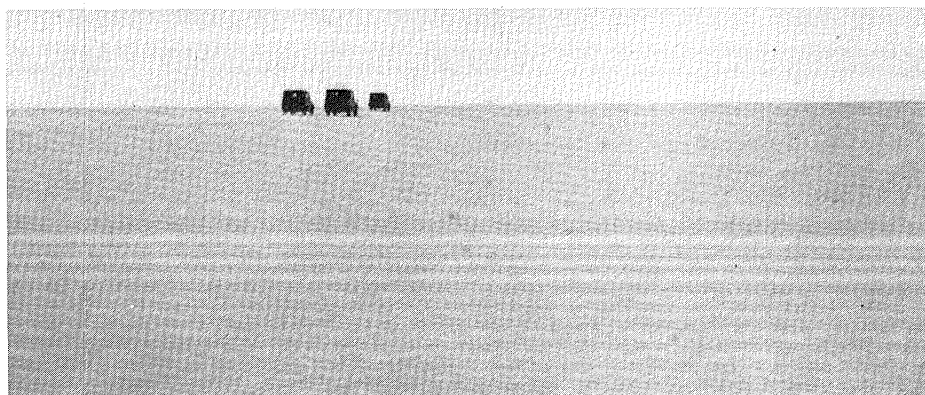


Figure 9.20 Sand (fine pebble) sheet between Bir Tarfawi and Black Hill is typical of the central part of the Darb El-Arba'in Desert.

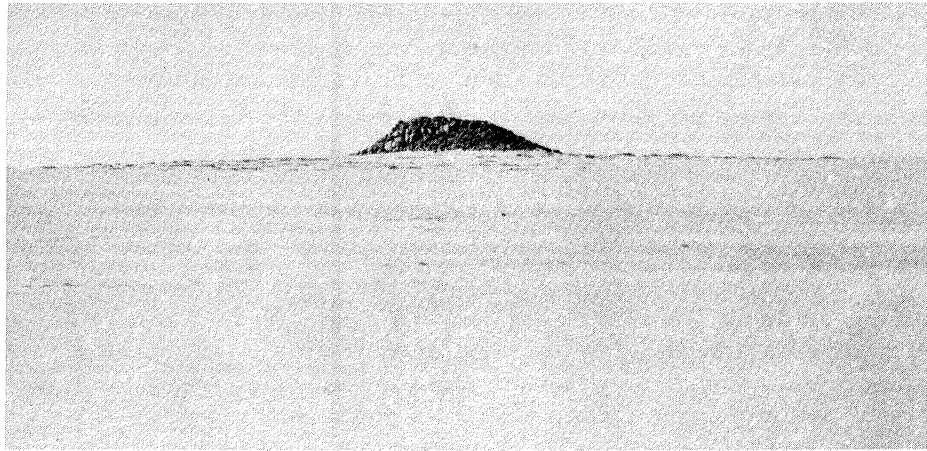


Figure 9.21 Qaret El-Maiyit, one of the few rounded hills of the Darb El-Arba'in Desert is spheroidally weathered granite.

stretch out in the prevailing wind direction across the sand sheets the largest of which, the Great Selima Sand Sheet, was first described by Bagnold (1933). Most of the sand sheets have a surface layer of coarse sand or fine pebbles (see Maxwell; Chapter 12). Their origin may be related to the vast flatness.

The surface of this area does not necessarily parallel the bedding, which is slightly undulatory with dips to the northeast seldom exceeding 3° and commonly less than 1° (Issawi, 1971). Instead the flat surface truncates the general bedding as well as shallow structures. Such areas have been referred to as desert peneplains by Sandford (1935a) and pediplains by Peel (1966) and Said (1975). The sporadic hills are either erosion remnants of sandstone protected by a more resistant cap, pyramid-shaped where the cap is gone, or are rounded outcrops of granite (Fig. 9.21). On a smaller scale, and less commonly, phreatophytic mounds of tarfa (Tamarix sp.) or Sayaal (Acacia ehrenbergiana) (Fig. 9.22) interrupt the flatness.

In the very center of the sand sheet area lie the miniature oases of Bir Tarfawi (Fig. 9.22) and Bir Tarfawi West in depressions 10 m or so below the surrounding plain which for 20 km or more in all directions is made up of dense, nodular, calcium carbonate; a calcrete, truncated by sandblasting and described and mapped by Bahay Issawi (see Schild and Wendorf, 1975). The calcrete is probably due to evaporation from an exposed capillary fringe, but patches of dense lithified marl indicate pond deposition. Both depressions contain shallow ground water, phreatophytic tarfa mounds, and archaeological sites associated with late Acheulean age springs and Mousterian-Aterian age lacustrine deposits. These Middle Stone Age people apparently lived by hunting and fishing with more advanced stone tools than their Acheulean predecessors (Wendorf and Schild, 1980).



Figure 9.22 Date palms indicate shallow ground water at the southern end of Bir Tarfawi. The phytogenic mounds are stabilized by tarfa (Tamarix). Foreground is calcrete, and late Pleistocene lake marl forms light streak in the background.

Origin of Sand Sheets

The depth of wind scour and deflation is limited by the depth of the water table. This is very likely the explanation for the extreme flatness of the sand sheet areas of the Arba'in Desert because the water table is relatively flat where it occurs in porous sandstone such as in the Nubia Formation. Some lesser irregularities in the surface of the sandstone are probably filled and thus smoothed over by the sand sheets.

Test pits excavated through a fine-pebble lag on the sand sheets east and west of the Kiseiba escarpment show the upper 20 to 50 cm to be made up of unconsolidated (soft) laminations of medium to coarse and coarse sand. Deeper sands are weakly cemented (slightly hard) and conspicuously browner with an abrupt smooth upper contact, similar to Bagnold's (1941) observations elsewhere. The lower zone is a buried paleosol representing a period of greater precipitation than today, during which clays and salts (eolian?) were translocated down the profile (Haynes, 1980a). Associated archaeology and a radiocarbon date show the paleosol (at the surface in some places) to be of Neolithic age (Haynes, 1980b).

The maximum thickness of the sand sheets is unknown, but from the way the edges feather out against flat surfaces of truncated bedrock it cannot be more than a few meters. Unfortunately, a report on two wells dug through the sand sheet by Beadnell (1931) made no mention of its thickness.

In several places in the Arba'in Desert, fine pebble sheets grade into medium coarse pebble sheets or lag hamadas (Haynes, 1980a) composed of obviously stream-rounded quartz and quartzite pebbles (Fig. 9.6). These areas are slightly elevated and are very likely the

last remnants of inverted stream beds. It is likely, therefore, that much of the sand and pebbles of the sand sheets is derived from the beds of former rivers and streams that once dissected the area in earlier Pleistocene times. The other significant source of sand is the one traditionally attributed to the deflation of the major depressions. In the fine to medium sand range, contributions from this source probably exceeded that from fluvial sources because these are the dominant grain sizes of the bedrock sandstones. In addition, the volume represented by the depressions probably greatly exceeds that of the former stream channels.

EOLIAN SAND

Overriding the bedrock landforms are the eolian deposits of the Western Desert studied by Bagnold (1941) and others. From satellite photography, the alignment of these mobile forms with prevailing winds of northeast Africa is outstanding (see El-Baz, Chapter 4). The sands are the bedload of a colossal braided air stream with major anabranches going around the east and west sides of the Gilf Kebir-Gebel Uweinat highlands and merging again to the southwest. To the north lies the Great Sand Sea with undulating mountains of sand (whalebacks) that finger out southward into remarkably parallel longitudinal (seif) dunes beyond which Landsat images show discontinuous, elongate clusters of crescentic dunes (barchans) aligned along the same arcuate stream lines as the seifs of the Great Sand Sea. Each procession of dunes maintains its alignment with the air stream whether it rises with the land or descends escarpments, most of which face southward (downwind). The barchan dunes are modern to late Holocene in age as they override the early to middle Holocene sand sheets, but the time of origin of the sand sea and its seif dunes is probably older.

The Great Sand Sea lies upon a subtle rise between the Qattara Depression and the sand sheets of the central Arba'in Desert. The distribution of the sand sea, longitudinal dunes and sand sheets is undoubtedly related to the topography but the aerodynamics remain unknown. It would be useful to learn if there has been a net gain or loss of sand during Holocene time. The geochronology of these features may eventually be interpreted by correlation of interdune playa deposits to deposits dated archaeologically or by radiocarbon.

GEOCHRONOLOGY

The chronology of the features of the Arba'in Desert and the rates of the processes involved in their origin are only now being ascertained by investigations at stratified archaeological sites. These sites reveal at least four major pluvial periods separated by periods of complete desiccation and intense eolian activity during the late Quaternary (Wendorf and others, 1976; 1977; Wendorf and Schild, 1980).

Late Acheulean time (approximately 200,000 \pm 100,000 years BP) was one of relatively intense spring activity at several localities in the Arba'in Desert resulting in the deposition of lacustrine marls containing late Acheulean hand axes at Bir Tarfawi and Tarfawi

West. Earlier dune sands cemented by spring and lake carbonates attest to an earlier episode of desiccation and eolian activity for which no evidence of human occupation or large animals has been found. At least one even earlier wet phase is represented by a few isolated low mounds of mudstones protected by an armor of autochthonous chert and quartz suggesting a hypersaline, lacustrine environment (Haynes, 1980a) and by the Plateau Tufa of the Kharga area (Caton-Thompson, 1952). A great age for the Plateau Tufa is indicated by the complete absence of associated artifacts and by the high degree of post-depositional lowering manifested by the Kharga depression. In the case of the chert-armored mudstones, the inverted topographic expression of what once was a basin and the complete absence of any shore features are suggestive of great age.

In the Kharga and Dakhla depressions the oldest artifacts are again late Acheulean, and are associated either with ancient springs (Caton-Thompson, 1952; Schild and Wendorf, 1977) or spring-laid tufa deposits. Along the plateau escarpment near Kharga, the artifacts are related to isolated terrace remnants of former drainages at higher levels than the present drainage (Caton-Thompson, 1952). Alluvial fan remnants high on the north slope of Gebel Nabta may correlate with these terraces or with the still older Plateau Tufa of Caton-Thompson (Haynes, 1980a).

Remnants of former elevated land surfaces were observed on gravel-capped benches at the base of Black Hill (Fig. 9.17) and the eastern side of the Gilf Kebir. The occurrences of Acheulean hand axes on these and lower surfaces suggest that the surfaces are older than $200,000 \pm 100,000$ years. At Myers' (1939) Acheulean site at the eastern side of the Gilf Kebir, hand axes occur in alluvial fan deposits lying below a gravel-capped ridge that is connected with the main plateau. Farther west and above the 1938 base camp (Bagnold and others, 1939), this ridge contains a channel fill of red, cross-bedded sand (Fig. 9.18) that may be even earlier Pleistocene age (Haynes, 1980b). Artifacts were not observed in either this channel sand or the overlying alluvial fan or pediment gravels.

The late Acheulean pluvial period ended with desiccation and dune formation which led to the abandonment of the Arba'in Desert by man and other large animals until the next pluvial. During Mousterian and Aterian time, reoccupation occurred sometime between 100,000 and 30,000 years ago. Bir Tarfawi and Tarfawi West were again inhabited by man and game animals, both making use of small lakes in the redeflated depressions. In the Kharga area, tufa depositing springs along the scarp and mound-springs on the floor of the depression were again occupied by prehistoric people (Caton-Thompson, 1952), and in the dike area between Kharga and Bir Tarfawi Mousterian artifacts were found associated with stabilized dune deposits (Schild and Wendorf, 1977).

From Aterian time to the time of reoccupation by terminal Paleolithic people, the last to live an Old Stone Age way of life (7500 B.C.), the desert was abandoned. Numerous basins were hollowed out by the wind, and dunes were again active on a grand scale, all of

which indicate hyper-arid conditions in the Sahara while late Pleistocene glaciation of the northern hemisphere was at a maximum. This out-of-phase relationship (Butzer, 1971, p. 333; Williams, 1975) is supported by other north African evidence (Street and Grove, 1976).

The Holocene pluvial period, 7500 to 4000 B.C., is evident from the large numbers of playa remnants in numerous hollows throughout the Arba'in Desert (Haynes and others, 1977). Invariably, abundant archaeological remains of Terminal Paleolithic and Neolithic age are associated with these playas, and three phases of the Neolithic occupation are associated with two distinct stands of playa lakes best displayed in the Gebel Nabta area (Wendorf and others, 1976; 1977; Wendorf and Schild, 1980).

Recognition of the large number and extent of the Neolithic playa deposits throughout the Arba'in Desert provides an insight into the extent of the pluvial represented. For every depression in which playa deposits are clearly recognizable as remnants of bottom sediments and beach deposits, there are many other hollows which in all probability contained such deposits that have since been destroyed by wind. All stages of deflation and corrasion have been observed. The occurrence of eolized (sand blasted) Neolithic artifacts in and around such hollows attests to the former presence of water to support the Neolithic occupation.

CLIMATIC CHANGES AND WATER TABLE FLUCTUATIONS

From the well-preserved stratigraphic record of Holocene climatic fluctuations, we can extrapolate back to Mousterian and earlier pluvials and assume that fluctuations were of comparable if not greater magnitude. Arguments as to whether the landforms derive from wind or water action have been reviewed by Peel (1966), and both are correct in that they represent the dominant processes in two parts of a cycle in which one climatic regime prepares the land for reworking by the other. Thus, pluvial episodes promote weathering which weakens exposures of bedrock, produce drainages that dissect the land, lakes that fluctuate and evaporate, and vegetated, dune stabilizing soils, all of which support life in relative abundance. The intense eolian activity of the hyper-arid episodes strips away the mantles weakened by weathering, erases many drainages, deflates the playa sediments, and reactivates the dunes that provide the abrasives for sand blasting. Under one regime, life flourished, similar to that of the arid regions to the south with 100 mm or more annual precipitation; under the other, it was possible for only the most adapted creatures.

The climatic extremes between full pluvial and interpluvial may have been great, even though the full pluvial precipitation was probably relatively small. Bagnold (1954) considers approximately 24 mm per year to be the minimum to be effective in supporting a nomadic existence, but this amount of precipitation could not produce the numerous lakes of Neolithic time. The present precipitation of 100-200 mm in northernmost Egypt and in north-central Sudan to the south (Oliver, 1965) is inadequate to support either lakes or rivers. It is likely, therefore, that full pluvial conditions were at least as

wet in the Arba'in Desert, and possibly augmented by reduced temperatures in order to support standing bodies of water of the size of Nabta Playa and pluvial Lake Kiseiba which extended along the Kiseiba escarpment. The water at Lake Kiseiba was deep and persistent enough to produce morphologically distinct beaches with rounded pebbles (Haynes and others, 1977). McHugh (1980) estimates 200-600 mm of precipitations were necessary to support the animals shown in the Neolithic rock art of Gebel Uweinat and the Gilf Kebir.

There are good indications that interpluvials were even drier than today (Wickens, 1975). Grove and Warren (1968) find support for this in central Sudan, where a succession of stabilized dunes (low and high Qoz) reflects late Pleistocene aridity extending to 10°N latitude. Cores taken at Merga Lake produced Holocene bottom sediments in which there is an evaporitic layer devoid of pollen, clear evidence that it was drier in the recent past (Haynes and others, 1979). Mehringer has made similar findings at Faiyum and the Siwa area (Mehringer and others, 1979). At Bir Tarfawi West, pre-Mousterian dune sands underlie the present basin floor and indicate deeper deflation and therefore a deeper water table during the interpluvial.

Solution features observed on the Limestone Plateau, wadi gravels of the Kharga area, and those on the limestone outlier of Gebel Nabta predate the Neolithic pluvial and have been severely modified by wind abrasion. Subsequent precipitation during the Neolithic pluvial failed to renew tufa deposition along the Kharga escarpment or to leave pronounced solution features on limestones other than possibly minor rillenstein. In addition, the Bir Tarfawi-Tarfawi West lacustrine deposits are for the most part chemical precipitates and not the slope-washed muds that make up the Neolithic lacustrine deposits. These findings suggest that significant differences existed in the character of the latest pluvial compared to the earlier ones.

Further evidence that the Acheulean pluvial and earlier ones were different than the Neolithic one is indicated by the abundant artesian springs active during late Acheulean time and by the terrace gravels along the scarp of the Limestone Plateau in the Dakhla-Kharga areas (Caton-Thompson, 1952).

A soil mantle over carbonate rocks can be very effective in accelerating their dissolution because enriched CO₂ of the soil gas combines with precipitation to produce carbonic acid. Such soils, relics of which have been observed on the Limestone Plateau and on Gebel Nabta, probably required several millenia to form and to be effective in producing the solution features observed. They suggest long sustained pluvial conditions (greater precipitation as well as reduced evaporation) as compared to the relatively brief intermittent rainy conditions indicated for the Neolithic pluvial by slope washed muds interbedded with dune sand and by the lack of all but minor solution features on limestones. Furthermore, several outcrops of granite, in the El-Tawila area (Issawi, 1971) in particular, display relict spheroidal weathering (Fig. 9.21) that probably formed under a soil mantle before the surrounding plain (Atmur El-Kibeish) was lowered to its present level.

Another indication of the differences in the nature of Neolithic and pre-Neolithic pluvials is the height of the water table. At Bir Tarfawi and Tarfawi West the Acheulean spring deposits indicate a water table at least 12 meters higher than today and at least 8 meters higher during Mousterian time, but there is no evidence of a Neolithic rise there. Elsewhere in the Arba'in Desert the Neolithic playas formed from runoff which created perched water tables and raised local ground water levels whenever local recharge could occur (Haynes and Haas, 1980). At Bir Tarfawi and Tarfawi West the catchment areas may have been too small, the infiltration rate too high, or the evaporation rates too high to create lakes in Neolithic times. On the other hand if such lakes existed all remains may have been lost to dessication because they would have had a weak, sandy composition with little clay available for cohesion. However, the near lack of Neolithic artifacts argues against there ever having been lakes there during this time. Isotopic studies on ground water are currently underway to see if infiltration may have been direct to the water table, thus producing a recharge bulge.

DISCUSSION AND CONCLUSIONS

If the extremes of Neolithic pluvial precipitation and post Neolithic hyperaridity were as great as indicated, the amplitude of earlier cycles must have been even greater and/or longer because the scale of alluvial deposition and deflation indicates that greater energy was expended in the earlier cycles. Each fluctuation in the water table would weaken the ground surface by salt weathering at the capillary fringe as water levels dropped with the onset of aridity. The water table would then be the ultimate control on deflation and because of its planar surface over most areas this mechanism may have been the major factor in creating some of the planar deflational surfaces of the Arba'in Desert such as the surface of the Atmur El-Kebeish. Once the capillary fringe had dropped permanently below the surface, and the destructive energy of wetting and drying was removed from the system, only the wind and local precipitation would be left to work on the surface rocks. This condition appears to have been reached before late Acheulean time because the major geomorphic features of the Arba'in Desert had been established by then.

The origin of the Atmur El-Kebeish appears to be related to a combination of persistent high velocity winds out of the NNW over the Great Sand Sea (a major source of abrasives) and a very low gradient (1:1400) capillary fringe fluctuating in permeable, friable sandstone. The El-Tawila granite is not so permeable, but surrounded as it is by Nubian sandstone, the concentration of water along the contact may have accelerated weathering, subsequent erosion, and slope retreat to leave the few positive features that occur on the Atmur El-Kibeish. Except for Gebel Tawila, a sandstone inlier within the outcrop of granite (Issawi, 1971), these are rounded hills of either granite (Fig. 9.21) or quartz pegmatite.

If during a hyperarid phase basins were scoured below the piezometric surface of a subsequent high water table, artesian springs could result where permeability factors and structural factors per-

mitted feeder paths to reach the surface. The chaotic stratigraphy of Acheulean-Mousterian age springs in Kharga reported by Caton-Thompson and Gardner (1932) support Beadnell's (1909; 1933) suggestion that some springs burst forth through the confining mudstone as the pressure of a rising water table exceeded the confining pressure of the deflated aquiclude.

The Acheulean springs at Bir Tarfawi and Tarfawi West probably formed as a result of a similar rise in the water table where the confining calcrete was thinnest in erosional hollows formed during the preceding hyperarid phase. The evaporation of and precipitation from the spring waters then produced the younger calcrete cementing the late Acheulean hand axes at Bir Tarfawi. This cycle may have occurred more than once at both Kharga and the Bir Tarfawi-Tarfawi West area, but the main effects in determining the present configuration of the Arba'in Desert occurred no later than late Acheulean time. If this model is correct, then the Atmur El-Kibeish became a relatively stable surface just prior to, or early in, late Acheulean time. The calcrete of the 200 m surface west of Gebel Nabta is similar to that on the Atmur and also has late Acheulean artifacts on it. It appears, therefore, that the Atmur El-Kibeish extended at least this far eastward over the Kiseiba-Dungal depression before the hyperarid interval during which the depression was deepened (Fig. 9.4).

Some deepening of the Kharga and Dakhla depressions may also have occurred in post Acheulean time. At present, all of the late Acheulean artifacts have been found within spring conduits, so it is not possible to reconstruct from living floors the height of the surface occupied by Acheulean people. However, the floor of the depressions is not likely to have been much more than about 20 m higher than today, if that.

It is not known when dissection of the Limestone Plateau began. If the relict terra rossa soil there is of Pliocene age, eolian destruction of the surface may have begun in response to Pleistocene climates. The soil may correlate with the relict red soils of central Sudan mentioned by Sandford (1935a) and apparently visible in Gemini II photographs (see El-Baz, Chapter 4). The Sudanese relict soil (it may be several soils) appears to be truncated on a grand scale by the deflational surface of the Arba'in Desert, and is overlain in places by eolian deposits, some of which may be Pleistocene in age.

Until more detailed investigations are undertaken, the origin of the Arba'in Desert and the effectiveness of various processes therein can only be outlined in the very general and qualitative terms expressed here. At present, it appears that in Pliocene time more warm humid conditions prevailed over a land surface several hundred meters higher than the central Arba'in Desert is today. The Pleistocene brought on desiccation that lowered water tables and converted rivers to wadis, and deflation that began to strip away the red soil presumably made vulnerable by a decreasing cover of protecting plants. Eventually wind erosion progressed to a point where drainages were destroyed and the armor provided by gravel stream beds left some reaches as pebble-armored sand sheets and others as sinuous, gravel-

capped ridges standing above wind scoured bedrock veneered with eolian sand.

If this stage had been reached by 500,000 years ago, as seems likely, and if the last major episode of lowering began near the beginning of the Pleistocene (approximately 2 m.y. ago), then roughly 200 m of lowering occurred in 1.5 m.y. for a rate of only 1.3 cm/100 yrs. Actual rates would have been higher because only part of this time was spent in hyperaridity. In the subsequent half million years, the rate of overall lowering of the Arba'in Desert has been slight. Only in localized areas of relatively soft sediments have rates exceeded the earlier estimate. Remnants of Neolithic playa deposits near Bulaq stand 15 m above the basin floor and their deflation probably did not begin until after 6000 BP. The minimum rate of deflation would be 25 cm/100 yrs. and could have been considerably greater if deflation started later in response to Roman agricultural practices (Haynes and others, 1977), but these soft, friable playa or semi-playa (Embabi, 1972) deposits are considerably more erodable than most bedrock.

During the late Acheulean, pluvial basins filled with spring-fed lakes, which attracted people from central Africa into the Sahara. Soils stabilized wind-driven sand and weathered bedrock, making another increment susceptible to deflation in the next arid part of the cycle.

By Mousterian-Aterian time, 100,000 to 30,000 BP, all but minor topographic features and lake basins had reached the configuration we see today. During Terminal Paleolithic-Neolithic times 9,500-6,000 BP, numerous (probably hundreds) basins filled with shallow ephemeral lakes whose sediments are in the final stages of complete removal by wind. Another millenium with present climatic conditions may see the destruction of virtually all remnants of the playa muds.

On the basis of their stratigraphic position and lack of even moderate paleosols, most of the major eolian deposits of the Arba'in Desert are clearly Holocene in age. The buried paleosols in the sand sheets indicate stability during Neolithic time, and older stabilized dune deposits are only minor deposits preserved at a few places such as Bir Tarfawi, Tarfawi West, and Nabta Playa. Such ancient dunes are more prevalent in Sudan south of the Darb El-Arba'in Desert (Grove and Warren, 1968).

A major unanswered question is the age of the Great Sand Sea. No paleosols have been recognized there, and their stratigraphy is unknown. Future effort in this regard should be directed toward investigation of playa deposits and archaeological sites around the southern borders of the Sand Sea with the hope that the sand could be stratigraphically related to datable sediments.

Of critical importance to the future of irrigation for agriculture in the oasis depressions is recognition of the fact that the best agricultural soils there, the Neolithic playa deposit and the early historic semi-playa deposits, are the most deflatable deposits.

This fact, in conjunction with the extremely high evaporation rate and the reliance on "fossil" ground water for irrigation, constitutes a very tenuous economic situation whereby a combination of 1) depletion of ground water, 2) soils poisoned by salts, and 3) high rates of deflation can result in gradual devastation just as it did when the aquifer in the "Shallow Water Sandstone" was depleted in Roman times (Haynes, not dated).

Furthermore, from the paleoclimatic history reviewed here it should be abundantly clear that the role of man in desertification is minor compared to that of natural change. In fact, except for the sensitive fringe areas and the oases where ground water is being over-exploited (Haynes, not dated), his role is insignificant. But these are the only inhabited areas of deserts, so from a provincial point of view the result of man's activities can be disastrous. Not until the next pluvial, perhaps thousands of years from now, will aquifers be recharged and stable vegetation established. In all probability the climate will at best be semi-arid.

Results of the Viking landings on Mars (Viking Lander Imaging Team, 1978) reveal that there are features on the surface that are more similar to some parts of the Western Desert of Egypt than to most other places on Earth (Bagnold, 1978; Haynes, 1978; El-Baz, 1978b) and salts resulting from evaporation from the capillary fringe in the Arba'in Desert are believed to be possible analogs for Martian surface crusts (Prestel and others, 1979). On the other hand, the physical-chemical conditions on Mars are so different from those on Earth that exact analogs seem unlikely. Considerable caution, therefore, should be exercised in proposing terrestrial analogs of Martian processes, landforms, and mineralogy, even if large-scale climatic cycles occurred there as they have during the Pleistocene on Earth.

ACKNOWLEDGEMENTS

This work was supported by the National Geographic Society, Smithsonian Foreign Currency Program grants FR4-60094 and FC 80140100, National Science Foundation Grants GS-36959 and EAR 77-10109, and was performed as part of the Combined Prehistoric Expedition sponsored by Southern Methodist University, the Polish Academy of Science, and the Geological Survey of Egypt. For this opportunity I owe special thanks to Fred Wendorf (SMU) and Bahay Issawi (GSE). I thank R. A. Bagnold, A. T. Grove, D. L. Johnson, P. J. Mehringer, Jr., R. F. Peel, and the late W. B. Kennedy Shaw for helpful discussion and constructive criticisms.

**Page Missing in
Original Document**

Chapter 10

WIND PATTERNS IN THE WESTERN DESERT

FAROUK EL-BAZ and R. W. WOLFE
National Air and Space Museum
Smithsonian Institution
Washington, D.C. 20560

ABSTRACT

The Western Desert is part of the driest region on Earth, where the incident solar radiation is capable of evaporating 200 times the amount of precipitation. For this reason wind is the main agent of erosion and deposition in a completely eolian environment. Data on wind velocity and direction are analyzed in this paper to establish their relationships to sand transport and orientation of dunes. Surface wind data are summarized for 42 meteorological stations between 15° and 35° N latitude and 15° and 41° E longitude. The summaries are presented in the form of graphs showing the patterns of sand-moving winds in wind roses, sand-drift potential in resultants, and streamlines. The basic patterns agree with the overall southward direction of prevailing wind, and thus of general sand transport directions. Variations from this general pattern are believed to be due to interaction between the wind and local topography. Prevailing wind directions in the Western Desert are also analyzed in terms of seasonal wind circulation patterns in North Africa. Because of the scarcity of data, it is recommended that automated meteorological stations be used to gather information on local winds in the open desert, particularly in the southwestern part, which is important for analog correlations with Mars.

INTRODUCTION

As part of the eastern Sahara, the Western Desert is one of the driest places on Earth. The "aridity index" of much of this desert is 200, which means that the incident solar energy is capable of evaporating 200 times the amount of precipitation received (Henning and Flohn, 1977). Because of this extreme aridity, wind is the main agent of sculpture in this desert. Wind, air moving more or less parallel to the surface of the ground, dismantles scarps, deepens hollows and erodes exposed rocks. The products of erosion are either hurled in the atmosphere as dust, accumulated in the form of sand sheets and dunes, or are left behind as coarse lag deposits.

Thus, an understanding of the prevailing wind directions and their variations is necessary to the study of eolian depositional and erosional features of this desert. In this paper we present a preliminary analysis of the available wind data and their relations to known directions of sand dunes.

Much of the basic research on dune classifications and sand movement has been carried out in the Western Desert. Based on his observations in this desert, Bagnold (1933; 1941; Bagnold and others, 1939) charted the major dune locations and discovered the basic principles of sand transport by wind. He attributed the main direction of dunes to a clockwise circulation of wind about a center near the Kufra Oasis in southeastern Libya.

Bagnold's early observations have recently been supported by studies of sand dune patterns as revealed by photographs taken from space (Fig. 10.1). Gifford and others (1979, p. 219) established that "the dune orientations change from north-northwesterly in the northern desert to north-northeasterly in the south. The dunes are intimately associated with scarps that bound numerous depressions in the Western Desert. This relationship is believed to result from the interactions between sand-carrying winds and scarps and other topographic variations."

A preliminary investigation of sand-moving winds from 21 stations in Egypt by Wolfe and El-Baz (1979, p. 299) revealed two major wind regimes: "a narrow band of predominantly westerlies along the Mediterranean seacoast and generally north-northwesterlies throughout the Western Desert. Imposed upon these regional trends are local variations that may be attributed to topographic effects."

It is important to note here that the northeasterly trend observed on the basis of dune orientations (Gifford and others, 1979) did not show up in the wind data analysis by Wolfe and El-Baz (1979). This is basically due to the lack of wind recording stations in the southwestern part of the desert, where the dunes veer towards a northeasterly orientation. In other localities, dune orientations were found to mimic prevailing wind direction. For this reason, the local topographic setting of meteorological stations in the Western Desert must be considered when using the wind data.

The wind data used in this study were obtained from the U.S. National Climatic Center in the form of U.S. Air Force N-type summaries (Summary Form 2 - surface winds). These summaries were produced from observations by World Meteorological Organization (WMO) stations, and cover periods ranging from 7 to 13 years.

GENERAL WIND CIRCULATION

The wind circulation of northern Africa including the Western Desert of Egypt is influenced by many factors, especially the presence of seasonally semi-permanent high pressure areas and the location of the Inter-Tropical Convergence Zone (I.T.C.Z.), a discontinuity separating southeasterly and northeasterly winds (Griffiths and Soliman, 1972). The location of the I.T.C.Z. generally follows the path of the Sun with the advance of the seasons (Fig. 10.2) and may play the greatest role in determining the winds of southern Egypt and the Western Desert.

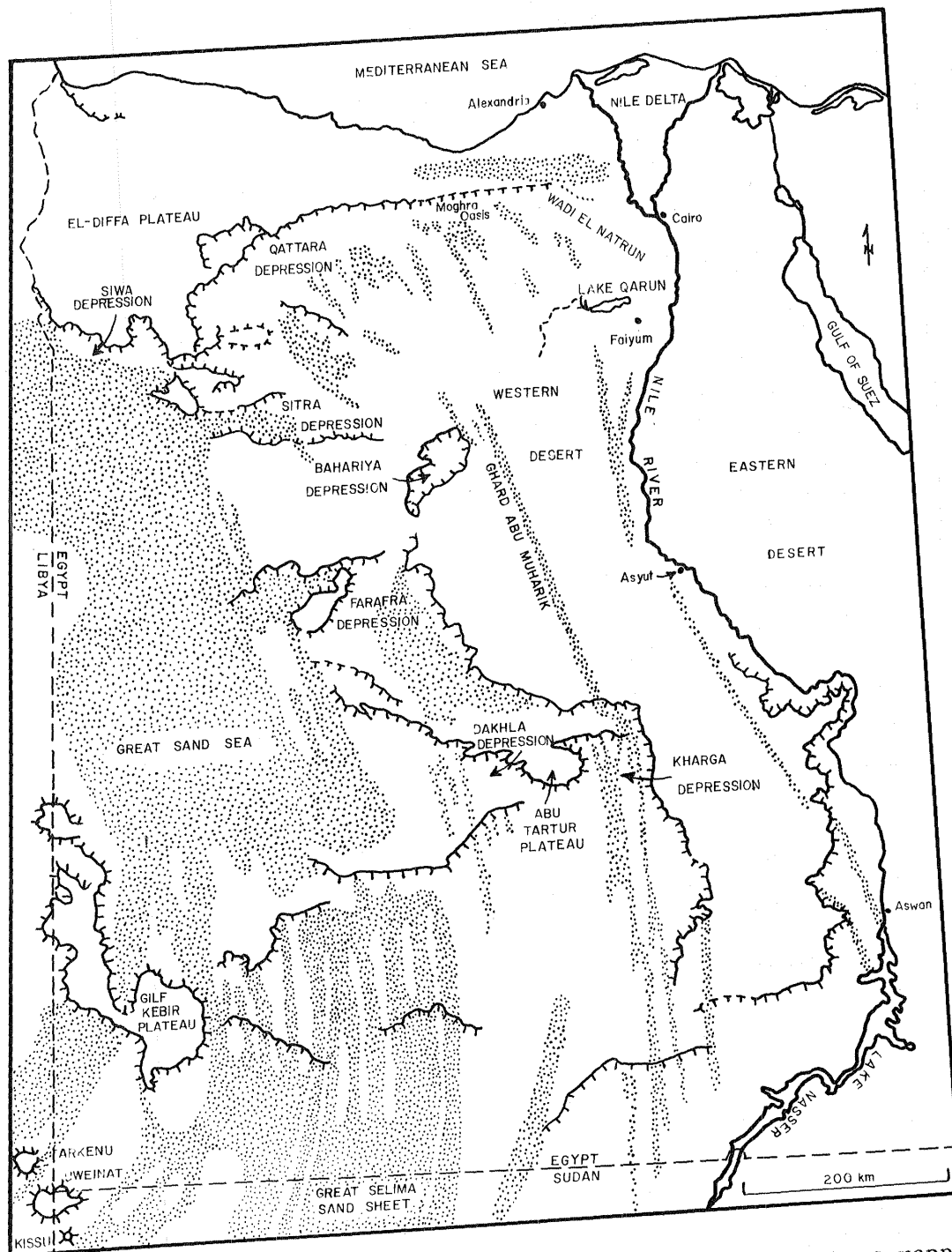


Figure 10.1 Sand dune belts of the Western Desert of Egypt as mapped from Apollo-Soyuz photographs and Landsat images. (Modified from Gifford and others, 1979, p. 225).

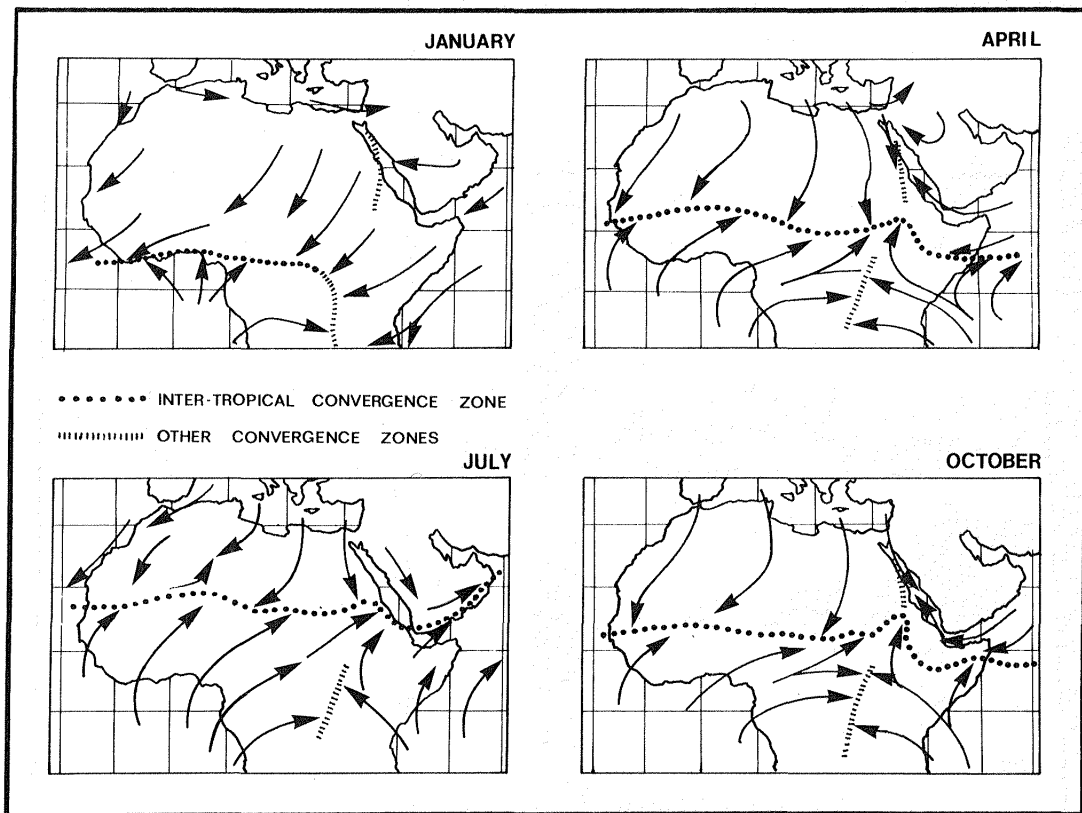


Figure 10.2 Wind circulation in North Africa as indicated by four months representing the seasons (After Griffiths and Soliman, 1972).

1. Winter (December-February): During this season, the I.T.C.Z. is far to the south and wind circulation is dominated by the presence of the large Saharan high situated in the western Sahara and modified by the passage of depressions across the Mediterranean Sea in northern Egypt. The winds, then, are generally north-northwesterly. In northern Egypt, winds are south-southwesterly in advance of the Mediterranean depressions and become northwesterly as the depressions pass. These two wind regimes are clearly seen in the wind map for January (Fig. 10.2).

2. Spring (March-May): During these months, the I.T.C.Z. begins to move northward (Fig. 10.2) and depressions become less frequent and follow tracks that are more southerly than in winter. Often these depressions are accompanied by strong southerly winds and may cause severe sandstorms.

3. Summer (June-September): The I.T.C.Z., which reaches its northerly limit during July, is located in northern Sudan (Fig. 10.2). During this season winds are generally northerly, even in northern Egypt. Generally, winds are stronger, blow more frequently, and are less variable than in other seasons.

4. Autumn (October–November): Like Spring, Autumn is a transition season with the I.T.C.Z. retreating southward. This retreat is more rapid than the Spring advance. With the exception of Aswan, this is the season of lowest wind speed (Griffiths and Soliman, 1972).

INTERACTIONS OF WIND AND SAND

Wind Data

Surface wind summaries for 42 observing stations between 15° and 35°N and 15° and 41°E listed in Table 10.1 were selected for analysis (Fig. 10.3). Of these, half (21 stations) are in Egypt, including the Sinai Peninsula. Only 9 stations cover parts of the Western Desert including eastern Libya, but none are located in the southern and southwestern parts of the desert. A guide to these and other weather summaries for the entire world is given by Ownbey (1978).

No details about the placement of anemometers or frequency and resolution of observation are included in the N-type summaries. However, World Meteorological Organization guidelines (WMO, No. 8 TPB)

Table 10.1. Name and designation of 42 wind stations whose data were studied in this report. See locations in Figure 10.3.

| STATION | WMO No. | STATION | WMO No. |
|---------------|---------|-------------------|---------|
| 1. Abu Hamed | 62640 | 22. Gulf of Suez | RS012 |
| 2. Abu Suer | 62438 | 23. Helwan | 62378 |
| 3. Agedabia | 62055 | 24. Jeddah | 40477 |
| 4. Alexandria | 62318 | 25. Jerusalem | 40184 |
| 5. Aswan | 62414 | 26. Kassala | 62370 |
| 6. Atbara | 62680 | 27. Kharga | 62435 |
| 7. Badanah | 40357 | 28. Khartoum | 62721 |
| 8. Bahariya | 62420 | 29. Kufra | 62271 |
| 9. Benina | 62053 | 30. Luxor | 62405 |
| 10. Cairo | 62366 | 31. Manqabad | 62393 |
| 11. Dakhla | 62432 | 32. Mersa Matruh | 62306 |
| 12. Derna | 62059 | 33. Port Said | 62333 |
| 13. Eilat | 40199 | 34. Port Sudan | 62641 |
| 14. El-Adem | 62063 | 35. Quseir | 62465 |
| 15. El-Arish | 62336 | 36. Red Sea North | RS011 |
| 16. El-Tor | 62459 | 37. Salum | 62300 |
| 17. Faiyum | 62318 | 38. Siwa | 62417 |
| 18. Farafra | 62423 | 39. Suez | 62450 |
| 19. Gaza | 62338 | 40. Tanta | 62438 |
| 20. Gialo | 62161 | 41. Turaif | 40356 |
| 21. Giarabub | 62176 | 42. Wadi Halfa | 62600 |

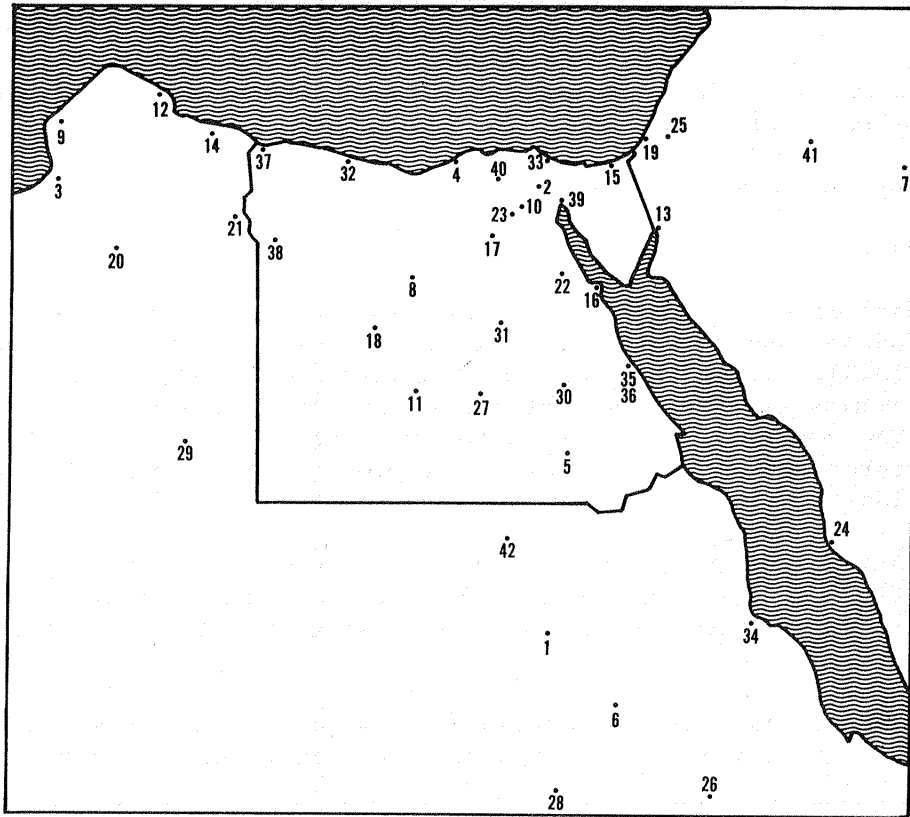


Figure 10.3 Location map of 42 wind stations from which data were analyzed (See Table 10.1 for name and number of individual stations).

recommend placement of anemometers 10 m above the surface and recording winds to the nearest one knot and to the nearest 10° direction. The data are summarized by month (in some cases an annual summary is available) and presented as frequency of occurrence in 15 (sometimes 8) directional classes corresponding to points of the compass, and 5 to 9 velocity classes shown in Table 10.2. Calm and variable winds are tallied separately.

Sand-Moving Winds

The basic expressions for the movement of sand by wind were developed by Bagnold (1941) based on field and laboratory observations. He assumed that a sand particle at rest would be about to move when the force of wind on the particle equaled the particle weight. The static threshold drag velocity, V_* describes these conditions, and is given by:

$$V_* = A \left(\frac{\rho_p - \rho_f}{\rho_f} g d \right)^{1/2} \quad (1)$$

Table 10.2 Wind velocity classifications in WMO data.

| 5 Classes | 9 Classes | |
|----------------------------------|----------------------|----------------------------------|
| 1 - 6 knots 0.5-3.1 m/sec | 1 - 3 0.5-1.5 | 4 - 6 knots 2.1-3.1 m/sec |
| 7 - 17 knots 3.6-8.2 m/sec | 7 - 10 3.6-5.1 | 11 - 16 knots 5.7-8.2 m/sec |
| 17 - 27 knots 8.7-13.9 m/sec | 17 - 21 8.7-10.8 | 22 - 27 knots 11.3-13.9 m/sec |
| 28 - 40 knots 14.4-20.6 m/sec | 28 - 33 14.4-17.0 | 34 - 40 knots 17.5-20.6 m/sec |
| > 40 knots > 20.6 m/sec | | > 40 knots > 20.6 m/sec |

where A is a constant; p , particle density; f , fluid (air) density; g , acceleration of gravity; and d , particle diameter. For medium sand (0.25 mm), the threshold drag velocity is about 0.22 m/sec. Once sand has begun to flow, the drag velocity decreases to 0.19 m/sec., which is called the dynamic threshold drag velocity, V_*' (Bagnold, 1941).

The wind velocity, v , at any height, z , near the surface can be related to the threshold drag velocity by:

$$v = 5.75 V_* \log z/k \quad (2)$$

where k is the height below which the velocity is zero. This height is related to the roughness of the surface and is approximately equal to 1/30 of the diameter of grains making up the ground surface (Fig. 10.4). For moving sands, a new roughness parameter, k' , is observed and may be approximated by height of ripples on the surface. This height ranges from 0.3 to 0.8 cm for sandy surfaces. The corresponding wind velocities, V_t , at height k' range from about 2.5 to 3.0 m/sec (Fig. 10.4).

To assess the sand-moving potential of winds recorded by meteorological stations, the wind velocity, v_t , at the height, z , of the recording instrument corresponding to the threshold wind velocity at height k' , must be determined from a modification of equation (2) as follows:

$$v_t = 5.75 V_* \log (z/k') + V_t \quad (3)$$

Table 10.3 Sand-moving potential of winds. See text for description of parameters.

| | k' | $V_* (10 \text{ m})$ |
|------------------------------------|--------|----------------------|
| Initiation of sand movement | 0.3 cm | 6.96 m/sec |
| | 0.8 cm | 6.92 m/sec |
| Maintenance of sand movement | 0.3 cm | 6.39 m/sec |
| | 0.8 cm | 6.42 m/sec |

where v_t is the threshold wind velocity at height z (10 m) and V_t is the threshold wind velocity at height k' . The results of these calculations for some cases are shown in Table 10.3. Although threshold wind velocities for sand movement as measured at 10 m range from 6 to 7.0 m/sec., other workers (Brookfield, 1970; McKee and others, 1977) have used the value 4.6 m/sec. To facilitate comparisons with previous studies, we also have chosen the same value. Possible errors arising from this choice will be discussed later.

Sand Drift Potential

Bagnold (1941) showed that the rate of sand transport, q , across a unit width is proportional to the cube of the dynamic threshold velocity, V_*' , namely:

$$q = C \left(\frac{d}{D} \right)^{1/2} \frac{\rho_f}{g} V_*'^3 \quad (4)$$

where C is a constant related to the degree of sorting of the sand, and ranges from 1.5 for well-sorted sand to 2.8 for poorly-sorted sand; D is 0.25 mm, the diameter of "standard" sand; d is the average diameter of sand in the area studied; ρ_f is the fluid (air) density; and g is the acceleration of gravity.

The rate of sand transport can be calculated from meteorological observations by substitution of equation (3) into equation (4) as in the following steps:

$$q = Bv_e^3 \quad (5)$$

where

$$B = C \left(\frac{0.174}{\log(z/k')} \right)^3 \left(\frac{d}{D} \right)^{1/2} \frac{\rho_f}{g} \quad (5a)$$

and

$$v_e = (v - v_t) \quad (5b)$$

v_e is the wind velocity in excess of the threshold velocity. The constant B is evaluated for several cases in Table 10.4. The amount of sand transported across a unit width, M, can be determined by multiplying the rate by the time wind is blowing, t, as follows:

$$M = qt = B(v - v_t)^3 t \quad (6)$$

PROCEDURES OF COMPUTATION

Wind data were converted to computer readable files as matrices of direction and velocity, and ordered by month and station. All computations of sand-moving winds and sand drift potential were performed on these raw data.

Winds of velocities less than the threshold wind velocity, v_t , at the height of the anemometer are not capable of moving sand and, therefore, are excluded from consideration. Because the threshold wind velocity falls within a velocity class interval rather than dividing classes (Fig. 10.5), the frequency of occurrence in that particular class must be weighted according to where v_t falls within the

Table 10.4 Evaluation of the constant B for sand transport potential.

| Sand Size | d(mm) | k'(cm) | C | /g | B (kg-sec ² /m ⁴) |
|------------------------------|-------|--------|-----|-----------------------|--|
| well-sorted medium sand | .25 | .3 | 1.5 | 1.25X10 ⁻⁶ | 2.26 |
| poorly-sorted medium sand | .25 | .8 | 2.8 | 1.25X10 ⁻⁶ | 6.21 |
| well-sorted coarse sand | 1 | .3 | 1.5 | 1.25X10 ⁻⁶ | 4.52 |
| poorly-sorted coarse sand | 1 | .8 | 2.8 | 1.25X10 ⁻⁶ | 12.4 |

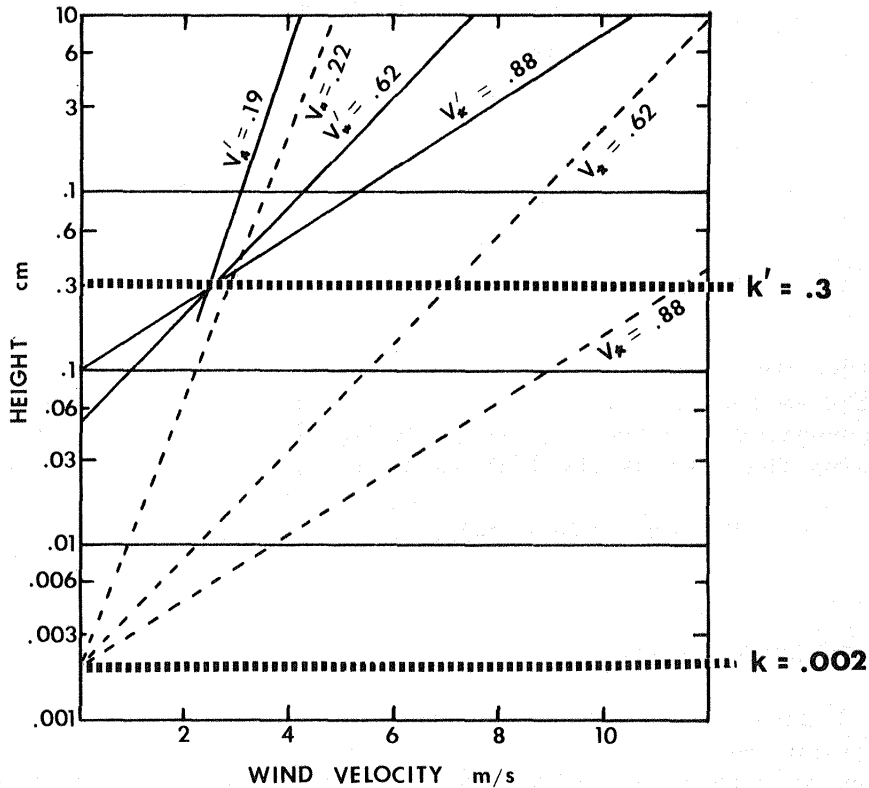


Figure 10.4 Plots illustrating relation of wind velocity to height. (See text for explanation).

interval. This assumes, probably unrealistically, that the frequencies of wind velocities are equally distributed within a given velocity interval. Most likely, this procedure tends to over estimate the frequency of sand-moving winds.

A similar sort of error arises from the compression of the data into fewer velocity classes as shown in Figure 10.5. Data originally summarized in nine velocity classes were compressed into five classes. Computation of frequency of sand-moving winds by the above method resulted in over-estimating their frequency by 20%. Wind distributions are commonly shown as circular histograms (wind roses) in which the arms are oriented in the direction from which the wind blows and their length is proportional to the frequency winds from that direction. The frequency of winds in each direction class, F_i , is:

$$F_i = \sum_{j=1}^n f_{i,j} \quad (7)$$

where n is the number of velocity classes; and $f_{i,j}$ the frequency of winds in each direction-velocity "bin".

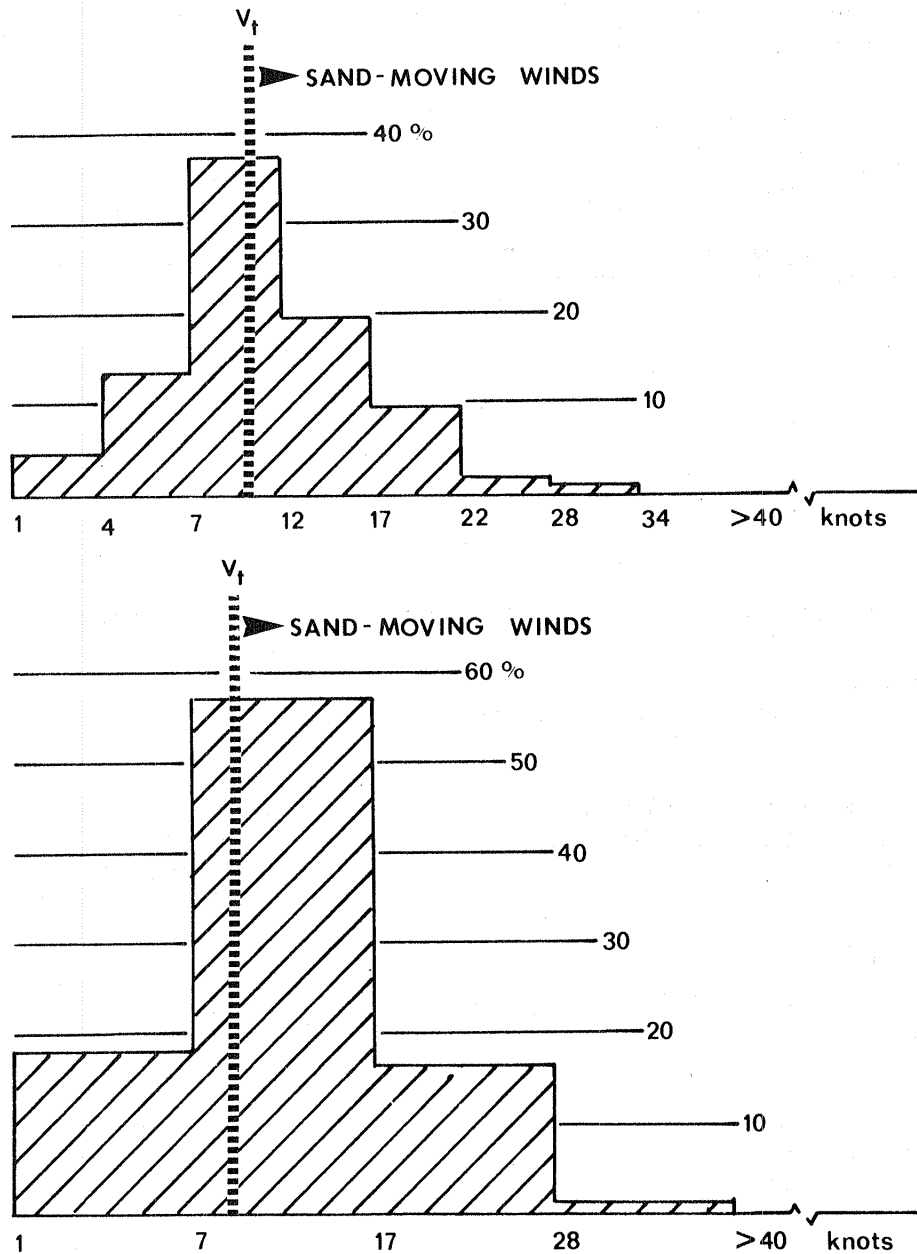


Figure 10.5 Cumulative graph of percentage of sand-moving winds as calculated in one station (Jeddah, number 24 in Figure 10.3 and in Table 10.1) during the month of January.

Wind roses may be constructed for sand-moving winds as well as for the total winds. Figure 10.6 illustrates the wind roses for all winds from stations in the Western Desert oases. Figure 10.7 shows the sand roses of the sand-moving winds in the same area covered by Figure 10.3. It is clear from this summary of the sand-moving winds in the Western Desert and adjacent regions that in the northern part of the desert a trend towards the southeast predominates. In the southern part of the desert, the trend of sand-moving winds is more toward the south.

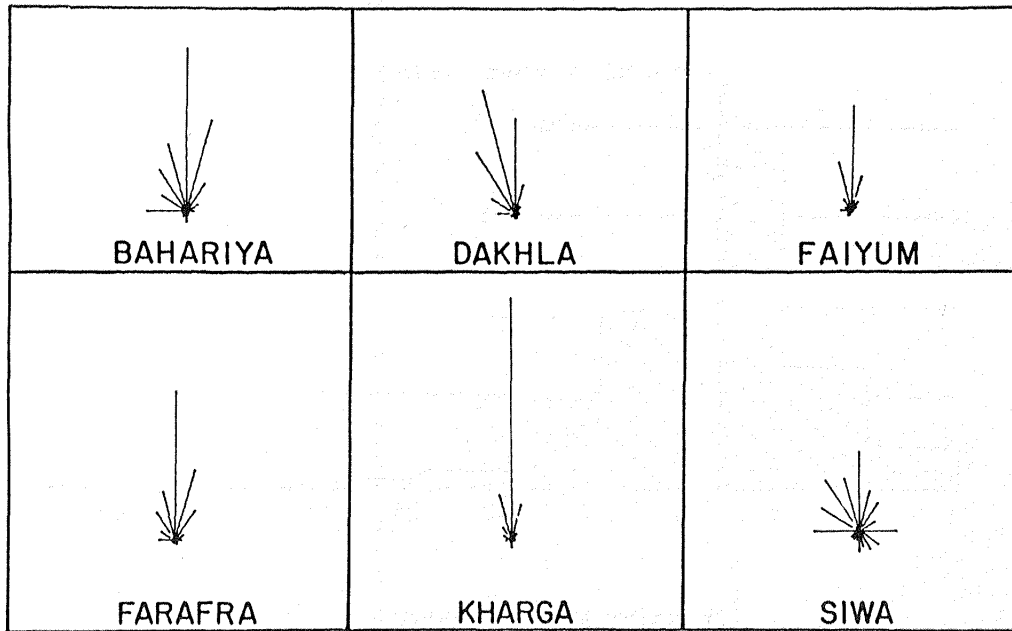


Figure 10.6 Annual summary of all winds in the six oases of the Western Desert of Egypt.

As shown previously, the potential for the drift of sand is proportional to the cube of sand-moving winds and their frequency. The sand drift potential, P_i , for a given direction is, therefore:

$$P_i \propto \sum_{j=1}^n (v - v_t)^3 f_{i,j} \quad (8)$$

where v is taken as the mid-point of each velocity class, j . Errors may be expected to arise for the same reasons outlined above. These errors are compounded by cubing the velocities and are especially prone to arise from the highest velocity class, for which there is no mid-point. Instead, an arbitrary "mid-point" is assumed, namely, 25.0 m/sec.

A summary of the sand drift potential in the studied area is shown in Figure 10.8. Comparisons of the directions in this figure with those in Figure 10.7 indicate that: (1) in the northern part of the desert, the sand drift potential is more easterly than the direction of sand-moving winds; and (2) in the southern part of the Western Desert, both sand-moving winds and sand-drift potential point to the same direction. The direction in Figure 10.8 represent resultants, which were calculated as discussed below.

For comparison with eolian features and sand distribution patterns, the wind data (recalculated as sand drift potential) are more conveniently studied as resultant (or effective) directions, r , and magnitudes, m . These resultant directions and magnitudes are com-

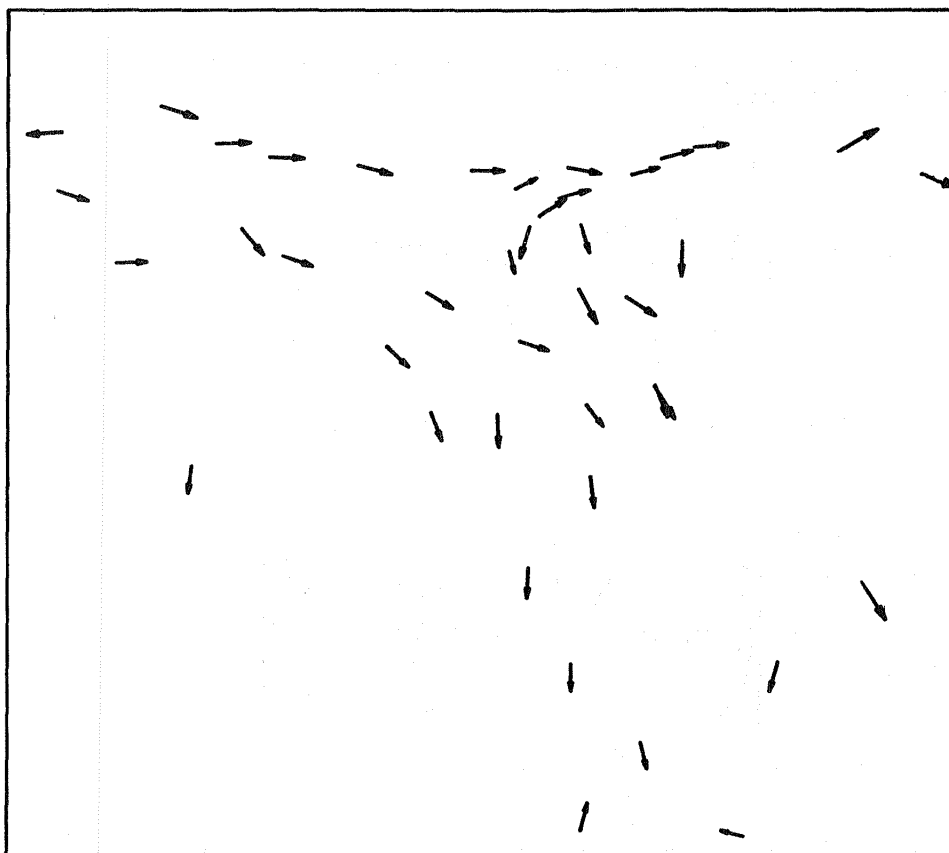


Figure 10.7 Annual summary of resultant winds at the stations shown in Figure 10.3.

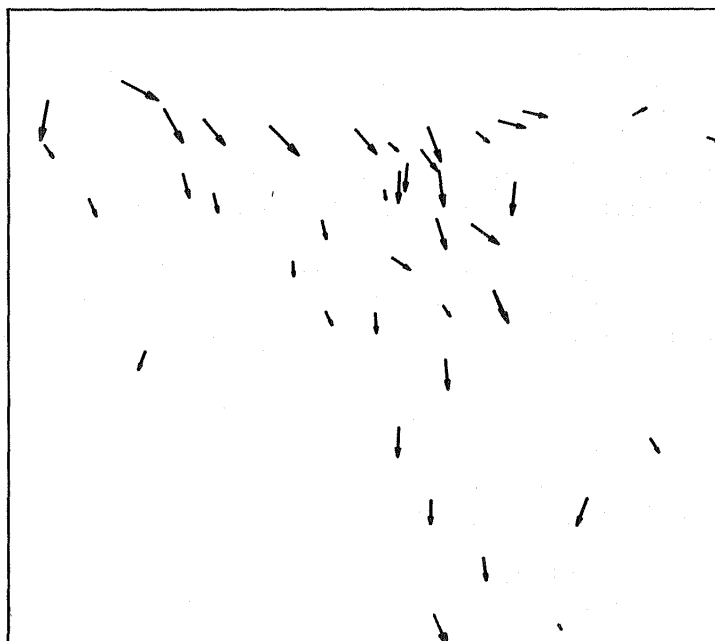


Figure 10.8 Annual summary of resultant sand drift potential at stations shown in Figure 10.3.

puted as the vector sums of frequency (sand drift potential) for each direction class by:

$$r = \tan^{-1} \left(\frac{\sum_{i=1}^n x_i \sin \theta_i}{\sum_{i=1}^n x_i \cos \theta_i} \right) + 180^\circ \quad (9)$$

and

$$m = \left[\left(\sum_{i=1}^n x_i \sin \theta_i \right)^2 + \left(\sum_{i=1}^n x_i \cos \theta_i \right)^2 \right]^{1/2} \quad (10)$$

where x_i is either the total of frequencies, or the drift potential for direction class, i , of n classes. The angle (in E-N coordinates) is the lower limit of each direction class.

Meteorological stations are scattered in the study region and are sparse in the area of most interest, the Western Desert (Fig. 10.3). This makes the patterns of wind and drift potential difficult to interpret. To alleviate this drawback, a regular, rectangular grid of points was overlaid on the region and values of direction and magnitude were interpolated from the locations of meteorological stations to the grid points. The computational procedure for this interpolation is the simple algorithm described by Davis (1973).

Essentially, the value at a given grid point is the average of the nearest n values (we chose $n=6$) weighted by the inverses of their distances from the grid point. The value, M_k , at a grid point is given by:

$$M_k = \frac{\sum_{i=1}^6 (M_i / D_{ik})}{\sum_{i=1}^6 (1 / D_{ik})} \quad (11)$$

where M_i is the value at one of the 5 nearest neighbors and D_{ik} is the Euclidean distance from that point to the grid point determined by:

$$D_{ik} = \left[(x_i - x_k)^2 + (y_i - y_k)^2 \right]^{1/2} \quad (12)$$

where x_i and x_k are the x-coordinates (longitude) of the station and grid point, respectively; and y_i and y_k the y-coordinates (latitude).

To interpolate orientations, two values were computed for each grid point, namely:

$$S_k = \frac{\sum_{i=1}^6 (\sin\theta_i / D_{ik})}{\sum_{i=1}^6 (1/D_{ik})} \quad (13a)$$

and

$$C_k = \frac{\sum_{i=1}^6 (\cos\theta_i / D_{ik})}{\sum_{i=1}^6 (1/D_{ik})} \quad (13b)$$

where D_{ik} is as previously defined and is the resultant vector orientation at station i . The orientation of a grid point, is then:

$$\theta_k = \tan^{-1} \left(\frac{S_k}{C_k} \right) \quad (14)$$

The general flow pattern of wind in the study area is shown in Figure 10.9 as annual summary of sand drift potential streamlines. This pattern clearly established the westerly flow of wind along the Mediterranean seacoast, which continues eastwards into the Arabian Peninsula. In the northern part of the Western Desert, the streamline wind flow pattern is to the south-southeast. In the rest of the desert the flow pattern is basically to the south. The veering to the

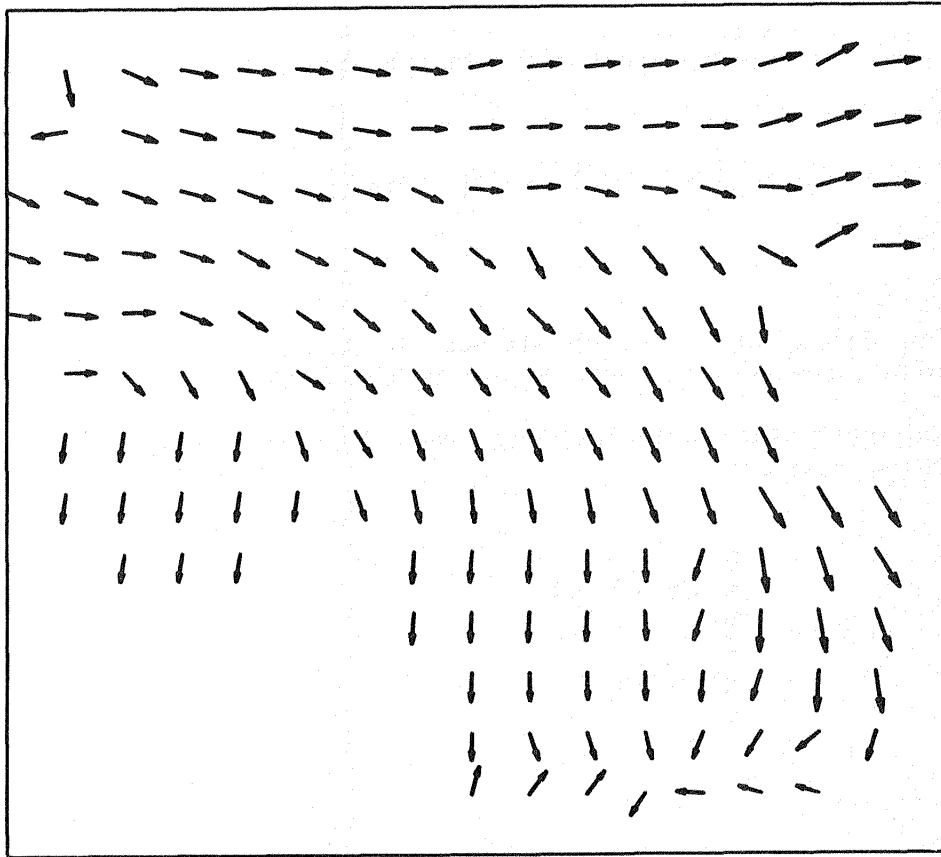


Figure 10.9 Streamlines of annual summary of resultant sand drift potential developed by trend surface analysis of data shown in Figure 10.8.

southwest near the convergence of the borders of Egypt, Libya and Sudan, which is displayed in the sand dune patterns (Fig. 10.10), is not indicated in these streamlines.

COMPARISONS WITH EOLIAN FEATURES

If we compare the annual summaries of sand drift potential in resultants (Fig. 10.8) with the orientation of dunes (Fig. 10.9) in the Western Desert of Egypt, numerous conflicts appear. Among these are:

1. In the north, the sand drift potential is basically to the east, while the dunes of Qattara are oriented in a southeasterly direction. This may be due to the fact that wind stations are placed in towns along the seacoast and reflect only the Mediterranean Sea system of winds, which may have little to do with the sand-moving winds inland.

2. In the central part of the desert, annual summaries of the sand drift potential are also more easterly than the dune orientations. This is most likely due to the fact that wind stations are in oases within depressions, which locally affect wind directions as discussed below.



Figure 10.10 Landsat image showing the deflection of dune bundles by topographic highs at the border intersection between Egypt, Libya and Sudan (E-2398-08044).

3. In the southern part of the desert, particularly the southwestern part, little correlation can be made, because of the lack of meteorological stations southwest of Kharga Oasis.

This shows that annual resultants of sand transport potential of the winds should not be used to establish dune orientation. Results of such correlations may be misleading. However, when the data are generalized by interpolation to produce annual summaries of sand drift potential streamlines (Fig. 10.9), the correlations of sand dunes in the Western Desert of Egypt (Fig. 10.1), correlate better with such streamlines.

RELATIONSHIP OF WIND DIRECTION TO LOCAL TOPOGRAPHIC SETTING

The Western Desert of Egypt is basically a rocky plain which slopes gently to the north. The Uweinat Mountain and the Gilf Kebir plateau in the southwest corner constitute the only prominences that are higher than 1900 m above sea level. The central and southern parts of the desert average 200 to 500 m in elevation, and rocks of the northern belt are less than 200 m above sea level. The generally flat plateau desert of sedimentary rocks is broken by seven major depressions including the Qattara and those that enclose the oases of

Siwa, Faiyum, Bahariya, Farafra, Dakhla, and Kharga (Fig. 10.1). Summaries of wind directions based on data from meteorological stations in the six oases are given in Figure 10.6.

Qattara Depression

The Qattara Depression is the largest of the Western Desert depressions and occupies approximately 19,500 km², or 1/15 the land area of Egypt. This depression also contains the lowest point on the continent of Africa, being 134 m below sea level. Much like other depressions in the Western Desert, its northern borders are clearly marked by a distinct scarp, whereas the depression grades into the terrain to the south (El-Baz, 1979b). The dunes of Qattara emanate from its southern part as bundles of longitudinal dunes that taper to the southeast (Fig. 10.1). This direction reasonably agrees with the inferred sand transport directions in Figure 10.8. Agreement between the orientation of dunes and inferred wind direction is probably due to the fact that southern Qattara can be considered an open plain, without scarps or other topographic barriers to affect wind circulation.

Siwa Depression

The Siwa depression is irregularly-shaped and generally elongate in an east-west direction. It is the farthest depression from the Nile Valley and is approximately 50 km long and covers 300 km²; parts of it are 60 m below sea level. About 15 km east of the Siwa depression is another depression about two-thirds its size (El-Baz, 1979c). Both depressions are bounded by faults that intersect in an "X" pattern. The southern borders of the Siwa Oasis blend with the northern boundary of the Great Sand Sea. Near Siwa, the dunes of this sand mass are sinuous and appear to have formed under varying wind regimes as suggested by the wind directions in Figure 10.6. However, yardangs along the western borders of the depression are all oriented in an east-west direction. This may have resulted from both structural control and strength of local winds from the west (Mediterranean wind system).

Faiyum Depression

The Faiyum depression is closest to the Nile Valley and occupies a circular area of approximately 1,700 km², much of which lies below sea level. The limestone cliffs of the Faiyum depression confine bundles of complex barchan chains. These dunes appear to be shifting in a south-southeast direction (Fig. 10.1). Some have reached the western borders of the fertile Nile Valley and have started encroaching on its agricultural land (El-Baz, 1979b). The alignment of the dunes along the scarp indicates the effect of that scarp in dividing the sand carrying wind towards the south rather than to the southeast (Fig. 10.1).

Bahariya Depression

The Bahariya depression is spindle-shaped and is elongate in a

northeast direction. It is approximately 95 km long and 45 km wide and covers an area of 1,800 km². The escarpment that completely encircles the depression is approximately 100 m high. The depression is unique among others in the Western Desert in that hills form a discontinuous line in its center. These hills appear to affect the local wind regime in the Bahariya depression as shown in Figure 10.6.

Farafra Depression

The Farafra depression is roughly triangular in shape and is bounded by high scarps on the east and west and a low scarp on the north. It is open towards the south where it meets the Dakhla escarpment some 200 km away. Most of the exposed rock in the depression is chalk of Maastrichtian age (Said, 1962). The eastern half of the depression is covered by dune sand. Field observations indicate that this sand mass is similar to that of the Great Sand Sea. The large dunes are gently sloping whaleback dunes, several kilometers across. Superposed on these dunes are sharp-crested, partly sinuous longitudinal dunes (El-Baz, 1979b). There is a small field of dunes that is enclosed in a small depression in the northern part of the larger Farafra depression. The dunes in this small field are oriented in the same direction as the scarps, approximately N 50°E (Manent and El-Baz, 1980).

Dakhla Depression

The Dakhla depression lies south of an escarpment that trends west-northwest from Kharga for approximately 250 km. South of the escarpment, the exposed rock belongs to the Nubian Sandstone, which covers most of the southern half of the Western Desert. The Dakhla



Figure 10.11 Landsat image showing dunes oriented in a NW-SE direction in the upper right corner and more southerly in the Kharga depression in the lower left corner (E-1110-07561).

depression is connected to the Kharga depression by level ground south of a large, arcuate escarpment known as the Abu Tartur Plateau. The wind pattern in the Dakhla depression appears to be identical to that of Kharga (Fig. 10.6). Because the Dakhla depression is open to the south, there are little if any topographic effects on wind direction and orientation of dunes.

Kharga Depression

The Kharga depression (Fig. 10.11) is aligned in a north-south direction. The succession of rocks from the floor upward begins with Nubian Sandstone, which is overlain by purple and variegated shales, phosphatic beds, Dakhla shale, chalk, Esna shales, Thebes limestone, and travertine and loess on top (Said, 1962). The depression is open to the south and southwest. The width of the depression varies from 20 km in the north to 80 km in the south. Within the depression numerous bundles of active barchans and barchan chains hamper the agricultural development of the land (El-Baz, 1979b). Hence, the effect on dune orientation of the north-south trending scarp on the eastern side of the depression are quite obvious (Fig. 10.1). North and east of the depression, the dunes point to the southeast, but within Kharga, they move due south.

Gilf Kebir and Uweinat

Beyond Kharga, and southwest of the other oases, the terrain of the Western Desert is flat to undulating; it is interrupted by a few topographic highs particularly in the southwestern corner (El-Baz and Maxwell, 1979a). The effects of the Gilf Kebir plateau and Uweinat Mountain on dune orientations are clearly visible on Earth orbital photographs (Fig. 10.10). However, the exact wind directions are not known because of the lack of recording stations in southwestern Egypt.

AUTOMATED METEOROLOGICAL STATIONS

As previously stated, a full understanding of the wind regime in the Western Desert is hampered by the lack of meteorological stations in the open desert. The present stations are located within depressions, and there are no stations in the southwestern part of the desert. This deficiency may be remedied by utilizing automated meteorological stations.

Space age technology has provided a wide variety of sensing devices that can, for example, measure air and water quality, monitor the flow within a pipeline, or detect earthquakes. It has recently been proposed that the same kind of technology be applied to monitoring climatic and meteorological conditions in remote desert regions (El-Baz, 1979d). Automated stations can obtain the measurements, average them over a period of time, and relay them to orbiting satellites. The satellites, in turn, can beam these data to Earth for analysis and synthesis.

A meteorological data collection scheme may use Earth orbiting satellites to relay data from a number of automated stations to one or

more receiving sites. There are three basic elements to such a scheme: 1) a data collection platform (DCP) connected to the sensor recorders; 2) a radio transponder with receiving and transmitting capabilities on board a satellite; and 3) a data receiving station for retrieval, processing, and dissemination of the collected data.

There are two experimental programs that utilize such a system for meteorological monitoring. These are for use in remote places that represent extremes of Earth weather: the perpetual ice sheets of Antarctica (T. Howard, pers. comm.) and the sun-scorched deserts of the American southwest (J. F. McCauley, pers. comm.).

Based on the above, it is recommended that testing of this method of meteorological monitoring via orbiting satellites be conducted in the western Desert of Egypt. The desert is ideal for this type of research, because "the free interplay of sand and wind has been allowed to continue for a vast period of time, and here, if anywhere, it should be possible in the future to discover the laws of sand movement, and the growth of dunes" (Bagnold, 1933, p. 121).

CONCLUSIONS

1. The general clockwise wind circulation pattern noted by Bagnold (1933) in the Western Desert of Egypt is supported by study of dune orientations from space images and photographs.
2. Annual wind summaries and sand drift potentials based on these summaries do not provide the same directions as those of the dunes. Generalizations by interpolation between stations correlate better with dune orientations.
3. Differences between directions of sand-moving potential and the dunes may be due to local topographic effects on the wind.
4. Depressions that are bound by north-south escarpments such as Faiyum and Kharga impose the same alignment of the dunes within these depressions.
5. Topographic highs such as the Gilf Kebir plateau and the Uweinat Mountain in the southwestern part of the desert also affect dune orientations, where the winds change directions to skirt these highs.
6. To fully understand the wind regime of the Western Desert, automated meteorological stations should be emplaced in the open desert, particularly in its southwestern parts.

**Page Missing in
Original Document**

Chapter 11

BARCHANS OF THE KHARGA DEPRESSION

NABIL SAYED EMBABI
Department of Geography
Qatar University
Doha, Qatar

ABSTRACT

The Kharga depression in the Western Desert of Egypt contains numerous north-south trending belts of barchan dunes, which create a serious problem for economic development of the region. The dune belts are oriented parallel to the long axis of the depression, and are here divided into three belts; the western belt consists of simple and compound barchans that extend from the Abu Muharik dune belt. The middle belt of barchans is smaller, but of great economic importance since it crosses the Kharga-Asyut highway. The eastern barchan belts, studied in detail, parallel the eastern scarp of the depression and consist of 261 barchans of various sizes. Analysis of barchan shape parameters indicates that the shape of the dunes remains essentially constant as growth takes place, although the degree of association of the parameters decreases as the dunes increase in size. The rate of barchan movement varies between 20 and 100 m/year, and exhibits strong correlation with dune size, ground length of the windward side and mean slope angle of the windward side. Thus, mapping of barchan distribution and measurement of their shape parameters may allow prediction of barchan movement, and will aid planning for future development in the depression.

INTRODUCTION

The Kharga Depression is one of the seven major depressions of the Western Desert of Egypt. It lies in the southern part of the desert, about 150 km west of the Nile Valley (24° to 26° N; $29^{\circ} 50'$ to $30^{\circ} 55'E$), and is the only depression that is aligned in a north-south direction. The interior of the depression is characterized by a relatively flat semi-playa or pediplain surface broken only occasionally by small, streamlined hills, groups of barchans, and barchanoid dunes. These dune belts are also elongated in a north-south direction, and are formed where sand has migrated southward across the northern scarp of the depression. Consequently, this area is well-suited to the study of barchan growth and movement (Embabi, 1967).

MORPHOLOGY OF THE KHARGA DEPRESSION

The depression is bounded by steep scarps on the east, north and northwest, and is open to the south and southwest. The surrounding plateaus vary in height from 300 to 500 meters above sea level. The

surfaces of the plateaus are characterized primarily by micro-relief landforms (small closed depressions, gullies, small wadis and yardangs). The most significant landform to the present study is the huge dune belt of the Ghard Abu-Muharik, which enters the Kharga Depression from the north. This dune belt represents the main source for barchan sands within the depression.

The depression scarps are characterized by concave, convex-concave, or step-like slopes, which are dissected by small wadis, and are covered by surficial deposits. Although the eastern scarp has a general north-south trend, it changes its alignment several times south of latitude 25°N. These changes have led to the development of several promontories, which obstruct the dunes of the eastern barchan belts. The northern and northwestern scarps have two general trends; east-west and north-south. The wadis of the northwest scarp act as passages for the sand of the Ghard Abu-Muharik, which spills over the scarp to the depression floor (Fig. 11.1).

The depression floor is a flat to undulating pediplain. Apart from the various projecting hills, the plain rises between 2 and 209 m above sea level, but most of it lies between 20 and 190 m above sea level. Most of the floor is covered either by water-laid deposits (outwash gravel and playa deposits), or by eolian deposits (dunes and sand sheets). Characteristic forms can be divided into two groups; scattered hills and eolian sculptured landforms. The hills consist of three types: the outlier hills (Taref, El-Teir, and Ganima), the en-echelon synclinal and anticlinal hills (Tarawan, El-Qarn, El-Qalaa, and El-Dibabah), and the granitic (inlier) hills in the south (Abu-Bayan hills).

Eolian landforms in the depression floor may be divided into two types: the first type is the clay plains of the semi-playa deposits, with wind-sculptured hummocks (Embabi, 1972, p. 84). These are typified by the Sherika plain in the north and the Paris plain in the south. The second type is the barchan dunes which occur in north-south trending belts in various parts of the floor. Barchan dunes can be considered the most significant landform in the Kharga Depression not only from the geomorphological point of view, but also from the viewpoint of economic development. Barchans are presently the most dynamic form in the area, and are a serious threat to existing and projected human activities.

BARCHAN DISTRIBUTION

The Kharga barchans are organized into belts that are approximately parallel to the longitudinal axis of the depression (Fig. 11.1). Although they are distributed in various parts of the floor, the barchan belts can be divided into three groups: the western, middle and eastern belts.

The western barchan belts are the extension of the great dune belt of the Abu Muharik, and form the main group of barchans in the depression. The sand dunes sweep down the northwestern scarp of the depression, forming several belts in the wadi floors, and then are

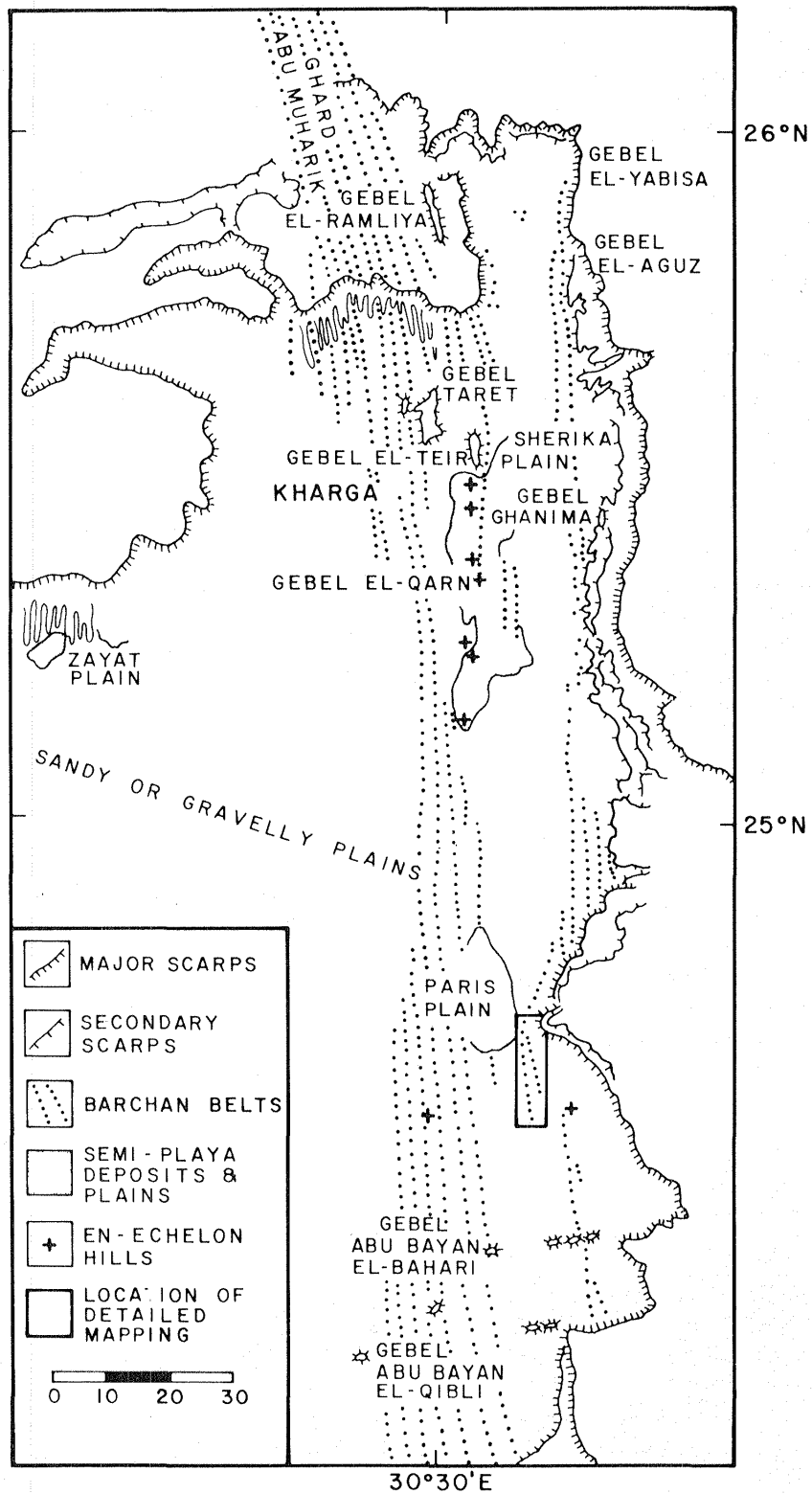


Figure 11.1 Morphologic features of the Kharga Depression. Inset shows location of Figure 11.4 (southeast of Paris Plain).

partially piled against Gebel Teref and Gebel El-Sheikh. South of these hills, the barchans are unhindered by any further obstacles. Along these belts, barchans change from simple to compound form, and are replaced by small climbing and descending longitudinal dunes or barchanoid ridges, according to local relief and sand supply.

The middle barchan belts are smaller and more localized than the western belts, although two of them are most significant. The first belt starts from the eastern tip of the northwest scarp and passes slightly to the east of Gebel El-Teir, Gebel Tarwan, Gebel El-Nadura downwind to the northern slopes of Gebel El-Qarn (Fig. 11.1). Along this belt, barchans cut the Kharga-Asyut highway and change from simple to compound to complex form due to local relief. The second important belt in this middle group consists of barchans which are trapped in the small, closed shallow basin 5 km east of Gebel El-Qarn (Fig. 11.1).

The eastern barchan belts extend from the foothills of the depression scarp opposite Gebel El-Yabisa downwind to the granitic hills in the southern part of the depression. They start and continue as one unit, running approximately parallel to the scarp before being checked by the northern slopes of the promontory facing the Paris plain. South of this promontory, three small barchan belts are present in the Doush plain.

BARCHAN MORPHOLOGY

Form

The barchans of Kharga vary between the simple compound and the complex crescentic shape. The simple form is present in various stages of development at many localities (Fig. 11.2). Generally, youthful forms are present at the upwind end of barchan belts, while older ones are present at the terminus of belts. Compound barchans develop when two or more dunes coalesce due to differential rate of movement (Fig. 11.3). The complex barchan is the largest dune, and a relati-

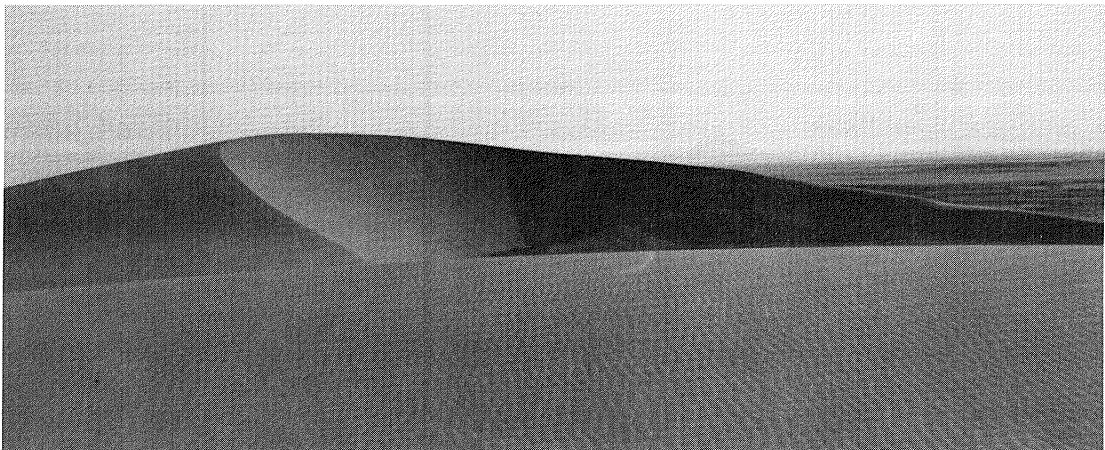


Figure 11.2 A simple barchan.



Figure 11.3 A compound barchan.

vely rare form at Kharga. It has a single major slip-face and many smaller ones on its windward slope. In many cases it acts as a source of sand for the development of new dunes.

Shape

Barchan shape parameters measured in this study include: height, length of dune, length of windward slope, width of horns, and length of horns. Kharga barchans vary from 0.5 to 25 m in height, from 30 to 650 m in length of dune, from 24 to 300 m in length of windward side, from 25 to 540 m in width of horns, and from 2 to 340 m in length of horns.

Statistical analysis of shape dimensions for a sample of 60 barchans suggests that there is a linear relationship with a high degree of association among the shape parameters (Embabi, 1978). This indicates that shape dimensions grow simultaneously at a constant rate, at any stage of development. However, because of modifications which occur during dune growth and movement, the degree of association decreases as dunes grow in size. This type of relationship exists between barchan shape dimensions in other arid regions of the world, such as southern Peru and California (Embabi, 1978).

Slope Angles and Form

Along the longitudinal axis, the barchan profile exhibits two asymmetric slopes which meet at the crest or brink of the dune. These are the leeward and windward slopes. In order to investigate the asymmetry of the two slopes, a slope profile survey was done on a sample of barchans from various localities at Kharga. In this survey, slope profiles of 34 dunes, varying between 0.9 and 15.2 m in height, were measured along the longitudinal axis. Measurements of slope angle to the nearest half degree were taken every 50 cm using an Abney level and a flat wooden rod. Although detailed results and field techniques will be the subject of another publication, the relevant characteristics of slope angles forms are the following:

1. Slope angle distribution is characterized by three sub-populations of low (0° - 12°), moderate (13° - 15°), and high (32° - 34°) angles. The low-angle group is the most prevalent on all dunes, and constitutes 92 to 97% of the total slopes on small dunes, and 82% on large dunes. This group is representative of the gentle slopes of the windward side. The second important group is the high-angle slopes which represent the slip-faces of barchans. It constitutes 7% and 15% of the total slopes of small and large dunes respectively.
2. The characteristic slope angle of both small and large barchans is 5 degrees, while on small dunes this angle is 4 degrees.
3. The slope form of the windward side is convex-concave on all dunes. Although convexities exceed concavities on all barchans, the ratio of convexity/concavity is 1.6 and 1.2 for small and large barchans respectively.
4. The leeward side is either convex, convex-straight, or straight in form. Convex and convex-straight slopes prevail on small dunes, whereas straight slopes dominate on the leeward side of large barchans.
5. The relationship between slope angles, form and dune size is supported by the following aspects: A) Slope angles of the windward side tend to increase as dunes grow in size, B) Slip-faces occupy a higher percentage of the total slope as barchans increase in size, C) The ratio of convexity/concavity on the windward side decreases as dune size increases, and D) The leeward side tends to change from convex to convex-straight, to straight as barchans grow in size.

Distribution

Barchans in Kharga, as in many other arid regions, are organized in belts parallel with the direction of the prevailing winds. In order to investigate the nature and properties of barchan distribution in belts (en masse), the belt which originates in the eastern scarp promontory facing the Paris plain (Fig. 11.1) was chosen as a repre-

sentative belt because of both its location and size. Except for a gently sloping small hill, this belt developed on a featureless plain. In addition to the absence of local vegetation and the presence of uni-directional winds, the location renders this site ideal for the propagation of crescentic dunes. In addition, the belt is of a considerable size; its length is about 20 km, and it comprises 261 dunes of assorted sizes.

The method adopted for the study of dune distribution is a modification of that used by Finkel (1959). A base map (Fig. 11.4) was prepared from aerial photographs originally at a scale of 1:20,000. The dune belt was divided into square kilometers along a base line of N 5°W for the first 6 km from the northern tip, and at N 15°W along the rest of the belt. These directions parallel the prevailing orientation of the dunes as measured on the base map. The squares parallel to the prevailing dune orientation were numbered, while those sides perpendicular to the wind direction were lettered increasing to the west. The number of barchans, regardless of size, was counted for each square. These numbers represent the density of barchans in a unit area of 1 km².

The total number of barchans in each unit area as well as the average number of dunes for each row and column are summarized in Figure 11.4. The area within the boundaries of the belt is 27 km², while the total number of dunes counted is 261. This represents an overall mean density of 9.7 dunes per km². The mean density in the numbered columns indicates a decrease in dune distribution as distance increases downwind from 37 to 5 dunes per km². The correlation coefficient between the mean of the two variables is 0.7, which indicates a relatively high degree of association between mean dune density and the distance downwind.

Similarly, the average density of the dunes in the rows transverse to the wind was computed. In this comparison, the mean dune density in row A (the western one) is lower (6.25) than that of row B (11.1), indicating that dune density also decreases in the westward direction. This tendency is in accordance with the fact that the level of the ground decreases generally in the same direction.

The decrease in dune density in a downwind direction is accompanied by an increase in dune size. This suggests that dunes merge together during their movement downwind, resulting in a decrease in the actual number of barchans and an increase in size. This rule is interrupted occasionally where newly-born dunes develop from large complex barchans, as in rows 16-18 (Fig. 11.4). In addition, the secondary reason for the decrease in dune density is the lateral spreading of dunes downwind due to the westward slope of the terrain.

BARCHAN GROWTH, MOVEMENT AND STRUCTURE

Naturally, the growth of a barchan depends on how much sand it gains or loses. This gain and loss occurs on a dune body due to sand removal from the lower part of the windward side, and deposition on the top and leeward side. Sand removal and deposition leads to the

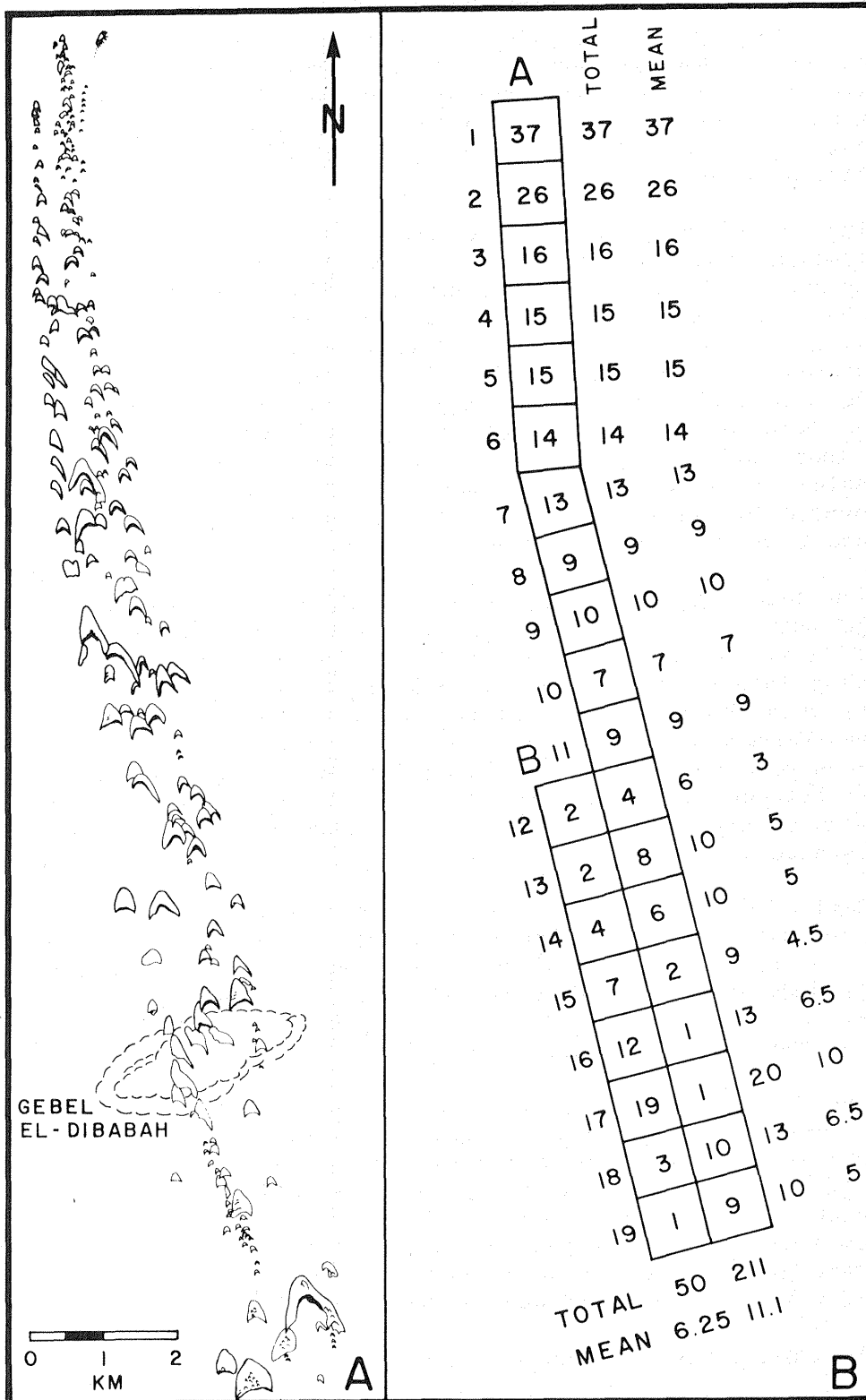


Figure 11.4 Distribution of barchans: A) Map of barchan belt south of the Paris Plain. B) Dune density (per km²) along barchan belt.

movement of barchans downwind and the development of their characteristic structure.

Barchan Growth

The presence of various sizes of barchans in the field indicates that any single dune may grow bigger with time. As shown by Embabi (1978), barchan shape dimensions grow simultaneously at a constant rate at any stage of development.

In the field, sand was observed to creep across the bare ground between barchans, especially in the lee of the horns. The sand which leaves a barchan usually accumulates on the next one which obstructs its path. For "steady-state" movement with no dune growth, the rate of sand loss must be balanced by sand gained from the upwind dune. Finkel (1959) mentioned that the rate of sand gained from the upwind dune nearly balances the sand loss in Southern Peru. Coursin (1964) has done two experiments to examine the sand balance sheet of a barchan in the region of Port-Etienne (Mauritania). In both experiments, the barchan lost more sand than it gained.

Another method of barchan growth was deduced from the study of the mass distribution of barchans east of the Paris Plain. Smaller, faster-moving dunes occasionally overtake the larger ones, and their sand blends together to form a still larger dune which soon develops the crescentic shape. This process can be seen in all its stages in Figure 11.4. It seems that the barchans of this belt grow in this manner rather than by movement of sand from the horn of one barchan to the windward side of the next. The gradual increase in the average dune size in the downwind direction supports this method of barchan growth.

Barchan Movement

Movement of barchans in the downwind direction is known to all research workers in desert geomorphology (Beadnell, 1910; Bagnold, 1941, p. 199-200; Finkel, 1959; Hastenrath, 1967). At Kharga, three attempts have been made to measure and study barchan movement. The first one was a pilot study based on field measurements (Beadnell, 1910). This study indicated that the annual displacement of dunes varied between 10.8 and 18.8 meters, and that there is an indirect relationship between dune height and rate of advance. The second study was based on a comparative study between two series of aerial photographs of 92 barchans at various localities (Ashri, 1970). This study revealed the same findings as those of Beadnell (1910).

The third study was carried out by Embabi (1979), and entailed periodic field measurements of the displacement of 25 barchans between February 1970 and February 1971. The sample of dunes was distributed at various localities in the Kharga depression, which was chosen to be representative of Kharga barchans. Dunes in this sample varied from 0.8 to 15.2 m in height, from 22 to 160 m in width, from 18 to 124 m in length of windward side, and from 2.0 to 11.8 degrees in mean slope of the windward side (Table 11.1).

Table 11.1 Shape dimensions of selected barchans in Kharga.

| Dune Displacement (m) | Dune Height (m) | Length of Windward Side (m) | Dune Width (m) | Mean Slope of Windward Side (deg.) | |
|--------------------------|--------------------|-----------------------------------|-------------------|--|-------|
| 1 | 49.6 | 2.6 | 36 | 27 | 4.33 |
| 2 | 37.0 | 9.2 | 76 | 110 | 7.30 |
| 3 | 43.5 | 4.0 | 54 | 56 | 4.60 |
| 4 | 33.7 | 10.0 | 124 | 120 | 4.58 |
| 5 | 75.5 | 2.0 | 38 | 26 | 4.34 |
| 6 | 87.0 | 1.8 | 38 | 30 | 2.60 |
| 7 | 60.8 | 2.3 | 40 | 30 | 2.80 |
| 8 | 81.0 | 1.8 | 30 | 40 | 3.06 |
| 9 | 29.6 | 7.4 | 108 | 125 | 4.78 |
| 10 | 29.6 | 8.0 | 80 | 88 | 5.83 |
| 11 | 20.8 | 15.2 | 74 | 160 | 11.79 |
| 12 | 22.0 | 11.2 | 76 | 160 | 8.38 |
| 13 | 23.1 | 12.4 | 98 | 150 | 6.65 |
| 14 | 53.0 | 1.8 | 28 | 45 | 5.07 |
| 15 | 53.5 | 3.2 | 28 | 40 | 6.64 |
| 16 | 59.5 | 3.6 | 40 | 38 | 6.35 |
| 17 | 70.0 | 2.6 | 46 | 42 | 3.93 |
| 18 | 28.0 | 7.1 | 60 | 117 | 7.78 |
| 19 | 100.0 | 0.8 | 20 | 20 | 2.00 |
| 20 | 79.0 | 2.4 | 18 | 22 | 7.22 |
| 21 | 35.0 | 5.0 | 58 | 42 | 4.55 |
| 22 | 41.0 | 4.5 | 42 | 60 | 4.50 |
| 23 | 31.5 | 6.0 | 50 | 72 | 4.56 |
| 24 | 27.5 | 9.0 | 85 | 110 | 4.57 |
| 25 | 37.5 | 4.2 | 50 | 56 | 4.65 |

As a result of this study, it was found that dune displacement varies between 20.8 and 100 meters per year (Table 11.1). Dune movement in the southern direction is controlled by several factors; the most important of which are the effective wind, dune size, slope angle and length of the windward side. The effective winds (20 km/hr) blow from the northern direction. Wind data of the Kharga meteorological station indicates that about 95% of the effective winds are from this direction. In addition, smaller dunes move faster than larger ones because the sand mass transported decreases as the dune gets smaller. The correlation coefficient between these two variables is 0.91.

High slope angles on the windward side decelerate wind velocity, resulting in a slower rate of movement. The correlation coefficient between these two variables is 0.62. The ground length of the windward side also affects the rate of dune movement. Time taken for sand grains to travel from the toe to the crest and leeward side is a function of the ground length of the windward side. The correla-

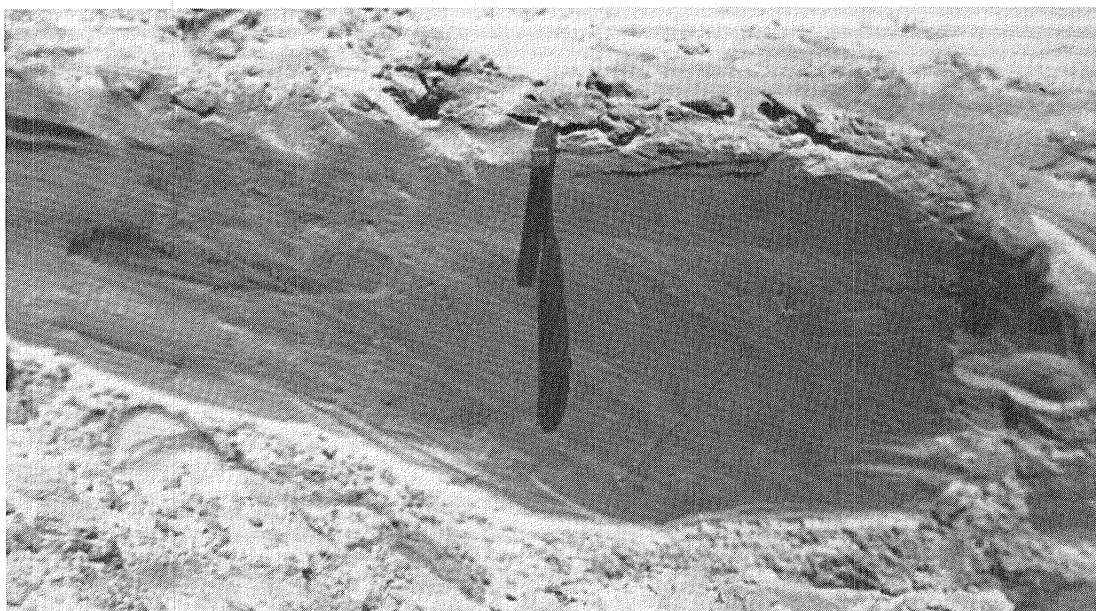


Figure 11.5 Internal structure of barchan.

tion coefficient between dune movement and ground length of the windward side is 0.84.

Consequently, 94% of the variations in the dune displacement of barchans can be correlated with three variables: dune size, ground length of the windward side, and the mean slope angle of the windward side.

Internal Structure

In order to investigate the type and scale of barchan sedimentary structures, vertical sections were cut along the longitudinal axis of two dunes in different stages of development (Embabi, 1970-1971). Analysis of the exposed stratification in both dunes reveals two major structures separated by a nearly horizontal bounding surface (Fig. 11.5). High-angle ($29-34^{\circ}$) cross stratification forms the lower part of the barchans. A set of low-angle to horizontally stratified cross-beds form the upper part of the dunes, and dip upwind.

The analysis of the exposed structures also reveals distinctive features that are characteristic of each dune. An ill-defined structure with no clear stratification forms the core of the smaller, and younger barchan. Two micro-structures (trough and reverse dipping beds) were found in the large barchan (Fig. 11.6). The angles of the dipping beds are constant in the large barchan, but decrease upwind from 34° to 18° in the small dune.

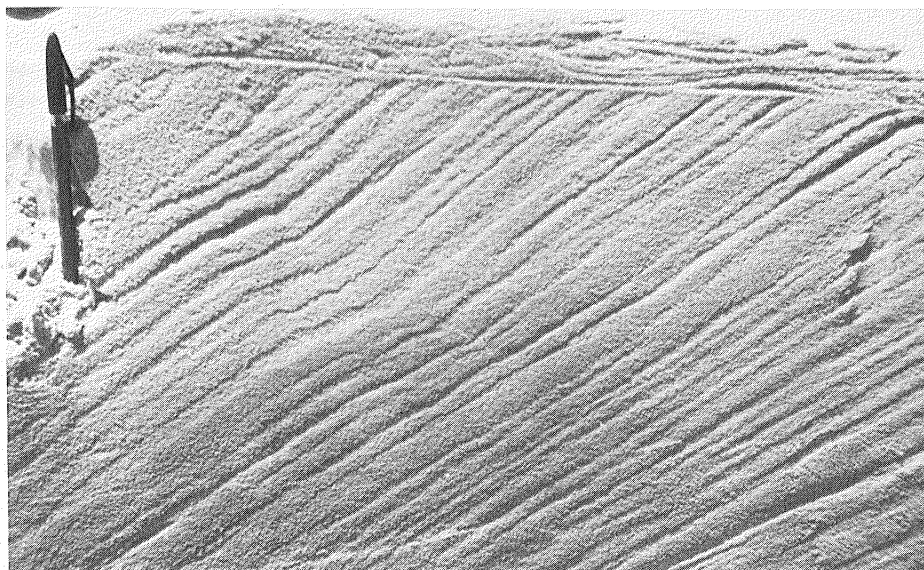


Figure 11.6 Trough structures in low-angle stratified deposits on the dune surface.

TEXTURAL PROPERTIES OF BARCHAN SAND

Grain Size

The predominant grain size of barchan dune sand is between 3.3 and 1.3ϕ (0.1 to 0.4 mm); the percentage of sand lying between these two sizes varies from 85% to 97% for all samples (Table 11.2). The foot of the windward side contains a higher percentage of coarse sand ($1.3 - 0.7 \phi$; 0.4 - 0.6 mm) than does the crest. In addition, the barchan crest contains a higher percentage of fine sand ($\leq 3.3 \phi$; 0.1 mm) than does the foot of the windward side.

The larger percentage of coarse grains at the foot of the windward side is due to sorting processes which occur at both the base of the windward side and at the dune crest. These characteristics have been observed in other desert regions of the world (Cook and Warren; 1973, p. 310-311).

Roundness

To study the roundness of barchan sand, a fraction of each particle size from four different samples was examined under the microscope. A series of photomicrographs were taken (for at least 100 sand grains) for each particle size (Fig. 11.7). Using Powers' roundness scale (Powers, 1953), roundness values were estimated for each particle size.

Differences in roundness values among the various particle sizes of the four samples are almost negligible. This is most likely due to the fact that all samples are composed of similar shaped quartz grains from the same origin (the Ghard Abu-Muharik).

Table 11.2 Grain size of barchan sand.

| Dune Location* | Size ϕ (mm) | | | | |
|-------------------|------------------|----------|----------|----------|----------|
| | 4.0(.063) | 3.3(0.1) | 2.3(0.2) | 1.3(0.4) | 0.7(0.6) |
| 1 C | - | 8.7 | 52.1 | 39.5 | - |
| T | - | 5.9 | 60.6 | 34.8 | - |
| 2 C | - | 3.3 | 27.0 | 69.7 | - |
| T | - | 4.3 | 49.0 | 41.0 | 5.7 |
| 3 C | - | 5.1 | 46.2 | 49.0 | - |
| T | - | 3.0 | 54.5 | 42.5 | - |
| 4 C | - | 5.7 | 50.6 | 34.4 | - |
| T | - | 4.1 | 43.7 | 61.4 | - |
| 5 C | - | 6.3 | 31.3 | 63.4 | - |
| T | - | 4.1 | 39.2 | 57.0 | - |
| 6 C | 2.5 | 7.3 | 39.5 | 50.6 | - |
| T | - | - | 53.0 | 44.2 | - |
| 7 C | 0.8 | 8.8 | 25.5 | 59.0 | 5.8 |
| T | - | 2.9 | 32.0 | 56.6 | 8.6 |
| 8 C | 1.0 | 10.6 | 34.8 | 50.8 | 2.9 |
| T | - | 0.6 | 23.8 | 67.0 | 8.8 |
| 9 C | - | 8.0 | 69.5 | 22.5 | - |
| T | - | 2.5 | 44.0 | 44.0 | 9.4 |
| 10 C | - | 3.8 | 42.3 | 51.0 | 2.9 |
| T | - | - | 27.9 | 67.4 | 4.7 |
| Mean C | 0.4 | 6.8 | 41.9 | 49.9 | 1.2 |
| T | - | 2.7 | 41.8 | 51.6 | 4.1 |

*C, crest of dune; T, toe of dune.

Roundness does, however, vary with grain size; the larger the grain, the greater the roundness values. Particles less than 3.3 ϕ (0.1 mm) have roundness values between 0.30 and 0.32 (subangular); particles 3.3 - 2.3 ϕ (0.1 - 0.2 mm) have values between 0.33 and 0.37 (subangular to subrounded), and particles 2.3 - 1.3 ϕ (0.2 - 0.4 mm) have values of 0.40-0.41 (subrounded). This may result from less abrasion at smaller grain sizes.

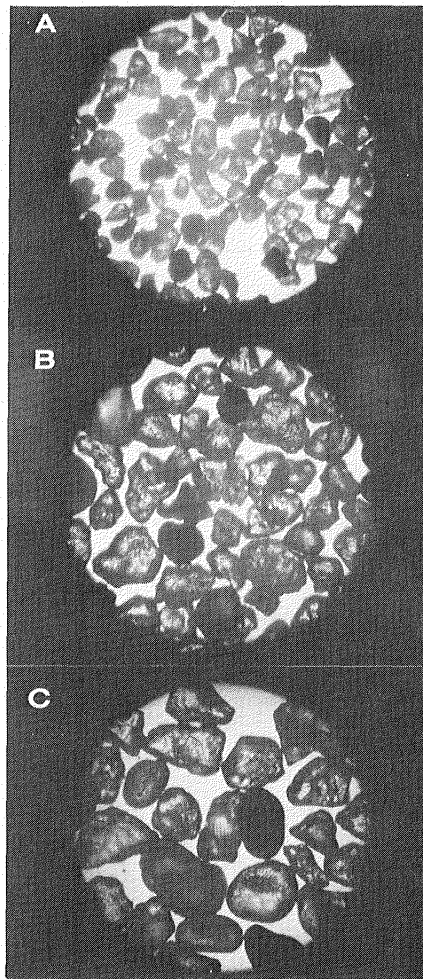


Figure 11.7 Photomicrographs of barchan sand: A) 3.3ϕ (0.1 mm) sand; B) 2.3ϕ (0.2 mm) sand; C) 1.3ϕ (0.4 mm) sand.

ECONOMIC IMPLICATIONS

Locally, several attempts to avoid dune encroachment have been made by both direct and indirect methods. These methods and some others were discussed by Embabi (1979). Dune stabilization by means of vegetation fences, plastic or petroleum spray, vegetation growth, or any mechanical means is impractical due to the nature of dune distribution, water shortage, climate, and importation of petroleum materials. Stabilization can be done by any of the above cited methods, or by covering the lower concave part of the windward side by a thin veneer of granule-size grains (0.0 to 1.6ϕ ; 1-3 mm).

Temporary divergence of highways at the crossing of barchan belts at times of dune encroachment can serve light traffic only. But if the Kharga area is going to be economically developed to absorb large populations, or to export its production, another method for avoiding barchan encroachment should be adopted. The author suggests the construction of tunnels or bridges at dune crossings.

Future research should concentrate on those methods which lead to co-existence with moving barchans. The present distribution of barchan belts should be mapped, especially in populated areas and in areas of future development. Areas of future development should be selected away from paths of dune belts. However, if there is a necessity to utilize areas lying along the paths of dune belts, the location should be proportionate to rate of barchan movement in the lower part of the belt, in order to avoid dune encroachment over a relatively long period (500-1000 years).

**Page Missing in
Original Document**

Chapter 12

SAND SHEET AND LAG DEPOSITS IN THE SOUTHWESTERN DESERT

TED A. MAXWELL

National Air and Space Museum
Smithsonian Institution
Washington, D.C. 20560

ABSTRACT

Based on size analyses of sand sheet and lag deposits in the southwestern desert of Egypt, it is possible to distinguish these sediments from the more commonly studied eolian dune deposits. Sand sheets consist of a bimodal mixture of sand-size grains and coarser lag fragments which vary from -1.0 to -2.5 ϕ (2.0 to 5.7 mm) in modal grain size, and are well sorted. In contrast, the sand-size fraction of these deposits is much more poorly sorted, and exhibits wider variations in both sorting and skewness than does dune sand. Except on a local scale, there is no evidence for selective removal of a saltation fraction in sand sheets. Instead, the wide range of grain sizes and poor sorting of the sand-size fraction support formation of sand sheets by relatively infrequent high winds that are capable of disturbing the protective lag surface.

INTRODUCTION

Since Bagnold's (1941) classic study on the physics of windblown sand, most studies of desert sediments have concentrated on the erosion and deposition of sand-size material in an eolian environment. These studies have dealt primarily with dune morphology and stratification (McKee and Tibbitts, 1964; McKee, 1966; Sharp, 1966; McKee and Moiola, 1975; Ahlbrandt, 1979; Moiola and Spencer, 1979) and the textural characteristics of eolian dune sand as compared to those of other environments (Amstutz and Chico, 1958; Friedman, 1961; 1967; 1973; Martins, 1965; Moiola and Weiser, 1968; Shepard and Young, 1961). However, studies of the size characteristics of desert lag surfaces typical of extensive sand sheets are less numerous in the geologic literature. McKee (1966) and McKee and Moiola (1975) have analyzed the interdune regions of the White Sands dune field in New Mexico, which essentially consist of deposits from former dunes. Folk (1968), in an extensive review of desert floor sediments, found that "reg" was universally bimodal, consisting of a mixture of several populations of sand. Ahlbrandt (1979) and Moiola and Spencer (1979) combined 40 interdune and serir samples from a variety of deserts, and presented additional evidence for bimodality and textural differences between interdune and dune sand. Studies of coastal dunes have concentrated primarily on the dune sand textures (Mason and Folk, 1958; Inman and others, 1966) rather than interdune sediments, because of

periodic reworking of the interdune sediments by water. Although these studies have provided much information on the nature of dune sands, these relatively small, interdune regions are not directly comparable to the vast expanses of sand sheet deposits in southwestern Egypt.

A wide variety of terms have been used to describe the sedimentary deposits in the open desert, including "desert pavement, hammada, lag gravel, interdune, reg, sand sheet and serir." In order to be consistent with Bagnold's (1933) naming of the Great Selima Sand Sheet the term "sand sheet" will be used in this paper to describe "A thin accumulation of coarse sand and fine gravel formed of grains too large to be transported by saltation, characterized by an extremely flat or plain-like surface broken only by small sand ripples" (AGI, 1974). Consequently, the term "sand sheet" is analogous to the "reg" samples described by Folk (1968), and some (but not all) of the "interdune" sediments of Ahlbrandt (1979). In this paper, the term "desert pavement" will be used to describe a surface of large, angular fragments (generally larger than a few centimeters) that may veneer a bare rock surface, or a layer of sand.

As described by Bagnold (1933), the Great Selima Sand Sheet occupies an area of about 52,000 km² stretching from Bir Tarfawi in the north to latitude 21° in the south. It is bounded on the west by the rocky terrain of the Gilf Kebir - Uweinat region, and on the east by Selima Oasis. In addition, numerous smaller sand sheet surfaces cover much of the Western Desert, where less than one fourth of the surface is covered by actively moving sand deposits and dunes (Gifford and others, 1979).

The study of sand sheet and associated deposits is important for several reasons: 1) These sediments provide a widespread, ubiquitous surface type in desert regions which can be correlated with tonal variations, visible on orbital images. 2) Larger size lag fragments protect the active moving sand, thus the size distribution of this material is important to studies of potential sand movement and desertification. 3) Surface materials with these size characteristics may be representative of windblown sediments on the surface of Mars (Maxwell and El-Baz, 1980).

Because of the dominant eolian environment on Mars, and the variations in sediment size seen at the Viking lander sites (Patterson and others, 1977; Zimmer and others, 1977), it is possible that large areas of Mars are made up of surface materials analogous to terrestrial desert pavements. 4) As suggested by Folk (1968), it is also possible that the desert floor environment may be present in ancient sandstones. Thus, investigation of the textural properties of the widespread sand sheets in the Western Desert will aid in the characterization of this environment.

The intent of this paper is first, to present the results of grain size analyses for sand sheet and dune samples, and second, to compare these two distinct desert environments on the basis of textural characteristics in the sand-size fraction alone (see below).

These results will then be compared to those reported from other major inland dune regions in order to typify the size characteristics of sand sheet deposits. Finally, some speculations on the nature of eolian sedimentary deposits on the martian surface will be made, based on data from the Western Desert.

METHODS

For the purposes of this study, the coarse and fine fractions of the bimodal sand sheet deposits are treated as two separate samples. While in the field, it became apparent that the method of sampling sand sheet deposits would greatly influence any later study of their textural characteristics. Sampling emphasis on the thin, surficial lag deposits would result in a greater weight percent of coarse material in the total sample (hence negative skewness), whereas emphasis on the underlying sand would fail to provide a representative sample of the coarse lag. Consequently, in order to provide data representative of both sediment modes and of the present-day eolian regime, only the top surface of the sand sheets was sampled.

All samples were obtained by scraping the top 2-3 cm of an area about 0.5 m² (about 600 gm). In some instances, where lag spacing was greater, wider areas of the sand sheets had to be scraped in order to provide a representative sample of the lag deposits. Samples were split and about 100 gm of each sample was sieved for 15 minutes at 1/4 ϕ intervals using a Rotap. Both frequency and cumulative frequency curves were plotted for each sample, and graphic textural parameters (Folk, 1974, p. 46-49) were calculated for the sand-size fraction. Because the width of the sampling field for the lag deposits is variable, it would not be valid to include the total samples of the lag and sand fractions in the calculation of graphic parameters. In any individual case, if the sample area were larger, the coarse fraction of the total sample would have been proportionally greater. Consequently, the lag and sand fractions are treated separately. For this study, the average size of lag was determined by visual estimate of the sieved separates which were compared with the bulk samples and photographs of the sampling sites.

DUNE SAND

Barchans

Samples of barchan dunes are from three localities: the dunes on the Kharga-Dakhla road within the Kharga depression, the Abu Hussein dune field west of Bir Sahara, and an individual low barchan south of Beacon Hill (Fig. 12.1). The individual barchans of the Kharga region are extensions of the longitudinal dunes north of the scarp bounding the depression, and range from 25 to 540 m wide (Embabi, 1967). Those of the Abu Hussein dune field are generally 300-500 m wide, and are not aligned in a north-south direction as are the barchans of the Kharga depression. Instead, the Abu Hussein barchans consist of laterally coalescing and individual dunes with a wide (almost 1 km) north-south interdune spacing. South of Beacon Hill, 2 samples were taken from a low barchan (approximately 2 m high).

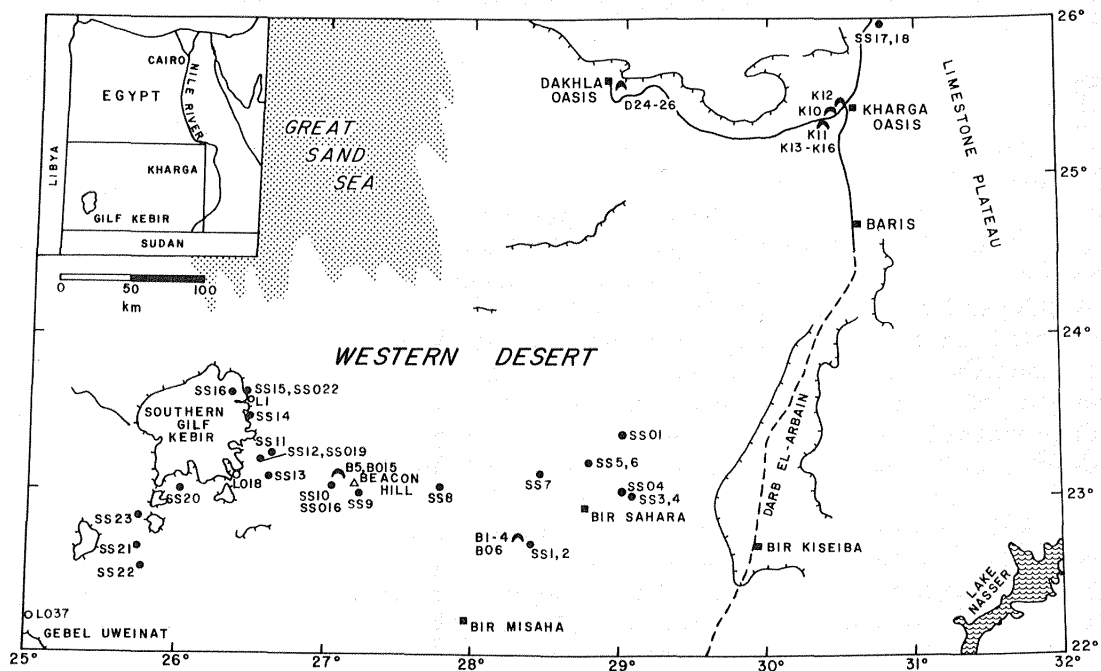


Figure 12.1 Location map of samples from sand sheets (solid circles), longitudinal dunes (open circles) and barchans (barchan-shaped outline) in the southern part of the Western Desert of Egypt.

The mean grain size of the barchans is 1.97ϕ (0.27 mm) (Table 12.1). Dune sand of the Kharga-Dakhla region is slightly finer-grained than that of the Abu Hussein dune field, although there is no statistically significant difference between any of the localities. All barchan samples are well- to moderately-well sorted (average $\sigma_1 = 0.61 \phi$), and 12 out of the 17 samples are slightly fine-skewed. Despite the fact that these samples are from a different dune type and a different continent, sorting and skewness are virtually identical to those of longitudinal dunes in the Simpson Desert, Australia (Folk, 1971), and to inland dunes of North America and North Africa (Moiola and Weiser, 1968). Mean grain size of these dunes is slightly larger than that reported for Simpson Desert dunes (2.7ϕ , 0.15 mm; Folk, 1971).

Longitudinal Dunes

The 19 samples of longitudinal dunes were taken from 3 dunes on the eastern side of the Gifl Kebir (Fig. 12.1), and 2 dunes in the Bahariya Oasis region north of Kharga. One dune in Bahariya was extensively sampled along the crest (10 samples), and was trenched in order to determine the internal structure. Samples from the Gifl Kebir include the longitudinal dune at the entrance to Wadi Mashi, the

Table 12.1 Summary of grain size statistics.

| Environment | Mz(ϕ) | σ_I (ϕ) | SK _I | K _G * |
|----------------------------|----------------|-----------------------|------------------|------------------|
| Barchans n=17** | 1.97 \pm .52 | 0.61 \pm .28 | +0.026 \pm .16 | 0.487 \pm .041 |
| Longitudinal Dunes n=19 | 1.80 \pm .32 | 0.54 \pm .19 | +0.146 \pm .15 | 0.521 \pm .043 |
| Coastal Dunes n=3 | 2.12 \pm .25 | 0.56 \pm .13 | +0.155 \pm .04 | 0.533 \pm .039 |
| Sand Sheets n=28 | 1.42 \pm .76 | 1.13 \pm .34 | -0.015 \pm .39 | 0.510 \pm .106 |

*Transformed Kurtosis ($K_G/(1 + K_G)$).

**Includes 11 samples from Kharga-Dakhla region.

dunes east of Bagnold's 1938 camp (see El-Baz and others, 1980) and a low (whaleback?) dune northwest of Uweinat.

As might be expected, grain size parameters of these dunes are similar to those of the barchans. Longitudinal dunes are composed of medium sand (average Mz = 1.80 ϕ ; 0.29 mm), are moderately well-sorted (σ_I = 0.54 ϕ), and are slightly fine-skewed (SK_I = +0.15). As is the case with barchans, sorting and skewness are similar to those reported for other inland dunes (Folk, 1971; Moiola and Weiser, 1968), whereas mean grain size is larger than Simpson Desert or "inland dune" sands, but is comparable to the medium-sand size reported for a seif dune in Libya (McKee and Tibbitts, 1964).

Coastal Dunes

For comparison with inland dunes of the Western Desert, 3 samples from the northern coast of Egypt are included in this analysis. All are from the crests of beach dunes in the Mersa Matruh region west of Alexandria, and are composed of calcareous sand rather than the quartz grains of the inland dunes. Unlike the north-south orientation of the inland dunes, the coastal dunes are oriented east-west, and have a seif-like appearance.

These calcareous sands have a smaller mean grain size (2.12 ϕ ; .23 mm) than the average mean for inland dunes (Table 12.1), although several inland dunes have mean grain sizes that are less than these coastal dunes. Sorting (σ_I = 0.56 ϕ) and skewness (SK_I = +0.15) are also similar to values of both barchans and longitudinal dunes.

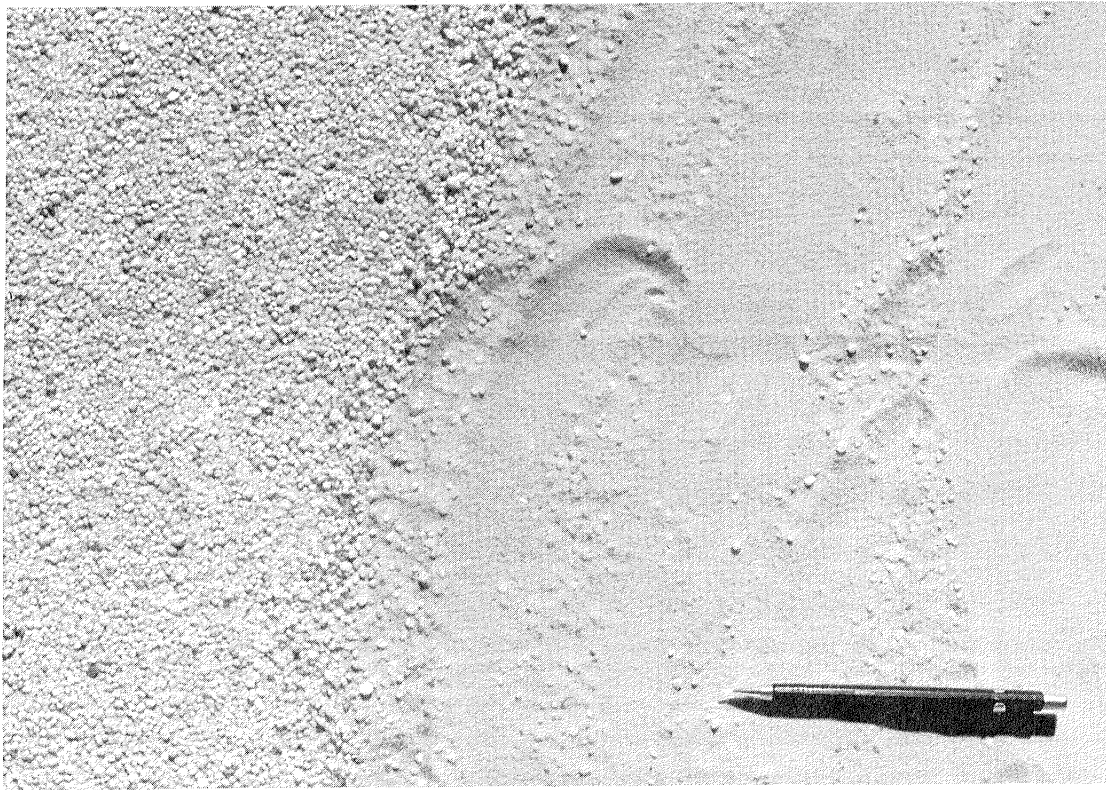


Figure 12.2 Typical lag-covered surface and underlying sand east of the Gilf Kebir plateau. Note the close spacing of the 1-grain thick lag surface; mean grain size of the coarse fraction is -1.25ϕ (2.4 mm). Pencil is 14.5 cm long.

SAND SHEETS

The 27 samples of sand sheets were taken from various locations ranging from the top of the plateau north of Kharga, to the southern end of the Gilf Kebir (Fig. 12.1). Although implied by the name given by Bagnold (1933), the Great Selima Sand Sheet is surfaced not by sand-size particles, but by coarser granule- to pebble-size lag that overlies and protects the sand. In a strict sense, only those samples between Bir Sahara and Beacon Hill, and the 5 samples southwest of the Gilf Kebir might be considered as belonging to a true sand sheet. On this extensive, featureless sand sheet, the spacing of coarse material is variable (Fig. 12.2). Granule-size grains may exhibit such close packing that they obscure the underlying sand. Such spacing was noted in both planar-bedded, featureless sand sheets, and in a field of flat-topped (truncated?) ripples east of the Gilf Kebir (Fig. 12.3).

Besides the rounded desert lag deposits that form the surface of the sand sheets, closely-spaced deposits of dark, locally-derived desert pavement occur near outcrops and in the lee of hills. These angular fragments range up to several cm's in diameter, and create dark streaks on the desert surface that emanate downwind from the topographic obstacle. In some cases, these dark streaks are large



Figure 12.3 (A) Flat surfaced (truncated?) ripples of coarse lag deposits east of the Gilf Kebir. Planar surface may result from high speed winds needed for redistribution of lag. (B) Closely-spaced lag and underlying sand deposits of flat-topped ripples. Mean grain size of lag fraction is -0.75ϕ (1.7 mm). Pencil is 14.5 cm long.

enough to be visible on orbital images, and attribute their characteristic streamlined shape to the pattern of movement of the surrounding lighter-colored sand sheets (El-Baz and Maxwell, 1979a). The size range of individual coarse fragments within these streaks is strongly dependent on the distance from the source outcrop. Because of the local size variations, the desert pavement is not included in this study. It is doubtful that the larger fragments of the desert pavement have been extensively transported by the wind, as have the coarse, rounded fragments of the sand sheet deposits.

Coarse Fraction

The average size of the coarse fraction of the sand sheet samples ranges from about -1.0ϕ to -2.5ϕ (2.0 to 5.7 mm; Fig. 12.4). However, one-third of the samples have a coarse mode at -1.25ϕ (1.0 to 1.2 mm). In an extensive review of the literature, Folk (1968) reported that the average size for desert lag varied from 1.4ϕ to -1.0ϕ (0.38 to 2.0 mm), and that for the Simpson Desert of Australia, the coarse mode was predominantly 0.25ϕ (0.84 mm). The large size of the granule to pebble-size lag fraction in the Western Desert deposits is most likely the result of the widespread Nubian sandstone, which

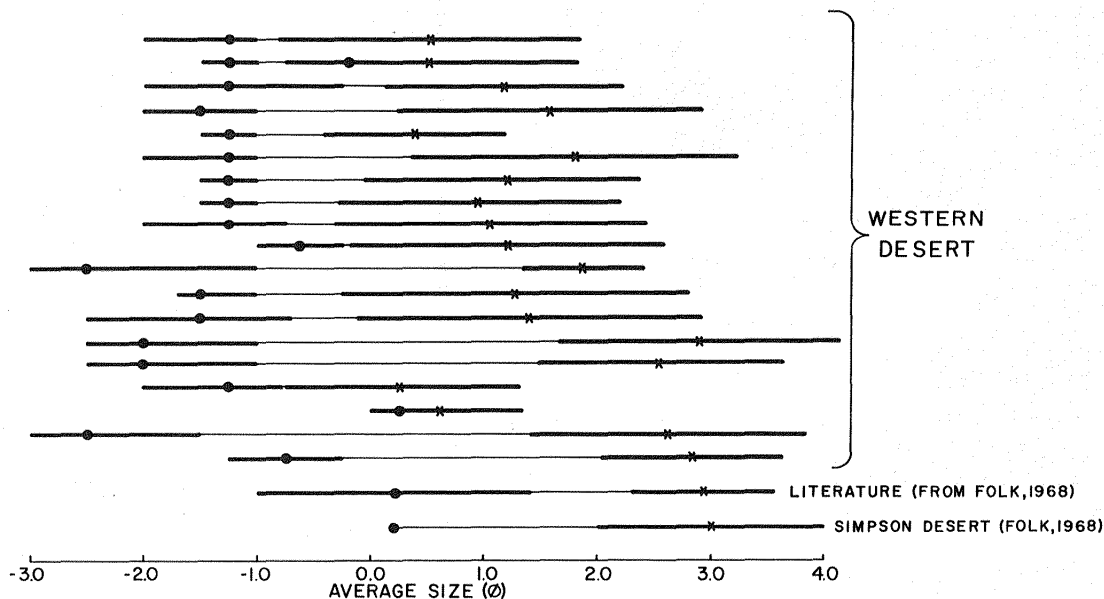


Figure 12.4 Average sizes for sand sheet deposits of Western Desert samples compared with those of previous studies. Average size for coarse fraction is visually estimated from field observations and sieved separates; average sand size is graphic mean. Sand sheet deposits are poorly sorted in the sand size fraction as indicated by heavy lines.

provides a source for the eolian sediments. However, the influence of locally derived material can only be documented where there are outcrops of rock other than sandstone (El-Baz and others, 1979b). The Eocene limestone north of Kharga provides one such example. Here, the lag fraction is composed almost entirely of limestone fragments that stand out against the background of reddish sand-size grains. South of the Kharga depression, however, quartz grains of the Nubian sandstone provide an immediate source for both lag and sand fractions of the sand sheets.

Fine Fraction

The fine fraction of the sand sheets (here used to denote the sand and smaller size fractions) exists both underlying and interspersed between lag pebbles and granules. Horizontally-bedded layers of sand separated by lag deposits were observed in several areas of the Great Selima Sand Sheet, although the total thickness of these deposits seldom exceeded a few 10's of centimeters (see Haynes, Chapter 9). Consequently, repeated episodes of deposition and winnowing have caused the build-up of the sand sheet surface, and have no doubt acted to smooth any pre-existing topographic relief.

As opposed to the lithologic variations noted within the coarse fraction, the sand-size grains are composed almost entirely of quartz (El-Baz and others, 1979b). Even north of Kharga, where the lag is composed entirely of limestone fragments, quartz grains predominate at sizes of 0.0ϕ (1.0 mm) and smaller. The influence of the Nubian sandstone source rock, together with compositional segregation during weathering and transport are both responsible for these monomineralic sands. In a similar manner, the variations in color of the sand fraction may also be inherited from original hematite coatings of grains in the Nubian sandstone. However, in situ modification of these coatings (precipitation of additional hematite or abrasion or the coating due to transport) nonetheless remains a possibility. On these samples, there are no specks of carbonaceous material such as those found on reg grains from the Australian Simpson Desert (Folk, 1976).

Within the sand-size fraction, the sand sheet samples are almost nonmodal in their size distribution. Mean grain size for all the samples averages 1.41ϕ (0.38 mm), larger than the average size for any of the dune environments, and the mean value for sorting is 1.13ϕ . As is true for the coarse fraction, these sands have a larger mean grain size than the sand fraction of most desert lag deposits from the Simpson Desert, or those reported in the literature (Folk, 1968). Both skewness ($SK_I = -0.015$) and kurtosis ($K_G = 1.14$) lie within the range of dune sands.

COMPARISON OF TEXTURAL PARAMETERS

Although textural parameters have been used extensively for discrimination among river, beach, beach dune and inland dune sands (Mason and Folk, 1958; Friedman, 1961; 1967; Moiola and Weiser, 1968), few studies have presented detailed size analysis data for the extensive sand sheet environment. In a study of seif and interdune areas

in northern Libya, McKee and Tibbitts (1964) presented histograms of the grain size distributions, noting that serir deposits were dominantly bimodal. Sharp (1966) discussed the dominantly unimodal sand of the Kelso dunes in southern California, but there are no extensive interdune tracts similar to sand sheets in this region. The first comprehensive analyses of grain size parameters for featureless desert plains are those of Folk on the Simpson Desert in Australia (Folk, 1968; 1971; 1976). Using graphic grain size parameters, Folk (1971) found systematic changes in the size distribution of sand from longitudinal dunes and the reg. According to his diagrams of the higher moments, there is considerable overlap in the fields of dune crests, windward flanks and leeward flanks. Warren (1972) presented cumulative curves for the size distribution of sands from seif, interdune flat and zibar (very gently undulating sand ridges) environments in the Tenere Desert of Niger. Both interdune flat and zibar sediments were found to have poorer sorting than dune sands.

In a study of the White Sands National Monument in New Mexico, McKee and Moiola (1975) found that the relatively small interdune areas are characterized by a high percentage of silt and clay, deposited from suspension and trapped by vegetation. Based on 40 interdune and serir samples, Ahlbrandt (1979) noted that the most significant textural differences within the eolian environment were between dune sands and those of the interdune and serir deposits. This distinction was further supported by the work of Moiola and Spencer (1979), who found that discriminant analysis of the quarter-phi weight fractions would separate inland dunes from interdune deposits. However, none of the above studies specifically treated a sand sheet type of environment, such as that which covers vast expanses of the southwestern Egyptian desert.

Sorting Versus Mean Grain Size

The poor sorting and wide variation of median grain size are responsible for the range of values for sand sheet sands compared to values from the dune environments (Fig. 12.5). Within the field of dune samples, there is no systematic relationship between size and sorting for the different dune types, nor any consistent variation with location on the dune. However, only three of the sand sheet examples fall in the field outlined by dune samples.

These results are consistent with those of Ahlbrandt (1979), in which interdune and serir samples were determined to be more poorly sorted than dune deposits (see Figs. 20 and 21 in Ahlbrandt, 1979). However, the major different between previous studies and the analyses presented here is in the treatment of the sand-size fraction as a discrete sample.

As shown in Figure 12.5, the sand sheets are characterized by moderate to poor sorting even within the sand fraction alone (excluding the coarse lag, which would create an additional tendency for poor sorting).

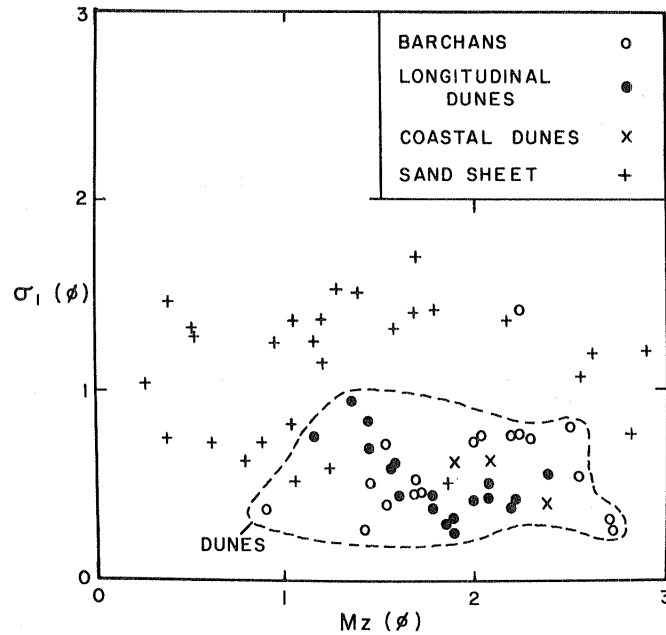


Figure 12.5 Relationship between sorting (σ_I) and mean grain size (Mz) for Western Desert sands. Poor values of sorting are characteristic of even the sand size fraction of sand sheet sands.

Skewness Versus Mean Grain Size

Although several early studies of dunes and associated eolian deposits suggested that positive skewness is characteristic of eolian sands (Mason and Folk, 1958; Friedman, 1961; Folk, 1971), more recent analyses of dune sands suggest that positive skewness is not a universal phenomenon (Bigarella, 1972; Friedman, 1973; Ahlbrandt, 1979). Results of the present study support the latter view, since one-third of the Western Desert dune samples are negatively skewed (Fig. 12.6). There is a lack of distinct fields of dunes and sand sheet sands on a plot of skewness versus mean grain size, although the larger mean size of the sand sheets provides a slight separation (Fig. 12.6). Coarse-grained sand sheet sands tend to have both positive and negative skewness values, and several of the samples fall in the field defined by dune sands, further suggesting that this pair of graphic parameters may not be the best for separation of environments.

Ahlbrandt (1975; 1979) found that for dune samples in the Killpecker Dune Field in Wyoming, and for interdune and serir deposits from various deserts, skewness was dependent on mean grain size. By using both coarse lag and sand-size material as one sample in the calculation of graphic parameters, however, this "dependence" naturally results from the bimodal nature of the sample. Positive (fine) skewness will result from a relatively coarse sand with another mode in the fines, whereas negative skewness will result from a sample with a finer mean grain size with an admixture of lag grains. As shown by the present study, there is no tendency for a grain-size

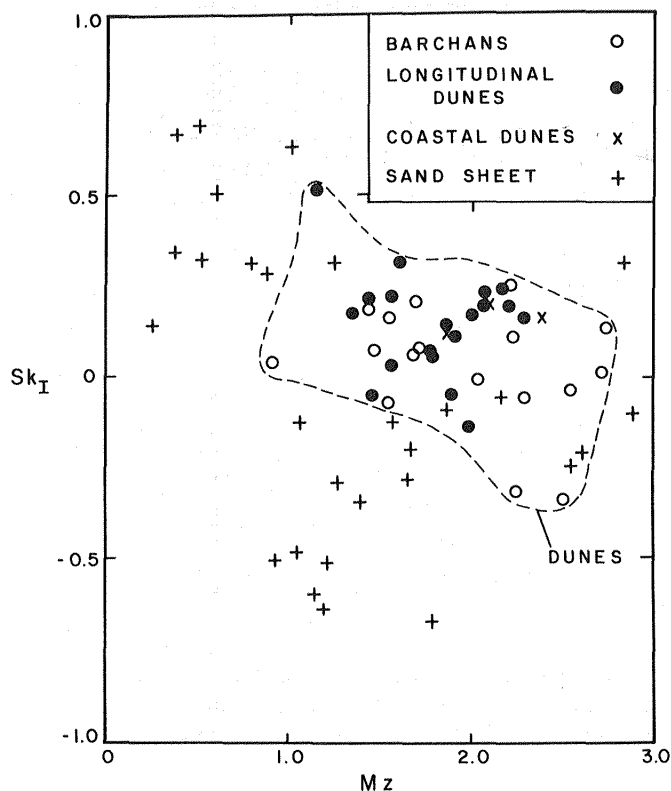


Figure 12.6 Relationship between skewness (SK_I) and mean grain size (Mz) for Western Desert sands. Note the negative skewness values for several dune sands, and more than half of the sand sheet sands.

dependence of skewness within the sand fraction of sand sheet deposits.

Skewness Versus Sorting

The combination of skewness and sorting provides the best separation of environments for Western Desert sands (Fig. 12.7). Separation is due primarily to the characteristic poor sorting of sand sheet sands, but it is aided by the narrow range of skewness of dune sands (-0.2 to +0.6). A similar grouping of inland dune sands is presented in Figure 5 of Moiola and Weiser (1968), although they found it difficult to separate dune from river sand on the basis of these parameters. The data of Folk (1971) would compare well in the dune field; Simpson Desert dunes have an average skewness of +0.09, and sorting values from 0.32ϕ to 0.71ϕ . The better sorting values and narrower skewness range for his reg samples, however, would cause his reg field to fall just to the right of the dune field outlined in Figure 12.7. Considering the number of variables involved in both source and transport on two different continents, the agreement is much better than would be expected.

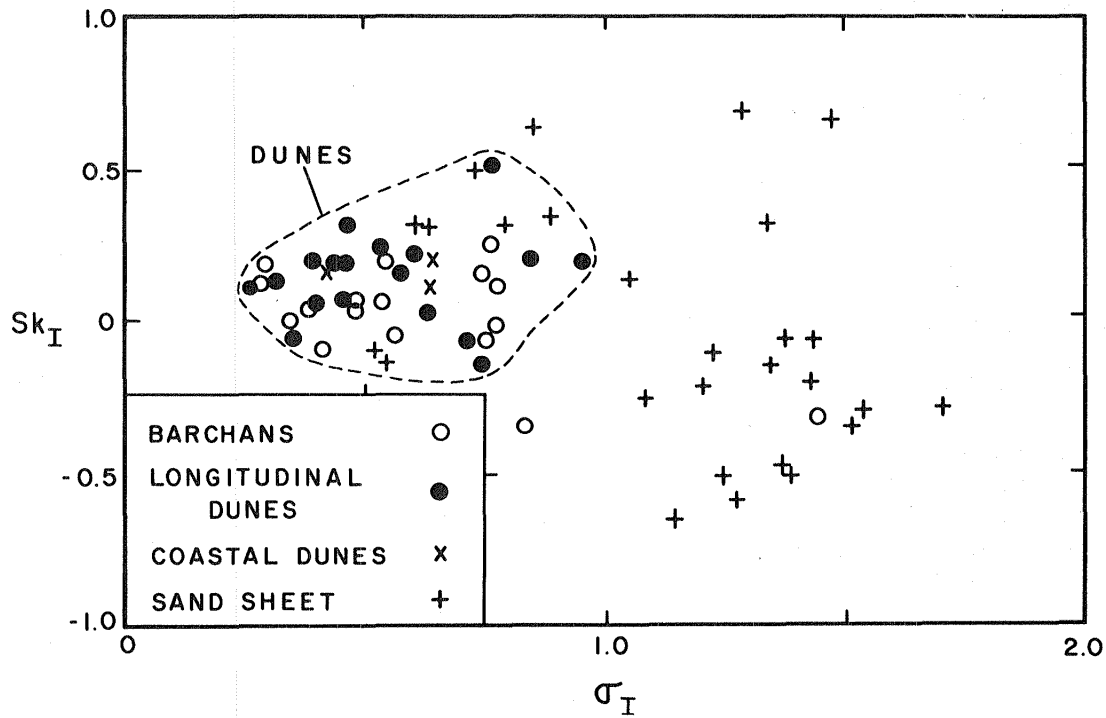


Figure 12.7 Skewness (SK_I) versus sorting (σ_I) for Western Desert sands. The combination of poor sorting of sand sheets and a relatively narrow range of skewness for dune sands suggest that these parameters are the most useful for distinguishing these environments.

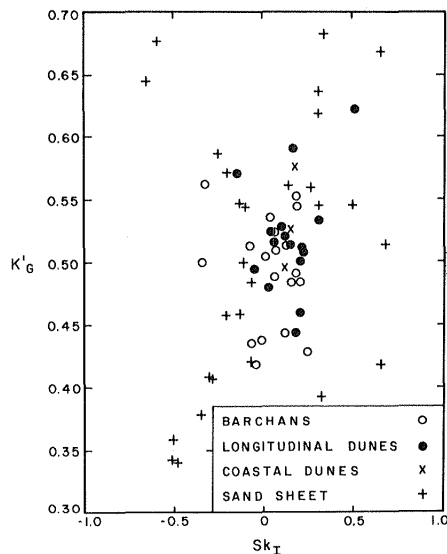


Figure 12.8 Kurtosis (transformed Kurtosis, $KG/(1 + KG)$) versus skewness (SK_I). Although specific fields are not well-defined, there is a tendency for the more platykurtic sand sheet samples to be characterized by negative values of skewness.

Skewness Versus Kurtosis

Since neither skewness nor kurtosis values individually exhibit any consistent variation with environment, the plot of these two parameters (Fig. 12.8) shows the expected high degree of scatter. Western Desert sands reveals more extreme variations in both SK_I and K_G than sands of the Simpson Desert (Folk, 1971), or eolian sands of Mustang Island, Texas (Mason and Folk, 1958). There is a general trend for platykurtic sand sheet sands to be negatively skewed, which is consistent with the polymodality and presence of the coarse grained fraction in these samples.

DISCUSSION

As shown by the present and previous studies of dune sands, no distinction has been made between the size and sorting characteristics of sands from different dune types, although a few studies have noted the textural differences between desert floor and dune sand. R. A. Bagnold provided the initial physical rationale for sand sheet sand, noting that "a desert surface is never composed entirely of fine dune sand, unprotected by a layer of coarser grains" (Bagnold, 1941; p. 168). Once deposited, the stability of sand sheets was thought to be maintained by the increased drag produced by the pebbles. Consequently, Bagnold regards the pebble surface as a reservoir in which sand is stored during periods of gentle wind, and removed in sudden storms (Bagnold, 1941, p. 169).

Recently, modifications of this basic theory have been proposed. Folk (1968) has proposed that selective removal of the saltation size fraction (1.5 to 4.0 ϕ ; .35 to 0.63 mm) is responsible for bimodal sands of the desert floor. Coarser grains from 1.0 to -1.0 ϕ which are too heavy for saltation would move primarily by rolling. This gave rise to Folk's (1971) "quantum theory" of eolian deposition, in which reg sediments were thought to be a combination of several populations, each having a normal distribution.

In contrast, Warren (1972) proposed that bimodal sands could not be explained by invoking high threshold velocities needed to move fine sands. Fine sands would be as likely to move because of bombardment by coarser grains. Therefore, Warren's (1972) "protectionist theory" involved a modification of previous selective transport models. According to this theory, the slightly coarser fraction of the saltation load would be too large to fit in the inter-particle voids of the surface creep fraction, and thus would be kept in transport to eventually end up as dunes.

The results of each of these methods for sand sheet development should be manifested in the size distribution of the sand fraction. According to Bagnold's (1941) near-surface drag theory and Folk's (1971) quantum theory, the mean grain size of the sand fraction should be highly variable, having been deposited by the less frequent, strong winds capable of disturbing the lag surface. However, if selective removal of the saltating, dune-forming fraction has occurred (Folk, 1968; Warren, 1972), then that size should be deficient in sand sheet

deposits. As a group, the widely distributed values for mean grain size of Western Desert sands suggest that selective transport, if it has occurred, has not been an efficient means of modifying the size distribution of sand sheets. The poor sorting of the sand-size fraction makes it difficult to single out any individual size populations within the sand sheets. The wide range of grain sizes present in the Nubia sandstone (Issawi, 1973b; Klitzsch and others, 1979) indicates that a continuum of source material in the Western Desert overrides any eolian sorting into "quanta." On a local scale, however, selective transport is supported by observations within the Abu Hussein dune field. Here, the mean grain size of the sand sheet is 2.83ϕ (.14 mm; sand fraction alone), finer than the 1.79ϕ (.29 mm) sand of the surrounding terrain.

INFERENCES FOR SURFICIAL DEPOSITS ON MARS

As shown in Mariner and Viking images of the surface of Mars, dunes and other eolian features have suggested the presence of a significant population of saltation-size particles that are available for eolian transport (Cutts and Smith, 1973; Greeley and others, 1974b). In addition, observations of the duststorms indicate that material in the $1 \mu\text{m}$ range is extensively redistributed on a planet-wide scale (Arvidson, 1972). In contrast to these observations, however, Viking lander images indicate an apparent deficiency of surficial material in the $1.75 - 2.5 \phi$ (.30 - .18 mm) size range (Patterson and others, 1977), and theoretical calculations of wind velocities needed for eolian entrainment both suggest that sand-size material should not be an important constituent in the martian eolian regime. According to Greeley (1979a), three possible explanations for the presence of sand on the martian surface are: 1) the dunes are remnants of a previous episode of a denser atmosphere, 2) the calculations suggesting the need of sand are incorrect, or 3) the eolian features may be formed of agglutinates of smaller grains that act as sand-size material during transport. Based on the size characteristics of sediments from the Western Desert, however, it is also possible that these seemingly conflicting lines of evidence are the result of the heterogeneity of eolian depositional environments.

Source materials for many present-day terrestrial deserts are found in previously consolidated sedimentary deposits, subjected to fluvial reworking during Pleistocene and Recent times (Folk, 1968). Eolian sands of the Western Desert are one example of this process, in that they were derived from highlands to the south, and transported northward by rivers only to be blown back southward by the prevailing winds (El-Baz and Maxwell, 1979a). In the southwestern desert, however, there is an additional local source of sand grains in the widespread Nubia sandstone that underlies the surficial deposits (Issawi, 1973b; Klitzsch and others, 1979). Consequently, there is likely to be a continuum of particle sizes present that are available for eolian sorting. The characteristics of source materials for martian deposits are much more difficult to specify. The effects of impact, thermal and chemical weathering, and possible fluvial erosion may all play an important role in generation of sand- and silt-size material. Because of our limited knowledge on the nature of martian

bedrock, however, the grain size of source materials on that planet still remains unknown.

On both Earth and Mars, the resultant size distribution of wind-transported material can be divided into two fractions: 1) Unimodal, saltation-sized grains that are the dune-forming population, and 2) A bimodal population of sand sheet, interdune and desert-pavement type of deposits. Locally, material derived from an immediate source will modify both populations in the form of large fragments let down from eroded outcrops. As indicated by the comparison of textural parameters, the deposits of dunes can be distinguished from those of sand sheets on the basis of textural parameters. Although both the gravity and the atmosphere differ on Mars, the basic processes of eolian sorting are likely to be the same. Differences in the martian environment suggest that the size of the saltation fraction may be greater than that of the Earth (Sagan and Bagnold, 1975), but that both wind speeds and net sediment transport rates are greater (Arvidson, 1972; White, 1979). Because of the differing modes of sand sheet deposition, it is likely that these environmental effects may be represented more by sand sheet and associated deposits rather than the relatively homogeneous dune deposits.

Unfortunately, data from the Viking landers are inconclusive with respect to particle size variations at the two locations on the martian surface. Limitations on pixel size and sampling rate of the lander cameras make it impossible to see surface particles finer than about 2.5ϕ (.18 mm). Based on an absence of false low frequency components in surface imaging, Patterson and others (1977) suggested that there is a deficiency in the medium to fine sand size range (1.75 to 2.3ϕ , .30 to .20 mm). On the basis of grain counting in the footpad of Viking Lander 2, Zimmer and others (1977) also suggested a depletion of fragments less than -1ϕ (2 mm) in diameter. Consequently, there is an apparent bimodal sediment distribution among the < 5 mm size material at both sites. Grains greater than a few millimeters are abundant on the surface, with finer material (less than about 2.5ϕ ;.18 mm) forming intervening areas and possibly the drifts.

The deficiency of sand-size material has been attributed to particle break-up due to reduced atmospheric density (the so-called "Kamikaze" particles of Sagan and others, 1977), or a debris-flow origin or material near the landers (Shultz and others, 1979). Based on sorting characteristics of Western Desert sands, however, it is also possible to consider this size distribution as the result of the sand-sheet mode of deposition transferred to the martian environment. On Mars, the larger gap between the modes of fine sand and silt versus clay material may be the result of the much higher wind speeds and wind speed variations present at the martian surface.

CONCLUSIONS

Different dune types studied in the Western Desert of Egypt are indistinguishable from each other on the basis of textural parameters. However, the median grain sizes of the sand fraction of sand sheet deposits are coarser than those of dunes, and there is a much wider

range of mean sizes for sand sheets than for dunes. On an individual sample basis, this is consistent with both the poor sorting of the sand fraction of sand sheets as opposed to the good sorting of dune sand.

The combination of skewness and sorting provides the best means of separating dune from sand sheets on the basis of the sand size fraction alone. Separation is due to the poor sorting of the sand sheet sands (even within the sand fraction alone) and the relatively narrow range of skewness of the dune sands. Although the selective transport of sand sheet sand may be represented on a local scale, the influences of a continuum of grain sizes present in the Nubian sandstone source is consistent with deposition of sand sheet sand from sporadic high winds that are needed to disturb the lag surface.

The presence of fine and coarse deposits, and apparent absence of a sand-size component at the Viking Lander sites is suggestive of eolian modes of deposition similar to those of terrestrial sand sheet deposits. It may be possible that the great variation of martian wind velocities is responsible for a greater spread between the coarse and fine sediment populations on the martian surface.

ACKNOWLEDGEMENTS

I thank R. L. Folk and F. El-Baz for their constructive comments on earlier versions of this paper, and Diane Cobb for pursuing the arduous task of sieving.

**Page Missing in
Original Document**

Chapter 13

COATINGS ON SAND GRAINS FROM SOUTHWESTERN EGYPT

FAROUK EL-BAZ
National Air and Space Museum
Smithsonian Institution
Washington, D.C. 20560

DONNA PRESTEL
Lockheed
1830 NASA Road 1, NASA/JSC
Houston, Texas 77058

ABSTRACT

Sand samples from the Gilf Kebir plateau region in southwestern Egypt were analyzed to study the coatings on quartz grains. Although some iron oxide (hematite) is present, kaolinite forms much of the coatings, making them chemically similar to classical "desert varnish". The coatings have pitted surfaces, with grooves and cracks that probably originate from eolian abrasion. Under high magnification (using a scanning electron microscope, SEM) the coatings show distinct platelet morphology, with books or layers of smaller platelets on top of larger ones. In addition to the Al- and Fe-rich material, some gypsum and halite were detected. The reflectance properties of sand deposits as depicted in Landsat images and space photographs are believed to be affected by the coatings on the quartz grains. Assuming that the red colored sands of southwestern Egypt are analogous to the reddish brown particles on the surface of Mars, their reflectance properties should be studied for correlation.

INTRODUCTION

Sands from the Western Desert of Egypt vary considerably in composition. Microscopic studies of samples from various parts of the desert have revealed that they are composed of at least 40% quartz, and varying amounts of calcareous grains (including chalk, limestone, dolomite, marl, and calcite), heavy minerals (including glauconite, phosphates, hornblende), shale, and gypsum (El-Baz and others, 1979b). Although these different minerals cause variations in the overall sand color, it is nonetheless believed that the color of the quartz grains themselves can be an indication of the time of exposure and distance from the sand source. This is based on the proposition that the red color of quartz sand is caused by the presence of hematite coatings on individual grains.

Reddened sands have been observed in deserts throughout the world. However, their mode of formation is a matter of controversy.

According to one hypothesis, the hematite is detrital having been formed in lateritic soils of hot, humid climates and later transported to desert basins (Van Houten, 1973). The second hypothesis contends that the hematite coating is post-depositional and results from weathering of iron-bearing minerals (Walker, 1967; 1979; Glennie, 1970).

Although the origin of the red color is controversial, the fact that the red color increases with the distance from the sand source has been established in many locations. Examples include the study of Skylab 4 photographs of the Namib Desert of Southwest Africa (McKee and others, 1977), the Apollo-Soyuz photographs of the Sturt (El-Baz, 1978a), and Simpson Deserts of Australia (Breed and Breed, 1979), and of the Western Desert of Egypt (El-Baz and El-Etr, 1979).

In addition, in the Algodones dunefield, the intensity of sand color increases from north to south; 25 to 60 percent of the grains are hematite-coated, with maximum values (60%) occurring in the south (Norris and Norris, 1961, p. 611). Because the sand transport direction in this field is to the southeast (Sharp, 1979, p. 908), the redder sands are farther from their source and have been exposed for a longer period of time.

Because of the importance of sand color variations, samples from the Western Desert of Egypt are being studied to investigate the nature of coatings on sand grains. Initially, samples from the southwestern part of the desert were selected because they fall near the end of the sand transport cycle in Egypt, which is generally from north to south (Gifford and others, 1979). This region showed increased reddening in Earth-orbital photographs and thus, the sand grains were presumed to show thicker coatings.

SAMPLE LOCATION

The sample discussed in this chapter was collected by T. A. Maxwell from the floor of Wadi El-Bakht (Fig. 13.1) during a journey

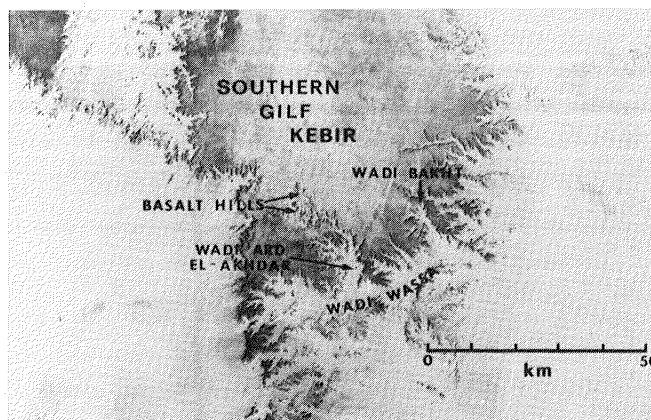


Figure 13.1 Part of the southern Gilf Kebir plateau as photographed by Landsat 1 (from Maxwell, 1980; Landsat Image E-1131-08141).

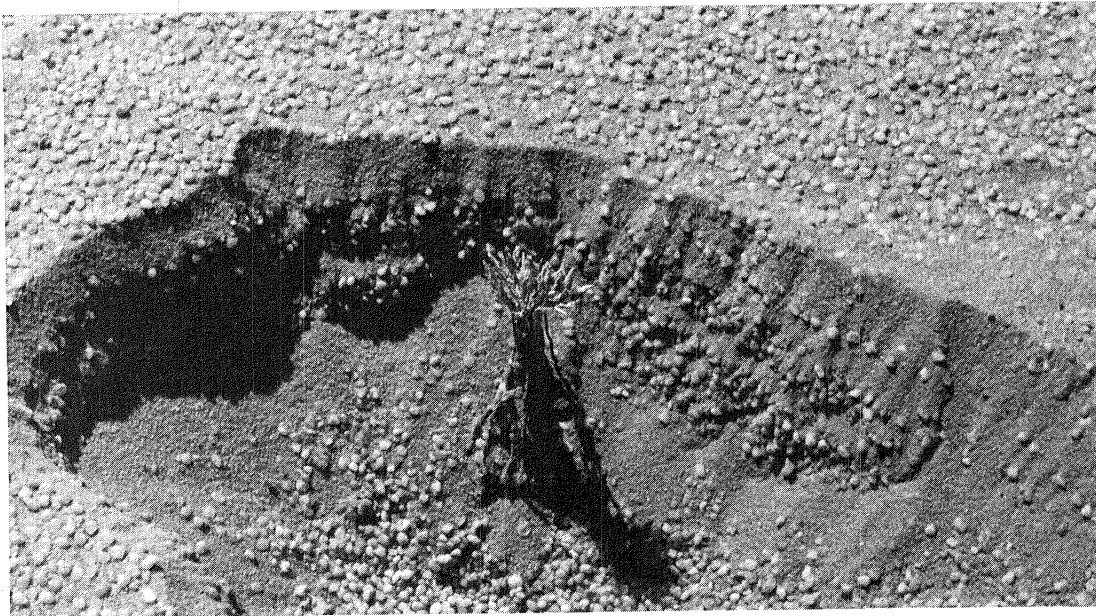


Figure 13.2 Layered coarse sand deposits in the floor of Wadi El-Diq on the eastern edge of the southern Gilf Kebir. Plant is about 12 cm high.

to the southeastern edge of the Gilf Kebir plateau (El-Baz and others, 1980). This plateau lies south of the gigantic dunefield of the Great Sand Sea. Grains from this sand mass travel southward with the prevailing winds, and field observations indicate that some sand climbs up and travels southward on top of the plateau. Thus, accumulations of sand south of the plateau come from either side or from its top. Some small component may result from the erosion of the hardened sandstones and quartzites that cap the plateau.

Numerous wadis incise the Gilf Kebir plateau, particularly along its southeastern margin. The floors of the wadis are flat with a sand cover, which is often coarse and laminated. Trenches in this sand reveal darker layers with a high percentage of heavy minerals intercalated with lighter, finer-grained layers (Fig. 13.2). This suggests that the sand was deposited by winds of varying velocities; the strongest winds deposit the coarser sands with the heavy minerals, and the weaker winds deposit finer, light-colored sands.

Wadi El-Bakht is located in the southeastern corner of the southern Gilf and trends toward the northwest. In the upper reaches of this wadi a thick deposit of mud indicates beds of ancient lakes. Here, "the old lake floor consisted of alternating thin sheets of mud and partly cemented sand with an upper capping of mud some 6 inches thick. Similar reddened and hard sand was found in the meander terraces in the wadi beds; probably iron oxides derived from the sandstones and basalts and washed into these sands during their transport are responsible for the alterations" (Peel, 1939b, p. 306). The Wadi El-Bakht sample was collected from a dune that crosses it (Fig. 13.3). The sand in the dune is well-sorted and contains small amounts

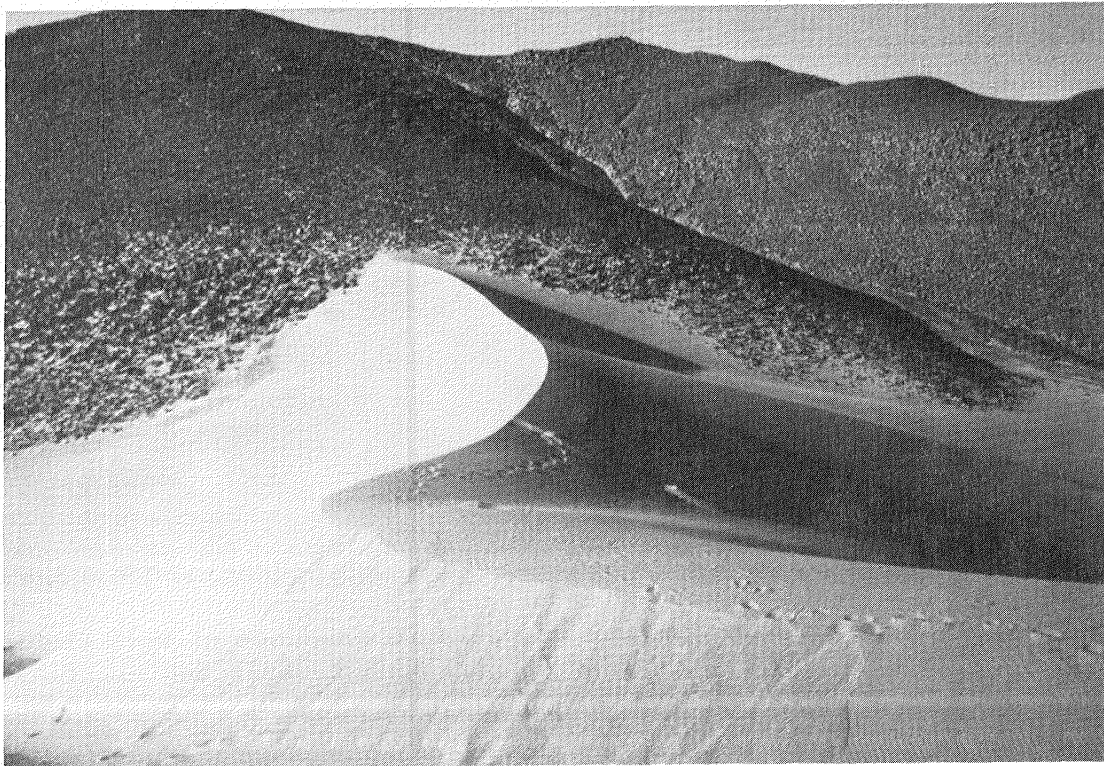


Figure 13.3 Dune partly blocking the upper reaches of Wadi El-Bakht in the southeastern edge of the southern Gilf Kebir (Photograph by N. S. Embabi).

of heavy minerals (Prestel and El-Baz, 1979; Prestel and others, 1980).

EXPERIMENTAL PROCEDURE

The quartz sand grains were initially examined with a binocular microscope to study the main textures and overgrowths. Single, small, heavily-coated grains were examined by X-ray powder diffractometry to characterize the mineralogy of the coatings. Due to the thin nature of the coatings, which occur in amounts below the detection limit (by volume) of the diffractometer, only quartz appeared in the diffraction pattern. Heavily-coated sand grains and those with coatings concentrated in pits or cracks were chosen for X-ray powder diffraction using the Gandolfi camera. The coating was gently scraped from many individual grains in order to collect sufficient material for analysis. The Gandolfi camera geometry allows precession of the sample in the X-ray beam so that crystals in all orientations can be brought into the diffraction condition, thereby enhancing diffraction lines produced by a small number of crystals. Fe K-alpha X-radiation was used to minimize fluorescence from iron in the sample. Concurrently, additional grains were fractured under liquid freon to expose the interior of the grains and a cross section of the coating. The grains were examined by scanning electron microscopy (SEM) at

magnifications from 100X to 200,000X. Energy dispersive X-ray analysis (EDXA) was used to qualitatively determine the chemistry of the coating and attached crystals.

MICROSCOPIC CHARACTERISTICS

Examinations using a binocular microscope indicate that the reddish-brown color of the sand grains may be attributed to: 1) an extremely thin coating or stain of reddish-brown material entirely covering the grains except on freshly broken surfaces, 2) small clumps of reddish-brown granules in pits on grain surfaces, 3) a reddish-brown material concentrated within cracks in the grains, and 4) detrital dark brown grains occurring within the sand grains, which were probably present in pore spaces when the parent sandstone was lithified.

Grains having either a relatively thick coating or a high concentration of material in pits or cracks were selected for X-ray diffraction analysis. The material concentrated in cracks was removed for detailed examination. The SEM study of the morphology of the

Table 13.1 X-Ray diffraction data on scrapings of quartz grain coatings.

| D Å | Kaolinite HKL | Hematite HKL | Quartz* HKL |
|-------|------------------|-----------------|----------------|
| 7.277 | 001 | | |
| 4.261 | | | 100 |
| 4.146 | 111 | | |
| 3.721 | 021 | | |
| 3.591 | 002 | | |
| 3.349 | | | 101 |
| 2.696 | | 104 | |
| 2.578 | 130,201 | | |
| 2.455 | | 110 | 110 |
| 2.282 | | | 102 |
| 2.235 | | | 111 |
| 2.123 | | | 200 |
| 1.980 | | | 201 |
| 1.817 | | | 112 |
| 1.693 | | 116 | |
| 1.671 | | | 202 |
| 1.541 | | | 211 |
| 1.488 | | 214 | |
| 1.452 | | 300 | 113 |
| 1.382 | | | 212 |
| 1.374 | | | 203 |
| 1.289 | | | 104 |
| 1.256 | | | 302 |

* + 10 additional quartz lines.

coatings in depressions corresponds to that on exposed grain surfaces, and associated EDXA chemical analyses supported the assumption that the material concentrated in the cracks was of the same composition as that on the grain surface.

MINERALOGY AND MORPHOLOGY OF THE COATINGS

X-ray diffraction analysis of the scrapings indicates that the coating on the quartz grains is composed of kaolinite (a 7Å clay mineral, indexed after kaolinite) and hematite. Table 13.1 shows the diffraction lines observed for each mineral present. Diffraction lines from kaolinite suggest a well-crystallized material. In contrast, hematite displays diffuse lines, which suggests poor crystallinity and very fine grain size.

A quantitative estimate of the amount of each mineral present cannot be made from these data. However, the greater number of diffraction lines corresponding to kaolinite compared to hematite, combined with the better resolution of the kaolinite lines suggests that kaolinite is either more abundant or better crystallized.

All of the grains examined had an irregular, pitted surface with a ubiquitous coating of fine-grained material. Figures 13.4 through 13.7 illustrate the variety of coating textures and morphologies observed. Figures 13.4a and b show the well-defined contact between the coating and its underlying quartz surface. The coating conforms closely to grain morphology. Although its thickness is roughly 2-5 μm, it has been observed to vary from 0.5 μm to 4.5 μm over the surface of a single grain. The sand grains exhibit a characteristically pitted surface with a rough, irregular, and slightly porous coating (Fig. 13.4c). Ridges protruding on the grains appear to have been smoothed during eolian transport.

At higher magnifications (Fig. 13.4d), the coating reveals a complex morphology consisting of a variety of sub-micrometer size particles and granules. Many of the particles are obviously crystals and frequently are hexagonal platelets (Fig. 13.5a). These platelets occur as randomly-oriented single grains or as books of platelets, with the individual platelets ranging in size from a few hundred angstroms to about 2 micrometers. Individual platelets have a powdery surface, with small platelets occurring on the surfaces of larger plates (Fig. 13.5b). This may indicate that books of platelets are formed as the result of in-situ growth of small platelets on larger, pre-existing ones.

Figures 13.6a and b are views of the coating in a depression in the surface of a grain. A well-defined contact and a lack of preferred orientation of coating particles are clearly shown. Some lineation along the quartz grain contact is indicated. Figure 13.6c shows books of platelets in a somewhat protected region along the contact with the fractured quartz grain surface. We observed incipient growth of coating crystals on a quartz grain surface (Fig. 13.6d), providing additional evidence that in-situ nucleation and growth processes are responsible for coating development. Thus, a mechanical

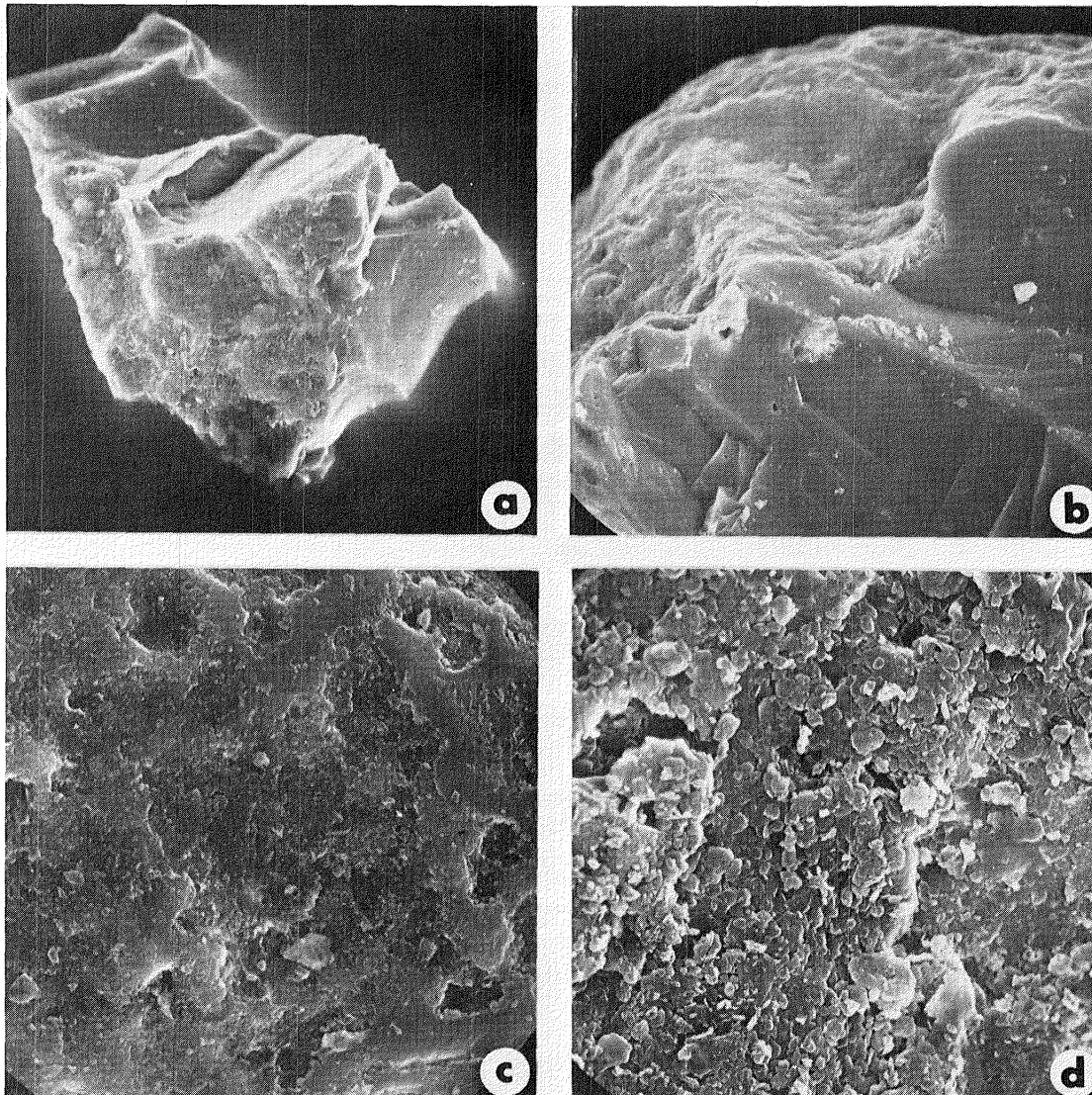


Figure 13.4 (a) A fractured sand grain showing a well-defined contact between the unweathered quartz and its surface coating (300X, width of field 300 μm); (b) An SEM view illustrating how the coating covers the entire grain surface and conforms to its morphology (300X, width of field 300 μm); (c) A sand grain exhibiting the characteristic pitted surface with ridges, probably smoothed during eolian transport (1000X, width of field 90 μm); (d) The same grain under higher magnification (8000X, width of field 11.25 μm) showing the porous nature of the coating and its complex morphology.

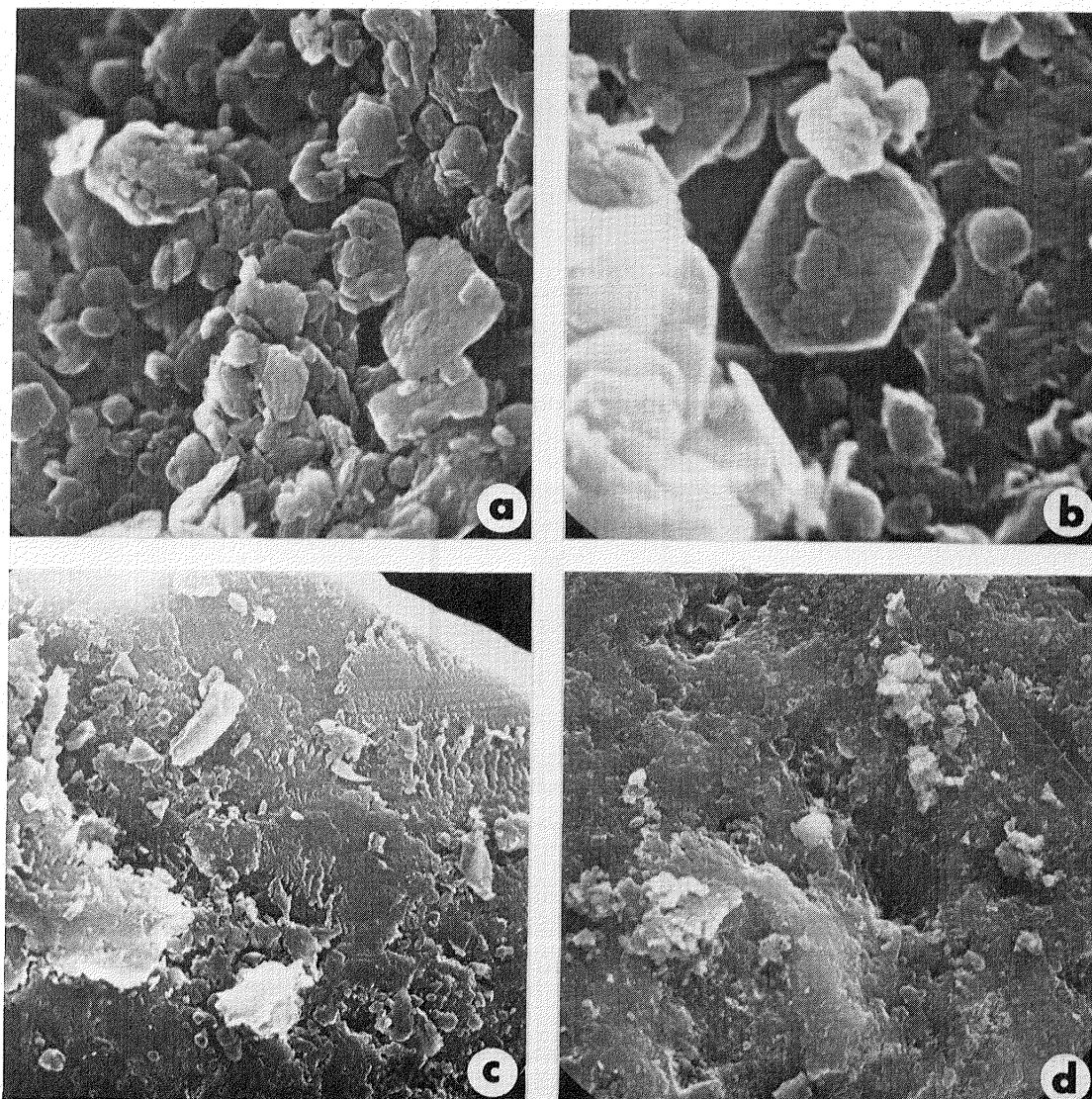


Figure 13.5 (a) Texture and morphology of hexagonal platelets of quartz grain coating (20000X, width of field 4.5 μm); (b) Books of platelets, small ones on top of a larger plate. The dusty appearance is probably due to fine grained hematite (80000X, width of field 1.12 μm); (c) An unusual, cracked coating with grainy rather than porous material. The grooves may be a result of extensive abrasion (6000X, width of field 15 μm); (d) A feathery silica deposit with white gypsum crystals especially in the lower left part of the view (6000X, width of field 15 μm).

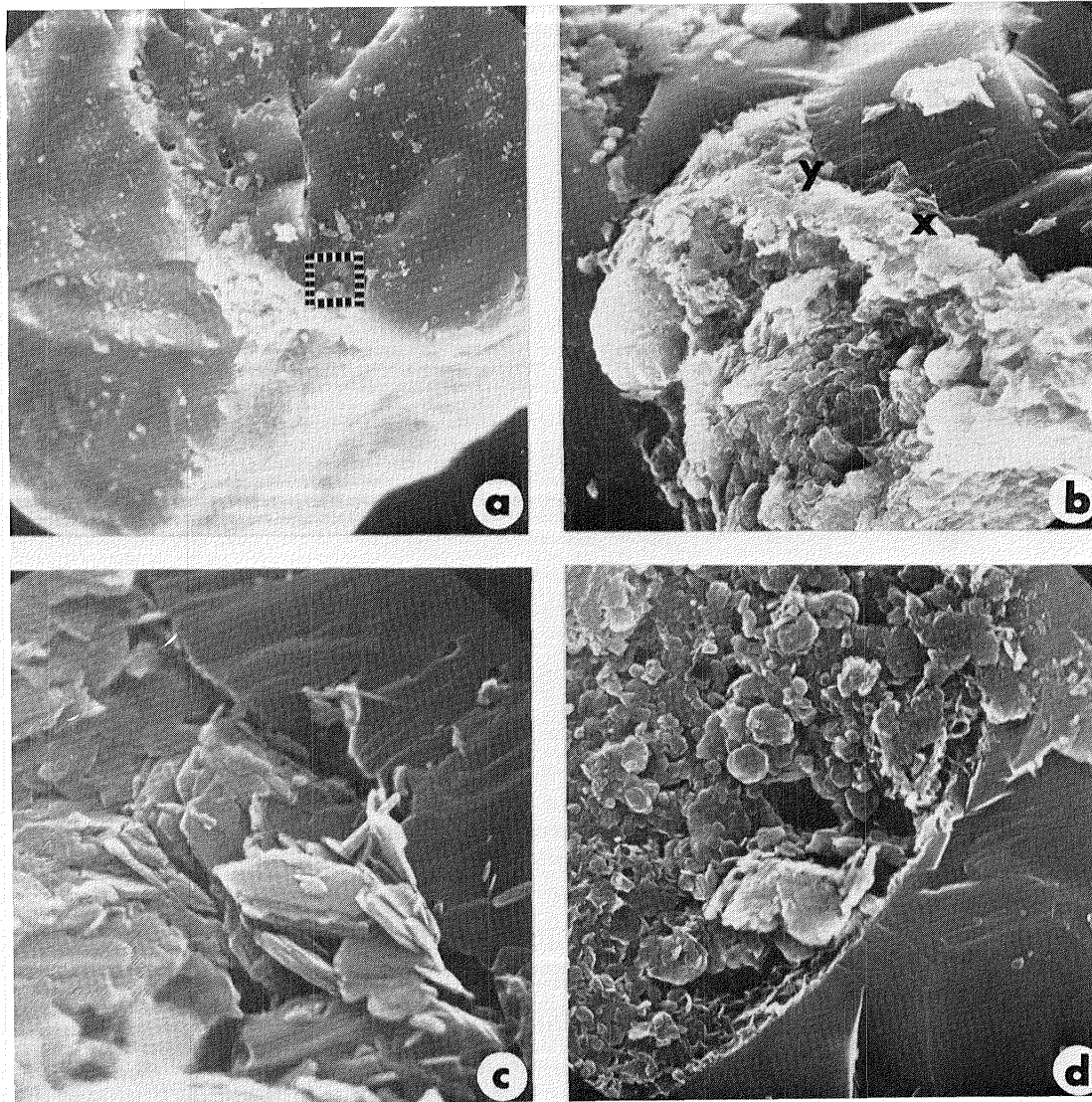


Figure 13.6 (a) A typical coating in a depression in a quartz grain (500X, width of field $180\mu\text{m}$; marked area is shown in Fig. 13.7b); (b) Enlargement of the same coating showing the lack of preferred orientation of particles, although some layering of the coating is visible along the contact with the grain surface (2000X, width of field $45\mu\text{m}$); (c) Additional enlargement of area X in Figure 13.6b, showing books of platelets on a somewhat protected area of the grain surface (20000X, width of field $4.5\mu\text{m}$); (d) Another enlargement, of area Y in Figure 13.6b, showing initial growth of coating crystals on the grain surface (10000X, width of field $9\mu\text{m}$).

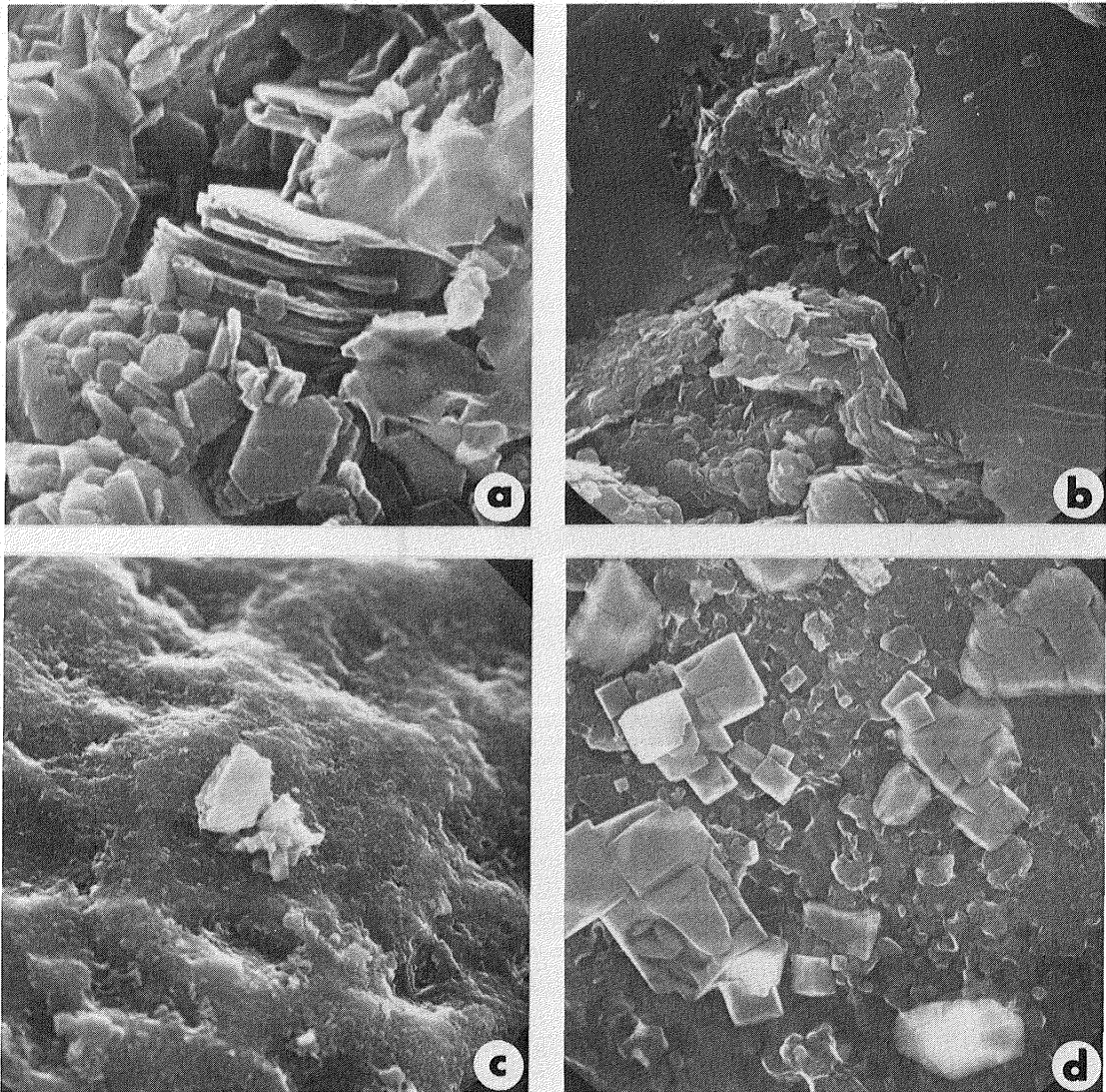


Figure 13.7 (a) Randomly oriented books of hexagonal platelets that appear powdery and delicate (30000X, width of field $3 \mu\text{m}$); (b) Examples of twisted platelets and of oriented platelets in a pit shown in Figure 13.6a (8000X, width of field $11.25 \mu\text{m}$); (c) Crystals of calcium sulfate (gypsum) attached to a coating on quartz grains (1500X, width of field $60 \mu\text{m}$); (d) Growth steps and penetrating crystals of sodium chloride (halite) attached to the coating (15000X, width of field $6 \mu\text{m}$).

plastering of clay particles on a quartz substrate cannot be a predominant process in coating formation. Figure 13.7a shows the randomly-oriented books of hexagonal platelets frequently observed.

Although the coating probably develops gradually during eolian transport, it shows little evidence of successive layers of deposition over most of the surface area of the grain. The lack of successive layering most likely precludes episodic growth periods with intervening erosion and is consistent with gradual, continuous growth. No systematic changes in morphology (crystal size or orientation), mineralogy or chemistry were observed in the coatings. However, in a few pitted regions, some preferred orientation of platelets in response to grain morphology was seen (Fig. 13.7b). Twisted platelets and oriented (flat-lying) platelets occur within pits and in areas surrounding pits.

Additional features of interest were secondary crystals and abrasion features on the coatings. Secondary crystals of gypsum (Fig. 13.7c and 13.8) and halite (Fig. 13.7d and 13.9) were observed attached to the coatings and were identified by EDXA. A silica deposit with superposed gypsum crystals (Fig. 13.5d) was also recognized. The crystals are believed to have grown in situ, since they exhibit growth steps on crystal faces and penetrating crystal forms. These deposits indicate that processes involving a fluid phase were encountered after the underlying coating was formed. Recognized abrasion features include extensive grooving, cracking, degrading of the coating to a grainy texture, and polishing of protruding ridges on the grains (some of these features are visible in Figure 13.5c).

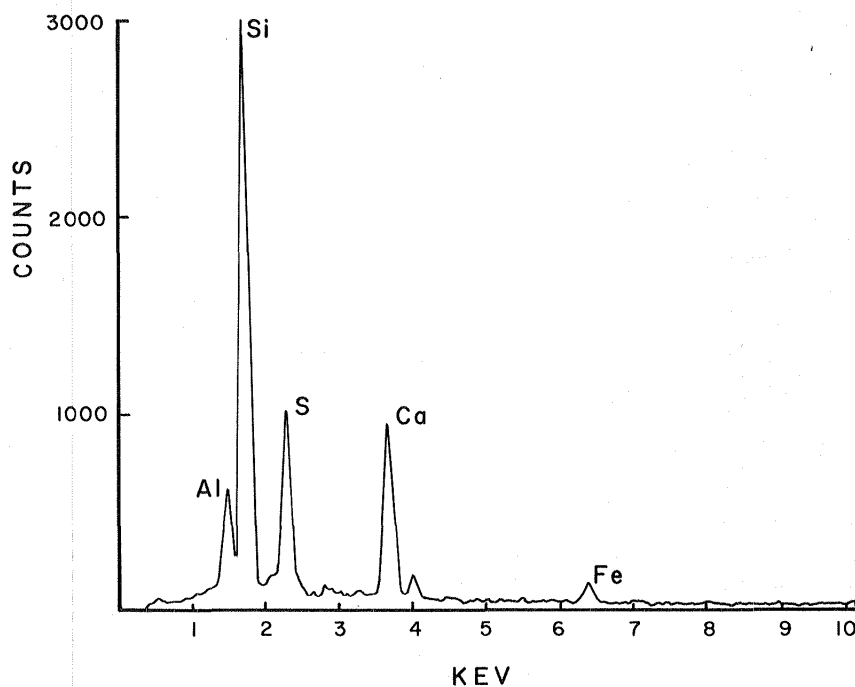


Figure 13.8 X-ray spectrum of calcium sulfate (gypsum) crystal attached to the coating.

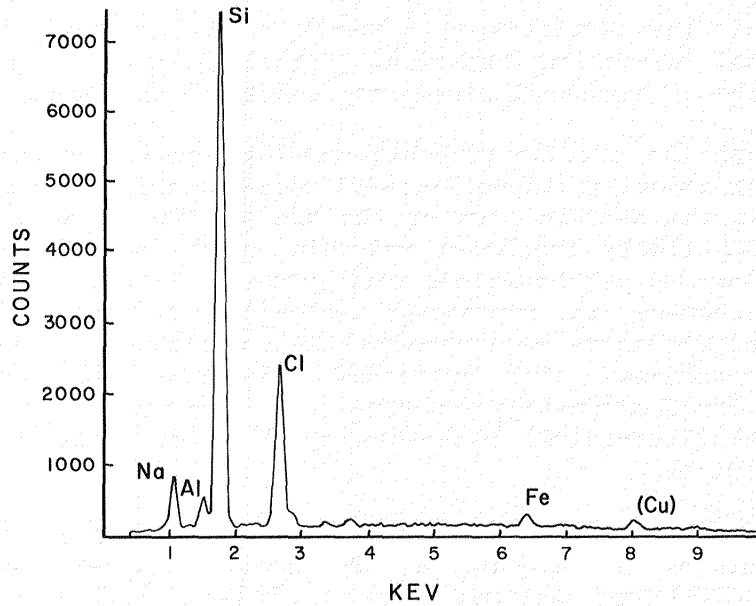


Figure 13.9 X-ray spectrum of sodium chloride (halite) crystals attached to the coating, using a Cu sample holder.

The hexagonal platelet nature of the coating agrees well with the presence of kaolinite and hematite, since both minerals are known to have a hexagonal, platy habit. Chemical analyses by EDXA indicate that the coating is much richer in Al than Fe (Fig. 13.10). This suggests that the coating is composed predominantly of a clay material with very finely disseminated hematite. The two minerals are probably growing either simultaneously or successively, since all attempts to separate them with SEM-EDXA have failed.

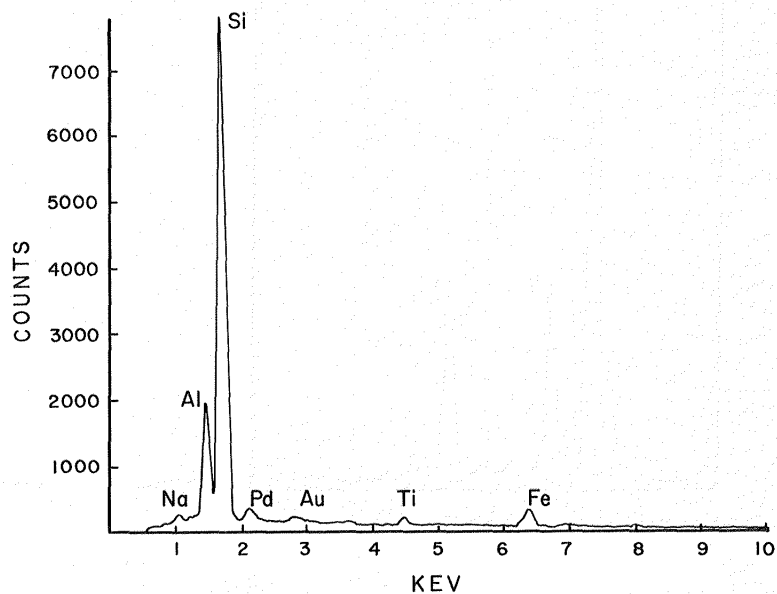


Figure 13.10 X-ray spectrum of overall coating on quartz sand grains.

DISCUSSION

From observations of fine drainage lines leading northward towards the Mediterranean and eastwards towards the Nile Valley, it is postulated that the sands of the Western Desert originated from the "Nubian" and from other sandstones exposed in the southern part of the desert. The sand was most likely transported to the northern part via the Nile and subsidiary drainage wadis, particularly during wetter climatic conditions in the past. After the climate became drier and an eolian regime dominated, the sands were driven southward by the action of wind. Most of the physical characteristics and chemical coatings were probably acquired in this eolian regime in an extremely arid environment.

The presence of large amounts of sand-sized grains not originally from the Nubian Sandstones is related to the nature of local rocks, particularly in the Western Desert depressions that enclose oases. Preliminary study of the sands from the northern and central parts of the desert supports this hypothesis. Sand samples from the various oases show varying compositions of sand-sized grains, with certain unique components such as phosphate, glauconite, shale, and carbonate (El-Baz and others, 1979b).

The detailed analyses of sand samples from the Gifl Kebir area in the southwestern part of the desert produced one major unexpected result. Although hematite is present in coatings of the quartz grains, there is a considerable amount of kaolinite. The presence of clays in the quartz sand coatings makes these coatings more like "desert varnish". (Recent studies of desert-varnished rocks indicate that clays constitute a significant component of the varnish; (Potter and Rossman, 1977, 1979.) The coatings in quartz grains in southwestern Egypt show complex morphology and mineralogy. Although kaolinite and hematite comprise the major part of the coatings, gypsum and halite do occur in minor amounts.

We are presently analyzing samples from other parts of the Western Desert. The purpose of these investigations is to study the quartz sand grain coating to determine its mineral components, and whether local components affect the composition of the coating. Additionally, samples from different localities will be studied to determine whether the observed geographic variations in desert color are due to varying thickness and mineralogy of the coatings on individual sand grains. These studies should allow us to further ascertain how the coatings develop and if they vary in different environmental conditions.

Also, the effects of these coatings on the reflectance properties of the sand accumulations will be studied. The chemistry and thickness of the coatings were assumed to affect the reflectance of the desert surfaces as measured by remote sensing (e.g., by the Landsat multispectral sensors). Attempts will be made to relate a measure of reflectance in the Landsat data to the nature of coatings on sand grains. In addition, there are possible correlations between the reddish brown sands of the extremely dry Western Desert and the yellowish

brown grains on the surface of Mars. Results of the Viking mission to Mars indicate that the color of the surface is consistent with an abundance of Fe⁺³-rich weathering products, notably nontronite (Huck and others, 1977, p. 4401). Thus, the study of the kaolinite/ hematite coated grains of the Western Desert of Egypt may provide an analog to the oxidized regolith on Mars.

Chapter 14

GEOLOGY OF THE SOUTHERN GILF KEBIR PLATEAU AND VICINITY, WESTERN DESERT, EGYPT

MAURICE J. GROLIER and PATRICIA A. SCHULTEJANN
U. S. Geological Survey
Flagstaff, Arizona 86001

ABSTRACT

The Gilf Kebir Plateau is located in the remotest and most arid part of the Western Desert. Bounded by irregularly dissected cliffs, it stands several hundred meters above the surrounding desert floor. Sandstone strata of Paleozoic and Mesozoic age, intruded here and there by volcanic rocks, are exposed in cliffs and walls of deeply incised wadis. The Gilf is a residual sandstone mass on which the successive (and alternating) imprints of running water, mass wasting and wind may be deciphered. Its interest to paleoclimatologists, geologists and archeologists lies in the paleoclimatic record retained in its erosional landforms and surficial deposits.

The geologic map of the southern Gilf Kebir Plateau and vicinity presented here is derived largely from analysis of a Landsat image. Several Landsat data products, such as false-color composites of bands 4, 5 and 7, linearly and sinusoidally stretched to enhance contrast, were used in map compilation. Geologic mapping of the sandstone strata that underlie the Gilf Kebir shows the extremely dissected outline of the plateau in greater detail than on earlier geologic maps of the region. Surficial deposits, mapped in detail for the first time, are differentiated into eight map units. These units include alluvium, colluvium and various types of eolian sand that mantle the floor of the Western Desert in the vicinity of the Gilf.

INTRODUCTION

The Gilf Kebir is a sandstone plateau bounded by high, steep-sided cliffs, which are broken here and there by incised but essentially abandoned stream valleys. These valleys are vestiges of past fluvial activity in the southwestern part of the Western Desert of Egypt. The shallow channels of underfit, ephemeral streams are the only morphological evidence of present fluvial activity on these valley floors (McCauley and others, Chapter 15).

The Gilf Kebir Plateau was approached on January 7, 1926, by Prince Kemal El-Din Hussein (Hussein, 1928, p. 324-325), and named by him in recognition of its bounding escarpment, which is, of all escarpments in the Western Desert, unusually high and forbidding.

Fifty-two years later, the El-Baz expedition to the Gilf Kebir and Uweinat (a dissected mountain massif astride the Egypt-Libya-Sudan borders, 120 km southwest of the southern tip of the Gilf) approached the Gilf Kebir from the eolian peneplain to the east. It came to a halt on September 30, 1978, at the base of east-facing bluffs (El-Baz and others, 1980), where Bagnold's 1938 camp still stands (Bagnold and others, 1939). Base camp was established 31 km to the south at the east entrance to Wadi Wassa, at a site used by Issawi while on reconnaissance surveys of the region (1971-1972, 1972-1973) for the Geological Survey of Egypt (Issawi, 1973a).

A preliminary geologic map of the southern Gilf Kebir Plateau and vicinity is shown in Figure 14.1. The map is based on analysis of Landsat image 1131-08141, December 1, 1972, and on visual interpretation of rock-stratigraphic units. Image analysis was supplemented by field observations made by John F. McCauley, Carol S. Breed, and Maurice J. Grolier during traverses along the east border of the plateau and en route to Uweinat in October 1978. Field observations by earlier workers during several pre- and post-World War II expeditions to the Gilf were helpful in compiling the map, and are incorporated wherever scale constraints allow.

The map is a product of the regional study of the Gilf first recommended by El-Baz and Mitchell (1975, p. 9) because of the similarities in climate and geomorphology between the Gilf and the deserts of Mars. It illustrates the kind of geologic map that can be prepared on a regional scale in the Western Desert, using computer-processed Landsat images as base maps (El-Baz and others, 1980).

PREVIOUS EXPLORATION AND GEOLOGIC WORK

The recorded expeditions to the Gilf Kebir are many. Among them are those of Prince Kemal El-Din (1925-1926), Bagnold (1930), P. A. Clayton (1931), R. C. E. Clayton and de Almasy (1932), Penderel and de Almasy (1933), R. C. E. Clayton (1932, 1934), Shaw (1935), Bagnold (1938), Muhammed Wasfi Bey (1939), Misonne (1969), Issawi (1971-1972, 1972-1973), Wendorf (1974), and El-Baz (1978). A historical account of the exploration of the Gilf has been summarized by Peel (1939b). Wright (1945), spent four days in 1942 adding topographic detail to the 1:250,000 scale map covering the region between Uweinat and the Gilf. In January 1969, after a lapse of 27 years, Misonne, the biologist on the Belgian scientific expedition to Uweinat (1968-1969), traveled for 600 km across the Gilf Kebir Plateau. He recorded the presence of wild sheep, small foxes and lizards, but stated that half the trees (mostly acacias) in the wadis of the northern Gilf were dead (Misonne, 1969a). During two field seasons (1971-1972 and 1972-1973), Issawi carried out a geologic reconnaissance of the southwestern part of the Western Desert, including the Gilf Kebir, for the Geological Survey of Egypt (Issawi, 1973a). In 1974, Wendorf paid a short visit to two archeological sites (described by Myers in Bagnold and others, 1939, p. 287-295) and dated them (Wendorf and others, 1977, p. 230). Since the winter 1976-1977, a geologic research program in southwest Egypt (including the Gilf Keber Plateau), sponsored by the Deutsche Forschungsgemeinschaft in cooperation with the Academy of Sciences of

Egypt, has been carried out by Klitzsch (1978, Klitzsch and others, 1979) with the support of the Continental Oil Company (CONOCO).

The geology of southwestern Egypt is described in reports by the geologists and archeologists attached to the expeditions listed above. It is generalized in the 1:2,000,000-scale geologic map of Egypt by the Geological Survey of Egypt (1979). This map incorporates some of the stratigraphic information gathered by Issawi (1973a) and earlier explorers, but except for the dune sand of the main linear dune belts, the regional distribution of surficial Quaternary units is not known.

BEDROCK GEOLOGY

The first mention of basement rocks in the area south of the Gilf Kebir Plateau was by P. A. Clayton (1933), who stated that the hills 10 km north of the peaks of Peter and Paul (35 km west of southwest map corner, Fig. 14.1) are mostly granite, and that the volcanic craters he had observed northeast of Uweinat rest on gneiss and granite. According to Sandford (1935a), the basement rocks that crop out between Uweinat and the Gilf consist of metamorphic rocks intruded by pink granite, aplite and pegmatites. A geologic map of basement rocks exposed in the Uweinat-Gilf Kebir area (south and east of area of Fig. 14.1) was compiled by El-Ramly (1972). Some of these rocks were also described by Issawi (1973a).

An older sandstone of Paleozoic age (unit Pzs) unconformably overlies basement rocks exposed at Uweinat (south of map area, Fig. 14.1), and in depressions between the Gilf and Uweinat (Sandford, in Bagnold, 1933, p. 127 and 214-225). Sandford (1935a, Fig. 6) noted that such a sandstone crops out in the hills east of the Gilf. Peel (1939b) reported a similar sandstone in the lower part of the cliffs along the western side of the Gilf, in the region of Wadi Sura (latitude 23° 35' N, longitude uncertain) in the northwestern part of the map area. The known regional distribution of this sandstone was extended by Issawi (1973a) to the area west and southwest of the Gilf, where he subdivided it into a basal unit of pre-Devonian age (a measured section near Gebel 1114, just west of area shown in Fig. 14.1, is 22.8 m thick), and an upper unit of Devonian-Carboniferous age, which is 104.5 m thick west of the Gilf Kebir Plateau near latitude 23° 50' N.

Igneous rocks, particularly those in the hills northeast of the peaks of Peter and Paul, and on Gebel Babein astride the Egypt-Libya border, are of uncertain Paleozoic age. The syenite layer interbedded in the basal unit of the Paleozoic sandstone, and some of the phonolite, trachyte and microsyenite sills and dikes known to occur in the upper unit (Issawi, 1973a) may be Paleozoic in age or younger. The igneous rocks (interstratified in Paleozoic sandstone unit Pzs) are not shown on the geologic map.

Within the Gilf Kebir Plateau, Paleozoic sandstone is unconformably overlain by a younger sandstone (unit KJs), which includes the Gilf Sandstone, named by Issawi (1973a) and probably of Jurassic age, and Nubia strata of Cretaceous age. At its type locality, in the

escarpment bordering the Gilf Kebir Plateau near the west entrance to Wadi Wassa, the Gilf Sandstone is about 165 m thick and dips very gently northeastward (1° - 3°) under younger "Nubia" sandstone and shale of Late Cretaceous age (Issawi, 1973a).

"Nubian sandstone" is a nomenclatural term traditionally applied to sandstone of almost any provenance and geologic age in Egypt and other Middle Eastern countries (Pomeyrol, 1968). Like Ball (1927) and Sandford (1935a), Issawi (1973a; 1973b) recognized this unsatisfactory situation, and was one of the first geologists to restrict usage of the term "Nubia" to sandstone of mostly Late Cretaceous age that crops out in southern Egypt and probably northern Sudan. However, the term "Nubia" is still used in the less restricted sense by other workers, particularly Klitzsch and others (1979).

The Nubia strata of Klitzsch and others (1979) have an aggregate thickness of 1000 to 2000 m in southwestern Egypt and include six units (Klitzsch, 1978). The lowermost is the Gilf Kebir unit of Jurassic age. Klitzsch and others' type area for the Gilf Kebir unit is on the west side of the southern Gilf Kebir Plateau, near Akaba Pass, 95 km north-northwest of the type locality of the Gilf Sandstone as defined by Issawi. The Gilf Kebir unit consists of channel and floodplain deposits that accumulated in a near-marine environment on a shallow shelf. According to Klitzsch (1978) and Klitzsch and others (1979, Fig. 2), the Gilf Kebir unit is the western lateral equivalent of three other newly defined Nubian strata: the basal clastics, the Lingula shale, and possibly the basal part of the Desert Rose unit of Jurassic age; west of the southern Gilf Kebir Plateau, the Gilf Kebir unit unconformably overlies the Paleozoic sandstone.

Despite these unreconciled differences of stratigraphic interpretation and nomenclature, most references to the Gilf Kebir region (Sandford, 1935a; Peel, 1939b; Issawi, 1973a; and Klitzsch and others, 1979) agree that both the older (unit Pzs) and younger (unit KJs) sandstones generally dip a few degrees northward or northeastward, and that the cliffs bordering the plateau are highest on the southern side of the Gilf, and lowest on the northern side. The triangular outline of the Gilf, and the bends of many reaches in the wadis incised into it, are strongly suggestive of a multi-joint pattern. Kadar (1937) reports three systems of fractures in Gilf rocks: NW-SE, NE-SW, and N-S. These fractures probably are mainly joints, for they show little or no apparent displacement on the Landsat image.

Obvious vertical displacement between north and south fault blocks is apparent only in a narrow northeast-trending graben, and along one local NW-trending fracture at the mouth of the second wadi enlargement south of Wadi Diyag in the north-central part of the map (Fig. 14.1). The sudden changes in direction along contiguous reaches of most of the wadis cut into the plateau can be explained by structural control of drainage by at least two joint sets. The anomalous bifurcation angles between main wadis and some of their tributaries, as alluded to by Peel (1941) and discussed by McCauley and others (Chapter 15), may also be explained in part by joint control of ancient river valleys.

Figure 14.1 Geologic map of the southern Gilf Kebir Plateau and vicinity, Western Desert, Egypt. Geographic base: Parts of Landsat scene 192/044 and image 1131-08141, December 1, 1972. Latitude and longitude lines are derived from tick marks and are approximately located.

EXPLANATION

DESCRIPTION OF MAP UNITS

Individual map units were delineated on a false-color composite (FCC) of Landsat image 1131-08141, Dec. 1, 1972. The FCC was prepared from three filtered bands (4-blue, 5-green, and 7-red) after the bands had undergone linear stretching of contrast. In the following descriptions, the numbers 4, 5, and 7 refer to the actual bands on which map units are most easily detected and identified; FCCs refers to the sinusoidally stretched FCC. Fraction symbols such as Qg/KJs are used wherever image interpretation suggests that a bedrock unit (KJs) is unevenly mantled by a thin veneer of a surficial rock unit (Qg).

All bedrock map units are rock-stratigraphic units. Eolian sand deposits as a whole also constitute one rock-stratigraphic unit, of dominantly quartz-grain composition. However, the subdivisions of eolian sand are morphogenetic, and thus are not based on compositional differences. They are facies divided primarily on the basis of variations in color and grain size (McCauley and others, Chapter 15), and secondarily on the basis of their variations in response to local and regional wind flow.

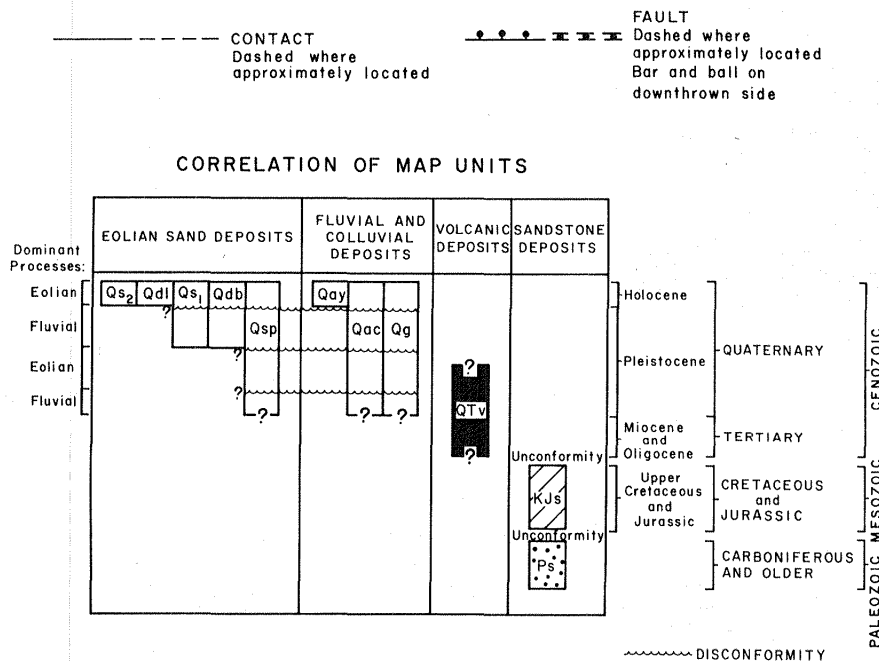


Figure 14.1 (continued)

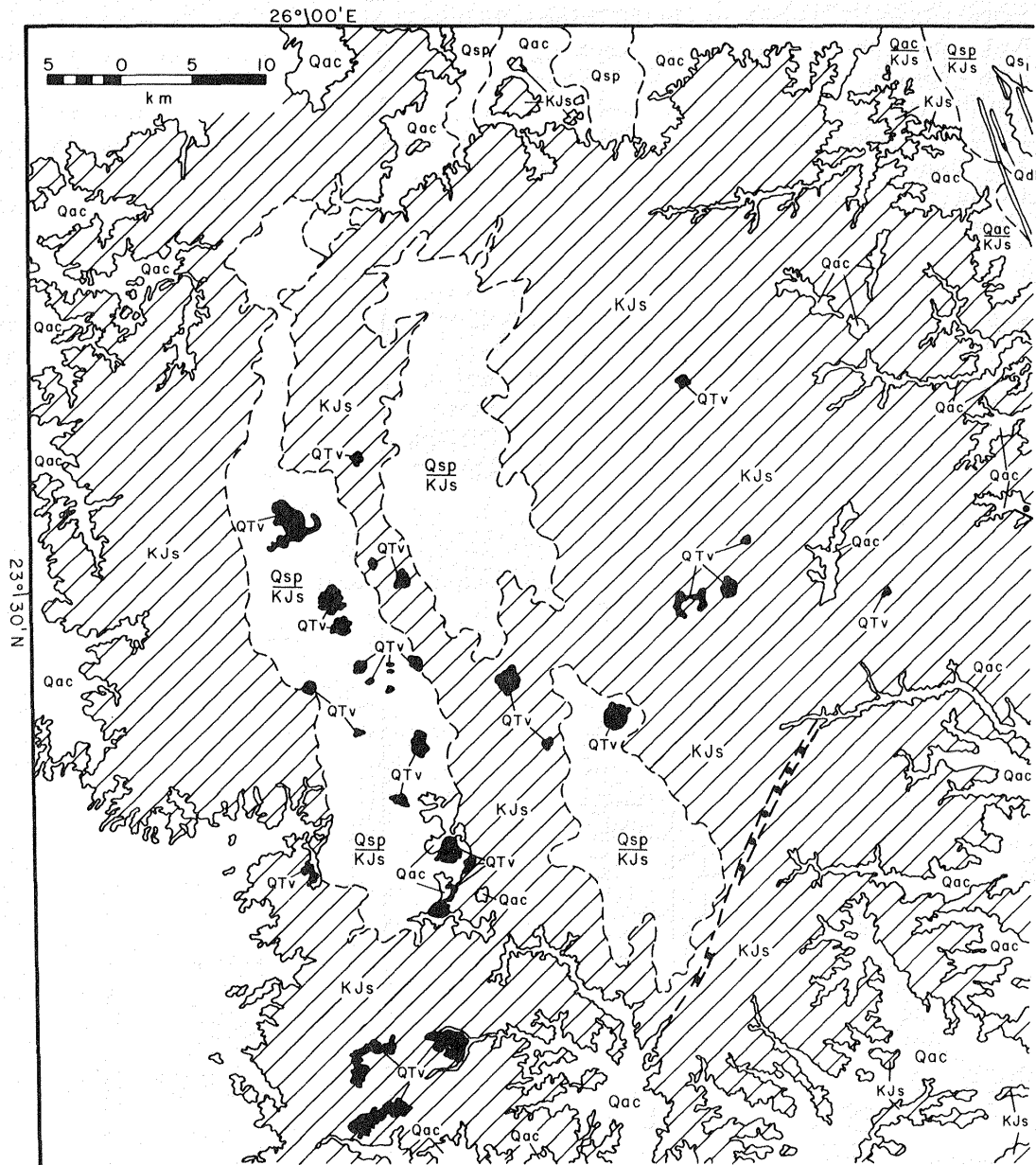


Figure 14.1 (continued)

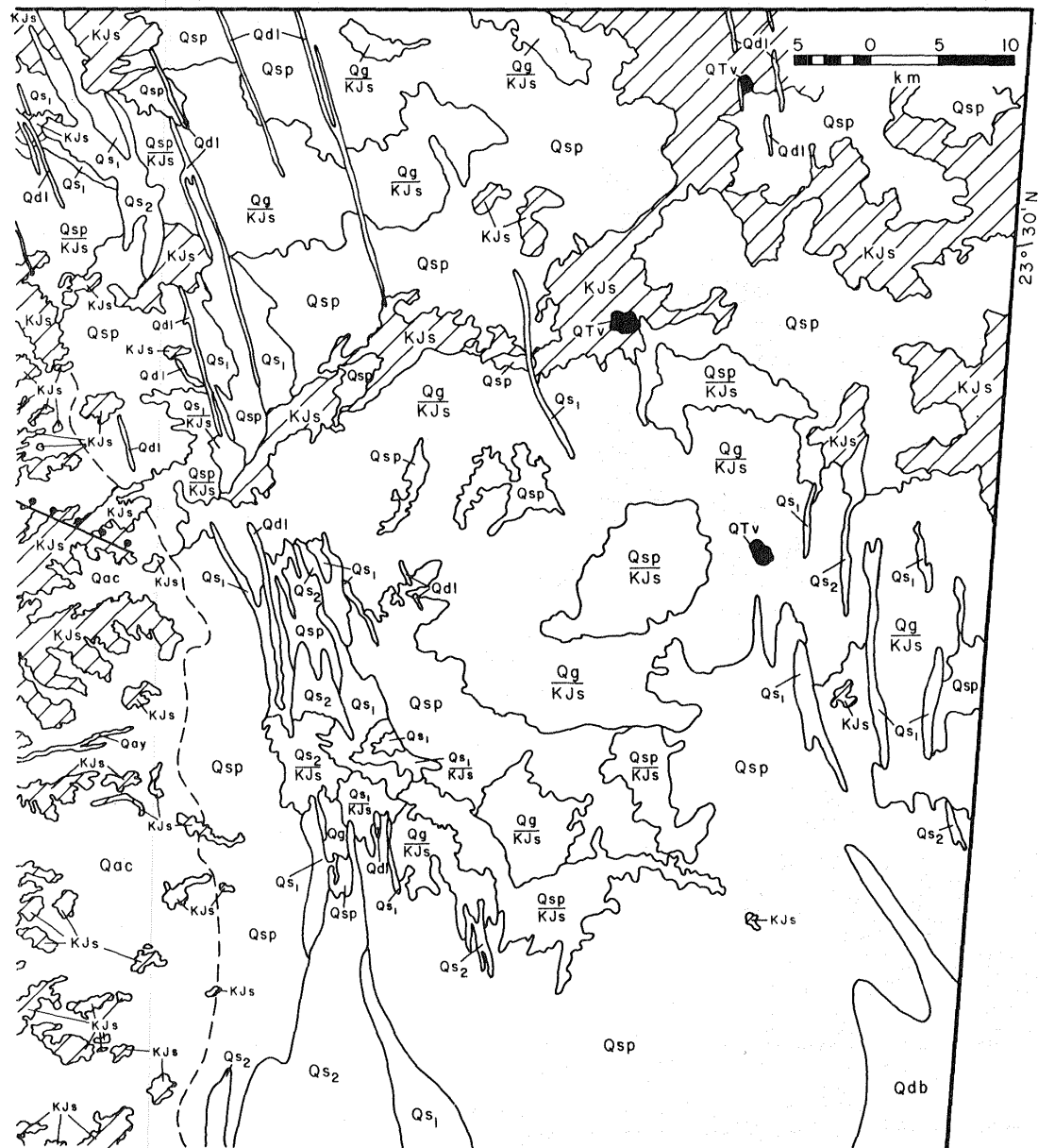


Figure 14.1 (continued)

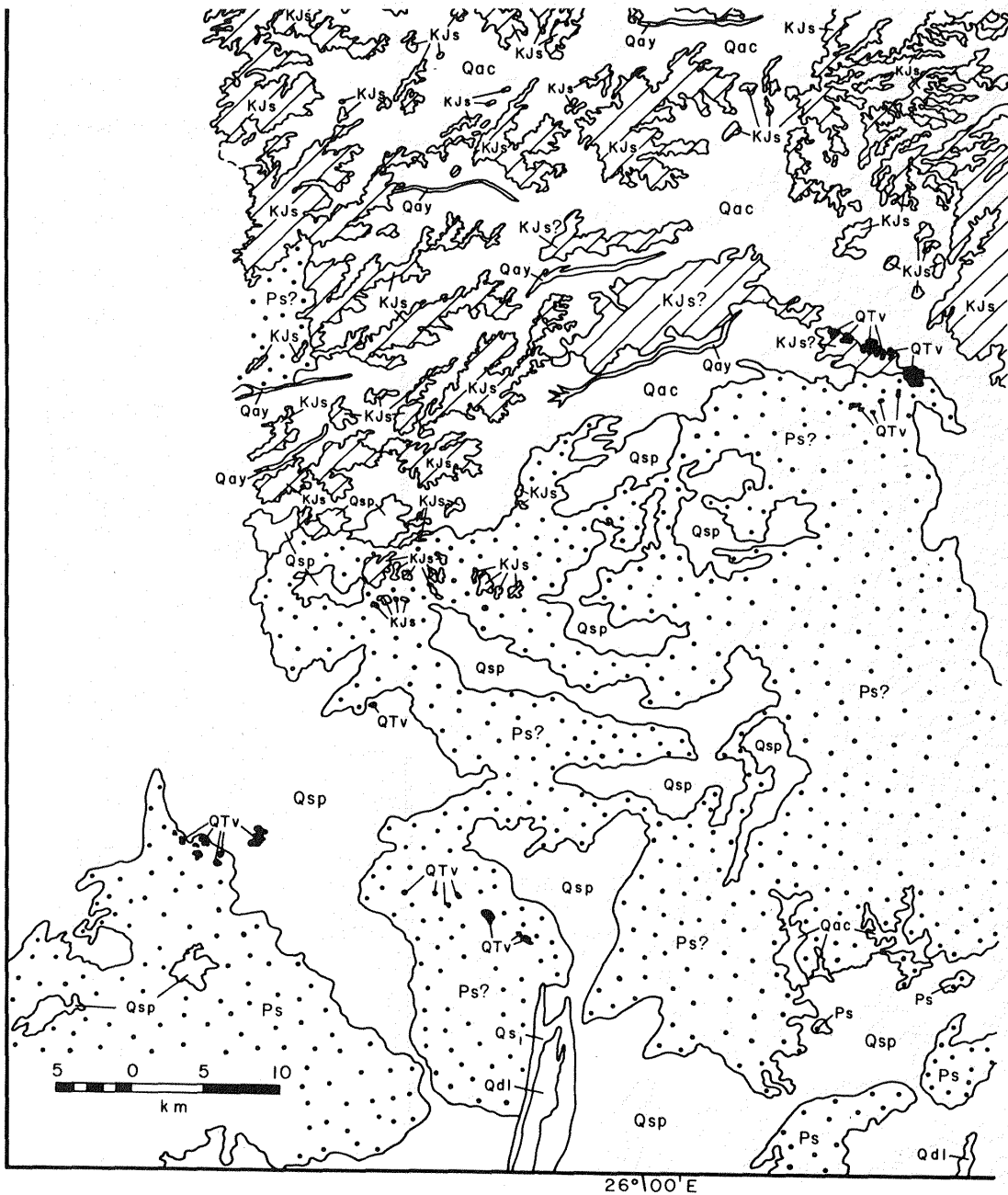
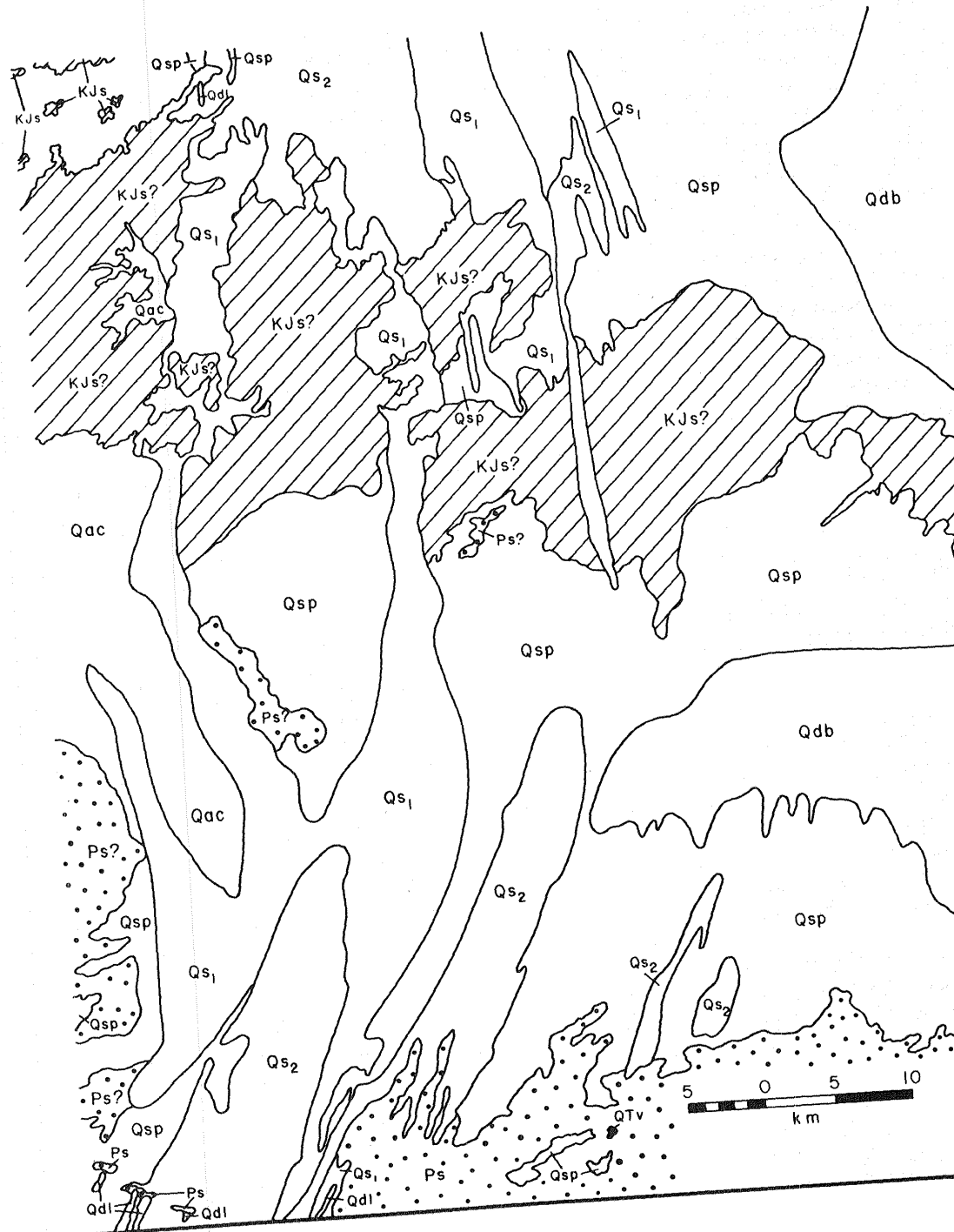


Figure 14.1 (continued)



EOLIAN SAND DEPOSITS

Qs₂ DRIFT SAND--Occurs in large, slightly curving swarms of mottled material in eolian thoroughfare on desert peneplain adjacent to east border of plateau. Many swarms oriented NNE-SSW or NE-SW, have a blunt convex northern end, and flare out southward; none of the blunt ends are located in immediate lee of an obvious adjacent topographic obstacle. Effective sand drift direction is southwestward. Overall shape of drifts is that of low, parabolic swarm of short transverse sand dunes, over the surface of which sand grains move southward from one superposed transverse dune (barchanoid ridge) to another. Wavy textural pattern, near limit of image resolution, is normal to long axis of swarm. Material cuts across or is superimposed on almost all adjacent rock units. Best defined as dark-gray mottled material on band 4, mottled light yellow on FCC, and orange on FCCs. Interpretation: Dune sand in large drifts or sheets with surface wave forms ("streaks" of Breed and Grow, 1979); also called sand shadows). Probably youngest of all eolian deposits. Probably consists of dune sand momentarily accumulated in drifts, but in transit from linear dunes of Great Sand Sea (north of map area) to western fringe of Selima dune field (south of map area).

Qd1 LINEAR DUNE SAND--Occurs mostly in northeastern part of map area, in single, narrow, long ridges, generally oriented NNW. Ridges are slightly sinuous, a few hundred meters to a few kilometers apart, and lie in eolian thoroughfare east of Gilf. Westernmost dunes extend southward in the lee of promontories

or isolated hills along plateau margin. Farther east, some sand ridges extend through gaps between east-trending bedrock ridges. Material crosscuts or is superimposed on adjacent rock units. Grain-size distribution shown by McCauley and others, Chapter 15. Best detected as light-dark-gray material on band 4, light-gray to white on band 7, light orange on FCC, and yellowish orange on FCCs. Ridges exhibit wavy pattern, nearly normal to their long axes. Medium gray on 7, light orange on FCC, and bright red on FCCs.

Interpretation: Dune sand migrating southward from Great Sand Sea (north of map area) to Selima dune field (south of map area). In southern part of map area, dune sand partly derived from local sources.

Qs₁ DRIFT SAND--Occurs as very thin veneer, not quite mantling pediplane surface beneath. Generally restricted in map area to one major elongate zone of wind transport ("eolian thoroughfare") described by McCauley and others, Chapter 15. Thoroughfare is 10-25 km wide, extends from north around east side of Gilf. Mantling material of unit thicker around groups of isolated hills, which protrude above eroded bedrock surface, but evenly spread elsewhere. Includes coarse lag of white quartz granules. Grain-size distribution shown by McCauley and others, Chapter 15, Fig. 15.7. Truncates all surficial map units except Qd1. Appears as white or very light gray on band 4, light gray on 7, white to very light orange on FCC, and red on SFCC. Interpretation: Drift sand deposited as thin sand sheets, along paths of northerly

prevailing winds that are topographically diverted around plateau. Sand sheet is thin where wind deflation and abrasion dominate over deposition.

Qdb BARCHANOID DUNE SAND--Occurs in two discrete areas on desert peneplain extending east of Gilf. Areas are distinctive because of wavy pattern of east-trending sinuous ridges. Ridges are many kilometers long, 0.5 km wide, and 0.5 to 0.75 km apart. Unit medium gray on 4 and 7, light pink on FCC, and red on FCCs. Interpretation: Barchanoid ridges of dune sand that trend east, transverse to northerly and southerly winds. Sand accumulation extends eastward outside mapped area.

Qsp SAND PLAIN MATERIAL--Forms extensive fine-textured surfaces on peneplain east south and west of Gilf. Truncated by all other surficial deposits. Light-gray on 4, dark gray on FCC, and green and red on FCCs. Interpretation: Thin, stable sand sheet, protected by residual lag cover of coarse sand or granules. Lag is well sorted, extremely mature, with closely fitted particles of sizes obviously in equilibrium with local peak wind energies. Grain-size distribution shown in McCauley and others (Chapter 15). Color differences on sine-stretched FCC probably due to variations in particle size and in clay and hematite coatings. Unit extends for hundreds of kilometers east of map area, and according to Bagnold (1933, p. 125) is confined to "Nubian Sandstone country". Oldest surficial unit in map area, and ultimate evolutionary stage of sandy desert peneplain developing under hyperarid climate. Age of unit increases with distance from Gilf, which results from gradual

retreat of the Gilf escarpment by fluvial erosion, mass wasting and deflation.

FLUVIAL AND COLLUVIAL DEPOSITS

Qay YOUNGER ALLUVIUM--Occurs in narrow, sinuous, braided and meandering tongues on floors of major wadis incised into edge of the Gilf Kebir Plateau. Best detected as dark-gray material on Bands 4, 7, and FCC, but generally lighter gray than alluvium and colluvium (Qac). Tongues trend east-northeast and cut across adjacent map unit (Qac). Only seven tongues delineated on map: In Wadi Maftuh (20 km long, 100 m wide); along north edge of Wadi Wassa, east of entrance to Wadi Ard El-Akhdar (9 km long, 75 m wide); in floors of three unnamed wadis west and northwest of Eight Bells; and in floors of unnamed wadis (9 km long, 100 m wide), 15 km and 25 km south of Wadi Diyaq. All tongues except the two last mentioned narrow gradually, and show gradual decrease in grain size, to east (downstream). Interpretation: Alluvium in channels, banks and flood plains of short, local, ephemeral streams, none of which appears to fit into an integrated regional drainage network.

Qac ALLUVIUM AND COLLUVIUM--Includes colluvium mixed with sheetflood deposits and eolian sand on valley slopes adjacent to wadi walls; alluvium includes older coarser grained wadi deposits, ranging in size from sand to boulders, and younger finer grained alluvium in channels and flood plains of present-day ephemeral streams and in alluvial cones at east and west mouths of major wadis; unit also includes lake beds at the heads of Wadis El-Bakht and Ard

El-Akhdar, and small playa deposits in depressions within wadis. Appears as dark-gray material on bands 4, 5, and 7, darkest on bands 4 and 7, very dark gray to dark orange on FCC, and aquamarine on FCC's; generally darker than younger alluvium (Qay), and locally striped with dark streaks. East boundary with lighter material of desert peneplain is a few hundred meters to 3 kms wide. This boundary, as defined by arcuate border of dark-brown materials on FCC, is tangential to east tips of promontories between major incised wadis; easternmost extension of boundary is east of Wadi El-Bakht. Interpretation: Dark streaks observed on Landsat image probably due to desert varnish. Colluvial and alluvial materials commonly covered with desert varnish may range from late Tertiary to late Pleistocene; younger alluvium is as young as late Holocene. None of these individual sub-units are mappable at 1:250,000 scale.

Qg GRAVEL--Occurs as desert pavement generally south of sandstone hills in northeastern part of map area. Dark gray on 4 and FCC, and green on FCCs. Interpretation: In places represents lag gravels sorted out of later Tertiary(?) and Quaternary alluvium by wind; elsewhere consists of angular gravel and hematite-bearing flagstones derived from mineralized sandstone bedrock. Commonly covered with desert varnish and fluted by wind erosion.

VOLCANIC DEPOSITS

QTv MAFIC AND INTERMEDIATE

VOLCANIC ROCKS--A) Form black to dark-gray subcircular constructs on surface of Gilf, and on floors and valley walls of some wadis; also occur as low subcircular and arcuate ridges that protrude above plateau surface. B) Occur as black peaks, open craters, or arcuate exposures that protrude above peneplain south of Gilf. Interpretation: A) Basalt cones, domes, or lava flows that intrude or overlie both older and younger sandstones (units Pzs and KJs). B) Trachyte in form of volcanic necks, plugs in craters, and lava flows capping isolated hills of sandstone, and materials of uncertain composition in diatreme-like craters. Several episodes of volcanic activity, ranging in age from Oligocene or Miocene to Quaternary, are probably represented.

SANDSTONE DEPOSITS

KJs YOUNGER SANDSTONE, UNDIFFERENTIATED--Underlies surface of Gilf Kebir Plateau and is exposed in its cliffs and wadi walls; also occurs on discontinuous, generally east-trending ridges and isolated hills east and southeast of the Gilf. Strongly jointed by at least three joint sets trending NNW-SSE, NNE-SSW, and, less strongly, E-W. Light to dark gray in 4 and 7 in northern and central parts of plateau, black along highly dissected southeastern plateau edge. Orange to black on FCC, and green to pink and light red on FCCs. Interpretation: Includes Issawi's (1973a) Gilf Sandstone of probable Jurassic age; also includes Klitzsch and others' (1979) Nubia strata of Late Cretaceous age, and possibly their Lingula shale and basal Desert Rose units. Baked and strongly silicified near lava flows and dikes; topmost layer at ground surface much silicified and indurated. Variations in gray tone and color observed on Landsat products from central part of plateau outward probably due to outward decrease in surficial sand and silt cover. Wadi walls and bordering cliffs have receded through headward erosion, pediplanation and groundwater sapping during former cycles of fluvial erosion, and through mass wasting and wind erosion during present-day and former cycles of hyperaridity. Sandstone cliffs are local source rock for much of mapped younger surficial deposits.

Pzs OLDER SANDSTONE, UNDIFFERENTIATED--Occurs as very rough, hilly fluvially dissected and wind-deflated material in southern part of map area. Strongly jointed by at least three joint sets trending NNW-SSE, NNE-SSW, and less strongly, E-W. Appears as light gray or dark gray on 4 and 7, yellowish orange on FCC, and light green or red on FCCs. Locally intruded by volcanic rocks (Q_{Tv}). Interpretation: Sandstone unconformably resting on Precambrian metamorphic rock, west and south of the Gilf Kebir Plateau and outside map area. According to Issawi (1973a, p. 13), basal layer of unit is kaolinized sandstone. Remnants of ancestral drainage pattern incised into this unit (long V-shaped benches open southward and southwestward) suggest slight dips northward, and former streamflow southward.

Peel (1939b) recorded the presence of rounded hills of basalt on the top of the Gilf Kebir Plateau and in the wadis. Among at least 50 such basaltic intrusions, he singled out as most representative the one in Wadi Ras El-Qibli on the south side of the Gilf. Issawi (1973a) confirmed Peel's earlier observations. These volcanic rocks, and other igneous rocks in southwestern Egypt that range in age from Early Cretaceous to early Miocene (Meneisy and Kreuzer, 1974), are now being studied by El-Baz and Issawi. Those igneous rocks of the Gilf plateau mapped as mafic and intermediate volcanic rocks (unit Qtv) are younger than the (Jurassic-Cretaceous) sandstone (unit KJs) that they intrude, and may be as young as Pleistocene in age on the basis of preservation of their volcanic landforms.

SURFICIAL GEOLOGY

The surficial units of the southern Gilf Kebir Plateau and vicinity consist of colluvium, alluvium, playa and lake deposits, and eolian deposits of late Tertiary (?) and Quaternary age. Neither colluvium nor eolian deposits in this area were described by previous workers, although Bagnold's (1931, p. 524) classification of sand formations in the Western Desert includes types that he observed in the Gilf region.

Alluvium consisting of very coarse, rounded, boulder gravel was observed by P. A. Clayton (1933) in a gorge located probably near Akaba Pass, and in wadis incised in the plateau. Bermann (1934, Fig. facing p. 469) illustrated fine alluvium in dry stream channels slightly entrenched in a wadi floor in the northern Gilf Kebir Plateau. Bagnold and others (1939, Fig. before p. 285) also illustrated alluvium in dry channels near the head of Wadi El-Bakht, and on the pediplane extending east of their camp. Peel (1939b, Fig. 3) described and sketched the alluvial channels issuing from volcanic craters northeast of the peaks of Peter and Paul.

Older and younger alluvium and colluvium can be differentiated in the Gilf region both on the ground (by differences in particle size and amounts of desert varnish), and on the Landsat image (by differences in surface reflectance). However, the map scale of Figure 14.1 requires that older alluvium and some of the younger alluvium and colluvium be lumped together and mapped as a single unit (Qac).

The older alluvium consists of fluvial materials ranging in size from sand to large boulders, which were deposited on wadi floors when the climate was more humid and streams more competent than now. The older alluvium, which may range in age from late Tertiary(?) to late Pleistocene, extends in places across wadi floors up to the foot of wadi walls, where it is interstratified with colluvium.

Since the onset of the latest cycle of hyperarid climatic conditions about 5000 years ago (Haynes, Chapter 9), the surface of the older alluvium-colluvium has been exposed to intense wind erosion, and locally is mantled by a thin accumulation of eolian sand. On the Landsat image, the surface of older alluvium-colluvium is generally darker than that of the younger alluvium (Qay), and is striped with dark streaks that suggest downslope movement of the debris, possibly

by slow creep. Its appearance and distribution contrast with that of the younger alluvium, which is lighter gray and is confined to a few narrow channels in the centers of major wadis (Fig. 14.1). The younger alluvium consists of finer particles deposited by recent, less effective, underfit ephemeral streams (McCauley and others, Chapter 15); its presence shows that sheet flooding and concentrated flow occur episodically even today inspite of the present hyperaridity.

Considerable stratigraphic, geomorphic and even archaeologic evidence indicates that lake, marsh, and playa deposits accumulated on wadi floors in the not-too-distant past, when the region was not as hyperarid as today (Issawi, 1973a; Haynes, 1980b, and Chapter 9; McHugh, 1980; McCauley and others, Chapter 15). R. C. E. Clayton and Penderel, during the first reconnaissance flight over the Gilf Kebir Plateau on April 26, 1932, observed that the surface was "seamed with water-ways" and held mud pans in depressions (Rodd, 1933). Peel (1939b) later confirmed these observations, and noted that "traces of mud occur in shallow depressions on the plateau itself," and that alluvium and eroded lake beds can be observed in the banks of some of the dry stream channels. Earlier, both Bagnold (1933) and Sandford (1936) observed mud pans while on their way to the Gilf and Uweinat. In 1938, lake beds were discovered in the upper reaches of Wadis El-Bakht and Ard El-Akhdar (Bagnold and others, 1939; Peel, 1939b). Sediment-filled pipes in the lake beds indicate soaking of these deposits since the lake was drained, and recent mud pans were observed on the deflated surface (McCauley and others, Chapter 15). These lake beds and playa deposits are not mappable at the scale of the geologic map (Fig. 15.1); they are all included in the older alluvium and colluvium unit (Qac), from which they cannot be differentiated, even though many are late Holocene in age (McHugh, 1980; Haynes, 1980b; McCauley and others, Chapter 15).

The distinctive characteristics of eolian deposits on the Landsat image permit mapping of their regional distribution in the vicinity of the Gilf Kebir Plateau for the first time (Fig. 14.1). Previous descriptions of these deposits are very few, consisting of brief mentions of a sand sheet that covers the floor of Akaba Pass and a complex dune field that abuts against the northern cliffs of the plateau (Penderel, 1934), and comments on the south-south-western trend of the linear dunes southwest of the Gilf Kebir (Ball, 1927). Bagnold (1931) published a map of the Great Sand Sea, but his map does not extend to the Gilf. He lamented (1931, p. 524) that "there appears to exist no recognized convention to show the general characteristics of systems of sand formations", but he had already recognized "such details as: A) land submerged by a sea of undulating or flat sand; B) longitudinal dunes resting either on bedrock or other sands; C) chains of barchan dunes; and D) fields of short-crested chaotic dunes." He further pointed out (1933, p. 125) that north of a line extending from the Gilf Kebir to Dakhla (an oasis 335 km to the northeast), seifs (linear dunes) are dominant, whereas barchans dominate to the south. Bagnold also gave an extended description (1933, p. 121-126) of four basic categories of eolian sand accumulation: sand drifts or sand shadows, dunes, whalebacks or undulations, and sand sheets.

METHODS OF STUDY AND LANDSAT DATA PRODUCTS

Most of the southern Gilf Kebir is located within Landsat scene 192/044. "Scene" refers to an area, 185 km by 185 km, which is part of the 185-km-wide swath of the Earth's surface scanned by the sensors of the Landsat spacecraft. Scene indexing is based on the path/row system of global subdivisions, which is utilized in the Landsat Index Atlas (World Bank, 1976). Only image 1131-08141, December 1, 1972, among those acquired by American receiving stations, was relatively cloud free and immediately available in the spring of 1979, when work on this geologic map began. In spite of blowing dust, haze, desert fog and clouds hanging low in the northwestern and central parts of the image, immediate availability of a computer-compatible tape dictated selection of this image for computer processing and geologic analysis. Thick cloud cover in the western part of the image casts shadows and alters the natural reflectance of the desert surface beneath; this part of the image was excluded from image analysis and geologic mapping. A southern strip, where stratigraphic data are uncertain, was also deleted.

Geologic mapping was done on the linearly stretched false color composite (FCC). Among the linearly stretched and sinusoidally stretched data bases, Band 4, and to a lesser extent Band 7, were the most useful in differentiating and delineating surficial deposits. The 4SG, 5SR, and 7SB sinusoidally stretched FCC was the more useful of the two sine-stretched FCCs available, because this particular color-filter combination brings out surficial deposits in various hues of red, which approach the natural colors of the desert floor. It was also useful in checking minute differences in spectral reflectance that were not immediately detectable on the linearly stretched FCC, but its overall usefulness was impaired by the reflectances of low-lying clouds and their shadows on the original image.

IMAGE INTERPRETATION

In the Gilf Kebir area, the synoptic view of the desert surface provided by a Landsat image makes possible the mapping of rock-stratigraphic units in greater detail and more accurately at a scale of 1:250,000 than heretofore possible. The regional distribution of surficial deposits in the area, and the relation of these units to one another, is shown for the first time. Several constraints are: 1) the spectral resolution of the Landsat sensors (which range only from blue green to near infrared); 2) spatial resolution of the sensors (about 80 m); 3) the restriction of our traverses to the eastern margin of the Gilf, to the valley floors of Wadis Mashī, Diyaq, El-Bakht, Wassa and its northern tributary, Wadi Ard El-Akhdar, and to our route to the peaks of Peter and Paul; and 4) the corresponding lack of field samples from all parts of the region. These constraints restrict image analysis to the identification of medium-scale stratigraphic units and landforms. Many questions of lithology, composition, provenance and morphology, therefore, are left unanswered. However, the method does allow us to pose pertinent field problems, and to direct the attention of future field investigators to them.

RESULTS AND CONCLUSIONS

The oldest rocks in the map area are the older and younger sandstones (units Ps and KJs). Volcanic rocks ranging in age from Oligocene to Quaternary (unit QTv) occur in sills, dikes, diatremes, volcanic necks and other volcanic edifices, but they could not be differentiated without extensive field sampling. Because band-ratio data products were not available, no attempt was made to differentiate individual strata of the younger sandstone that underlie the plateau, despite subtle differences in spectral reflectance observable on the Landsat image. However, the older sandstone in the southern part of the map area was distinguished from the younger sandstone by its distinctive spectral reflectance (light yellow versus dark gray on the FCC). The older sandstone crops out southeast of the Gilf Kebir Plateau on a low, stripped structural surface that appears to be of fluvial origin (V-shaped notches in northeast-dipping layered rocks), but modified by wind erosion. This surface lies near the junction of the defunct, south-flowing Eight Bells wadi system (McCauley and others, Chapter 15) with the defunct valley of the south-flowing master stream (now an eolian thoroughfare), to which most of the incised wadis that debouched from the eastern Gilf Kebir Plateau are graded.

The textural and color contrasts detectable on linearly and sinusoidally stretched FCCs made possible the detection and identification of either different types of surficial deposits. Three of these - younger alluvium (Qay), alluvium and colluvium, undifferentiated (Qac), and gravel (Qg) - attest to the roles played by running water and mass wasting. The five eolian deposits mapped - drift sand (Qs₁ and Qs₂), linear dune sand (Qdl), barchanoid dune sand (Qdb), and sand plain material (Qsp) - provide abundant evidence for the hyperarid conditions that alternated with more humid conditions during most of Pleistocene and Holocene time. These hyperarid conditions still prevail. Erosional landforms detectable on the Landsat image include the deeply incised wadis noted above, irregularly dissected cliffs that characterize the Gilf Kebir Plateau, isolated residual hills (inselbergs) and palimpsest valleys on the intermediate pediplain, and the eolian thoroughfares that sweep around the borders of the Gilf. These landforms and the erosional processes by which they were formed are described and discussed in a companion paper (McCauley and others, Chapter 15). When the surficial deposits observed on the Landsat image and outlined on the geologic map are considered jointly with the erosional landforms also shown on the Landsat image and even better observed on the ground, the stage is set for an analysis of the interplay of running water, mass wasting, and of the wind in the Gilf Kebir region (McCauley and others, Chapter 15).

ACKNOWLEDGEMENTS

Travel funds and salary were provided by the Office of International Geology and the Energy Lands and Climate Programs, U. S. Geological Survey (Grolier). The U. S. Department of the Interior, Minority Participation in Earth Sciences Program, also paid salary for Patricia A. Schultejann. We thank all of these agencies for their support of the research reported in this paper.

Chapter 15

THE INTERPLAY OF FLUVIAL, MASS-WASTING AND EOLIAN PROCESSES IN THE EASTERN GILF KEBIR REGION

JOHN F. McCAULEY, CAROL S. BREED and MAURICE J. GROLIER
U. S. Geological Survey
Flagstaff, Arizona 86001

ABSTRACT

The Western Desert of Egypt provides many analogs for interpreting landforms on Mars. In this hyperarid region of Earth, as on Mars, eolian erosional and depositional processes are now dominant. In the Western Desert, wind and mass wasting have severely altered landscapes whose basic patterns were established long ago by running water. Relict drainage basins, reconstructed on a Landsat image of the Gilf Kebir region, formerly contained integrated, mature stream networks. These restored networks share certain morphometric characteristics with drainage systems developed under far more humid climatic conditions. Streams of probable mid- to late-Tertiary age drained the Gilf highlands to the north, east, west, and south; their restored patterns indicate that the Gilf Kebir was formerly a major drainage divide in southwestern Egypt. Under present conditions of hyperaridity, the trunk streams are defunct, and their valley-side slopes are being reduced mainly by mass wasting and wind erosion.

The distribution of old interfluves on Landsat images clearly shows that the former streams within the plateau were continuous with watercourses that extended far beyond the present plateau escarpment on the surrounding desert plains. The newly recognized Eight Bells system drained 3,400 km² or more of the southern Gilf region and discharged to the south hundreds of kilometers beyond the present plateau scarp. In more humid intervals such as the late Tertiary, this system must have been part of a larger system of internal drainage in the east central Sahara.

Remnant interfluves used to map the now defunct Gilf drainage basins are identified by clusters of conical hills on wadi floors and on the pediplain that surrounds the plateau. The symmetrical, conical shape of the most isolated residuals reflects dynamic equilibrium with present-day slope-forming processes. In the Western Desert, this equilibrium form apparently develops when inselbergs initially isolated by fluvial dissection are further reduced principally by wind and mass wasting in the virtual absence of running water.

The broad, flat-floored wadis within the Gilf plateau are characterized by wind-eroded lake beds, ventifacted stream cobbles, residual conical hills, dunes, ripples, and ephemeral underfit gullies choked with windblown sand. These features record a complex interplay of running water, wind, and mass wasting under Quaternary climatic fluctuations, in which long intervals of hyperaridity were punctuated by episodes of semiaridity with savannah-like conditions. On the pediplain outside the escarpment, windblown debris is in transit along broad eolian thoroughfares that follow the apparent courses of defunct master streams. Loose particles driven south by northerly prevailing winds are segregated according to grain size into dunes and sheet deposits of varying mobility. These eolian plains deposits overlie and obscure much of the formerly fluvial landscape around the plateau.

The fretted terrain along the northern margin of the martian highlands is a belt of dissected plateaus, protected by caprocks, from which relict fluvial channels debouch onto the smooth, flat northern plains. The plains are partly veneered with eolian deposits and dotted with clusters of inselbergs, including mesas and conical hills that resemble in general those of the Gilf region. The geomorphic relations of the "wadis", dissected plateaus, inselbergs, and plains of the fretted terrain on Mars may be at least partly explained in terms of an interplay between fluvial processes, wind, and mass wasting, such as described herein for the Gilf Kebir region of southwestern Egypt, one of the best terrestrial analogs for the surface of Mars.

INTRODUCTION

Since discovery of the Gilf Kebir Plateau by modern explorers, this 12,000 km² erosional remnant of sandstone strata has been of intense interest to geologists and geomorphologists. Peel (1941), in an account of general relations of the Gilf Kebir to the surrounding desert plains, focused on the problem of development of the large wadis that embay the plateau (Figs. 15.1 and 15.2). Subsequent work by Maxwell (1980) and Haynes (Chapter 9) emphasized the unusual character of these almost-defunct watercourses. Broad but steep-walled valleys incised in the Gilf are now occupied only infrequently, perhaps as seldom as 20 year intervals, by water that runs briefly in underfit channels partly choked with windblown sand (Fig. 15.2B). Present-day fluvial processes play a very minor role in the region. Collected sheetwash runs off only a short distance into the desert sands, and the tracks left by expeditions more than 40 years ago show no signs of erosion by running water (Fig. 15.3). However, in and near the plateau, abundant evidence remains of earlier erosional and depositional fluvial activity. Complex but topographically subordinate sequences of local damming, lake formation, and wadi floor cutting and filling attest to several Quaternary pluvial episodes that postdate the probable Tertiary incision of the regional drainage pattern.



Figure 15.1 Landsat image of southeastern part of Gilf Kebir Plateau region with overlay map of now-defunct drainage networks extending well beyond present plateau margin. Lines of drainage divides are dashed where approximately located, queried where uncertain. Restored network patterns are consistent with patterns of active stream systems in less arid regions. Bright zones adjacent to plateau are eolian thoroughfares, where sediments reworked by wind are blown southward across the pediplain toward dune fields in the east-central Sahara. A geologic map of the region included in Figure 15.1 is shown in Grolier and Schultejann (Chapter 14). (Landsat 1131-08141, Dec. 1, 1972).

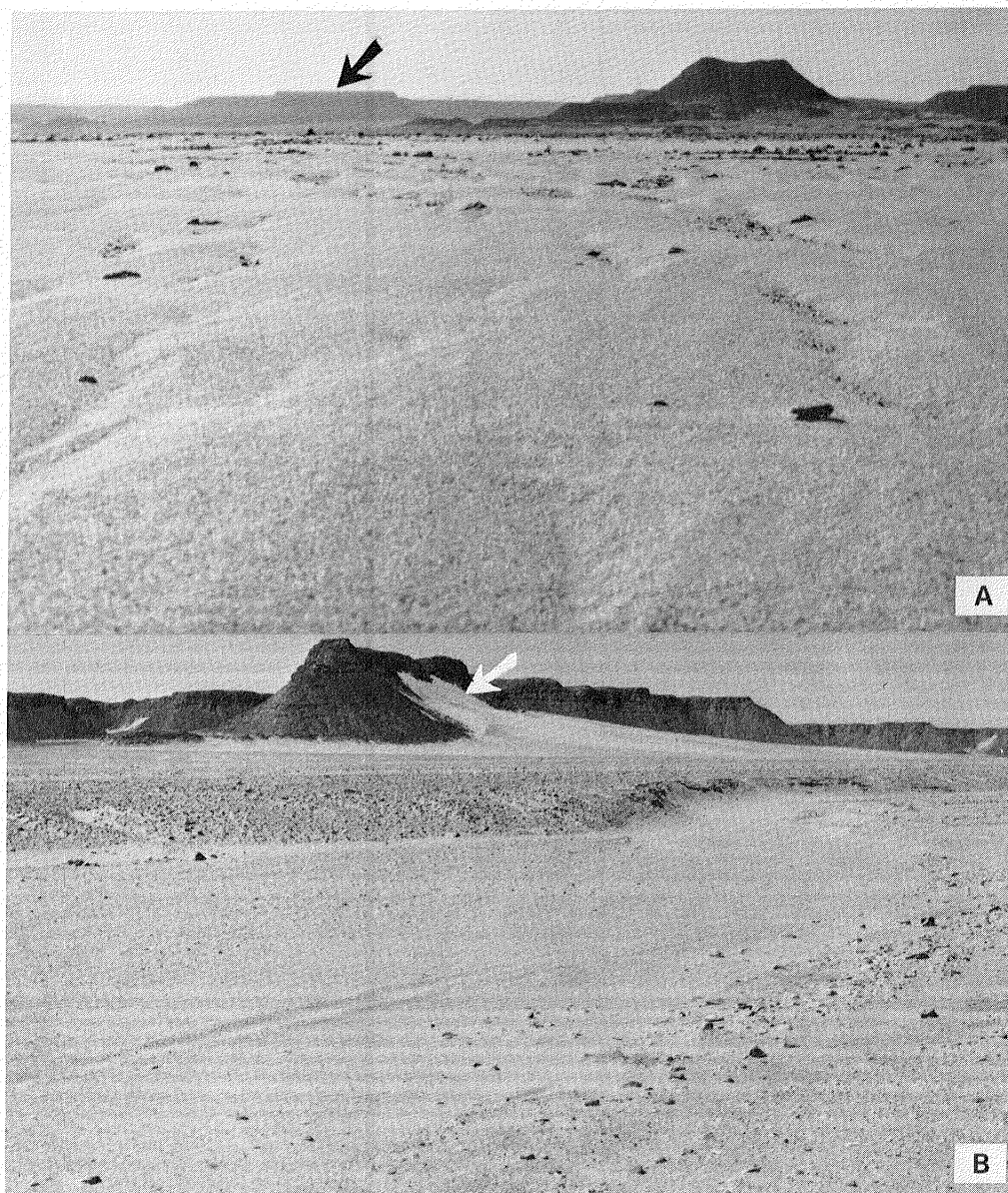


Figure 15.2 A) View west near locality H, Figure 15.1, showing 300 m high, flat-topped escarpment (arrow) that marks margin of Gilf Kebir Plateau. Stream gravels on desert floor are covered by wind-rippled eolian deposits characteristic of eolian thoroughfares. Cobble in right foreground (arrow) about 15 cm long. B) View southwest across Wadi Mashi, showing steep wadi walls and the broad, flat wadi floor cut by an underfit channel, approximately 6 m wide, which is choked by wind-rippled sand. Streamflow from right background, toward viewer. Expedition botanist (Boulos, 1980, p. 69) estimates from conditions of dried vegetation that no precipitation or runoff have occurred in the wadi in about 20 years. A climbing dune (arrow) occupies part of south wall next to conical spur remnant.

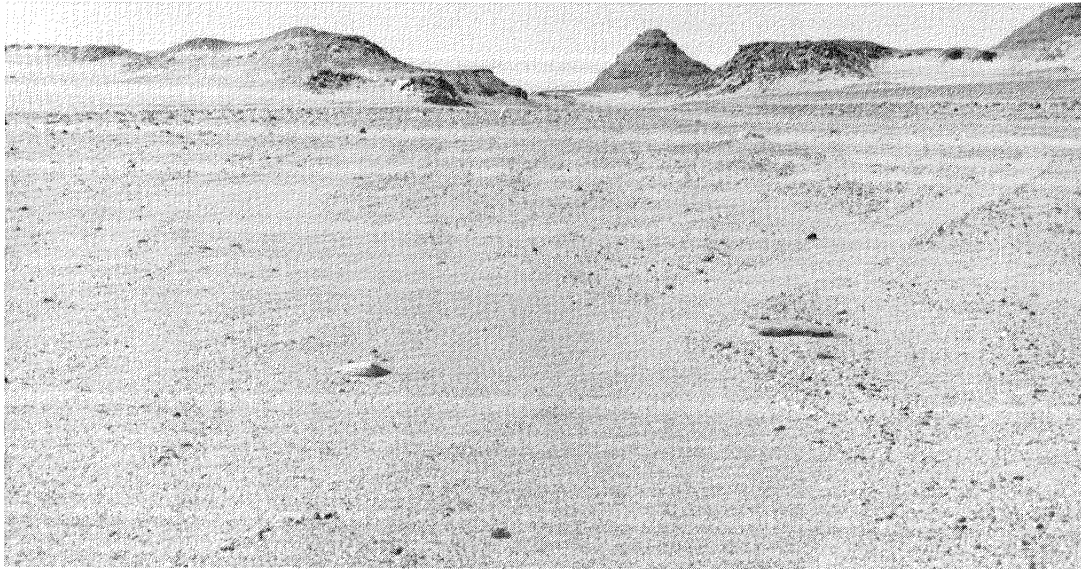


Figure 15.3 Tracks near gap leading south from Wadi Wassa toward Eight Bells (locality C, Fig. 15.1) show no evidence of erosion by running water, but are filled with windblown sand. Narrow widths of tire tracks indicate they were made by vehicles of the type used in early expeditions such as those of Bagnold and Peel in 1939.

During the period from September 30 to October 4, 1978, we reconnoitered the east and south sides of the Gilf Kebir and conducted brief field studies on the top of the plateau and in Wadis Mashi, El-Bakht, Wassa, and Ard El-Akhdar (Fig. 15.1). We found that many of the peculiar geomorphic characteristics of the Gilf region are the results of an eolian and mass-wasting overprint on a landscape whose basic patterns were established by running water. Much-degraded drainage basins, now invaded by windblown sand, are relicts of an ancient (mid-Tertiary?) landscape that had probably reached a mature or "quasi-equilibrium stage" (Strahler, 1952) of fluvial dissection. During later episodes of aridity, these ancient stream valleys were altered to wadis (steep-sided, flat-floored dry washes); even today, though all but defunct, these wadis retain certain characteristics in common with those in semiarid plateau areas of the American southwest. The present unusual characteristics of the Egyptian landscape, however, have evolved under climatic conditions of hyperaridity peculiar to the Western Desert, which is about 200 times more arid (Henning and Flohn, 1977) than the driest parts of the American deserts.

The Gilf Kebir lies near the center of what is now the largest expanse of hyperarid terrain on Earth (Henning and Flohn, 1977) and is almost completely lacking in vegetation. It is one of the few places on Earth where wind, not water flow, is now the most effective agent of surface sculpture. In less arid regions, landscapes most familiar to European and North American geologists are formed principally by the interplay of running water and mass wasting processes. In

contrast, the Western Desert of Egypt has been episodically mostly hyperarid since at least early Quaternary time (Haynes, 1978; Chapter 9), and wind processes are an added and important factor in landscape evolution. As a consequence, the area displays peculiarities that include relict drainage systems, broad, essentially horizontal sand plains beyond the scarps of the Gilf, and clusters of conical inselbergs, fields of yardangs, unusual ventifacts scattered on the desert floor, and chains of migrating sand dunes.

Our investigations in the Western Desert of Egypt may provide insights into some terrain features of probable eolian origin on the hyperarid planet Mars (McCauley and others, 1979a, 1980a, b; El-Baz and others, 1979a; Breed and others, 1979, 1980a, b). Both in southwestern Egypt and on Mars, wind erosion and mass wasting have obscured former fluvial landscapes. Surface debris, derived at least in part from fluvial processes, has been redistributed in the form of windblown sand sheets, streaks, and dunes. In Egypt, dune sand is still in transit southward toward sites of deposition in the great ergs of the east-central Sahara; on Mars, most of the dune "sand" is already concentrated in the north circumpolar erg (Cutts and others, 1976; Breed and others, 1979, 1980a).

Haynes (Chapter 9) has discussed the climatic cycling that has occurred in the Egyptian desert through Quaternary time. This cycling, as in most older desert regions of the world, has caused numerous "stops and starts" in geomorphic evolution: no one model or inferred sequence of events can be invoked. The observations presented here come from numerous localities in the eastern part of the Gilf Kebir, on part of the "desert peneplain" (Sandford, *in* Bagnold, 1933) between the Gilf Kebir and the Nile Valley, and from interpretations of certain regional geomorphic patterns studied on Landsat images (Fig. 15.1).

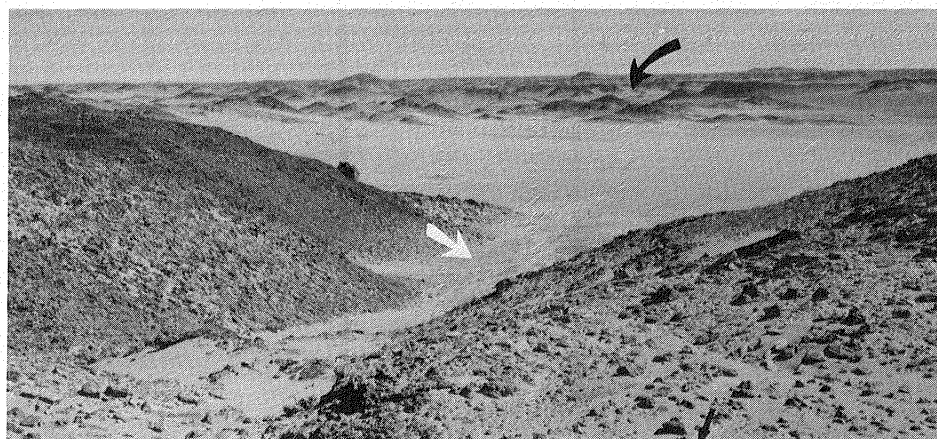


Figure 15.4 Clusters of conical hills (curved arrow) to the south mark positions of old interfluves in Wadi Mashī (locality B, Fig. 15.1). Large talus blocks in foreground (straight black arrow) are less than 0.3 m long. Minor gully system (white arrow) in tributary valley partly obscured by windblown sand.

FEATURES OF THE GILF KEBIR PLATEAU

General Description of the Wadis

As described by Peel (1941, p. 12), the incised wadis of the Gilf seem to differ from river valleys of more humid regions in that "there are none of the swinging curves of the normal river valley. Tributaries run into them at all sorts of abrupt angles, some even pointing upvalley." The wadis at some places are enlarged into broad open bays and at other places are constricted; they are bounded by high steep walls that rise as much as 300 m along the west edge of the Gilf.

Myriads of small sandstone inselbergs (isolated residual hills) are clustered on the wadi floors and on the pediplain (Howard, 1942) immediately adjacent to the plateau (Figs. 15.3; 15.4). Peel (1941, p. 7) recognized these inselbergs as "relict features, left outstanding by the lowering of the desert surface around and between them." On the Landsat image (Fig. 15.1), the inselbergs are interpreted as remnants of the interfluves of much-degraded, relict drainage basins. Ancient drainage networks, only partly recognizable on the ground, extend tens of kilometers or more to the east and south, beyond the present retreating plateau scarps. Although greatly modified by wind erosion and mass wasting, the relict patterns appear to be part of a former regional drainage system, and are clearly continuations of the wadi systems within the plateau. Beyond the region shown in Figure 15.1, the pediplain surrounding the Gilf Kebir grades into the great penplain of central Egypt and northwestern Sudan, from which rocks of the type remaining in the Gilf plateau have largely been stripped; this stripped surface is now covered by a nearly ubiquitous eolian veneer.

From the Landsat image we have reconstructed the patterns of ancient interfluves by tracing the outlines of residual outliers. The streams inferred to have flowed between these interfluves are shown restored in Figure 15.1. The reconstructed patterns indicate that several drainage systems, integrated to at least sixth-order main streams (Horton, 1945), formerly drained sizeable catchment areas in the southern and eastern parts of the Gilf region. One or two of these relict systems extended across the entire plateau. The larger of these, now almost entirely erased from ground view, drained an area of approximately 3,400 km² south of Wadi Wassa and discharged to the south more than 100 km beyond the present position of the retreating Gilf scarp. We suggest the name "Eight Bells" for this former drainage system, after a prominent landmark visible from a gap in the divide separating it from Wadi Wassa (locality C, Fig. 15.1).

Mass wasting and wind erosion have altered many parts of the former drainage networks almost beyond recognition, either in ground view or on the best available Landsat images, and topographic maps are inadequate for morphometric analyses. However, some characteristics of the "fossil" Gilf drainage nets can be reconstructed and compared with characteristics, such as Horton's (1945) Law of Stream Numbers, which are common to all "normal" stream systems (Shreve, 1966; Smart,

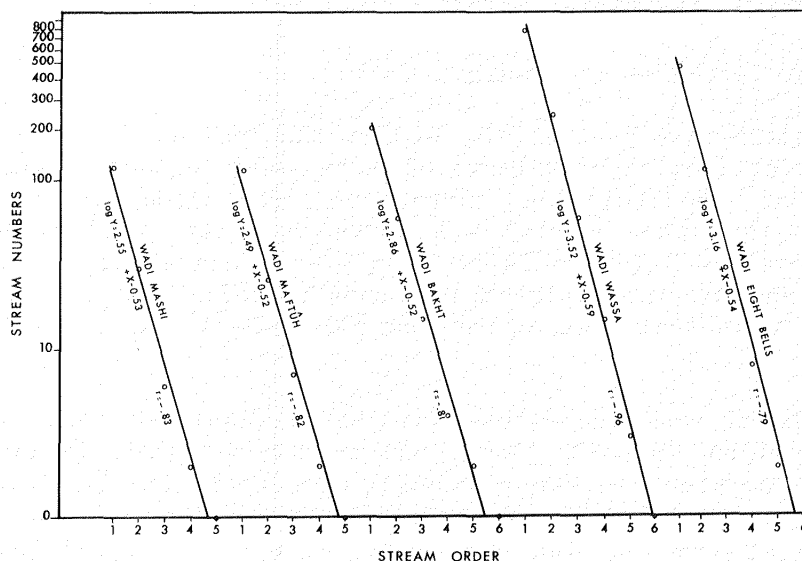


Figure 15.5 Graphs illustrating close adherence of reconstructed Gilf Kebir drainage networks (Fig. 15.1) to Horton's (1945) Law of Stream Numbers. Numbers of streams of each order in each drainage basin form an inverse geometric series, each having a very high coefficient of correlation (r). The trend equations have the form $\log Y = \log a + Xb$. Regression coefficient (b) of the equation for Wadi Eight Bells is close to the mean for Gilf wadis. It does not differ significantly (at the .95 confidence level) from regression coefficients of "normal" stream networks in less arid regions.

1978). Using Horton's method as modified by Strahler (1952, p. 120), numbers of streams of each order in the reconstructed drainage nets of Wadi Mashi, Wadi Maftuh, Wadi El-Bakht, Wadi Wassa, and Wadi Eight Bells systems were plotted (Fig. 15.5). As shown in Figure 15.5, in each basin the relation takes the form of an inverse geometric series, as demonstrated by Horton (1945, p. 286-291 and Table 1) for humid areas in New York and Michigan, for drainage networks in clay badlands in New Jersey (Schumm, 1956, Fig. 2); for an ephemeral stream system incised in terrace sediments near Poquonock, Connecticut (Carter, 1957); and for ephemeral stream systems in semiarid New Mexico (Leopold and Miller, 1956, Fig. 13) and South Dakota (Smith, 1958, Fig. 17).

The slopes of the graphs in Figure 15.5, expressed by the coefficient of regression, b, provide a dimensionless standard for comparing drainage networks of different sizes, geographic settings, and drainage densities (Chorley, 1957). The covariance of the coefficients of regression (Walker and Lev, 1953, p. 387) shows no difference among drainage nets in New Jersey, Connecticut, and the Eight Bells system in the Gilf region. The "fossil" Gilf networks thus share certain basic characteristics with "normal" streams. We suggest that they were normal streams that formed under climatic conditions

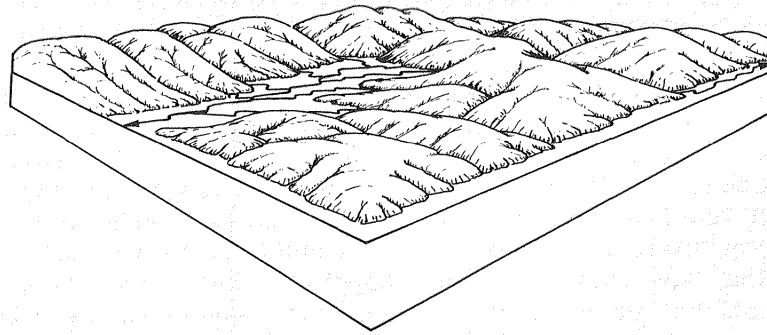
sufficiently humid to provide rainfall, which collected in runoff that carved integrated valleys in the bedrock of the Gilf region.

The reconstructed streams of the Gilf region were drawn as if each flowed in a straight course down the midline of each present wadi to join the nearest higher order stream segment. Possible twists and turns were necessarily omitted, so that the length of each segment is the minimum required to join it to the next. Furthermore, beyond the present topographic margin of the plateau only faint, ephemeral traces remain, like the grin of the Cheshire cat, to show the former existence of tributary streams; on the peneplain farther from the plateau, such traces have disappeared from the present surface. For these reasons, more sophisticated morphometric analyses using stream link lengths and basin areas (Shreve, 1975) were not feasible.

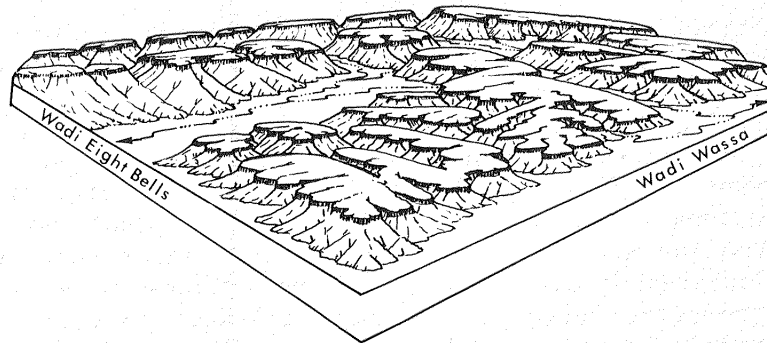
The degree of dissection of the plateau indicated by the reconstructed stream patterns (Fig. 15.1) suggests that the inferred drainage basins received precipitation in sufficient quantities to provide runoff with considerable erosive force. The appearance of the Gilf Kebir area during this stage of dissection is suggested in Figure 15.6A. Haynes (1978) hypothesized that initial fluvial dissection of the plateau took place in less resistant shales that have since been stripped from the highly resistant quartzitic layer that now caps the plateau. Topographic maps of the Gilf region lack elevation contours, so that hypsometric curves cannot be calculated to estimate the mass of rock eroded from the basins; the vertical relief suggested in Figure 15.6 is an approximation. Observations suggest, however, that the inferred former streams eroded their basins to equilibrium "maturity" of Strahler, 1952, defined by him as the point at which 40% or more of the mass of rock above the base plane had been removed.

The morphometric clues are incomplete due to the limits and paucity of ground data. However, they indicate that the relict drainage patterns in the Gilf Kebir area are parts of major regional stream systems. These streams almost surely reduced parts of southwestern Egypt to a maturely dissected fluvial terrain before the onset of hyperaridity in Pleistocene time.

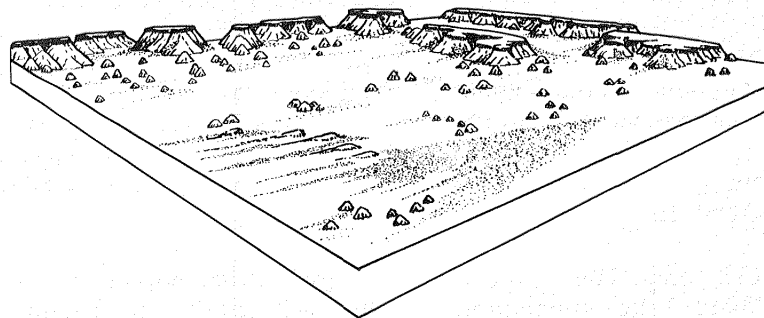
The Gilf and its surroundings probably began to take on the semiarid, desertlike appearance suggested in Figure 15.6B during late Tertiary or early Quaternary time. Much of the denudation probably occurred as a result of Quaternary climatic cycling, as described by Haynes (1978), whereby surfaces made vulnerable by weathering and fluvial processes during subhumid intervals were stripped by the intense eolian erosion that prevailed during arid intervals. Cliffs undercut by spring sapping, sheetwash, and episodic flash flooding retreated by mass wasting, as in semiarid to arid parts of the world today. In many localities, divides between adjacent drainage basins were breached. Many of the resulting gaps have since been partly filled with blown sand. Such gaps may now appear to be tributary valleys that enter the main valleys at peculiar angles, as observed by Peel (1941). Patterns observed on the Landsat image and in the field suggest that stream capture may have occurred in many localities, including capture of parts of the Wadi Wassa system by streams to the west and south (Fig. 15.1).



A



B



C

Figure 15.6 Block diagrams illustrating main stages in a suggested sequence of development of the southern Gilf Kebir landscape, viewed from the southeast margin of Eight Bells drainage basin (Fig. 15.1): A) Mid- to late-Tertiary dissection of drainage basins by dendritic, perennial stream systems under humid climatic conditions. B) Modification of stream valleys to broad, open wadis as climate became arid later in Quaternary time. C) Further modification of wadis by mass wasting, wind erosion and deposition, and occasional fluvial activity under fluctuating Quaternary climatic conditions culminating in present hyperaridity.

Wadis of the Gilf Kebir, though greatly modified, retain certain characteristics of this stage, which resemble those of the "dry washes" of intermittent stream systems in plateau and canyon regions of the semiarid American Southwest (Fig. 15.7). For example, certain tributary valleys incised in resistant strata in the Grand Canyon region are commonly steep walled and appear to lack sufficient catchment areas. Some of the tributaries of the Grand Canyon, like those on the Gilf plateau, are at least in part structurally controlled (Grolier and Schultejann, Chapter 14) and some join the master valleys at odd angles - even in an apparent upgradient direction (Fig. 15.7).

Such "barbed tributaries" can be caused by reversal of drainage due to migration of divides and stream capture. Incised barbed tributaries occur on the erosionally stripped, flat surface of Marble Platform in the eastern Grand Canyon region (Fig. 15.7B). They are described by Billingsley and Breed (1973) as subsequent streams, controlled partly by cliff retreat of less resistant overlying rocks and partly by joint patterns in the caprock. Although this analogy should not be carried too far, some general similarities seem to exist in the patterns of dissection of the two plateau surfaces.

During Quaternary time, climate in the Western Desert of Egypt cycled between arid and semiarid with possible short spans of subhumid conditions (Haynes, 1978; Chapter 9). As the region became increasingly arid, large ephemeral streams disappeared, and the wadis were subjected to further modification by mass wasting, wind erosion, and wind deposition. The present result of climatic cycling is illustrated in Figure 15.6C. Scattered inselbergs dot the pediplain formed by retreat of the Gilf scarps. Large southward moving dunes and sand sheets are present along with some yardangs (wind-streamlined residual hills; McCauley and others, 1977). According to Haynes (1978), the latest cycle of hyperaridity set in about 5000 BP, after which water ceased to be a significant factor in landform development.

Since the onset of the present cycle of hyperaridity, water erosion in the wadis has been so infrequent that resistant cobbles of sandstone lying on older stream terraces have become severely wind eroded (Fig. 15.8B). The oriented pits, flutes, and grooves on sandstone and quartzite cobbles of the terraces just a meter or less above the most recent erosion channels are secondary in origin. Haynes (Chapter 9) corroborates the efficacy of the wind in eroding stream-channel deposits in western Egypt. We observed similar wind-erosion features on a flash-flood deposit near Bir Abu El-Hussein, about 340 km east of the Gilf Kebir Plateau. Stream-deposited boulders of quartzite and limestone, in place on the wadi floor, are severely wind eroded on their north-facing sides, but retain normal, stream-rounded shapes on their downwind sides. Similar wind pitting and fluting of ventifacts in crystalline limestone, basalt, quartzitic sandstone, and other rock types in the Western Desert are described in earlier reports (Hume, 1925, p. 62-73; Grolier and others, 1980; McCauley and others, 1979a; 1980a,b). Wind-pitted fragments of massive basalts and orthoquartzites in the Western Desert are described by McCauley and others (1979a, 1980b) as analogs of similar-appearing rocks at the Viking Lander sites; pits in the martian rocks were earlier thought, by many workers, to be vesicles.

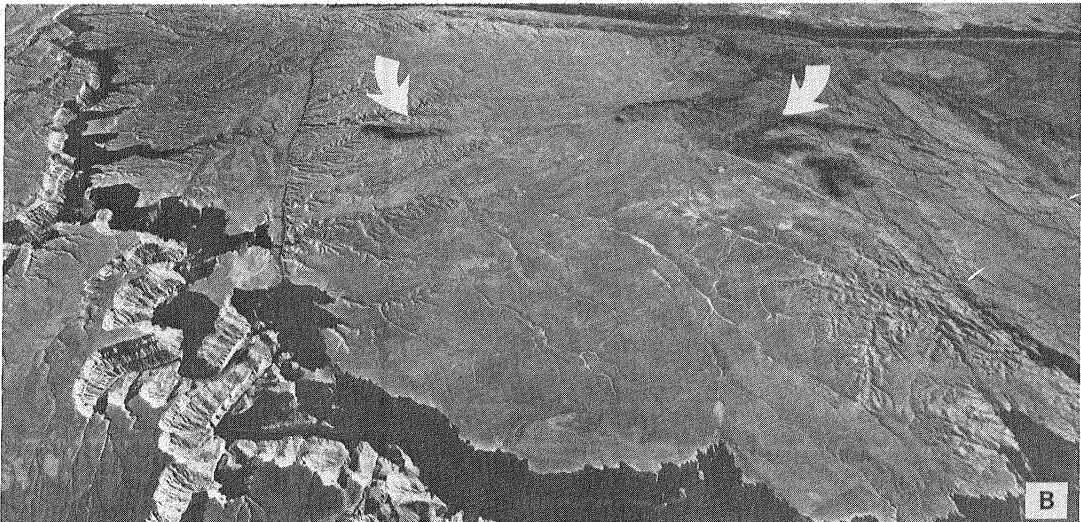
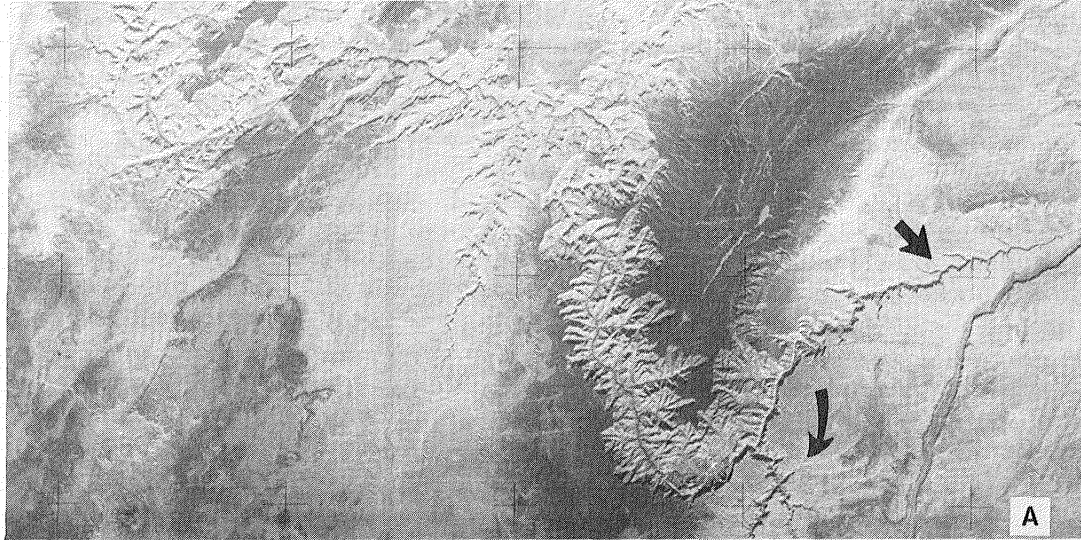


Figure 15.7 A) Skylab photograph (SL3-122-2581) of the semiarid Grand Canyon region, Arizona, showing intermittent tributary stream valleys incised into flat-lying rocks of the Colorado Plateau. View north. The caprock is resistant Kaibab Limestone of Permian age from which overlying softer shales and sandstones of Mesozoic age have been eroded. Barbed tributaries of Marble Canyon (straight arrow) resemble those of some Gila drainages; compare also with Nirgal Vallis, Mars (Fig. 15.19A). Curved arrow indicates Marble Platform shown in (B). B) Patterns of intermittent stream valleys incised in stripped caprock of Marble Platform in eastern Grand Canyon region, Arizona. View east. Arrows indicate erosional remnants of soft shales of Moenkopi Formation of Triassic age. Compare with patterns of defunct stream valleys incised in stripped caprock of the Gila Kebir Plateau (Fig. 15.1). (U.S. Air Force oblique high-altitude photograph 008 374R Sept. 6, 1968).



Figure 15.8 A) Dry underfit watercourses cut into terraces of probable Holocene age in Wadi El-Bakht (locality D, Fig. 15.1). Talus cones and rock falls on north wadi wall (background) define incipient conical segments. Wind-eroded stream pebbles about 8-10 cm long on terrace in left foreground. B) Wind-eroded stream cobble with finger-like projections pointing in local upwind direction (eastward, to right) on terrace in same locality as (A). Knife is about 10 cm long.

The following sections discuss features shown diagrammatically in Figure 15.6C: the wadis, conical hills, yardangs, sand sheets, and dunes of the Gilf region, including both the plateau and parts of the adjacent plains. Interpretations are based on field observations made during the 5-day reconnaissance of the eastern Gilf area described in preliminary reports by El-Baz and others (1980) and Maxwell (1980). Suggested models relate the geomorphic features to climate change and to the roles of running water, wind, and mass-wasting processes in landscape development.

Wadis El-Bakht and Ard El-Akhdar

Wadis El-Bakht and Ard El-Akhdar preserve partial records of fluvial, mass-wasting, and eolian activities that varied in effectiveness with episodic climate change. These records illustrate some aspects of the complex geomorphic history of the Gilf.

Both of these steep-walled valleys were dammed by natural obstacles in narrow parts of their upper reaches, creating lakes in which 6 m or more of lacustrine sediments accumulated. Both wadis were occupied by Man during pluvial episodes in Neolithic time, as shown by artifacts from the surface of the lake-bed deposits (McHugh, 1980; Haynes, 1980b). As yet no fossils or artifacts have been found to establish the age of the lake bed deposits; the finding of such evidence would be a worthwhile goal for future expeditions. A sequence of events in Wadi El-Bakht is proposed by McHugh (1980). Our tentative interpretation of the sequence of geologic events at Wadi Ard El-Akhdar is as follows:

1. Stream erosion in post-Oligocene time, postdating some of the basaltic eruptions in the region (Meneisy and Kreuzer, 1974, p. 25-29), results in valley cutting and exposure of a basaltic plug.
2. With the onset of episodic aridity during late Tertiary or early Quaternary time, streamflow becomes ephemeral. During arid intervals, the wadi is invaded by dunes, similar to the modern dune shown in Figure 15.9. Mass wasting and occasional sheet-

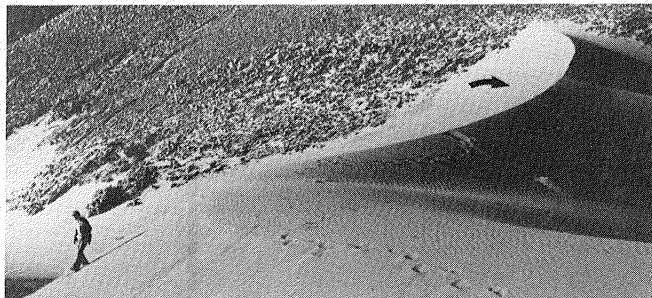


Figure 15.9 View north toward modern dune near breached dam in Wadi Ard El-Akhdar. Wind that formed slipface (arrow) blew upvalley from east; regional prevailing wind, outside the wadis, is northerly. Exhumed basalt intrusion forms wadi wall in background.

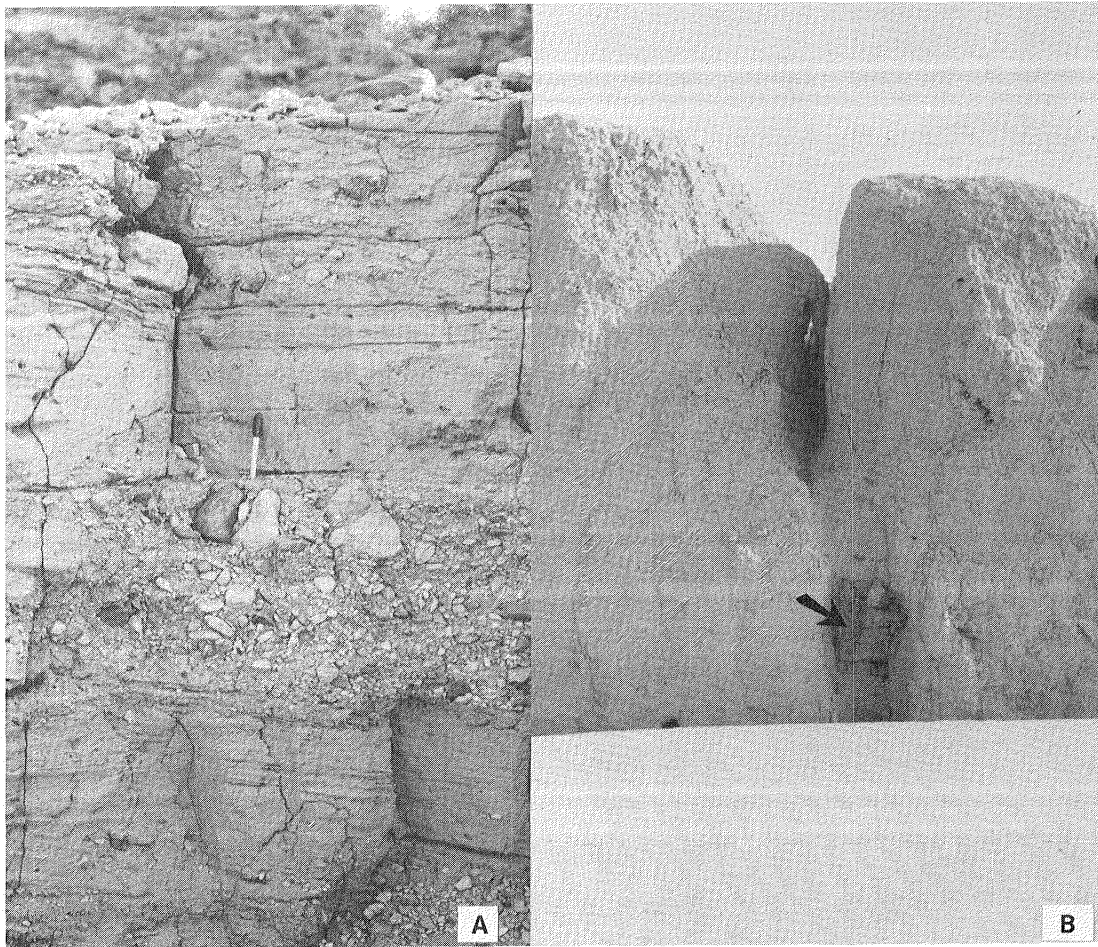


Figure 15.10 A) Interbedded reworked dune sand, sheetwash deposits, and talus fragments form breached dam at Wadi Ard El-Akhdar (white arrow, Fig. 15.11B). B) Pipes in lacustrine deposits at Wadi Ard El-Akhdar (arrow, Fig. 15.11A) indicate episodic soaking of the lake beds since draining of lake. Arrow indicates part of a sediment-filled pipe about 20 cm wide.

wash result in continued formation of talus slopes on wadi walls. Fanglomerates interbedded with reworked dune sands are deposited in the constricted neck of the wadi (Fig. 15.10). This deposit, indicated by the white arrow in Figure 15.11, forms a natural dam that traps runoff from cloudbursts and reactivated springs, and a shallow lake accumulates upstream.

3. The colluvial-eolian dam is breached, resulting in sudden, catastrophic draining of the lake. Such breaching would account for erosion of the unusually large, deep stream channel that excavated the lake beds to a depth of about 4-5 m (Fig. 15.11A). Pottery and deflated fire pits on the surface of the lake beds indicate Neolithic occupation of the exposed lake bottom (McHugh, 1980; Fig. 15.12).

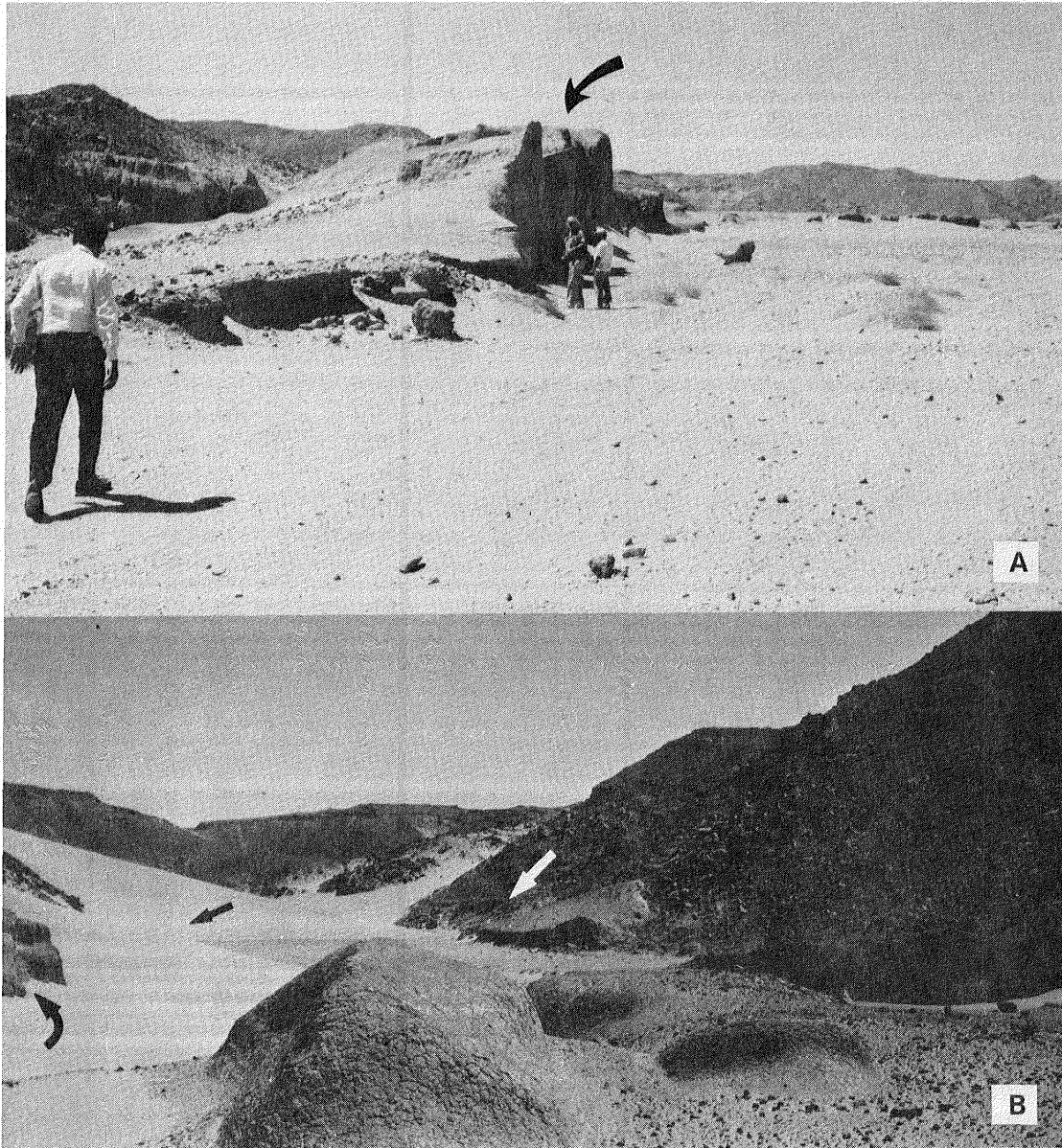


Figure 15.11 Erosion of lacustrine deposits and invasion by windblown sand in Wadi Ard El-Akhdar (locality E, Fig. 15.1) indicate change from a dominantly fluvial to a dominantly eolian environment. A) View upstream (west) along the main drainage channel cut to depth 4-5 m in lake beds (arrow) following breakout of the dam in Wadi Ard El-Akhdar. B) View east at constricted neck of Wadi Ard El-Akhdar where colluvial-eolian dam (white arrow), now breached, blocked the wadi. Deposit shown in detail in Figure 15.10A. Keel of well-streamlined, meter-high yardang in lake beds (foreground) points in the upwind, but downstream (eastward) direction, toward the notch. A modern dune (dark straight arrow and Fig. 15.9) occupies north side of notch. Part of basalt intrusion is indicated by curved arrow.



Figure 15.12 Deflated Neolithic hearth of baked sediments (arrow) on surface of lake bed in Wadi Ard El-Akhdar. Wind action has modified the channel walls, carved parts of lake bed into meter-size yardangs (background and right of photo), and deposited sand in channel.

4. Wind erosion carves the dessicated lacustrine deposits into aerodynamically shaped hillocks (yardangs) with an east-west orientation (Fig. 15.11B). The most streamlined of these lie within about 100 m of the narrow neck of the wadi, probably because of the venturi effect. Tops of the yardang keels extend upward to within a few centimeters of the top surface of the lake bed deposits; thus the heights of these excavated hills represent nearly the total depth of wind erosion since the lake was drained. Recent easterly winds at this locality are indicated by sand tails deposited in the lee of rock fragments on the wadi floor, and by orientation of the slipface on the dune at the notch (Fig. 15.9).

5. During the present interval of extreme aridity, active dunes again accumulate near the site of the earlier dam. Occasional runoff flows in an integrated but minor, very shallow gully system in the upper reaches of the wadi. Older sheetwash deposits of poorly sorted pebbles are preserved as low terrace remnants between the gullies. An extensive talus apron mantles the loose dune sand surface at the notch, setting the stage for development of another colluvial-eolian dam.

The Conical Hills: Remnant Interfluves

Steep-sided conical or flat-topped hills that rise abruptly from surrounding plains are landforms common to most deserts; they are generally referred to as inselbergs. Unlike yardangs, which result

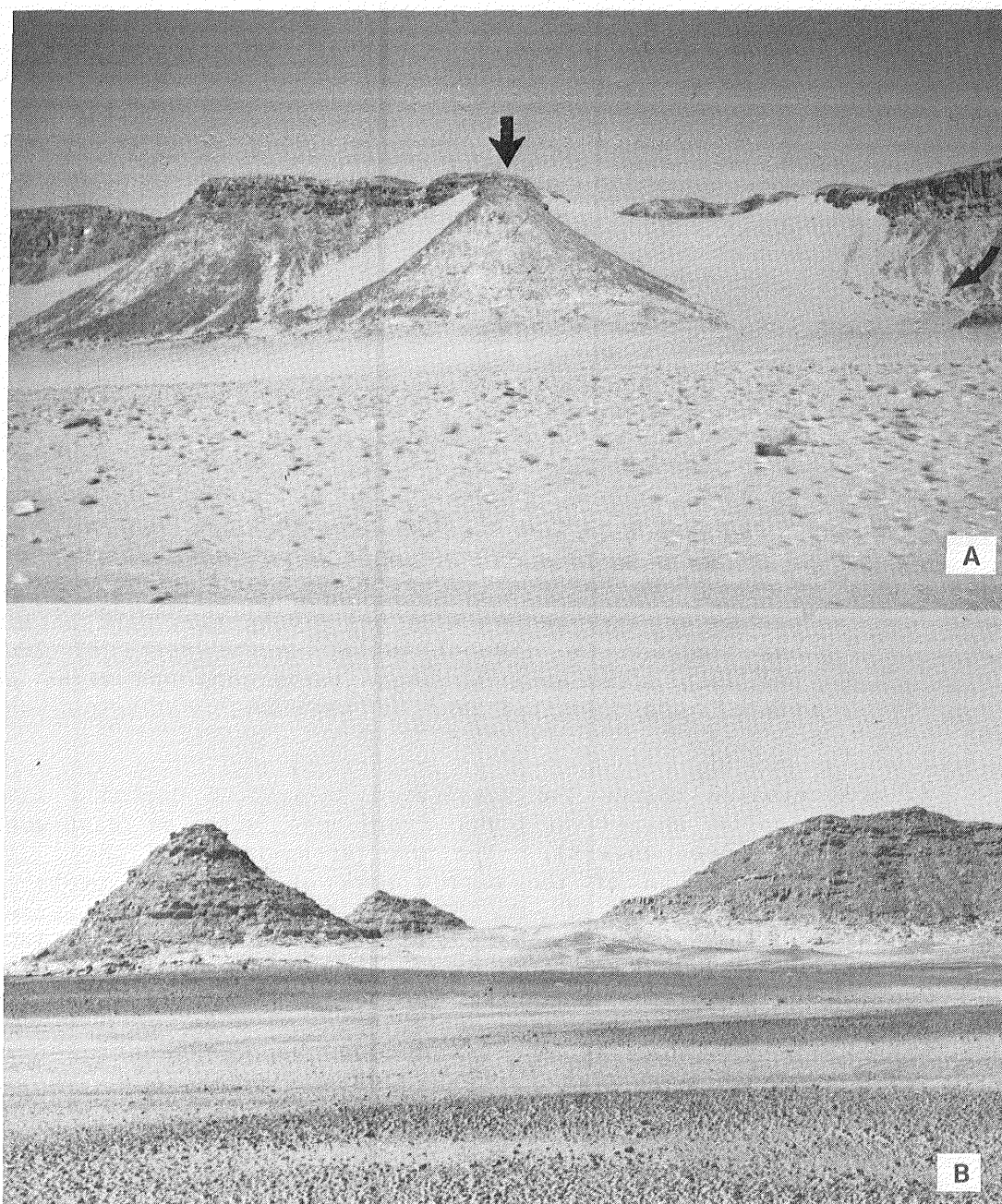


Figure 15.13 Sequence showing suggested evolution of conical hills from wadi side walls and spurs. A) Semi-detached segment (arrow) of wadi wall near junction of Wadi Ard El-Akhdar with Wadi Wassa. Dune sand blankets much of wadi wall and obscures underlying remnants of alluvial fans (curved arrow). B) Conical spur detached from side wall of Wadi Eight Bells, about 500 m south of divide from Wadi Wassa (locality C, Fig. 15.1). Pediment slopes gently southward (to left across photo) from base of wadi wall and inselbergs and is veneered with lag deposits of varnished stream pebbles and drifts of windblown sand.



Figure 15.13 C) Isolated flat-topped mesas and conical hills are remnants of wadi walls standing as inselbergs on pediplane east of Gifl Kebir Plateau. Scarp of Gifl Plateau in far distance, in right of photo (arrow). View south (downwind) from top of 6 m high linear dune in lee of bedrock ridge at Bagnold's 1938 camp (Bagnold and others, 1939) in the eolian thoroughfare (locality F, Fig. 15.1). The south terminus of this dune has migrated 40 m southward in 40 years (Haynes, 1980).

from excavation of intervening troughs by wind erosion, inselbergs owe their relief to dissection of highlands, usually by stream erosion. They commonly evolve from dissected plateaus capped by resistant, nearly horizontal bedrock: when the caprock disappears, the irregular buttes and mesas gradually become conical hills standing in groups, chains, or in isolation.

The shapes of inselbergs evolving in hyperarid deserts differ significantly from those in arid to semiarid deserts, because slope-forming processes vary in relative effectiveness under different climatic conditions. In semiarid deserts, undercutting of caprock occurs by weathering, spring sapping, and slopewash; comminuted debris is removed mainly by running water, and wind erosion plays a subordinate role. Inselbergs in semiarid deserts are typically bounded by pediments veneered by alluvium and graded to valleys of nearby ephemeral streams (Bryan, 1925; Rahn, 1965).

In the hyperarid Western Desert of Egypt, where annual precipitation is less than 1 mm, running water is now virtually absent. Flat-topped interfluvial areas of the dissected Gilf plateau surface are now being reduced to conical inselbergs mostly by dry mass wasting and wind erosion, with only rare and sporadic episodes of spring sapping and slopewash. In this desert, wind is now the dominant agent for removal and transport of comminuted slope debris. Mass wasting, wind erosion and deposition have erased most traces of gullies, fans, and pediments from the wadi side slopes, except in areas deep within the dissected plateau (Fig. 15.13A, B). Many of the divides between the wadis, like the outliers of the plateau scarp, are reduced to groups of low hills (Fig. 15.4). The most isolated hills on wadi floors and on the plain outside the Gilf scarp are conical in shape, and they rise abruptly, with slope angles of about 35°, from the essentially flat desert floor, which is veneered with windblown sand. Although all of these hills owe their relief to regional downcutting by long-vanished streams, those that are farthest removed from the wadi walls and the Gilf scarp are highly symmetrical and typically lack gullies, fans, and pediments (Fig. 15.13C).

The symmetrical, conical shape of these remnant hills seems to be an equilibrium form that results when slopes are reduced primarily by weathering, mass wasting, and wind erosion, in the virtual absence of running water. This shape, much like that of the upper part of tents used by the Geological Survey of Egypt, is probably a form of dynamic stability in winds of variable direction. Most bedrock remnants in and near the Gilf Kebir are eroded to such conical forms rather than to streamlined forms (yardangs) that typically form in desert areas with unidirectional winds (McCauley and others, 1977). Although regional winds in southwestern Egypt are highly directional, in and near the Gilf they are topographically deflected (Fig. 15.14). These winds are only locally unidirectional, and they do not have as long a fetch as winds on the open plains. Diversion of the regional northeasterly winds into local flow patterns within the wadis is shown by the orientations of yardangs and dunes. In Wadi El-Bakht, for example, trimodal local wind directions are indicated by the presence of a star dune (Fig. 15.14A) and giant ripples of coarse sand oriented transverse to the wadi and to the direction of transport of sand in climbing dunes on the south wall (Fig. 15.14B). In those parts of the Western Desert where winds are highly directional, the sandstones, granites, and even crystalline limestones are eroded to well-streamlined yardangs (Grolier and others, 1980; El-Baz and others, 1979a).

Wind modifies the shapes of inselbergs during arid intervals by abrasion and deflation of weathered rockfall debris. Falling and breaking of bedrock blocks comminutes and preconditions fragments for weathering, abrasion, and deflation. Observations of wind-erosion grooves in bedrock around the base of conical hills in Farafra Oasis (Breed and others, work in progress) suggest that isolated hills may act as centers of vorticity, producing local turbulent wind currents. Such wind currents sweep around and between isolated hills and remove loose particles from all sides, thus helping to maintain the shape of the hills while reducing their size, in the same way as demonstrated

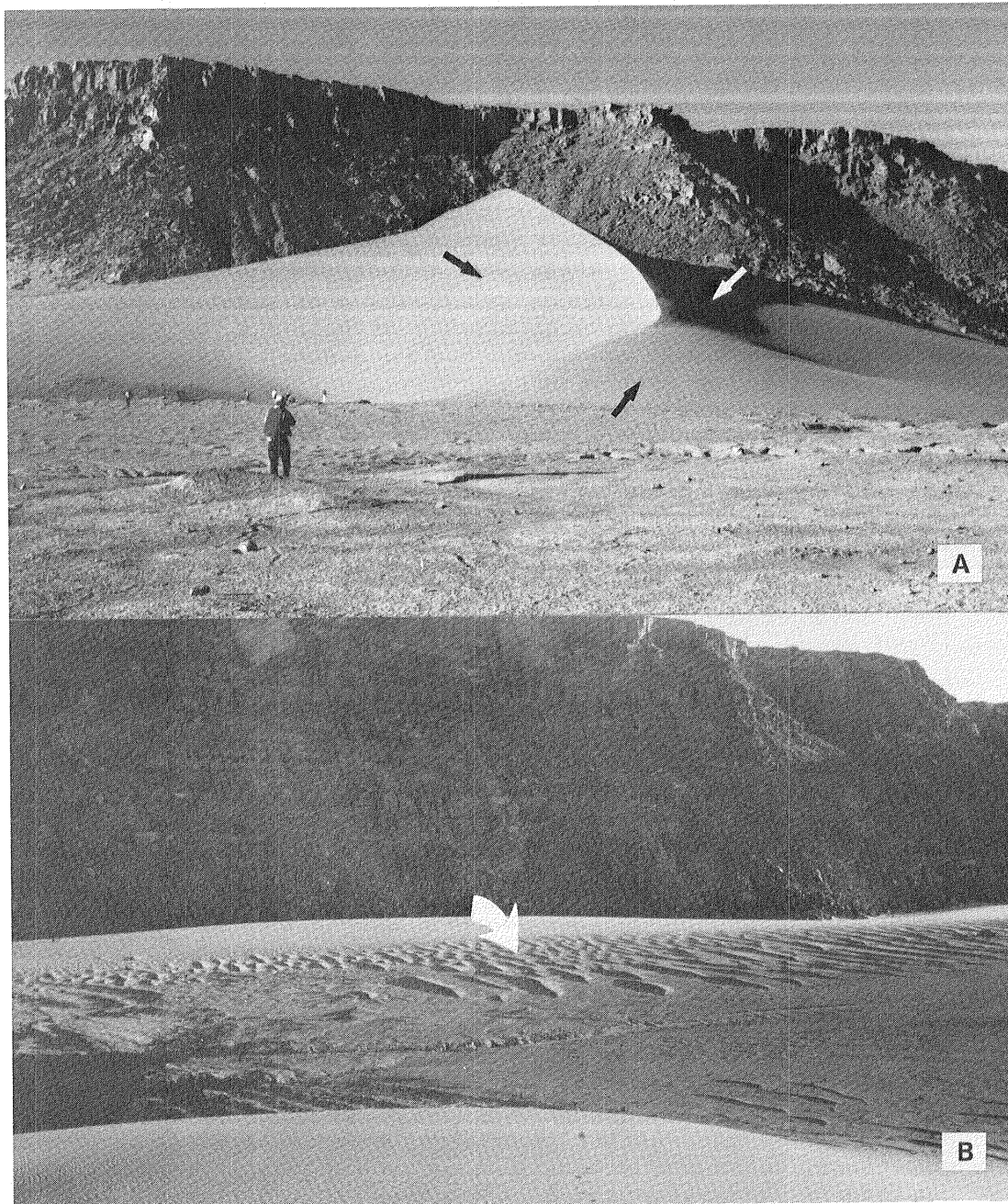


Figure 15.14 A) Star dune in lee of north wall in upper part of Wadi El-Bakht. Multiple slipfaces (arrows) indicate that prevailing north winds are locally diverted and channelled by the wadi. Sand is driven southward over the surface of the plateau and down wadi side walls by prevailing winds. The sand is then secondarily shifted back and forth, more or less in place, by upvalley (east) and downvalley (west) winds, so that the trapped falling dune assumes a starlike shape. B) View south from top of dune at the notch in Wadi El-Bakht, showing giant ripples (arrow) formed by local winds blowing along valley axis. Footprints on dune show scale.

for small features in laboratory experiments and field observations by Whitney (1978).

A key concept for inselberg evolution under hyperarid climatic conditions is that wind, unlike water, is not confined to downslope movements (Udden, 1894); wind transports the fines of comminuted slope debris up and away in suspension, not simply down onto the surrounding floor. Winds carrying coarser grains abrade grooves in exposed bedrock floors and deflate them, but do not produce pediments. As pointed out by Peel (1939b, 1941), one of the most peculiar aspects of the Gif landscape is the general absence of pediments at the foot of the plateau scarps and inselbergs. The conical hills that rise directly from the flat plains of southwestern Egypt lack the intervening break of slope (piedmont angle) characteristic of inselbergs developed in less arid regions (Kesel, 1972). Steep sides are maintained on the inselbergs of the Western Desert as they are reduced in size from hills tens of meters high to small nubbins. Slope debris, comminuted by weathering, mass wasting, and wind abrasion, is removed rapidly as material is almost continually deflated.

Reduction of Gif interfluves to groups of conical hills (Fig. 15.13) may occur as follows:

1. Dissection of the plateau by running water accompanied by mass wasting produces steep slopes on valley sides and isolates flat-topped remnants (buttes and mesas) characteristic of plateau canyonlands in semiarid regions. Alluvial fans accumulate at the foot of gullies along the scarps and on pediment slopes graded to the valleys of nearby streams. Depths of erosion are controlled by a regional base level that is the intersection of the water table with the ground surface; this level was formerly controlled by master streams from which the bordering cliffs of the Gif receded by headward and lateral erosion.

Some of the residual hills and wadi walls deep within the dissected Gif Plateau rise from remnants of old pediments veneered by stream gravels, and a few have minor debris aprons or fans (Fig. 15.4; 15.13A). These parts of the Gif wadis retain the imprint of earlier fluvial erosional and depositional processes, which are thought to have been highly effective during Quaternary intervals of subhumid climatic conditions. Some of the Gif inselbergs thus have complex slopes typical of inselbergs that have evolved in both humid temperate regions and in semiarid to arid deserts (Bryan, 1925; Cotton, 1952, p. 260-262; King, 1960; Rahn, 1965; Kesel, 1972).

2. Hyperaridity sets in, and active downcutting by running water ceases except for sporadic, local episodes of torrential downpour. Vegetation disappears, except for a few scattered bushes and clumps of grass in ephemeral stream channels (Boulos, 1980). Backwearing of wadi walls by weathering, cliff sapping, and mass wasting gradually isolates conical segments on the wadi side slopes and spurs (Fig. 15.13A).

As these segments become detached from the parent wadi walls, their potential catchment and storage areas for sporadic rainfall diminish, so that sheetwash cannot collect and carve gullies on their slopes. Continued slumping of debris further isolates the slope segments and allows increased flow of abrasive winds around them.

Wind gaps develop around the semi-isolated cones, which have become centers of vorticity (Fig. 15.13A, B). Comminuted debris is carried away from the hillsides by wind, rather than washed down slope by running water. Pediment slopes are no longer maintained, and fans no longer accumulate. Eventually the conical wall segments become isolated conical hills whose slopes approach equilibrium with the forces of wind and gravity (Fig. 15.13C). These more fully evolved forms are typically found on the broad, flat floors of the larger wadis and on the open plains away from the Gilf scarp, as recognized by Peel (in Bagnold and others, 1939; Bagnold, 1941, Fig. 10).

Meanwhile, as lowering of the wadi floors by ephemeral streams essentially ceases, sediments are redistributed by wind into eolian deposits that surround the conical inselbergs, and fill in the low lying areas, forming smooth, essentially flat plains. Except for a few dry, underfit drainage channels here and there, most traces of fluvial activity in the wadis are buried beneath the eolian plains.

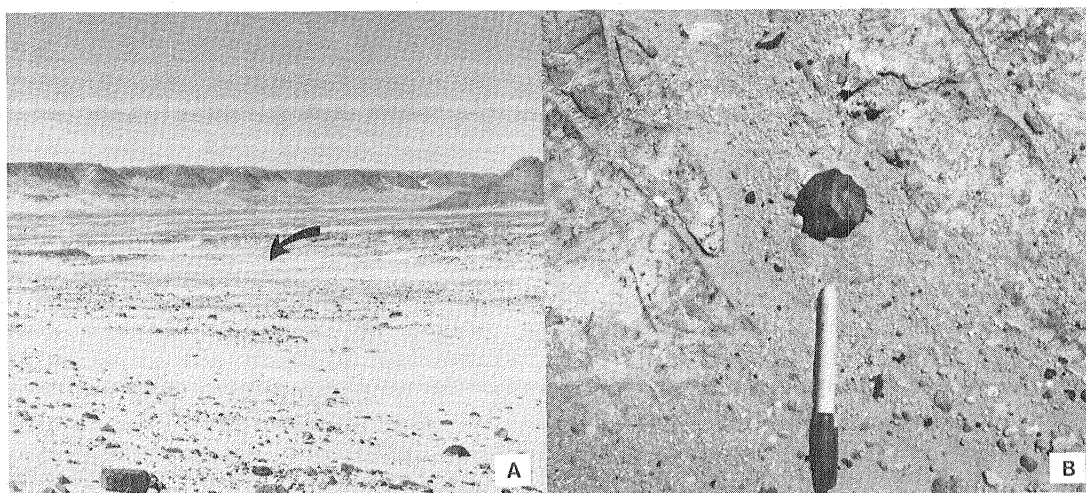


Figure 15.15 A) View west from eolian thoroughfare toward dissected Gilf escarpment at mouth of wadi near location G, Figure 15.1. Isolated conical spur remnant on right. Concentrations of white lag particles veneer pediplain and mark course of former master stream that flowed southward in channel across middle of photo (arrow). B) Beveled "Nubian" strata (Grolier and Schultejann, Chapter 14) about 5 km east of Gilf escarpment (locality H, Fig. 15.1). Rocks that litter pediplain are stream pebbles; many are now ventifacts.

FEATURES ON THE PLAINS

Surficial Deposits

Elongate bands of mobile eolian sediments occupy broad zones along both the east and west sides of the plateau just beyond the wadi mouths (Fig. 15.1; Grolier and Schultejann, Chapter 14, Fig. 14.1). The surfaces of these "eolian thoroughfares" consist of dunes, sand sheets, and coarse but well-sorted lag deposits that truncate and override the fluvial deposits where the wadis of the Gilf debouch on the pediplain. Migrating windblown sand piles up against north-facing (upwind) slopes of isolated hills and ridges, and extends downwind from these obstacles in the form of drifts and numerous elongated, linear lee dunes. A view of the eolian thoroughfare on the east side of the plateau from a locality (G, Fig. 15.1) about 9 km north of Bagnold's 1938 camp (Bagnold and others, 1939) shows traces of former bedrock outliers of the Gilf and relict drainage systems (Fig. 15.15A). Still farther east (locality H, Fig. 15.1), the beveled sandstone of the pediplain is overlain by ventifacts that are old stream pebbles (Fig. 15.15B).

Segregation by wind of grains of certain sizes into discrete types of surficial deposits is typical of deserts (Folk, 1968), and is particularly well advanced in southwestern Egypt. Most grains capable of saltation (Bagnold, 1941) have been winnowed and heaped into isolated dunes, while finer and coarser grains lag behind to form an extensive flat plains deposit. This sand plain surface is commonly armored by a layer, one grain thick, of evenly distributed coarse sand or granules.

Drifts of very coarse, white quartz sand and granules (included in Qs₁ of Grolier and Schultejann, Chapter 14) are distributed throughout the eolian thoroughfare along the east side of the plateau. Distribution of these lag deposits on the Landsat image (Fig. 15.1) coincides rather closely with the inferred locations of one or more master streams to which the wadis of the Gilf may have once been tributary. Large drifts of the coarse material are concentrated downwind from wind gaps in east-trending ridges of sandstone strata that protrude above the pediplain. The white lag is here interpreted as windworked stream deposits from which finer, more mobile grains have been winnowed. In this interpretation, the coarse grains have not been blown far from their sources in old fluvial deposits. However, winds whose velocities are enhanced by the venturi effect in the wind gaps are competent to move and concentrate these coarse particles. Thus the coarse-grained deposits appear as white streaks in these localities on the Landsat image (Fig. 15.1).

Finer, more mobile sands have been segregated into dunes that are migrating south-southwestward along the thoroughfares, driven by northerly prevailing winds (Fig. 15.13C). In the thoroughfare adjacent to the extreme northern and southern parts of the plateau (Fig. 15.1), linear dunes whose long axes are aligned essentially parallel to prevailing winds extend in an oblique direction across the concentrations of white lag granules.

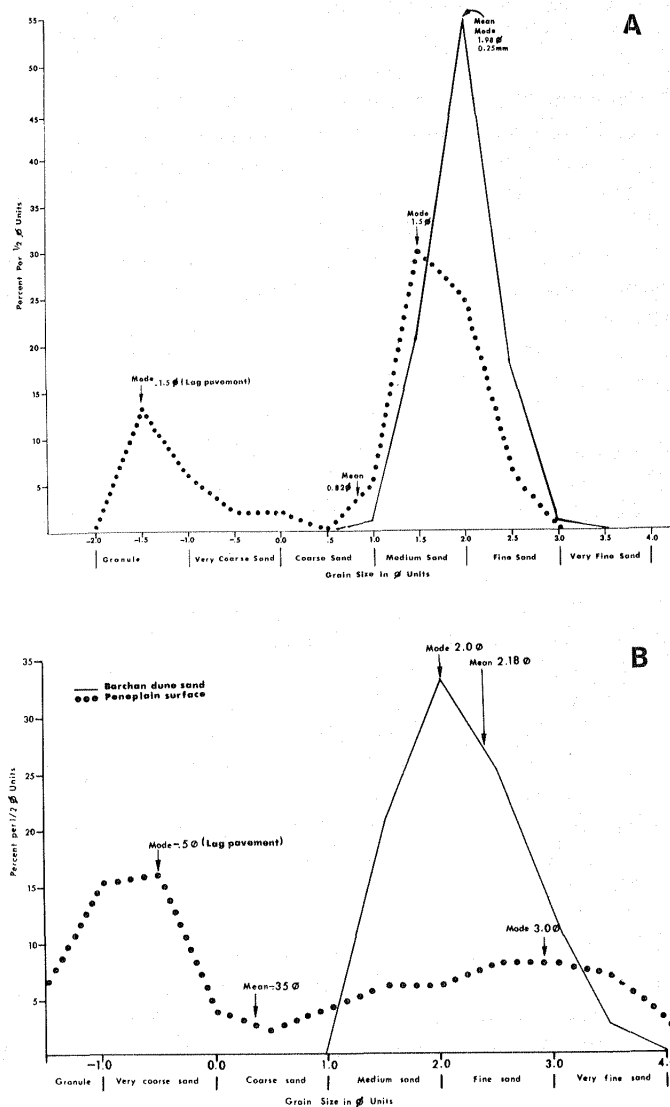


Figure 15.16 Size-frequency diagrams showing distributions of grain size in dunes and on the desert floor: A) in eolian thoroughfare at locality F, Figure 15.1, immediately east of Gilf Kebir (Fig. 15.13C), and B) on penepplain about 180 km east of the Gilf. Both curves illustrate segregation, by wind, of surface sediments by grain size. The characteristic bimodality of grain sizes of desert floor deposits (pediplain surface, (A); penepplain surface, (B)) is discussed by Folk (1968). In both (A) and (B), coarse grains on desert floor represent lag pavement composed of particles left behind as winds removed finer grains from surficial debris. On the pediplain surface, near the mouth of a Gilf wadi, coarsest particles (mode 1.5 ϕ) probably are reworked stream gravels. Finer particles on desert floor have a narrow size range; they probably represent well-sorted sand washed from windblown deposits in the wadi during infrequent flash floods.

Many of the linear dunes in the thoroughfares appear to have migrated into the Gilf region from the Great Sand Sea to the north (Peel, 1941). On satellite pictures these arrays of migrating dunes can be traced beyond the margins of the Gilf southward for hundreds of kilometers. Eolian thoroughfares diverge around Uweinat Mountain (El-Baz and others, 1980, Plate 5), and continue in the direction of the ergs of the east-central Sahara. The regional pattern of migrating sand is shown by Mainguet (1977, Fig. 1). Near the Gilf, many of these elongate "streams" of eolian sand deposits appear to follow the abandoned valleys of ancient watercourses (Fig. 15.1), as if the migrating sand, like running water is "channelled" in the lowlands and is "discharging" toward basins of deposition in "downstream" areas.

Among the southward-migrating, presently mobile materials in the eolian thoroughfares near the Gilf and on the peneplain farther east are numerous fields of barchanoid dunes. We sampled a field of migrating barchans (the Abu Hussein field: McHugh, 1980) about 180 km east of the Gilf Kebir Plateau (Fig. 15.16). The actively saltating sand grains of these dunes have a mean diameter of 2.18ϕ (about 0.22 mm: fine sand). The sand is moderately well sorted and yellow (7.5 YR 7/6 on the Munsell Soil Color Chart). We also sampled actively saltating sand from dome dunes (considered incipient barchans; McKee, 1966) 75 km east of the plateau. One of these dunes has moved 20 m in 8 years (Breed and others, 1980a). Distribution of grain sizes in this dome dune, characterized by relatively coarse and poorly sorted sand, is shown on Figure 15.17A. This distribution contrasts sharply with that of well-sorted grains in less active lee and stabilized dunes (Figs. 15.16; 15.17B).

Rather rapid migration of transient features such as dome and barchan dunes makes their initial presence in the vicinity of archeological remains discovered nearby (McHugh, 1980) somewhat doubtful. On the other hand, many dunes located in the lee of topographic obstacles are relatively stable, built of sand that has been accumulating in those sites repeatedly during episodes of aridity. Star dunes and falling dunes, such as those observed in Wadi El-Bakht (Fig. 15.14A) and in the lee of the cliff behind our 1978 camp at Wadi Wassa (locality A, Fig. 15.1), are good examples of dunes trapped in the lee of obstacles; they are "topographically stabilized" dunes. Relations of the topographically trapped dunes to underlying deposits, artifacts, and fossils may be of long duration and thus useful for interpreting sequences of events in certain localities.

DISCUSSION AND IMPLICATIONS

Former Drainage in Southwestern Egypt

The basic geomorphic framework of the Gilf region is derived from fluvial dissection that appears to have been much more extensively developed and mature than is generally recognized. In a sense, the ancient drainages in the southeastern part of the Gilf region represent that "most senile valley" (Peel, 1941, p. 10) whose supposed absence might have lent credence to the hypothesis of marine planation

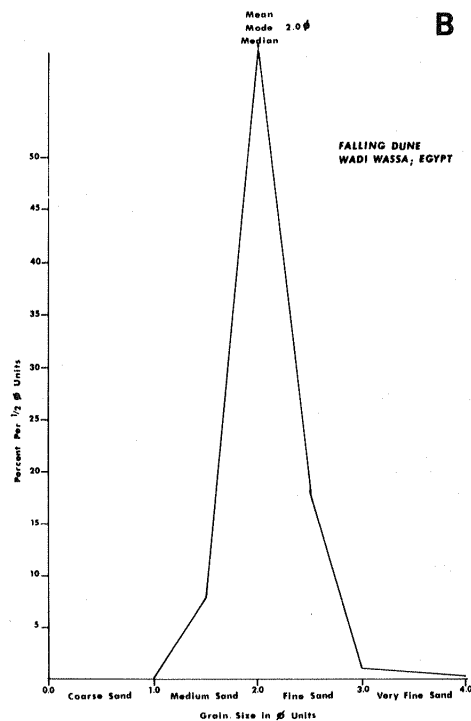
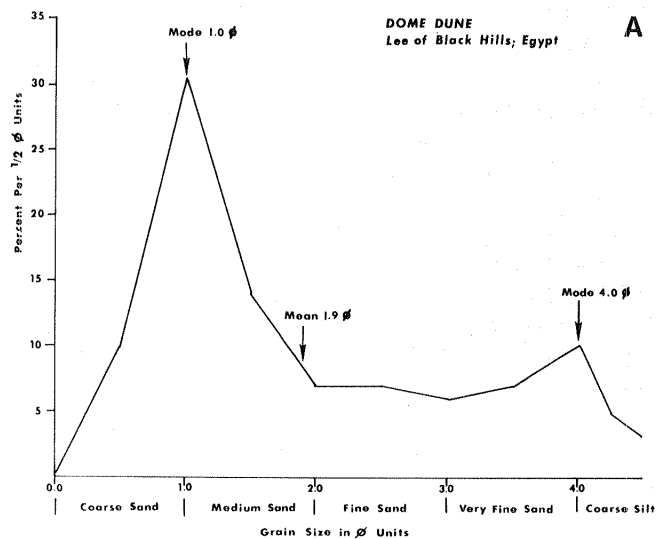


Figure 15.17 A) Size-frequency diagram showing poorly sorted, coarse sand in a highly mobile, transient dome dune near Black Hills in the Western Desert east of the Gif. Compare with well-sorted sand in a less mobile, linear lee dune (Fig. 15.16A) and fairly well sorted sand in a barchan (Fig. 15.16B), whose mobility is probably intermediate between that of the dome and the lee dune. B) Size-frequency diagram showing extremely well sorted, narrow size-distribution of sand in an inactive, topographically trapped, falling dune in the lee of wadi walls at Wadi Wassa (locality A, Fig. 15.1).

of the plateau surface. A more plausible explanation for the planation may be erosional stripping of the plateau surface by long-vanished streams, followed by wind scouring of the resistant caprock according to the mechanism suggested by Haynes (1978; Chapter 9).

The presence of the Eight Bells drainage system, which extended tens of kilometers south of the present physiographic boundary of the Gilf, raises interesting questions as to the eventual destination of the stream systems that formerly debouched from the plateau. Other workers have postulated integrated drainage in parts of southwestern Egypt in earlier, more humid times (Haynes, Chapter 9), but have considered that it probably flowed eastward. The pattern of the Eight Bells system on the Landsat image (Fig. 15.1), as well as field observations in its headwater tributaries (Fig. 15.13B), indicate that it discharged to the south, whereas Wadi Wassa and other streams on the east and north sides of the plateau discharged to the east and north. The Gilf highlands thus apparently were the location of several major regional drainage divides in southwestern Egypt.

If south-flowing drainage from the southern Gilf highlands did not join Wadi Howar and thence discharge into the Upper Nile, where did it go? If a master stream existed south of the Gilf, where was its course on the peneplain now mantled by the Selima sand sheet and what was its ultimate destination? These are tantalizing questions on which we can only speculate with the inadequate photographic, cartographic, and field data presently at hand.

The present regional slope of the land surface in the southwest corner of Egypt is, according to Said (1962, p. 11), generally northward, but the detailed topography of the region is poorly known and essentially unmapped. Capture of some of the Wadi Wassa system by the south-flowing Eight Bells system and by streams eroding headward into the west side of the plateau (Fig. 15.1) implies steeper gradients to the south and west than to the north in these areas. Relief maps of North Africa (Raisz, 1952) suggest that, if the Gilf Kebir were indeed once a major divide separating east and north-flowing from south-flowing drainages, the latter might have eventually discharged into the Bodele Depression in the Borkou region of northern Chad.

In the southern part of the Bodele Depression is the present Lake Chad, a much shrunken relic of a lake formerly about the size of the Caspian Sea (Grove, 1970). The Bodele Depression was a major catchment of internal drainage during Quaternary Pluvial episodes. At the latest time of maximum extent, about 5000 BP, Lake Chad filled the Bodele Depression to a level of at least 320 m (Grove and Warren, 1968), extending to within about 600 km of the south margin of the Gilf Kebir. During humid intervals of mid- to late Tertiary time, as well as during the Quaternary pluvials, Lake Chad might have been at least as extensive. If so, at such times the Eight Bells drainage network may have discharged from the Gilf uplands into this great inland basin. Concentrated, extensive field studies are needed to test these hypotheses; further reconnaissance of key localities would be a worthwhile goal for future expeditions.

APPLICATIONS TO PLANETARY GEOLOGY

Comparisons with Landforms on Mars

Investigations in Western Egypt have proved useful in analysis and interpretation of landforms on other planets, particularly Mars (El-Baz and others, 1979a; McCauley and others, 1979a; Breed and others, 1979). On the Earth, Moon, Mercury, and Mars, primary landforms are created by impact, volcanism, or tectonism; secondary landforms result from numerous complex processes among which running water, wind activity, and mass wasting are most important. These processes continuously compete for dominance of the landscape. Current states of the surfaces of the Earth, Moon, Mercury, and Mars can be illustrated qualitatively by three-component diagrams that use these parameters of primary and secondary landform development (Fig. 15.18).

On the Moon and Mercury, ballistic redistribution of materials by meteorite impact is the main process of primary surface development. Dry mass wasting, triggered by volcanic or seismic activity, is the main agent of secondary landform development. Both of these bodies lack atmospheres, and no evidence exists for past fluvial or eolian activity.

On most of the Earth, secondary landform development is now and probably has nearly always been dominated by the multitudinous effects of running water. These effects are well known and reasonably well understood by geomorphologists. Mass wasting, abetted by running water, ground water, and ice, is also an important agent of slope development. Glacial activity dominates in polar and subpolar regions, and in the recent past has episodically left its imprint in the mid-latitude and high mountainous regions. The deserts of the world are less well understood.

Whereas the Moon and Mercury have little in common with the Earth in terms of landform development, many surface features on Mars resemble those in hyperarid terrestrial deserts, particularly the Western Desert of Egypt (Haynes, 1978; Chapter 9; Breed and others, 1979, 1980a,b; El-Baz and others, 1979a; Grolier and others, 1980; McCauley and others, 1979a,b; McCauley and others, 1980a,b; Maxwell, 1980). On Mars, as in western Egypt, inferred former fluvial activity has been replaced by mass wasting and wind processes, and wind is now the dominant agent of erosion and transport. Mars apparently had at least one climatic period when conditions were very different. Climate change would explain numerous martian gullies and large channels that are inferred to have resulted from erosion by fluvial processes, possibly including collected runoff, or from collapse associated with movement or seepage of moisture from ground ice, or even from erosion by glaciers (B. K. Lucchitta, oral commun., 1980).

Figure 15.19 illustrates some of the martian features that we consider analogous to the dissected plateau, dry wadis, dunes, ripples, sand plains and inselbergs of the Gilf region. Although martian rock types, particle sizes, wind regimes, and degrees of hyperaridity differ greatly from those on Earth (Mutch and others,

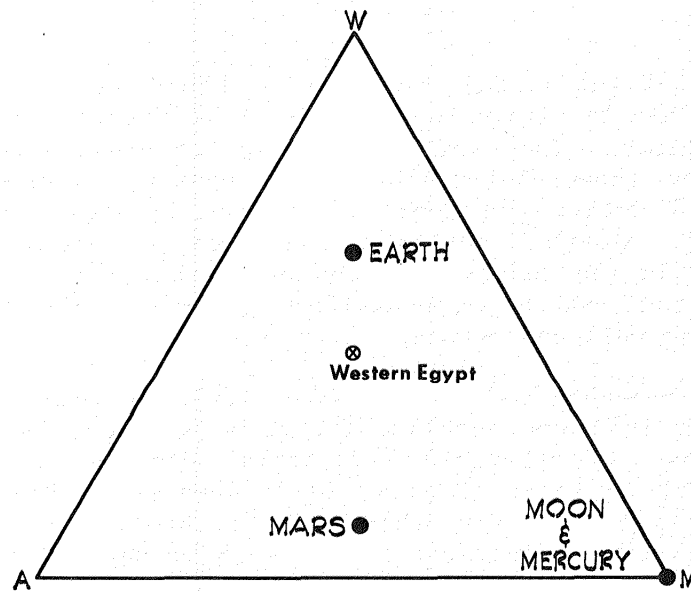
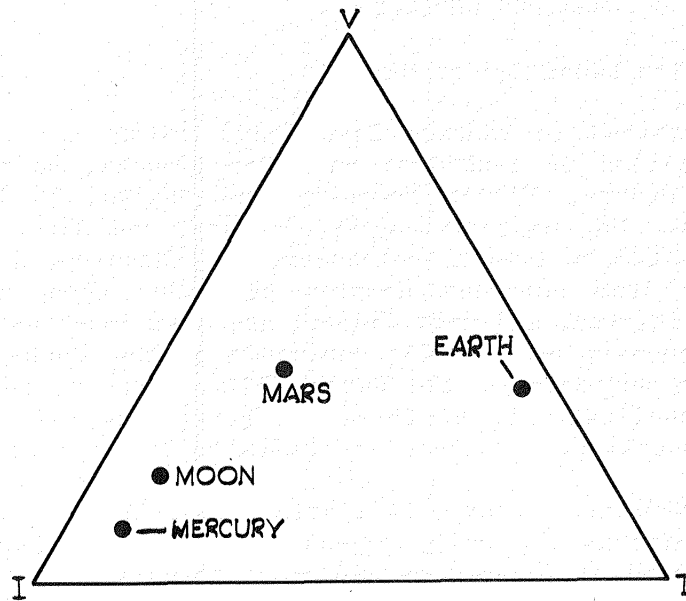


Figure 15.18 Schematic diagrams suggesting relative importance of water (W), wind (A), and mass-wasting processes (M) in modification of primary landforms produced by volcanism (V), impact (I) and tectonism (T). The Western Desert of Egypt is probably more like Mars than any other large region on Earth, in terms of the relative effectiveness of wind and mass wasting versus water in sculpting the landscape.

1976, and many others), surface materials in terrestrial deserts and on Mars have apparently responded in generally similar ways to the forces of water, wind, and mass wasting.

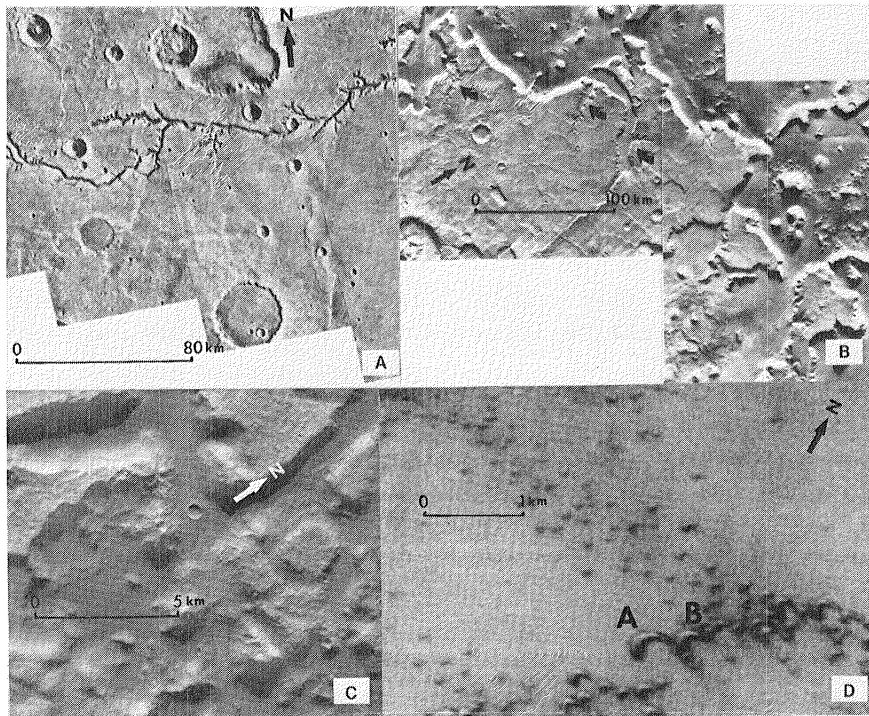


Figure 15.19 Images of the martian surface from the Viking Mission, showing erosional and depositional features similar to those in the Gilf Kebir region. A) The relict fluvial Nirgal channel (Sharp and Malin, 1975); compare with patterns of relict drainages in the Gilf (Fig. 15.1) and intermittent valleys on the Colorado Plateau (Fig. 15.7A). Mosaic of Viking images 466A 49-57. B) Fretted terrain along the boundary between highlands and smooth northern plains in the Ismenius Lacus region of Mars. Numerous flat-topped and conical hills are outliers of a plateau protected by caprock and incised by "wadis" (arrows) that resemble the wadis of the Gilf Kebir (Fig. 15.1). Groups of martian inselbergs may represent remnant interfluves between valleys that extend beyond present plateau scarp. Mosaic of Viking images 675B66, 67. C) Transverse bed forms of windblown sand(?) trapped in broad flat valleys in the equatorial region at about 15°S , 189°W . Orientation of the bed forms varies from valley to valley, but is consistently transverse to each valley axis. Despite scale differences, the pattern resembles that of ripples in Wadi El-Bakht (Fig. 15.14B). Viking image 763A16. D) Barchan dune field in the north polar sand sea. The large dune A has collided with dune B, indicating that rates of barchan migration vary with size (proportional to slipface height), as on Earth. These martian dunes are strikingly similar in shape to barchans observed on the penplain and in the Kharga Depression east of the Gilf Kebir (El-Baz and others, 1979a, Fig. 4). Part of Viking image 488B27.

Inselbergs standing in groups on the plains outside the martian plateau in the fretted terrain (Sharp, 1973; Fig. 15.19D) appear to be remnants of divides between valleys that are continuous with the incised wadis within the plateau. Similar groups of hills beyond the margin of the Gifl Plateau in Egypt mark the positions of interfluves between once-vigorous, integrated streams that extended at least 100 km beyond the present plateau scarp (Fig. 15.1, 15.3, 15.13C). If the Gifl analogy is useful, then the patterns of martian inselbergs may also indicate the traces of ancient watercourses that extended beyond the present margin of the uplands, through the fretted terrain, and onto the low northern plains (Breed and others, 1980b).

One of the unsolved problems of martian geomorphic history is the origin of the north circumpolar erg or "sand" sea. These dunes, which extend over a region of at least 1×10^6 km² around the ice cap, have been attributed to various "sand" sources, including aggregates of dust particles carried to the polar region in suspension (Greeley, 1979b), or solid particles derived from impact, volcanism, and fluvial activity, and transported to the circumpolar region in saltation by surface winds (Breed and others, 1979). Two constraints on the second hypothesis have been 1) the lack of recognizable fluvial deposits on the plains north of the martian highlands, and 2) the absence of north-blowing winds in that region under current climatic conditions, which are controlled by the presence of the north polar ice cap.

Channels of apparent fluvial origin occur near the Viking 2 Lander site on the northern plains at 48°N, 226°W. Channels containing deposits of probable fluvial origin have recently been described below the plateau scarp in the fretted terrain. Martian climatic change could account for a cyclic presence and absence of the ice cap, a denser atmosphere, and episodic running water with erosive force sufficient to carve valleys and transport rock particles from the highlands to depositional sites on the northern plains. Given these as yet unproven climatic conditions, fluvial erosion of the highlands materials may have provided a supply of solid particles susceptible to saltation by surface winds blowing toward the pole. Later, as freezing and dessication set in and running water ceased to flow, evidence of fluvial transport and deposition on the martian plains may have been obliterated, as on the plains of southwestern Egypt. The fluvial characteristics of the martian valleys, where glacial processes may have been added to those of mass wasting and wind, were probably modified to a much greater extent than occurred in and around the Gifl Kebir.

Whereas in Egypt, large, linear accumulations of dune sand are still in transit across the plains toward basins of deposition in the southern Sahara (Mainguet, 1977), most of the dune material on Mars appears to be trapped in the form of barchanoid dunes concentrated in the north circumpolar region (Breed and others, 1979). Some of the north polar dunes on Mars are seasonally active, reversing their slip-faces in response to thermal winds generated by seasonal shrinkage and expansion of the ice cap, but dune sands are not presently migrating into the north circumpolar region; cold air, always descending over the ice cap, causes present-day surface winds to blow generally outward (southward) from the pole (Ward and others, 1980).

Perhaps the advanced stage of segregation of dune materials on Mars implies that upwind sources of saltating sand are exhausted. Martian sands, unlike the sands of the Sahara, have probably not been frequently replenished during repeated intervals of fluvial activity. Furthermore, sand-size particles derived from weathering and from comminution of basaltic rocks on Mars are likely to be far less abundant than sands derived from quartz-rich rocks on Earth (Breed and others, 1979, 1980b). At present, the northern plains on Mars appear to be mantled with eolian dust blankets, deposited from suspension, which obscure the underlying materials. In southwestern Egypt, dunes are migrating along eolian thoroughfares whose locations seem to be determined by the ancient courses of defunct master streams. If similar eolian thoroughfares for migrating sand formerly existed on Mars, they may lie buried beneath accumulations of volcanic and eolian materials on the northern plains.

ACKNOWLEDGMENTS

Salaries for the three U. S. Geological Survey participants were provided by the Office of International Geology, U. S. Geological Survey (Grolier), the Energy Lands and Climate Programs, U. S. Geological Survey (Breed), and the Planetary Geology Program, U. S. National Aeronautics and Space Administration (McCauley). We thank all of these agencies for their support of the research reported in this paper, and in earlier papers that are listed in the references.

**Page Missing in
Original Document**

Chapter 16

BOULDER TRACKS ON HILLSLOPES IN SOUTHWEST EGYPT AND SIMILAR FEATURES ON THE MOON

FAROUK EL-BAZ

National Air and Space Museum
Smithsonian Institution
Washington, D.C. 20560

ABSTRACT

Tracks of mass wasted boulders are examined on the slope of a steep hill 3 km east of Peter and Paul in the southwestern desert of Egypt. The hill is what remains of a volcanic neck of trachytes and basal conglomerates. The hill is surrounded by an apron of debris in which the tracks are grooved. One 2 m boulder left a straight trail and its motion appears to have been smooth. It continued to slide on the level surface surrounding the debris apron for about 5 m, perhaps lubricated by the fine sand that covers this surface. Another boulder left a chain of depressions suggesting that it bounced as it moved downslope. This boulder appears to have disintegrated just before reaching the level ground. Erosional products from previous wetter climatic conditions appear to have been completely washed away in this region, where eolian conditions predominate. The motion of boulders downslope seems to be basically controlled by gravity, or mass wasting. The resulting features are analogous to those on the Moon. Boulder tracks in southwestern Egypt are compared to those on walls of lunar craters such as Hyginus, and mountain slopes such as the massifs at the Apollo 17 landing site. On the Moon, boulder tracks occur as straight or curved depressions with sharp parallel borders, or as chains of depressions. The similarity of the tracks left by mass-wasted boulders in the two places attests to the extremely dry conditions in southwest Egypt. From this correlation it is speculated that similar tracks will be observed on martian hillslopes, when those are revealed by high resolution photographs.

BOULDER TRACKS ON TRACHYTE HILL

On the way from the Gilf Kebir to Gebel Uweinat, a hill about 3 km east of Peter and Paul was examined (Fig. 16.1). Like many other hills in the region, this one is composed of volcanic rock and rises steeply from the otherwise flat terrain of Paleozoic sandstones. The hills are composed of either trachyte or basalt. The trachyte hills form piles about 30 m high on the average, but may reach heights of up to 80 m.

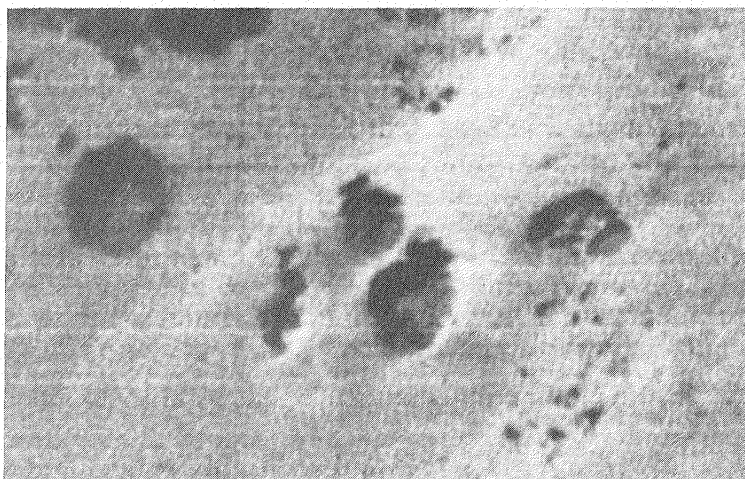


Figure 16.1 Enlargement of Landsat image (E-1131-08141) showing four trachyte hills in southwest Egypt. The two hills in the center are known as Peter and Paul; the 3 km long hill to the east (right) is illustrated in Figure 16.2.

Fluvial landforms in the Gifl Kebir and Uweinat region, in the form of wadis and small catchment basins, attest to wet conditions in the past. However, today the whole area appears to be completely enveloped in an extremely dry climate that is characterized by an eolian regime. In fact, this area is part of the driest region on Earth, where the incident solar radiation is capable of evaporating 200-times the amount of rainfall (Henning and Flohn, 1977).

The desert surfaces on which the volcanic hills occur appear to have eradicated the climatic history of the area. Results of water erosion in previous episodes appear to have been completely blown away. Today each hill is skirted by an apron of rock rubble, which is most likely due to both gravity-induced mass wasting and wind erosion.

The unnamed hill east of Peter and Paul typifies the locality. It stands approximately 25 m above the plain. The upper half is composed of trachyte with characteristic jointing that gives it a columnar, steep-sided appearance. The lower half is composed of a mixture of trachyte and basal conglomerate with a distinct apron of debris (Fig. 16.2a).

As shown in Figure 16.2a, the area beyond the apron does not show remains of the hill's erosional products. These are concentrated only in the debris apron, beyond which an eolian sand sheet thinly covers the rock surface. Mass wasting caused by gravity and wind action is clearly visible on the hillslopes. Large boulders are dislodged from the very steep walls of the trachyte mass. As these boulders land on the apron of debris surrounding the basal conglomerate their downward motion leaves trails behind.

In one case, the approximately 2 m fallen boulder left a nearly straight trail with a sharp rim (Fig. 16.2b). Only one slight bend is

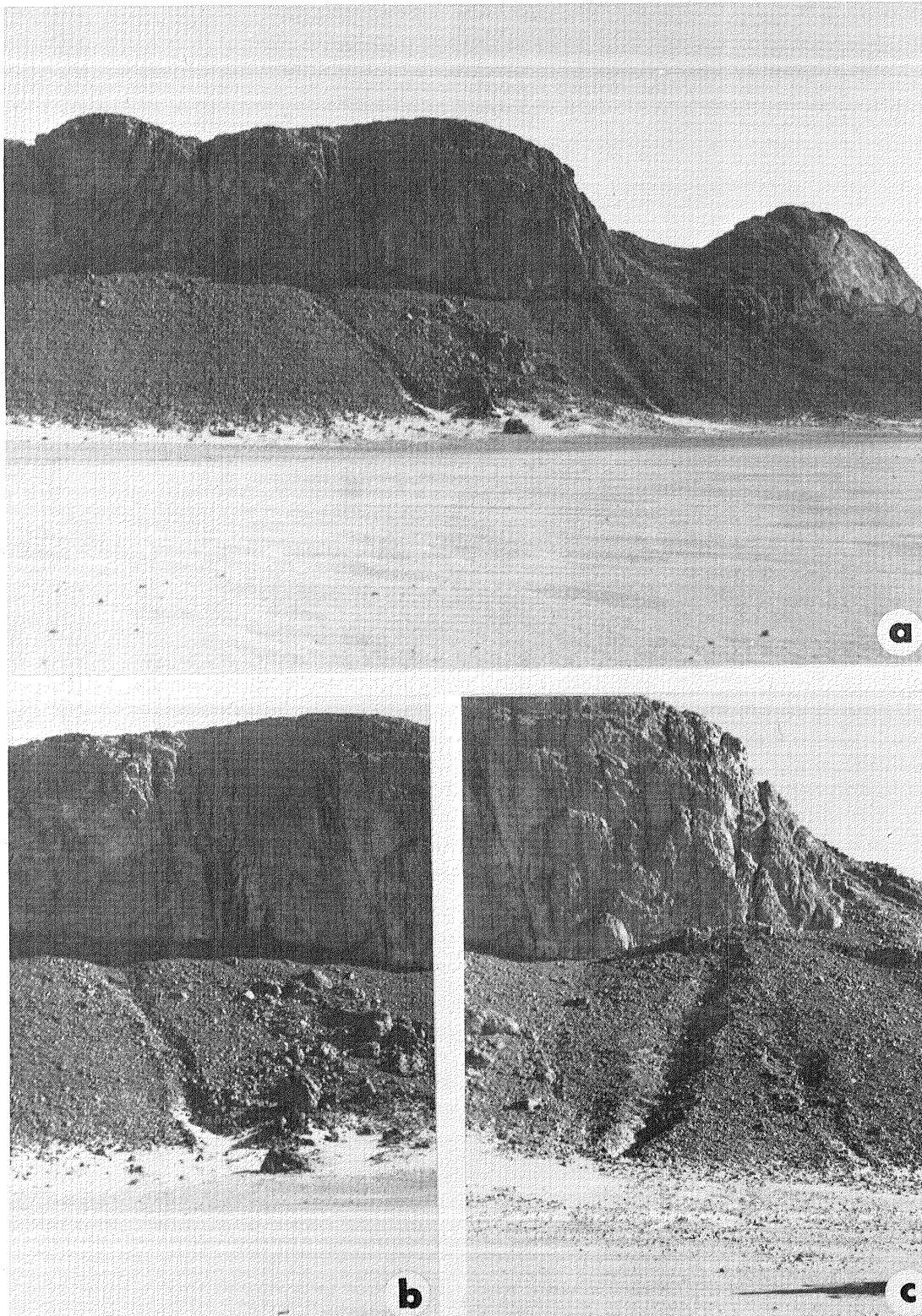


Figure 16.2 Photographs of a hillslope showing the vertical jointing in the upper part and the apron of debris in the lower half (a), with a straight boulder track (b) and one that is made of a chain of depressions (c).

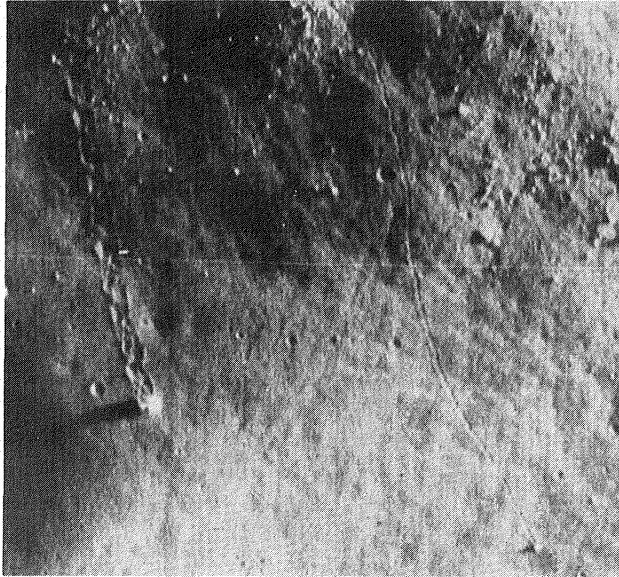


Figure 16.3 Blocks on the south wall of the crater Hyginus, including many that have rolled and left trails of their downslope movement along the crater wall. Framelet width is 440 m (Lunar Orbiter V H-95).

noticeable in this boulder track, suggesting a reasonably fast and unimpeded downward motion. The rapid motion is also supported by the fact that the boulder did not settle at the break in slope; it continued moving until coming to rest some 5 m away from the hill. The movement on the level plain may have been lubricated by the fine sand on the surface. As will be discussed below, some boulders that moved downslope on the Moon also continued to move away from the break in slope onto the level lunar terrain, perhaps also lubricated by the fine lunar dust.

A second prominent track on the same (north) side of the hill shows distinctly different morphology (Fig. 16.2c). In this case, the track is made of a chain of depressions, suggesting that the boulder had bounced on the surface as it made its way downslope. However, in this case, no boulder can be found at the end of the track. Only small pieces of rock remain. This suggests that the boulder disintegrated before reaching the level ground.

BOULDER TRACKS ON LUNAR SLOPES

The boulder tracks on hillslopes in southwestern Egypt are reminiscent of those photographed on lunar slopes. Large numbers of these occur on the walls of fresh appearing craters, rilles and massifs. By far, the largest number of boulder tracks is displayed along the walls of Hyginus crater at $7^{\circ}40'N$, $6^{\circ}20'E$. Most of these tracks are in the form of chains of small depressions; some are up to 1 km long. In most cases the boulder is clearly visible at the end of the slope, in other cases the boulder appears to have disintegrated into small pieces (Fig. 16.3), similar to the track on the trachyte hill in



Figure 16.4 Photograph taken by the Apollo 17 astronauts of boulder tracks on the slopes of the North Massif. The larger boulders are approximately 15 m in diameter (AS17-144-21991).

southwestern Egypt. Tracks in the Hyginus walls and also on the walls of Rima Hadley are depicted in Kosofsky and El-Baz (1970).

Other occurrences of boulder tracks on lunar hillslopes are those investigated and photographed by the Apollo 17 astronauts in the Taurus-Littrow landing site at $20^{\circ}10'N$, $30^{\circ}45'E$. The astronauts observed that the tracks led from outcrops high on the slopes to large boulders near their bases (Fig. 16.4). They also observed that "once a boulder is jarred loose and begins to roll, only a decrease in slope or the disintegration of the boulder will stop it.

"The tracks are made up of chains of small depressions. These chains are generally straight; however, gradual curves were noted in some instances. Not all tracks are exactly perpendicular to the contours, and, in some cases, the tracks curve noticeably.

"Most boulders stopped rolling at least a few tens of meters before reaching the base of the massif slope. However, two large boulders in the crater Nansen moved across the base of the slope and up the other side of the crater for several tens of meters" (Schmitt and Cernan, 1973, p. 5-17).

The use of boulder tracks to find the original location of the boulder was helpful in constructing the stratigraphy of the Apollo 17 site, and the origin of the returned samples. Details of the utilization of the tracks is discussed by Muehlberger and others (1973).

The morphological similarity between the tracks observed on hillslopes in southwestern Egypt and those photographed on the Moon attests to the very dry conditions prevailing today in the Egyptian

desert. This leads to the speculation that similar features may exist on hillslopes on Mars. Confirmation of this will have to wait acquisition of high resolution photographs of martian scarps.

ACKNOWLEDGMENTS

The author benefited from discussion of the boulder tracks in southwestern Egypt with two field companions: Maurice Grolier and Bahay Issawi.

Chapter 17

ANALOGS OF MARTIAN EOLIAN FEATURES IN THE WESTERN DESERT OF EGYPT

TED A. MAXWELL and FAROUK EL-BAZ
National Air and Space Museum
Smithsonian Institution
Washington, D.C. 20560

ABSTRACT

Dark, streamlined streaks observed in orbital images of the Western Desert of Egypt are similar in scale and form to crater- and knob-related streaks on the martian surface. In Egypt, dark streaks form in the lee of topographic highs, ranging in size from small hills a few meters across, to the 60 km wide Uweinat massif. On the surface of Mars, streaks may be either lighter or darker in tone than the surrounding plains. Individual streaks occur primarily in the lee of craters, although in the Cerberus region, several light-toned streaks occur in the lee of irregular knobs, similar to those in southwestern Egypt. Knob- and crater-related wind streaks on both Earth and Mars owe their characteristic patterns to the local deviation of wind around topographic barriers. Knob streaks on both planets most often display a convergent pattern, whereas crater streaks on Mars are more often divergent. Field investigation in southwestern Egypt indicates that the characteristic shape of wind streaks is a function of the transport and deposition of material surrounding the streak rather than erosion or deposition in the lee of the obstacle.

In addition to these landform analogies visible at orbital altitudes, many near-surface features in the Western Desert are similar to those seen in Viking lander images from the surface of Chryse Planitia on Mars. Sand drifts and small dunes are present in both deserts, as are pitted and faceted rocks that occur in both non-vesicular basalt and in sandstones. Evidence of wind pitting and erosion in the Western Desert suggests that rocks in the Viking 1 landing site may not necessarily consist of vesicular basalt, but may owe their surficial features to wind erosion.

INTRODUCTION

Wind-dominated landforms are the most abundant features throughout northern Africa and particularly in the Western Desert of Egypt. Although the major eolian landforms of the Sahara were known well before the advent of orbital data, photographs from the Gemini through the Apollo-Soyuz missions, and images from Landsat satellites allow comparison of these features on an interplanetary basis. In

1972, when the Mariner 9 spacecraft returned images of the surface of Mars, it became clear that eolian activity was the most dominant process on the martian surface. One of the first clear indications of this fact was the presence of wind-produced bright and dark streaks extending from many craters.

Both bright- and dark-toned wind streaks occur in the Western Desert. Bright streaks are composed of sand dunes and dune belts, sand sheets, and lag deposits of light-colored bedrock, whereas dark-toned streaks are predominantly local lag fragments and desert pavement (El-Baz and Maxwell, 1979a). As seen from orbit, the dark streaks in the Western Desert are present in the lee of topographic obstacles to the predominant northerly wind flow, and create stream-lined patterns similar to those in the lee of craters and knobs on Mars.

As a result of the 1978 investigation of the Western Desert, however, it was found that geomorphic features on a much smaller scale are also analogous to several of those seen in Viking Lander 1 and 2 images of the surface of Mars. In addition to the eolian drifts that are a commonplace occurrence in the Western Desert, numerous pitted and fluted rocks of differing lithologies are present on the desert surface. Similarities of these eolian pitted rocks to those on the martian surface have been described by McCauley and others (1979a).

Consequently, the scale-independent resemblance of both Egyptian and martian landforms suggests that the Western Desert, with its present-day hyperarid climate, provides one of the closest terrestrial analogs for the study of martian geomorphic processes. The purpose of this study is to present detailed comparisons of dimensional parameters for both martian and Egyptian wind streaks and to discuss their inferences for the origin of martian streaks. Based on our field observations of surface materials in the Western Desert, it is also possible to speculate on the origin of martian eolian features seen in Viking lander images.

REGIONAL SETTING

In the Western Desert, knobs of protruding bedrock and associated wind streaks form an irregular line between the Kharga depression and the Gifl Kebir plateau. Bedrock exposures are composed of highly resistant, Fe-rich sandstones and conglomerates of the Nubia series, although east of the Bir Tarfawi region, the protruding knobs consist of outcrops of the Tawel granite (see Dardir, Chapter 7). The linear nature of the Nubia sandstone outcrops is created by the gently northward dipping attitude of the beds, which have been partially submerged by sand driven from the north. It is possible that these linear outcrops mark the positions of low cliffs retreating northward, now represented by isolated hills that create the streak patterns seen from orbit. The location of streaks measured for this study is shown in Figure 17.1.

In several areas on Mars, wind streaks have formed in the lee of irregular positive features as well as craters. Streaks may form behind groups or rows of knobs as well as behind isolated hills.

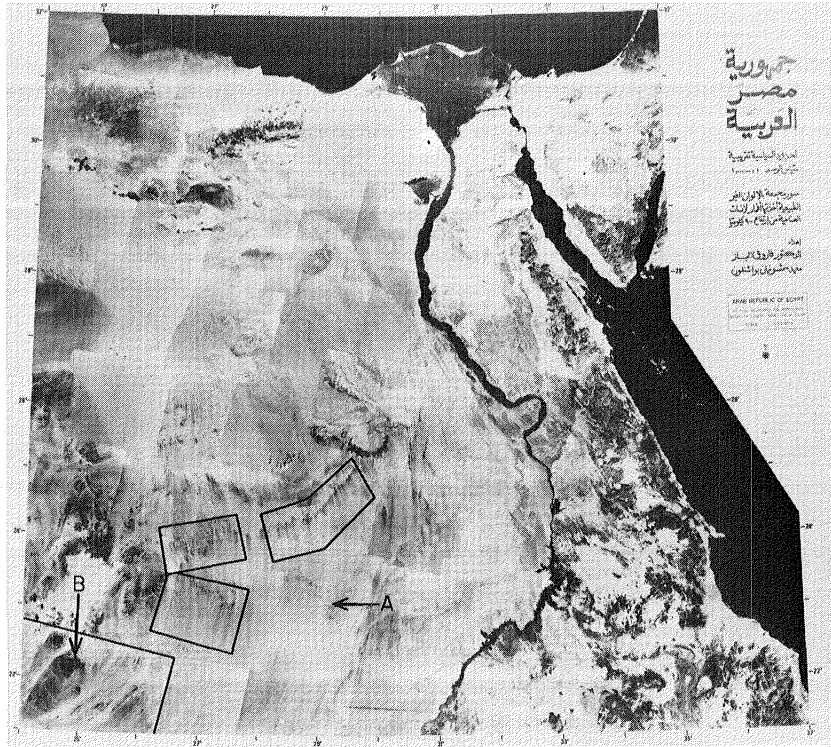


Figure 17.1 Landsat mosaic of Egypt showing location of wind streaks used for comparison with martian streaks. Arrows indicate the locations of streaks investigated during 1978 field trip: A) Qaret El-Maiyit, a granitic hill approximately 1 km across, and B) Uweinat Mountain, a 60 km wide mountain composed of granite and syenite.

Knob-related streaks are well-developed in the Cerberus region of Mars (15°N, 200°W), where the knobs consist of roughly equidimensional faceted appearing hills that occur on a smooth plains unit of probable volcanic origin (Fig. 17.2). Comparisons of Mariner 9 and Viking images of this region have shown that subtle changes in the patterns of dark and light streaks have occurred in the 5 years between the two missions (Chaikin and others, 1980). With this evidence of surficial erosion and deposition, and the presence of knob-related streaks, Cerberus provides a suitable location for comparison with the wind streaks of the Western Desert.

WIND STREAKS

Comparison of Scale

For comparison of the scale of wind streaks on both planets, measurements of knob widths and streak lengths were made from enlarged Viking images and Landsat images placed in an opaque projector. Knob widths were measured perpendicular to the streak direction, and in the case of martian craters, rim crest diameter was measured. Streak lengths were measured from the downwind edge of the knob or crater to

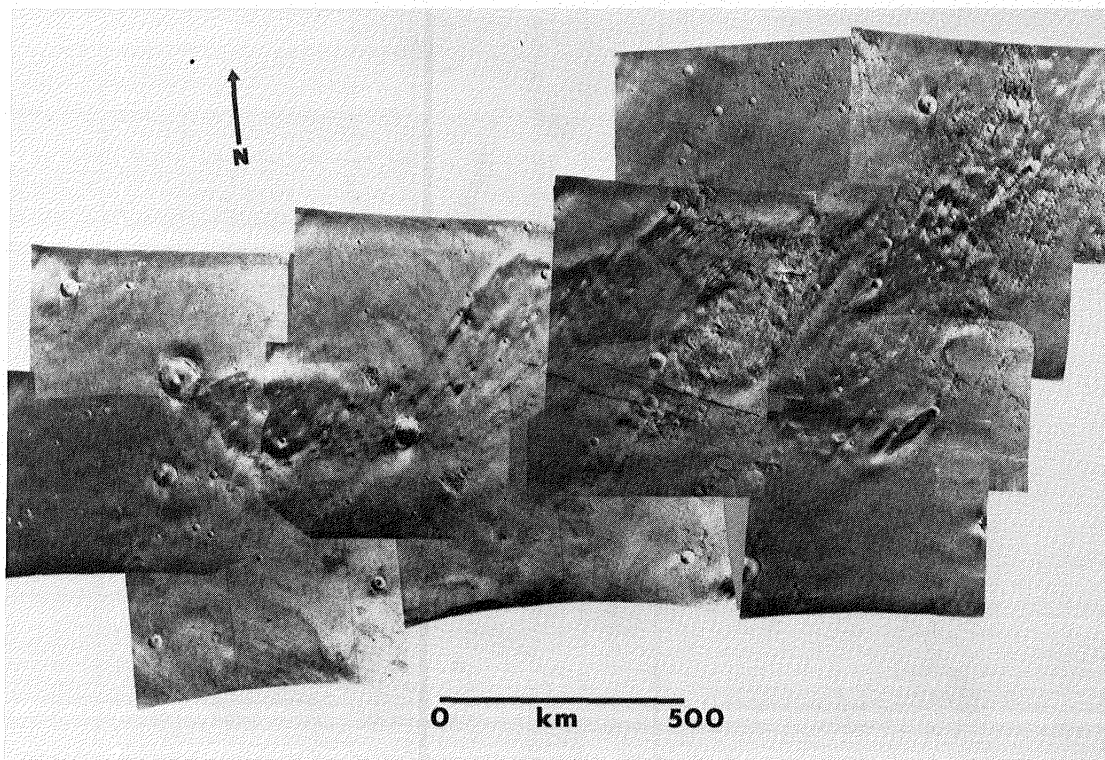


Figure 17.2 Mariner 9 mosaic of the Cerberus region of Mars showing dark- and light-toned streaks. Note dark crater streak in lower right, and the numerous light streaks within the dark albedo feature.

the tip of the streak. If the streak had a ragged downwind edge, as with some divergent streaks, an average length was measured, this being necessarily a subjective measurement. Both the knob widths and streak lengths of Egyptian and martian wind streaks are within the same scale. Knob widths seen from orbit range from 1 to 25 km, although most knobs in the Western Desert occur between 2 and 7 km. Streak lengths range from 5 to 75 km, although most cluster at lengths of 5 to 25 km (Fig. 17.3). The scale and overall form of knob streaks on both planets are similar to those of crater-related streaks on Mars, which are shown in Figure 17.3 for comparison. The average streak length/knob width ratio for Egyptian streaks is 4.8, and for martian knob streaks is 3.0, consistent with the range of crater streak parameters noted by Arvidson (1974). Because of these similarities between knob- and crater-related streaks, we believe that any implications resulting from our study of knob streaks in the Western Desert may apply equally well to the formation of both knob and crater streaks on Mars.

Streak Patterns

In addition to the similar scale of wind streaks, the patterns of knobs protruding through smooth, plain surfaces is also similar on both planets. This suggests that the local geologic setting may be

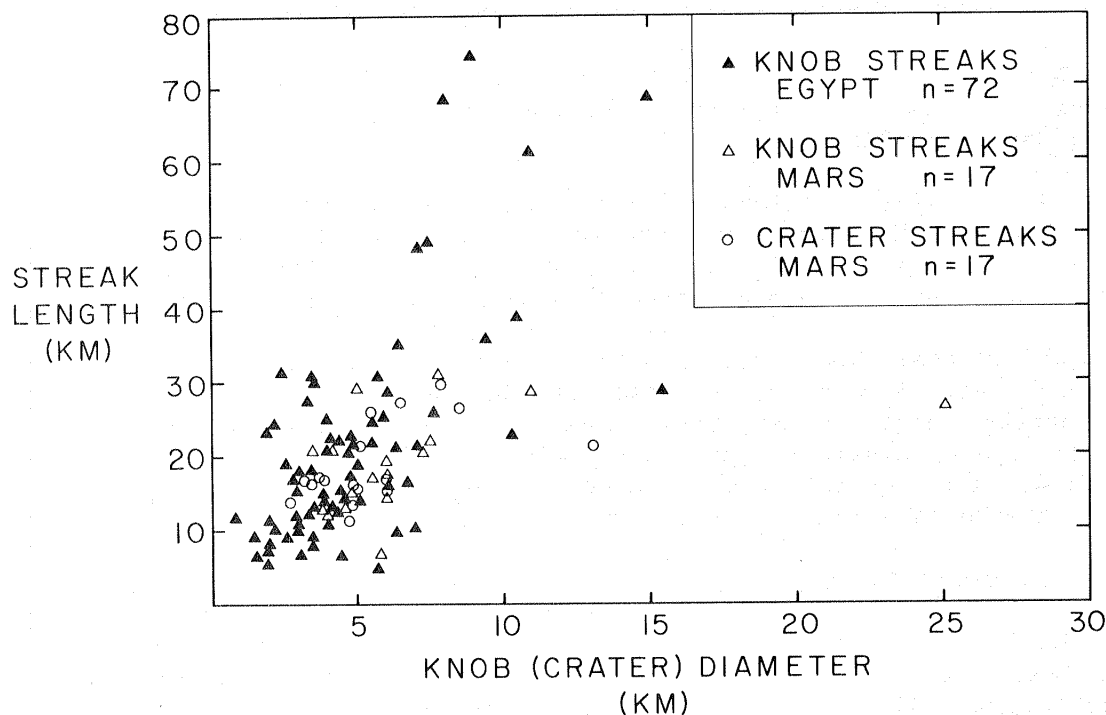


Figure 17.3 Scatter diagram of knob width versus streak length for both Egyptian streaks in the Western Desert, and knob and crater streaks in the Cerberus region of Mars. Both Egyptian and martian streaks occur at the same scale, although some of the larger Egyptian streaks (particularly Uweinat) are longer than those in the Cerberus region.

important in controlling both the placement and morphometric characteristics of streaks. In the Western Desert, the pattern of exposure of dark material is controlled by the locations of numerous light-colored longitudinal dunes that have migrated southward (El-Baz, 1977; p. 77). Composite streaks are generally much smaller, and average 9 km long. In contrast to large streaks (such as that in the lee of Uweinat), smaller ones form in response to local bedrock outcrop patterns, and are affected more by local wind directions than by the regional wind regime. For example, composite streaks north of Uweinat deviate to the east and west around the mountain. As is the case with individual large streaks, light-colored sand deposits surround the dark material (local desert pavement?) of the composite streaks, resulting in an irregular pattern.

Streak Form

For comparisons of streak form, Mars streaks were measured from enlarged Viking Orbiter images of the Cerberus region at a scale of 1:425,000. Martian crater and knob streaks range up to 36 km in

length and 17 km in width, and the maximum area of 179 knob streaks is 450 km², whereas that of 62 crater streaks is 342 km². Because of the less distinct outline of the larger Egyptian streaks, only smaller streaks were used for shape comparison. The 239 knob streaks in southwestern Egypt, outlined at a scale of 1:200,000 from Landsat false color images range up to 21 km² in area, and are up to 12 km long and 5 km wide.

A plot of the maximum width and length of martian crater and knob streaks, and Egyptian knob streaks (Fig. 17.4) indicates that all three streak types follow the same general curve, although the degree of scatter increases from crater to knob streaks. Knob streaks in the southwestern corner of Egypt exhibit the greatest scatter ($r = 0.618$), but are generally narrower than their martian counterparts. The relatively small width of the Egyptian streaks is also indicated by a plot of streak length versus total area. As shown in Figure 17.5, the total area of distinct Egyptian streaks is much less than that of martian streaks. In both places, however, the range of values is similar for streaks less than about 50 km² in area.

In order to compare the degree of streamlining for streaks on both planets, we have chosen a dimensionless shape parameter (K) used by Chorley (1959) to analyze the shape of drumlins, and more recently by Baker (1978a) for loess islands in the channeled scablands of Washington. The value of K indicates the deviation of the observed form from that of a circle:

$$K = \frac{l^2 \pi}{4 A} \quad (1)$$

in which l is the length of the form, and A is the area. Thus, a circle would have a value of $K = 1$. For streamlined forms in the channeled scablands, Baker (1978a, p. 92) found that K varies between 2 and 5, and may be related to the calculated Reynolds number for maximum scabland flood flows.

For crater streaks on Mars, values of K range from 0.6 to 4, and can be correlated with the length of the streak (Fig. 17.6); the longer the streak, the greater degree of streamlining. Although this relationship holds for knob streaks on both planets, there is a significant difference in the slope of the regression curve between martian and Egyptian knob streaks. Values of K for the Egyptian streaks range from 0.3 to 9, and exhibit a higher degree of streamlining than do martian crater or knob streaks. The relatively high values of K associated with the Egyptian streaks are most likely a function of the near-surface transport of material, and the unidirectional wind flow. Among the larger streaks visible in the Western Desert, parallel types are the dominant form. Many of the larger dark streaks have a constant width and extend for as much as 140 km before grading into the surrounding brighter sand. Thus, deposition of material from martian duststorms, and variability of wind direction are likely causes for the lower values of K exhibited by martian streaks.

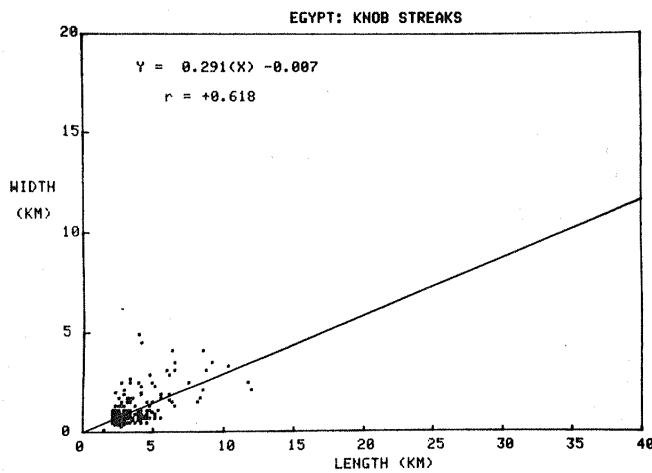
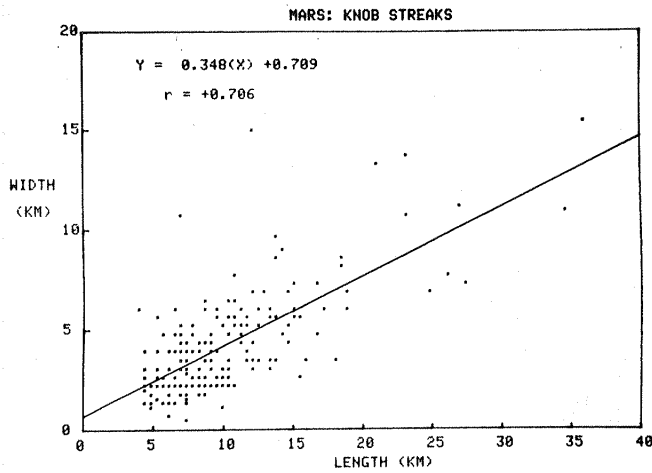
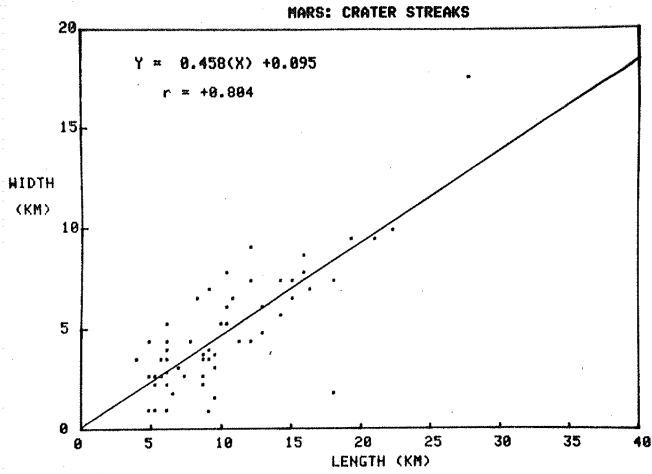


Figure 17.4 Width versus length for martian and Egyptian wind streaks. The distinct knob streaks in Egypt are smaller than their martian counterparts, but follow a similar size relationship.

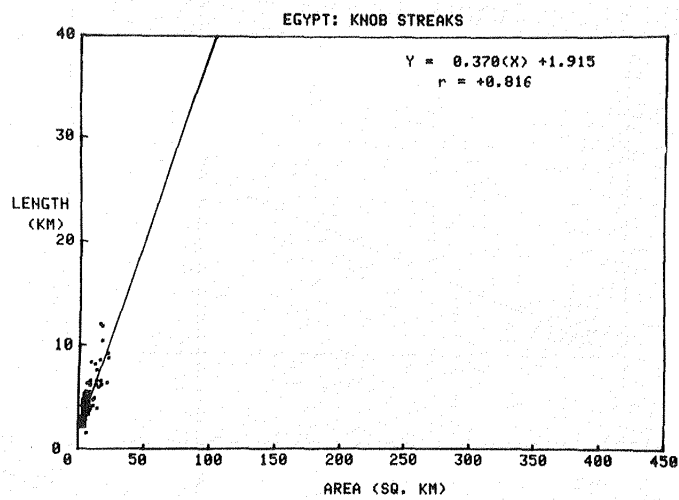
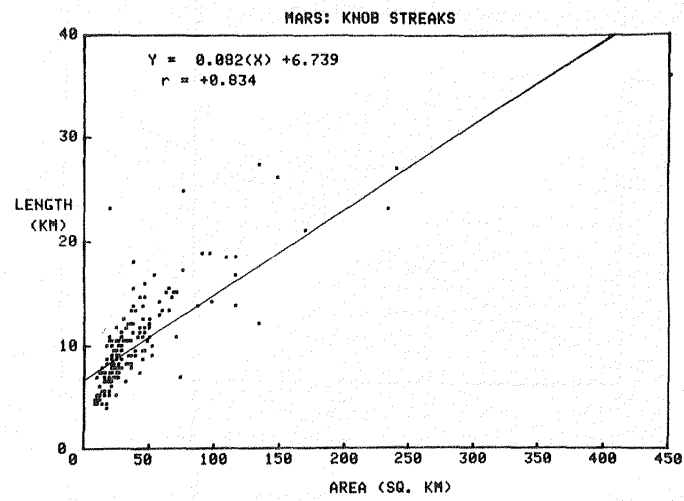
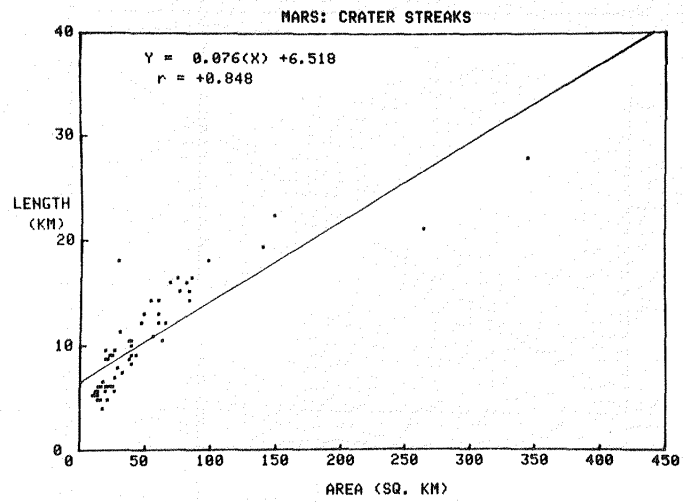


Figure 17.5 Length versus area for martian and Egyptian wind streaks.

Surface Characteristics

A combination of photogeologic evidence (Veverka, 1975; Veverka and others, 1978) and wind tunnel simulations with model craters (Greeley and others, 1974a) have been used as evidence that most dark streaks on Mars are erosional scars which change in response to the redistribution of the brighter material surrounding the streak. This method of change in streak form has recently been supported by observations of streaks in the Western Desert (El-Baz and Maxwell, 1979a). Bright streaks on Mars are most likely fine grained material deposited in the wind shadow in the lee of craters. These streaks may not be affected by the lower velocity winds that occur between the martian dust storms.

Both bright and dark streaks are present in the Western Desert; bright streaks are depositional and consist of sand accumulations in longitudinal dunes, relatively thin sand sheets, and coarse lag surfaces. Dark streaks are erosional products of mountains and hills and consist of irregular chips of rock.

The importance of local bedrock outcrops as a source of material for dark streaks in southwestern Egypt is demonstrated in the lee of Qaret El-Maiyit hill. This streak is composed of 5-7 mm size granitic pebbles eroded from the hill, and the dark surface is surrounded on both sides by a light-colored sand sheet. The surface of the streak itself is more than 1 m below the level of the surrounding sand sheet, thus providing a minimum estimate of the sand sheet thickness. Because of their large size, the dark pebbles of the streak are less likely to be moved due to the more frequent sand moving winds than are the finer particles of the sand sheet. Consequently, the shape of the dark streak will change mainly in response to the shifting of light-colored sand on both sides.

The area surrounding Ras El-Abd, a trachyte hill east of Gebel Uweinat typifies the conditions resulting in light- and dark-colored streaks in the Western Desert of Egypt (Fig. 17.7). North of the dark trachyte mass, the terrain is an eolian peneplain covered by coarse sand with numerous 15 cm and smaller pieces of rock. The wind seems to be less effective just north of the topographic high than on either side of it. Near the sides of the hill the terrain is covered by a coarse lag composed of 20 cm size chunks of sandstone and trachyte. Stringers of sand up to 10 m long occupy low areas between patches of the rocky desert floor. On the lee side of the hill, however, only a dark, trachyte lag exists with no light-colored sand. The lag consists of fragments a few cms in diameter, and appears to have formed solely from erosional products from Ras El-Abd.

COMPARISONS WITH THE MARTIAN SURFACE

The extreme aridity of southwestern Egypt causes it to appear more like the deserts of Mars than any other desert on the Earth. This is suggested not only from an orbital perspective, but also from the nature of the surface materials. Rocks of various sizes cover many parts of this desert with a matrix of very fine grained sands,

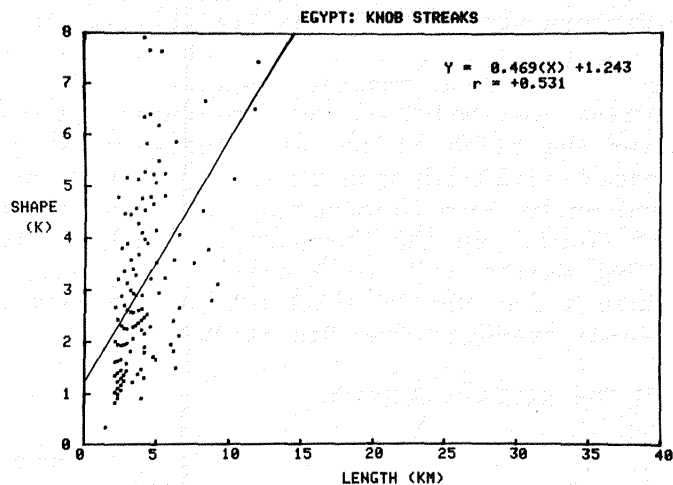
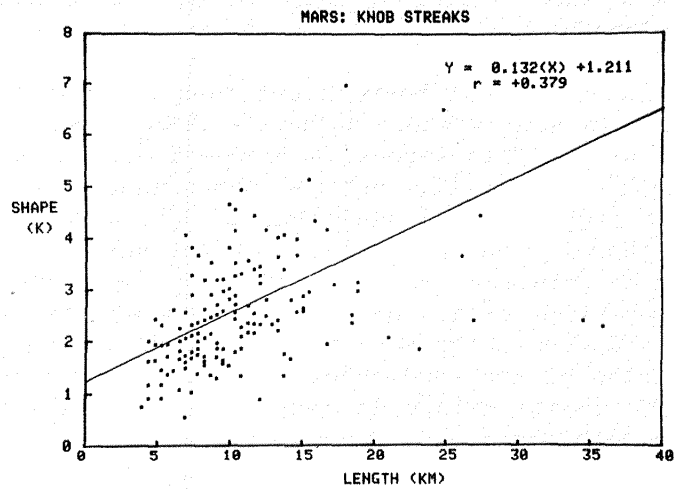
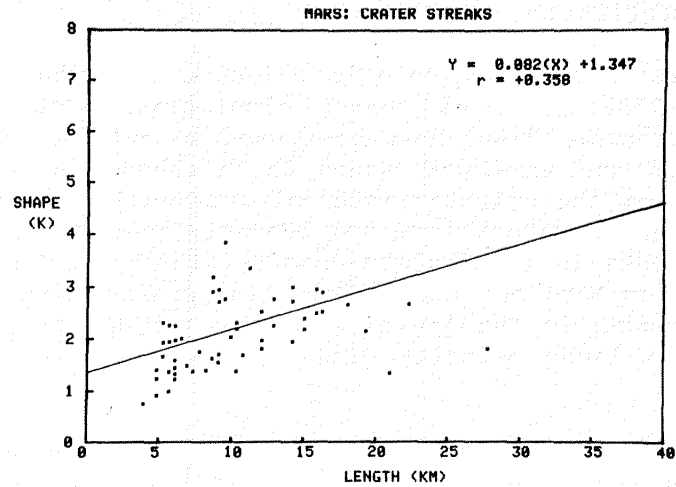


Figure 17.6 Shape factor (K) versus length of wind streaks; knob streaks in Egypt exhibit a greater degree of streamlining than do martian streaks.

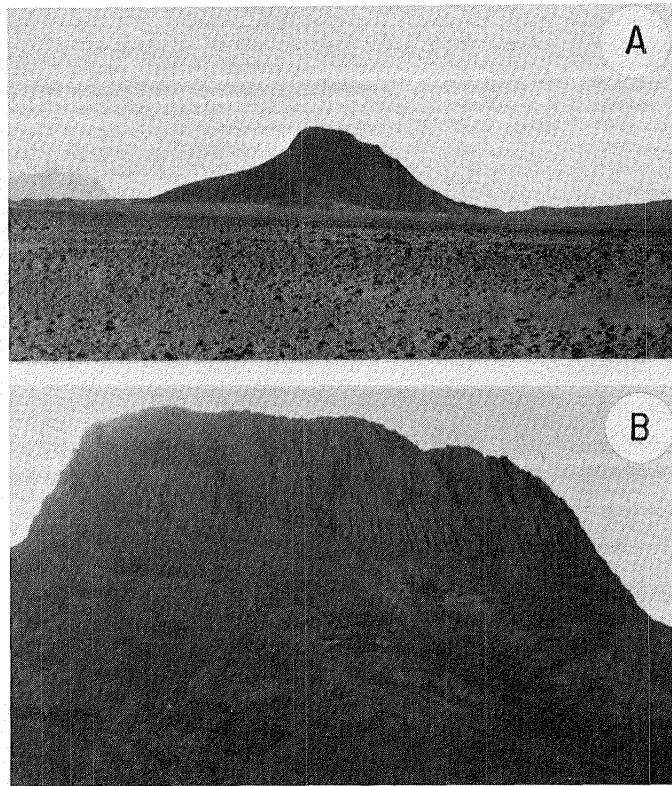


Figure 17.7 A) View of Ras El-Abd, a trachyte mountain east of Uweinat. Rocks in the foreground consist of both trachytes and fragments of the underlying sandstone. Gebel Uweinat is visible to the southwest (left side of picture). B) Close-up of Ras El-Abd, showing exterior talus deposits surrounding the mountain.

not unlike the setting on the surface of Mars as viewed by the Viking landers (Viking Lander Imaging Team, 1978).

Of special significance are the pitted rocks strewn on the surface of the southwestern desert (Fig. 17.8). These pits, usually smaller than 2 cm, occur in rocks of numerous types including sandstones, ferruginous quartzites, and basalts in the Uweinat region, and limestones north of Kharga. The basalts were always pitted on the surface, while dense and finely crystalline on the inside. One large basalt hill in the Gilf Kebir exhibited columnar jointing. All pieces strewn around it were dense inside with no evidence of vesicles, but contained windformed pits, a few mm across on the outer surface. Many of these pits had sand grains trapped within. It is believed that such entrapped grains act as grinders and enlarge the pits with each wind gust.

The similarity between such pitted surfaces and the pitted rocks on Mars was first noted by El-Baz and others (1979a) with additional work reported by McCauley and others (1979a), including results of wind tunnel simulations. These comparisons suggest that the pits on the

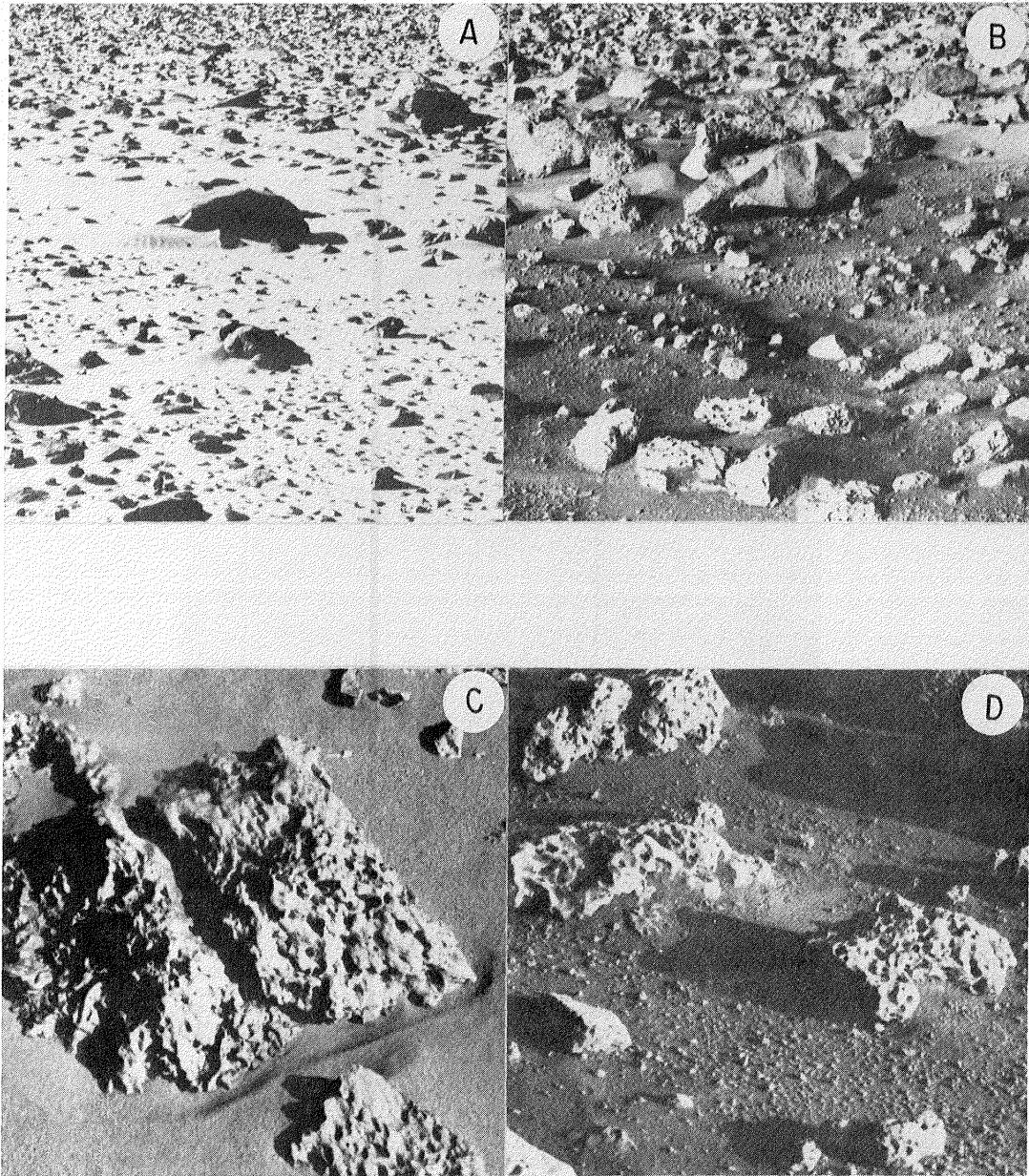


Figure 17.8 A) Windswept surface of faceted rocks and sand drifts near Black Hill. B) The Viking Lander 1 site in Chryse Planitia, Mars. C) Pitted and fluted quartzarenite from the Gifl Kebir. D) Pitted rocks at the Viking Lander 1 site.

martian rocks may have originated, or at least been enlarged by wind action.

In addition, some rocks show a transition between pits and flutes. Rows of elongate pits on the windward facing slopes of the Uweinat Mountain appear to grade into flutes. Some of the rocks in the Viking lander 2 site also show what appears to be flutes (McCauley

and others, 1979a). These flutes, like those in the Western Desert of Egypt, may also be windsculpted and are being studied as possible indicators of prolonged wind directions at this site.

SUMMARY

Analogues of martian eolian features in the Western Desert of Egypt range in scale from the large streaks visible in orbital images and photographs, to the millimeter-size pits evident in rocks of various lithologies. Although both martian and Egyptian wind streaks occur at the same scale, the smaller, more distinct wind streaks in the Western Desert are generally narrower and more streamlined than their martian counterparts. Field observations indicate that dark streaks are composed of material derived from the hill or mountain on the upwind end of the streak, and that changes in the shape of the streak may result from the redistribution of the surrounding sand. In addition, pitted and fluted rocks, common in many areas of the Western Desert, provide evidence that rocks at the Viking landing sites may be extensively modified by wind erosion.

ACKNOWLEDGMENTS

We are indebted to A. L. Chaikin for supplying streak data from the Cerberus region of Mars, and to Ellen Stofan, an intern at the Center for Earth and Planetary Studies of the National Air and Space Museum during the summer of 1980, for assistance in measurements of the wind streaks.

**Page Missing in
Original Document**

Chapter 18

CHARACTERISTICS OF ROCK POPULATIONS IN THE WESTERN DESERT AND COMPARISON WITH MARS

J. B. GARVIN

Department of Geological Sciences
Brown University
Providence, Rhode Island 02912

ABSTRACT

Detailed morphologic analysis of two basaltic boulder fields in the hyperarid Western Desert of Egypt reveals the importance of eolian modification in determining their general appearance. Comparisons with Viking lander sites on Mars provides evidence for the presence of isotropic, homogeneous, wind-pitted rock fragments at two martian localities. Interplanetary rock morphology analyses appear to be a useful means for investigating the formation, emplacement, and modification processes affecting rocks on planetary surfaces.

INTRODUCTION

The dominance of eolian processes in the Western Desert of Egypt over the last 6000 years or more is reflected in the rocks exposed at the surface on the Gilf Kebir plateau in this desert. A recent (1978) expedition to the Gilf Kebir has produced an excellent photographic record of many fields of rocks in this area (El-Baz and others, 1980). Unidirectional northerly winds carrying fine particles and sand are known to be operating in the Gilf Kebir at present. By studying the morphology of wind weathered rocks of a common lithology in this hyperarid, nonvegetated terrestrial environment, we can extend our understanding of rock modification on planetary surfaces, including Mars. For this reason, two basaltic block fields from the Western Desert were analyzed in a fashion analogous to that used in a recent study of the Viking lander sites (Garvin and others, 1981). Images of these Egyptian blockfields were available in the form of 35 mm black and white negatives taken on location by Farouk El-Baz. Sixteen by twenty inch photographic prints were made from the negatives to facilitate analysis.

The two sites were chosen to be as similar as possible, but differ in one or two critical respects. One locality is located at the base of a 0.5 km basalt hill in Wadi Mashi (WMB). The talus fragments at the base of this Quaternary age basalt plug are fine grained, non-vesicular, and internally homogeneous except for 1 mm size olivine crystals in their matrix. All of these blocks are pitted and fluted, in spite of their massive or non-vesicular character. The WMB site has a sandy substrate devoid of lag gravels and there is little evidence for any fluvial deposition.

The second Egyptian site consists of basalt blocks embedded in a desert pavement of lag gravels and coarse sands in the eolian pediplain of the Gilf Kebir region (GKR). The flat nature of such a stony desert or "reg" permits occasional floods resulting from infrequent rains to deposit gravels and cobbles that serve to armor the surface. The origin of the larger basalt blocks (i.e., 30-50 cm in diameter) is unclear, but they may have been water transported to their present location.

Both sites (WMB and GKR) have similar basaltic lithologies and have been most recently modified by predominantly eolian action. Saltation of sand-sized particles is not an everyday occurrence in this region, but buffeting by dust-laden winds of less than 30 km/hr has apparently produced the pits, flutes and associated features observed on the rocks at the two localities (McCauley and others, 1979a). The effects of different modes of emplacement for WMB (mass wasting) and GKR (fluvial deposition) might be discernible from consideration of rock morphologies.

Each rock considered in this study was "digitized" on a digitizing table -- the set of morphologic parameters appearing in Figure 18.1 was used in the systematic collection of the data. This is the same technique used by Garvin and others (1981) in studying the rock populations at the Viking sites on Mars. Due to lack of adequate viewing-geometry control for the Egyptian photographs, detailed rock size analysis was not attempted at this time.

From the data collected on the rocks at WMB and GKR characteristics and trends in certain morphologic parameters can be documented (Tables 18.1 and 18.2). The purpose of this paper is to characterize two terrestrial environments in order to provide a framework for the understanding of the significance of the characteristics of surfaces of other planets.

Table 18.1 Characteristics of study areas in Egypt and on Mars.

| | Wadi Mashi Basalt Hill (n=101) | Gilf Kebir Stoney Desert (n=51) | Mars VL-1 (n=250) | Mars VL-2 (n=210) |
|------------------------|--------------------------------------|---------------------------------------|-------------------------|-------------------------|
| Area Studied | 5.5 m ² | 9.6 m ² | 7 m ² | 7 m ² |
| Rock Size Range | 7-50 cm | 4-45 cm | 2-25 cm | 2-30 cm |
| Form Ratio | -0.27 | -0.56 | -0.25 | -0.30 |
| Roundness (Average) | Angular | Subangular | Subangular | Subangular |

| FORM | ROUND-NESS | OCCULTATION | CAVITY SIZE | CAVITY SHAPE | CAVITY ORIENT. | MOAT | FLUTE MODALITY | FLUTE DEPTH | FLUTE SHAPES WAVY | FLUTE GROOVE | CROSS CUTTING FLUTES | FLUTE DENSITY | FACETS | REL. ALBEDO | DUST EFFECT | BASAL PARTICLES | LOCAL ENVIRON | LINEAR FEATURES |
|----------------|----------------------------------|-----------------|--------------|-------------------------|--------------------|----------------|----------------|-----------------------|-------------------|---------------------|----------------------|---------------|-------------|----------------|---------------------------|------------------|------------------------|-----------------|
| COMPACT | VERY ANGULAR | NONE | NO CAV.S | NO CAV.S | NO CAV.S | NO | NO FLUTES | NO FLUTES | NO FLUTES | NO FLUTES | NO FLUTES | NO FLUTES | NO | LOW | NONE | NO | TROUGH | NO |
| COMPACT/PLATY | ANGULAR | SHADOW | SMALL | ROUND | NO | YES | UNIFORM | SHALLOW | NO | NO | NO | LOW | YES | MED | DUST ON ROCK | YES | DRIFT | YES |
| COMPACT/ELONG. | SUB-ANGULAR | ROCK | MED. | ELLIP-TICAL | YES | INDET | BIMODAL | MOD. | YES | YES | YES | MED. | INDET | HIGH | DUST IN CAVITIES + FLUTES | INDET | DURI-CRUST | INDET |
| PLATY | SUB-ROUND | ROCK + SHADOW | LARGE | IRREG-ULAR | INDET | APRON (FILLET) | HETERO-GENEOUS | DEEP | INDET | INDET | INDET | HIGH | FACET STYLE | VARIES | DUST ON + IN CAVS | FRAGMENT OF ROCK | BEDROCK | NOTCH IN ROCK |
| ELONG. | ROUND | OTHER | INDET | ROUND + ELLIPT. | TAIL (STREAK) | NO | INDET | INDET | FLUTE WEDGE | PARALLEL FLUTE ROWS | PITS IN FLUTE | INDET | NO FACETS | INDET | INDET | NO | RIDGE OR RISE | NO |
| VERY PLATY | INDET | INDET | CAVITY DEPTH | ROUND + IRREG | NO | YES | FLUTE SIZE | FLUTE SHAPE: STRAIGHT | NO FLUTES | NO FLUTES | NO FLUTES | | ONE-FACED | FRACTURE STYLE | UNDER-GROUND SHAPE | YES | FLATS | YES |
| VERY ELONG. | ROCK SURFACE TEXTURE HOMOGENEOUS | CAVITY DISTRIB. | NO CAV.S | ELLIPT. + IRREG. | YES | INDET | NO FLUTES | NO FLUTES | NO | NO | NO | | TWO-SIDED | NOT SIGNIF. | NOT BURIED | INDET | ROCK ON ROCK (CONTACT) | INDET |
| INDET | UNIFORM | NO CAV.S | SHALLOW | ROUND, ELLIPT. + IRREG. | ROCK IN TAIL | | SMALL | NO | YES | YES | YES | | THREE-SIDED | CON-CHOIDAL | INCREASE WITH DEPTH | | INDET | |
| | BIMODAL | UNIFORM | MOD. | INDET | IN TAIL + HAS TAIL | | MED | YES | INDET | INDET | INDET | | MULTI-FACED | PLANAR | DECREASE WITH DEPTH | | | |
| | HETERO-GENEOUS | BIMODAL | DEEP | | INDET | | LARGE | INDET | | | | | INDET | CONCH + PLANAR | INDET | | | |
| | INDET | HETERO-GENEOUS | INDET | | | | INDET | | | | | | | INDET | | | | |
| | | INDET | | | | | | | | | | | | | | | | |

Figure 18.1 Rock morphology "menu" used in systematically cataloging rocks in images from Mars and Egypt.

Table 18.2 Morphologic attributes for total rock populations in Egyptian and Martian study areas.

| | Wadi Mashi Basalt Hill (n=101) | Gilf Kebir Stoney Desert (n=51) | Mars VL-1 (n=250) | Mars VL-2 (n=210) |
|----------------------------|--------------------------------------|---------------------------------------|-------------------------|-------------------------|
| FORM | | | | |
| Compact | 38% | 27% | -- | 23% |
| Elongate | 20% | 35% | 23% | 21% |
| Compact- elongate | 32% | 25% | 21% | 30% |
| ROUNDNESS | | | | |
| Subrounded | -- | -- | 33% | 20% |
| Subangular | 33% | 33% | 43% | 54% |
| Angular | 52% | 33% | 21% | 22% |
| CAVITY DISTRIBUTION | | | | |
| Uniform | -- | 31% | 46% | 39% |
| Bimodal | 75% | 57% | 40% | 42% |
| Heteroge- neous | 19% | -- | -- | -- |
| CAVITY SIZE | | | | |
| Medium | 50% | 59% | 47% | 54% |
| Small | 48% | 27% | 37% | 32% |
| FLUTES | | | | |
| Present | 100% | 96% | 48% | 45% |
| Absent | -- | -- | 22% | 28% |
| Indetermi- nant | -- | -- | 33% | 27% |
| FACETS | | | | |
| Present | 80% | 61% | 48% | 31% |
| Absent | 19% | 29% | 28% | 43% |
| Indetermi- nant | -- | -- | 25% | 6% |
| FRACTURES | | | | |
| Planar | 57% | 45% | 27% | 29% |
| Indetermi- nant | -- | -- | 33% | 25% |
| Not Signif- icant | 14% | 37% | 22% | 25% |

Table 18.2 (Continued)

| | Wadi Mashī Basalt Hill (n=101) | Gilf Kebir Stoney Desert (n=51) | Mars VL-1 (n=250) | Mars VL-2 (n=210) |
|------------------|--------------------------------------|---------------------------------------|-------------------------|-------------------------|
| DEGREE OF BURIAL | | | | |
| High | 33% | -- | 35% | 22% |
| Slight | 60% | 57% | 46% | 40% |
| Not Buried | -- | 29% | -- | 34% |
| LINEAR FEATURES | | | | |
| Present | 57% | 69% | 36% | 40% |
| Absent | 41% | 27% | 46% | 36% |
| Indeterminant | -- | -- | -- | 23% |
| SEDIMENT MOATS | | | | |
| Present | 28% | -- | 38% | -- |
| Absent | 67% | 98% | 40% | 94% |
| Indeterminant | -- | -- | 23% | -- |
| APRONS (fillets) | | | | |
| Present | 29% | 22% | 68% | 36% |
| Absent | 53% | 63% | 21% | 44% |
| SURFACE TEXTURE | | | | |
| Uniform | 16% | 24% | 58% | 56% |
| Bimodal | 74% | 75% | 41% | 42% |
| RELATIVE ALBEDO | | | | |
| Medium | 53% | 45% | 38% | 40% |
| Varying | 40% | 45% | 31% | 35% |

GENERAL OBSERVATIONS

Wadi Mashī Basalt Hill Blocks (WMB):

1. Rocks are primarily equidimensional (60% compact or compact-elongate).
2. Angular, faceted rocks are by far most common.
3. Small and medium sized cavities (approximately 4 cm) dominate the rock surfaces (bimodal distribution).
4. Virtually all rocks have some visible flutes (most are linear or wedge shaped).

5. Planar fractures are frequently observed on the blocks (probably from columnar joints).
6. Most rocks are slightly embedded in the sandy substrate; perched or unburied rocks are rare.
7. Over 50% of the blocks have linear features such as cracks or fissures.
8. Fillets of sand are not common about rocks.
9. Sediment moats and other wind scour features are generally absent.
10. Most blocks have an intermediate albedo and highly reflective surfaces are uncommon.

The Gilf Kebir desert pavement blocks (GKR):

1. Rocks are primarily elongate (60% are elongate or compact-elongate).
2. Subangular rocks dominate.
3. Most fragments have medium sized cavities (approximately 4 cm).
4. Bimodal surface textures (variable) are common.
5. Many rocks display planar fractures, but equally many are lacking such fractures.
6. Highly buried rocks are rare; most rocks appear to be slightly embedded in the stony substrate.
7. Cracks and fissures occur on most rocks (69%).
8. Virtually no wind scour features are observed (moats or tails).
9. Relative rock albedos are variable; rarely are reflective rocks seen.

Next, in considering modification of the rocks resulting from wind action, we list the observations most pertinent in this regard. Fluting is important in this context (Whitney and Dietrich, 1973), so its nature can be used in making observations and comparisons of the two sites.

FLUTING AND FACETING

A. Wadi Mashi basalt hill blocks (massive, aphanitic basalts with 1 mm olivine phenocrysts):

1. Bimodal flute distribution (2 kinds).
2. Flutes are mostly medium size and moderate depth (approximately 1 cm long).
3. The most common flutes are linear (straight) or wedge (scallop) shaped.
4. A significant percentage of rocks have sinuous flutes (approximately 43%).
5. Few blocks have grooves.
6. Parallel flute arrangements frequently occur (79%).
7. Crosscutting flutes are often observed (78%).
8. Many flutes have internal pits (65%).
9. The relative density of flutes on rocks is low to medium.
10. Most rocks have facets (80%).
11. Multifaceted rocks occur most frequently among faceted rocks (i.e., 4 facets or more).

B. Gilf Kebir reg fragments (basalt boulders on a basalt fragment pavement):

1. Many rocks have uniform flute distributions but bimodal distributions are most common (57%).
2. Medium size, moderate depth flutes are typical.
3. Linear or wedge shaped flutes dominate.
4. Wavy or sinuous flutes are rare.
5. Parallel flutes are common.
6. Crosscutting flutes are generally absent.
7. Pits are observed in 39% of the fragments but the majority of flutes are "pit-free."
8. Rocks with a high concentration of flutes are rare.
9. Over 60% of the rocks are faceted, with keel-like facets the most common.



Figure 18.2 A) Wadi Mashi basalt hill survey image. Rocks in the foreground of this scene were studied in this investigation.



Figure 18.2 B) Wadi Mashi basalt hill (WMB) study area (bottom half of this image).

DIFFERENCES BETWEEN EGYPTIAN SITES

Two localities from the hyperarid Western Desert of Egypt (Fig. 18.2) were found to differ in terms of their rock morphologies. Both sites have basaltic lithologies and have been exposed to dust laden unidirectional desert wind (<30 km/hr) over at least the last 6000 years. Thus, eolian modification has dominated their recent histories. Periods of intense fluvial erosion and deposition are likely to have affected the GKR locale. There is no evidence for such activity at WMB. The talus blocks at WMB lie in a coarse sand substrate and probably rolled to their present positions from somewhere on the basalt hill. The mode of emplacement for the larger (>20 cm) fragments at both sites varies considerably from fluvial deposition to unloading and mass-wasting.

The major morphologic differences between the rocks at the two sites can be summarized as follows:

1. Rocks at WMB are more equant than their elongate GKR counterparts.
2. WMB blocks are multifaceted and highly angular, unlike the sub-angular, simply faceted GKR rocks.
3. Planar fractures are ubiquitous at WMB.
4. Linear features such as cracks and fissures abound at GKR, but are far less common at WMB.
5. Almost all rocks at WMB have small and medium sized cavities; GKR rocks are more uniform in their cavity distribution.
6. Sinuous flutes are rare at GKR but significant at WMB.
7. Crosscutting flutes are rare at GKR but common at WMB.
8. Pits occur inside most WMB flutes, but not in most GKR ones.
9. A wider variety of rock sizes are observed at GKR than at WMB (in the areas studied).
10. The substrate at WMB is reflective sand while that of GKR is composed of gravel fragments mixed with very coarse sand, hence darker.

SIMILARITIES BETWEEN EGYPTIAN SITES

The WMB and GKR sites in the hyperarid Western Desert of Egypt are fundamentally similar in terms of lithology, most recent modification history, and lack of vegetation. Both sites are dominated by massive, almost aphanitic basalts. These rocks are non-vesicular and internally homogeneous. Over at least the last 6000 years both sites have been subject to extreme aridity coupled with unidirectional northerly winds normally less than 30 km/hour. These winds carry fine

particles (dust), and occasionally are strong enough to saltate sand grains. There is evidence for wetter periods in these areas in the past 10,000 years (McCauley and others, 1979a). Even at present dews can form at both locations (El-Baz and others, 1980). The WMB basalts were observed to contain small (<1 mm) olivine crystals within their groundmass when broken open. It is not known if such is the case for the GKR basalts.

The important rock morphologic similarities for these sites are:

1. Highly pitted and fluted character of the rocks.
2. Slightly buried nature of most rocks.
3. Bimodal surface texture.
4. Variable or medium albedo (no high albedo).
5. Lack of rounded rocks.
6. Predominance of planar fractures.
7. Existence of facets at both sites (60% at either).
8. Lack of obstacle scour features at either site (result of substrate character?).
9. Overall trend to elongation in rock form (both sites have negative form ratios).

In considering what we have learned from our study of two Egyptian localities (WMB and GKR), we must ask the following fundamental questions. How were the rocks at each site formed and how were they transported to their present location (i.e., emplacement mechanism)? Finally, how have the rocks been modified; what processes have altered their morphologies and with what intensity and duration? These critical questions are applicable to rock populations anywhere on the earth, and are hereafter referred to as the "FEM" processes for Formation, Emplacement, and Modification.

Since both Egyptian sites are made up of isotropic rocks of a similar, uniform lithology, i.e., massive, homogeneous basalts, their formation is likely related to volcanic processes. The WMB locality is at the base of a basalt plug, so there is no question of its volcanic origin. There are numerous basalt plugs and ring dikes in the Western Desert, and one of these is likely the source for the GKR blocks.

It is clear the WMB blocks were emplaced by falling, rolling, or tumbling from elevated portions of the basalt hill nearby. Contraction cooling produced numerous fractures which, in combination with weathering and tectonic processes, could unseat blocks of basalts along these fractures. These blocks could then tumble to the base of the hill due to their positional instability. The emplacement process



Figure 18.3 Gilf Kebir reg study area (bottom half of image). Larger blocks in foreground are basalts, most of which are tens of cms in diameter.

at GKR is not as well defined. It appears GKR blocks were carried from their source by a water-related process; occasional torrential rains in an arid region are known to be able to carry large amounts of debris in suspension over kilometer-scale distances and create wadis. Basalt blocks were probably transported from a nearby volcanic construct during one of these infrequent floods to their present location at the GKR site (Fig. 18.3).

While the formation and modification processes have obviously contributed to the morphology of the rocks at GKR and WMB, it is their subsequent modification history that is most probably reflected by the morphologic data gathered in this study. The formation of wind erosional features such as flutes, pits, sediment moats, tails, and facets must be attributed to the modification stage of the FEM sequence. Little water is available in the Western Desert, so we must call upon the action of wind-driven dust and sand (El-Baz and others, 1980; McCauley and others, 1979a) to explain the overall morphology of the rocks at GKR and WMB. Differences in degrees of modification can be explained by variable ages of exposure along with differences in the intensity of the emplacement process. For instance, recently emplaced blocks at WMB would have been protected from wind and water weathering processes and would be less pitted, fluted, and display a lower albedo than rocks at GKR which experienced a more intensive transport process and have been exposed to surface weathering con-

tinuously since their emplacement. In addition, very localized effects such as morning dews or fogs, along with protection from wind-driven materials by other rocks could be responsible for some of the observed variations in the rock morphologies. Slight variations in the homogeneity of the basalt blocks themselves (i.e., olivine phenocrysts) might also be responsible for morphologic variations. However, in general the basalts at both the WMB and GKR localities appear to have behaved similarly under mechanical weathering by windblown particles based on their general morphology. Differences in the degree of faceting, planar fracturing, and cracking between the sites are probably most reflective of the original mode of formation and subsequent emplacement of the rocks and not to their modification.

CLUSTER ANALYSIS

Multiparameter cluster analysis can be used to objectively discover related subgroups of rocks within large (>50) populations. This is especially the case when there are several morphologic parameters that should be given equal weight in a statistical analysis. Garvin and others (1981) applied multiparameter clustering to rock morphology data collected for the Viking lander sites on Mars. Here the same approach is applied to Egyptian rock morphologies from the WMB and GKR sites. When using this technique, a subset of the complete set of morphology parameters (Fig. 18.1) must be chosen. We have selected a set of 23 attributes all of which relate to erosional or modification features on the rocks. Cavity distribution, size, depth, shape and orientation along with flutes, facets, linear features, fracture style, burial, dust effects, and obstacle scours were considered (see Fig. 18.1). The results observed are illustrated in Figures 18.4 and 18.5 in dendogram format.

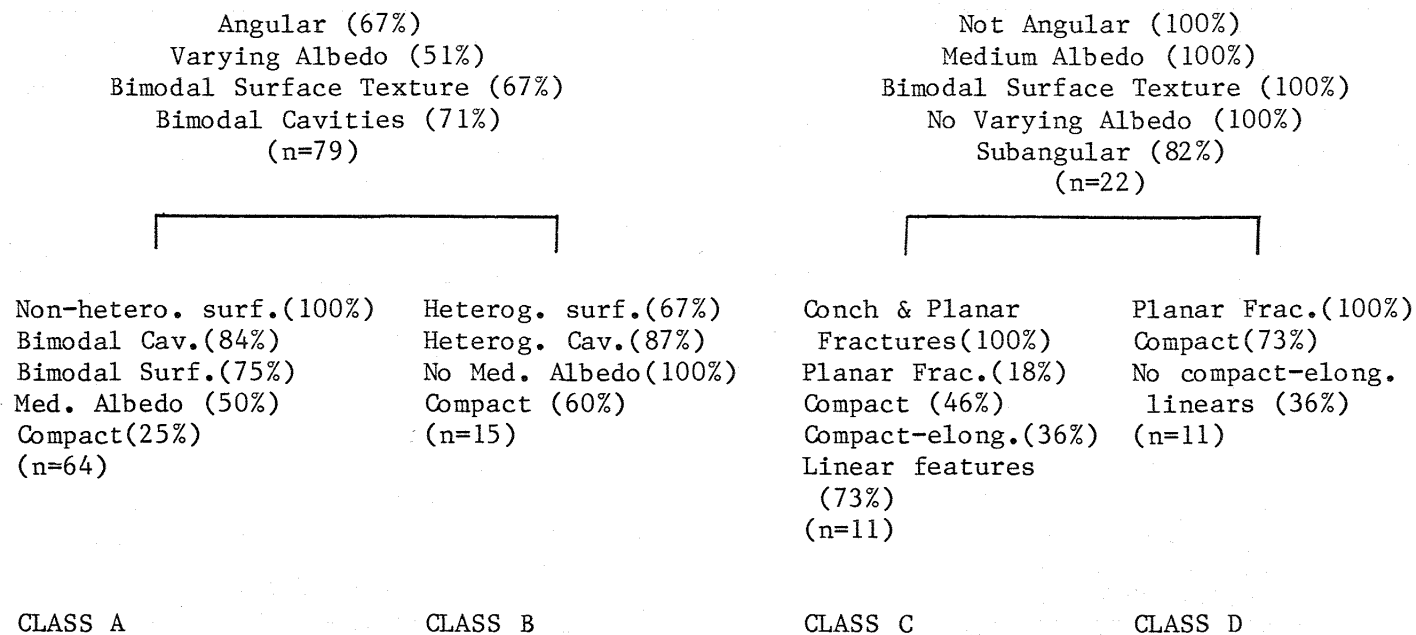
For WMB the following observations can be made:

1. Most of the rocks fall into subgroups (class A or C) which are distinguished by cavity size (small vs medium), cavity distribution, and presence of aprons; otherwise, they are similar.
2. The primary separation criteria used in subdividing the entire population of rocks are relative cavity size and depth.
3. The smallest cavities are not the shallowest; medium size cavities are often shallow.
4. Facets are not useful in separating subgroups.
5. Planar fractures, oriented cavities, and aprons are useful in finely subdividing rock morphologic subgroups.

At GKR we observe the following trends from the clustering analysis (Fig. 18.5):

1. Cavity distribution is the primary separation criterion: uniform rocks are subdivided from non-uniform ones at the first stage.

ROCK SHAPE AND GENERAL FEATURE CLUSTERING: EGYPT
Wadi Mashi, Basalt Hill
(n=101)



-273-

Figure 18.4 A) Dendograms of rock subgroups produced by clustering rock morphologic data collected for Wadi Mashi basalt hill site; general feature clustering.

EROSIONAL FEATURES-BASED CLASSIFICATION: EGYPT
Wadi Mashi, Basalt Hill
(n=101)

Small Cavities (100%)
No Med. Cavities
Moderate Cavity Depth (100%)
No Shallow Cavities
High Burial (40%)
Slight Burial (53%)
Aprons (38%)
Planar Fractures (49%)
Bimodal Cavities (83%)
(n=47)

Medium Cavities (93%)
No Small Cavities
Moderate Cavity Depth (100%)
Shallow Cavities (24%)
High Burial (26%)
Slight Burial (67%)
Aprons (20%)
Planar Fractures (65%)
Bimodal Cavities (69%)
(n=54)

-274-

Slight Burial (56%)
High Burial (42%)
All Cavity Shapes present (56%)
Bimodal Cavities (84%)
Dust on Rocks (49%)
Facets (76%)
Planar Fract. (51%)
Aprons (40%)
(n=45)

Not Buried (100%)
Only round & elong. cav. (100%)
Bimodal Cavities (50%)
Heterog. Cavities (50%)
Dust on Rocks (100%)
Facets (100%)
No Planar Fract.
No Aprons
(n=2)

CLASS A

CLASS B

Moderate Depth Cav. (72%)
Oriented Cavities (56%)
Linear Features (70%)
Facets (79%)
All Cavity Shapes (67%)
Heterogeneous Cav. (37%)
Bimodal Cavities (63%)
High Burial (30%)
Slight Burial (63%)
(n=43)

CLASS C

Shallow Cavities (82%)
No Oriented Cavities
Linears (18%)
Facets (100%)
Only Round & Elong. cavities (64%)
No Heterog. Cavities
Bimodal Cavities (91%)
High Burial (9%)
Slight Burial (82%)
(n=11)

CLASS D

Figure 18.4 B) Dendograms of rock subgroups produced by clustering rock morphologic data collected for Wadi Mashi basalt hill site; erosional features clustering.

2. Cavity depth is an important feature in grouping rocks.
3. Facets are not a useful subgroup separator.
4. Degree of burial is somewhat diagnostic in grouping the rocks.
5. Most rocks fall into one class (A) which is distinguished by its bimodal cavity distribution and moderate cavity depth.

At both sites, erosional features such as flutes and facets are too pervasive to be significant separators of rock morphologic subgroups. On the other hand, obstacle scour effects (tails, moats, aprons) are too uncommon to be critical in subdividing the populations.

When other sets of attributes are used in clustering the rocks other trends emerge. For instance, surface texture and albedo differences were seen to be significant separation criteria at GKR, while angularity and fracture style were critical parameters at WMB. These other trends are secondary, however, since they can only be seen when erosional features are excluded from the cluster analysis.

Cluster analysis of two sites in the Western Desert of Egypt in terms of erosional parameters illustrates how the same lithologies subjected to similar weathering processes are affected in analogous ways. Differences in the degree of erosion as manifested by cavity size, depth, and distribution of rock surfaces is the critical factor in determining morphologic groups. Other local weathering or modification effects play a secondary role when similar rock types are subjected to similar weathering phenomena. In terms of the FEM processes, this result supports our contention that modification stage effects are best demonstrated by the morphologies of wind-affected basalt blocks.

COMPARISONS WITH VIKING LANDER SITES

The two Egyptian desert sites may be compared with the Viking sites on Mars on a rock morphologic basis (Fig. 18.6 and 18.7). In terms of aridity, lack of vegetation, dominance of eolian processes, and rock type, the GKR and WMB localities represent some of the most comparable terrestrial analogs to the martian sites. Differences in substrate character and in the nature of chemical weathering between the Egyptian and martian blockfields are important, and must not be overlooked. From a first order comparison, however, several generalizations can be made:

1. The WMB site correlates very well with the Viking sites in terms of overall rock form: form ratios in the range -0.25 to -0.30 are characteristic of isotropic rocks (Garvin and others, 1981).
2. The GKR site closely matches the Viking sites in average rock roundness.

ROCK SHAPE AND GENERAL FEATURE CLUSTERING: EGYPT
 Gifl Kebir Reg (desert pavement)
 (n=51)

-276-

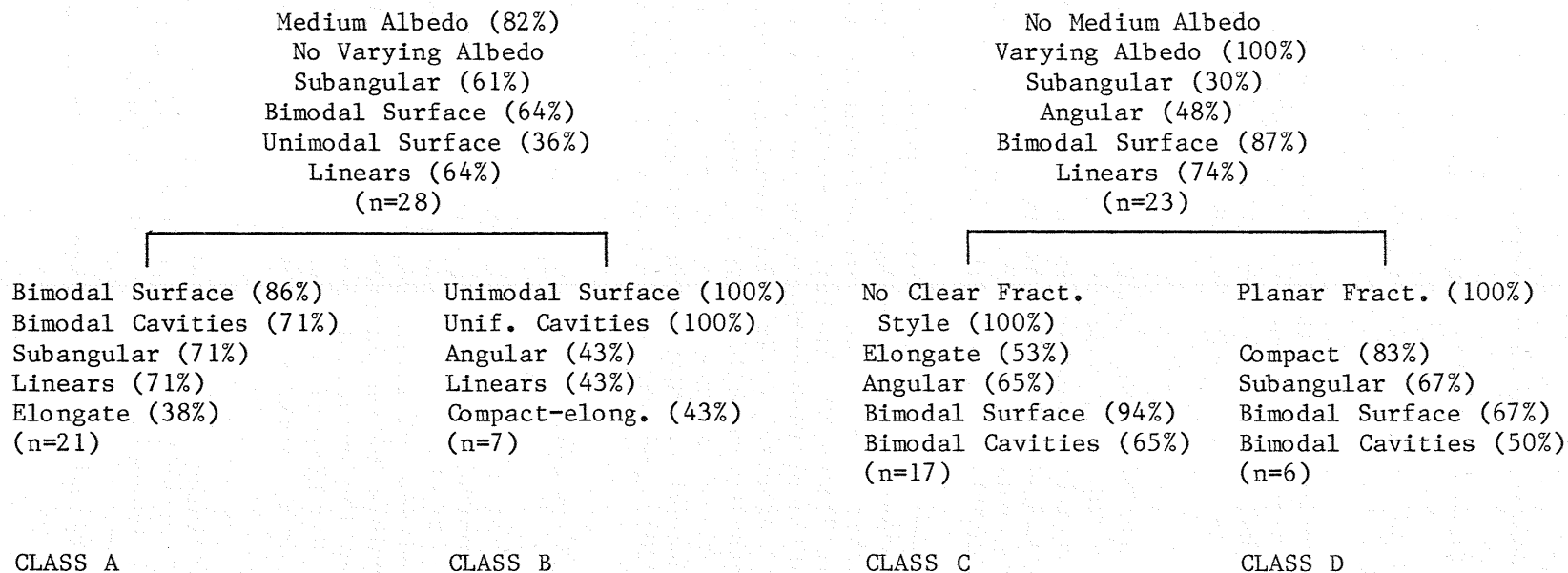


Figure 18.5 A) Dendograms for Gifl Kebir reg site; rock shape and general feature clustering.

EROSIONAL FEATURES-BASED CLASSIFICATION: EGYPT
 Gilf Kebir Reg (desert pavement)
 (n=51)

Bimodal Cavity Distribution (83%)
 Moderate Depth Cavities (49%)
 Medium Cavities (69%)
 Facets (54%)
 Slight Burial (60%)
 Linears (77%)
 (n=35)

Uniform Cavity Distribution (100%)
 Moderate Depth Cavities (69%)
 Small Cavities (50%)
 Medium Cavities (37%)
 Facets (75%)
 Not Buried (50%)
 Slight Burial (50%)
 Linears (50%)
 (n=16)

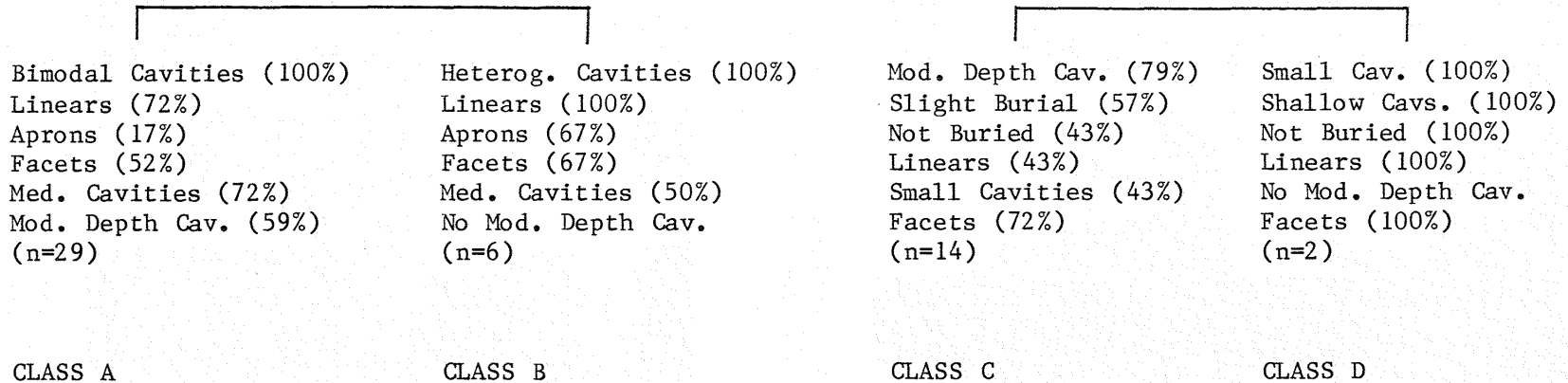


Figure 18.5 B) Dendograms for Gilf Kebir reg site; erosional features-based classification.

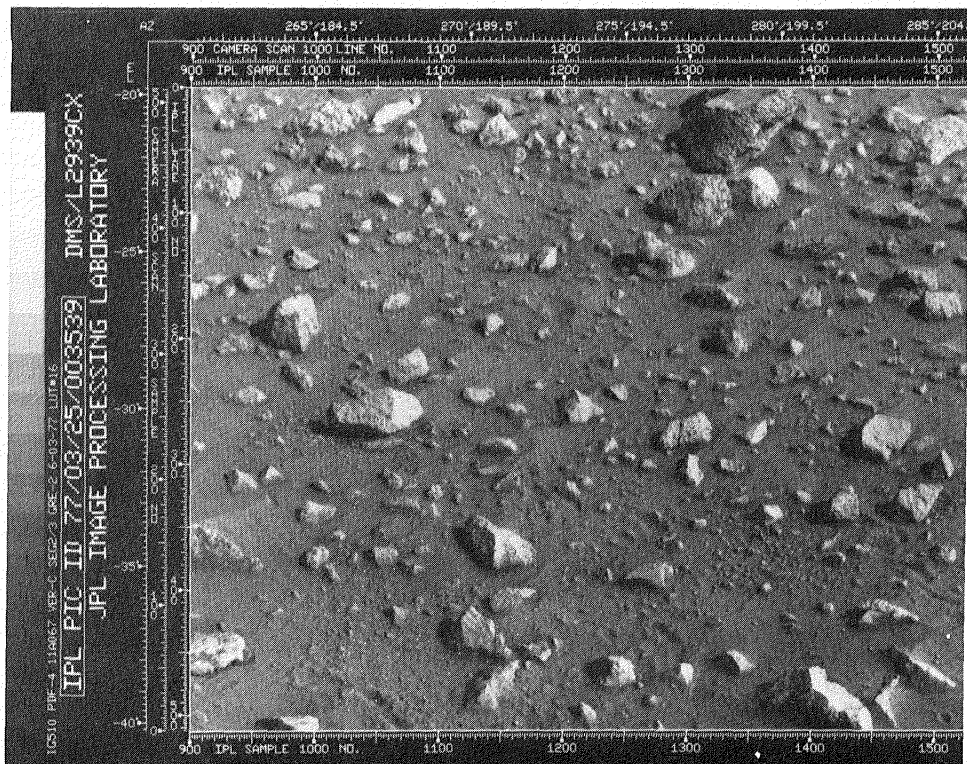


Figure 18.6 Part of Viking Lander 1 Frame 11A067, showing one of the study areas on Mars. The largest rocks in this image are 25 cm across.

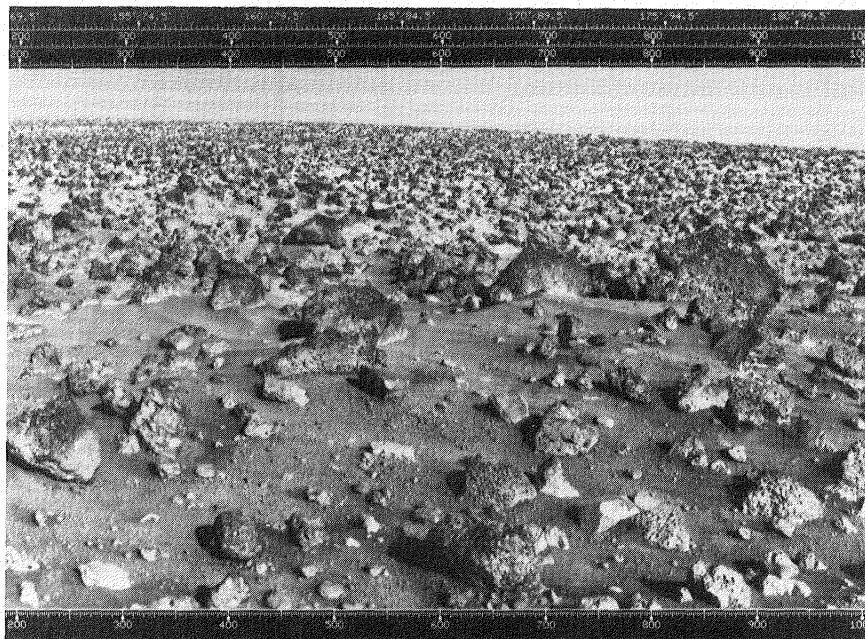


Figure 18.7 Part of Viking Lander 2 Frame 21A164, showing one of the study areas on Mars. The largest blocks in the lower half of the image are 40 cm across.

3. Fluting on Mars is less pronounced than in the hyperarid desert of Egypt, possibly due to the higher relative intensity of eolian abrasion on the Earth relative to Mars.
4. Facets at VL-1 are almost as common as at GKR.
5. The Viking sites have far fewer linear features and planar fractures than the Egyptian ones.
6. Obstacle scours (moats, tails) are more common at VL-1 than at any of the other martian or Egyptian sites.
7. Martian blocks are more uniform in their surface textures.
8. VL-1 and VL-2 are correlative with GKR and WMB in terms of cavity size patterns.
9. There are more unburied rocks on Mars than at either of the Egyptian desert sites.

From these observations and cluster analyses of the Viking sites (Garvin and others, 1981) it is possible to conclude that there are rocks on Mars that morphologically resemble those from the Western Desert of Egypt -- these rocks could be massive basalt fragments that have been modified by dust-laden martian winds. It is not necessary to require that all martian pitted blocks be originally vesicular. If there are significant numbers of basalt fragments at the lander sites on Mars then one can assess the strength of eolian modification processes on Mars from their morphologies. It appears blocks on Mars are eroded much more slowly than those on Earth under similar weather regimes. The key result of the Mars-Egypt surface comparison is indirect evidence for a basalt lithology on Mars at both lander sites.

CONCLUSIONS

A detailed morphologic analysis of the rocks at two sites in the hyperarid Western Desert of Egypt has been completed. Both localities have similar rock types (basalts) and have recently been subjected to eolian processes under some of the driest conditions on Earth. The effects of weathering on massive basalts by dust-laden unidirectional winds has been assessed. Despite differences in their modes of emplacement, the rocks at GKR and WMB appear to have been modified in a grossly similar fashion. Pitting, fluting, and faceting are significant features on most of the observed blocks. Differences probably relating to ages of exposure and transport history can be observed in rocks from WMB and GKR.

Comparisons with Viking lander sites on Mars are instructive as well, since the Egyptian sites have proven to be good analogs in terms of their general rock morphologies and modification histories. Pitting and fluting on Mars and in Egypt need not be attributed to vesicles if a suitable eolian regime is operative. We conclude from our study of Egyptian basalt block morphology that there is good evidence for the existence of massive, wind-pitted rock fragments at both

VL-1 and VL-2, possibly basaltic in composition. Studies of single lithology block fields under known weathering processes should prove useful in constraining the possible lithologies and processes present on Mars.

ACKNOWLEDGMENTS

This research was made possible by NASA Grant NSG-7569 of the Mars Data Analysis Program. I am grateful for the assistance and encouragement of Jim Head in this project. Farouk El-Baz provided the Egyptian images and invaluable information on the nature of the eolian processes in the Western Desert. Helpful discussions with Ted Maxwell are also acknowledged. Also, I'd like to thank Sam Merrell for his superb photographic work with Viking lander images. Lastly, I am appreciative of the excellent manuscript preparation provided by Sally Bosworth.

Chapter 19

EROSIONAL PATTERNS OF THE GILF KEBIR PLATEAU AND IMPLICATIONS FOR THE ORIGIN OF MARTIAN CANYONLANDS

TED A. MAXWELL
National Air and Space Museum
Smithsonian Institution
Washington, D.C. 20560

ABSTRACT

The relict fluvial topography of the Gilf Kebir plateau provides ample evidence for previous episodes of running water, with present-day domination by an active eolian environment. The caprock of the plateau is composed of quartzarenite, which locally has been recemented into extremely hard quartzite by silica overgrowths and vein fillings most likely accompanying adjacent Tertiary intrusions. Orbital photographs and images show both light- and dark-toned caprock, as well as eolian sand transported from the Great Sand Sea to the north, and redder sand that may in part be locally derived. Incised into the plateau are numerous wadis 10-40 km long that exhibit broad mouths with extensive alluvial fans. The upstream portions of the wadis are narrow canyons with flat floors, bounded by 100 m cliffs of sandstone. Within Wadi El-Bakht and Wadi Ard El-Akhdar, sporadic discharge of the wadis has apparently been blocked by dunes formed in the lee of south-facing slopes, which resulted in periodic damming of the channels and deposition of lacustrine silts and muds upstream from the dunes. More than 10 m of lacustrine sediments was deposited in Wadi El-Bakht, and in both wadis, interbedded mud and eolian sand are exposed where eolian and fluvial erosion has stripped away the recent playa deposits. Because of the absence of tributaries on the plateau surface, the linearity of wadi segments, and the evidence for structural control of Wadi Ard El-Akhdar, it is hypothesized that subsurface drainage, perhaps in the form of piping, has been responsible for the headward erosion of the wadis. This method of canyon development may also apply to several runoff channels on Mars, such as Nirgal Vallis, where tributary canyons in the upstream portions are similar in both scale and form to the blunt-shaped, abrupt headcuts of the Gilf Kebir wadis. Several of the martian canyons terminate at the location of scarps and ridges on the upland plains, suggesting structural control. These similarities in morphology and proposed origin provide justification for future investigations into the origin of the wadis of the Gilf Kebir.

INTRODUCTION

The Gilf Kebir consists of a broad elliptical plateau capped by extremely resistant sandstones of the Nubia Series (Peel, 1939b). Since its first sighting in 1909 by W. J. Harding King (see discussion in Bagnold, 1931), the Gilf Kebir and surrounding region has been the destination of several expeditions to southwestern Egypt, although the remote setting and harsh environment have not allowed extensive field work. Many of the early expeditions concentrated on mapping the extent of the plateau, exploring the many archaeological sites, and finding ways to go around it. Legendary accounts of the lost city of Zorzura, reported to be in the interior of the plateau (Bermann, 1934), no doubt were responsible for several of these trips. Serious investigation of the geomorphic history of the Gilf, however, began in 1938, and was due primarily to the efforts of Ronald F. Peel.

The massive, steep cliffs and extensive wadi networks that characterize the Gilf Kebir were of interest to the early explorers. In 1933, P. A. Clayton noted that the wadis commence at the scarps, yet have no drainage on top of the plateau. This suggested to him that the canyons must be the remains of an older system of drainage (Clayton, 1933). Studies by Peel (1939b) resulted in the first detailed interpretations of wadi and cliff morphology. The major unanswered questions of drainage pattern origin, channel incision and cliff retreat were raised by Peel, and still suffer today from lack of quantitative information.

Recently, photographs from the Gemini and Apollo missions, and images from Landsat spacecraft have greatly improved our view of this part of southwestern Egypt. The geographic division between the northern and southern Gilf Kebir discovered by Penderel in 1933 (see below) is well-documented on earth-orbital pictures, as are the extensive wadi systems that are cut into the plateau (Fig. 19.1). Consequently, although field studies are still sparse, there is much new data available on the large-scale relationships within the plateau.

The intent of this paper is to present both the field and orbital data in light of existing theories for the geomorphic development of the Gilf Kebir. New field data include profiles of Wadi El-Bakht and Wadi Ard El-Akhdar, and observations on the sandstones that make up the caprock of the plateau. In conjunction with previous maps of Peel (1939b), several volcanic hills can be tentatively identified on Landsat images. If the association between volcanically modified sandstones and early human settlement sites (El-Baz and Maxwell, 1979b) holds up under further field studies, then Landsat images may provide a useful means of predicting potential archaeological sites in this region.

In addition, orbital images of this region provide us with the large aerial view necessary for interplanetary comparisons. As on Mars, landforms of the southern Gilf Kebir show the effects of previous episodes of running water, yet are now dominated by an eolian environment. Fluvial canyons on both planets have been ascribed to

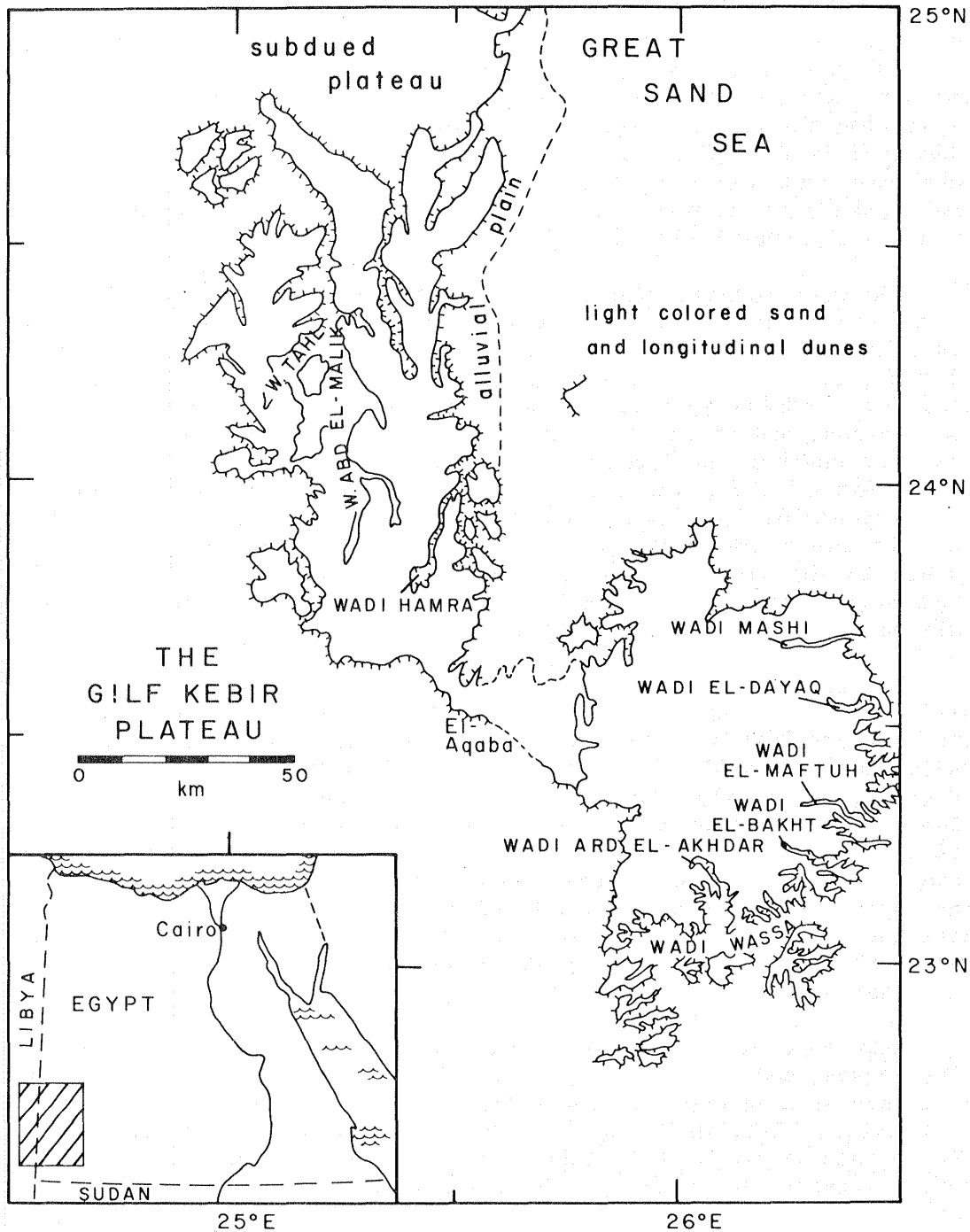


Figure 19.1 Map of Gifl Kebir region showing major named features and locations of wadis discussed in text.

the action of subsurface drainage and cliff retreat (Maxwell, 1979a), and the wadi systems of the Gilf Kebir provide a viable terrestrial analog for the results of these processes.

PHYSIOGRAPHY

In early 1933, while on a reconnaissance flight for the Royal Air Force, H. W. G. J. Penderel flew northwards over the western escarpment of the Gilf Kebir, and discovered the separation between the northern and southern parts of the extensive plateau. The gorge separating the northern and southern Gilf Kebir Plateau is 25 to 30 km wide, and is floored by numerous longitudinal dunes that have migrated southward from the Great Sand Sea (Fig. 19.2). Consequently, east-west passage is extremely difficult, although P. A. Clayton was able to cross the area later in 1933.

The most notable feature of both the northern and southern Gilf is the prevalence of steep-sided wadis that deeply incise the edges of the plateau. In some cases, wadis have completely separated portions of the plateau. This is especially true in the northern Gilf, where Wadi Abd El-Malik penetrates nearly the entire north-south length of the plateau, and on the southern edge of the plateau, where dissection has left several outliers. With the exception of the Clayton-Almasy expedition of 1932, there has been little work done on the wadis of the northern Gilf, although drainage dissection is more complete here than in the southern Gilf. In addition, the existence of trees and bushes in the wadis of the northern Gilf suggested to Clayton (1933) that water was either more plentiful here, or that it could have existed for longer periods of time.

In contrast, much more is known about the wadis of the southern Gilf, resulting mainly from the work of Bagnold's expedition of 1938. The southern Gilf occupies an area of 5800 km², and is penetrated by 5 wadis more than 15 km long. Wadi dissection appears to have progressed primarily from East to West, and the extreme southern portion of the plateau has been completely isolated by the east-west trending Wadi Wassa. The western side of the southern Gilf differs from the eastern side in that it has steeper cliffs (Bagnold, 1939; and Haynes, pers. comm.) and only minor incursions into the relatively straight walls of the plateau. East of El-Aqaba (Fig. 19.2), the few wadis that penetrate the plateau are elongate in a north-south direction.

Knowledge of the plateau surface of the southern Gilf comes from transverses made by Peel and Bagnold in 1938. The surface was described as rough and hilly by Peel (1939b), and nearly 50 exposures of basaltic hills were mapped. As can be seen from orbital images, the surface of the western half of the plateau is covered with reddish sand, similar in tone to the longitudinal dunes on the plains northeast of the plateau. In the northern part of the Gilf Kebir, inundation of the plateau is nearly complete; remnants of the dark, plateau-forming sandstone are barely visible through the haze of sand drifting southwards from the Great Sand Sea.

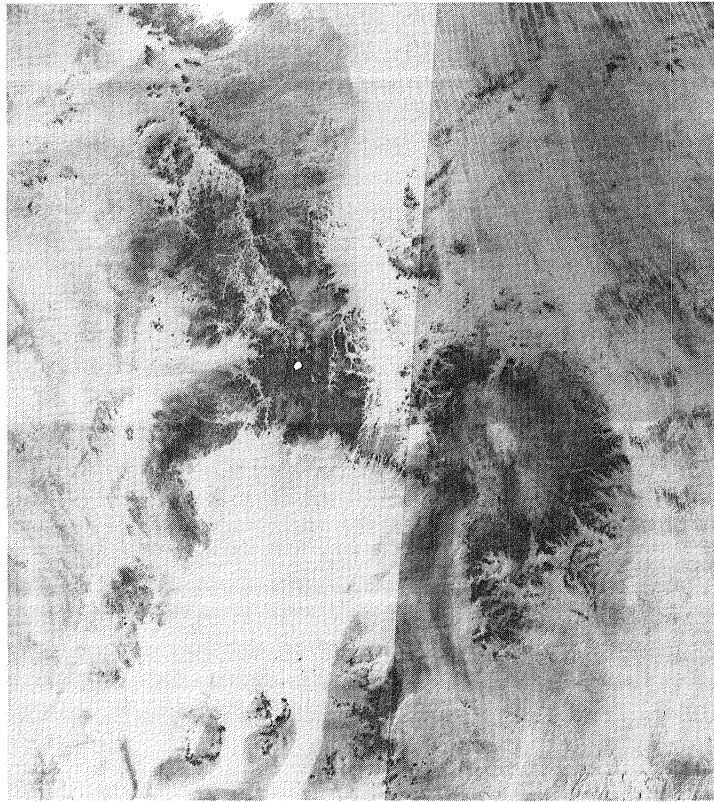


Figure 19.2 Mosaic of Landsat images of the Gilf Kebir plateau. Caprock of northern plateau disappears to the east under sand from the Great Sand Sea to the north (note the numerous longitudinal dunes). The northern plateau is more completely dissected than the southern part, primarily by north-south oriented wadis.

GEOLOGIC SETTING

The sedimentary series comprising the southern Gilf plateau consists primarily of sandstones, although individual beds may range from siltstones to conglomerates. The sandstone of the northeastern part of the plateau is believed to be conformable with the Jurassic-Cretaceous age Nubia Sandstone exposed south of the Kharga depression (Issawi, 1980), supported by the existence of upper Cretaceous fossils in the northeastern part of the plateau. The name "Gilf Sandstone," proposed by Issawi (1980), is reserved for that part of the section that unconformably overlies the Paleozoic rocks south of the plateau, and extends upsection to the dark, siliceous caprock of the northern Gilf. In contrast, Klitzsch (1978) proposed the name "Gilf Kebir Formation" for the sandstone section best exposed in El-Aqaba, where it consists of a cyclical cross-bedded silt to fine sandstone. Regardless of which stratigraphic model is preferred, the relatively soft siltstone cliffs of the Gilf Kebir are capped by layers of hard, siliceous sandstone that may range from several meters to tens of meters thick. These resistant ledge-formers create a stepped appearance to the scarps on the southeastern edge of the

plateau, but appear to be thicker in the plateau interior where exposed in the wall of the wadis.

Samples of caprock and prominent ledge-formers from six locations on the edge of the plateau consist of quartzarenites (or orthoquartzite), although there is a great variation in texture, cementation and porosity of the sandstones. At the northeastern edge near Wadi Mashi, for example, the caprock consists of a bimodal mixture of coarse- to fine-sand-size quartz grains with almost no porosity. Almost 40% of this sandstone consists of a microcrystalline quartz and calcite matrix, with quartz slightly more abundant than calcite. Near a basalt intrusion in the same wadi, however, the caprock consists of a mottled white and brownish-red mixture of well-rounded medium sand (.20 mm) and angular medium- to coarse silt size grains. The matrix of both white and red portions is composed of microcrystalline quartz, with the reddish stain probably made up of iron oxides. Numerous bright red specks of hematite, 10 μ m in diameter are present. The porosity of this rock is 10-15%, but has been somewhat reduced by late-stage precipitation of calcite as vein fillings.

In the upstream portions of Wadi El-Bakht (approximately 15 km from the mouth), the caprock consists of a unimodal, fine quartzarenite with abundant grain-to-grain contacts that pre-date quartz overgrowths in some cases (Fig. 19.3A). Although the rock is fairly strongly foliated, it is difficult to tell whether this fabric resulted from deposition, or later diagenesis. A primary stratification is favored, however, since quartz extinction is not related to the direction of foliation, and there is no other evidence for pressure-related phenomena. The rock is cemented by a mixture of microcrystalline quartz and hematite. For comparison, a resistant ledge-forming sandstone from near the mouth of Wadi El-Bakht is composed of a bimodal mixture of subangular silt to fine-sand and well-rounded coarse sand (0.60 mm) grains. This sample exhibits much higher porosity (10-15%), and similar to the other Gilf sandstones, is

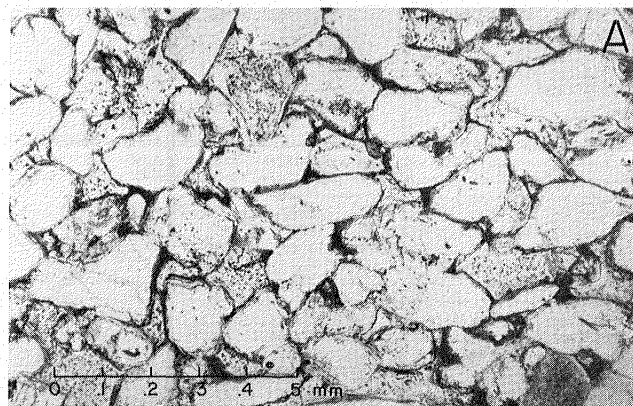


Figure 19.3 Photomicrographs of sandstone from the eastern edge of the Gilf Kebir plateau. A) Caprock sample from Wadi El-Bakht showing fairly strong (original?) foliation of angular grains.

cemented by microcrystalline quartz with minor calcite as the latest stage authigenic mineral. A sample of unimodal fine-sand size quartz-arenite from the caprock at the eastern edge of Wadi Wassa also suggests late-stage carbonate deposition in the form of narrow (20 μm) veinlets filled with microcrystalline calcite.

As shown by these analyses of caprock samples from locations scattered on the eastern edge of the plateau, there is an abundant source for silica both in detrital grains and in the matrix. The numerous Tertiary basalt intrusions mapped by Peel (1939b) provided a source of heat that aided local precipitation of silica as grain overgrowths and vein fillings. An example of this process is apparent at the constricted part of Wadi Ard El-Akhdar. Here, the hill on the northern side of the wadi consists of a basalt intrusion, whereas the southern hill is composed of an almost pure quartzite. The sandstone consists of an extremely siliceous mosaic of interlocking grains (0.08 mm; very fine sand) cemented by quartz overgrowths up to 50 μm wide (Fig. 19.3B). The porosity of this rock is much less than 5%, and where pores are present, they are bordered first by chalcedony, and then by calcite filling the center of the void. Since there are very few original grain-to-grain contacts, it is not likely that pressure solution played an important role in diagenesis. Instead, remobilization of silica was most likely due to the proximity of the intrusion, which reduced porosity and locally produced an extremely resistant caprock. An archaeological reduction site on top of the quartzite hill suggests that early man took advantage of the local geologic conditions, and used this material for production of implements (El-Baz and Maxwell, 1979b).

Surficial Deposits

As seen on Earth-orbital images and photographs, the surficial deposits of the Gifl Kebir consist primarily of exposed caprock, and eolian sand alluvial deposits within the wadis. Variations in degree of cementation and possibly even composition of the caprock make it



Figure 19.3 B) Extensive quartz overgrowths in a sample from Wadi Ard El-Akhdar adjacent to a basalt hill.

possible to distinguish a dark-toned and light-toned caprock. The dark-toned caprock is most prevalent on the surface of the northern Gilf Kebir, although it is also present on the northwestern and southern edges of the southern Gilf. It is possible that this tonal distinction is solely the result of covering by recent eolian deposits, but investigation of cliff heights in Wadi El-Bakht suggests that stratigraphically different units may also be responsible. The light-toned caprock on the north side of Wadi El-Bakht varies from 70 to 96 m above the wadi floor, whereas the dark-toned caprock on the south side of the wadi occurs at elevations of 115 to 140 m. Consequently, exposure of a stratigraphically higher sandstone unit (20-70 m thick) should not be discounted as a possible cause for tonal variations within the caprock. Locally, some circular patches of dark caprock most likely result from low grade metamorphism of the sandstone surrounding basalt intrusions.

Based on an Apollo 7 color photograph of the southern Gilf and numerous false-color Landsat images, it is also possible to divide the sand into two color zones. Relatively white sand similar in color to that of the Great Sand Sea surrounds the northern part of the plateau, and forms longitudinal dunes and linear chains of barchans within El-Aqaba. Reddish sand occurs in the middle of the plateau, as an extensive deposit off the southeastern edge of the plateau, and as a group of longitudinal dunes that have spilled over a short wadi on the western edge of the plateau. It is possible that part or all of the reddish color may be due to the addition of sand grains from the Gilf Sandstone, although the influence of a possible lag surface on the deposits cannot be discounted.

WADI MORPHOLOGY

Although only two wadis were investigated in detail, it is possible to make some generalizations on the overall morphology of several wadi canyons based on the experience gained from Wadi El-Bakht and Wadi Ard El-Akhdar, and the appearance of other wadis in orbital images. Minor tonal variations near the mouth of Wadi El-Bakht are the result of an extensive fan deposit shed off the south wall of the canyon, forcing the stream channels to the north side of the valley (Fig. 19.4). A similar process is also affecting Wadi El-Maftuh, where light-toned alluvial deposits occur only in the northern half of the valley.

In contrast to the wide mouths of the wadis, the upstream portions are narrow, linearly segmented box canyons characterized by flat alluvial floors. Channel incision ranges from less than a few tens of centimeters in Wadi El-Bakht to more than 3 m in Wadi Ard El-Akhdar, and the steep cliffs bounding the wadis rise to more than 100 m above the floor (Fig. 19.5). The investigation of the upstream portions of wadis El-Bakht and Ard El-Akhdar indicate that eolian activity has locally had a major effect on the floors of these wadis, although not on the morphology of the canyons as viewed from orbit.



Figure 19.4 View to the southwest at the mouth of Wadi El-Bakht. The relatively gentle slopes on the south side of the wadi are composed of coalescing alluvial fans and local deposits of eolian sand leading up to the sandstone cliffs.

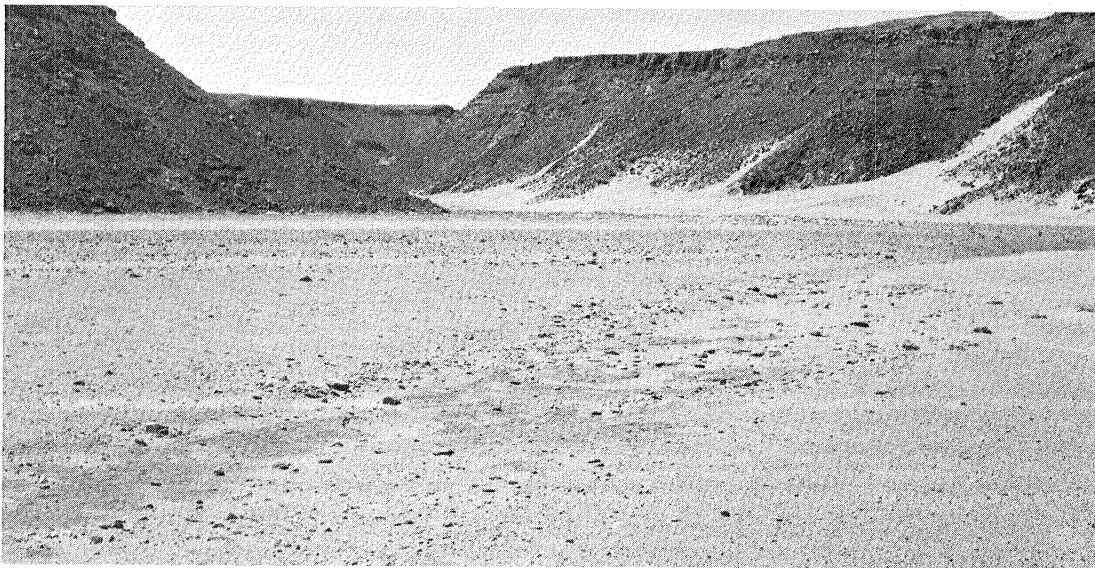


Figure 19.5 Upstream portion of Wadi El-Bakht. Note the steep cliffs (approximately 100 m high), lack of extensive fan deposits and only minor channel incision.

Wadi El-Bakht

Approximately 15 km upstream from the mouth of Wadi El-Bakht, the effects of the comparatively recent eolian dominance can be seen in the valley floor morphology and sediments. Here, a 30 m high sand dune rests against the north wall of the wadi, and extends 200 m to the south, almost half way across the canyon floor. Because of its placement on the north wall of the wadi, and its north-south orientation, it is probable that this dune originated as a lee dune, formed from sand blown across the plateau surface. Although the position of the crest may have shifted to the east or west in response to (diurnal) up- and down-valley winds, the position of the dune itself has been remarkably stable as indicated by the presence of neolithic implements found on the upper dune surface (see McHugh, Chapter 20).

The presence of the dune has had a marked effect on both the stream profile and on the type of sediments found in the wadi floor. Upstream from the dune, more than 10 m of interbedded lacustrine mud and eolian sand was deposited, although these deposits are now exposed in a gorge at the present-day southern tip of the dune (Fig. 19.6). The valley floor above the dune is graded to the level of the playa surface (approximate channel gradient = 0.0028), suggesting that either channel incision was limited by the temporary base level imposed by the dune dam (Fig. 19.7), or that a significant thickness of alluvial valley fill has been deposited upstream from the lake bed. In either case, the continuous gradient of the wadi floor indicates a cumulative effect of fluvial erosion and deposition for more than the past 7000 years since man lived on the latest lake deposits (Wendorf and others, 1976). It is possible that once the initial lake sediments were deposited behind the dune, they may have provided a positive-feedback mechanism for the stability of the dune. Sand carried by the up- and down-valley winds would be deposited at the topographic break between the valley floor and lacustrine deposits, and thus would have aided dune growth during times of increased aridity. Near the present-day cliff of lake deposits, the bedding dips at low angles to the west (upstream), suggesting that at least during the latest episodes of playa formation, growth of the dune and consequent damming kept pace with formation of the intermittent lake.

Artifacts found within the top few meters of the lake deposits indicate that human habitation took place contemporaneously with the last stages of deposition of the lake. The single ^{14}C age of 7280 ± 90 BP of an eggshell in Wadi El-Bakht (Wendorf and others, 1976) suggests that the latest major periods of lake sedimentation took place as recent as the "Terminal Paleolithic-Neolithic Wet Phase" of Wendorf and others (1977), although more youthful lake sediments may have been stripped by wind erosion. The detailed topographic survey of the archaeological sites on the playa sediments indicates a minimum of 1 m of deflation from the highest hummocks of lacustrine semi-consolidated mud to the level plain consisting of the most recent mud-cracked playa surface.

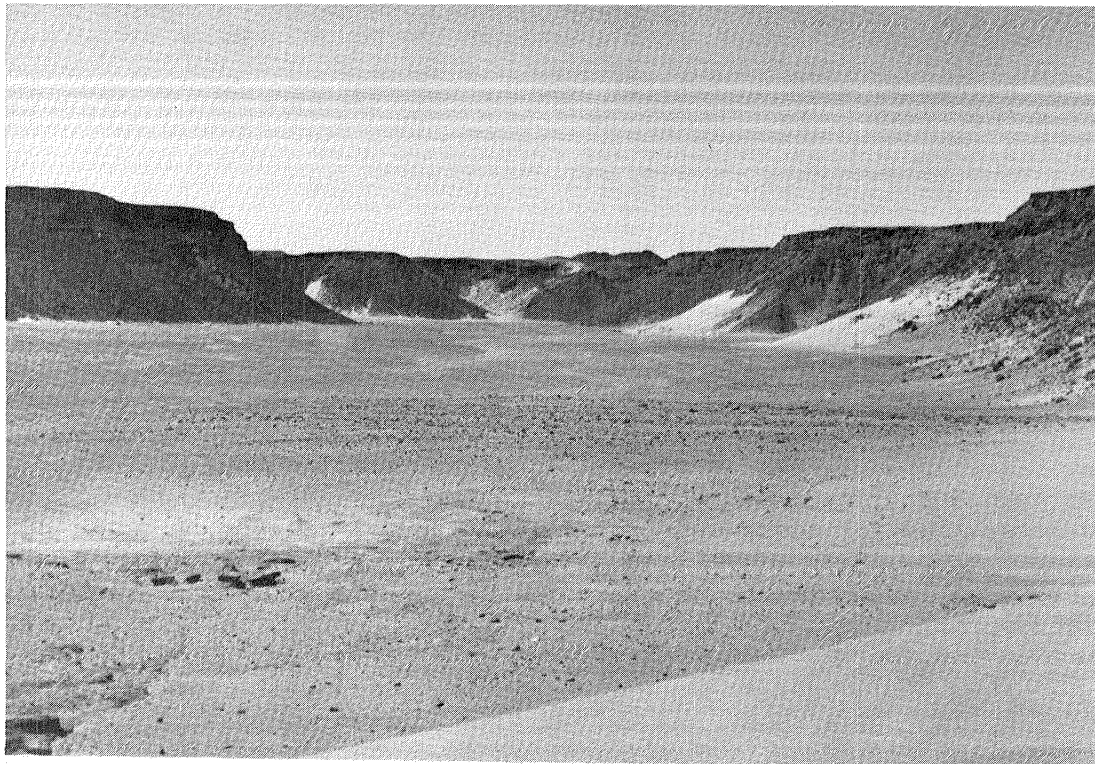


Figure 19.6 View looking upstream from the crest of the dunes in Wadi El-Bakht. Recent playa deposits are in the foreground, and present-day channel and gorge are at lower left.

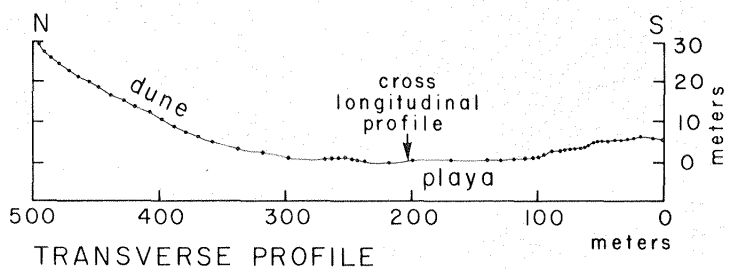
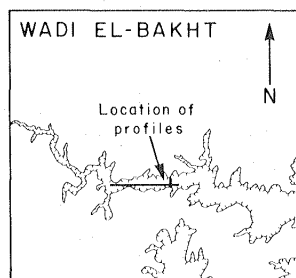
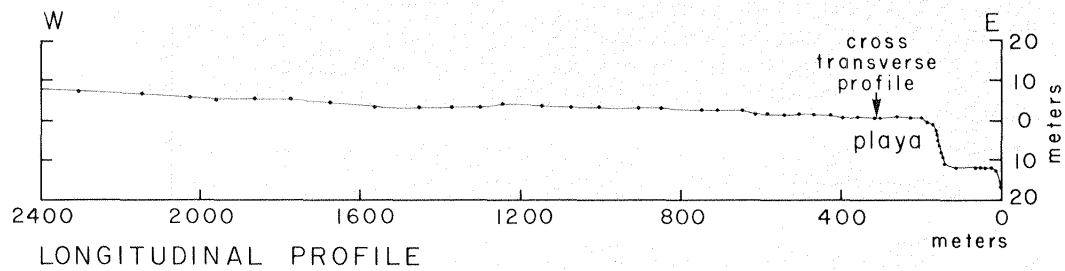


Figure 19.7 Longitudinal and transverse profiles of Wadi El-Bakht. Longitudinal profile was surveyed by pace and hand level and transverse profile by tape and level.

Wadi Ard El-Akhdar

As can be seen in orbital images, the upstream ends of Wadi Ard El-Akhdar abruptly terminate in circular, amphitheater-like depressions, with no evidence for channelized flow over the surface of the plateau (Fig. 19.2). Similar to Wadi El-Bakht, the downstream (southern) portion of Wadi Ard El-Akhdar is 10 km wide and is characterized by broad alluvial fans sloping down from the base of the steep cliffs of the plateau. The 2 km wide circular depression at the head of Wadi Ard El-Akhdar was investigated by Peel (1939b), who noted the presence of numerous basalt hills surrounding the depression. In addition, scree slopes of extremely hard, silica rich sandstone make up the southern side of the narrow mouth of the amphitheater, and a basalt hill forms the northern side of the wadi (Fig. 19.8). Although wadi formation by headward erosion versus inherited drainage remains an open question, it seems plausible that the incision of the canyon was here controlled by the bedrock. Whether inherited or headwardly eroded, the stream channel most likely took advantage of the highly fractured and metamorphosed sandstone at the contact with the Tertiary intrusion.

Within the gorge at the mouth of the amphitheater, a sharp crested dune is present, stretching from the basalt hill on the north approximately 2/3 of the way across the wadi (Fig. 19.8). On the south side of the constriction, channel incision has exposed a 3.4 m section of sediments, composed primarily of poorly-sorted pebbles and cobbles set in a matrix of silt and clay. However, alternating with these structureless beds are well-sorted red sand lenses with low-



Figure 19.8 Canyon constriction and dune in Wadi Ard El-Akhdar. View from quartzite hill on south side of wadi. Hill on opposite side is basalt. Note jeep in lower right corner for scale.

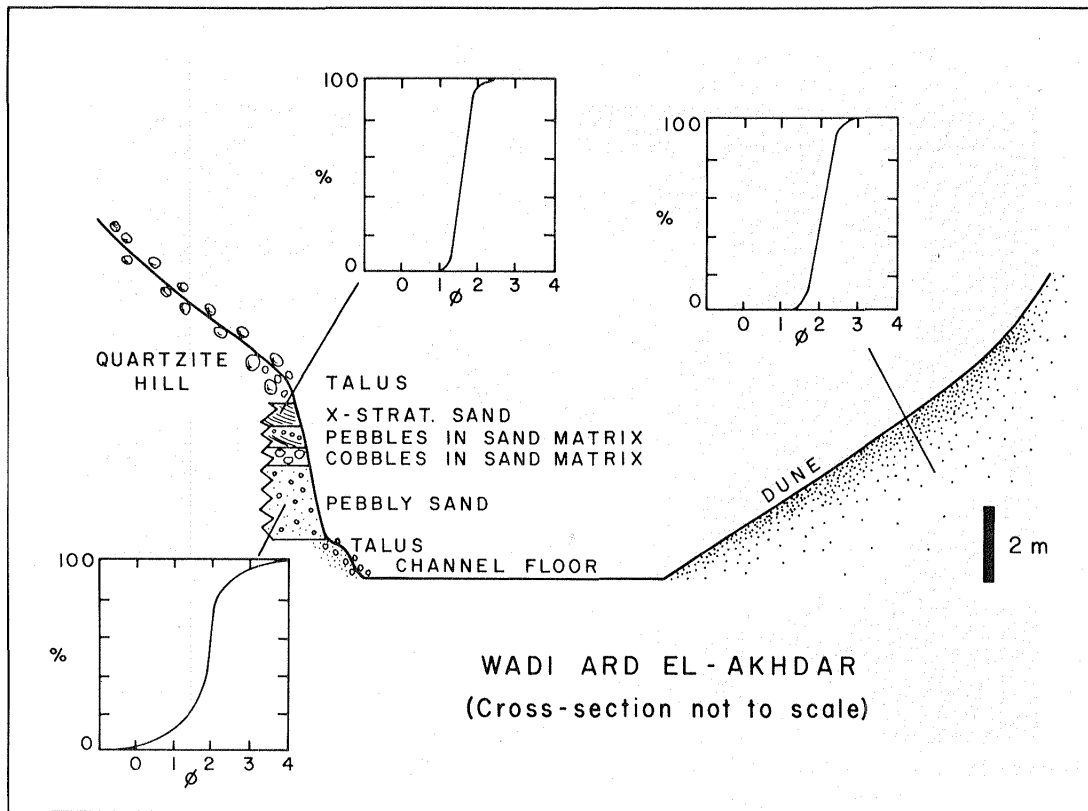


Figure 19.9 Vertical section and grain-size distributions for sediments in the constriction of Wadi Ard El-Akhdar. Note similarity in size distribution of modern dune sand and planar cross-stratified sand exposed on the south side of the wadi.

angle ($6-14^\circ$), planar cross stratification dipping to the west (Fig. 19.9). As evidenced by a comparison of the modern dune sand with that exposed on the southern wall of the wadi, and the stratification observed in cross-section, it is most likely that this dune has experienced several episodes of growth across the wadi, resulting in the damming of the channel, and consequent playa mud deposition upstream from the dune.

In contrast to the limited extent of the playa deposits at Wadi El-Bakht, those at Wadi Ard El-Akhdar cover the entire floor of the amphitheater, and are extensively eroded by later periods of channel incision (Fig. 19.10). The main channel is incised up to 3 m into the lacustrine sediments, and secondary channels, now choked with sand, are perched 0.5 to 1.0 m above the level of the main channel. This lack of adjustment of drainage within the amphitheater is consistent with highly localized rainfall on the upper part of the basin. Although the pace and hand-level survey of the constriction of Wadi Ard El-Akhdar is not as long as that of Wadi El-Bakht, it is evident that the gradient of the main channel is much steeper in Wadi Ard El-Akhdar (Fig. 19.11).



Figure 19.10 Incised playa sediments of Wadi Ard El-Akhdar; view to the northwest. Dark hill on north side of the amphitheater (upper right corner) is composed of basalt intrusions.

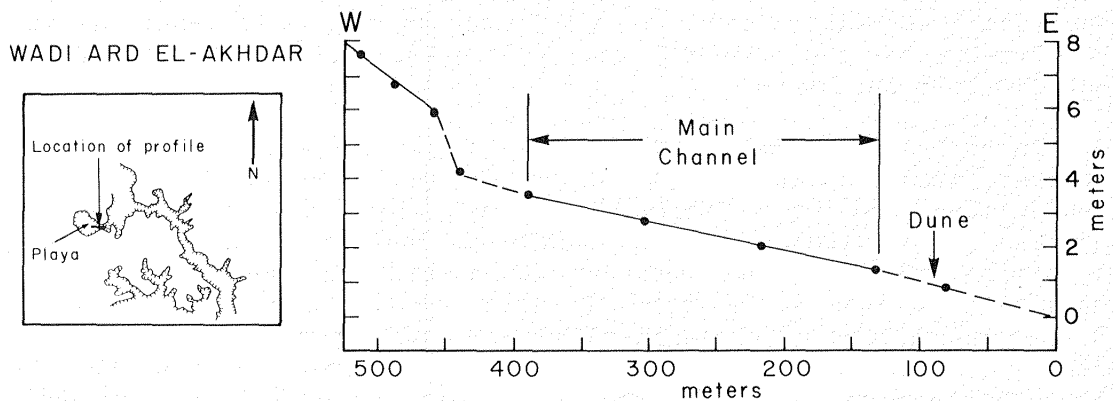


Figure 19.11 Longitudinal channel profile of Wadi Ard El-Akhdar near the constriction in the canyon.

DRAINAGE EVOLUTION

The conflict between the absence of surficial drainage patterns on top of the plateau, and the presence of the extensive wadi systems was explained by Bagnold in 1939 (in Peel, 1939b) as the result of subsurface drainage forming the wadis from rainfall seeping through the plateau surface. This hypothesis is supported by the observation of a discolored, friable sandstone alcove found midway up the southern cliffs of Wadi Ard El-Akhdar. However, the record of interbedded dune sand and lacustrine deposits found in both Wadi Ard El-Akhdar and Wadi El-Bakht suggests sporadic, high magnitude floods that were able to breach the dune dams in recent times (<6000 years).

An alternative model for the development of the wadis has been suggested by Haynes (pers. comm., 1978). Since less resistant shales (e.g. the Lingula Shale of Klitzsch, 1978) once covered the surface of the plateau, it is possible that the present-day canyons of the southern Gifl Kebir represent inherited channels from pre-existing drainage networks on the surface of the plateau. According to this theory, any evidence for pre-existing integrated drainage has been swept away by eolian planation of the surface of the plateau. Drainage patterns that are present in dark-toned portions of the northern plateau (Fig. 19.2) may support this hypothesis, if they are incised into stratigraphically higher units than the caprock on the southeastern edge of the plateau. However, considerable modification of the wadi headcuts must have occurred since the destruction of possible pre-existing drainage, as evidenced by the abrupt cliffs that are not at grade with the top of the plateau.

The lack of extensive widening of the wadis incised into the southeastern edge of the plateau, and the preservation of interfluvial ridges south of Wadi Wassa (Fig. 19.2) indicate the importance of headward erosion in the geomorphic development of the plateau. However, the occurrence of the canyons as linearly segmented reaches, with short, stubby tributaries often joining the main canyon at right angles (Peel, 1939b) suggests the influence of structural control on headcutting. Consequently, it is possible that subsurface, channelized flow occurred through piping, a phenomenon that occurs in several arid regions of the earth (Parker, 1964). However, more field work needs to be done on the surface of the plateau in order to test this hypothesis, with particular attention paid to the nature of the plateau surface at the heads of the major wadis. Playa lakes may have formed on the plateau where the water table reached the surface. If so, then these areas would have been attractive to the early inhabitants of this region, and thus may be opportune sites for future archaeological investigations.

MARTIAN CANYONS

The interpretation of erosional processes and their results in the canyons of the Gifl Kebir plateau are particularly suited to the martian problems of canyon erosion in stable headlands, cliff retreat by possible subsurface drainage, and eolian modification of fluvial valleys and channels. In addition, the climatic change from a relatively

humid to an extremely arid environment in southwestern Egypt is similar to the change experienced on Mars, where liquid water could have existed on the surface earlier in the planet's history (Pollack, 1979; Cess and others, 1980). Analogous features include flat upland surfaces with no integrated drainage, the abrupt, blunt-shaped headcuts, and the prevalence of straight channel segments possibly controlled by regional structure. Although several types of channels exist on the surface of Mars, these characteristics are typical of those classified as "runoff" channels by Sharp and Malin (1975). The spectacular outflow channels of the martian equatorial region generally do not share these attributes (Baker and Milton, 1974; Baker, 1978b), but terminate in chaotic, slumped terrain suggestive of a catastrophic release of water (Carr, 1979).

As viewed on orbital images, the stubby, linear segmented canyons of the southeastern Gilf Kebir resemble the tributary canyons on the south side of Ius Chasma on Mars (Maxwell, 1980), although there is a major difference in valley morphology. Instead of the characteristic flat floors of the canyons in the Gilf Kebir, the Ius Chasma tributary canyons are dominantly V-shaped, and very little floor is visible in the upstream portions of the canyons. Here, smooth surfaced talus slopes form the valley sides, extending to the base of the canyon (Fig. 19.12). However, the absence of tributaries on the surrounding upland plains, and the termination of the canyons in subcircular, amphitheater-like depressions are suggestive of erosion by drainage of

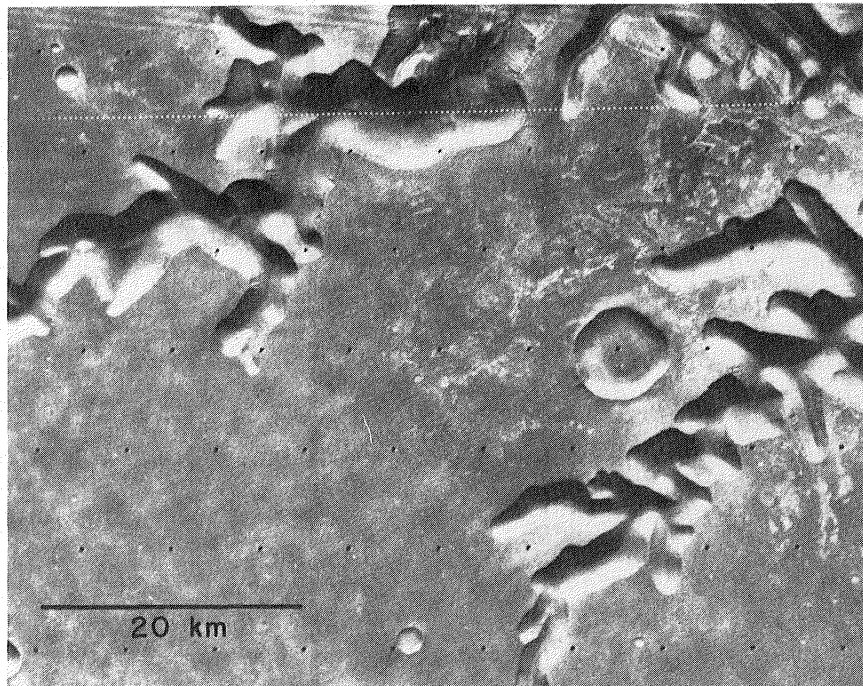


Figure 19.12 Tributary canyons on the south side by Ius Chasma on Mars. Note lack of low order channels on surrounding plains and abrupt termination of canyons in amphitheater-like depressions.

subsurface water (Sharp, 1973). It is possible that the differences in valley morphology may result from a less resistant "caprock" layer in the Ius Chasma region, which combined with the previously active tectonic formation of Vallis Marineris (Frey, 1979), would create conditions that favor unstable valley walls.

In the tectonically stable plains 500 km southeast of Vallis Marineris, the canyons of Nirgal Vallis display an outline similar to the wadis of the Gilf, and are also characterized by flat floors. This 700 km long canyon in the Mare Erythraeum region is characterized by abrupt headcuts of numerous tributaries, widening of mid-valley reaches, and an increase in width downstream, which led Sharp and Malin (1975) to suggest sapping and runoff as the principal mechanism for formation of the channels. Aided by Viking Orbiter images, it is possible to see finer details within the canyon than were evident in Mariner 9 images, which provide further evidence for subsurface drainage.

Near the upstream end of the valley, small tributaries are much more subdued than the main canyon possibly the result of mantling by eolian material. Sharp and Malin (1975) noted that the upstream portion of Nirgal Vallis exhibits a darker floor than the surrounding plains, which could result from the trapping of dark, mobile material. Consequently, the absence of low order tributaries to Nirgal Vallis may be in part due to infilling by eolian debris, although the similarities of canyon outlines to those in southwestern Egypt support an origin by subsurface drainage rather than by surface runoff (Fig. 19.13).

The effects of structural control on the location of canyons is evident in both the Gilf Kebir and Nirgal Vallis. In Wadi Ard El-Akhdar, the location of the constriction of the upper channel at the boundary between the basalt intrusion and the quartzite suggests that headward erosion took advantage of this weakness in the bedrock. In addition, the predominant north-south alignment of wadis in the northern Gilf Kebir may have resulted from drainage localized by fractures that originated during uplift and eastward tilting of the plateau (Maxwell, 1979b). Structural control on the location of tributaries to Nirgal Vallis is represented by north trending ridges and scarps that terminate at the headcuts of several tributaries, and continue on the opposite side of the canyon (Fig. 19.14). Assuming that these ridges represent folding or faulting of the local bedrock, it is possible that the flow of subsurface water was localized along these discontinuities resulting in an enhanced zone of headward erosion. Of the four tributary canyons that exhibit this phenomenon, three are incised into the south side of Nirgal Vallis, possibly suggesting a more abundant source of water to the south.

As shown by our field investigations in the southern Gilf wadis, the relatively recent eolian regime has had a great effect on the type of sediments deposited on the wadi floors, but has done little to mask the effects of the original fluvial processes that created the canyons. Instead, the location of wind-blown deposits has been controlled by pre-existing forms (such as south-facing cliffs),

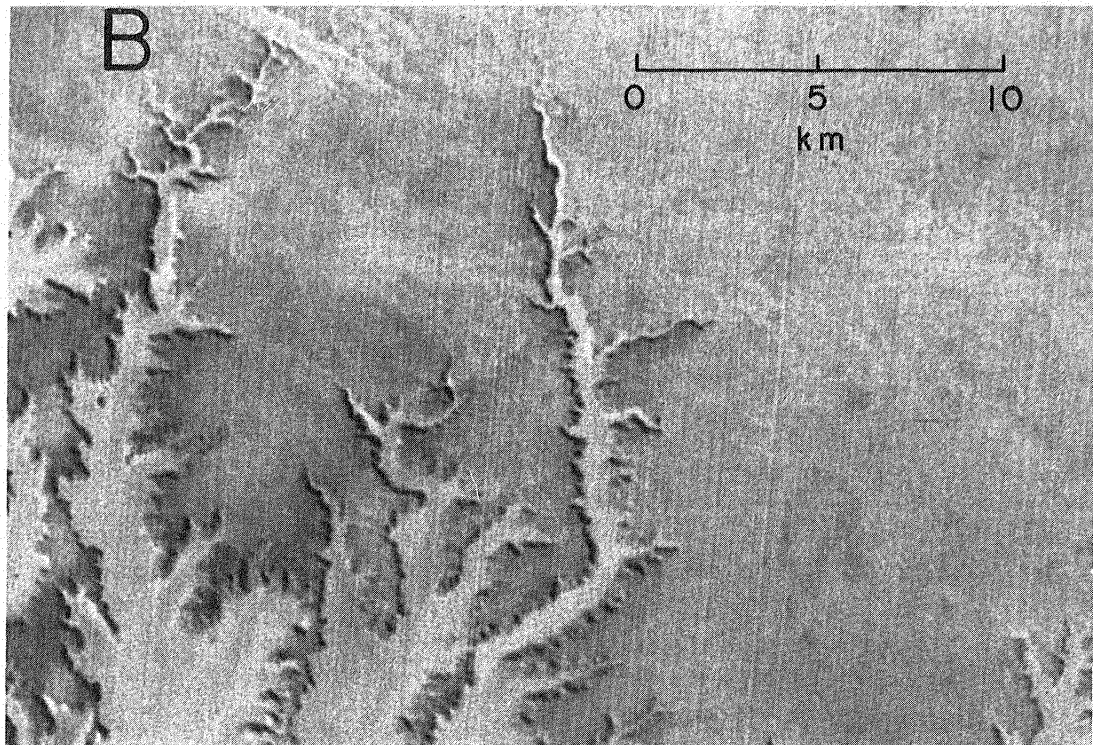
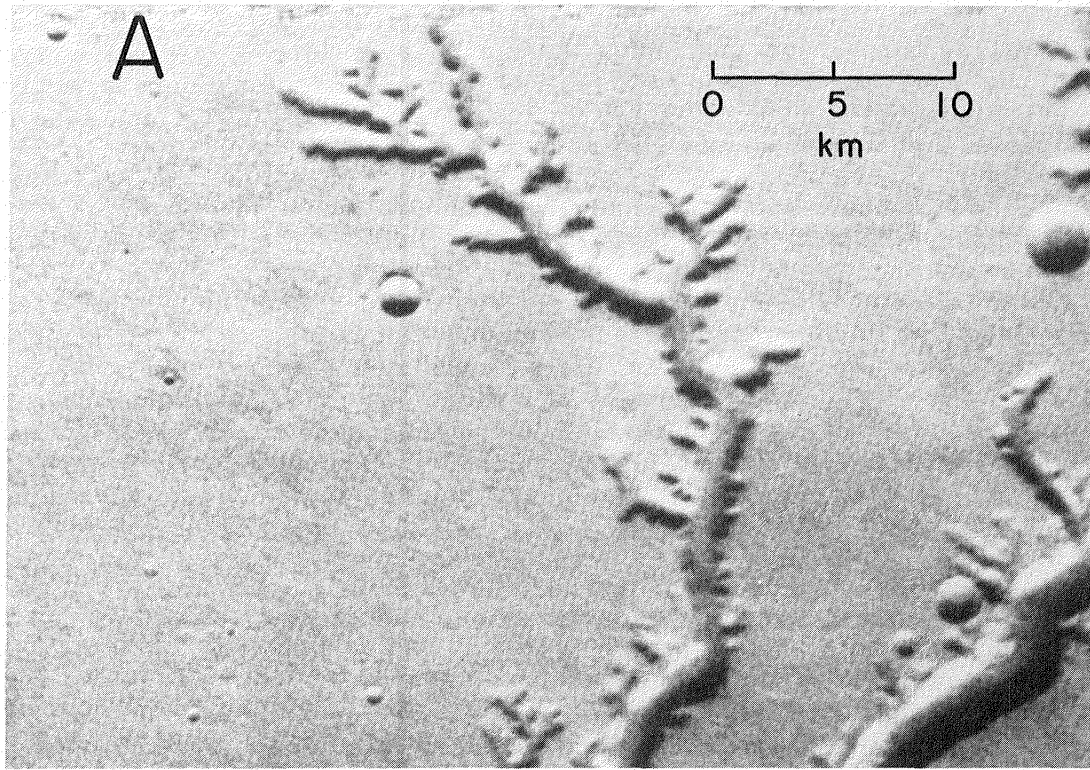


Figure 19.13 Tributary canyons to Nirgal Vallis on Mars (A) and drainage canyons of the southeastern Gifl Kebir (B). Canyons in both places abruptly terminate in subcircular depressions, and are dominantly flat floored.

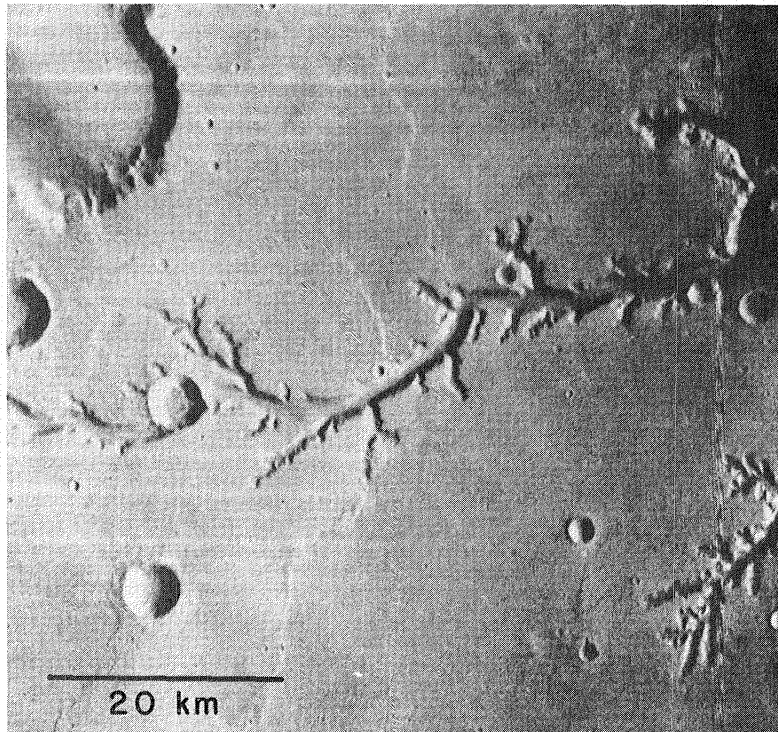


Figure 19.14 Tributary canyon on the south side of Nirgal Vallis that is suggestive of structural control. Canyon terminates at location of ridge in the upland plains.

resulting in the formation of lee-side dunes in Wadi El-Bakht and Wadi Ard El-Akhdar. Since they are transient features, the dunes have imposed temporary base levels, locally affected the gradient of the wadi channels, but have not caused any change in canyon outline or in the dominant flat-floored character of the valley floors. These observations thus suggest that many of the morphologic characteristics of martian canyons may truly be relict fluvial topography, with relatively little recent modification.

CONCLUSIONS

Erosion patterns of the Gifl Kebir plateau provide evidence for previous fluvial activity, which has now been taken over by the eolian regime of the present-day hyperarid climate. The extensive systems of wadis that are carved into the resistant quartzarenite and quartzite caprock of the plateau are dominantly flat-floored, and terminate in abrupt headcuts in the plateau interior. In the upstream reaches of Wadi El-Bakht and Wadi Ard El-Akhdar, lee dunes have dammed the channels, resulting in extensive deposits of playa mud. It is apparent that early man took advantage of these geologic conditions, the lakes for storage of intermittent rain water, and the quartzite for the production of implements.

Both field investigations and observations of orbital images support Bagnold's early hypothesis of subsurface drainage of the plateau.

The absence of surficial drainage networks and the steep cliffs that characterize the upstream ends of the wadis may best be explained by eastward drainage of water trapped beneath the caprock of the plateau. Headward erosion of the wadis took advantage of the pre-existing structure, as shown by the location of the constriction of Wadi Ard El-Akhdar at the contact between basalt and quartzite, and by the north-south alignment of wadis in the northern Gilf Kebir. It is suggested that subsurface water may have been channelized by piping in the siltstones of the plateau, thus accounting for the linear segments of the wadis.

The similarities in canyon outline and valley shape between the Gilf Kebir wadis and the tributary canyons of Nirgal Vallis on Mars suggest that similar mechanisms may be responsible for their formation. Subsurface runoff, perhaps in the form of piping may have substantially contributed to headward erosion on both Earth and Mars (Baker, 1978b), resulting in the abrupt headcuts and amphitheater-like terminae of the canyons.

Chapter 20

ARCHAEOLOGICAL INVESTIGATIONS IN THE GILF KEBIR AND THE ABU HUSSEIN DUNEFIELD

WILLIAM P. MCHUGH
G.A.I. Consultants, Inc.
Pittsburgh, Pennsylvania 15156

ABSTRACT

Investigations at Wadi EL-Bakht and Wadi Ard EL-Akhdar, in the southern Gilf Kebir, amplify previously published accounts by Myers, Bagnold, Peel, and McHugh. New data demonstrate that Neolithic pastoralists who raised cattle and goats (or sheep) occupied these two wadis during and shortly after the existence of small lakes. The vertebrate remains have been identified by Achilles Gautier (University of Gent) and a single ^{14}C date (7280 ± 90 BP, SMU-273), previously obtained by Vance Haynes, suggests a sixth millennium B.C. age for the pastoral groups. This age estimate is supported by the single determination, also on ostrich egg shell, of 8170 ± 120 BP (A-1966), from the Big Barchan 1 site in the Abu Hussein Dunefield; this site produced one truncated skull of a juvenile Bos among a scatter of flakes and blades of silicified quartzite and conglomerate chunks, all of which lay on or were slightly embedded in a reddish ("Neolithic") soil. A similar soil development is reported for the Gilf Kebir plateau surface at a reduction station where lithic artifacts are embedded in 30 cm of this soil. The lithic technology at wadis EL-Bakht and Ard EL-Akhdar demonstrate that the occupants also utilized plant remains, processed them on their grinding stones, and stored or cooked them in their pottery. Aspects of this pastoral Neolithic complex are widespread across the southern Egyptian Desert, from the Gilf and Uweinat to Napta Playa and the implications of the presence of this adaptation for Egyptian and Nilotic prehistory are only beginning to be realized.

INTRODUCTION

The archaeology and cultural history of southwestern Egypt are barely known. Only a handful of publications report on limited aspects of the prehistoric archaeology of the vast southwest quarter of the Western Desert. The rock art of Gebel Uweinat is reasonably well reported in the works of Winkler (1939b), Rhotert (1952), Van Noten (1978), and a few others. Rhotert's work also covers the rock art of a large area in southwest Egypt and northwest Sudan, including the Gilf Kebir, and provides the most comprehensive sample of rock art of the region.

In spite of the numerous publications on rock art, none of the original archaeological investigators have reported the details of the settlement sites. The artifact collections made by the Frobenius 1933-35 expeditions were destroyed in World War II and never reported. The collections made by W. B. Kennedy-Shaw were deposited in various museums and never described. The collections made from several localities by Oliver Myers on the 1938 Bagnold-Mond expedition have ended up in the Department de Prehistoire, Musee de l'Homme, and have not been fully analyzed. I have studied part of the collection and reported the results of my analysis and interpretations in three papers (McHugh, 1974a; 1974b; 1975). A preliminary account of the settlement sites and associated artifacts from the plain north of Karkur Talh, investigated by the Belgian scientists, has been published (de Heinzelin and others, 1969).

The reported settlement site archaeology is thus limited essentially to one wadi (Wadi El-Bakht) in the southern Gilf Kebir, and to the plain north of Karkur Talh. This paper will report on the settlement or specialized activity sites in three additional locales, one in the Abu Hussein dunefield, the second in Wadi Ard El-Akhdar, and the third on the Gilf plateau surface. In addition, further information on the settlement archaeology in Wadi El-Bakht, originally studied by Oliver Myers, will be provided.

Archaeological Investigations of the Bagnold-Mond 1938 Expedition

During the 1938 Bagnold-Mond expedition to the Gilf Kebir and Gebel Uweinat, systematic archaeological investigations were conducted by Oliver Myers and Hans Winkler over a period of seven weeks. Myers (1939) investigated sites at the eastern edge of the southern Gilf Kebir, in the wadis El-Bakht and Ard El-Akhdar, and along the Karkur Talh near Uweinat mountain. In their wide-ranging surveys, Peel and Bagnold (1939; Peel, 1939b) discovered and reported numerous sites, many on the Gilf surface, and others, including some with rock art (Peel, 1939a), in the Gilf and Uweinat wadis, and between the Gilf and Uweinat. Myers spent almost 3 weeks at the large Acheulean station near Birket El-Shaitan, north of the mouth of Wadi El-Maftuh at the eastern edge of the southern Gilf. He spent a few days each in the wadis of El-Bakht and Ard El-Akhdar, and (apparently) a couple of weeks in Uweinat. He was assisted by three laborers (Quftis), one driver-mechanic, and at various times by other members of the party.

Myers' purpose in joining Bagnold was to look for evidence of what he called the "Saharan culture", a term he used to denote the assemblages (lithic implements and pottery) he had discovered in his explorations in the low desert around Armant on the west bank of the Nile. He was convinced that the source of this culture was to be found far to the west of the Nile Valley, for he had examined ceramics from several remote places in the Sahara which he thought were of the same tradition as the "Saharan" ceramics from Armant. Some of this pottery had, in fact, been collected by W. B. Kennedy-Shaw in the southern Gilf and in the surrounding country (Shaw, 1936a). It is indeed curious then, that Myers first elected to investigate the large Acheulean site near the base camp which we revisited in 1971,

and only subsequently examined the ceramic-bearing locales in the southern Gilf.

Myers published only one short paper on the results of his research (Myers, 1939). I was able to study the materials from wadis El-Bakht and Ard El-Akhdar which he had deposited in the Musee de l'Homme in Paris. These were accompanied by fragmentary notes and three short manuscript drafts (Myers, ms. a, b, and c). Nevertheless, enough information existed in the papers by Myers, Bagnold and Peel to indicate that these two wadis contained artifact assemblages and associated physiographic settings of unique importance for understanding the paleogeography and cultural ecology of southwestern Egypt. Thus, my objective on the 1978 expedition was to visit these two wadis to reappraise their tantalizing potential and to conduct whatever investigations our limited time would allow.

Impatient as I was to get there, other requirements of the expedition dictated spending several days at other places and in traveling to the Gilf. These excursions provided the opportunity to examine other locales with evidence of prehistoric settlement in the southern Western Desert, an extremely impressive introduction to this vast area. In the following sections, I will describe the major archaeological localities I was able to investigate (in each case, all too briefly). I will offer some very tentative models of the geomorphic events in wadis El-Bakht and Ard El-Akhdar, and will suggest the paleoclimatic implications of these events. Finally, I will review the major elements of a testable model of human adaptation, or the cultural ecology of the Gilf-Uweinat area in late prehistoric times.

THE BIG BARCHAN SITES

The Big Barchan Site 1 was found accidentally on September 27, 1978. While visiting the Abu Hussein dunefield, Vance Haynes called our attention to the presence of an isolated concentration of lithic artifacts adjacent to a large barchan. At that time, Haynes collected some ostrich eggshell fragments from within the soil, and I excavated and removed a fragmentary mammalian skull which had been partially exposed and truncated at the surface. A collection of lithic implements was made by the party. I returned to the site on the following day to make a map of the distribution of the remaining lithic materials, and to put in some test pits to ascertain the vertical extent of the cultural materials and to provide soil samples. A second concentration of implements was noted on this second visit. It is located about 70 m southwest of the first, and is designated Big Barchan Site 2. The lithics were collected at this site also, and a test pit was excavated.

Setting

The Abu Hussein dunefield is an extensive series of large barchan dunes covering hundreds of square kilometers southwest of Bir Sahara at about 22° 55' N, 28° 25' E. The large barchan near the two sites is located at the eastern edge of the dunefield. The approach to the dune from Bir Sahara, some 37 km to the east-northeast, is across an

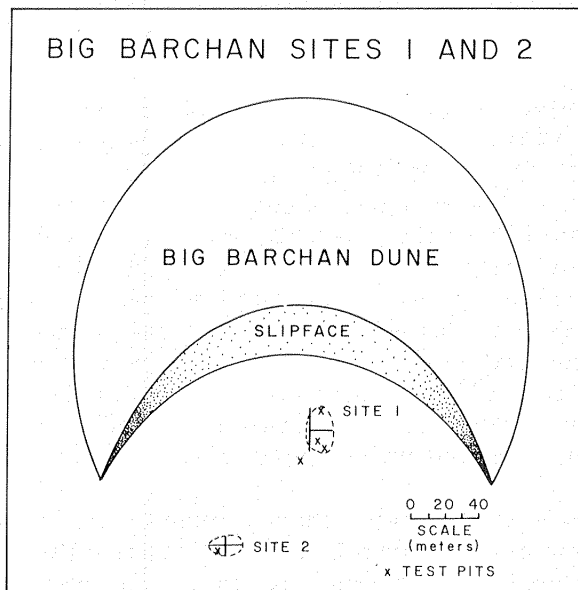


Figure 20.1 Sketch map of the Big Barchan sites in the Abu Hussein dunefield southwest of Bir Sahara.

almost featureless sand plain. The absence of noticeable drainage channels, rock outcrops, or vertical relief is probably noteworthy in evaluating the significance of the sites.

Site 1 is situated well within the horns of the barchan and about 32 m from the south-facing slip-face of the dune (Fig. 20.1). The tips of the horns are roughly 220 m apart, and Site 1 is located a little east of the midpoint between the two horns. The quartzite implements and abundant fragments of conglomerate at Site 1 were distributed over an area measuring about 26.5 m (N-S) and 15.8 m (E-W). The lithics were primarily on the surface, although a few were slightly embedded within the sand.

Site 2 consists of a scatter of quartzite artifacts and a few conglomerate fragments covering an area about 11 m N-S and 20 m E-W. The artifacts here were fewer in number and less dense than at Site 1. Both sites occupy flat surfaces, so flat as to suggest the surface has been graded level by eolian processes. The truncated skull indicates the operation of such processes as, of course, do the barchans themselves.

The location of the two sites within the wind-shadow of the dune poses a quandary. Although we didn't have time to explore widely around the sites, I made a brief survey in their vicinity to look for other sites within and beyond the dunefield, but found none. As mentioned above, no detectable water courses are to be found nearby, although my survey around the sites and passage across the sand plain to the east can hardly be considered an adequate search for such features.

Archaeological Observations

No quantified description of the artifact assemblages can be offered since time was insufficient for their study. The artifacts remain in Egypt awaiting future analysis. However, it can be said that the assemblages are unusual in several respects. First, they contain two different components, flaked quartzite implements and fragmentary conglomerate rocks. The quartzite implements were mainly blades of moderate to large size (50 mm to greater than 100 mm in length). There is no minute debitage and there are no blade cores; thus, the production of the blades was carried out elsewhere and they were carried to the site. The conglomerate fragments are generally of small to moderate size, easily lifted in one hand. They too must have been intentionally brought to the site. For what purpose, we cannot say at this time. Second, no pottery and no ground stone implements were found with the assemblages. The absence of pottery and milling stones may have chronological significance, but given the location of the sites and their lithic contents, a functionally-based explanation may be reasonable.

Pedological Observations

The excavations on the first day revealed the presence of an interesting soil immediately below the granules on the surface. A description of the deposits of Test Pit #1 represents the soil profile to a depth of about 70 cm. The top 2-3 cm is comprised of a mantle of loose sand and coarse granules. This layer overlies a dull, reddish zone comprised of compact, reasonably consolidated, coarse and very fine elements. This zone also reveals narrow desiccation cracks running vertically through it to a depth of at least 35 cm. Surprisingly, tiny rootlets permeate this reddish zone. These appear as fine tubular sand castings about 1 mm wide. Within the sand tube is a very fine fiber, presumably that of a rootlet. The question of the age of these rootlets naturally arises. According to Dr. Loufy Boulos, expedition botanist, these rootlets cannot be very old (oral comm., 1978). Their presence and probable recent age suggest vegetation cover in the not too distant past, and the possibility of recent pedogenic processes as well. The relative age of this soil needs further study.

Without question, the sand-granule zone has been in place for a long time, since before the arrival of the implements. A radiocarbon date of 1870 ± 120 BP (A-1966, Haynes, pers. comm., 1978) on the ostrich eggshells gives a lower limit for this layer. Relatively moist conditions are reasonably inferred from the degree of soil development and from the presence of the desiccation cracks. It is also likely that the deposit has been reduced by eolian processes because of the very level surface, the location of almost all the artifacts completely on the surface, and the truncation of the skull.

The chronological relationship between the sites' occupation and the presence of the large barchan cannot be estimated. Only some questions can now be posed:

1. Were the barchans in existence when the sites were occupied?
2. Were sites 1 and 2 ever covered by the southward-moving barchans? (We should look for artifactual assemblages coming out from under the tail of the barchans.)
3. What was the pre-dune morphology of the area?
4. What was the drainage pattern in the area? Are the ancient water courses completely mantled by the sand and dunes?

Interpretation

The extremely limited artifact typology of the two site assemblages suggests that these were specialized settlement situations. Their locations on, and slightly within an old soil formation permits the deduction that relatively moist conditions existed locally when these sites were occupied. The soil formation indicates the presence of vegetation. The ostrich eggshell fragments and the truncated skull, identified as a juvenile Bos. by A. Gautier (Chapter 21), indicate the local presence of the species represented by these remains. The apparently specialized nature of the artifact assemblages (blades of varying sizes, and absence of milling stones and pottery) indicates that only limited activities were conducted by the site inhabitants. It would seem that these sites represent rather transitory settlement, such as that of a small group of hunter collectors out after game (ostriches, cattle, ostrich eggs), or perhaps pastoralists en route. Based on the quartzite implements, with no apparent local source, it is possible that these people came from afar. The absence of pottery and milling stones in the assemblages calls for no other explanation than to point out that a group of hunters or pastoralists on an expedition would likely not carry such impedimenta.

The significance of the Big Barchan sites lies in the following:

1. They show human settlement at some time in the past in what is now an incredibly hostile environment.
2. They indicate that local conditions were sufficient to support soil development, vegetation growth, and probably the presence of wild species and domestic cattle (?).
3. The radiocarbon date of the ostrich egg shell gives an estimate of the time of occupation of the sites, and when the climatic conditions were favorable for habitation.
4. They reveal a specialized functional situation with an extremely limited inventory of tools, far removed from the source region of the lithic materials, from a base camp, or from an obvious source of water.

ARCHAEOLOGICAL SITES IN THE SOUTHERN GILF KEBIR

We reached the eastern flanks of the Gilf Kebir in mid-afternoon on September 29, 1978. Soon after, a few of us went scouting for Bagnold's 1938 camp near the large Acheulean site examined by Myers. I examined the extent of Myers work at the Acheulean site (the trenches and surface areas collected) and left impressed with his industry, and sorry he hadn't been able to publish the results of his work. Late in the afternoon, we departed for our camp at the eastern end of Wadi Wassa, arriving well after dark following a blistering chase of Haynes' lead car.

The locations of Myers' Acheulean site, and the others we visited in the southern Gilf are shown in Figure 20.2. The following pages detail our archaeological investigations at Wadi Diyaq, Wadi El-Bakht and Wadi Ard El-Akhdar.

Reduction Station at Wadi Diyaq

On October 1, 1978, while attempting to find a place for the vehicles to get to the plateau surface of the southern Gilf, we chanced upon a remarkable site. Walking up the slope toward the plateau surface, I noticed some blades and flakes among the slope scree. Just over crest, I stepped onto a surface which was littered with a continuous cover of flakes, blades, and cores.

Description of the Site. The flakes, blades, and cores were spread over a small flat area approximately 12 by 20 m. The artifacts were mainly of large size with specimens commonly exceeding 10 cm. A few large cores were scattered among the flakes and blades, and near the center of the concentration was a circular area of small-scale debitage apparently marking the location where the flaking took place (Fig. 20.3). Off to one side of the concentration of flakes and blades was an area with rough, large blocks of dark quartzite. Some of the blocks bear large detachment scars, and scattered among these blocks are more flakes, apparently the product of removing materials for reduction.

A collection of reduction specimens was made from the circular concentration of small debitage and the area immediately surrounding it. In making this collection, we observed that some flakes and blades were imbedded in the soil. A small test pit was excavated to determine the depth of the reduction materials, but limited time allowed only partial completion. Flakes and blades were present to a depth of at least 30 cm, embedded in a reddish soil matrix. Desiccation cracks filled with a soft, buff-colored sand penetrated 20 cm into this soil (Fig. 20.4). The reduction specimens from below the surface had the red soil adhering to them.

Interpretation. The identification of this site as a reduction station is based on: 1) The tremendous quantity of large and small debitage on the surface, and below, only one bifacially flaked implement; and 3) The nearby presence of the large quartzite blocks with detachment scars and the debitage around their bases.

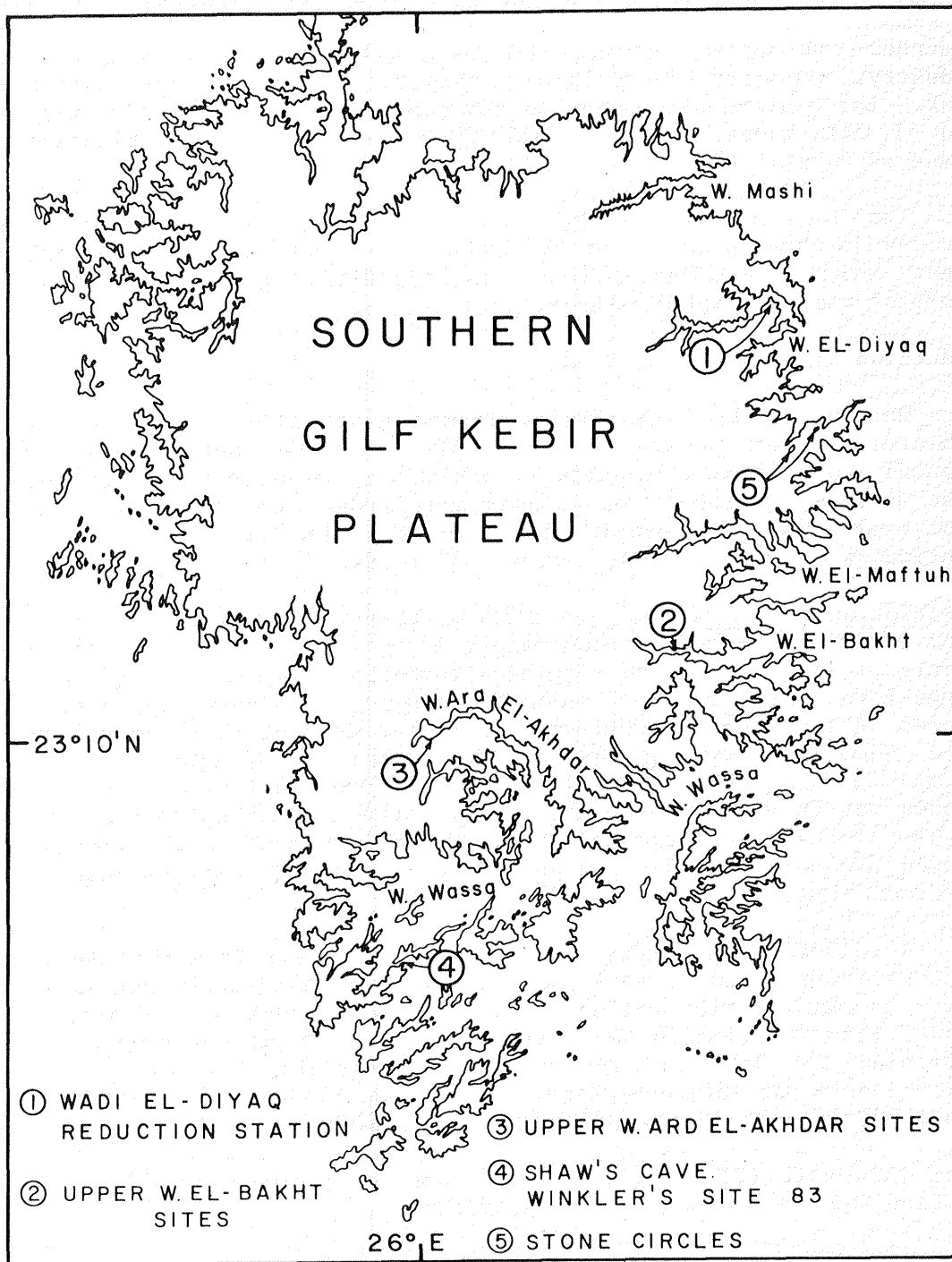


Figure 20.2 Map of the southern Gilf Kebir showing the archaeological locations investigated during 1978 expedition.



Figure 20.3 Reduction station near Wadi Diyaq; note that the surface is littered with lithic debitage.



Figure 20.4 Subsurface deposits at the Wadi Diyaq reduction station showing in situ artifacts and desiccation cracks.

The depth of the debitage within the paleosol raises the question, what mechanisms could explain the depth of lithic implements in the soil? Extended production while soil deposits were accumulating seems indicated. Yet this area still seems to represent a partially deflated surface with the continuous mantle of quartzite artifacts functioning as a lag surface. If anything, the deposit since abandonment should have been lowered through the eolian removal of sediments. The 30+ cm depth of implements mixed in the paleosol demands a process of sediment accretion during the production of the implements, or their downward displacement from original positions on the surface. Desiccation cracks are present extending more than 20 cm below the surface, but such cracks could not be the routes taken by the artifacts to lower depths. The subsurface artifacts have the red soil adhering to them, indicating the processes of soil formation and desiccation post-date the stage in which the artifacts became incorporated in the sediment.

The reduction station above Wadi El-Diyag is the only one of the Gilf sites with any substantial depth to the artifactual remains. Although deflation seems to have been the most recent dominant process, accretionary processes have been important, during which sediments and artifacts were either deposited synchronously, or the implements were lowered in a previously existing soil deposit.

It would be unwise to attempt a reconstruction of the deposition/erosional sequence at the Wadi El-Diyag reduction station on the basis of so short an examination. The substantial soil development incorporating some 30 cm of cultural remains is intriguing, to say the least. It is encouraging, moreover, to find such evidence on the Gilf plateau surface, evidence suggesting not only specialized human activity (quarrying), but also geographic and climatic conditions under which the soil could develop (moisture and vegetation). Such conditions fit nicely with the evidence of moist conditions which the wadis El-Bakht and Ard El-Akhdar contain. The reduction station near Wadi El-Diyag indicates the importance of studying the plateau surface for data on human settlement systems and correlated paleogeographic conditions. The potential significance of the plateau surface will be considered below after the discussion of the finds in wadis El-Bakht and Ard El-Akhdar.

Wadi El-Bakht

The Wadi El-Bakht was explored and mapped by members of the 1938 expedition (Bagnold and others, 1939). Near the head of the wadi, they found lacustrine deposits behind a large, wadi-straddling sand dune. During this expedition, R. F. Peel mapped the wadi, and Oliver Myers made a longitudinal profile across the ancient lake bed and blocking dune. Myers also made controlled collections from several areas on the dune and from the surface of the lake sediments (Myers, 1939). I studied the artifact remains in the Musee de l'Homme (McHugh, 1971), published a description of them, and offered a model of the late Prehistoric geographic conditions and the cultural adaptive mode as indicated by these remains and their physiographic setting (McHugh, 1974a; 1974b; 1975). On October 2 and 3, 1978, Carol



Figure 20.5 Blocking dune in upper Wadi El-Bakht, view looking west.

Breed, Jack McCauley, Ted Maxwell, Nabil Embabi, three laborers, and I investigated the archaeology, geology, and geomorphology of the upper Wadi El-Bakht.

Setting. The Wadi El-Bakht is one of the numerous, steep-sided canyons which penetrate the eastern and southern margins of the southern Gilf Kebir, and extends about 22 km into the Gilf plateau following a westerly course. Eighteen km above the mouth, the wadi turns abruptly from a short northerly course to the west and about one km farther, a sizeable dune extends across the floor (Fig. 20.5). West of the dune are the deep sediments of the ancient lake which formed behind the dune. The dune has since been breached, and a deep erosional gorge has formed in the eastern edge of the lake sediments (Fig 20.6). This deep gorge climbs steeply to the west continuing as a shallow, sand-filled, 2-3 meter wide channel which crosses the playa surface from east to west (Fig. 20.7).

The lake deposits are composed of irregularly alternating levels of hard, greyish silt and reddish sand which are exposed in the vertical walls of the gorge. These stratified deposits are generally horizontal but they do rise gradually to the east where they once abutted the blocking dune (Fig. 20.8). The reduction and planation of these ascending levels by eolian processes has produced a rough, saw-tooth-like surface in the southeastern part of the playa, south of the gorge. A 1.0-1.5 m thick, homogeneous unit of hard grey silt underlies the thin, alternating silt and sandy levels in the eastern

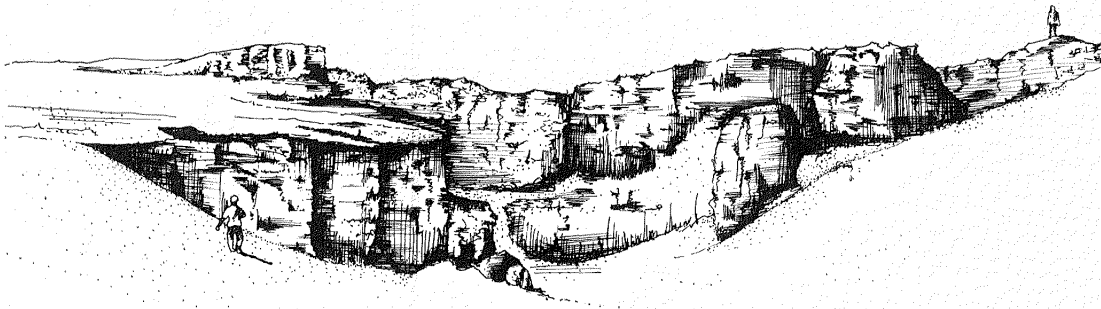


Figure 20.6 Eastern part of eroded lake deposits and breached dune in Wadi El-Bakht; view to the southwest.



Figure 20.7 Shallow, sand filled channel on the playa surface west of the gorge in Wadi El-Bakht, view to the southwest.



Figure 20.8 Northeast corner of the eroded lake deposits in Wadi El-Bakht, showing small yardangs and Area C (see Fig. 20.10) being collected.

section of the lake deposits and is exposed as the playa surface at about the western limit of the gorge. This depositional sequence is approximately 10 meters thick according to Ted Maxwell's longitudinal transect (see Maxwell, Chapter 19). Clearly, the thickness of the lake sediments must have been greater in the past as there are a series of small yardangs rising a meter or more above the general level of the playa surface along its northeastern margin.

The playa is confined within the steep walls of the 500 m wide canyon, which rise about 120 m above the playa surface. Talus deposits extend well up the sides of the canyon walls, and sand covers the lowest levels of the talus. The lake deposits abut the western edge of the dune, although an erosional moat or trough is present along the northeastern margin of the playa, below and west of the dune (Fig. 20.9). This part of the playa surface is heavily eroded; small yardangs dot the surface and indicate that the playa surface has been reduced over a large area. The visible playa deposits extend about 300 meters west of the eastern margin of the gorge and almost 200 meters north to south. Each border is covered by eolian or alluvial deposits, so these dimensions are only approximate. Near the center of the playa is a shallow depression covered by a thin (10-15 mm) deposit of recent silt, among which are some desiccated plants. This association must be the result of a fairly recent accumulation of water in this area, although there is no data for the actual age of

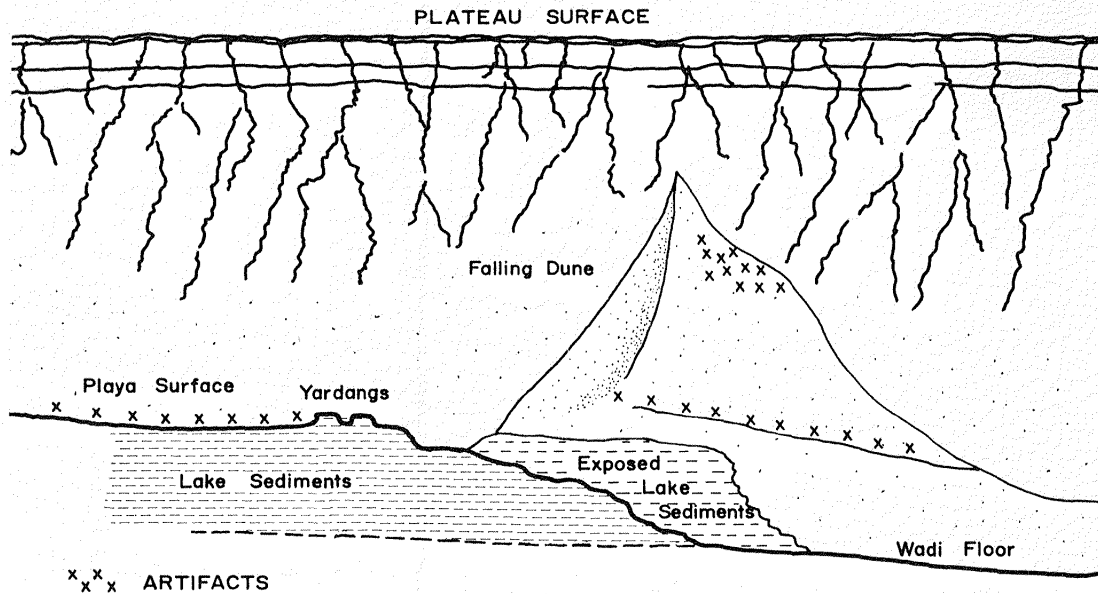


Figure 20.9 Schematic longitudinal section of upper Wadi El-Bakht showing relationships among the blocking dune, erosional gorge, playa and plateau surfaces, and locations of artifacts.

these silts and plants. We observed no other obvious evidence which could be associated with this recent wet episode, although it is conceivable that the plant stems protruding from the dune surface might be related to recent moisture.

The blocking dune at the eastern margin of the lake sediments is composed of a northern component, a falling dune, and a lower, southern component. The two components of the dune are separated by a depression where the dune has been breached, apparently by water pouring through the gorge. The dune exhibits at least three different levels which are shown in Figure 20.6.

The breached area is flanked by two shoulders whose surfaces are a little higher than the level of the playa surface. Abundant artifacts cover broad areas on both shoulders. North of the north shoulder, the dune climbs steeply up the canyon wall, and a well-defined linear crest rises to approximately 50 meters above the playa surface. East of this crest, but 10-15 meters lower, the sloping dune surface is again covered by numerous quartzite implements, a little pottery, and some ostrich egg fragments. These artifacts disappear under the crest of the dune, indicating dune development since the prehistoric settlement ended. A third surface of the dune, also lit-

tered with artifacts, is located about 80-100 meters to the east; this surface lies below that of the surface of the dune shoulders bordering the breach.

Archaeological Remains. Due to limited time, investigations in the Wadi El-Bakht were confined to the northern part of the ancient lake deposits and the north shoulder and crest of the blocking dune. Eroded channel banks downstream from the blocking dune were superficially inspected for artifacts, but only one large flake was discovered. cursory inspection of several locales along the course of the wadi failed to reveal any concentrations of artifactual materials, but it can scarcely be concluded that they do not exist. None were reported by Peel or Myers, however, although Peel recorded the location of a site on the plateau surface at the head of Wadi El-Bakht. Myers reported that he had made controlled collections at four places: one on the playa surface, two on the dune (lower dune and upper dune), and a fourth just below the blocking dune. The precise loci of these samples cannot be determined.

To facilitate our brief examination, a grid was laid out on part of the playa. A number of areas with concentrations of lithic implements or fragmentary faunal remains were identified, and both controlled and nonsystematic samples were collected. Several hearths were carefully excavated, and baked earth and charcoal were collected from them. A sketch map based on the grid system has been prepared showing the areas where we collected faunal remains, lithics, and hearth materials (Fig. 20.10). Ted Maxwell assisted in laying out the

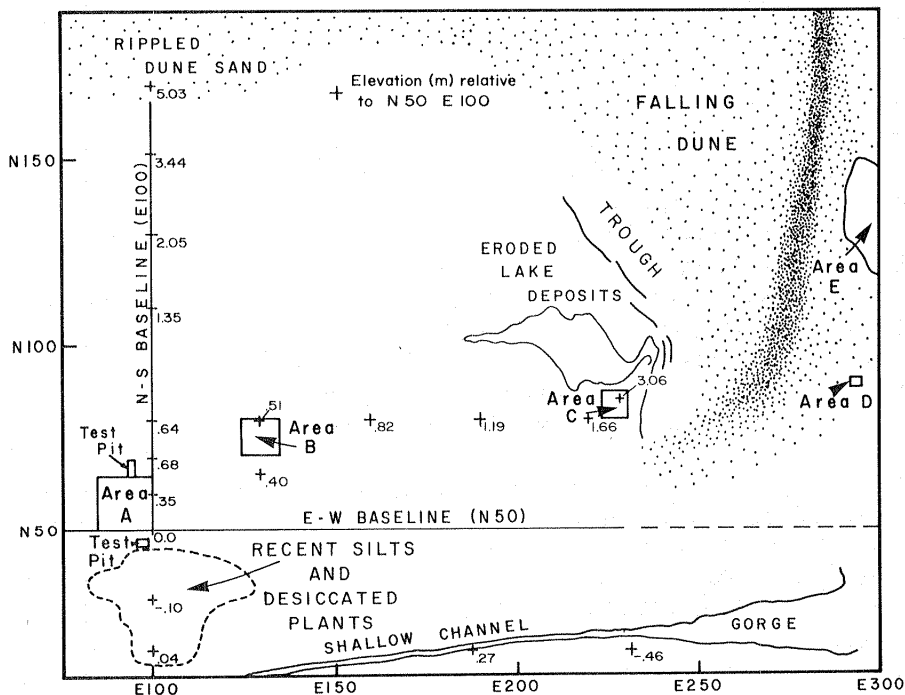


Figure 20.10 Sketch map of upper Wadi El-Bakht showing locations of artifacts collected.

grid, made the longitudinal and transverse profiles, and surveyed the elevations that appear on the sketch map. Photographs of the general area and of specific features were also taken.

My investigations of the settlement archaeology began on the north side of the central part of the playa surface, from which I moved eastward, ending on the dune surfaces. Immediately north of the recent silts mentioned above was an area with scattered artifacts and a concentration of subfossil bone fragments. The bone fragments were systematically collected from a 15 m x 15 m square, designated Area A, at N50-N65, E85-E100 (Fig. 20.10). A narrow test pit (3 m by 0.5 m deep) was excavated at the northern edge of Area A to ascertain if faunal and artifactual remains extended below the surface, but none was found. Among the bone fragments were articular processes, teeth and numerous bone splinters. The mammalian species represented by these bone remains have been identified by A. Gautier (Chapter 21) and will be discussed below.

Area B, a 10 m by 10 m square at N60-N70, E125-E135, produced a series of potsherds entirely on the surface. Area C, a 7 m by 7 m square at N80-N87, E224-E231, contained a concentration of lithic implements (f=48), one hand milling stone, abundant debitage (quartzite specimens, f=622; chalcedony or chert specimens, f=10), ostrich egg fragments and abundant pieces of rough rock. Area C is adjacent to the eroded north eastern margin of the playa and close to the small yardangs.

Systematic collections were also made at two other areas. Area D is a 2 m x 2 m square located on the northern shoulder of the dune at the western edge of a large artifact concentration (Fig. 20.11). Its exact grid location was not plotted. This square was investigated in order to determine the number of flaked versus non-flaked stone specimens and thus to evaluate Carol Breed's suggestion that this concentration of lithic materials was a naturally deposited lag surface. The counts are: flaked implements, f=362; fragments of conglomerate, sandstone, and quartzite, f=310. My interpretation based on this limited but carefully collected sample is that all these lithic materials were introduced onto the dune surface by human and not by natural agencies. These materials may indeed be remnants of a deflated surface, or lag surface, but one whose origin is artificial. The amount of possible deflation, however, needs further study. Similarly, the effect of the breaching of the dune on the distribution of dune-shoulder artifacts needs to be studied.

On the opposite shoulder of the dune, however, is another large area of artifacts within which is a local (1-2 m diameter) concentration of small-scale lithic debitage, the product of chipping at this location. This concentration cannot have been introduced by other than human activity. Interestingly, abundant plant stems protrude from the lithic remains on the south shoulder; however, it hardly seems likely that these can date from the time of the prehistoric occupation. These plant stems may be due to growth generated by the same wet episode which resulted in the very recent accumulation of silt and plant growth in the playa.



Figure 20.11 Concentration of artifacts forming a lag surface on the north shoulder of the blocking dune (Area D in Fig. 20.10).

North of Area D, high up on the east-facing slope of the falling dune, but 10-15 m below the crest, is another concentration of artifacts (lithic implements, potsherds, and also ostrich eggshell fragments). A selected sample was collected from part of this area (Area E). The western edge of this artifact concentration disappears under the crest of the dune, indicating the post-occupational movement of the present dune crest. The presence of these artifacts suggests occupation on the higher part of the falling dune surface when it must have been stabilized by moisture and perhaps vegetation. A few plant stems still protrude through the surface here.

It seems reasonable at this time to propose the following hypothesis regarding the timing and persistence of human settlement at Wadi El-Bakht: 1) Human occupation occurred late in the history of the lake; 2) Human occupation was not continuous, and two or more cultural facies are represented in the artifacts; 3) Human occupation persisted beyond the local edaphic (and climatic?) optimum; and 4) The adaptive mode of some of the groups at Wadi El-Bakht included the use of milling stones, presumably for the grinding of some unidentified plant product.

The presence of several classes of artifacts on the surface of the playa (flaked stone tools and debitage, milling stones and

ceramics) and in situ hearths and fragmentary faunal remains (bones, ostrich egg shell) make it clear that the late prehistoric occupants of Wadi El Bakht were living on the lake bed when it was dry or partially dry. The in situ hearths indicate that the present surface, or one very near to it, was occupied. The aforementioned yardangs protruding a meter or so above the main playa surface indicate that the lake deposits were formerly deeper and subsequently have been reduced, largely by eolian erosion. On the scooped out (concave) and rounded (convex) yardang surfaces, stone artifacts are found. Unfortunately, these were not collected or examined, and we cannot say at this time whether or not they were placed on the yardangs after deflation of the surface.

Based on these observations, the following conclusions can be made:

1. No Pleistocene-age Acheulean, Mousterian, or Aterian artifacts were found in the upper Wadi El-Bakht. The lake may well have formed in post-Pleistocene times. No artifacts were exposed in the lower two-thirds of the lake sediments and only one non-diagnostic flake was observed deep within the lake deposits, in the gorge, about 3 meters below the eroded and lowered playa surface. I believe that the implements on the surface of the southeastern part of the playa, where the slightly dipping lake deposits are truncated, are not eroding out of the sediments but were rather left on the already partially deflated surface.
2. It is reasonable to assume that the lake surface could not be occupied when the playa was full of water. At this time, the adjacent dune surfaces, apparently stabilized by vegetation and sub-surface moisture, were the original loci for human settlement while the blocked basin contained water.
3. Occupation of the playa surface took place during a phase when the lake was partially or completely dried up, but when water was still locally present. The water may have been confined to a limited central basin, beneath the playa surface, or in springs along the base of the wadi cliffs.
4. The occupants of both the dune and the playa surfaces utilized milling stones; presumably the plant products exploited were locally available, even when the lake was (temporarily?) dried up. The wadi floor above and below the blocking dune provides hundreds of hectares where grain-bearing plants could have grown. This suggestion does not require the presence of domesticated cereals, although the possibility of their presence cannot be discounted. In a climatic regime with rainfall sufficient to produce the playas in wadis El-Bakht and Ard El-Akhdar, seasonal moisture could well have supported the natural growth of grain-producing plants which may have been exploited by the human occupants of the two wadis.

Wadi Ard El-Akhdar

Wadi Ard El-Akhdar is a complex of canyons which penetrates the southern Gifl Kebir from its broad opening along the east-west trending Wadi Wassa. The wadi describes an arc-like course to the north, west, and finally southwest where it terminates some 35 km from its mouth. Several shorter but still impressive wadis branch away from Ard El-Akhdar. Peel and Bagnold discovered the locale of the lake deposits in the upper Wadi Ard El-Akhdar, and Peel (1939b) described it as a two-kilometer-wide basin filled with lake deposits and rich in archaeological sites. Myers apparently spent several days here, but little specific information about his work in Wadi Ard El-Akhdar accompanied the few artifacts recovered there.

Lake Deposits and Archaeological Setting. The sediment-filled basin is more accurately described as a widening of the Wadi Ard El-Akhdar above a pronounced constriction caused in part by the presence of a large basaltic intrusion. Slope talus further constricts the wadi and, at present, a falling dune partly blocks the northern half of the wadi. It would seem that an earlier dune completely blocked the wadi at some time(s) in the past, causing the formation of the lake within which were deposited some 4 to 5 m of sediment. Remnants of these sediments are perched 4 to 5 m above the wadi floor on the steep slope of the cliffside which forms the southern border of the wadi at its narrowest point (Fig. 20.12). The perched sediments require the presence of some kind of a dam, behind which the lake was impounded for a



Figure 20.12 Perched sediments on the south wall of Wadi Ard El-Akhdar at the point of greatest constriction (photo courtesy T. Maxwell).

period of time sufficient for sediments to be deposited at their present elevation above the wadi floor. This dam could have been an extended talus dam, a sand dune, or some combination of two. Whatever the cause, the wadi was blocked and during a period of enhanced precipitation, water and sediments accumulated behind the dam. On the basis of present evidence, human occupation of the area did not begin with the initial stages of the development of the lake. Additional investigations will be needed to demonstrate when humans discovered the lake and began to settle at its edges.

The setting is more complex than that of Wadi El-Bakht, where the lake was confined within a narrower canyon, where most of the blocking dune still remains, and where the playa surface shows little evidence of fluvial erosion. The Wadi Ard El-Akhdar playa is much larger than that of Wadi El-Bakht, perhaps on the order of ten times, and is much more heavily dissected by drainage channels (Fig. 20.13). The playa surface at Ard El-Akhdar varies between relatively broad areas which are almost level, to those which are undulating, to those which are deeply eroded. A wide (approximately 30 m) channel winds through the lake deposits between steep banks about 4 m high. Numerous smaller gullies dissect the playa sediments and grade, often steeply, to the main channel. Locality 100 displays the moderately undulating surface relief in the southeast corner of the playa, where artifacts are present and deflated hearths are partly embedded in the silts (Fig. 20.14). Locality 101, about .5 km west-northwest of Locality 100, occupies a flatter block of silt where concentrations of artifacts often cap the slightly higher knolls (Fig. 20.15).



Figure 20.13 Oblique view to the southwest of the dissected lake deposits in upper Wadi Ard El-Akhdar; archaeological site 100 is located at far left of photo, and site 101 is located at far right (photo courtesy C. V. Haynes).

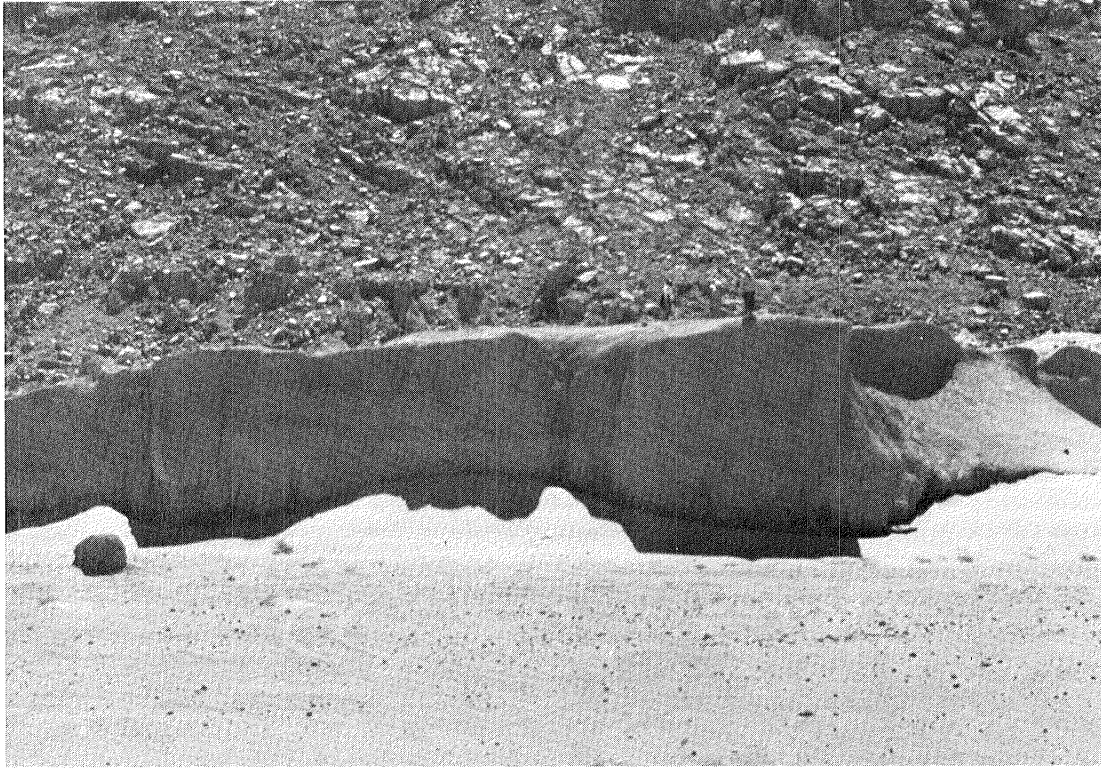


Figure 20.14 Deeply eroded lake deposits at archaeological site 100 in Wadi Ard El-Akhdar.

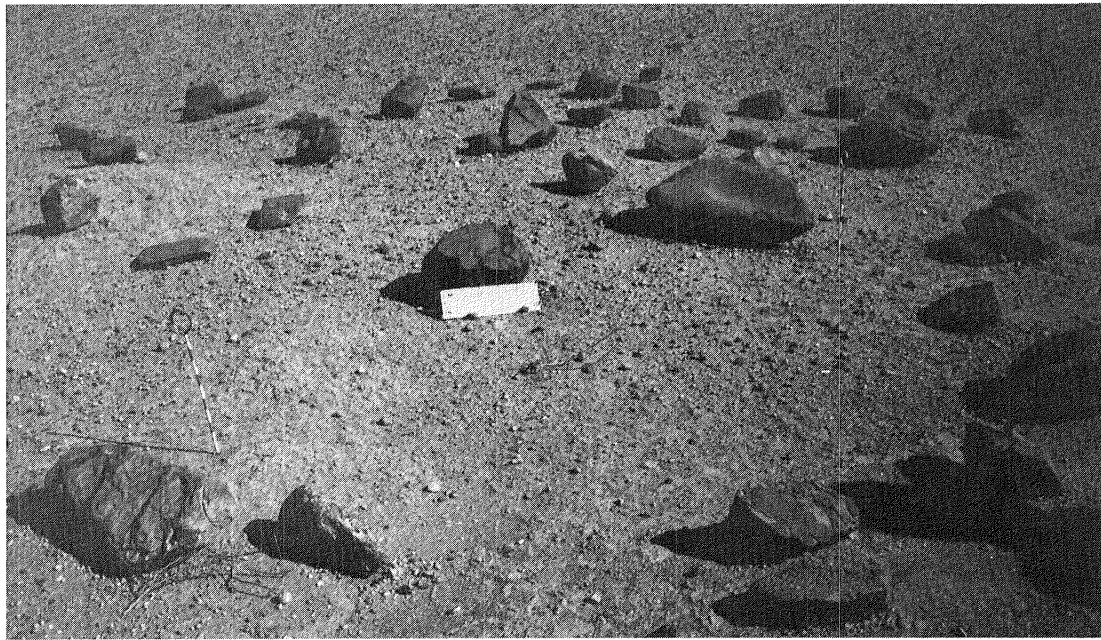


Figure 20.15 Circular concentration of large quartzite rocks and two milling stones on the surface of lake silts at site 101 in upper Wadi Ard El-Akhdar.

Geomorphic Evolution. The depositional and erosional events in the Wadi Ard El-Akhdar can be outlined as follows: 1) The wadi itself was formed over millions of years through the agencies of fluvial and eolian action, perhaps along lines of structural weakness in the sandstone of the plateau. 2) Late in prehistoric times, toward the early or middle Holocene, sand and/or fanglomerates accumulated and blocked the wadi at a constricted point. 3) In a time of rather pronounced precipitation, a lake or marsh developed behind the blocking dune, and silty sediments were deposited at the bottom of the lake. The lake must have experienced alternating dry and wet periods, for vertical "pipes" formed within the silts from the present surface to a depth of 3-4 m. 4) When the water of the lake disappeared exposing the sediments, human groups occupied the surface, making and leaving stone implements, and making fires on the surface. Presumably, water must have still been present locally, in the deeper channels or at least below the surface. 5) Sheet flooding seems to be indicated by the wide-spread gravels on the present surface in some areas. Channel incision took place in playa deposits on which artifacts were already present, for the lithic artifacts are often found in the gullies. 6) Eolian erosion caused lowering of the playa surface overall, but left remnants of the higher lake levels, and rounded off the dissected sediments. Deposition of sand took place in the main channel and other depressions. 7) Occasional, torrential rains caused the partial clearing of the main and tributary channels, and the deposition of rather coarse materials along the edges of the main channel near the constriction. This outline must be considered extremely oversimplified and provisional. In particular, the role of eolian action may be understated, being masked by the more conspicuous evidence of water-caused erosion.

The playa sediments themselves deserve some comment. First, they are not nearly as thick as those in the Wadi El-Bakht (i.e. 4-5 m as compared with 10 m). Nor do the Wadi Ard El-Akhdar sediments reveal the alternating layers of silt and sand which are so marked in the Wadi El-Bakht playa sediments. The Ard El-Akhdar sediments show evidence of more extensive fluvial erosion than those at El-Bakht where only the narrow gorge and the very shallow channel testify to running water eroding the playa deposits.

The Ard El-Akhdar sediments might have resulted from a shorter period of deposition in which persistent conditions resulted in the accumulation of a rather homogeneous deposit, without the alternation of silt and sand. This episode might equate with the "thick silt block" period at Wadi El-Bakht depositional sequence. The "thick silt block" period at El-Bakht largely predates the initial appearance of man there, and underlies the archaeological sites.

Inter-Wadi Comparisons

The playa deposits of wadis El-Bakht and Ard El-Akhdar are separated by only 30 km. Very little is known about the topography of the southern Gilf Kebir plateau surface which separates the two wadis. The term "Rough Hilly Country" occurs on Peel's map, indicating a fair degree of relief. Presumably, the two wadis have

separate catchment areas and drainage systems. Peel (1939b), however, found no evidence of developed drainage systems on the plateau surface. Such systems, perhaps never deeply entrenched in the hard, capping formations of the Gilf, may have been largely obliterated by mass-wasting at the wadi edges and by eolian erosion on the surface.

We have reason to be optimistic regarding the potential for research on the Gilf plateau surface itself, for we know that pre-historic archaeological sites exist there, and at least parts of the surface retain soil profiles. Where such soils have developed in the past, there was vegetation and, hence, rainfall. Consequently one can further deduce that some of the water falling as rain on the Gilf surface drained into the major wadis, directly by surface drainage systems or indirectly by percolating through the ground. Given the proximity of wadis El-Bakht and Ard El-Akhdar, and the contiguous relation of their respective catchment areas, the hydro-geomorphic events experienced by the two wadis may have been roughly synchronous.

According to this simplified model, rainfall in the Gilf was sufficient at some period in the past to support vegetation on the plateau surface and to collect in certain natural depressions, there to form ponds or lakes, such as in wadis El-Bakht and Ard El-Akhdar. Where no impoundments existed in the wadis, the water poured down the wadis and out onto the plains. Indeed, along the courses of the wadis the evidence of water transport and alluvial deposition is abundant; we drove along dry water-courses sometimes between cut-banks one to two meters high. The alluvial deposits in the debouchement of Wadi El-Bakht are gradually masked by wind-blown sand at its eastern margin. Wadi Ard El-Akhdar empties directly into the broad Wadi Wassa, which is full of coarse alluvial materials. In sum, the evidence of water transport and deposition of materials in the southern Gilf wadis is overwhelming. While the processes of thermal weathering, mass wasting, and eolian erosion may be the primary ones operating today, fluvial processes were significant in the past, perhaps as recently as the middle of the Holocene if our archaeological interpretations are correct.

TECHNOLOGY

Technology is that subsystem of a culture which includes the body of knowledge involved in the production of useful things, both the organization for production, as well as those things produced. The artifactual remains of any society, modern or ancient represent only part of the technology of that society. The organization for production and the body of knowledge behind the production must be inferred from that extent of the artifacts (from their morphology, inferred function, distribution and associations, age, and sources of material).

It is exceedingly difficult, if not impossible, to define a pre-historic society and to determine the total range of its activities, many of which will not be expressed in the archaeological record. It is, on the other hand, very possible to mistakenly treat artifact assemblages of different societies as being the product of a single

society. These problems plague the study of the cultural ecology of the Western Desert of Egypt as they do other areas. Nevertheless, using our relatively crude analytic and synthetic methods, we will try to understand the industries we have located, because they are manifestations of mankind's adaptations to changing environmental conditions. These cultural adaptations shed light on the last major occupation of this area before the onset of hyperarid conditions.

The lithic debitage of the four locales described above is dominated by quartzite blades of moderate to large size. The blades exhibit varying amounts of edge retouch, but complete edge modification is not common and bifacial retouch is very rare. Thus, the flake stone industries are not complex in terms of the diversity of tool types and extensiveness of retouch. This situation is not unexpected, at least for the reduction station above Wadi Diyaq. The reduction station (by definition) would not be expected to produce a variety of completed lithic implements. It was a specialized functional locality used to procure resource material (quartzite flakes and blades), which was then removed to other places for final modification and use.

The "other places" could have been the two wadis in the southern Gilf, or a campsite like the Big Barchan sites. At the Big Barchan Sites, only a select group of quartzite blades and flakes was recovered. None had been converted into fully finished implements, but each could easily have been used as is, or have been retouched to convert it into any of a number of types useful to a small group of hunters or pastoralists on an extended trip far from the sources of quartzite raw material. The extremely limited typological variation of the Big Barchan assemblage is seen as reflecting a basic tool kit of readily modified blades adaptable to different needs as determined by the success of the hunting-foraging party. No implication that the Big Barchan assemblages were brought from the southern Gilf, more than 200 km to the west, is intended.

The Wadi Diyaq reduction station could have served both Wadis El-Bakht and Ard El-Akhdar, but this seems unlikely because sources of quartzite closer to these wadis are present. In fact, Ted Maxwell (oral comm., 1978) found what may be another reduction station on a bluff overlooking the Ard El-Akhdar playa. The artifact assemblage of Wadi El-Bakht will be taken to represent those of both wadis because it has had more extensive study. In the previously published analysis of the Wadi El-Bakht materials, I described the lithic implements collected by O. Myers in 1938 (McHugh, 1974a). That sample, from four localities, lacked the smaller debitage (small flakes and bladelets, shatter) one would expect with a representative sample from a multi-functional habitation site. However, this component is indeed present at Wadi El-Bakht; we observed it in situ, and collected it from two controlled areas.

Myers' collection was also without much evidence of milling stones, but we found these to be common if not abundant. Milling slabs are present both on the dune (Fig. 20.16) and on the playa surfaces, and hand stones, some of the distinctive expanded-head pestle-shape type (sometimes termed "phallic"), were found at several

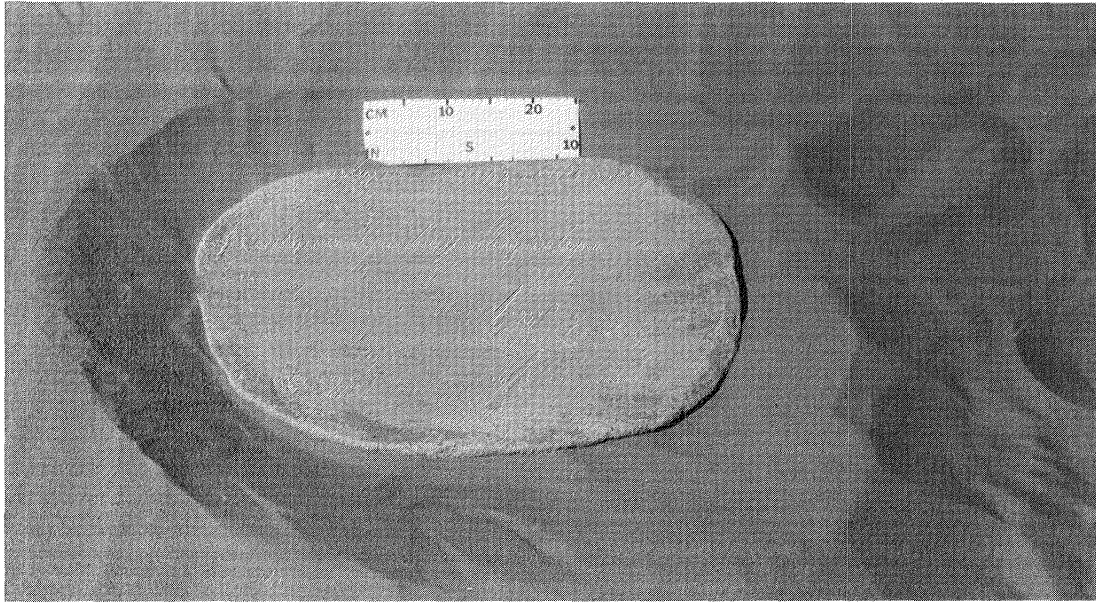


Figure 20.16 Large milling basin with shallow superior depression found buried in the sand on the blocking dune, upper Wadi El-Bakht.

locations on the playa surface (Fig. 20.17). Someone, perhaps Myers, had left a group of hand stones on a small yardang at the eastern edge of the playa. It is now clear that milling stones are an integral part of the Wadi El-Bakht assemblages, and that the activities represented by this class of implements must have been practiced there.

The final major component of the wadi assemblages is pottery, found at both the dune and playa localities at Wadi El-Bakht and at some playa localities at Wadi Ard El-Akhdar. In the Myers' collection from Wadi El-Bakht, a thin ware (3-8 mm) was common at the playa locality, and a thick ware (8-15 mm) was more common on the dune (McHugh, 1974a). This dichotomy is a real one according to our recent observations. In fact, we found some very thick (18-20 mm) sherds with extraordinarily coarse temper (granules) among the dune sherds. Some of the thin ware sherds feature incised or impressed surface designs, including chevrons and dotted-line motifs (Fig. 20.18). These designs were not present in the sample Myers collected, probably because the rim sherds and decorated sherds had been removed from the collection.

The pottery at Wadi El-Bakht, then, seems to belong to two different wares representing two different ceramic traditions, one of which, that from the dune locality, may pre-date the other. This inference on the chronological relationship of the dune and playa pottery is based both on the degree of technical refinement displayed by the pottery and their different physiographic situations.

The presence of ceramic technology at Wadi El-Bakht indicates not only a relatively late prehistoric age for settlement, but also a degree of occupational persistence and a variety of activities

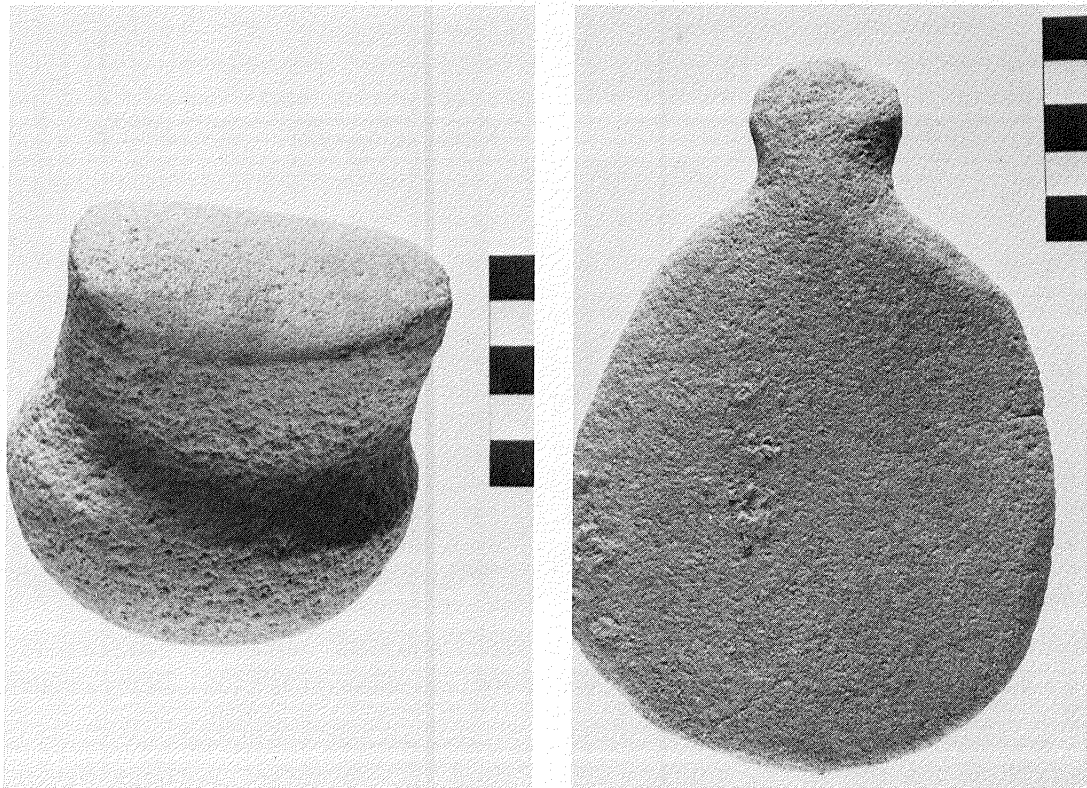


Figure 20.17 Artifacts from Wadi El-Bakht. A) Expanded head stone pestle; B) Small, flat milling stone with projecting knob.



Figure 20.18 Rim and body sherds from Wadi El-Bakht. Note the mending or suspension holes (one incompletely drilled) in three specimens, and the chevron and parallel linear surface decorations on several sherds.

involving manufacture and use of pottery. If manufactured in the wadi itself, the pottery demands, in addition to the technological knowledge and skills, the presence of suitable raw materials, clays and flammable materials (vegetation). The presence of pottery presumes the need for solid vessels for storing and transporting foodstuffs and liquids, and for cooking and preserving foods. Pottery is, after all, peculiarly related to food. The presence of pottery and milling stones in the Wadi El-Bakht assemblage combine to form a strong case for the utilization of some kind of a cereal grain.

Obvious killing implements (projectile points) are conspicuously absent from the Wadi El-Bakht assemblage, as well as from the other three sites. No bifacially flaked, tanged, basally- or corner-notched projectile points occur in any of the collections. This fact was noted in the study of the Myers collection and remains true, according to my recent observations. Also absent from all four assemblages is any significant number of geometric microliths. Microlithic implements are common in the later prehistoric industries along the Nile Valley, at Kharga Oasis, and elsewhere in north and east Africa. What the apparent absence or extreme paucity of microliths in the Gilf and nearby assemblages means in techno-economic terms cannot be determined at present. It may relate to an economic orientation or adaptive mode, still not widely recognized or understood, which existed in the southern Western Desert of Egypt in early and mid-Holocene times. This adaptive mode will be discussed after we consider the implications of the settlement system represented by the four sites.

SETTLEMENT PATTERNS AND ADAPTIVE MODES

The concept of settlement patterns is one employed by archaeologists to attempt to relate prehistoric societies and their adaptations to the natural environment. It can be a rewarding approach when data pertinent to paleogeographic conditions and temporal variations are available. The distribution of human settlements and specialized activity areas can be seen as expressions of cultural adaptations to the existing geographic conditions. During our brief expedition, we located innumerable archaeological sites, only a few of which we were able to study. Almost everywhere we stopped, where ever there was rock and in one instance where there was only sand, there were artifacts. Although the Big Barchan sites may have no relationship to the Gilf sites, they may represent the kind of site frequently reported to exist in the desert away from the Gilf and Uweinat (Shaw, 1936a). The rock art sites of the Uweinat and Gilf wadis represent another mode of prehistoric human activity, but not studied on this trip. In addition, sites with stone circles have been reported from the Gilf plateau (Bagnold and others, 1939), were observed near Uweinat by El-Baz (oral comm., 1979), and are present near Qaret El-Maiyit east of Bir Sahara.

Confining ourselves to the best studied sites, we can see three basic modes of settlement: the first within the wadis, the second on the plains surrounding the Gilf and Uweinat, the third on the Gilf plateau surface. The first is exemplified in the Wadis El-Bakht and Ard El-Akhdar and in several Uweinat wadis (karkurs). It may be an

over-simplification to group the Uweinat rock art sites with the playa-dune habitations of the Gilf wadis, but the former surely mean nearby habitation as well as graphic production. The second mode is represented by the sites around the basin northeast of Karkur Talh, Uweinat, by Van Noten (1978; p. 29), some of those reported by Shaw (1936a), and perhaps by the Big Barchan sites. A third mode may be represented by the plateau surface reduction station and the stone circles. These three settlement/activity modes can be hypothetically related by employing a diachronic model of human adaptation in the region.

The proposed model is based on the assumptions that each of the prehistoric societies represented by the artifact and graphic assemblages employed multiple strategies and a variety of techniques in gaining their subsistence requirements. It also assumes that the producers of the graphic art left traces of their other activities in other places, and that the fauna depicted in the rock art, whether wild or domestic, was present in the area when the depictions were produced. However, it is not necessary that the graphic depictions fully reflect the fauna (artistic traditions are notoriously selective). Another assumption is that the groups that inhabited the wadis, with or without lakes, were not confined to these locales, but exploited large areas on the plateau surface and the adjacent plains.

The representations of human groups and animals seen in the rock art of Gebel Uweinat and the Gilf Kebir lends itself both to chronological ordering and paleogeographic reconstruction. The following scheme, based on the data published by several authors (Shaw, 1936a; Peel and Bagnold, 1939; Winkler, 1939b; Rhotert, 1952; and Van Noten, 1978), is offered as a provisional sequence of rock art production reflecting changing adaptive modes.

Early Holocene (8000 - 6000/5000 B.C.)

The Gilf-Uweinat area was settled by scattered small groups of nomadic hunter-gatherers who gathered available plant foods and hunted such local species as giraffes, scimitar oryx, gazelles, Barbary sheep, and ostriches using dogs, clubs, shields, wheel traps, lassos, and perhaps the bow and arrow. This mode is evidenced by engraved scenes on boulders and wadi walls in Uweinat, and to a lesser extent in the Gilf.

Middle Holocene (6000/5000 - 3000/2000 B.C.)

1. Initial: Appearance of cattle (Bos sp.) in the region as graphically shown in engraved scenes, but still featuring mainly wild species.
2. Middle: Cattle become the dominant animal depicted in the engravings with wild species, dogs, and humans becoming rare.
3. Mature: Paintings replace engravings, cattle remain the dominant element but many animated human figures are portrayed, often featuring body decorations and adornment, and posed in social

activities. Dogs and wild fauna are almost entirely absent; outlines of structures are present, and there are examples of scenes depicting armed combat, perhaps ritual, between groups of opposed archers.

4. Final: Goats appear in scenes with cattle and then by themselves (perhaps heralding the on-set of the modern hyperarid regime). The latest graphics are historic age productions of camel-caravaneers and do not immediately concern us here.

The rock art sequence is still hypothetical and must be tested further. If correct, it reveals the replacement of a hunting-gathering adaptive mode by one dominated by cattle pastoralism, itself supplemented and finally replaced by goat herding. As depicted in the rock art, these replacements are not sudden or disastrous. Cattle raising may have been adopted by the autochthonous hunter-gatherers, although it seems clear that cattle were not an indigenous species in the Gilf-Uweinat area, since they were not depicted in the earliest engravings. The adoption of goats by cattle pastoralists raises no problems, but may indicate that climatic conditions suitable for extensive cattle pastoralism were beginning to deteriorate. This suggestion is supported by the paintings showing only goats in the latest prehistoric phase.

A settlement pattern model can only make sense when combined with a model of paleogeographic conditions. The rock art vividly portrays the native fauna of the region when the hunter-gatherers were the only occupants. These species (giraffes, ostrich, and scimitar oryx, but not gazelles and Barbary sheep, which are still present; Misonne, 1969b; Haynes, pers. comm., 1978) need vegetation of the savannah type. The absence of elephants and rhinos, present elsewhere in north African rock art, suggest these species were locally absent because the mesic conditions they required did not exist. The general vegetation mosaic which would support giraffes, ostriches, and scimitar oryx must be considered the minimal one which would support domestic cattle with their requirements for extensive pasturage and free water. Thus, from the fauna of the rock art, a floral pattern consisting of widespread grassy plains interspersed with trees and low brush is inferred. This picture must be coupled with seasonal variations in precipitation, solar insolation, and temperature. A semi-arid regime with summer rains and winter drought is suggested, the analog being the regime now present in the Sudanic zone to the south.

Incorporation of this seasonal analog in the paleogeographic model introduces a dynamic aspect into the model of prehistoric settlement patterns. If seasonally alternating moist and dry conditions prevailed in the Gilf-Uweinat area in late prehistoric times, the human populations would have to make adjustments to these alternations. The following scheduling adjustments are offered. During the rainy season (May-June through September-October), the vegetation over broad areas would germinate, flower, and reproduce. Water would be present in drainage channels, in inter-dune troughs, and in closed basins. Accordingly, this would be the period when native fauna, especially the giraffes, scimitar oryx, ostriches, and

gazelle would range widely across the plains and plateau surface. The Barbary sheep would have remained confined to the mountains and plateaus. The prehistoric hunter-gatherers presumably would have hunted their quarry across these same plains and during the same time collected plant foods to meet their subsistence needs.

Hunting populations are all too often considered to be solely or mainly dependent on meat for survival when, in fact, plant foods are often the more important. Significant reliance on plant foods (wild grains, especially) may have been characteristic of the late prehistoric hunter-gatherers of the Gilf-Uweinat area. The milling stones present in numerous assemblages may reflect this adaptation rather than an agricultural one. This pattern of plant exploitation would necessarily have drawn these populations onto the plains during the rainy season. In the dry season, both animal and human populations would gradually contract to those zones maintaining surface water sources, mainly the mountain and plateau wadis and playas retaining water. Initially, post-rainy season conditions would be very favorable to man and animal. Then, wadi settlement would be free from the threat of calamitous gully-washers but water and vegetation would still be abundant and life comfortable. (Is this the season when the engravings were produced?) Later, in the dry season (February-May), conditions became increasingly stressful as the dormant vegetation deteriorated and water became less plentiful and more difficult to obtain. The last month or so of the dry season may have been a crucial period in terms of human survival. Human populations which had plant collecting, especially wild grain exploitation, as a major adaptive technique had the basis of a successful survival strategy, since grain can be amassed and stored for long periods. When supplemented by the hunting of giraffes, ostriches, oryx, and Barbary sheep, species probably attracted to the wadis for water and food in the dry season, the hunter-gatherers had a viable, balanced economy well-adjusted to the prevailing geographic conditions.

This apparently well-balanced adaptive mode gave way, as shown in the rock art, to one in which domestic cattle became a predominant concern to the subsequent human populations. Domestic cattle must have been introduced into the Gilf-Uweinat area from outside as cattle are not present in the earliest engravings. Whatever their source, cattle became an economic mainstay and hunting of wild animals, but not plant collecting, retreated into the background. The cattle pastoralists also had to follow a transhumant schedule, taking their herds onto the plains during the rainy season, remaining there until pasture conditions and the lack of surface water forced retreat to the confines of the wadis where water and progressively limited vegetation existed during the dry season. Again, initially this was a season (October-December) of relative plenty, perhaps the time of feasting, ceremonies, weddings, and production of rock art. As the new year progressed, pasture for the cattle became scarce and inferior in nutritional quality and water also became scarce. As the quantity of milk declined, cereal grains collected the previous season plus butchered cattle and hunted animals served to sustain the cattle pastoralists. With the onset of the first rains in May or June, the pastoralists began returning to the plains. To remain in the wadis

would court disaster, in many instances because of torrential rains.

Such might not be the case in Wadis El-Bakht and Ard El-Akhdar which had been blocked by dunes and/or talus detritus. Water impounded here in the rainy season may have persisted longer than in typical unblocked wadis. But it is clear from our investigations that both of these wadi lakes disappeared at times and human groups moved onto the lake sediments during these dry episodes. The paleogeographic model virtually requires the Wadi El-Bakht and Ard El-Akhdar inhabitants to leave the wadis for the plains where abundant pastures and free water would be undeniably attractive. Likewise, the Gifl plateau surface may have been a locus of human exploitation during the rainy season, for it apparently also supported plant growth and settlement (reduction station soil, the sites with stone circles). The reliance of the Wadi El-Bakht and Wadi Ard El-Akhdar occupants on plant foods is indirectly but forcibly indicated by the common presence of milling stones. These plants must have, in part, been collected away from the immediate vicinity of the two wadi lakes. The presence of pottery in these two wadis is perfectly compatible with the bi-modal economic system (cattle pastoralism, grain-collecting or cultivating).

The addition of goats to this economic system presents a problem of origins, but not one of economics. In a semi-arid environment, goats would provide another important source of milk and meat (not to mention hair) to that provided by cattle. That goats contributed to the final environmental degradation of the Gifl-Uweinat flora is easy to accept, especially since Van Noten (1978, p. 22, Figure 197) describes and illustrates scenes in which the branches of trees are pulled down by goatherds for consumption by these animals.

FAUNAL REMAINS

Until now, the hypothetical model of human adaptation in southwestern Egypt derived from the rock art and settlement sites has been lacking support from paleo-osteological evidence. While the rock art proclaims the presence of a limited number of native mammals and domestic cattle and goats, no assuredly prehistoric mammalian remains associated with human occupation have been reported. The osteological remains we collected at the Big Barchan 1 site and in the two southern Gifl wadis have been identified by A. Gautier, University of Gent, who discusses them in Chapter 21.

Cattle (Bos sp.) are definitely present in Wadi El-Bakht and most probably in Ard El-Akhdar and at the Big Barchan 1 site. These are almost certainly domestic cattle. Either goat (Capra sp.) or sheep (Ovis sp.) are definitely present at El-Bakht and Ard El-Akhdar. Thus, the suggestion that the inhabitants of these two wadis were pastoralists raising cattle and goats (sheep seem unlikely) is now completely credible, if not proven. This interpretation is in keeping with the model of prehistoric cultural adaptation I have previously offered (McHugh, 1971; 1974b) although goat-herding was not included in this model.

Knowing that the late prehistoric inhabitants of the southern Gif wadis raised domestic cattle strongly reinforces the interpretation based on the geomorphic evidence from the two wadis that the Gif-Uweinat area experienced long-term mesic conditions in the early to middle Holocene. The localities in El-Bakht and Ard El-Akhdar, although perhaps unique in their preservation of a suite of intimately related geomorphic and archaeological evidence, were surely only special locales in a broad environmental zone which was amenable to the pastoralists. Therein lies the significance of the Big Barchan 1 site in the Abu Hussein dunefield with its single calf skull and soil development.

AGES

Chronometric evidence supporting the proposed model is skimpy. The suggested time periods are obviously arbitrary and only suggestive. From the Gif and Uweinat, only a few radiometric age determinations exist. From Wadi El-Bakht, a sample of ostrich egg shell gave a radiocarbon date of 7280 BP \pm 90 years (SMU-273; Wendorf and others, 1977). Vance Haynes (oral comm., 1978) reports this sample was collected from the northeastern corner of the playa. This ^{14}C date fits the model very nicely, indicating that Wadi El-Bakht was occupied at about 5300 B.C. (uncorrected for radiocarbon flux). Unfortunately this is the only radiometric date from the Gif at present, and solitary ^{14}C dates are always suspect.

The only other radiometric dates for the area are those reported by Van Noten (1978; p. 29) from the plain north of Karkur Talh, northeast of Uweinat. The sites from which the samples came are associated with a closed basin containing progressively decreasing water levels. The four dates are 6115 \pm 70 BP (GrN 6018; on wood), 4305 \pm 60 BP (GrN 7237, on ostrich egg shell), and 3320 \pm 35 BP (GrN 6018, on tree wood). These determinations translate to a range of from 4165 B.C. to 1370 B.C. (uncorrected for radiocarbon flux). The ostrich egg shell samples are reported to be associated with neolithic artifacts, and the tree wood sample from an apparent neolithic surface (Van Noten, 1978, p. 29). These dates indicate that the neolithic occupations may have spanned some 2800 years near Uweinat. It seems unlikely that this neolithic settlement was continuous. The basin probably contained water at several times attracting groups to the playa edge who remained for undetermined periods only as long as the water remained. This interpretation implies a series of recurrent moist episodes in the Uweinat area between 4200 and 1400 B.C.

The single ^{14}C date from Wadi El-Bakht (7280 \pm 90 B.P.) and its application to the occupation by pastoralists should not be considered remarkable. It is supported by the ^{14}C date of 8170 \pm 120 B.P. (A-1966, also on ostrich egg shell) from the Big Barchan 1 site which produced a solitary juvenile Bos skull and a developed soil profile. Additional support for early cattle and goat domestication comes from Napta Playa, about 100 km west of the Nile. Here Fred Wendorf and his colleagues have uncovered remains of neolithic settlements including the osteological remains of domestic cattle and goat (or sheep) dating to before 7150 \pm 130 B.P. (SMU-242; Wendorf and others, 1976; and pers. comm., 1978).

Thus, it would appear that a broad zone across southern Egypt was suitable for raising cattle and goats in early and middle Holocene times. The implications of these discoveries for our constructs of Egyptian and Nilotic prehistory are dramatic. It would seem, on present evidence, that the southern Western Desert of Egypt, or more broadly the northeastern Sahara, may have begun to experience the so-called "Neolithic Revolution" before the Nile Valley did.

SUMMARY

Our brief expedition to the southern Western Desert of Egypt and especially to the Gilf-Uweinat area has produced abundant evidence indicative of the paleogeographic and cultural ecological potential of this vast region. This evidence takes on new significance in relation to recent discoveries elsewhere in southern Egypt (outside the Nile Valley). This region was not uninhabited during the early and mid-Holocene but was rather extensively occupied by wide-ranging hunter-gatherers and, later, cattle pastoralists-cultivators. These interpretations may force a reappraisal of Nilotic culture history during this period. The paleogeographic evidence from the Gilf Kebir and Abu Hussein dunefield must have implications for the Nile borderlands as well. The geographic discontinuity between the southern Egyptian and Nubian Nile Valley and the Western Desert, so long assumed in constructs of Nilotic culture history must now be seriously questioned.

Disregarding the Nilotic connections and confining ourselves only to the paleogeographic and cultural ecological potential of the Gilf-Uweinat area, the research problems are formidable. The previous sections of this paper have obviously concentrated on the late prehistoric cultural adaptation (early to middle Holocene). While artifactual evidence is clearly abundant, the total range of settlement modes and exploitative practices is very poorly known. The associated geographic conditions are even less well known. Several seasons of research could easily be devoted to this time period covering only a few millenia.

Yet there remain scores of millenia to be studied, for human occupation as old as one hundred to two hundred millenia exists in the area (e.g. the Acheulean site discovered by O. Myers). The nature of Acheulean adaptation in the Gilf and Uweinat is a mystery, and the cultural stages between the Acheulean and the Holocene cultures is even more so. What paleographic conditions existed in Acheulean and in the late Pleistocene to the Gilf and Uweinat cannot even be sketched. Thus, the known period of human occupation is in need of an immense amount of research.

Although the discoveries of archaeologists will be of some interest to the geologists, especially those concerned with the results of changing climatic conditions of the past 200,000 years on the landscape, the results of eons of geologic processes remain to be studied. The value of coordinated archaeological and geological research is obvious. The archaeologist can potentially provide dates for deposits and climatic episodes for the recent past (2×10^5 years

ago). A comprehensive sequence of paleoclimatic episodes covering this period, developed through coordinated archaeological and geological research, could provide the geologists with analogs useful for the study of earlier periods.

ACKNOWLEDGMENTS

I am deeply indebted to Farouk El-Baz for inviting me to join this expedition and to Bahay Issawi for making it at all possible. I also want to thank all the other members of the expedition for sharing their specialized knowledge, equipment and supplies with me. I am especially thankful to Vance Haynes for a ¹⁴C date and other information, and to Achilles Gautier, University of Gent, for the identification of the osteological remains collected on this expedition.

Chapter 21

NEOLITHIC FAUNAL REMAINS IN THE GILF KEBIR AND THE ABU HUSSEIN DUNEFIELD, WESTERN DESERT, EGYPT

ACHILLES GAUTIER

Laboratorium voor Paleontologie
Rijksuniversiteit Gent
Gent, Belgium

ABSTRACT

Faunal remains from the archaeological site in Wadi El-Bakht and from the region surrounding the Gilf Kebir consist of elephant, bovid, addax, gazelle, goat, jackal, ostrich, wild donkey and dog. Several of these animals are depicted in the rock art at Gebel Uweinat, although presently only sheep, goat and donkey have been reported from this area. Identification of remains found by W. P. McHugh during the 1978 expedition indicates the prior existence of domestic cattle and sheep or goat in the upstream portions of Wadi El-Bakht, and the probable existence of cattle in Wadi Ard El-Akhdar. A single sample from the Abu Hussein dunefield, 200 km east of the Gilf Kebir, consists of a poorly-preserved skull that may represent a calf or small-size bovid. These native faunal remains provide evidence for the occupation of the area by Neolithic-age pastoralists.

PREVIOUS STUDIES

Evidence for animal life in Neolithic times in the Gilf Kebir and in Gebel Uweinat is provided both by faunal remains and rock art. Faunal remains from the Gilf Kebir were collected by O. H. Myers in 1938 (Bagnold and others, 1939) and are housed in the British Museum of Natural History in London. According to preliminary identification by D. M. A. Bate and J. W. Jackson, this collection includes Elephas sp. (elephant), Bos sp. (large bovid); Addax cf. nasosulcatus (addax), Damaliscus sp., Gazella sp. (gazelle), Capra sp. (goat), Canis cf. anthus (jackal), Struthio camelus (ostrich, presumably in the form of eggshell fragments) and Equus asinus (wild donkey) (J. Cluttonbrock, pers. comm.). Unfortunately, the exact provenance of these remains is not known, though it is likely that some of them were associated with the cultural materials recorded or collected by Myers, especially at the site on the playa in the upstream portion of Wadi El-Bakht (McHugh, 1974a; 1975).

In 1975 the Combined Prehistoric Expedition (Wendorf and others, 1977) visited the Gilf Kebir area and collected prehistoric cultural and faunal materials from the site at Wadi El-Bakht previously recorded by Myers. A sample of ostrich eggshell fragments (SMU-273) gave a radiocarbon date of 7280 B.P. \pm 90 years (Wendorf and others, 1977). The scanty mammalian remains include vestiges of large dog

(Canis lupus f. familiaris), dorcas gazelle (Gazella dorcas), and sheep or goat (Ovis ammon f. aries or Capra aegragus f. hircus) (Gautier, not dated). This assemblage is basically comparable with part of the Myers collection (Bos sp., Gazella sp., Capra sp., Struthio camelus, Canis cf. authus, which may rather be a domestic dog). In this report, faunal remains collected by W. P. McHugh in October 1978 will be described.

RECENT FAUNAL OCCUPATION

Notes on the rock art from Wadi Hamra and Wadi Sura in the Gilf Kebir were published by Rhotert (1952). The animals depicted include ostrich, a medium sized antelope, giraffe, gazelle, domestic cattle and dog. A detailed study of the rock art at Gebel Uweinat was recently published by Van Noten (1978), who tentatively distinguishes five phases of faunal occupation: (1) engravings with wild herbivores and ostriches; (2) engravings with game as well as domestic cattle (not well documented); (3) engravings with cattle (predominantly long-horn); (4) paintings with short horn cattle and later goats; and (5) engravings with dromedaries and other domesticates. Neolithic surface materials found by Van Noten include ostrich eggshell fragments, grinding stones and lithics, and faunal remains of Gazella soemmeringi in the plain to the north of Karkur Talh, which are dated between 6100 and 3300 BP (Van Noten, 1978; p. 29). An elephant molar fragment (Elephas africanus) was also found associated with pottery near the entrance of Karkur Ibrahim. These sites are thought to be contemporary with the shorthorn pastoralist phase. The faunal remains of caprovid (goat or sheep) and domestic cattle from the Gilf Kebir can also be attributed to that phase, or more precisely to the second part, in which small livestock appear. The finds in Myers' collection of Elephas sp., Addax cf. nasosulcatus, Damaliscus sp. and Equus asinus may date from the first part of the second rock art phase, though it is also possible that they represent game contemporaneous with the shorthorn pastoralist phase. A reinvestigation of this material is necessary in order to further define the age relationships.

The present large mammalian faunal remains of large mammals at Gebel Uweinat and the Gilf Kebir is very limited. Only Barbary sheep (Ammotragus lervia) and gazelle (Gazella dorcas, G. leptoceros) are recorded from Gebel Uweinat. Human settlement is also almost non-existent, but in 1968-69 one Toubous family with about sixty goats, twelve dromedaries and a dozen or so semi-wild donkeys was living at Gebel Uweinat (Van Noten, 1978; p. 22). Fifty years ago, however, this area was still visited regularly by small numbers of Toubous shepherds. It is possible that the degradation of the environment, initially due to climatic change, continues very probably as a result of the destructive influence of man and his livestock. Indeed, some of the younger rock paintings depict herds of goats accompanied by men busily tearing off branches to feed animals (Van Noten, 1978; p. 32). Goats may have been introduced in the area after desiccation set in, but they certainly contributed more than other livestock to the destruction of the delicately balanced and sparse vegetation.

SETTING

The first assemblage comprises finds from prehistoric settlements on the playa, the blocking dune, and upstream from the playa in Wadi El-Bakht, a steep-sided canyon which penetrates some 20 km into the southern Gilf plateau. The second assemblage was collected from a playa accumulation with associated prehistoric sites (site 100 and site 101) in Wadi Ard El-Akhdar, formed in a way comparable to the playa in Wadi El-Bakht. The alluvial sequence at Wadi Ard El-Akhdar, which consists of compact silts, may be contemporaneous with the comparable sequence in the Wadi El-Bakht playa, where compact silt deposits, apparently devoid of archaeological material are followed by alternating silts and sands. A third assemblage consists of one sample only, collected at the Big Barchan site I in the Abu Hussein dunefield, well east of the Gilf and about 35 km southwest of Bir Sahara. The dune site is associated with a dull, reddish soil containing fine rootlets, the age of which remains unknown. The associated lithics form a rather poor assemblage, suggesting a very transitory occupation and only limited economic activities.

In the following inventory, the locations of remains refer to the grid lines of McHugh (Chapter 20). Identifications were made with the aid of comparable materials from the same area and elsewhere in Egypt (the Nabta playa), and the recent osteological collections of the Laboratorium voor Paleontologie. The remains described below are now included in the collections of this laboratory under Number P2532.

WADI EL-BAKHT ASSEMBLAGE

- No. 9: Playa surface between N52-N62.5 and E87-E97.5; bone splinters and flakes mainly of large long bones, and one fragment of the symphysis of a large bovid jaw (domestic cattle, Bos primigenius f. taurus).
- No. 10: Playa surface at about N71, E116; one fragmentary scapula of a large bovid, possibly domestic cattle.
- No. 13: Playa surface at N53, E97.5; probably of a large bovid; two fragments of a distal humeral epiphysis of a large bovid, probably domestic cattle. The width of the articular end is approximately 61 mm, which suggests an animal of rather small size when compared to the measurement of the large series on Latene cattle of Manching (approximately 125 mm; Boessneck and others, 1971). One jaw fragment with damaged P4, M1 and M2 is either sheep (Ovis ammon f. aries) or goat (Capra aegragus f. hircus).
- No. 15: Wadi above the playa, exact provenance unknown; some pelvic fragments of a medium sized bovid, in all probability sheep or goat.
- No. 16: Playa surface at N101, E207; completely fragmented jaw of sheep or goat.

- No. 17: Playa surface, eastern area, precise provenance unknown; one proximal moiety of a caprovid metacarpal, probably derived from a goat (see Fig. 66A in Boessneck and others, 1964); proximal transverse diameter: 21.0 mm.
- No. 19: Area E, dune on north side of wadi, eastern face; one vertebral fragment of a large animal, possibly large bovid; one flake of a large long bone.
- No. 20: Area C, surface of eastern edge of playa, N80-N87; E224-E231; cluster of teeth fragments of a large bovid, indistinguishable from analogous fragments of relatively small domestic cattle.
- No. 28: Playa surface at N103.5, E106-107.5; several splinters and flakes predominantly of a large bone (or bones). This sample was recorded as being from Wadi Ard El-Akhdar, but both the collection date (10/3/78) and the coordinates recorded on the label indicate that it is from the Wadi El-Bakht playa (McHugh, pers. comm., 1979). It is therefore included in the Wadi El-Bakht assemblage.

WADI ARD EL-AKHDAR ASSEMBLAGE

- No. 25: Playa surface, site 100, at about N99, E114; four eolized fragments of a large long bone (or bones).
- No. 26: Playa surface, area A; six eolized fragments apparently all derived from a large long bone (or bones).
- No. 27: Playa surface, area B; several eolized fragments of a large long bone (or bones).
- No. 35: Playa surface, site 101, area E; one jaw fragment with incomplete and much worn M1 and M2; either sheep or goat.

ABU HUSSEIN DUNEFIELD SPECIMEN

- No. 21: Big Barchan site 1; very fragmentary and poorly preserved skull remains embedded in sediment and partially truncated by eolian activity. The recognizable fragments include a bullae tympanica and skull base elements (condyle and basioccipital). These specimens cannot be attributed to Gazella dorcas (dorcass gazelle), Ammotragus lervia (Barbary sheep), sheep, goat or other medium sized bovids, because of morphological and overall size differences. They are, however, morphologically comparable to their analogs in domestic cattle, but smaller. The bullae are about 0.8 times smaller, and the condyle and basioccipital are about 0.6 times smaller. This suggests that we are dealing with a juvenile animal (calf), but unfortunately no comparative material of this developmental stage of cattle is available to me. Moreover, the remains are very poorly preserved. The identification must therefore remain tentatively as a medium-sized bovid, possibly juvenile cattle.

SUMMARY

As can be seen, the Wadi El-Bakht and Ard El-Akhdar assemblages contain both small livestock and remains derived from large animals, most likely cattle. Undeniable evidence for cattle was found at Wadi El-Bakht only, probably because the samples from that area are larger than those from Wadi Ard El-Akhdar. At any rate, both assemblages are comparable with the one collected at Wadi El-Bakht by the combined Prehistoric Expedition, which fits in the later rock paintings phase of Gebel Uweinat (shorthorn cattle and small livestock). Presumably, this phase is related to younger neolithic settlements in that area and in the Gilf Kebir. The size of the cattle is consistent with this interpretation, since we can assume that the shorthorn cattle was probably smaller than the longhorn cattle preceding it.

The sample from the Abu Hussein dunefield is tentatively ascribed to domestic cattle. The poor contextual data, however, are confusing and several explanations are possible: a transitory camp site of hunters, cattle raiders, pastoralists in search of lost cattle, or maybe a poorly defined activity area at the edge of a large (now inaccessible) site of less transitory nature (see McHugh, Chapter 20). Further research in both the Gilf Kebir and Gebel Uweinat could be very rewarding for the assessment of the marked faunal changes (disappearance of native fauna, including elephant, etc.) which occurred there in the late Quaternary.

**Page Missing in
Original Document**

Chapter 22

THE FLORA OF GEBEL UWEINAT AND NEIGHBORING REGIONS, SOUTHWEST EGYPT

LOUTFY BOULOS

National Research Centre
Dokki, Cairo, Egypt

ABSTRACT

Only a few investigations have been made of the flora of Gebel Uweinat or surrounding terrain, although these previous studies have resulted in the listing of 55 plant species from the region. In this paper, the results of 165 identifications of samples collected during 1968, and 32 identifications of samples collected during 1978 are summarized. In the Uweinat region, 73 species are now known to exist, of which 7 are cultivated.

PREVIOUS BOTANICAL EXPLORATION

Among the several expeditions to Gebel Uweinat, only few have paid some attention to the study of its flora. Gebel Uweinat is not unique in this regard, however, since few investigations have been made of the flora of the Gilf Kebir or surrounding desert regions. The pioneer works of Hassanein Bey (1924b) and Prince Kemal el Din Hussein (Hussein, 1928) provided very little botanical information about the newly-discovered Gebel Uweinat and Gilf Kebir plateau. Shaw (1931) and Shaw and Hutchinson (1931; 1934) gave the first accurate botanical information about Gebel Uweinat and the Gilf Kebir, as a result of the collections made by Shaw during the two expeditions of Major R. A. Bagnold in 1929-1930 and 1932. Hutchinson (1933) gave an additional brief botanical account on the 1929-1930 expedition.

In 1933, the expedition of Marchesi to southern Cyrenaica reached Gebel Uweinat, where plant collections were made by Di Caporiacco. One year later, Monterin collected specimens from Gebel Uweinat during the expedition of the Royal Geographical Society of Italy. Botanical results of both Italian expeditions in 1933 and 1934 were published by Corti (1939), in which he identified and provided information about 27 species from Uweinat.

The Trans-Saharan Belgian expedition of the winter of 1964-1965 passed by Uweinat. Leonard (1966) gave a brief account about the expedition and reported the presence of 25 different flowering plants from the foot of Gebel Uweinat, but did not give their names.

In 1967, the United States Naval Medical Research Unit Number Three (NAMRU-3) visited Uweinat. Osborn and Krombein (1969) gave an account on its flora, and provided a list of 55 plant species of which 45 were covered by the collections of Osborn. The extra 10 species were compiled from Shaw (1931) and Shaw and Hutchinson (1931; 1934).

From October 1968 to January 1969, a Belgian-Libyan expedition visited Uweinat. The Belgian group camped in Karkur Talh, with a small camp near Gilf Kebir. I joined the expedition for the first two months, representing the University of Libya, and camped independently near Ain Zuwia. The published results of the Belgian expedition included a chapter on the flora (Leonard, 1969), and another account on the flora and vegetation of Gebel Uweinat was presented by Leonard (1971). In both papers, Leonard described the vegetation, often citing the plants by their generic names without giving names of the species.

My unpublished collections of 1968 (165 identifications from Gebel Uweinat) as well as those from the 1978 expedition (32 identifications from Uweinat and southwestern desert of Egypt) form the basis for the comments on the vegetation presented here.

The main collections from Gebel Uweinat, the Gilf Kebir and the neighboring areas are deposited in the following herbaria: Jardin Botanique National de Belgique (BR); Botany Department, Faculty of Science, Cairo University (CAI); Field Museum of Natural History, Chicago, Illinois (F); Istituto Botanico, Firenze (FI); Royal Botanic Gardens, Kew (K) and University of Libya (now Al Faateh University), Tripoli (ULT).

VEGETATION

The scarceness of rain, which may fall once every seven to ten years in Uweinat, and up to twenty years or more in the Gilf Kebir and other areas, may explain the extremely scattered spots of vegetation, sometimes separated by hundreds of miles of sterile desert. The rain is not only erratic in terms of intervals but also in terms of quantity. In the area studied during the 1978 expedition, four vegetation types are recognized (Boulos, 1980).

Ephemeral Vegetation

Ephemeral, or annual plants appear after occasional rains, continue to grow and complete their life cycle in a period from several days to one year, and then dry up. The length of their life span usually depends on the amount of rain water available to them. The seeds of ephemerals are known to be resistant to the drought and heat characteristic of this and similar deserts, and may remain in the soil for several decades until the next rain, and then germinate.

In the Gilf Kebir region, the dry remains of some plants suggest that certain perennials may behave as ephemerals in order to produce seeds in a shorter time, e.g. Zilla spinosa (Turra) Prantl, Trichodesma africanum (L.) R.Br. var. abyssinicum Brand and Citrullus colocynthis (L.) Schrader. I propose here, to call these and other perennials which can possibly acquire the life form of annuals as "pseudo-annuals".

According to a NOAA satellite image, it was cloudy December 16-17, 1977 over an area 5 km southeast of Peter and Paul mountains,

50 km northeast of Gebel Uweinat. As our expedition passed by a small wadi with sandy soil and trachyte boulders, some plants were still growing on October 20, 1978. The only species which was rather green and bore flowers and fruits, though showing some signs of senility was Fagonia arabica L., while Stipagrostis plumosa (L.) Munro ex T. Anders. was almost dry. Farsetia ramosissima Hochst. and Trichodesma africanum var. abyssinicum were perfectly dry. Considering that these plants have germinated after the rain of December 1977, 10 months before we saw them, it may be concluded that the perennial Fagonia arabica and Trichodesma africanum var. abyssinicum changed their growth form from perennials into pseudo-annuals to meet these severe and unfavorable conditions. Stipagrostis plumosa and Farsetia ramosissima, which are known to be annuals or perennials, successfully acquired the annual habit by producing their seeds that are now kept in the soil for the next unpredictable shower.

Ephemeral and Perennial Vegetation

Ephemeral and perennial plants occur mixed together in wadis and water catchments. They are entirely dependent on rain where no perennial ground water or other permanent water supply is available. The difference between this and the previous category, where only perennial vegetation could occur, is the availability of rain and run-off, which form a layer of temporary underground moisture available to the root system of perennial plants. The life time of perennials is usually 3 to 4 years in this region. This temporary moisture ceases to exist due to the irregularity of rainfall and rapid evaporation. The difference between this and the next category, where perennial vegetation occurs near wells, is that the continuous supply of water from the wells allows long-living trees to exist as well as smaller plants, irrespective of rain.

Ephemeral and perennial vegetation is typified by vegetation in some wadis of the Gilf Kebir, particularly Wadi El-Bakht and Wadi Ard El-Akhdar. During our 1978 visit, the vegetation was quite dry. However, it was possible to identify the following species: Panicum turgidum (perennial), Zilla spinosa (perennial), Stipagrostis plumosa (perennial or annual), Trichodesma africanum var. abyssinicum (pseudo-annual), Anastatica hierochuntica L. (annual).

Perennial Vegetation Near Wells

The conspicuous perennial vegetation in the vicinity of wells consists of trees, shrubs and perennial herbs. Around the five wells (Bir Tarfawi, Tarfawi West, Bir Kiseiba, Bir El-Shab and Bir Kurayim) which we visited during our 1978 expedition, several species grow and cover small to large areas, depending on the abundance of water and its availability to the plants. The most luxuriant growth is certainly that at Bir Tarfawi, where palm trees of Hyphaene thebaica (L.) Mart. (dom palm) and Phoenix dactylifera L. (date palm) as well as Tamarix nilotica (Enrenb.) Bunge, grow in dense groves. Some huge trunks of Tamarix nilotica trees were found lying on the ground mixed with the debris of its leaves and branches, suggesting that Tamarix trees flourished in the not too distant past. This may also suggest



Figure 22.1 Dense growth of Typha domingensis (foreground) and Imperata cylindrica (background) around Ain Brins, Karkur Murr, Gebel Uweinat. October 27, 1978.



Figure 22.2 Close-up view of Cassia italica shrubs in the bed of Karkur Bu-Hleiga at Gebel Uweinat. November 7, 1968.

that the ground water has become depleted and may no longer support large trees as it did a hundred to probably a few hundred years ago.

In the vicinity of other wells, Tamarix nilotica grows as shrub-forming hummocks. At Bir Tarfawi West, these hummocks unite and form enormous crescent-shaped hills of pure stands without being associated with any other plant species. Acacia ehrenbergiana Hayne, a shrubby form about one meter high, was recorded 25 km northwest of Bir Kiseiba, on a hummocky sand dune.

The herbaceous perennials are mainly grasses; Sporobolus spicatus (Vahl) Kunth grows around the wells very close to where the water level approaches the soil surface, normally a saline soil. Imperata cylindrica (L.) Beauv. and Phragmites australis (Cav.) Trin. ex Steud. grown near and around Bir Kiseiba and Bir Kurayim. Stipagrostis vulnerans (Trin. & Rupr.) de Winter, another perennial grass with stiff sharp spiny leaves, formed a pure stand extending over one kilometer on the sand dunes near El-Shab. Alhagi mannifera Desv., a perennial leguminous shrublet with spiny-tipped twigs and dull brown lomentoid fruits, was recorded from Bir Tarfawi and Bir Kurayim, covering extensive parts of the ground in the drier, or seemingly dry areas near the wells. It constitutes an excellent fodder, especially for camels.

Perennial Vegetation in Gorges

The perennial vegetation in the winding gorges (Karkurs) of Gebel Uweinat depend on ground water. Occasional rains may feed the ground water and allow ephemeral vegetation to appear shortly after showers. The following three vegetation types are recognized in the gorges.

Vegetation near springs. This vegetation, which is restricted to the vicinity of springs within the gorges, may be compared to the perennial vegetation near wells described previously. The difference between these types of vegetation near wells lies in the open desert (or an oasis-like vegetation), while spring vegetation is located within a closed system and consists of gorge or wadi-like vegetation. Ain Brins at Karkur Murr provides an example of wadi vegetation, where the following perennial water-loving plants grow near the springs: Typha domingensis Pers. Phragmites australis, Imperata cylindrica and Juncus rigidus Desf. (Fig. 22.1). The date palm, Phoenix dactylifera is also recorded; however, only small scattered trees occur. Some annuals grow on the muddy borders of the springs; Eragrostis aegyptiaca (Willd.) Del., Polypogon monspeliensis (L.) Desf. and Portulaca oleracea L.

Herbs and Small Shrubs. This type of vegetation is commonly found in the gorges (Karkurs) of Gebel Uweinat. It comprises perennial herbaceous and small shrubby species, almost in the complete absence of trees. The following are the most characteristic: Aerva javanica (Burm.fil.) Juss. ex J. A. Schultes var. bovei Webb, Cassia italica (Mill.) Lam. ex Steud (Fig. 22.2), Citrullus colocynthis (L.) Schrad., Pulicaria crispa (Forssk.) Benth. & Hook. fil., Crotalaria thebaica (Del.) DC., Pergularia tormentosa L., Cleome chrysantha Decne, Cleome

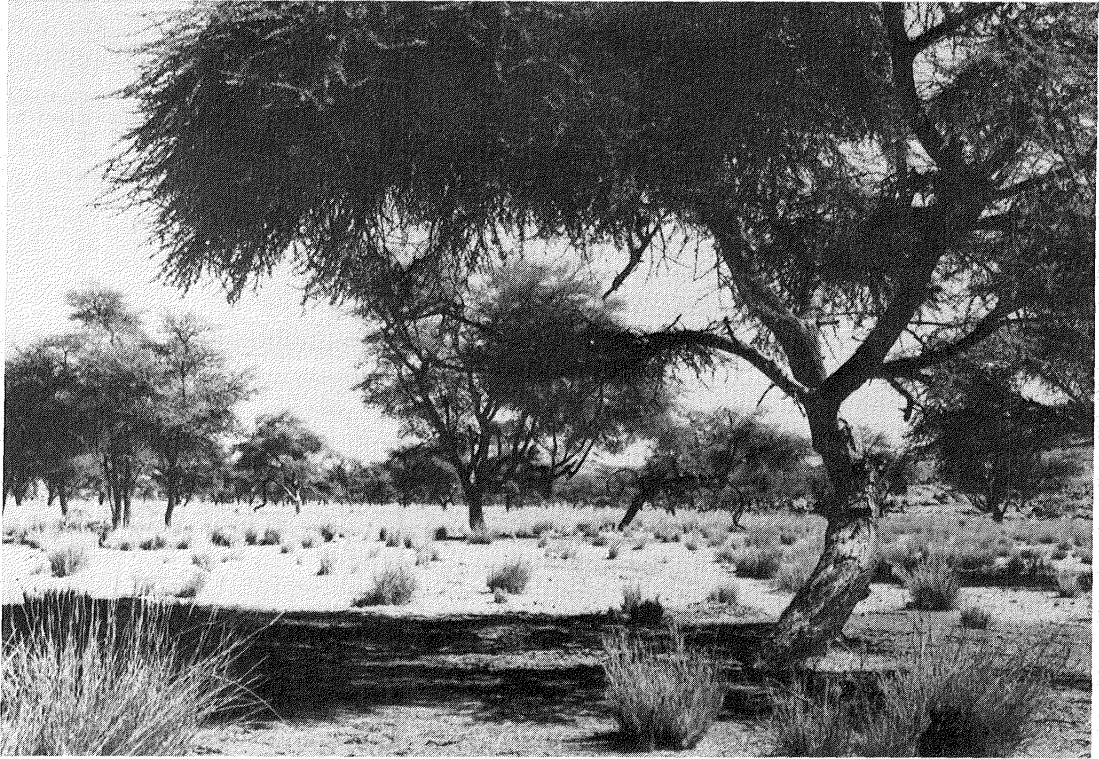


Figure 22.3 Luxuriant growth of Acacia raddiana trees in Karkur Talh, Gebel Uweinat. Note the tufts of the perennial grass Panicum turgidum. October 28, 1968.



Figure 22.4 Ficus salicifolia, a small tree growing between granite boulders at 850 m altitude, Wadi Abd El-Malek, affluent of Karkur Ibrahim, Gebel Uweinat. November 15, 1968.

droserifolia (Forssk.) Del. and Fagonia thebaica Boiss. One or a few species may stretch over the greater part of a gorge. Toward the mouth of gorges, where they join the open desert, Fagonia indica Burm. fil. and Stipagrostis plumosa are more common.

Trees. These are restricted to four species: Acacia raddiana Savi., A. ehrenbergiana, Maerua crassifolia Forssk. and Ficus salicifolia Vahl; the last three species are also known in shrubby forms in this area. Usually the two Acacia species grow together and are associated with perennial grass Panicum turgidum (e.g. in Karkur Talh; Talh is the local vernacular name of A. raddiana). The conspicuous element of the vegetation is mainly due to the luxuriant growth of A. raddiana (Fig. 22.3), which forms an open thorny forest together with the less common A. ehrenbergiana. Dense tufts of Panicum turgidum cover a high percentage of the Karkur bed.

In Wadi Abd El-Malek, however, Acacia trees are almost absent, while Maerua crassifolia trees are abundant, and Ficus salicifolia trees start to appear at about 850 m altitude (Fig. 22.4).

Vegetation of Higher Altitudes

According to Leonard (1971), Ochradenus baccatus occurs between 900 and 1400 m, while Lavandula, Salvia, Heliotropium and Monsonia occur between 1250 and 1850 m. Some of the last four species are considered by him as Mediterranean elements.

ACKNOWLEDGMENTS

Professor M. N. El-Hadidi and Miss H. A. Hosni, Cairo University Herbarium, kindly checked the determinations of Fagonia and Tribulus specimens, respectively.

**Page Missing in
Original Document**

REFERENCES

- AGI (American Geological Institute), 1974, Glossary of Geology: Gary, M., McAfee, R. Jr., and Wolf, C. L., eds., Amer. Geol. Institute, Wash., D.C., 805 p.
- Ahlbrandt, T. S., 1975, Comparison of textures and structures to distinguish eolian environments, Killpecker Dune Field, Wyoming: *The Mountain Geologist*, v. 12, p. 61-73.
- , 1979, Textural parameters of eolian deposits: in McKee, E. D., ed., *A Study of Global Sand Seas*: U. S. Geol. Survey Prof. Paper 1052, p. 21-51.
- Akaad, M. K. and El-Ramly, M. F., 1961, Geological history and classification of the basement rocks on the Central-Eastern Desert of Egypt: *Geol. Surv. Egypt Paper No. 9*, Cairo, Egypt, 24 p.
- Akaad, M. K. and Noweir, A. M., 1964, Trachyte plugs and breccia cones east of Gebel Um Hombos, Eastern Desert, Egypt: *Bull. Sci. and Tech.*, v. VII, Assiut Univ., Assiut, Egypt, p. 51-60.
- Almasy, L. B. de, 1936, Récentes explorations dans le Désert Libyque (1932-1936): *Publications de la Société Royal de Géographie d'Égypte*, Cairo.
- Almasy, K. E. de, 1940, Unbekannte Sahara; Mit flugzeug und auto in der Lignschen Wüste: *F. U. Brockhaus*, Leipzig.
- Amstutz, G. C. and Chico, R., 1958, Sand size fractions of South-Peruvian barchans and a brief review of the genetic grain shape function: *Bull. Ver. Schweizer. Petrol.-Geol.*, v. 24, p. 47-52.
- Arvidson, R. E., 1972, Aeolian processes on Mars; Erosive velocities, settling velocities, and yellow clouds: *Geol. Soc. America Bull.*, v. 83, p. 1503-1508.
- Arvidson, R. E., 1974, Wind-blown streaks, splotches, and associated craters on Mars; Statistical analysis of Mariner 9 photographs: *Icarus*, v. 21, p. 12-27.
- Ashri, A. H., 1970, The movement of sand dunes at Kharga Oasis (abstract): in *Papers presented at the Eighth Annual Meeting, Geol. Soc. Egypt, Cairo, The National Information and Documentation Centre, Cairo*, 21 p.
- Bagnold, R. A., 1931, Journeys in the Libyan desert 1929 and 1930: *Geogr. Jour.*, v. 78, p. 13-39 and 524-535.
- , 1933, A further journey through the Libyan desert: *Geogr. Jour.*, v. 82, p. 103-129 and 211-235.
- , 1941, *The Physics of Blown Sand and Desert Dunes*: Methuen and Co. Ltd., London, 265 p.

- , 1945, Early days of the Long Range Desert Group: *Geogr. Jour.*, v. 105, p. 30-46.
- , 1953, Navigation ashore: *Jour. Inst. of Navigation*, v. 6, p. 184.
- , 1954, Physical aspects of dry deserts: in Clovosley-Thompson, J. L., ed., *Biology of Deserts*, p. 7-12.
- , 1978, Wind-sand interactions (abstract): in Greeley, R. and Black, D., eds., *Abstracts for the Planetary Geology Field Conference on Aeolian Processes*, NASA Publication TM-78, 455, Wash. D. C., p. 8.
- Bagnold, R. A., Newbold, D., and Kennedy-Shaw, W. B., 1931, Journeys in the Libyan desert, 1929 and 1930: *Geogr. Jour.*, v. 78, p. 524-535.
- Bagnold, R. A., Peel, R. F., Myers, O. H., and Winkler, H. A., 1939, An Expedition to the Gilf Kebir and Uweinat, 1938; *Geogr. Jour.*, v. 93, p. 281-313.
- Baker, V. R., 1978a, Large-scale erosional and depositional features of the Channeled Scabland: in Baker, V. R. and Nummedal, D., eds., *The Channeled Scabland*, NASA, Wash. D.C., p. 81-115.
- , 1978b, A preliminary assessment of the fluid erosional processes that shaped the martian outflow channels: *Proc. Lunar Planet Sci. Conf.*, 9th, New York, Pergamon, p. 3205-3223.
- Baker, V. R. and Milton, D. J., 1974, Erosion by catastrophic floods on Mars and Earth: *Icarus*, v. 23, p. 27-41.
- Ball, J., 1927, Problems of the Libyan desert: *Geogr. Jour.*, v. 70, p. 21-38, 105-120, and 209-224.
- , 1928, Remarks on "Lost" Oases of the Libyan desert: *Geogr. Jour.*, v. 72, p. 250-258.
- Ball, J. and Sandford, K. S., 1971, Nodular masses of manganese in volcanic rocks around Gebel Uweinat: *First Symposium on Geology of Libya*, Tripoli, Libya, p. 333-339.
- Beadnell, H. J. L., 1909, *An Egyptian Oasis*: Murray, London, 262 p.
- , 1910, The sand dunes of the Libyan Desert: *Geogr. Jour.*, v. 35, p. 379-394.
- , 1931, Zerzura: *Geogr. Jour.*, v. 77, p. 245-250.
- , 1933, Remarks on the pre-historic geography and underground waters of Kharga Oasis: *Geog. Jour.*, v. 81, p. 128-139.

- Bermann, R. A., 1934, Historic problems of the Libyan desert: Geogr. Jour., v. 83, p. 456-470.
- Bigarella, J. J., 1972, Eolian environments: Their characteristics, recognition and importance: in Rigby, J. K. and Hamblin, W. K., eds., Recognition of Ancient Sedimentary Environments: Soc. Econ. Paleontologists and Mineralogists Spec. Pub. 16, p. 12-62.
- Billingsley, G. H. and Breed, W. J., 1973, The origin of barbed tributaries in Marble Canyon, Arizona: Plateau, Museum of Northern Arizona, v. 45, p. 128-132.
- Boessneck, J., Muller, H. H., and Teichert, M., 1964, Osteologische Unterscheidungsmerkmale zwischen Schaf (Ovis aries Linné) und Ziege (Capra hircus Linné): Kuhn-Archiv., v. 78, p. 1-129.
- Boessneck, J., Von Den Driesch, A., Meyer-Lempeneau, U., and Wechsler, O. E., 1971, Die Tierknochenfunde aus dem Oppidum von Maching: F. Steiner Verlag, Wiesbaden.
- Boulos, L., 1980, IV. Botanical results of the expedition: in El-Baz, F. and others, Journey to the Gilf Kebir and Uweinat, Southwest Egypt, 1978: Geogr. Jour., v. 146, p. 68-71.
- Breed, C. S. and Breed, W. J., 1979, Dunes and other wind forms of central Australia (and comparisons with linear dunes on the Moenkopi plateau, Arizona): in El-Baz, F. and Warner, D. M., eds., Apollo-Soyuz Test Project Summary Science Report, Volume II: Earth Observations and Photography: NASA SP-412, Wash. D. C., p. 319-358.
- Breed, C. S. and Grow, T., 1979, Morphology and distribution of dunes in sand seas observed by remote sensing: in McKee, E. D., ed., A Study of Global Sand Seas: U. S. Geol. Survey Prof. Paper 1052, p. 253-282.
- Breed, C. S., Embabi, N. S., El-Etr, H. A., and Grolier, M. J., 1980a, Wind deposits in the Western Desert: in El-Baz, F. and others, Journey to the Gilf Kebir and Uweinat, Southwest Egypt, 1978: Geogr. Jour., v. 146, p. 88-90.
- Breed, C. S., Grolier, M. J., and McCauley, J. F., 1979, Morphology and distribution of common "sand" dunes on Mars: Comparison with the Earth: Jour. Geophys. Res., v. 84, p. 8183-8204.
- Breed, C. S., McCauley, J. F., and Grolier, M. J., 1980b, Evolution of inselbergs in the hyperarid Western Desert of Egypt -- comparisons with martian fretted terrain (abstract): in Reports of Planetary Geology Program - 1980, NASA TM-82385, Wash. D.C., p. 309-311.
- Brookfield, M., 1970, Dune trends and wind regime in Central Australia: in Ann. Geomorph. Suppl. 10 Piedmont Plains and Sand Formations in Arid and Humid Tropic and Subtropic Regions, p. 121-153.

- Bryan, K., 1925, The Papago Country, Arizona: U. S. Geol. Survey Water-Supply Paper 499, 436 p.
- Burollet, P. F., 1963, Reconnaissance géologique dans le Sud-est du bassin de Kufra: Inst. Francais Petrole v. 18, p. 1537-1545.
- Butzer, K., 1971, Environment and Archaeology: Aldine-Atherton, Chicago, New York, 703 p.
- Butzer, K. and Hansen, C. L., 1968, Desert and River in Nubia: Madison, Wisconsin, University of Wisconsin Press.
- Caporiacco, L. di, 1933, Le Pitture preistoriche oi Ain Dova (Auenat): Archivio per l'Antropologia e le Etnologia. Firenze, v. 63, p. 275-282.
- Caporiacco, L. di and Graziosi, P., 1934, Le pitture rupestri di Ain Doua: Edit. Centro. de Studi Coloniali el Instit. Geogr. Milit., Firenze, Italy.
- Carr, M. H., 1979, Formation of Martian flood features by release of water from confined aquifers: Jour. Geophys. Res., v. 84, p. 2992-3007.
- Carter, C. S., 1957, Morphometry and evolution of a rapidly expanding drainage basin at Poquonock, Connecticut: unpublished M.S. Thesis, Brown University, Providence, Rhode Island, 62 p.
- Carter, W. D. and Paulson, R. W., 1978, Introduction to monitoring dynamic environmental phenomena of the world using satellite data collection systems: COSPAR Tech. Man. Ser. Man. No. 8.
- Caton-Thompson, G., 1952, Kharga Oasis in Prehistory: London, Athlone Press.
- Caton-Thompson, G. and Gardner, E. W., 1932, The prehistoric geography of Kharga Oasis: Geog. Jour., v. 80, p. 369-409.
- Cess, R. D., Ramanathan, C., and Owen, T., 1980, The Martian paleoclimate and enhanced atmospheric carbon dioxide: Icarus, v. 41, p. 159-165.
- Chaikin, A. L., Maxwell, T. A., and El-Baz, F., 1980, Photogeologic studies of the Cerberus albedo feature of Mars: in Reports of Planetary Geology Program, 1979-1980: NASA TM-81776, Wash. D. C., p. 43-45.
- Chorley, R. J., 1957, Illustrating the laws of morphometry: Geological Magazine, v. 94, p. 140-149.
- , 1959, The shape of drumlins: Jour. Glaciology, v. 3, p. 339-344.

- Clayton, P. A., 1933, The western side of the Gilf Kebir: *Geogr. Jour.*, v. 81, p. 254-259.
- , 1937, The south-western desert survey expedition 1930-31: *Société Royale de Géographie Égypte* Cairo, v. 19, p. 241-265.
- Cook, R. U. and Warren, A., 1973, *Geomorphology in Deserts*: Batsford Ltd., London, 347 p.
- Corti, R., 1939, Le raccolte botaniche nel Sud Cirenaico del Prof. L. Di Caporiacco (1933 *Spediz. Marchesi*) e del Prof. U. Monterin (1934 - *Royal Soc. Geogr. Italiana*) e la Florula delle Oasi di Cufra e del Gebel Auenât: *Nuovo Giornale Botanico Italiano*, Nuovo Serie 45, p. 202-260.
- Cortright, E. M., 1968, *Exploring Space with a Camera*: NASA SP-168, Wash. D.C., 214 p.
- Cotton, C., 1952, *Geomorphology*: Christchurch, N.Z., Whitcombe and Tombs, 503 p.
- Coursin, A., 1964, Observation et expériences faites en Avril et Mai 1956 sur les barkhanes du Souehel el Abiodh (région est de Port Etienne): *Bull de l'Institute Francaise, d'Afrique Noire*, v. 26 Ser. A, no. 3, p. 989-1022.
- Cutts, J. A., Blasius, K. R., Briggs, G. A., Carr, M. H., Greeley, R., and Masursky, H., 1976, North polar region of Mars: Imaging results from Viking 2: *Science*, v. 194, p. 1329-1337.
- Cutts, J. A. and Smith, R. S. U., 1973, Eolian deposits and dunes on Mars: *Jour. Geophys. Res.*, v. 78, p. 4139-4154.
- Dardir, A., 1973, Geology of the northern part of the Arabo-Nubian Shield: *New Resh. Geology*, no. 5, Leningrad, p. 9-20 (in Russian).
- Davies, M. E., Dwornik, S. E., Gault, D. B., and Strom, R. G., 1978, *Atlas of Mercury*: NASA SP-423, Wash. D.C., 128 p.
- Davis, J. C., 1973, *Statistics and Data Analysis in Geology*: New York, Wiley, 550 p.
- Dietz, R. S., 1961, Astroblemes: *Scientific American*, v. 205, p. 51-58.
- Dietz, R. S. and McHone, J. F., 1979, Volcanic landforms and astroblemes: *in* El-Baz, F. and Warner, D. M., eds., *Apollo-Soyuz Test Project Summary Science Report, Volume II: Earth Observations and Photography*: NASA SP-412, Wash. D. C., p. 183-191.
- Doughri, A. K., Sinha, D. S., and Yeats, R. S., 1978, Syenite and carbonatite west of Jabal Awaynat, Southeastern Libya (abstract): *in* *Second Symposium on Geology of Libya, Tripoli, Libya*, p. 3.

- Doyle, F. J., 1979, A large format camera for shuttle: Photogramm. Eng. and Remote Sens., v. 45, p. 73-78.
- El-Baz, F., 1977, Astronaut Observations from the Apollo-Soyuz Mission: Smithsonian Studies in Air and Space, No. 1, Wash. D. C., Smithsonian Institution Press, 400 p.
- , 1978a, The meaning of desert color in Earth orbital photographs: Photogramm. Eng. and Remote Sens., v. 44, p. 69-75.
- , 1978b, Analogs of Martian eolian features in southwestern Egypt: Paper presented at meetings of the Committee on Space Research, Innsbruck, Austria.
- , 1979a, Egypt as seen by Landsat: Cairo, Egypt, Dar Al-Maaref.
- , 1979b, The Western Desert of Egypt, its problems and potentials: in Bishay, A. and McGinnes, W. G., eds., Advances in Desert and Arid Land Technology and Development, v. 1, New York, Harwood Academic Pub., p. 67-84.
- , 1979c, Siwa: Resort of kings: Aramco World, v. 30, no. 4, p. 30-35.
- , 1979d, Monitoring the desert environment from space: in Bishay, A. and McGinnes, W. G., eds., Advances in Desert and Arid Land Technology and Development, v. 1, New York, Harwood Academic Pub., p. 383-398.
- El-Baz, F., Boulos, L., Breed, C., Dardir, A., Dowidar, H., El-Etr, H., Embabi, M., Grolier, M., Haynes, V., Ibrahim, M., Issawi, B., Maxwell, T., McCauley, J., McHugh, W., Moustafa, M., and Yousif, M., 1980, Journey to the Gifl Kebir and Uweinat, Southwest Egypt, 1978: Geogr. Jour., v. 146, p. 51-93.
- El-Baz, F., Breed, C., Grolier, M. J., and McCauley, J. F., 1979a, Eolian features in the Western Desert of Egypt and some applications to Mars: Jour. Geophys. Res., v. 84, p. 8205-8221.
- El-Baz, F. and El-Etr, H. A., 1979, Color zoning in the Western Desert of Egypt: in El-Baz, F. and Warner, D. M., eds., Apollo-Soyuz Test Project Summary Science Report, Volume II: Earth Observations and Photography: NASA SP-412, Wash. D. C., p. 203-217.
- El-Baz, F. and Maxwell, T. A., 1979a, Eolian streaks in southwestern Egypt and similar features in the Cerberus region of Mars: Proc. Lunar and Planetary Science Conf., 10th, New York, Pergamon, p. 3017-3030.
- , 1979b, Geological constraints on archaeological sites in the Western Desert of Egypt: Abstracts with Programs, Geol. Soc. America, v. 11, p. 420.

- El-Baz, F. and Mitchell, D. A., 1975, Remote sensing as a tool for development: Islamic Solidarity Conf. on Science and Technology, Univ. of Riyad, Saudi Arabia, Vol. II, p. 1-11.
- , 1976, Earth observations and photography experiment MA-136: in Apollo-Soyuz Test Project Preliminary Science Report: NASA TMX-58173, Wash. D. C., p. 10-1 - 10-64.
- El-Baz, F. and Ondrejka, R. J., 1978, Earth Orbital Photography by the Large Format Camera: Proc. 12th Internat. Symp. on Remote Sensing of Environment, v. 1., Environmental Research Institute of Michigan, Ann Arbor, p. 703-718.
- El-Baz, F., Sleazak, M. H., and Maxwell, T. A., 1979b, Preliminary analysis of color variations of sand deposits in the Western Desert of Egypt: in El-Baz, F. and Warner, D. M., eds., Apollo-Soyuz Test Project Summary Science Report, Volume II: Earth Observations and Photography: NASA SP-412, Wash. D. C., p. 237-262.
- El-Etr, H. A., 1967, The technique of lineaments and linears analysis and its application in the minerogenic province of southeast Missouri: unpublished Ph.D. Dissertation, Univ. Missouri, Rolla, Missouri, 249 p.
- , 1976, Proposed terminology for linear features: in Hodgson, R. A., Gay, S. P. Jr., and Benjamins, J. Y., eds., Proc. First Internat. Conf. on New Basement Tectonics: Salt Lake City, Utah Geol. Assoc. Pub. No. 5, p. 480-489.
- El-Etr, H. A. and Abdel Rahman, M. A., 1976, Airphoto lineations of the southern part of the Gulf of Suez region, Egypt: in Hodgson, R. A., Gay, S. P. Jr., and Benjamins, J. Y., eds., Proc. First Internat. Conf. on New Basement Tectonics: Salt Lake City, Utah, Utah Geol. Assoc. Pub. No. 5, p. 309-326.
- El-Ramly, M. F., 1972, A new geological map for the basement rocks in the Eastern and South Western Desert of Egypt: Annals Geol. Survey Egypt, v. 2, p. 1-12.
- El-Shazly, E. M., 1964, On the classification of the pre-Cambrian and other rocks of magmatic affiliation: Inter. Geol. Cong. India, Section 10.
- Embabi, N. S., 1967, A morphological study of the Kharga Oases depression, the Western Desert, Egypt: unpublished Ph.D. Dissertation, Univ. Bristol, Bristol, England, 326 p.
- , 1970-1971, Structures of barchan dunes at the Kharga Oases depression, the Western Desert, Egypt and a comparison with structures of two aeolian micro-forms from Saudi-Arabia: Bull. de la Societé de Géographie d'Égypte, v. 43-44, p. 53-71.

- , 1972, The semi-playa deposits of Kharga depression, the Western Desert, Egypt: Bull. de la Societ  de G ographie d' gypte, v. 41-42, p. 73-87.
- , 1978, Statistical relationships between barchan shape dimensions: Egyptian Computer Science Jour., v. 1, no. 2, p. 29-51.
- , 1979, Barchan dune movement and its effect on economic development at the Kharga Oases Depression: Jour. Middle East, The Middle East Research Centre, Ain Shams Univ, Cairo, v. 6, p. 1-20 (in Arabic).
- Ezzat, Mohamed Aly, 1974, Ground water series in the UAR exploration of ground water in El Wadi El-Gedid (New Valley) project: Part II: Hydrologic conditions, Dakhla-Kharga area.
- Farid, H., 1978, Al-Tariq el-a Al-Merikh Yabda bil Sahara Al-Gharize (The road to Mars starts with the Western Desert): October Magazine, Cairo, No. 104, p. 25-27; No. 106, p. 28-29; No. 108, p. 34-35; No. 109, p. 32-33 (in Arabic).
- Finkel, H. J., 1959, The barchans of Southern Peru: Jour. Geol., v. 67, p. 614-647.
- Folk, R. L., 1968, Bimodal supermature sandstones: Product of the desert floor: in 23rd Session Internat. Geol. Cong., Proc. Sect. 8, Prague, Academia, p. 9-32.
- , 1971, Longitudinal dunes of the northwestern edge of the Simpson Desert, Northern Territory, Australia, 1. Geomorphology and grain size relationships: Sedimentology, v. 16, p. 5-54.
- , 1974, Petrology of Sedimentary Rocks: Hemphill Pub. Co., Austin, Texas, 182 p.
- , 1976, Reddening of desert sands: Simpson Desert, N. T., Australia: Jour. Sed. Petrology, v. 46, p. 604-615.
- French, B. E., Underwood, J. R., and Fisk, E. P., 1974, Shock-metamorphic features in two meteorite impact structures, Southeastern Libya: Geol. Soc. Amer. Bull., v. 85, p. 1425-1428.
- Frey, H., 1979, Thaumasia: A fossilized early forming Tharsis uplift: Jour. Geophys. Res., v. 84, p. 1009-1023.
- Friedman, G. M., 1961, Distinction between dune, beach and river sands from their textural characteristics: Jour. Sed. Petrology, v. 31, p. 514-529.
- , 1967, Dynamic progresses and statistical parameters compared for size frequency distribution of beach and river sands: Jour. Sed. Petrology, v. 37, p. 327-354.

- , 1973, Textural parameters of sands: Useful or useless? (abstract): Abstracts with Programs, Geol. Soc. America, v. 5, p. 626.
- GPC (General Petroleum Company), 1979, Gravity and basement relief maps of the Western Desert of Egypt: Internal Report, General Petroleum Company, Cairo, Egypt.
- Garvin, J. B., Mouginis-Mark, P. J., and Head, J. W., 1981, Characteristics of rock populations on planetary surfaces at the Viking lander sites and comparisons with Venus: The Moon and the Planets, v. 24, p. 355-387.
- Gautier, A., not dated, Some animal remains from a Neolithic site on Wadi El Bakht, Gilf Kebir: manuscript on file at Southern Methodist University, Dallas, Texas.
- Geological Survey of Egypt, 1979, Geological Map of Egypt: Cairo, Egypt (Scale 1:2,000,000).
- Giengengack, R. F., 1968, Late Pleistocene history of the Nile Valley in Egyptian Nubia: unpublished Ph.D. Dissertation, Yale University, New Haven, Conn.
- Giegengack, R. F. and Issawi, B. 1975, Libyan Desert silica glass, a summary of problem of its origin: Annals Geol. Survey Egypt, v. 5, p. 105-118.
- Gifford, A. W., Warner, D. M., and El-Baz, F., 1979, Orbital observations of sand distribution in the Western Desert of Egypt: in El-Baz, F. and Warner, D. M., eds., Apollo-Soyuz Test Project Summary Science Report, Volume II: Earth Observations and Photography: NASA SP-412, Wash. D. C., p. 219-236.
- Glennie, K. W., 1970, Desert Sedimentary Environments: Amsterdam, Elsevier, 222 p.
- Greeley, R., 1979a, A model for the formation of windblown sand-size particles and related structures on Mars (abstract): in Second Internat. Colloquium on Mars, NASA Conf. Pub. 2072, Wash. D. C., p. 32.
- , 1979b, Silt-clay aggregates on Mars: A model for the formation of sand: Jour. Geophys. Res., v. 84, p. 6248-6254.
- Greeley, R., Iverson, J. D., Pollack, J. B., Udovich, N., and White, B., 1974a, Wind tunnel studies of Martian aeolian processes: Proc. Roy. Soc., v. 341, p. 331-360.
- , 1974b, Wind tunnel simulations of light and dark streaks on Mars: Science, v. 183, p. 847-849.

- Griffiths, J. F. and Soliman, K. H., 1972, The northern desert (Sahara): in Griffiths, J. F., ed., *Climates of Africa*: Amsterdam, Elsevier, 604 p.
- Grolier, M. J., McCauley, J. F., Breed, C. S., and Embabi, N. S., 1980, IX. Yardangs of the Western Desert: in El-Baz, F. and others, *Journey to the Gilf Kebir and Uweinat, Southwest Egypt, 1978*: *Geogr. Jour.*, v. 146, p. 86-87.
- Grove, A. T., 1970, Rise and fall of Lake Chad: *Geogr. Magazine*, v. 42, p. 432-439.
- Grove, A. T. and Warren, A., 1968, Quaternary Landforms and climate on the south side of the Sahara: *Geogr. Jour.*, v. 134, p. 194-298.
- Hall, D. N., 1967, A simple method of navigation in deserts: *Geogr. Jour.*, v. 143, p. 192-205.
- Harding-King, W. J., 1913, The Libyan desert from native information: *Geogr. Jour.*, v. 42, p. 271-283.
- , 1925, *Mysteries of the Libyan Desert*: London, Seeley, Service and Co. Ltd., 348 p.
- Hassanein Bey, A. M., 1924a, Through Kufra to Darfur: *Geogr. Jour.*, v. 64, p. 213-291 and 353-366.
- , 1924b, Crossing the untraversed Libyan desert: *National Geographic Magazine*, v. 46, p. 233-278.
- , 1925, *The Lost Oasis*: New York, London, Century Co., 363 p.
- Hastenrath, S. L., 1967, The barchans of the Arequipa Region, Southern Peru: *Zeitschrift fur Geomorphologie*, v. 11, no. 3, p. 300-331.
- Haynes, C. V., 1978, The Nubian Desert: A product of Quaternary climatic cycles (abstract): in Greeley, R. and Black, D., eds., *Abstracts for the Planetary Geology Field Conference on Aeolian Processes*: NASA publication TM-78, 455, Wash. D. C., p. 22-23.
- , 1980a, Geological evidence of pluvial climates in the El Nabta area of the Western Desert, Egypt: in Wendorf, F. and Schild, R., eds., *Prehistory of the Eastern Sahara*: New York, Academic Press, p. 353-371.
- , 1980b, II. Quaternary geology and archaeological observations: in El-Baz, F. and others, *Journey to the Gilf Kebir and Uweinat, Southwest Egypt, 1978*: *Geogr. Jour.*, v. 146, p. 59-63.
- , not dated, Late Quaternary geochronology and irrigation agriculture, Western Desert, Egypt: in preparation.
- Haynes, C. V. and Haas, H., 1980, Radiocarbon evidence for Holocene recharge of ground water, Western Desert, Egypt: Paper presented at 10th Internat. Radiocarbon Conf., Berne and Heidelberg.

- Haynes, C. V., Mehringer, P. J. Jr., and Zaghloul, S., 1979, Pluvial lakes of northwestern Sudan: *Geogr. Jour.*, v. 145, p. 437-445.
- Haynes, C. V., Said, R., and El Hennawi, M., 1977, Quaternary lakes of the Nubian Desert: Paper presented at 10th Congress, INQUA, Birmingham, England.
- de Heinzelin, J., 1968, Geologic history of the Nile Valley in Nubia in Wendorf, F., ed., *The Prehistory of Nubia*, v. 1: Dallas, Texas, Fort Burgwin Research Center and Southern Methodist University Press, p. 19-55.
- de Heinzelin, J., Haesaerts, P., and Van Noten, F., 1969, Geologie recente et prehistorie an Jebel Uweinat: *Africa-Tervuren*, v. 15, p. 120-125.
- Henning, D. and Flohn, H., 1977, Climate Aridity Index Map: U. N. Conference on Desertification, UNEP, Nairobi, Kenya.
- Hermina, M. and Issawi, B., 1971, Rock-stratigraphic classification of the Upper Cretaceous-Lower Tertiary exposures in southern Egypt: in Gray, C., ed., *Symposium on the Geology of Libya*: Faculty of Science, University of Libya.
- Honvault, C., 1980, The earth resources satellite programme of the European Space Agency (abstract): in *Summaries*, 14th International Symposium on Remote Sensing of the Environment: Ann Arbor, Mich., Environmental Research Inst. of Michigan, p. 8.
- Horton, R. E., 1945, Erosional development of streams and their drainage basins: Hydrophysical approach to quantitative morphology: *Geol. Soc. America Bull.*, v. 56, p. 275-370.
- Howard, A. D., 1942, Pediment passes and the pediment problem: *Jour. Geomorph.*, v. 5, p. 1-31 and 95-136.
- Huck, F. O., Jobson, D. J., Park, Wall, S. K., Arvidson, R. E., Patterson, W. R., and Benton, F. D., 1977, Spectrophotometric and color estimates of the Viking lander sites: *Jour. Geophys. Res.*, v. 82, p. 4401-4411.
- Hume, W. F., 1925, *Geology of Egypt, Vol I*: Cairo, Egypt, Egyptian Survey Dept.
- , 1934, *Geology of Egypt, Vol. II, The Fundamental Precambrian rocks of Egypt and the Sudan, Part I, The Metamorphic Rocks*: Cairo, Egypt, Egyptian Survey Department, 300 p.
- , 1935, *Geology of Egypt, Vol. II, Part 2*: Cairo, Egypt, Geol. Survey Egypt, p. 301-688.
- Hussein, Prince Kemal El-Din, 1928, L'exploration du desert Libyque: *la Geographie*, v. 50, p. 171-183 and 320-336.

- Hussein, Prince Kemal El-Din and Breuil, H., 1928, Les gravures rupestres du Djebel Ouenat: *Revue Scientifique Illustree*, v. 66, p. 105-117.
- Hutchinson, J., 1933, Botany: Appendix III: in Bagnold, R. A., A further journey through the Libyan Desert: *Geogr. Jour.* v. 82, p. 226.
- Inman, D. L., Ewing, G. C., and Corliss, J. B., 1966, Coastal sand dunes of Guerrero Negro, Baja, California, Mexico: *Geol. Soc. America Bull.*, v. 77, p. 787-802.
- Issawi, B., 1968, Geology of Kurkur-Dungul area: *Geol. Survey Egypt Paper No. 46*. Cairo, Egypt, 102 p.
- , 1971, Geology of Darb el Arbain, Western Desert, Egypt: *Annals Geol. Survey Egypt*, v. 1, p. 53-92.
- , 1972, Review of Upper Cretaceous-Lower Tertiary stratigraphy in central and southern Egypt: *American Assoc. Petroleum Geol. Bull.*, v. 56, p. 1448-1463.
- , 1973a, Nubia Sandstone, type section: *American Assoc. Petroleum Geol. Bull.*, v. 57, p. 741-745.
- , 1973b, Contribution to the geology of Uweinat-Gilf Kebir area, Western desert, Egypt: *Geol. Survey Egypt Internal Rept.*, 42 p.
- , 1978, New findings in the Gilf-Uweinat area: *Annals Geol. Survey Egypt*, v. 8, p. 275-293.
- , 1980, V. Geology, stratigraphy and structure of southwest Egypt: in El-Baz, F. and others, *Journey to the Gilf Kebir and Uweinat*, Southwest Egypt, 1978: *Geogr. Jour.*, v. 146, p. 72-75.
- Jones, G. H. S., 1977, Complex craters in alluvium: in Roddy, D. J., Peppin, R. O., and Merrill, R. B., eds., *Impact and Explosion Cratering*: New York, Pergamon Press, p. 163-183.
- Judson, S., 1950, Depressions of the northern portion of the Southern High Plains of eastern New Mexico: *Geol. Soc. America Bull.*, v. 61, p. 253-273.
- Kadar, L., 1937, La morfologia dell'altopiano del Gilf Kebir: *Bolletino della Reale Societa Geografica Italiana*, ser. 7, v. 2, p. 485-503.
- Kesel, R. H., 1972, The comparative morphology of inselbergs in different environments with emphasis on a humid temperate and an arid area: unpublished Ph.D. Dissertation, University of Maryland, College Park, Maryland, 267 p.
- King, D., 1960, The sand ridge deserts of South Australia and related aeolian landforms of the Quaternary arid cycles: *Transact. Royal Soc. South Australia*, v. 83, p. 99-108.

- Khein, V. F., 1971, Regional geotectonics of North and South America, Antarctica and Africa: Moscow, Nedra, 547 p. (in Russian).
- Klerks, J., 1978, Age and metamorphic evolution of the basement complex around Jebel Uweinat (abstract): in Second Symposium on Geology of Libya, Tripoli, Libya, p. 2.
- Klitzsch, E., 1966, Comments on the geology of the central parts of southern Libya and Northern Chad: Petroleum Explor. Soc. Libya, Amsterdam, Holland, Druckhary, p. 1-18.
- , 1970, Die Strukturgeschichte der Zentral-Sahara: Geol. Rundschau, v. 59, p. 459-527.
- , 1971, The structural development of parts of north Africa since Cambrian time: in Gray, C., ed., Symposium on the Geology of Libya: Tripoli, Libya, p. 253-262.
- , 1978, Geologische Bearbeitung Sudwest-Agyptens: Geologische Rundschau, v. 67, p. 509-520.
- , 1979, Zur Geologie des Gifl Kebir Gebietes in der Ostsahara: Clausthaler Geologische Abhandlungen, v. 30, p. 113-132.
- Klitzsch, E., Harms, J. C., Lejal-Nicol, A., and List, F. K., 1979, Major subdivisions and depositional environments of Nubia Strata, Southwestern Egypt: American Assoc. Petroleum Geol. Bull., v. 63, p. 967-974.
- Knetsch, G. and Yallouze, M., 1955, Remarks on the origin of the Egyptian oasis depression: Bull. de la Societe de Geographie d'Egypt, v. 28, nos. 21-23.
- Kosofsky, L. J. and El-Baz, F., 1970, The Moon as viewed by Lunar Orbiter: NASA SP-200, Wash. D.C., 152 p.
- Leonard, J., 1966, The 1964-65 Belgian Trans-Saharan expedition: Nature, v. 209, p. 126-128.
- , 1969, Expedition scientifique Belge dans le desert Libye: Africa-Tervuren, v. 15, p. 102-105 and 110-116.
- , 1971, Apercu de la flore et de la vegetation du Jebel Uweinat (Desert de Libye) Resume: Mitt. Bot. Staatissamml, Munchen, v. 10, p. 476-477.
- Leopold, L. B. and Miller, J. P., 1956, Ephemeral streams - hydraulic factors and their relation to the drainage net: U. S. Geol. Survey Prof. Paper 282-A, 37 p.
- Mahrholz, W. W., 1965, Geological exploration of the Kufra region: Geological Section Bull., Ministry of Industry, Libya, n. 8, 76 p.

- Mainquet, M., 1977, Analyse quantitative de l'extremite sahelienne du courant eolien transporteur de sable au Sahara nigerien (Note presented by Theodore Monod): Geomorphologie, Academie Sciences, Comptes Rendus, Paris, France, ser. D, no. 285, p. 1029-1032.
- Manent, L. S. and El-Baz, F., 1980, Effects of topography on dune orientation in the Farafra region, Western Desert of Egypt, and implications to Mars: in Reports of Planetary Geology Program - 1980, NASA TM-82385, Wash. D. C., p. 298-300.
- Martin, A. J., 1969, Possible impact structure in southern Syrenaica, Libya: Nature, v. 223, p. 940-941.
- Martins, L. R., 1965, Significance of skewness and kurtosis in environmental interpretation: Jour. Sed. Petrology, v. 35, p. 768-770.
- Mason, C. C. and Folk, R. L., 1958, Differentiation of beach, dune, and aeolian flat environments by size analysis, Mustang Island, Texas: Jour. Sed. Petrology, v. 28, p. 211-226.
- Mason, M. H., 1936, The paradise of fools: London, Hodder and Stoughton.
- Masursky, H., Colton, G. W., and El-Baz, F., 1978, Apollo over the Moon: A view from orbit: NASA SP-362, Wash. D.C., 255 p.
- Maxwell, T. A., 1979a, Field investigations of martian canyonlands in southwestern Egypt (abstract): in Second Internat. Colloquium on Mars, NASA Conf. Pub. 2072, Wash. D. C., p. 54.
- , 1979b, Erosional development of the southern Gilf Kebir plateau, southwestern Egypt (abstract): Abstracts with Programs, Geol. Soc. America, v. 11, p. 473.
- , 1980, VII. Geomorphology of the Gilf Kebir: in El-Baz, F. and others, Journey to the Gilf Kebir and Uweinat, Southwest Egypt, 1978: Geogr. Jour., v. 146, p. 76-83.
- Maxwell, T. A. and El-Baz, F., 1979, Fluvial landforms in Southwestern Egypt: Implications for surface processes on Mars (abstract): in Lunar and Planetary Science X, Lunar and Planetary Institute, Houston, Texas, Part 2, p. 786-788.
- , 1980, Transportation and deposition of particulate material on the surface of Mars: Inferences from sand sheet deposits in the Western Desert of Egypt (abstract): in Reports of Planetary Geology Program, 1979-1980, NASA Tech. Memorandum 81776, Wash. D. C., p. 393-395.
- McCauley, J. F., Breed, C. S., El-Baz, F., Whitney, M. I., Grolier, M. J., and Ward, A. W., 1979a, Pitted and fluted rocks in the Western Desert of Egypt: Viking Comparisons: Jour. Geophys. Res., v. 84, p. 8222-8232.

- McCauley, J. F., Breed, C. S., and Grolier, M. J., 1980a, The Gilf Kebir and the Western Desert of Egypt -- Insights into the origin of the north polar erg on Mars (abstract): in Reports of Planetary Geology Program - 1980, NASA Tech. Memorandum 82385, Wash. D. C., p. 312-313.
- McCauley, J. F., Breed, C. S., Grolier, M. J., and Collins, P. S., 1979b, The eolian features of the north polar region of Mars (abstract): in Second Internat. Colloquium on Mars, NASA Conf. Pub. 2072, Wash. D. C., p. 55.
- McCauley, J. F., Breed, C. S., Grolier, M. J., and El-Baz, F., 1980b, VIII. Pitted rocks and other ventifacts in the Western Desert: in El-Baz, F. and others, Journey to the Gilf Kebir and Uweinat, Southwest Egypt, 1978: Geogr. Jour., v. 146, p. 84-85.
- McCauley, J. F., Grolier, M. J., and Breed, C. S., 1977, Yardangs: in Doehring, D. O., ed., Geomorphology in arid regions: Geomorphology Symposium 8th, Proceedings, State University of New York, Binghamton, N.Y., p. 233-269.
- McHugh, W. P., 1971, Late prehistoric cultural adaptation in the southeastern Libyan desert: unpublished Ph.D. Dissertation, University of Wisconsin, Madison, Wisconsin, 373 p.
- , 1974a, Cattle pastoralism in Africa - A model for interpreting the archeological evidence from the eastern Sahara Desert: Arctic Anthropology, Suppl., v. 11, p. 236-244.
- , 1974b, Late prehistoric cultural adaptations in southwest Egypt and the problem of the Nilotic origins of Saharan cattle pastoralism: Journal American Research Center in Egypt, v. 11, p. 9-22.
- , 1975, Some archaeological results of the Bagnold Mond expedition to the Gilf Kebir and Gebel Uweinat, southern Libyan Desert: Journal of Near Eastern Studies, v. 34, p. 31-62.
- , 1980, III. Archaeological sites of the Gilf Kebir: in El-Baz, F. and others, Journey to the Gilf Kebir and Uweinat, Southwest Egypt, 1978: Geogr. Jour., v. 146, p. 64-68.
- McKee, E. D., 1966, Structures of dunes at White Sands National Monuments, New Mexico (and a comparison with structure of dunes from other selected areas): Sedimentology, v. 7, p. 1-69.
- McKee, E. D., Breed, C. S., and Fryberger, S. G., 1977, Desert sand seas: in Skylab Explores the Earth: NASA SP-380, Wash. D. C., p. 5-47.
- McKee, E. D. and Muiola, R. J., 1975, Geometry and growth of the White Sands dunes field, New Mexico: U. S. Geol. Survey Jour. Research, v. 3, p. 59-66.

- McKee, E. D. and Tibbitts, G. C., 1964, Primary structures of a seif dune and associated deposits in Libya: Jour. Sed. Petrology, v. 34, p. 5-17.
- Mehring, P. J. Jr., Peterson, K. L., and Hassen, F. A., 1979, A pollen record from Birket Qarun and the recent history of the Fayum, Egypt: Quaternary Research, v. 11, p. 238-256.
- Menchikoff, N., 1926, Observation geologique faites au cours de l'expedition de S.A.S. Le Prince Kemal El Din Hussein dans le Desert de Libya 1925-1926: C. R. Akad Sci., v. 183, p. 1047-1049.
- , 1928, Les roches cristallines et volcanique du centre du Desert de Libye: C. R. Akad. Sci., v. 184, p. 215-217.
- Meneisy, M. Y. and Kreuzer, H., 1974, Potassium-Argon ages of Egyptian basaltic rocks: Geol. Jahrbuch, ser. D, v. 9, p. 21-31.
- Missone, X., 1969a, Historique de l'exploration du Jebel Uweinat: Africa-Tervuren, v. 15, p. 105-108.
- , 1969b, La faune: Africa-Tervuren, v. 15, p. 117-119.
- Moiola, R. J. and Spencer, A. B., 1979, Differentiation of eolian deposits by discriminant analysis: in McKee, E. D., ed., A Study of Global Sand Seas: U. S. Geol. Survey Prof. Paper 1052, p. 53-58.
- Moiola, R. J. and Weiser, D., 1968, Textural parameters: An evaluation: Jour. Sed. Petrology, v. 38, p. 45-53.
- Muehlberger, W. R., Batson, R. M., Cernan, F. A., Freeman, V. L., Hait, M. H., Holt, H. E., Howard, K. A., Jackson, E. D., Larson, K. B., Reed, V. S., Rennilson, J. J., Schmitt, H. H., Scott, D. H., Sutton, R. L., Stuart-Alexander, D., Swann, G. A., Trask, N. J., Ulrich, G. E., Wilshire, H. G., and Wolfe, E. W., 1973, Preliminary geologic investigation of the Apollo 17 landing site: in Apollo 17 Preliminary Science Report, NASA SP-330, Wash. D. C., p. 6-1 - 6-91.
- Muratov, M. K., 1975, The origin of continents and ocean basins: Nodra, Moscow, 191 p. (English Translation by MIT Publishers, 1977, Moscow).
- Murray, G. W., 1952, Water beneath the Egyptian Western Desert: Geogr. Jour., v. 118, p. 443-452.
- , 1967, Dare me to the desert: London, Geo. Allen and Union Ltd., 214 p.
- Mutch, T. A., Arvidson, R. F., Head, J. W., Jones, K. L., and Saunders, R. S., 1976, The Geology of Mars: Princeton, New Jersey, Princeton University Press, 400 p.

- Myers, O. H., 1939, The Sir Robert Mond Expedition of the Egypt Exploration Society: Geogr. Jour., v. 93, p. 287-291.
- , not dated, a, Notes concernant les gisements fouilles: Manuscript in the Musee de l'Homme, Paris.
- , not dated, b, Evidence of the Lower Palaeolithic in the Gilf al Kabir region: Manuscript in the Musee de l'Homme, Paris.
- , not dated, c, Some problems in the later prehistory of the Sudan, the southern Sahara, and south Arabia: Manuscript in the Musee de l'Homme, Paris.
- Newbold, D., 1924, A desert odyssey of a thousand miles: Sudan Notes and Records, v. 7, p. 43-92.
- , 1928, Rock-pictures and archaeology in the Libyan desert: Antiquity, v. 2, p. 261-291.
- , 1931, Survey methods and results, Appendix 1: in Bagnold, R. A. and others, Journeys in the Libyan Desert 1929 and 1930: Geogr. Jour., v. 78, p. 526-530.
- Newbold, D. and Shaw, W. B. K(ennedy), 1928, An exploration in the south Libyan desert: Sudan Notes and Records, v. 11, p. 103-194.
- Nicks, O. W., 1970, This Island Earth: NASA SP-250, Wash. D. C., 182 p.
- Norris, R. M. and Norris, K. S., 1961, Algodones dunes of southeastern California: Geol. Soc. America Bull., v. 72, p. 605-620.
- Oliver, J., 1965, Evaporation losses and rainfall regime in central and northern Sudan: Weather, v. 20, p. 58-64.
- Osborn, D. J. and Krombein, K. V., 1969, Habitats, flora, mammals, and wasps of Gebel Uweinat, Libyan desert: Smithsonian Contributions to Zoology, v. 11, p. 1-18.
- Ownbey, J. W., 1978, Guide to Standard Weather Summaries and Climatic Services: National Tech. Information Service, Wash. D.C., AD-A047482.
- Parker, G. G., 1964, Piping, a geomorphic agent in landform development of the drylands: in Internat. Assoc. Scientific Hydrology, Pub. 65, p. 103-113.
- Patterson, W. R., Huck, F. O., Wall, S. D., and Wolf, M. R., 1977, Calibration and performance of the Viking Lander Cameras: Jour. Geophys. Res., v. 82, p. 4391-4400.
- Paulson, R., 1978, Use of Earth satellites for automation of hydrologic data collection: in Collection, Storage, Retrieval and Publication of Water Resources Data: U. S. Geol. Survey Circular 756, p. 8-14.

- Peel, R. F., 1939a, Rock-paintings from the Libyan desert: *Antiquity*, v. 13, p. 389-402.
- , 1939b, The Gilf Kebir: Part 4 *in* Bagnold, R. A. and others, *An Expedition to the Gilf Kebir and Uweinat, 1938: Geogr. Jour.*, v. 93, p. 295-307.
- , 1941, Denudational landforms of the central Libyan Desert: *Jour. Geomorph.*, v. 5, p. 3-23.
- , 1942, The Tibbu people and the Libyan desert: *Geogr. Jour.*, v. 100, p. 73-87.
- , 1966, The landscape in aridity: *Inst. British Geographers Transact.*, no. 38, p. 1-23.
- Peel, R. F. and Bagnold R. A., 1939, *Archaeology: Additional notes: Geogr. Jour.*, v. 93, p. 291-295.
- Penderel, H. W. G. J., 1934, *The Gilf Kebir: Geogr. Jour.*, v. 83, p. 449-456.
- Pesce, A., 1968, *Gemini Space Photographs of Libya and Tibesti: A Geological and Geographical Analysis: Petroleum Exploration Society of Libya, Tripoli, Libya*, 81 p.
- Pollack, J. B., 1979, Climatic change on the terrestrial planets: *Icarus*, v. 37, p. 479-553.
- Pomeyrol, R., 1968, *Nubian Sandstone: American Assoc. Petrol. Geol. Bull.*, v. 52, p. 589-600.
- Potter, R. M. and Rossman, J. R., 1977, Desert varnish: The importance of clay minerals: *Science*, v. 196, p. 1446-1448.
- , 1979, The manganese and iron oxide mineralogy of desert varnish: *Chemical Geology*, v. 25, p. 79-94.
- Powers, N. C., 1953, A new roundness scale for sedimentary particles: *Jour. Sed. Petrology*, v. 23, p. 117-119.
- Prestel, D. J. and El-Baz, F., 1979, Microscopic characteristics of quartz sand from the arid environment of the Gilf Kebir, southwest Egypt (abstract): *in* *Reports of Planetary Geology Program, 1978-1979, NASA Tech. Memorandum 80339, Wash. D. C.*, p. 293-295.
- Prestel, D. J., McKay, D. S., and Haynes, C. V., 1979, Mineralogy and caliche-like salt crusts from the Western Desert. Egypt: Implications for Martian duricrust formation (abstract): *in* *Reports of Planetary Geology Program, 1978-1979, NASA Tech. Memorandum 80339, Wash. D. C.*, p. 200-202.

- Prestel, D. J., Wainwright, J. E., and El-Baz, F., 1980, Studies of coatings on sand grains from the Gilf Kebir, southwest Egypt (abstract): Reports of Planetary Geology Program, 1979-1980, NASA Tech. Memorandum 81776, Wash. D. C., p. 43-45.
- Rahn, P. H., 1965, The inselbergs of southwestern Arizona: unpublished Ph.D. Dissertation, Pennsylvania State University, University Park, Pennsylvania, 140 p.
- Raisz, E., 1952, Landform map of North Africa: 130 Charles St., Boston, Mass.
- Rhotert, H., 1952, Libysche Felsbilder: Ergebnisse der XI und XII Deutschen Inner-Afrikanischen Forschungs-Expedition (DIAFE) 1933: Wittich, Damstadt.
- Rodd, F. J. R., 1933, A reconnaissance of the Gilf Kebir by the late Sir Robert Clayton East Clayton: Geogr. Jour., v. 81, p. 249-254.
- Roddy, D. J., 1977, Large scale impact and explosion craters: Comparisons of morphological and structural analogs: in Roddy, D. J., Peppin, R. O., and Merrill, R. B., eds., Impact and Explosion Cratering: New York, Pergamon Press, p. 185-246.
- Rodis, H. G., Hassan, A., and Wahadan, L., 1964, Ground water geology of Kordofan Province: Bull. Geol. Survey Sudan, no. 14, 91 p.
- Rodis, H. G. and Iskander, W., 1963, Ground water in the Nahud Outlier of the Nubian Series, Kordofan Province Sudan: U. S. Geol. Survey Prof. Paper 475-B, p. 179-181.
- Saad, S. I. and Ghazaly, G., 1976, Palynological studies in Nubia Sandstones from Kharga Oasis, pollen et spore: Museum National Histoire Naturelle, v. 18, p. 407-470.
- Sagan, C. and Bagnold, R. A., 1975, Fluid transport on Earth and aeolian transport on Mars: Icarus, v. 26, p. 209-218.
- Sagan, C., Pieri, D., Fox, P., Arvidson, R., and Guinness, E., 1977, Particle motion on Mars inferred from the Viking Lander Cameras: Jour. Geophys. Res., v. 82, p. 4430-4438.
- Said, R., 1962, The Geology of Egypt: Amsterdam, Elsevier Pub. Co., 377 p.
- , 1975, Some observations on the geomorphological elevation of the south western desert of Egypt and its relation to the origin of ground water: Annals Geol. Survey Egypt, v. 5, p. 61-70.
- Sandford, K. S., 1933a, Geology and geomorphology of the southern Libyan desert: Geogr. Jour., v. 82, p. 213-219.
- , 1933b, Past climate and early man in the southern Libyan Desert: Geogr. Jour., v. 82, p. 219-222.

- , 1933c, Volcanic craters in the Libyan Desert: *Nature*, v. 131, p. 46.
- , 1935a, Geological observations on the northwest frontiers of the Anglo-Egyptian Sudan and the adjoining part of the southern Libyan desert: *Quarterly Jour. Geol. Soc. of London*, v. 91, p. 323-381.
- , 1935b, Sources of water in the northwestern Sudan: *Geogr. Jour.*, v. 85, p. 412-431.
- , 1935c, Extinct volcanoes and associated intrusions in the Libyan desert: *Trans. Roy. Geol. Soc. Cornwall*, v. 16, p. 331-358.
- , 1936, Appendix II: Notes on geological data from the southern Libyan desert: *Geogr. Jour.*, v. 87, p. 211-214.
- Sandford, K. S. and Arkell, W. J., 1933, Paleolithic man and the Nile Valley: *in* Nubia and Upper Egypt: Univ. Chicago Orient. Inst., Publ. 17, 92 p.
- Schild, R. and Wendorf, F., 1975, New explorations in the Egyptian Sahara: *in* Wendorf, F. and Madsen, A. E., eds., *Problems in Prehistory: North Africa and the Levant*: Dallas, Texas, Southern Methodist Univ. Press, p. 65-112.
- , 1977, *The Prehistory of Dakhla Oasis and Adjacent Desert*: Warsaw, Polish Academy of Science, 259 p.
- Schmitt, H. H. and Cernan, E. A., 1973, A geologic investigation of the Taurus-Littrow valley: *in* Apollo 17 Preliminary Science Report: NASA SP-330, Wash. D. C., p. 5-1 - 5-21.
- Schumm, S. A., 1956, Evolution of drainage systems and slopes in badlands at Perth Amboy, New Jersey: *Geol. Soc. America Bull.*, v. 67, p. 597-646.
- Sharp, R. P., 1966, Kelso Dunes, Mojave Desert, California: *Geol. Soc. America Bull.*, v. 77, p. 1045-1074.
- , 1973, Mars: Fretted and chaotic terrains: *Jour. Geophys. Res.*, v. 78, p. 4073-4083.
- , 1979, Interdune flats of the Algodones chain, Imperial Valley, California: *Geol. Soc. Amer. Bull.*, Part I, v. 90, p. 908-916.
- Sharp, R. P. and Malin, M. C., 1975, Channels on Mars: *Geol. Soc. America Bull.*, v. 86, p. 593-609.
- Shaw, W. B. K(ennedy), 1929, Darb el Arbain: The Forty Days Road: *Sudan Notes and Records*, v. 12, p. 63-71.

- , 1931, Botanical Notes: Appendix IV: in Bagnold, R. A. and others, Journeys in the Libyan Desert 1929 and 1930: Geogr. Jour., v. 78, p. 534-535.
- , 1934, The Mountain of Uweinat: Antiquity, v. 8, p. 63-72.
- , 1936a, Rock paintings in the Libyan desert: Antiquity, v. 10, p. 175-178.
- , 1936b, An expedition in the southern Libyan desert: Geogr. Jour., v. 87, p. 193-221.
- , 1936c, Two burials from the south Libyan desert: Jour. Egyptian Archaeology, v. 22, p. 47-50.
- , 1945, Long Range Desert Group: Collins; London.
- Shaw, W. B. K(ennedy) and Huchinson, J., 1931, The Flora of the Libyan Desert: Bull. Misc. Information of the Royal Botanical Gardens, Kew, v. 4, p. 161-166.
- , 1934, The Flora of the Libyan Desert: Botanical notes: Bull. Misc. Information of the Royal Botanical Gardens, Kew, v. 7, p. 281-289.
- Shepard, F. P. and Young, R., 1961, Distinguishing between beach and dune sands: Jour. Sed. Petrology, v. 31, p. 196-214.
- Sheppard, T. H., 1970, Desert navigation: Geogr. Jour., v. 136, p. 235-239.
- Shreve, R. L., 1966, Statistical law of stream numbers: Jour. Geol., v. 74, p. 17-37.
- , 1975, The probabilistic-topologic approach to drainage basin geomorphology: Geology, v. 3, p. 527-529.
- Shultz, A., Sutner, L. J., and Basu, A., 1979, Terrestrial debris flow deposits as analogs of martian strewn fields (abstract): in Second Internat. Colloquium on Mars, NASA Conf. Pub. 2072, Wash. D. C., p. 74.
- Slezak, M. H. and El-Baz. F., 1979, Temporal changes as depicted on orbital photographs of arid regions in North Africa: in El-Baz, F. and Warner, D. M., eds., Apollo-Soyuz Test Project Summary Science Report, Volume II: Earth Observations and Photography: NASA SP-412, Wash. D. C., p. 263-272.
- Smart, J. S., 1978, The analysis of drainage network composition: Earth Surface Proc., v. 3, p. 129-170.
- Smith, K. G., 1958, Erosional processes and landforms in Badlands National Monument, South Dakota: Geol. Soc. America Bull., v. 69, p. 975-1008.

- Stigand, C. H., 1916, Observations on the northern section of the Tanganyika-Nile rift valley: *Geogr. Jour.*, v. 48, p. 145-149.
- Strahler, A. H., 1952, Hypsometric (area-altitude) analysis of erosional topography: *Geol. Soc. America Bull.*, v. 63, p. 1117-1142.
- Street, F. and Grove, A. T., 1976, Environmental and climatic implications of late Quaternary lake-level fluctuations in Africa: *Nature*, v. 261, p. 385-390.
- Underwood, J. R., 1979, Review of Libyan Desert Glass, SW Egypt and report on 1978 expedition: in Reports of Planetary Geology Program, 1978-1979, NASA Tech. Memorandum 80339, Wash. D. C., p. 87-90.
- Udden, J. A., 1894, Erosion, transportation and sedimentation performed by the atmosphere: *Jour. Geol.*, v. 2, p. 318-331.
- Vail, J. R., 1978, Outline of the geology and mineral deposits of the Democratic Republic of the Sudan and adjacent areas: *Inst. Geol. Sci.*, London, no. 49, p. 11-12.
- Van Houten, F. B., 1973, Origin of red beds: A review: *Ann. Rev. Earth and Planet. Sci.*, v. 1, p. 39-61.
- Van Noten, F., 1978, Rock Art of the Jebel Uweinat: Graz, Austria, Akademische Drucku. Verlagsanstalt, 42 p., 186 plates.
- Veverka, J., 1975, Variable features on Mars, V, Evidence for crater streaks produced by wind erosion: *Icarus*, v. 25, p. 595-601.
- Veverka, J., Cook, K, and Goguen, K., 1978, A statistical study of crater-associated wind streaks in the north equatorial zone of Mars: *Icarus*, v. 33, p. 466-482.
- Viking Lander Imaging Team, 1978, The Martian Landscape: NASA SP-425, Wash. D. C., 160 p.
- Walker, H. M. and Lev, J., 1953, Statistical inference: New York, Henry Holt, 501 p.
- Walker, T. R., 1967, Formation of red beds in modern and ancient deserts: *Geol. Soc. Amer. Bull.*, v. 78, p. 353-368.
- , 1979, Red color in dune sand: in McKee, E. D., ed., A study of global sand seas, U. S. Geol. Survey Prof. Paper 1052, p. 61-81.
- Ward, W. A., Helm, P. J., Witbeck, N., and Weisman, M., 1980, Digital map of martian eolian features (abstract): in Reports of Planetary Geology Program - 1980, NASA Tech. Memorandum 82385, Wash. D. C., p. 330-332.
- Warren, A., 1972, Observations on dunes and bi-modal sands in the Tenere Desert: *Sedimentology*, v. 19, p. 37-44.

- Wendorf, F., Close, A., Schild, R., Sard, R., Haynes, C. V., Gautier, A., and Hadid, N., 1977, Late Pleistocene and Recent climatic changes in the Egyptian Sahara: *Geog. Jour.*, v. 143, p. 211-234.
- Wendorf, F. and Schild, R., 1980, *Prehistory of the Eastern Sahara*: New York, Academic Press, 414 p.
- Wendorf, F., Schild, R., Sard, R., Haynes, C. V., Gautier, A., and Kobusienwicz, M., 1976, *The Prehistory of the Egyptian Sahara*: *Science*, v. 193, p. 103-114.
- White, B. R., 1979, Soil transport by winds on Mars: *Jour. Geophys. Res.*, v. 84, p. 4643-4651.
- Whiteman, A. J., 1971, *The geology of the Sudan Republic*: London, Clarendon Press, 290 p.
- Whitney, M. I., 1978, The role of vorticity in developing lineation by wind erosion: *Geol. Soc. America Bull.*, v. 89, p. 1-18.
- Whitney, M. I. and Dietrich, R. V., 1973, Ventifact sculpture by windblown dust: *Geol. Soc. America Bull.*, v. 84, p. 2561-2582.
- Wickens, G. F., 1975, Changes in the climate and vegetation of the Sudan since 20,000 B. P.: *Boissiera*, v. 24, p. 43-65.
- Williams, M. A. J., 1975, Late Pleistocene tropical aridity synchronous in both hemispheres: *Nature*, v. 253, p. 617-618.
- Williams, M. A. J. and Hall, D. N., 1965, Recent expeditions to Libya from the Royal Military Academy, Sandhurst: *Geogr. Jour.*, v. 131, p. 482-501.
- Williams, R. S. Jr. and Carter, W. D., eds., 1976, *ERTS-1, A new window on our planet*: U. S. Geol. Survey Prof. Paper 929, Wash. D. C., 362 p.
- Winkler, H. A. 1939a, Rock-pictures at Uweinat: *Geogr. Jour.*, v. 93, p. 307-310.
- , 1939b, *Rock-drawings of southern Upper Egypt II (including Uweinat)*: The Egypt Exploration Society, London, Oxford Univ. Press.
- Wolfe, R. W. and El-Baz, F., 1979, The wind regime of the Western Desert of Egypt (abstract): *in* Reports of Planetary Geology Program, 1978-1979: NASA Tech. Memorandum 80339, Wash. D. C., p. 299-301.
- World Bank, 1976, *Landsat index atlas of the developing countries of the world: Europe and North Africa*: IBRD 1180.

Wright, J. W., 1945, War-time exploration with the Sudan Defense Force in the Libyan desert: Geogr. Jour., v. 105, p. 100-111.

Zimmer, H., Moore, H. J., Shorthill, R. W., and Hutton, R. E., 1977, Grain size distribution of the martian soil inside the Viking Lander 2-footpad 3: Paper presented at Twentieth Plenary Meeting, COSPAR, June 7-18, 1977.

End of Document